Proceeding of
2015 9th International Conference on Telecommunication Systems Services and Applications (TSSA)
November 25-26, 2015
Bandung, Indonesia

Table of Content

10dB Planar Directional Coupler on FR4 Substrate for Automatic Gain Control

Arie Setiawan and Taufiqqurrachman Taufiq (Indonesian Institute of Sciences, Indonesia); Yusuf Nur Wijayanto (National Institute of Information and Communication Technology & Indonesian Institute of Sciences, Japan)

Performance Evaluation of Inter-cell Interference of LTE-A System Using Carrier Aggregation and CoMP Techniques

Desiana Ginting and Arfianto Fahmi (Telkom University, Indonesia)

Improving Bio-Cryptography Authentication Protocol

Ari Moesriami Barmawi (Institut Teknologi Telkom, Indonesia); Irfan Fadil (Telkom University, Indonesia)

Spectrum Sensing of OFDM Signals Using GLRT Detector with Bootstrap Approach

Suhartono Tjondronegoro (Institut Teknologi Bandung, Indonesia); Fiky Suratman and Fajar Nugraha (Telkom University, Indonesia)

The Effects of Apodization profile on uniform Fiber Bragg Gratings

Rumadi Antartika (University of Al Azhar Indonesia, Indonesia); Ary Syahriar, - (University al Azhar Indonesia & Faculty of Science and Technology, Indonesia); Dwi Astharini and Ahmad H. Lubis (University of Al Azhar Indonesia, Indonesia)

A Conceptual Framework of Engaged Digital Workplace Diffusion

Dinda Lestarini, Sarifah Putri Raflesia and Kridanto Surendro (Bandung Institute of Technology, Indonesia)

An Emulation of Transparent Interface Design Based on TCP/IP Implemented onto FPGA of an Altera Nios® Board

Arthur Silitonga (President University, Indonesia); Mervin Hutabarat (Institut Teknologi Bandung, Indonesia)

Design of Wireless Battery Charger Using Near-field Induction Method

Firdaus Firdaus (Universitas Islam Indonesia, Indonesia)

Wireless Sensor Network Application for Carbon Monoxide Monitoring

Firdaus Firdaus (Universitas Islam Indonesia, Indonesia)

Early Warning System for Infectious Diseases

Selvyna Theresia and Inayatulloh Achtar (Binus University, Indonesia)

Outage Probability Analysis for Optical Inter-platform HAPS-Link over Log Normal Turbulence Channels

Iskandar Iskandar (Institut Teknologi Bandung, Indonesia); Hasbi Akbar (Bandung Institute of Technology, Indonesia)

Telemetry, Tracking and Command Subsystem for LibyaSat-1

Faisel Tubbal (University of Wollongong & The Libyan Center for Remote Sensing and Space Science, Australia); Akram Alkaseh and Asem Elarabi (The Libyan Center for Remote Sensing and Space Science, Libya)

Utilizing Mean Greedy Algorithm using User Grouping for Chunk Allocation in OFDMA Systems with Carrier Aggregation

Arfianto Fahmi, Rina Pudjiastuti, Linda Meylani and Vinsensius Prabowo (Telkom University, Indonesia)

Designing Gamified-Service Towards User Engagement and Service Quality Improvement

Sarifah Putri Raflesia and Kridanto Surendro (Bandung Institute of Technology, Indonesia)

A Conceptual Framework for Implementing Gamified-Service to Improve User Engagement by Using ITIL

Sarifah Putri Raflesia and Kridanto Surendro (Bandung Institute of Technology, Indonesia)

Smart Home Platform Based on Optimized Wireless Sensor Network Protocol and Scalable Architecture

Trio Adiono, Rachmad Vidya Wicaksana Putra, Maulana Yusuf Fathany, Muhammad Ammar Wibisono and Waskita Adijarto (Institut Teknologi Bandung, Indonesia)

Analysis of Camera Array On Board Data Handling using FPGA for Nano-Satellite Application

Whildan Pakartipangi, Denny Darlis, Budi Syihabuddin, Heroe Wijanto and Agus D. Prasetyo (Telkom University, Indonesia)

Use of Clustering Concept for Chunk Forming based on Constellation Signals on OFDMA Resource Allocation Systems

Budi Prasetya (Institut Teknologi Bandung & Telkom University, Indonesia); Adit Kurniawan (ITB, Indonesia); Iskandar Iskandar (Institut Teknologi Bandung, Indonesia); Arfianto Fahmi (Telkom University, Indonesia)

Comparison Performance Analysis of OWDM and OFDM System on Multipath Fading Rayleigh Channel

Yuyun Siti Rohmah and Ahmad Muayyadi (Telkom University, Indonesia); Rina Puji Astuti (Institut Teknologi Telkom, Indonesia)

On Comparison of Multigrid Cycles for Poisson Solver in Polar Plane Coordinates

Nurhayati Masthurah (LIPI, Indonesia); Iftitahu Ni'mah, Furqon Hensan Muttaqien and Rifki Sadikin (Research Center for Informatics, LIPI, Indonesia)

Efficient Implementation of EC based Key Management Scheme on FPGA for WSN

Priya Mathew (National Institute of Technology Calicut & CDAC Knowledge Park Bengaluru, India); Jilna P (National Institute of Technology, Calicut, India); Deepthi P.p (NIT Calicut, India)

An agent-based approach for resource allocation in the Cloud Computing environment

Mohamed El-kabir Fareh (Biskra University, Algeria); Kazar Okba (Algeria, Algeria); Manel Femmam and Samir Bourekkache (Biskra University, Algeria)

Application - state A ware Scheduling for Video Delivery over LTE Network

Farhan Pervez (COMSATS Institute of Information Technology, Pakistan); Muhammad Raheel (University of Wollongong, Australia)

Coverage and Capacity Trade-off Using Admission and Power Controlled CDMA System for Wireless Internet Services in Rural Environments

Adit Kurniawan (ITB, Indonesia); Irma Zakia (Institut Teknologi Bandung & School of Electrical Engineering and Informatics, Indonesia); Enok Wartika (Institut Seni Budaya Bandung, Indonesia); Azmi Austin (Institut Teknologi Bandung, Indonesia)

Development of AVR Microcontroller-based Antenna Measurement Tool for Student Experimentation

Muhammad Ammar Wibisono and Achmad Munir (Institut Teknologi Bandung, Indonesia)

Analysis of Wave Characteristics between Cylindrical and Cartesian Coordinate System-based Structure Using FDTD Method

Nabila Husna Shabrina and Achmad Munir (Institut Teknologi Bandung, Indonesia)

Adult Image Classifiers Based On Face Detection Using Viola-Jones Method
Muhamad Putro (Universitas Sam Ratulangi, Indonesia)

Design of Geographic Information System for Tracking and Routing Using Dijkstra Algorithm for Public Transportation
Muh. Aristo Indrajaya, Achmad Affandi and Istas Pratomo (Institute Technology of Sepuluh Nopember, Indonesia)

Application and Data Level Interoperability on Virtual Machine in Cloud Computing Environment
Soffa Zahara, Istas Pratomo and Djoko Rahardjo (Institut Teknologi Sepuluh Nopember Surabaya, Indonesia)

Effect of Electromagnetic Radiation on Rice Plant Growth in Microgravity Environment
Arda Editya, Istas Pratomo and Gatot Kusrahardjo (Institut Teknologi Sepuluh Nopember Surabaya, Indonesia)

The Implementation of Communication System Based on FPGA
Hong Lv, Zhixiang Hua, Fei Pan, Xiaoxuan Li, Yong-Lin Yu and Xinwen Tao (Anhui Jianzhu University, P.R. China)

Performance Analysis of 10-Gigabit-capable Passive Optical Network (XGPON) with Splitting Ratio of 1:64
Nana Rachmana Syambas (Institute of Technology Bandung, Indonesia)

Link Failure Analysis in SDN Datacenter using RipL-POX Controller
Iffah Nisrina, Andre Aginsa and Elsa Vinietta (Institut Teknologi Bandung, Indonesia); Nana Rachmana Syambas (Institute of Technology Bandung, Indonesia)

The Simulation of SDN Network Using POX Controller: Case in Politeknik Caltex Riau
Dwina Siswanto, Suci Ramadona and Beni Hidayatulloh (Institut Teknologi Bandung, Indonesia); Nana Rachmana Syambas (Institute of Technology Bandung, Indonesia)

Effect of Material Thickness on Resonance Characteristics of Anisotropic Artificial Circular Dielectric Resonator
Hepi Ludiyati (School of Electrical Engineering & Informatics Bandung Institute of Technology (ITB) & Politeknik Negeri Bandung (POLBAN), Indonesia); Andriyan B. Suksmono (Bandung Institute of Technology, Indonesia); Achmad Munir (Institut Teknologi Bandung, Indonesia)

Simulation of Network Migration to Software-Defined Network Case Study ITB Ganesha Campus
Mukti Rahim, Muhammad Rizky Hikmatullah and Gede Arna Jude Saskara (Bandung Institute of Technology, Indonesia); Nana Rachmana Syambas (Institute of Technology Bandung, Indonesia)

Network Migration to SDN Using Pareto Optimal Resilience Controller (POCO): Case Study in the UPI Network
Arif Irawan, Maya Rahayu and Fidyatun Nisa (Institut Teknologi Bandung, Indonesia); Nana Rachmana Syambas (Institute of Technology Bandung, Indonesia)

FMCW-based SAR Transmitter for Remote Sensing Application and Its Characterization
Edwar Baihaqi (Bandung Institute of Technology, Indonesia); Achmad Munir (Institut Teknologi Bandung, Indonesia)

Implementation of Load Balancing and Automatic Failover for Application Internet Banking
Fronita Saputra (Indonesia University, Indonesia); Raka Yusuf (Mercu Buana University, Indonesia)

On Relay Selection in Cooperative Communications
Ferzia Firdousi (National University of Sciences and Technology, Pakistan)

Migration Strategies of Terrestrial Digital TV Broadcasting in Indonesia
Case Study West Java Area
Hadi Putra Masrul, Hendrawan (ITB)

Video Processing for Traffic Monitoring Application Using Optical Flow Technique
Bagas Abisena Swastanto, Hendrawan (ITB)

A High Availability (HA) MariaDB Galera Cluster Across Data Center with Optimized WRR Scheduling Algorithmof LVS - TUN
Bagus Aditya, TutunJuhana (ITB)

Implementation Parallel Duplicate Address Detection (PDAD) Mechanism for Macro Handover on HMIPv6
Hamzah U. Mustakim, Tutun Juhana (ITB)

Non-Intrusive Load Monitoring Using Bluetooth Low Energy
Arif Indra Irawan, Tutun Juhana (ITB)

Analyzing Impacts of Physical Interference on a Transmission in IEEE 802.11 Mesh Networks

Trong-Minh Hoang and Van-Kien Bui
Posts and Telecoms Inst of Technology
Hanoi, Vietnam
Email: hoangtrongminh@ptit.edu.vn

Thi Nguyen
Voice of Vietnam
Hanoi, Vietnam
Email: nguyenthi@vov.org.vn

Abstract—Interference is an inherent property of wireless multi-hop networks. In 802.11 wireless multi-hop networks, the impacting of physical interference on a transmission is complexity phenomenon that is the cause of degraded network performance. Several previous studies use analytical model to clarify the issue as a common approach. However, the models did not take fully considerations of physical interference on a transmission such as back-off freezing phenomenon and inter-flow interference. Hence, this paper proposes a novel analytical model based on Markov chain to model the 802.11 MAC based multi-hop mesh networks under fully physical interference. The model is developed to overcome these existed challenges of previous studies and validated by numerical results.

Keywords: IEEE 802.11 MAC; physical interference; analytical model; sensing range; back-off freezing.

I. INTRODUCTION

The IEEE 802.11 DCF (Distributed Coordination Function) is the fundamental mechanism to access the shared medium and available for both the infrastructure and the ad-hoc configurations [1]. It employs the carrier sense multiple access/collision avoidance (CSMA/CA) protocol which has been widely employed in wireless multi-hop networks such as IEEE 802.11 based wireless mesh network.
Interference in wireless multi-hop networks is complicated issue because it is depended on various network conditions such as node density, transmission power, receiver sensitivity threshold or back-off algorithm, etc. Moreover, the concurrent transmissions in overlapping carrier sense range can cause to an inter-flow interference problem for a transmission. Hence, analyzing of the impacts of physical interference on a transmission is critical but not easy task because their concerns to all phases of a connection procedure.
To evaluate the network performance parameters of IEEE 802.11 based wireless multi-hop networks, several studies used to analytical model approach as a popular method.The paper proposes a novel analytical model which covers all impacts of physical interference to compensate the shortfall in the previous studies. The paper is organized as follows: In section II we briefly review the state of the art of related studies. Section III presents our proposed model in both single hop network and multi-hop network scenarios. We adopt some main simulation results with our analysis in section IV. The conclusion is drawn in Section V with the indication of our future work in the last.

II. RELATED WORK

Using analytical models as a tool for evaluating the IEEE 802.11 network performance has been attracted by many researchers in recent years. Since the originated analytical model proposed by Bianchi [2], a number of papers have enhanced this basic model to evaluate the network performance under practical conditions such as finite retransmission attempts [3], back-off algorithm [4], or unsaturated condition [5], etc. However, several practical problems have been not investigated thoroughly in 802.11 based wireless multi-hop networks.
In a wireless multi-hop mesh network, interference issue is significant problem effected to a transmission. When a node initiates a transmission that can force other nodes in its carrier sense range to back-off freezing state then get unfair access. This problem is mentioned in [6] [7] for wireless single hop network case. Otherwise, a transmission can not be completed due to the hidden node problem. The issues can be presented by physical interference model in an analytical model. However, this is not easy task due to its complexity. In our previous work [8] used physical interference model with fixed interference range. The analytical model in [9] [10] based on the combination of the model in [6] and interference model in [11] to present back-off freezing and physical interference impact simultaneously. Unfortunately, the back-off freezing is described in these models is not accuracy as the results proved in [7].
Moreover, these previous proposed models are mostly focused to the impact of concurrent DATA transmissions only. In fact, the impact of interference can appear at any given time of a transmission phase [12]. The study in [13] indicated that in a high density network, the interference caused by ACK packet can create unexpected collisions. Hence, interference impacts of concurrent transmissions including both DATA and ACK transmissions need to be studied. In this paper, we propose a novel analytical model to overcome several challenges in previous studies with main numerical results for evaluating the network performance of 802.11 based wireless multi-hop networks.

III. ANALYTICAL MODEL

A. Assumptions and the proposed analytical model

1) Assumption and network model: Consider a generic IEEE 802.11 wireless mesh network which nodes are uniformly distributed and employed the CSMA/CA mechanism. Every node has already a packet to send out its interface at any time (saturated traffic condition). We focus on the performance

IEEE 802.11 CSMA/CA basic access for both single hop and multi-hop scenarios.

To evaluate performance of IEEE 802.11 based single hop networks, the analytical models in [2] [7] use the concept of discrete time scale based on virtual slot time. Otherwise, a physical slot time concept is used in [14] to describe the remained back-off decrement stage on its time axis. For a long probability, two concepts are in the same meaning then physical time slot is chosen in our approach because it is best suited in a common case. Following that, a meaning of the transmission probability obtained from system of equations (1) and (2) in [2] [7] is redefined as the transmission probability when the previous slot is idle.

$$\tau = \frac{1 - p^{R+1}}{1 - p} \frac{2}{\sum_{i=0}^{R} p^i (W_i + 1) - (1 - p^{R+1})} \quad (1)$$

$$p = 1 - (1 - \tau)^{n-1}. \quad (2)$$

In which, p is the conditional collision probability, $R + 1$ is the maximum retransmission number, W is equal to minimum contention window plus 1, and n is number of nodes in the single hop network.

TABLE I.   NOTATIONS AND SYMBOLS IN OUR ANALYTICAL MODEL

α	Ratio of the sensing range and the transmission range
$A_H ACK(x)$	The hidden area interfered to ACK transmitting session
$A_H DATA(x)$	The hidden area interfered to DATA transmitting session
σ	The length of physical slot time
$g(x)$	The probability density function between two nodes
$f(x, R_1, R_2)$	Calculation function for intersection area
N	Average number of nodes in the transmission range
M	Average number of nodes in the carrier sensing range
$p_e(x)$	The concurrent transmission probability in sensing range
p_o	The transmission probability in a generic slot time
p_t	The transmission probability with the idle channel condition
P_s	The probability that a transmission is successful
T	The length of a transmission duration
Th	The aggregate throughput over a transmission area
R_t	Radius of a transmission range
R_s	Radius of a carrier sensing range
$R_i(x)$	Radius of a interference range
γ	Density distribution function of nodes

2) The proposed analytical model: The proposed model is illustrated in figure 1. In which, the actions of each node can be modeled by a 5 states Markov chain. The five states of a node A are: *Wait (W)* is the state when node A stays in back-off process; *Success (S)* is the state when node A can complete its transmission to another node; *Contention (C)* is the state when the transmission of node A is collided with other transmission; *Freezing type 1 (F)* is the state when node A stops its back-off counter caused other node is transmitting; and *Freezing type 2 (N)* is the state when another node around node A initiates a successful handshake. When node A goes to freezing back-off type 1 or type 2, it can also be the receiver. By having two freezing states, this model can totally describe the status of the channel around a node. The transition probabilities from *Wait* to *Wait*, *Wait* to *Success*, *Wait* to *Contention*, *Wait* to *Freezing type 1*, *Wait* to *Freezing type 2*, *Success* to *Success* and *Freezing type 2* to *Freezing type 2* are denoted as $p_{ww}, p_{ws}, p_{wc}, p_{wf}, p_{wn}, p_{ss}, p_{nn}$, respectively. There are some transition probabilities equal to 1 such as $p_{sw} = p_{cw} = p_{nw} = p_{fw} = 1$.

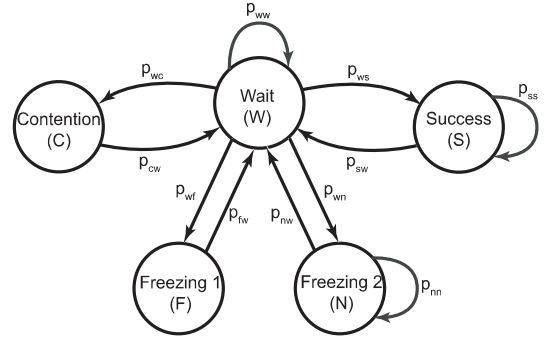

Fig. 1.   The proposed model based on Markov chain

B. The model for IEEE 802.11 based wireless single network

We defines a transmission probability is p_t. The transition probabilities in our model are briefly explained below.

- *Wait* to *Wait*: p_{ww} is the transition probability from state *Wait* to itself. This probability is given by $p_{ww} = (1 - p_t)^n$.

- *Wait* to *Success*: The back-off counter of node A reaches 0, and then, node A initiates a successful transmission to node B; $p_{ws} = p_t(1 - p_t)(1 - p_t)^{n-2} = p_t(1 - p_t)^{n-1}$.

- *Wait* to *Contention*: The transmission of node A is collided due to some concurrent transmissions of other nodes in the network; $p_{wc} = p_t(1 - (1 - p_t)^{n-1}) = p_t - p_{ws}$.

- *Wait* to *Freezing type 1*: In this case, node A does not transmit and there are more than two remaining nodes initiating to transmit; $p_{wf} = (1 - p_t) \times (1 - p_t(n-1)(1 - p_t)^{n-2} - (1 - p_t)^{n-1})$.

- *Wait* to *Freezing type 2*: Node A has to stop its back-off process caused by a successful handshake of another node; $p_{wn} = (1 - p_t) \times p_t(n-1)(1 - p_t)^{n-2}$.

- *Success* to *Success*: node A can transmit consecutively several packets with the probability equal to $p_{ss} = 1/W$ [7].

- *Freezing type 2* to *Freezing type 2*: Its the event when node A continues to freeze its back-off counter due to a consecutively successful transmission of other nodes; $p_{nn} = p_{ss} = 1/W$. The steady-state probabilities of Markov chain are determined as follow:

$$\pi_w = \frac{1}{1 + p_{wc} + p_{wf} + p_{wn}/(1 - p_{nn}) + p_{ws}/(1 - p_{ss})}; \quad (3)$$

$$\pi_c = \pi_w \times p_{wc}; \pi_s = \pi_w \times p_{ws} \frac{p_{ws}}{1 - p_{ss}};$$
$$\pi_f = \pi_w \times p_{wf}; \pi_n = \pi_w \times p_{wn} \frac{p_{wn}}{1 - p_{nn}}.$$

We have the expression to evaluate the one-node throughput as the number of payload bits successfully transmitted in an average slot time:

$$Th(1) = \frac{\pi_s \times E[P]}{E[T]}, \quad (4)$$

where $E[P]$ is the average payload of DATA packet (bits) and $E[T]$ is the average slot time:

$$E[T] = \pi_w T_w + \pi_s T_s + \pi_c T_c + \pi_f T_f + \pi_n T_n \\ = \pi_w T_w + (1 - \pi_w)T. \quad (5)$$

Then, the aggregate throughput of the network is given by:

$$Th = \frac{n \times \pi_s \times E[P]}{E[T]}. \quad (6)$$

The rightness of the proposed model for IEEE 802.11 wireless single hop networks is examined in the same conditions with other analytical models [2] [6] [7] which based on IEEE 802.11a standard [15]. The figure 2 shows the aggregate throughput versus the number of contending nodes in the experiment network. We can recognize that our throughput curve is identical with the result presented in [7].
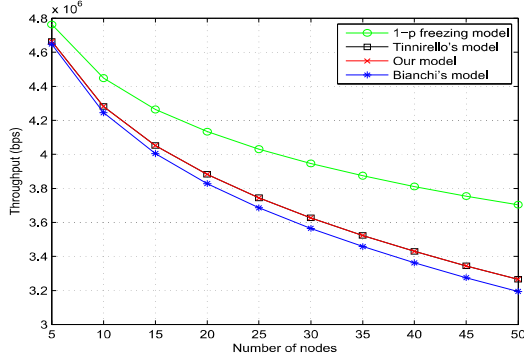

Fig. 2. Network throughput vs number of nodes - Basic mechanism

C. The model for IEEE 802.11 based wireless mesh network

1) Interference description: Considering an IEEE 802.11 wireless mesh network which nodes are distributed on the two dimensional plane with uniform density γ. The probability to find out a number of nodes in an area S is $N(S) = \gamma S$. Denote R_s is radius of a carrier sensing range and R_t is radius of a transmission range. The average number of nodes in these areas is presented as $N = \gamma \pi R_t^2$ and $M = \gamma \pi R_s^2 = N\alpha^2$ with R_s is normalized by $\alpha = R_s/R_t$ and $R_t = 1$. These areas are illustrated in figure 3. The radius of the interference range
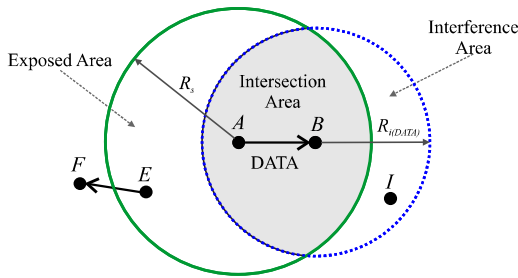

Fig. 3. Exposed area, interference area and intersection area

is $R_i = \sqrt[L]{SINR} \times x$ [11], we choose path loss parameter $L = 4$ in all our experiments. Following the IEEE 802.11b standard, the SINR thresholds are 10 dB (1 Mbps) and 15 dB (11 Mbps) [16]. We assume that the DATA packet is sent at the maximum speed rate. Therefore, $R_{i(ACK)}(x) = 1.78x$ and $R_{i(DATA)}(x) = 2.37x$.

Denote $A_{int} = f(x, R_1, R_2)$ is the intersection area between two circles (A, R_1) and (B, R_2) with the Euclid distance between node A and node B is x [8]. To calculate this function,

we need consider three cases as bellows:

if $R_2 - x > R_1 \rightarrow A_{int}^1 = f(x, R_1, R_2) = \pi R_1^2$;
if $R_2 - x \leq R_1 \leq R_2 + x \rightarrow$
$A_{int}^2 = f(x, R_1, R_2) = \theta R_1^2 + \beta R_2^2 - R_1 R_2 \sin(\theta + \beta)$;
if $R_2 + x < R_1 \rightarrow A_{int}^3 = f(x, R_1, R_2) = \pi R_2^2$,

$$(7)$$

where $\theta = \arccos(\frac{R_1^2 + x^2 - R_2^2}{2x R_1})$, $\beta = \arccos(\frac{R_2^2 + x^2 - R_1^2}{2x R_2})$.
The hidden area interfered to DATA and ACK transmitting sessions as a bellows:

$$A_H DATA(x) = \pi R_{i(DATA)}^2 - f(x, R_s, R_{i(DATA)}) \quad (8)$$

$$A_H ACK(x) = \pi (R_{i(ACK)}^2 - R_s^2) - \\ f(x, R_{i(ACK)}, R_{i(DATA)}) - f(x, R_s, R_{i(DATA)}) \quad (9)$$
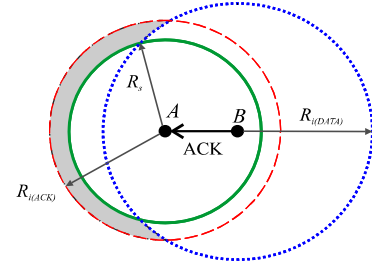

Fig. 4. A hidden area interfered to ACK transmission

2) Probabilities calculation: In IEEE 802.11 multi-hop mesh networks, we redefine some main probabilities such as p_t is the transmission probability of a node with the idle channel condition, P_c is the conditional collision probability which presents the average collision probability of a transmission on a link. At the given slot time, P_c is depended on the transmission probability (p_e) of a node in node A's carrier sensing range, and transmission probability (p_o) of a node outside of node A's carrier sensing range. These probabilities are calculated as bellows.

When node A senses the channel is idle during the previous slot, only node A can certainly reduce its back-off value, while other nodes around node A can be in freezing status, thus $p_e < p_t$. The p_e of a node E is a function of the distance x between node A and node E as follows:

$$p_e(x) = p_t \frac{\pi_w T_w}{\pi_w T_w + (1 - \pi_w)T \times S(x)/\pi\alpha^2}, \quad (10)$$

where $S(x)$ is the sensing area of node E that is not covered by node A's sensing area.

A node outside of the carrier sensing range of node A may be fallen in one of three status as back-off processing, transmitting or freezing back-off. Then, the p_o is:

$$p_o = \pi_s \frac{\sigma}{E[T]} + \pi_f \frac{\sigma}{E[T]} = (\pi_s + \pi_f) \frac{\sigma}{E[T]}. \quad (11)$$

In a uniform distribution mesh network, an average number of node in an area of radius x is proportional to x^2. Thus, the probability density function of a transmission distance between two nodes is $g(x) = \frac{2x}{R_t^2}$, $0 \leq x \leq R_t$.

Let $P_s = 1 - P_c$ be an average successful transmission probability of a practical link. P_s is depended on vulnerable events from other transmissions effecting to a transmission.

We have, $P_s = \int_0^{R_t} g(x)p_s(x)dx$, and $p_s(x)$ is calculated as follow:

$$p_s(x) = p_{in}(x)p_{D-D}(x)p_{D-A}(x)p_{A-D}(x)p_{A-A}(x). \quad (12)$$

In which, $p_{in}(x)$ is the probability that none of nodes within the intersection area is transmitting at the given time. We use **Riemann** method to find the probability with the step division is $\triangle x$. Denote m_i is number of node in i^{th} sub-region of the sensing area of node A, where lying between the $(i-1)^{th}$ arc (radius r_{i-1}) and the ith arc (radius r_i). Thus,

$$p_{in}(x) = \lim_{n \to \infty} \prod_{i=1}^{n} (1 - p_e(r_i))^{m_i}. \quad (13)$$

- The $p_{D-D}(x)$ is a probability that none of nodes in hidden area of node B is transmitting a DATA packet. The vulnerable time is $2 \times t_{DATA}$. We have:

$$p_{D-D}(x) = (1 - p_o)^{2A_H DATA(x)\gamma \times t_{DATA}/\sigma}. \quad (14)$$

- The $p_{D-A}(x)$ is the probability that none of nodes in hidden area of node B is transmitting a ACK packet in DATA transmitting session. The vulnerable time is $t_{DATA} + t_{ACK}$. We have two cases as $x + R_i + R_t > R_s$ and $x + R_{i(DATA)} + R_t \le R_s$.
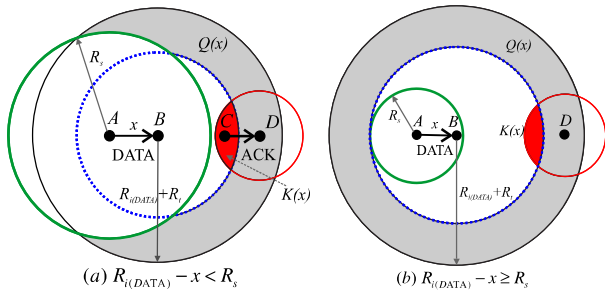

Fig. 5. Areas affected to DATA transmitting session by ACK

In the first case (figure 5a, 5b), we denote the annular grey area created by two circles $(B, R_{i(DATA)})$ and $(B, R_{i(DATA)} + R_t)$ is the $Q(x)$ area. All nodes located in this region (node D) have chances to send DATA packet to another node in the interference area of node B (node C). After receiving DATA packet successfully, node C immediately responses ACK packet to node D and can corrupt the current DATA transmission between node A and node B. The area of Q(x) is:

$$Q(x) = \left[\pi(R_{i(DATA)} + R_t)^2 - f(x, R_s, R_{i(DATA)} + R_t)\right] - \left[\pi R_{i(DATA)}^2 - f(x, R_s, R_{i(DATA)})\right] \quad (15)$$

The average probability of node D transmits has a transmission with a node in the interference area of node B is:

$$p_D(x) = \left[1 - (1 - p_o)^{Q(x)\gamma(t_{DATA}+t_{ACK})/\sigma}\right]\frac{K(x)}{\pi R_t^2}, \quad (16)$$

where $K(x) = f\left(R_{i(DATA)} + \frac{R_t}{2}, R_{i(DATA)}, R_t\right)$. Hence, we derive:

$$p_{D-A}(x) = 1 - \left[1 - (1 - p_o)^{Q(x)\gamma(t_{DATA}+t_{ACK})/\sigma}\right]\frac{K(x)}{\pi R_t^2}. \quad (17)$$
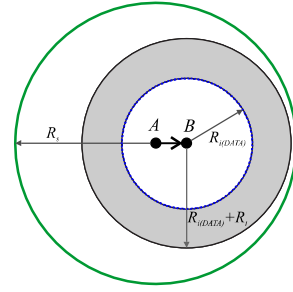
Fig. 6. The sensing range of node A covers the $Q(x)$ area

The second case is shown in figure 6. The $Q(x)$ area is located in the sensing range of node A, thus, there is no ACK packet session from the interference area.

- $p_{A-D}(x)$ is the probability that none of nodes in hidden area of node A have concurrent DATA transmission with ACK transmission of node B. The vulnerable time is $t_{DATA}+t_{ACK}$. If the interference range of node A is less than the sensing range, $p_{A-D}(x)$ is defaulted to 1. Otherwise, if $x \ge \frac{R_s}{1.78}$, then:

$$p_{A-D}(x) = (1 - p_o)^{A_H ACK(x)\gamma \times (t_{DATA}+t_{ACK})/\sigma}. \quad (18)$$

- $p_{A-A}(x)$ is the probability that none of nodes within hidden area of node A has a ACK transmission while node B has a ACK transmission. The vulnerable time is $2 \times t_{ACK}$. There are 3 cases as follows: $R_{i(ACK)} \le R_s - R_t$; $R_s - R_t < R_{i(ACK)} < R_s$ and $R_{i(ACK)} \ge R_s$. In the first case (figure 7a), $p_{A-A}(x) = 1$. The calculation of the remaining parts (as shown in figure 7b and 7c) are similar to the $p_{D-A}(x)$. We also have:

$$p_{A-A}(x) = 1 - \left[1 - (1 - p_o)^{Q(x)\gamma \times 2t_{ACK}/\sigma}\right]\frac{K(x)}{\pi R_t^2}. \quad (19)$$

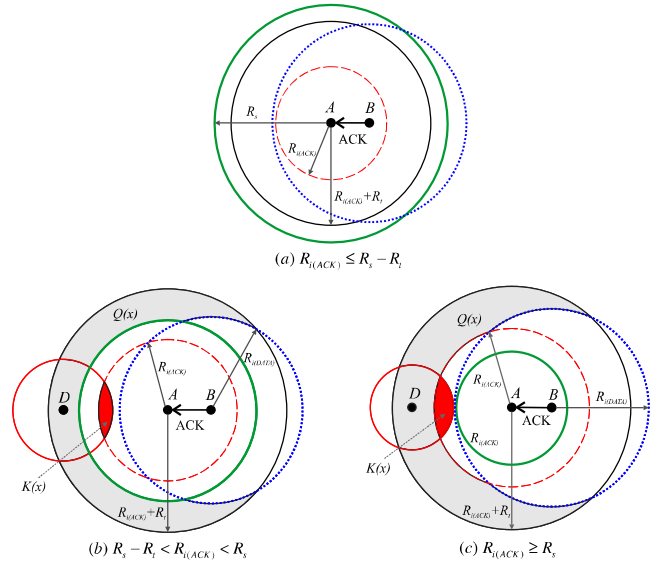Fig. 7. The Q(x) area in ACK-ACK collision

3) *Transition probabilities*: As shown in figure 1, the transmission probabilities are explained below:

- *Wait* to *Wait*: Denote m_i is number of nodes in the ith sub-region of the sensing area of node A with the outside radius r_i as illustrated in figure 8. m_i is approximately equal to: $m_i = \left[\pi(r_i + \Delta x)^2 - \pi r_i^2 \right] \times \gamma \approx 2\pi \gamma r_i \Delta x$. The probability that none of nodes in the sensing range transmits in the next slot time is given by:

$$p_{ww}(x) = \lim_{n \to \infty} \prod_{i=1}^{n} \left(1 - p_e(r_i) \right)^{m_i}. \qquad (20)$$
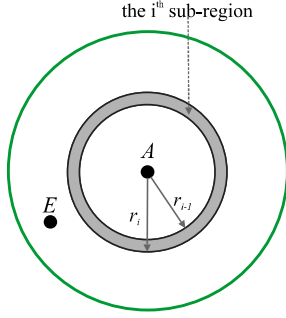

the ith sub-region

Fig. 8. Dividing the carrier sensing area into n sub-regions

- *Wait* to *Success*: We have $p_{ws}(x) = p_t p_s(x)$, where $p_s(x)$ is the probability that a transmission at distance x becomes success. Hence:

$$\begin{aligned} p_{ws} &= \int_0^{R_t} g(x) p_{ws}(x) dx = p_t \int_0^{R_t} g(x) p_s(x) dx \\ &\Rightarrow p_{ws} = p_t P_s. \end{aligned} \qquad (21)$$

- *Wait* to *Contention*: A transmission can't be completed if there is an unsuccessful transmission of DATA or ACK packet. Thus, the transition probability from *Wait* state to *Contention* state is: $p_{wc} = p_t - p_{ws}$.
- *Wait* to *Freezing type 2*: This event occurs when node A keeps silent and there is another node inside its carrier sensing range initiates a successful transmission.

$$p_{wn} = (1 - p_t) \times \lim_{n \to \infty} \sum_{i=1}^{n} \left(p_e(r_i) m_i \right) \times P_s. \qquad (22)$$

- *Wait* to *Freezing type 1*: We have $p_{wf} = 1 - p_{ww} - p_t - p_{wn}$.
- *Success* to *Success* and *Freezing type 2* to *Freezing type 2*: A node has a chance to transmit several continuous data packets if and only if after extracting new zero back-off value, there will be no interference impacts in both DATA-ACK transmission phases. Thus,

$$p_{ss} = p_{nn} = \frac{1}{W} \int_0^{R_t} p_{D-D}(x) p_{D-A}(x) p_{A-D}(x) p_{A-A}(x) dx. \qquad (23)$$

IV. NUMERICAL RESULTS AND DISCUSSIONS

To validate our proposed model, we use MATLAB Tool to verify throughput and packet drop performance parameters. We determine the stationary probabilities to obtain the throughput per one node as:

$$Th(1) = \frac{\pi_s \times E[P]}{E[T]}. \qquad (24)$$

The aggregate throughput over the transmission area of a node (Th) is given by:

$$Th = \frac{N \times \pi_s \times E[P]}{E[T]}. \qquad (25)$$

We use this value to evaluate the performance of the multi-hop mesh network. Assume that the length of the queue is infinite and the maximum retransmission retry is 7, the packet drop rate is:

$$P_{drop} = (1 - P_s)^7. \qquad (26)$$

The analytical model will be examined under standard parameters of IEEE 802.11b [16]. Let L_{DATA} is the average length of DATA packet, $L_{DATA} = H + E[P]$, where H is the length of header which composes physical header and MAC header. The transmission durations of ACK and DATA packet are: $t_{DATA} = \frac{L_{DATA}}{R_{data}}; t_{ACK} = \frac{L_{ACK}}{R_{basic}}$. Ignoring the propagation delay, the duration of each state in basic mechanism is given by:

$$\begin{aligned} T_w &= \sigma, T_S = T_C = T_F = T_N = T \\ T &= t_{DATA} + SIFS + t_{ACK} + DIFS. \end{aligned} \qquad (27)$$

From equations (25) and (26), we verify throughput and packet drop rate of wireless mesh networks based on 802.11b in multi-hop fashion by varying input parameters such as density distribution, ratio of the sensing range and the transmission range, and payload packet size.

As shown in Figure 9, the single-node throughput decreases when number of nodes in transmission area increases. This result reflects to collisions of concurrent transmissions which depend on varying of carrier sense range. In case $\alpha \geq 4$, there is no hidden node area then we have a result as in single hop case.
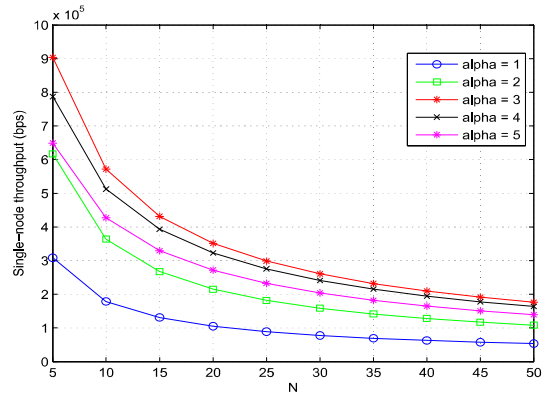
Fig. 9. Single-node throughput vs number of nodes

Figure 10 illustrates the aggregated throughput which has best performance with $\alpha = 3$ around, and the throughput is strongly decreased while $\alpha \geq 4$ due to the influence of back-off freezing phenomenon.

The influence of α on network performance on packet drop rate is illustrated in figure 11. This work focused on BEB algorithm with varying number of nodes in transmission area. The packet drop rate reaches maximum value with $\alpha = 1$.

Figure 12 illustrates the aggregated throughput depends on vary of the ratio α and payload size when $N = 5$. It is seen
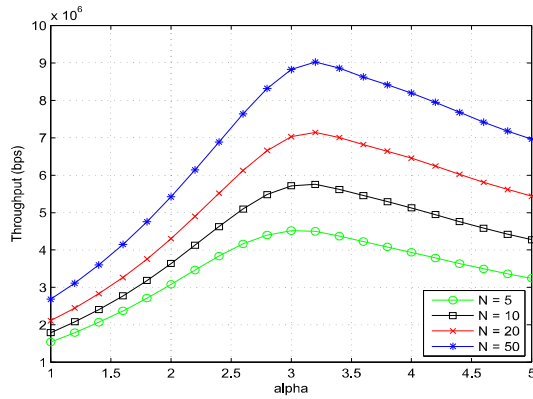
Fig. 10.   The aggregated throughput
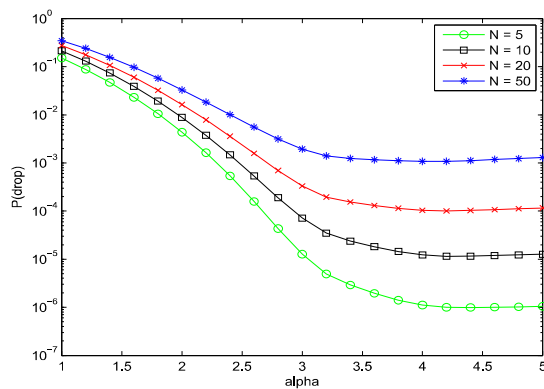
Fig. 11.   Packet drop rate vs alpha

from the figure that the aggregated throughput is maximum when the payload size is reached maximum data unit with α around 3.
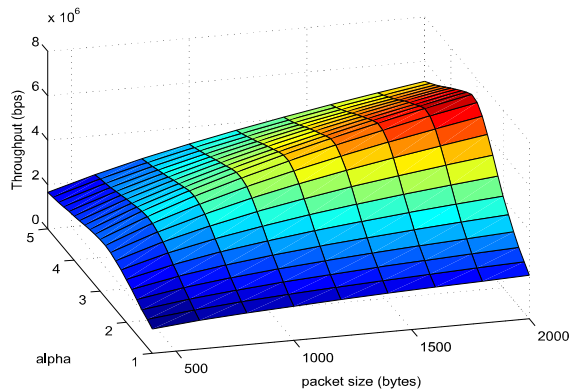
Fig. 12.   Aggregate throughput vs alpha and the packet size

V.   CONCLUSION

In this paper, we propose a novel analytical model to analyse the impacts of physical interference on a transmission in 802.11 multi-hop mesh networks. The model provides a detailed view of interference phenomenon on every stage of a transmission in the saturated multi-hop mesh network. To prove the exact of our model, our numerical result has been examined and compared with other previous studies in saturated 802.11 single hop networks. Our model taking into account the practical conditions of 802.11 multi-hop networks were neglected in previous studies as the back-off freezing phenomenon and interference of concurrent transmissions. To exploit the impacts of physical interference on the network performance, throughput and drop rate parameters of saturated 802.11 multi-hop mesh networks are validated by some main numerical results. We have learned from the results that there is existed an optimal carrier sensing range which strikes a balance value between the back-off freezing phenomenon and collision events on a practical transmission.

REFERENCES

[1] IEEE 802.11 standard, Wireless LAN Medium Access Control (MAC) and Physical Layer (PHY) specifications, 2007.

[2] G. Bianchi, "Performance analysis of the IEEE 802.11 distributed coordination function", IEEE J. Sel. Areas Commun., vol. 18, no. 3, pp. 535547, Mar. 2000.

[3] H. Wu, Y. Peng, K. long, S. Cheng, and J. Ma, "Performance of reliable transport protocol over IEEE 802.11 WLAN: Analysis and enhancement" in Proc. IEEE INFOCOM, 2002, vol. 2, pp. 599607.

[4] C. Ye, Y. Li and A. Reznik, "Performance Analysis of Exponential Increase Exponential Decrease Back-off Algorithm" in Proc. IEEE Globecom, 2010.

[5] J. M. Pitts, and O. M. Shepherd, "Analyzing the Transition Between Unsaturated and Saturated Operating Conditions in 802.11 Network Scenarios", IEEE MILCOM, Nov. 2008.

[6] E. Ziouva and T. Antonakopoulos, "CSMA/CA performance under high trafc conditions: Throughput and delay analysis", Comput. Commun., vol. 25, no. 3, pp. 313321, Feb. 2002.

[7] I. Tinnirello, G. Bianchi and Y. Xiao, "Refinements on IEEE 802.11 distributed coordination function modeling approaches", IEEE Trans. Veh. Technol., vol. 59, no. 3, pp.1055 -1067 2010.

[8] Trong-Minh Hoang, Minh Hoang, "A Novel Analytical Model to Identify Link Quality in 802.11 Mesh Networks", CICSyN, 2012.

[9] J. He, D. Kaleshi, A. Munro, Y. Wang, A. Doufexi, J. McGeehan and Z. Fan, "Performance investigation of IEEE 802.11 MAC in multihop wireless networks", Proc. IEEE/ACM MSWIM, pp.242 -249 2005.

[10] B. Alawich, C. M. Assi and H. Mouftah, "Investigating the performance of power-aware IEEE 802.11 in multi-hop wireless networks", IEEE Trans. Veh. Technol., vol. 58, no. 1, pp.287 -300 2009.

[11] K. Xu, M. Gerla, and S. Bae., "Effectiveness of RTS/CTS handshake in IEEE 802.11 based ad hoc networks", Journal of Ad Hoc Networks, pages 107123, 2003.

[12] H. Zhai and Y. Fang, "Physical carrier sensing and spatial reuse in multirate and multihop wireless ad hoc networks", INFOCOM, 2006.

[13] Wei Wang, Qiang Wang, Wai Kay Leong, Ben Leong, and Yi Li, "Uncovering a HiddenWireless Menace: Interference from 802.11x MAC Acknowledgment Frames", SECON, 2014.

[14] H. Ma , H. M.K Alazemi and S. Roy, "A stochastic model for optimizing physical carrier sensing and spatial reuse in ad hoc networks", Proc. IEEE International Conference on Mobile Ad-hoc and Sensor Systems - MASS, pp.615 -622 2005.

[15] IEEE 802.11a-1999, Supplement to Part 11: Wireless LAN Medium Access Control (MAC) and Physical Layer (PHY) specifications: High-speed Physical Layer in the 5 GHZ Band, 1999.

[16] IEEE 802.11b-1999, Supplement to Part 11: Wireless LAN Medium Access Control (MAC) and Physical Layer (PHY) specifications: Higher-speed Physical Layer Extension in the 2.4 GHz Band, 1999.

Mobile Based Radars using Eclipse IDE with OpenStreetMap for Tracking Object Locked by ISRA Radar Console

R. Priyo Hartono Adji
Research Center for Electronics and Telecommunication
Indonesian Institute of Sciences (LIPI)
Bandung, Indonesia
r.priyo.hartono.adji@lipi.go.id

Octa Heriana
Research Center for Electronics and Telecommunication
Indonesian Institute of Sciences (LIPI)
Bandung, Indonesia
octa.heriana@lipi.go.id

Arief Nur Rahman
Research Center for Electronics and Telecommunication
Indonesian Institute of Sciences (LIPI)
Bandung, Indonesia
arief.nur.rahman@lipi.go.id

Abstract—**This paper presents about design of mobile-based data integration application system from one radar station for displaying information about objects detection results from multiple object locked by radar for tracking needs, AIS receiver data, long range camera monitoring and also weather information. The system proposed in this paper can be a guidance for commander for taking decision. A sample implementation of the system is also given.**

Keywords—Android SDK, Eclipse, OpenStreetMap, Phonegap, Leaflet.js.

I. INTRODUCTION

Radar is an electronic system that transmits radio frequency (RF) in the form of electromagnetic waves (EM) towards / desired areas and receiving also detecting the EM wave when reflected by objects in the area [1]. The reflected signal is processed to obtain information about the existence of an object, such as position, velocity, and other relevant information. Any information received will be displayed on the display console.

Eclipse is an integrated development environment (IDE). It contains a base workspace and an extensible plug-in system for customizing the environment. Written mostly in Java, Eclipse can be used to develop applications in Java. The Eclipse software development kit (SDK), which includes the Java development tools, is meant for Java developers. Users can extend its abilities by installing plug-ins written for the Eclipse Platform, such as development toolkits for other programming languages, and can write and contribute their own plug-in modules [2].

Android Developer Tools (ADT) is a plugin for Eclipse that provides a suite of tools that are integrated with the Eclipse IDE. It offers you access to many features that help you develop Android applications[3]. A mobile based implementation has been proposed in this work to ensure mobility, speed and also for commander guidance for how to respond the situation immediately. In this paper authors making application by using phonegap for making hybrid app

(Native & HTML5) and Leaflet.js for helping to generate OpenStreetMap data.

The next section first explains related work and introduction about OpenStreetMap. The subsequent section provides principle and system model, and implementation details and finally the chapter explains future directions.

II. RELATED WORK

The OpenStreetMap (OSM) project is the most successful collaborative geospatial content generation project. The distinguishing attribute of OSM is free access to huge amounts of geospatial data, which has resulted in hundreds of commercial and non-commercial web and mobile applications and services. The OSM data is freely available and that is why the data can be used within many data infrastructure applications and value-added services. In addition, the free access to data has led to the growth of OSM as a replacement of propriety systems in academic and business environments. It was inspired by the success of Wikipedia and the preponderance of proprietary map data in the UK and elsewhere. Since then, it has grown to over 2 million registered users, who can collect data using manual survey, GPS devices, aerial photography, and other free sources. This crowdsourced data is then made available under the Open Database License.

OpenStreetMap has been widely used in numerous scientific and research endeavors. Godwin Yeboah and Seraphim Alvanides propose a research by undertaking a route choice analysis using the cycling-friendly version of OpenStreetMap (OSM) as the transportation network for analysis, alongside GPS tracks (7 days) and travel diary data for 79 Utility Cyclists around Newcastle upon Tyne in North East England. They examined specific variables as proposed in the relevant cycling literature and used these to develop a model testing the null hypothesis that network restrictions (i.e. one way, turn restrictions and access) do not have any significant influence on the movement of commuter cyclists.

The findings suggest that OSM can provide a robust transportation network for cycling research, in particular when combined with GPS track data[4].

Pouria Amirian, et. al. demonstrated a next generation of navigational services using OpenStreetMap data with augmented reality and graph databased, they describes the implementation of a navigational application using OSM data as part of the eCampus project in Maynooth University. The application provides users several navigation services with navigational instructions through standard textual and cartographic interfaces and also through augmented images showing way-finding objects[5].

Jorge Gil [6] presents the process of building a multimodal urban network model using Volunteered Geographic Information (VGI) and in particular OpenStreetMap (OSM). The spatial data model design adopts a level of simplification that is adequate to OSM data availability and quality, and suitable to the measurement of the sustainable accessibility of urban neighborhoods and cityregions. The urban network model connects a private transport system (i.e. pedestrian, bicycle, car), a public transport system (i.e. rail, metro, tram and bus) and a land use system (i.e. building land use units).

III. OPEN STREET MAP

OpenStreetMap is a free, editable map of the entire world. Unlike proprietary datasets, the OpenStreetMap license allows free access to the full map data set. This massive amount of data may be downloaded in full but is also available in other useful formats such as mapping, geocoding or other web services. Unlike popular map sources like Google Maps, OSM relies mostly on data from portable GPS devices, aerial photography or simply local knowledge. This implies that there is no guarantee to the accuracy of the map data. Nevertheless, since every user is allowed to edit the map content, there is a high chance of the rectification of errors with the passage of time. Currently, the OSM API provides almost all the functionality needed for AGV guidance and control. The advantage of using OSM is that it does not have stringent license issues and hence a wide variety of applications can be created using OSM at the expense of MAP accuracy[7].

The Google maps API's terms of service[8] explicitly prohibit the application of the service for automobile guidance and tracking applications. Map accuracy keeps improving with the passage of time as more and more sources are added to the OSM map data and keeping in view the progress OSM has made in the last few years, we can safely predict that in the future, OSM maps will be considered as much authentic as Google or any other mapping service for that matter. OSM maps rely on Javascript for displaying their maps and all the map functions are derived from the OpenLayers mapping library. A map is created by instantiating the OpenLayers.Map object which takes the ID of a DIV tag in which the map is to be displayed as its parameter. OSM maps offer numerous features like a collection of controls, markers (also called permalinks), event handlers, Asynchronous Javascript and XML (AJAX), etc. [9].

IV. PRINCIPLE & SYSTEM MODEL

Principle in this system is to monitoring object locked by ISRA Radar Console by hitting tracking button ON (Radar Console) and then sending latitude and longitude to mobile for tracking, and also for AIS the data is sent in the form of values latitude, longitude, type and timestamp, coupled with the data from the identity of the ship name. MJPEG are sending by long range camera and also weather info by using Leaflet Weather. Overall application are illustrated in this use case diagram (Figure 1).
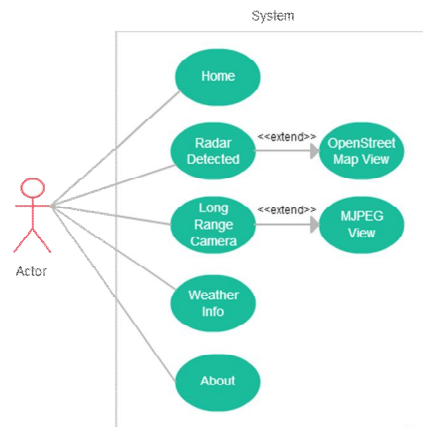
Fig. 1. Use Case Diagram Mobile Based Radar.

The following is a system model of mobile based radar application (Figure 2).
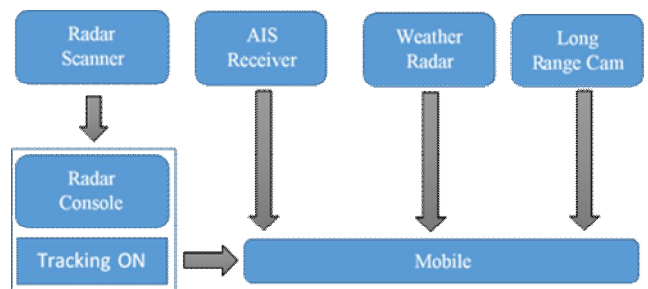
Fig. 2. System Model of Mobile Based Radar.

V. IMPLEMENTATION

A. Tracking Process

Radar console software is designed to be able to transmit information which contains the latitude and longitude, then given marker type data set that is sent is reading data from the radar data with label "Type", and put a mark on each data with label "Timestamp". The radar desktop application software that is used is a modified version of the software radar ISRA [10]. The workflow system in general can be shown by Figure 3.

Data Processing Flow

Fig. 3. Data Processing Flow of ISRA Radar.

Software system of a radar developed with the structure as shown in Figure 4 below.
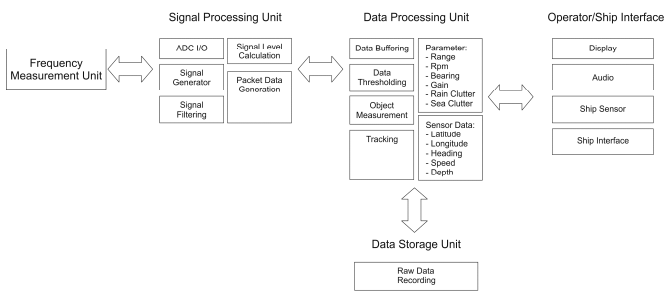
Fig. 4. Software Function Block Diagram of ISRA Radar.

Computer parts Signal Processing are ADC IO Handling, Signal Generator DDS, Counting Signal Level, Filter Signal and Preparation Package Data. Overall signal processing on the computer signal processing is handled by the application a snap. SNAP is a signal processing program based on Visual C ++ on a radar applications that perform several major functions, namely Raw Data Capture, FFT Processing, CFAR (Constant False Alarm Rate) Processing and Data Compression.

Object tracking process can be described as follows:

- when start (tracking on);
- Input data point user clicked;
- Windowing the data around a central point when sweep past the point of data

- Calculating the center of the data points in the window and calculate point next prediction
- Receive data prediction
- Previous point move in accordance with the prediction data received and describes the track is formed
- Did Sweep past the point of the selected data? If yes then back to windowing the data around a central point when sweep past the point of data if not Input Tracking OFF and END.
- When user clicked the object then sending the coordinates to mobile which containing data.

While mobile obtaining data in the following way :

- Click the button "TRACKING".
- Place cursor to echo image object and then "CLICK".
- Windowing process PictureBox coordinates in one of the function in VB to develop a matrix that will be processed by clustering in java.
- Conducting the process of sending data matrix coordinates (x, y) to the java application.
- Java process data matrix, calculate the cluster center of the clustering process, and make predictions of further movement of the cluster center.
- The calculation result obtained cluster center, and sent back to VB.
- VB then make a plot of the cluster center coordinates into the PictureBox (Picture box standard component in VB to plot the drawing, the operation has no built-in function of its own).

Data tracking results for the current version now does not display the string Latitude or Longitude. But in principle, can be shown by calculating the formula :

$Latitude = Round(Lon + ((x - CenterX) * RangeByPixel /RangeDegreeUnit), 7)$

$Longitude = Round(Lat - ((y - CenterY) * RangeByPixel/RangeDegreeUnit), 7)$

With explanation :

- The value of x and y are the coordinates of the tracking results
- CenterX, CenterY is the circle center point coordinates on a display in a PictureBox
- Mr = Radius of the earth to the position Latitude (origin radar position), calculated based on the radius of the earth's equator and the polar radius of the earth.
- RangeDegreeUnit = RangePerDegPrecision / 1000
- RangePerDegPrecision = 3.1415926536 * Cos (Lat) * Mr / 180

- $M_r = Sqr(((A^4 * Cos(Lat)^2) + (B^4 * Sin(Lat)^2)) / ((A * Cos(Lat))^2 + (B * Sin(Lat))^2))$

- A = 6378137 'diameter of the earth's equator in meters

- B = 6356752.3 'Earth's polar diameter in meters

- Latitude is the value placed Latitude radar position

- Longitude is the value placed Longitude radar position

B. *Sample Implementation*

By sending its latitude and longitude from radar console to mobile and by processing of Leaflet.js that would plot object on OpenStreetMap as shown in figure 5(c).
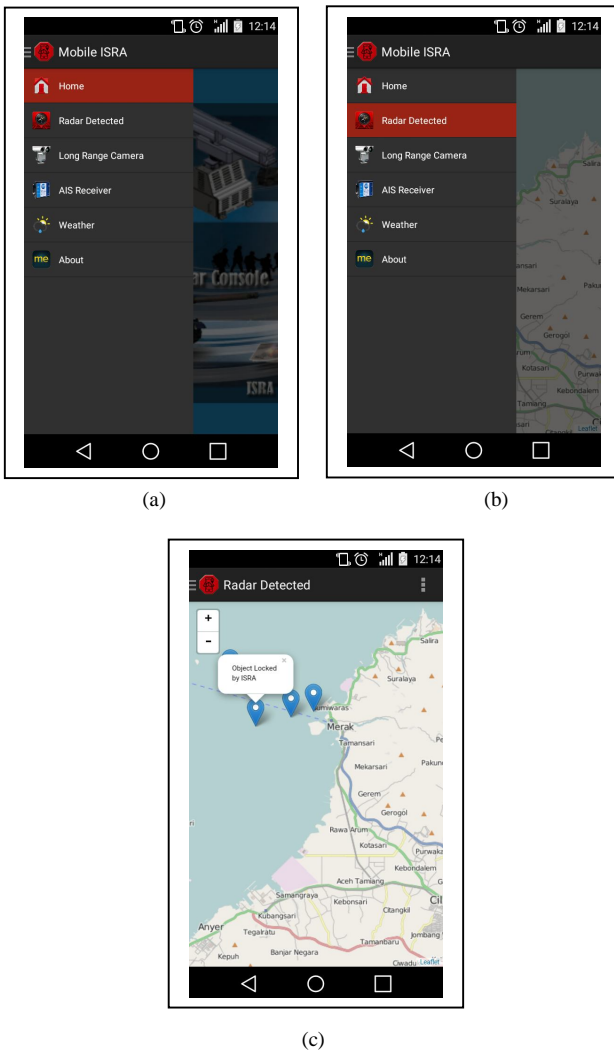

(a)   (b)

(c)

Fig. 5. Screenshot of Mobile ISRA (a) Home; (b) Radar Detected; (c) Object Locked by ISRA Radar Console.

VI. Conclusion and Future Work

Design of mobile-based radar has been done by using data connection from Radar console application to a web server. Data shown are data from radar detection, decoding of data from AIS receiver, MJPEG from Long Range Camera and weather information.

As mentioned in paper of Pouria Amirian and teams authors should have using augmented reality that would make visual navigation service using augmented reality provides an intuitive interface that could be integrated into augmented reality systems. By using augmented reality for long range camera and connected with graph database and AIS that would more give information for commander about the object detected by radar. With the proliferation of augmented reality and gadgets in the very near future, and with the availability of reliable OSM data coupled with the multi-dimensional nature of graph databases, there will be huge opportunities for innovative and creative applications in the next generation.

References

[1] Mashury Wahab and ISRA Radar Team, Techniques Reference Book for FM-CW ISRA RADAR, PPET-LIPI, 2014.

[2] Garima Pandey and Diksha Dani, "Android mobile application build on eclipse", International Journal of Scientific and Research Publications, Vol. 4, Issue 2, February 2014.

[3] https://developer.android.com/tools/help/adt.html

[4] Godwin Yeboah and Seraphim Alvanides, "Route Choice Analysis of Urban Cycling Behaviors Using OpenStreetMap: Evidence from a British Urban Environment", OpenStreetMap in GIScience Experiences, Research, and Applications, Springer, pp 189-210, November 2014.

[5] Pouria Amirian, Anahid Basiri, Guillaume Gales, Adam Winstanley and John McDonald , "The Next Generation of Navigational Services Using OpenStreetMap Data: The Integration of Augmented Reality and Graph Databases", OpenStreetMap in GIScience Experiences, Research, and Applications, Springer, pp 211-228, November 2014.

[6] Jorge Gil, "Building a Multimodal Urban Network Model Using OpenStreetMap Data for the Analysis of Sustainable Accessibility", OpenStreetMap in GIScience Experiences, Research, and Applications, Springer, pp 229-251, November 2014.

[7] Fahad Ullah, Qaiser Habib, Muhammed Irfan, and Khawaja M. Yahya, "Autonomous Vehicle Guidance and Control using OpenStreetMap and Advanced Integration Techniques", International Journal of Computer Theory and Engineering, Vol. 3, No. 5, October 2011.

[8] Goolge Maps/Earth Terms of Services. Available: http://www.google.com/help/terms_maps.html.

[9] OpenLayers Javascript Mapping Library Developer Docs. Available: http://www.dev.openlayers.org/docs/

[10] Octa Heriana and Arief Nur Rahman, "Design of Web Based Radars Data Integration System", The 2nd International Conference on Radar, Antenna, Microwave, Electronics and Telecommunications (*ICRAMET),* March 2013.

Pilot-Based Estimation for SC-FDMA LTE in High Altitude Platforms (HAPS) Channel

D. Hidayat and Iskandar

School of Electrical Engineering and Informatics, Bandung Institute of Technology
Jl. Ganesha No.10 Bandung 40132 Indonesia
E-mail: dicky.hidayat@gmail.com, iskandar@stei.itb.itb.ac.id

Abstract–**This paper aims at evaluating pilot-based estimation technique for SC-FDMA LTE deployed via high altitude platforms (HAPS) channel. HAPS is a novel wireless infrastructure in which one of its applications is to carry cellular system such as 4G LTE. The problem of SC-FDMA LTE signal transmission over HAPS channel is due to multipath from objects nearby the mobile user. Signal at the receiver, which in this case receiver is an eNB onboard the platform, will be suffering from fluctuation due to fading. Since the channel conditions fluctuate, immediate channel state information (CSI) needs to be estimated in a short time. Pilot signal or a so-called training sequence is a popular approach to estimate CSI. HAPS channel is known to follow Ricean fading distribution. In our work, pilot-based estimation is evaluated under HAPS Ricean channel. The channel variation is governed by user's elevation angle. Modulation type and LTE channel bandwidth are also investigated.**

Keywords–**LTE, SC-FDMA, HAPS, pilot-based channel estimation, Ricean fading channel.**

I. INTRODUCTION

In LTE, two multiple access schemes are used namely Orthogonal Frequency Division Multiple Access (OFDMA) for downlink and Single Carrier Frequency Division Multiple Access (SC-FDMA) for uplink. The characteristic of orthogonality between the users make those schemes are able to reduce interference and improve network capacity. For the uplink, user specific allocation is continuous to transmit in a single-carrier mode, while in the downlink users can use resource blocks from different parts of the spectrum freely. Another reason for the uplink single-carrier solution is also to allow efficient terminal power. LTE technology has many options to use spectrum bandwidth, starting from 1.4 MHz, 3 MHz, 5 MHz, 10 MHz, 15 MHz and 20 MHz. This bandwidth flexibility brings LTE to be the best technology ever of cellular communication and potential to offer high-speed data rate. Using MIMO 2x2 and MIMO 4x4 LTE can provide data rate up to 150 Mbps and 300 Mbps with 20 MHz bandwidth for the downlink, respectively. For the uplink peak data rate is 75 Mbps [1]-[2]. The above LTE specification was originally designed for terrestrial-based cellular system formulated in 3GPP Release 8. However, LTE is not much investigated to be deployed over HAPS or satellite network.

SC-FDMA is designed in LTE uplink to reduce multipath fading effect. The basic principle of SC-FDMA is equal to the QAM modulation. Each symbol is sent one at a time such as in TDMA of GSM. Therefore, the receiver which in this case is the eNB onboard the HAPS still needs to deal with inter-symbol interference because of preventing inter-symbol interference between a block of symbols. The transmission occupies the continuous part of the spectrum allocated to the user, and for LTE the system facilitates a 1 ms resolution allocation rate.

In this paper, we propose a deployment of LTE uplink using SC-FDMA multiple access scheme through HAPS channel. Our goal is to investigate pilot-based channel estimation performance on the uplink direction of LTE via HAPS channel. As we may know that uplink is a bottleneck and often causes major problems in cellular network. Objects nearby the users on the ground are the main problem of multipath fading experienced by the uplink signal. Elevation angle of users in looking at the HAPS determines fading level. Users who have high elevation angle or located beneath the platform will experience less fading compared with those who are located at the edge coverage.

HAPS has been proposed to be a novel wireless delivery method floating on the stratospheric layer about 17 – 22 km above the ground [3]. HAPS has a unique geometry in terms of communication link compared with terrestrial tower or satellite system [4]-[5]. Today we are witnessing the terrestrial tower system and satellite as a common infrastructure of wireless technology. In terrestrial system, we need the ground allocation and large numbers of tower to cover large areas. In satellite system, we require only 3 satellite GEO to cover the global coverage of earth. However, both terrestrial and satellite technology encounter their unique problem. HAPS is developed as a solution to the problem that is encountered by terrestrial and satellite system. Compared with satellite system, HAPS advantage includes low propagation delay, low power consumption, and smaller user equipment. Whereas compared with terrestrial, HAPS advantage includes high elevation angle which broaden Line of Sight (LOS), better coverage areas, relatively low operational costs and easy to mobilize in emergency conditions. HAPS also is able to minimize the problems of multipath [6]-[8].

As an infrastructure that utilizes the medium of air, characterization of the channel is important, because it greatly affect the performance of the system. Meanwhile, channel estimation technique by using pilot signal is used to

compensate channel characteristic to the system. Integrating HAPS on LTE provide a positive impact on the world of mobile communications today. These two technologies are expected to answer the need of safety, reliable and revolutionary telecommunication technology with high bit rates at low cost.

In this paper, SC-FDMA's performance on HAPS with pilot-based channel estimation will be analysed. SC-FDMA's performance on a HAPS channel is evaluated based on a computer simulation. The result will be analysed to determine the effect of elevation angle, channel bandwidth, modulation type and Doppler frequency on system's performance. Characteristic of channel is taken from research of HAPS in Hokkaido, Japan [1]. HAPS is using ricean channel that modelled the condition of Line of Sight (LOS) and multipath due to user's location and landmark circumstances. K factor is used as a parameter to indicate LOS ratio.

The rest of paper is organised as follows. Section II reviews SC-FDMA on LTE while in section III we review High Altitude Platforms channel model and characteristic. In Section IV, we explain simulation model for signal transmission of LTE uplink over HAPS channel. Then simulation results is analysed in Section V. We focus our analysis on the effect of users elevation angle, LTE spectrum bandwidth, modulation type, and Doppler frequency shift. Finally, conclusions are drawn in Section VI.

II. INTRODUCTION TO SC-FDMA SCHEME IN LTE

SC-FDMA is LTE's multiple access scheme for uplink. SC-FDMA can be regarded as DFT-spread orthogonal frequency division multiple access, where time domain data symbols are transformed to frequency domain by DFT before going through subcarrier mapping process. The only different between OFDMA dan SC-FDMA is an additional DFT block on transmitter and IDFT block on receiver [9]-[11].

Resource block structure on SC-FDMA can be described as in Fig. 1. A resource block has a duration of 0.5 ms and bandwidth of 180 kHz (12 subcarriers). All the resource blocks constitute a resource grid. The number of blocks in the resource grid ranges from 6, for 1.4 MHz channels, to 100, for 20 MHz channels. Each uplink slot carries seven SC-FDMA symbols. The smallest element in a resource block is called Resource Element which contains a subcarrier for the duration of one SC-FDMA symbol.

Pilot signal is used as reference signal that is required to perform channel estimation at the receiver output. Pilot signal is inserted at specific symbol and when it pass through the channel, it will be processed with a method that estimates channel condition and then compensate it to another symbols. Pilot signal is generated based on Zadoff-Chu sequence. Zadoff-Chu sequence commonly referred as Constant Amplitude Zero Auto Correlation (CAZAC) sequence. Here is the equation.

$$x_q(m) = e^{-j\frac{mqm(m+1)}{N_{ZC}}}, 0 \leq m \leq N_{ZC-1} \qquad (1)$$
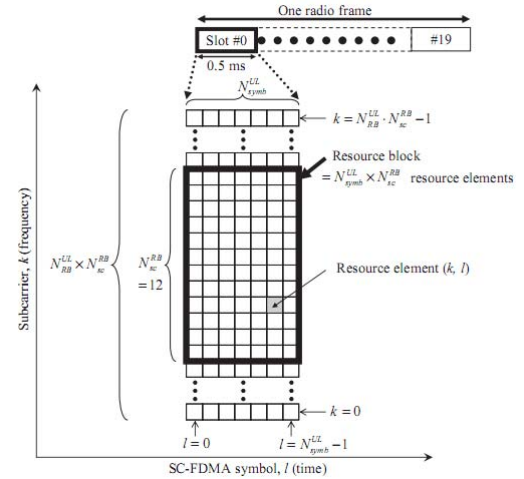
Fig. 1 SC-FDMA resource grid [1].
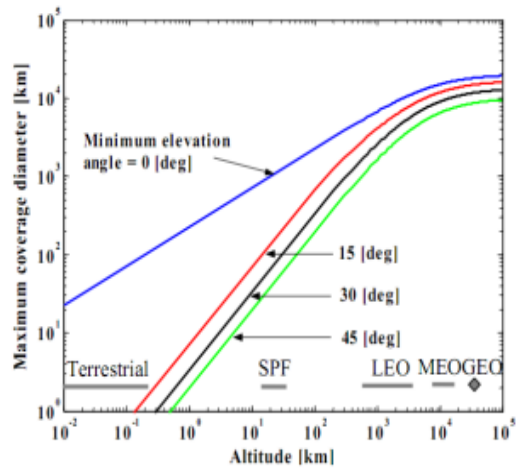
Fig.2 Altitude vs HAPS coverage [2].

where q is Zadoff-Chu *sequence root index*, Nzc is sequence length and m = 0,1,….Nzc – 1. Zadoff-Chu has constant amplitude, so does it's Nzc-point DFT and PAPR.

III. HIGH ALTITUDE PLATFORMS (HAPS) CHANNEL MODEL

High Altitude Platforms located in the stratosphere, at an altitude between 17 and 22 km above the earth surfaces. HAPS have a rapid roll-out capability and the ability to serve a large number of users, using considerably less communications infrastructure than required by a terrestrial network. HAPS located in the stratosphere which has constant temperature rise and constant wind speed rise. There is no weather phenomenon occurs in this layer because this layer has low content of water. That is also this layer is stable with only slight turbulence. No clouds on this layer thus allow effective use of solar power [2].

HAPS coverage depends on several factors such as altitude, users elevation angle, and earth dimension. In Fig. 2, we can see relation between altitude and HAPS coverage. HAPS
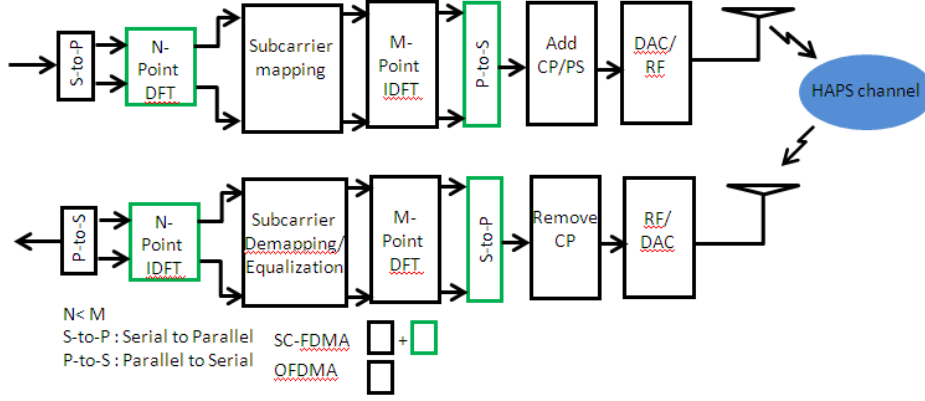
Fig. 3 Simulation model.

coverage are expressed in maximum diameter of LOS communication. Fig. 2 shows the diameter of LOS communication at altitude ranging from 1 to 10^5 km as a function of elevation angle. The graph was made with the assumption that the propagation is straight, so it can be said that the higher HAPS, the broader the scope, but with a limitation that the coverage area is smaller than earth diameter.

In case of HAPS channel, Ricean fading is a general case of fading channel model that there are two components of signal arrive at the receiver. First component arrives at receiver through line of sight (LOS) path while the second comes from scattered signal. In SPF communication scenario, it is probably to get both components because SPF is highly located above the ground. Consequently, it was found that the Ricean fading channel is an appropriate model for the case of SPF link with K factor varies depending on the elevation angle and the frequency. SPF channel can be characterized using Rician distribution as follows.

$$x(t) = \sqrt{\frac{K}{K+1}} e^{j(2\pi f_D \cos(t))} + \sqrt{\frac{1}{K+1}} h(t) \qquad (2)$$

where K is Rice factor, $\theta(t)$ is the users elevation angle, f_D is Doppler shift from receiver movement, and $h(i)$ is the scattered component. If the total power of scattered signal is denoted by $2\sigma^2$ and power of LOS signal represented as A^2, then the total received power and K factor are given by:

$$E[x^2(t)] = A^2 + 2\sigma^2 \qquad (3)$$

$$K = \frac{A^2}{2\sigma^2} \qquad (4)$$

Then the equation (1) can be rewritten as follows:

$$H = \sqrt{\frac{K}{K+1}} H_d + \sqrt{\frac{1}{K+1}} H_s \qquad (5)$$

where H_d is LOS component, and H_s is scattered component.

IV. SIMULATION MODEL

Performance of pilot-based channel estimation, which is used to estimate the performance of signal transmission of SC-FDMA LTE on HAPS channel, was evaluated through computer simulations. The structure of simulation model is depicted in Fig. 3. At the transmitter, the series of bit is generated, then modulated into symbol. Pilot signal is then inserted at each first symbol in all subcarrier. These modulated symbols and pilots perform M-point discrete fourier transform (DFT) to produce a frequency domain representation of the symbols. It then maps each of the M-point DFT outputs to one of the orthogonal subcarriers mapping that can be transmitted.

In this paper, Distributed method is used for subcarrier mapping. In this method, the outputs are allocated equally spaced subcarrier with zeros occupying the unused subcarrier in between. Then IDFT block followed by Cyclic Prefix (CP) insertion. Cyclic prefix is a copy of the last part of symbol that placed in front of symbol that can eliminate Inter Symbol Interference (ISI). Then the signal is transmitted through the AWGN + Ricean channel. At the receiver, the opposite set of the operation is performed. CP is removed then the signal is processed by the DFT. Pilot signal then being extracted to get the channel condition. Channel condition then being compensated to the other symbols. The received signals are demapped, then IDFT operation is performed. These received signals are demodulated to get the bit stream. Bit stream in the receiver then being compared with bit stream in the transmitter to get Bit Error Rate (BER).

V. PERFORMANCE ANALYSIS

A. Users Elevation Angle Analysis

Simulation parameters of the SC-FDMA LTE on High Altitude Platforms are summarized in Table I and the results is shown in Fig. 4. This figure shows that the higher the elevation angle, the performance of SC-FDMA will be better. This is consistent with the notion that the greater the LOS signal power received by the receiver, then the better the performance of SC-FDMA.

Parameters	Value
Channel Bandwidth (MHz)	1.4
Modulation	QPSK
Resource Block (RB)	6
Subcarrier	72
Cyclic Prefix (CP)	9
DFT size	128
Doppler Frequency (Hz)	50
Bitrate (Mbps)	0.9

Simulation Parameters	Value
Channel Bandwidth (MHz)	1.4, 3, 5, 10, 15, and 20
Number of Resource Block	6, 15, 25, 50, 75, and 100
Number of Subcarrier	72, 180, 300, 600, 900, and 1200
Number of Cyclic Prefix	9, 18, 36, 72, 108, and 144
DFT size	128, 256, 512, 1024, 1536, and 2048
Bit rate (Mbps)	0.9, 2.2, 3.6, 7.2, 10.8, and 14.4
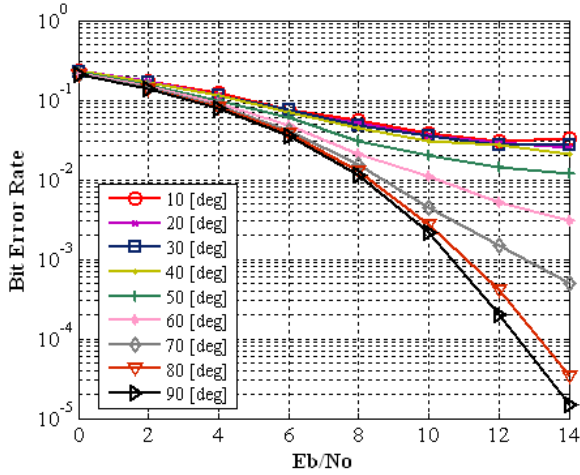
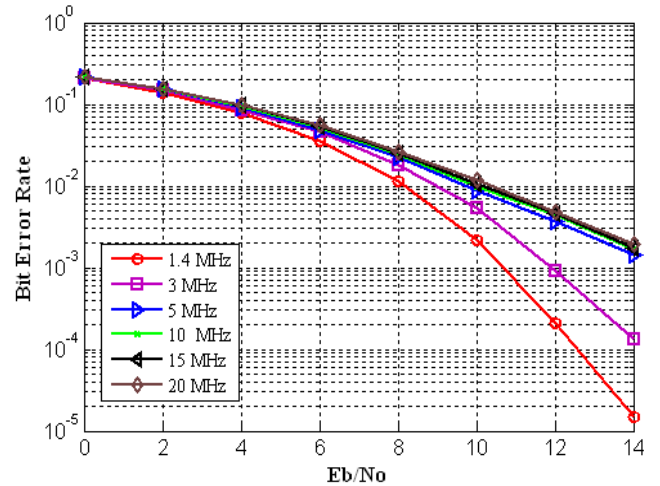Fig. 4 BER performance of pilot-based estimation scheme as a function of user's elevation angle.

Fig. 5 BER performance of pilot-based estimation as a function of channel bandwidth with 90^0 elevation angle.

High elevation angle wmeans high k factor, because k factor is ratio between average LOS power and average Multipath signal's power, so when the elevation angle is high, more LOS signal will be received by receiver. When the elevation angle is high, it will have bigger probability of LOS communication. Performance differences due to changes in elevation angle will more significant when Eb/No is more than 6 dB. Eb/No represents the ratio between signal with noise, so when Eb/No is less than 6 dB, influence of the elevation angle is less clearly visible because the signal to noise ratio is too small. When Eb/No is more than 6 dB, significant differences will be shown between 10^0-40^0 elevation angle and 50^0-90^0 elevation angle. So, communication will be optimal when the elevation angle between the transmitter and HAPS is more than 40^0 and Eb/No is more than 6 dB. At that condition, we can obtain BER difference about 0.0182 to 0.090546 at same elevation angle.

B. Channel Bandwidth Analysis

Simulations performed at 6 channel bandwidth, which is 1.4 MHz, 3 MHz, 5 MHz, 10 MHz, 15 MHz and 20 MHz. Simulation parameters are summarized in Table 2.

Fig. 5 shows that the greater the bandwidth of the channel, then the performance will drop. BER decreases ranging from 1.4 MHz to 20 MHz. This is because the greater channel bandwidth, the greater noise bandwidth. Noise power is a function of Boltzmann constant, absolute temperature and

noise bandwidth, so when the noise bandwidth increase, noise power will be increase to which will affect system performance. Based on simulation results, performance will be decreased from half to 12 time when compared with 1.4 MHz bandwidth performance.

C. Modulation Type Analysis

Simulation performed at two different modulations, QPSK and 16-QAM. Fig. 6 shows the simulation results with 40^0 and 90^0 elevation angle. There is big difference between performance of SC-FDMA with QPSK modulation and with the 16-QAM modulation. This is because QPSK only use 2 bits per symbol while the 16-QAM use 4 bits per symbol, so the 16-QAM will be more susceptible to noise during transmission. In the 16-QAM, constellation of each point is closer to the other point than QPSK, so that the noise would be more likely to occur. Average distance of points on QPSK constellation is $2\sqrt{2}$ while 16-QAM average distance is $2\sqrt{10}$. If that distance is compared on dB, we will get 7 dB difference. This means that to get the same BER, 16-QAM requires approximately 7 dB from the QPSK need. From the simulation results, for QPSK with 90^0 elevation angle with $E_b/N_0 = 0$ dB, we get 0.2067 BER. So, 16-QAM will need $E_b/N_0 = 7$ dB to get the same BER. However, because in the simulation, Eb/No is increasing by 2dB, then the closest E_b/N_0 is 8 dB which have 0.2277 BER Difference between the simulation results with the calculation
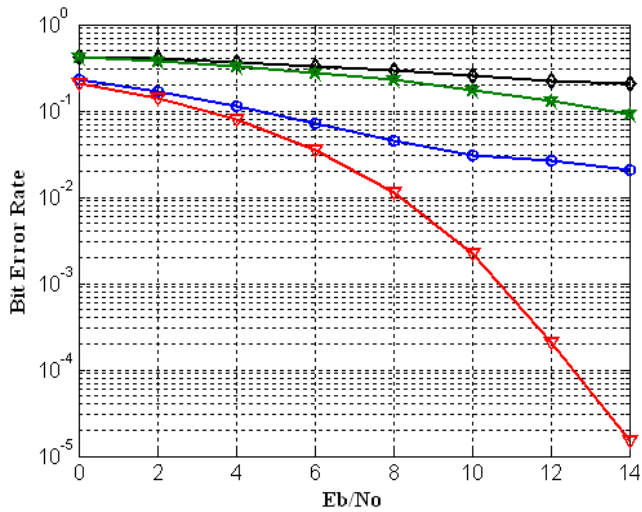
Fig. 6 BER performance of pilot-based estimation as a function of modulation type using 40^0 and 90^0 user's elevation angle.
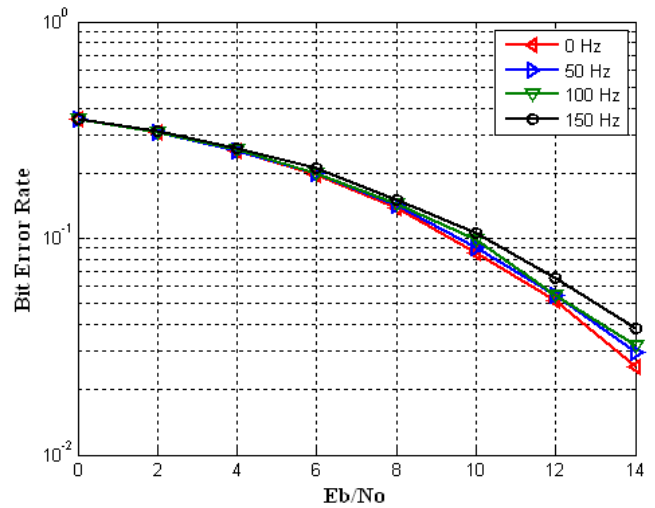

Fig. 7 BER performance of pilot-based estimation as a function of Doppler frequency using 70^0 user's elevation angle.

D. Doppler Frequency Analysis

Simulation performed with parameter shown in Table I, but with 4 different Doppler frequencies which is 0, 50, 100 and150 Hz. Fig. 7 shows the simulation result. It shows that the performance is better when the Doppler frequency is smaller.

Doppler frequency of HAPS is less influential on greater elevation angle.This is due to the doppler effect is influenced by transmitter movement toward or away from HAPS. The greater the angle, the effect will be less significant, just like what we get from elevation angle analysis.

VI. CONCLUSIONS

We have evaluated pilot-based channel estimation performance for uplink LTE SC-FDMA schemes via HAPS channel. Some important variables have been considered in our evaluation such as user's elevation angle, LTE channel bandwidth, modulation scheme, and Doppler shift. Simulation result shows for user's elevation angle above 400, the performance of pilot-based estimation increases significantly. However, the large channel bandwidth we used, the performance decreases due to the increased of noise. The lower level of modulation type shows more robust compared with high level modulation. Finally, the Doppler frequency shift experienced by the users of up to 150 Hz gives insignificant difference of performance compared with the users who experience no Doppler shift.

REFERENCES

[1] H. Holma and A. Toskala. LTE for UMTS Evolution to LTE-Advanced Second Edition, John Wiley and Sons, Ltd., 2011.

[2] I. Toufik, M. Baker, and S. Sesia. LTE The Long Term Evolution from Theory to Practice, John Wiley and Sons Ltd., 2009.

[3] D. Grace and M. Mohor_ci. Broadband Communications via High Altitude Platforms, John Wiley & Sons Ltd, 2011.

[4] Iskandar and S. Shimamoto, "Prediction of propagation path loss for stratospheric platforms mobile communications in urban site LOS/NLOS environment," in Proceedings IEEE International Conference on Communication (ICC), vol. 12, pp. 5643 - 5648, June 2006.

[5] Iskandar and S. Shimamoto, "Channel characterization and performance evaluation of mobile communication employing stratospheric platform," IEICE Transactions on Communications, vol. E89-B, no. 3, pp. 937-944, March 2006.

[6] Iskandar, A. Kurniawan, E. B. Sitanggang, and S. Shimamoto, "Step Size Optimization for Fixed Step Closed Loop Power Control on WCDMA High Altitude Platforms (HAPs) Channel," in Proceedings of IEEE Global Telecommunication Conference (GLOBECOM), vol. 1, pp. 1-5, Dec. 2008.

[7] Iskandar and S. Shimamoto, "On the downlink performance of stratospheric platform mobile communications channel," in Proceedings of IEEE Global Telecommunication Conference (GLOBECOM), vol. 1, pp. 1-5, Dec. 2006.

[8] Iskandar, A.Kurniawan, and M.E. Ernawan, "Closed Loop Power Control with Space Diversity to Improve Performance of Low Elevation Angle Users in HAPs-CDMA Communication Channel," in Proceeding of The 8th International Conference on Telecommunication Systems, Services, and Applications (TSSA 2014), vol 1, pp. 1-5, Oct. 2014.

[9] Hyung G. Myung and David J.Goodman, Single Carrier FDMA, A New Air Interface for Long Term Evolution. UK: John Wiley and Sons, Ltd., 2008.

[10] 3GPP TS 36.211 v8.9.0, 3GPP; Technical Specification Group Radio Access Network; Evolved Universal Terestrial Radio Access (E-UTRA); Physical Channel and Modulation (Release 8), 2009.

[11] David Grace and Mihael Mohorcic, Broadband Communications via High Altitude Platforms. UK: John Wiley and Sons, Ltd., 2011.

Cognitive Access Control
(An Artificial Access Control Decision making)

Ubaidillah[1], Budiman Dabarsyah[2], Yusep Rosmansyah[3], John Euk Choi[4]

School of Electrical and Informatics Engineering
Bandung Institute of Technology, Indonesia

[1]ubaidillah@students.itb.ac.id
[2]dabarsyah@gmail.com
[3]yusepros@yahoo.com
[4]juchoi@markany.com

Abstract---Cognitive access control is an alternative authentication that perform access control mechanisms through the artificial process based on the human brain intelligence processing in determining permit priorities, effectiveness, the authority until the security risk level in any object usage scenarios. apart from the design, this paper also describes the advantages expectation and implementation of Cognitive Access Control simulation
Keyword : Authentication, Access Control, security, artificial.

I. Introduction

Access control is a mechanism to protect the information and corporate data from misuse and the risk of data theft that can harm to the organization [1].

Several case that related is the theft of 400 million credit card records of CardSystem in June 2005 committed by hackers, suspicion because the weakness of access control mechanism, which resulted the lost of two main customers, visa and american express. later on 27 January 2006, recording 4,117 credit card stolen in Rhode Island, this is caused by the vulnerability of the data access control from the branches [2].

Nowadays, there is many kinds of access controls that have been implemented by all organizations worldwide, mandatory access control (MAC) [3], Role based access control (RBAC) Attribute based access control (ABAC) [4] until the Risk adaptable access control (RAdAC) [5], but in general, the method of control in every mechanism models only focused by one or two-dimensional functions, e.g. in object-oriented access control (such as the MAC) control is done only to manage permission to use the object in accordance with the mandate, not the calculation access based on the role, resources and capabilities of across domains

management. the next modern ABAC, has been better, in terms of managing the object, also allowing the environment to be part of the access control, but the secure factor is beyond of ABAC capabilities.

By taking all existing models above, selecting the excess and build a new access control mechanism with all these advantages, but with improved the weakness function, and use the human brain's ability abstractions to think for determining access control, we can design and build an access control that can think, identify, acknowledge to determine the permission access.

Through artificial consciousness-based access control, it can be a solution for organizations with limited resources to implement similar access control that more complex and expensive to manage the organizations information and data more efficiently without reducing other important factors such as cross domain, management of efficiency and security.

II. Access Control Model

There are many type of model or mechanism of access control, the advantages and disadvantages of each model :

1) Role Based Access Control
   Is a rule-based access control or authority of any user who has the rights to distribute an object within an organization. through RBAC, users can define those authorized to access an object based on a command line or position or role of each user [6].

   The excess of RBAC is it can ensure system integrity and availability with strict control, not only how some resources is accessible but also how to occurred

The disadvantages of RBAC is the flexibility of data sharing level that very rigid, and became the administrative problem for a large system environment.
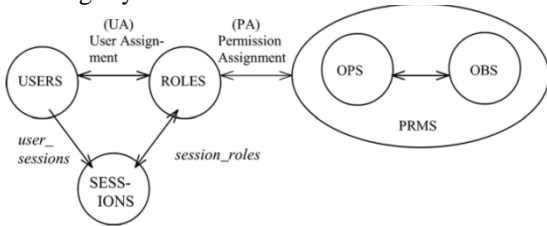

figure 1. Role Based Access Control Model[7]

2) Attribute Based Access Control

Access control based on the attributes of each object in a process that occurs, the attributes of the requestor (user / device / system), resource (database) until the environment attributes (mutualism between divisions cross-domain) [8]

The ABAC advantages is it can provide the flexibility of permission to an object within an organization in accordance with the attribute of requestor, resources and cross domain environment.

The ABAC disadvantages is with increasingly complex cross-domain environment within an organization, then the frequency of the possibility of role conflict will be higher so that ABAC is not efficient for the organizations with high information sharing among divisions[13][14].
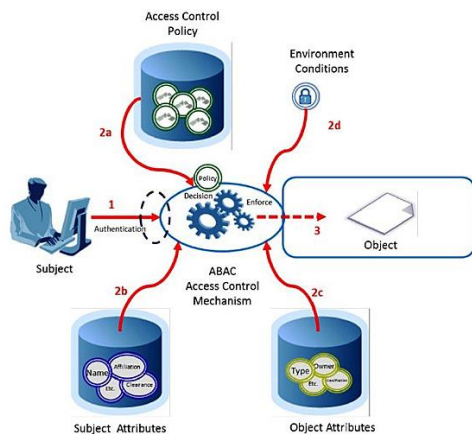
1. Subject Requests Access to Object
2. Access Control Mechanism Assesses a) Rules, b) Subject Attributes, c) Object Attributes, and d) Environment Conditions to Determine Authorization
3. Subject is Given Access to Object if Authorized and Denied Access if Not authorized
Source: NIST

figure 2. Attribute Based Access Control Model[9]

3) Risk Adaptable Access Control (RAdAC)

Risk Adaptable Access Control (RAdAC) is an emerging concept in access control, conceived in context of modern large-scale computing environments such as the US Department of Defence Global Information Grid (GIG). The vision for such systems is a global interconnected, end-to-end set of information capabilities for collecting, processing, storing, disseminating, and managing information on demand [5].

The RAdAC excess is the ability of the permissions process mechanism in giving permission to access an object with considering the possible risks that may occur to the system environment.

The disadvantage of RAdAC is the implemented process complexity is only suitable for large organizations that are able to run the whole mechanism simultaneously.
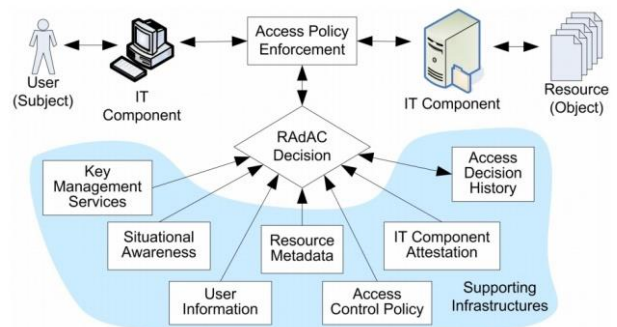
figure 3. risk adaptable access control model[10]

4) Multi Layer Access Control (MLAC)

Is one type of access control that is quite interesting, MLAC make every resource as a filter of a permitting process . through MLAC, user must pass through each layer of access control. this is done to ensure access licensing is done in accordance with the user capacity and security attributes[2] [11].

The excess of MLAC is any demand for dynamic data object can be controlled so that the receiver object is the user who actually fit the criteria object permissions.

The weaknesses is by increasing the number of permits which is comparable with a layer of organizational resources.

Considering the advantages and disadvantages of every model types of access control, we can mapped the strengths and weaknesses to gain the best alternative suits against the request, role, resource, environment, cross-domain and security in an organization.

III.   *Human Cognitive Process*

Humans have complicated mechanism of thinking process, but can be grouped according to

the input, process and output, the following is description of the process of human thinking.
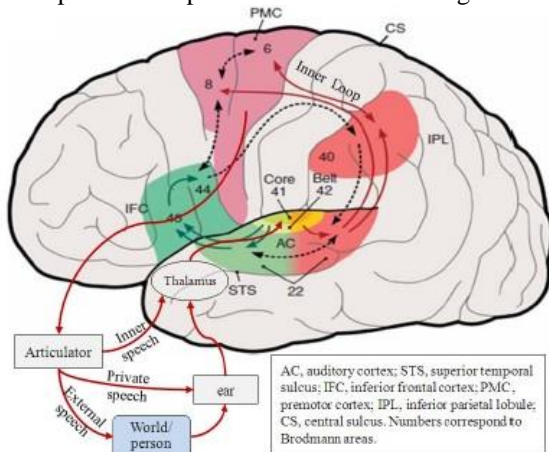
figure 4. Cognitive Human Thinking[12]
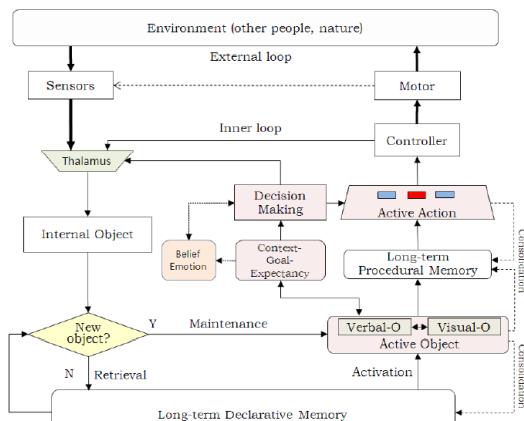
figure 5. Cognitive Human Mechanism[12]

Cognitive process begins with the inputs that go into the system, either from the object, subject and the environment, these inputs then be identified by the sensors, either motor or sensory sensor to be store into memory.

Incoming input will be identified and give different reactions according to the input, processing occurs in the main part is identification, memory reading and analysis until decision making form of action of grant or deny.

For input a new object, the system written and stored into memory as new input, but what if the input is from the same subject with same policy for the same goal? the system will be able to provide the action immediately in accordance with previous history in memory.

The advantages if we adopt a process cognitive is we can minimize repeatedly Process without having to rewrite those processes into memory, in addition, from the security factor, a input that has been written and processed have been getting security input based on environmental

attribute and other that may be a potential risk, so it will greatly help organizations to simplify the control that have large members as well as divisions and the complex cross-domain, it can also minimize the security process in each layer as in multi-layer access control that consume the resources[12].

Cognitive can also minimize role conflict, because it is through memory-owned, access control can search the best decision for the process as well as the decision to an object for the same input request.

IV.   Cognitive Architecture Mechanism Modelling

From the description, we can group the processes into four processes, are:

a) Catching Up
Like nerve as receptor catching input from the sense, the mechanism of cognitive access control also need the stimulate from the input, in this case input are the attribute of object, subject and another input that related with the systems.

Each input will be decompose to attributes and stored and kept into modular memory that used to main processing as attribute input according the process needs.

b) Main Process
The main process is place that all attribute will be calculate, the main process contain of calculation part, consideration with another input to anomaly checker. And checker for calculation from new or existing object

–   "Remembering"
Is the process of collecting the entire memory / input needed to perform the process permission. This requires dataset attributes, policyset and inputs from the environment to examine the risks that may occur, all inputs are then gathered into consideration mechanism.
–   Consideration
Is a process to considering permits issued in accordance with the rules and the risks are acceptable or not, all input request could be appropriate but may cause a risk of leakage because the request did not go in at a reasonable time or performed many times at the same time. the result of this consideration is permission license.

– Origin Input Request

Is a recognition input request process whether it has been recorded or not, if not then it will go to the long term memory and if it is then it will be paired with the previous memory to check is an anomaly or not.

All process automatically run every single input come in to the system, make the process works like artificial system that can work with their own every time.

c)   Decision Making

Decision making is the goal of the control mechanism, its part give the requestor deny or grant position for each object the he request from the systems.
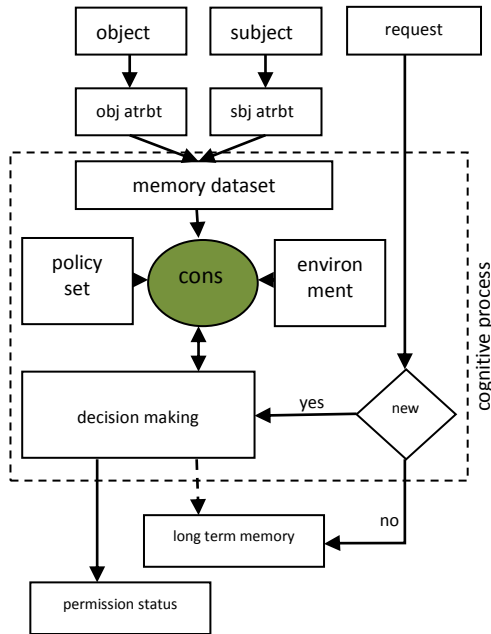
figure 6.propose cognitive access control mechanism

V.   Simulation

We perform simulation tests for attributes distribution process input, simple consideration process until decision making, using three scenarios organization : small organization (simple hierarchy management), medium(with several cross domain division) and large(complex organization), and using matlab from mathwork as computation tools.

The test focused on role conflict that one of the most vulnerable area, higher role conflict make organization more vurnerable, not only make bureaucracy going slower, it also make higher information leak to unknown party even bigger
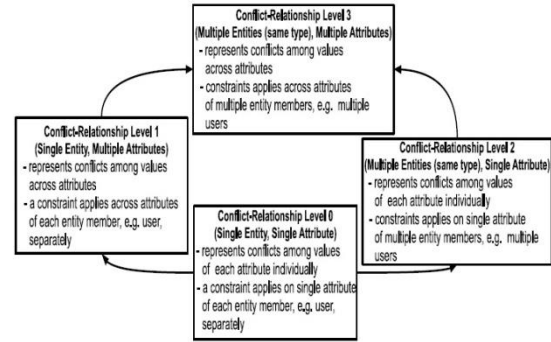
figure 7. role conflict level [14]

from the test results, we are not found problems in the flow diagrams process, and the outputs results is line with initial expectations, from the test results, we also discovered the potential of role conflicts for each level of the organization, thanks to consideration process, all the risks role conflicts can be passed in accordance with recommendations issued by the system.

Referring to the test results, we can draw the conclusion:

a. coac could theoretically meet the shortcomings of the previous access control

b. because its flexibility to organization input, coac can be implemented from the low level until large level organization, without compromising the ability in every sector, such as security and cross-domain.

Type orgz	Level type	Hie	N	M	P	O
Low	1	4 layer	14	4	6	2
Medium	2	6 layer	31	6	15	7
Large	3	7 layer	77	7	35	13

	level	$\mathcal{O}$	Coac ($\mathcal{O}$)	RP
Result	1	280	0	Low
	2	43.245	1002	Low
	3	1.156.155	5.693	Low

N = User   Lvl0= NxMxP
M = Attribute Set   Lvl1 = Nx(M+O)xP
P = Predicates Expression   Lvl2= N^2xMxP
O = cross attribute set   Lvl4 = N^2x(M+O)xP
Hier = Hierarchies
$\mathcal{O}$ = Role(constraint) Conflict
RP = Risk Potential

VI.   Discussion

The next step is artificial complex test on the main process, testing is will using the tools ACT-R 7,

ACT-R is a commonly used for cognitive modelling based on levels of functionality[12].

ACT-R used to simulate the artificial intelligence that is Symantic into systematic logic. but due to the limit of these tools, the test will be performed into 3 stages :

1) Developing Declarative Knowledge
   Is a declaration of human reasoning processes into systematic logic that can be understood by the computer language, the declaration example is when the computer is giving grants to the subject, given grant decision is the result of processing data from the memory to the policy set that exist within the system (with other attributes also). it is like how humans react to something as a result of stimulation received.
2) Developing Procedural Knowledge
   Is how do we determine a goal, this process involves a memory which contains datasets and policy set which must be translated into a procedural form to deciding a decision.
3) Goal Setting
   Goal setting is a cognitive program that has been extracted by the system in the form of systemic

VII.   Conclusion

With the development of the digital world as well as the different needs of an organization in managing data and information, access control became a key in providing control over every movement of such data and information. cognitive control access proved capable of providing solutions to organizations in providing a robust access control that can be tailored to the needs of the organization without having to configure the excess. coac also proven to provide data and information management solutions without forgetting the other factors that should be owned by a system that is efficient, effective and secure

VIII.   References

[1]. Qing-hai.Bai , *Study on The Access Control Model,* Cross Strait Quad-Regional Radio Science And Wireless Technology Conference (CSQRWC), 2011 (Volume:1), IEEE, 2011
[2]. Wen. Zhichao, Wu .Di, *Three Layer Role Based Access Control Framework In Large Financial Web Systems*, Zhejiang University, IEEE, 2009
[3]. Jiang. Yixin, Lin. Chuang, Yin. Hao, Tan. Zhangxi, *Security Analysis of Mandatory Access Control Model*, Tsinghua University, International Conference on Systems, Man and Cybernetics, IEEE, 2004
[4]. Ferraiolo. David, Khun. Richard, The *NIST model for role based access control : towards a unified standard*, National Institute of Standards and Technology, 15th National Computer Security Conference, Baltimore MD pp. 554 - 563, 1992
[5]. Kandala. Savith, Sandhu. Ravi, Bhamidipati. Venkata, *An Attribute Based Framework for Risk Adaptive Access Control Models*, 6th International Conference on Availability, Reliability And Security, IEEE, 2011
[6]. Khun. Richard, *Vulnerability Hierarchies in Access Control Configuration, National Institute of Standards and Technology*, 4th Symposium on Configuration Analytics and Automation, IEEE, 2011
[7]. Ravi S. Sandhu, Edward J. Coynek, Hal L. Feinsteink and Charles E. Youmank, *Role-Based Access Control Models*, IEEE Computer, Volume 29, Number 2, February 1996, pages 38-47, IEEE, 1996
[8]. Xu. Dianxiang, Zhang. Yunpen, *Specification and Analysis of Attribute Based Access Control Policies : An Overview*, 8th International Conference on Software Security and Reliability, IEEE, 2014
[9]. Hu. Vincent, Schnitzer. Adam, Sandlin. Ken, *NIST Special Publication 800-162 Attribute Based Access Control Definition and Considerations,* National Institute of Standards and Technology, 2013
[10]. Robert W. McGraw, *Information Assurance Architecture and Systems Security Engineering Group*, National Security Agency, 2009
[11]. Tao. Cai, Dejiao. Niu, Shiguang. Ju, *Two Layer Access Control for Storage Area Network*, 8th International Conference on Grid and Cooperative Computing, IEEE, 2009
[12]. Guangzuo. Cui, Xuefeng. Wei, Lili, Boling. Wang , *A Cognitive Model Of Human Thinking,* 7th International Conference on Natural Computation, IEEE, 2011
[13]. Long. Yi-Hong, Tang. Zhi-Hong, Liu. Xu, *Attribute Mapping for Cross Domain Access Contro*l, International Conference and Information Application(ICCIA), IEEE, 2010
[14]. Dan. Ni, Yuan. Chen, Hua-Ji. Shi, Jia-Hu. Guo, *Attribute Based Access Control (ABAC) Based Cross Domain Access Control in Service Oriented Architecture (SOA),* International Conference on Computer Science and Service System, IEEE, 2012

PTS-Based PAPR Reduction in Fixed WiMAX System With Grouping Phase Weighting (GPW)

Chaeriah Bin Ali Wael, Nasrullah Armi, Budiman P.A. Rohman
Research Center for Electronics and Telecommunication
Indonesian Institute of Sciences
Bandung, Indonesia
chae003@lipi.go.id

Abstract—**WiMAX is a wireless technology that was developed to overcome the limitations of wireline networks to meet the needs of Broadband Wireless Access (BWA) services to customers. As standardized, fixed WiMAX uses OFDM as its physical air interface. Therefore, it also suffers from high PAPR. To solve this problem, Partial Transmit Sequence (PTS) is used in this paper due to its better performance among other PAPR reduction techniques. Unfortunately, in conventional PTS, an exhaustive search over all combinations of allowed phase weighting factors is needed. This process leads to high computational complexity. Hence, Grouping Phase Weighting (GPW) is used to simplify search complexity and still maintain to provide effective PAPR reduction as conventional PTS. The simulation is conducted to IEEE 802.16d system with various mandatory modulation types and channel coding rates. The derived results show that the choice of modulation type does not give significant effect on the PAPR value. The higher channel coding rate gives higher PAPR reduction.**

Keywords— Fixed WiMAX; IEEE 802.16-2004/d; OFDM; PAPR Reduction; Partial Transmit Sequence (PTS); Grouping Phase Weighting (GPW)

I. INTRODUCTION

In today's world, the demand for broadband connectivity is growing rapidly. Broadband access is currently offered through digital subscriber line (xDSL), cable and Broadband Wireless Access (BWA). Although cable and DSL are already deployed widely, BWA has several advantages, such as solving distance limitations of DSL and high costs of cable, high scalability and lower maintainance and upgrade costs. WiMAX (Worldwide Interoperability for Microwave Access) is a promising broadband wireless technology which can offer high speed data, voice and video service to the end customer in a large geographical area, which is presently dominated by the cable and digital subscriber line (DSL) technologies. The WiMAX standards (IEEE 802.16) is also known as Wireless Man (WMAN) because of its goal to implement broadband wireless access for wireless metropolitan area networks. It supports two types of usage models, fixed WiMAX (IEEE 802.16d) and mobile WiMAX (IEEE 802.16e). The fixed WiMAX system has subscriber terminals located at fixed place, whereas the mobile wimax system has mobile subscriber terminals [1].

The fixed WiMAX physical layer is based on Orthogonal Frequency Division Multiplexing (OFDM). OFDM-based system gives high spectral efficiency, supports very high data

rate transmission and provides greater robustness to communications channel perturbations such as frequency selective fading and multipath fading effects [1]-[2]. However, such system prefaces high Peak to Average Power Ratio (PAPR) problem since its transmitted signal is the sum of many subcarrier components via an Inverse Fast Fourier Transformation (IFFT) operation. High peak signals will saturate power amplifier (PA). As a consequence, PA operates at its nonlinear region which leads to high out of band radiation and inter-modulation distortion [3]. One of the approaches used for solving PAPR problem is using highly linear PA. However, it is usually complicated to build and very expensive. Another solution is modifying the signal by reducing its PAPR.

Various methods have been studied for PAPR reduction which are summarized in [3] - [6]. Generally, PAPR reduction methods are classified into two main categories, scrambling and distortion techniques [6]. Scrambling techniques include selected mapping (SLM), Partial Transmit Sequence (PTS), Tone Reservation (TR), Tone Injection (TI) and block coding techniques. Peak windowing, envelope scaling and clipping are kinds of distortion techniques. Among these techniques, PTS can reduce PAPR significantly without signal distortion and has no restrictions to the number of subcarriers [7], [8]. Unfortunately, it has highly computational complexity due to an exhaustive search over all combinations of allowed phase weighting factors. One of the techniques which focus on simplifying search complexity in conventional PTS (C-PTS) is proposed in [9]-[11], called Grouping Phase Weighting (GPW).

In this paper, PTS with GPW is applied in Fixed WiMAX system to solve high PAPR problem considering various modulation types and channel coding rates. The rest of this paper is organized as follows : section II describes fixed WiMAX (IEEE 802.16d) physical layer. PAPR problem is reviewed in section III. Simulation results are given in section IV and conclusion of all research is written in section V.

II. IEEE 802.16-2004 PHYSICAL LAYER

IEEE 802.16-2004 (802.16d) applied to NLOS transmission at 2-11 GHz. This system can work in the frequency division duplex (FDD) or time division duplex (TDD) mode. It uses OFDM as its physical layer technology. Physical layer of 802.16d transceiver block diagram is shown

in Fig. 1. The tasks performed in this system are explained as follows :

- The first stage is channel coding. It consists of three parts ; randomization, Forward Error Correction (FEC) and interleaving. The randomizer block aims to scramble a long sequences of zeros and ones into randomized data. Then, FEC is applied on certain fixed-block lengths of data, which have been defined based on modulation type as shown in table 1. FEC encoder in IEEE 802.16d consists of concatenation of Reed Solomon (RS) code as outer code and convolutional code (CC) as inner code. The last block of channel coding is interleaver. It is used for improving the performance of error correcting codes.

- The coded bits will be mapped by the constellation modulator. In fixed WiMAX, QPSK, 16-QAM and 64-QAM are mandatory for downlink. Meanwhile, uplink only support of QPSK and 16-QAM is required.

- A representation of OFDM modulation process is given in Fig. 2. The output of mapper which in form of symbols is devided into N substreams each with bit rate B/N bps where N is number of OFDM carriers. In fixed WiMAX, $N = 256$ which number of used data subcarriers is 192, 8 pilot subcarriers to perform synchronization and channel estimation and 56 Null subcarriers. These streams are subsequently input to IFFT after Serial-to-Parallel (S/P) conversion. IFFT processing is then applied to each stream to generate OFDM carriers in the baseband. The cyclical prefixes are added to the symbols to achieve the guard bands. After multiplexing the subcarrier streams through Parallel-to-Serial (P/S) converter, the OFDM signal is transferred to RF transmission modules via Digital-to-Analog (D/A) converter. The OFDM receiver implements the same operations as performed by transmitter in reverse order.

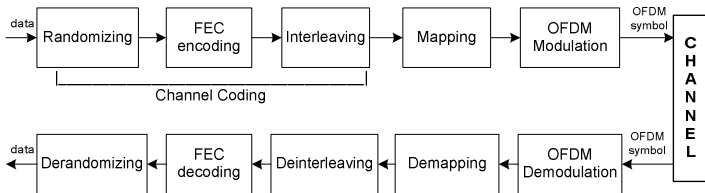- The reverse process takes place in the WiMAX receiver.

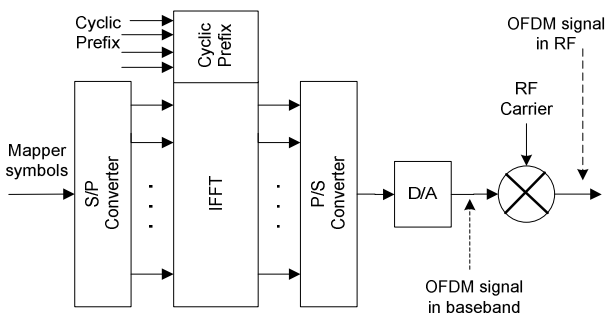Fig 1. Block diagram of WiMAX transceiver physical layer

Fig 2. Block diagram of OFDM modulation

TABLE I.   MANDATORY CHANNEL CODING PER MODULATION

mod type	uncoded block size (bytes)	CC rate	RS rate	overall coding rate	coded block size (bytes)
BPSK	12	1/2	(12, 12, 0)	1/2	24
QPSK	24	2/3	(32, 24, 4)	1/2	48
QPSK	36	5/6	(40, 36, 2)	3/4	48
16-QAM	48	2/3	(64, 48, 8)	1/2	96
16-QAM	72	5/6	(80, 72, 4)	3/4	96
64-QAM	96	3/4	(108, 96, 6)	2/3	144
64-QAM	108	5/6	(120,108,6)	3/4	144

III.   PAPR PROBLEM

A. PAPR Definition

The use of a large number of subcarriers causes a high PAPR in OFDM-based systems, incuding WiMAX system. PAPR can be defined as the ratio between the maximum power of a sample in a transmit OFDM symbol and its average power. A discrete form of OFDM signal $x(n)$ is given by :

$$x(n) = \frac{1}{\sqrt{N}} \sum_{k=0}^{N-1} X_k e^{j2\pi \frac{k}{N} n} \ , \ \ 0 \le n \le N - 1 \qquad (1)$$

Where $x(n)$, X_k, N represent discrete OFDM signal, modulated input symbols and total number of subcarriers respectively.

For a discrete OFDM signal, PAPR is computed from L time oversampled OFDM signal. Oversampling needed to prevent aliasing. This process is done by padding $(L - 1)N$ zeros in frequency domain. Mathematically, PAPR of OFDM signal is expressed in (2).

$$PAPR_{(dB)} = 10 \log_{10} \frac{P_{peak}}{P_{average}}$$

$$= 10 \log_{10} \frac{\max_{n}\{|x(n)|^2\}}{E\{|x(n)|^2\}}, 0 \le n \le LN - 1 \quad (2)$$

Where P_{peak} represents peak output power, $P_{average}$ means average output power, $E\{.\}$ denotes the expected value and L represents oversampling factor. The peak power of received signals is N times the average power when phase values are the same. So, theoretically, maximum PAPR of baseband signal will achieve $10\log N$ (dB). For fixed WiMAX with 256 subcarriers, the expected maximum PAPR is about 24,08 dB.

B. PAPR Distribution

Complementary Cumulative Distribution Function (CCDF) often used to express the distribution of PAPR. CCDF can be used to estimate the bounds of PAPR and usually used for performance evaluation parameter of PAPR reduction techniques. Its values are obtained by checking how often PAPR exceeds the threshold (= $PAPR_0$).

$$CCDF = P(PAPR > PAPR_0)$$
$$= 1 - P(PAPR < PAPR_0) \qquad (3)$$

C. PTS-based PAPR Reduction

PTS is one of the scrambling techniques to reduce PAPR. The basic idea of this technique is to form a weighted combination of the V disjoint subblocks, then choose one which has the smallest PAPR value for transmission. Block diagram of conventional PTS (C-PTS) can be seen in Fig. 3 which can be explained as these following steps :

1. Output sequences of modulator, X, is partitioned into V disjoint subblocks. There are three ways of subblock partition in PTS; adjacent, interleaved and pseudo-random partition. Each subblock has equal size.

$$X_v = \{X_v^0, X_v^1, \ldots, X_v^{N-1}\}, \quad v = 0, 1, \ldots, V- \qquad (4)$$

2. Apply LN point IFFT to each X_v to get time domain subblocks x_v.

$$x_v = IFFT\{X_v\} \qquad (5)$$

3. Each time domain subblock x_v is multiplied by a corresponding complex weighting factors w_v.

$$x = \sum_{v=0}^{V-1} w_v\, x_v \qquad (6)$$

Where w_v, $v = 0, 1, \ldots, V\text{-}1$, are weighting factors or phase factors. $w_v = e^{j\phi_v}$, with $\phi_v \in [0, 2\pi)$.

4. Choose one suitable rotation factor which gives minimum PAPR. Rotation factor is the combination of weighting factors.

$$\widetilde{w}_v = \arg\min_{w_v}\left(\max_{0<n<LN-1}\left|\sum_{v=0}^{V-1} w_v\, x_v\right|\right) \qquad (7)$$

Where $\widetilde{w}_v = \{\widetilde{w}_0, \widetilde{w}_1, \ldots, \widetilde{w}_{v-1}\}$ is the optimum rotation factor.

5. Optimized transmitted signal ($\tilde{x}$) is expressed as following equation :

$$\tilde{x} = \sum_{v=0}^{V-1} \widetilde{w}_v\, x^{(v)} \qquad (8)$$

It has been already pointed out that PTS gives better PAPR reduction. Unfortunately, computation of optimal PTS weighting factors requires exponential complexity in the number of subblocks. In consequence, many suboptimal strategies have been proposed such as [8-11]. In [8], suboptimal PTS has been developed using iterative flipping algorithm. It has linear complexity proportional to the number of subblocks. It also does not give better performance of PAPR reduction compared to conventional PTS. On the other hand, PTS with Grouping phase Weighting in [9-11] can reduce computational complexity of conventional PTS and still can maintain to achieve good performance of PAPR reduction as conventional PTS.

In GPW-PTS, all subblocks from step (1) in conventional PTS are separated into several groups. Phase weighting process is applied to every subblock in each group by using the same set of phase weighting factors and bring out subcandidate sequences. Thereafter, subcandidate sequences
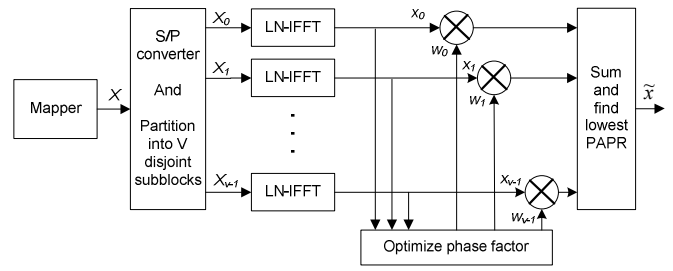

Fig 3. Block diagram of C-PTS technique.

from different groups are combined to yield all OFDM candidate sequences. OFDM transmitted signal is then selected from these sequences which has the minimum PAPR. Mathematically, OFDM candidate sequences in equation (6) can be written as follows :

$$
\begin{aligned}
x &= \sum_{i=1}^{V} w_i x_i \\
&= \sum_{i=1}^{r_1} w_i x_i + \sum_{i=r_1+1}^{r_2} w_i x_i + \cdots + \sum_{i=r_{R-1}}^{V} w_i x_i \qquad (9) \\
&= G_1 + G_2 + \ldots + G_R \\
& \qquad 1 < r_1 < r_2 < \cdots < r_{R-1} < V
\end{aligned}
$$

Where r_i, i = 1, 2, …, $R-1$, is the subblock index, R is number of groups and G_j, j = 1, 2, …, R, is subcandidate sequences of jth group.

IV. SIMULATION RESULT AND ANALYSIS

In this section, simulations have been conducted to evaluate performance of PTS with GPW to overcome high PAPR problem in fixed WiMAX system in terms of CCDF. Matlab simulation is performed on a fixed WiMAX based OFDM system (IEEE 802.16-2004) with 1000 block of OFDM signal for iteration. All parameters that used in simulation are shown in table 2. The simulation is done in the following way :

- An OFDM block consists of 256 subcarriers are splitted into $V = 4$ disjoint subblocks using adjacent partition.

- These subblocks are grouping into two group :

  Group 1 : x_1, x_2

  Group 2 : x_3, x_4

  The phase weighting sequences is chosen from $\{\pm1\}$ or allowed weighting factors, W = 2. In this simulation, the phase weighting sequences of each group are devided as follows :

  Group 1 : $[1, 1]^T$, $[1, -1]^T$

  Group 2 : $[1, 1]^T$, $[1, -1]^T$, $[-1, 1]^T$, $[-1, -1]^T$

- The OFDM candidate sequences, *x'*, are obtained by combining candidate sequences from both groups according to (9).

$$x'_1 = x_1 + x_2 + x_3 + x_4$$
$$x'_2 = x_1 + x_2 + x_3 - x_4$$
$$x'_3 = x_1 + x_2 - x_3 + x_4$$
$$x'_4 = x_1 + x_2 - x_3 - x_4$$
$$x'_5 = x_1 - x_2 + x_3 + x_4$$
$$x'_6 = x_1 - x_2 + x_3 - x_4$$
$$x'_7 = x_1 - x_2 - x_3 + x_4$$
$$x'_8 = x_1 - x_2 - x_3 - x_4$$

- From these OFDM candidate sequences, choose one with minimum PAPR as OFDM transmitted signal.

WiMAX systems use adaptive modulation and coding to take advantage of fluctuations in channel. This simulation aims to evaluate PAPR reduction using GPW-PTS of such system with various modulation types and channel coding rate. Fig. 4 shows CCDF performance of 802.16d system considering different types of modulation at channel coding rate = 3/4. From Fig. 4, it is clear that the choice of modulation type does not give significant effect on the PAPR value. As an example, CCDF of 10^{-2} is reached when PAPR are around 6,2 dB for QPSK, 6,44 dB for 16-QAM and 6,16 dB for 64-QAM after GPW-PTS is applied. PAPR reduction performance in dB of various modulation types is summarized in table 3. It shows that QPSK gives highest PAPR reduction. In addition, for QAM modulation, the higher order of modulation type gives less PAPR reduction.

Fig. 5 depicts CCDF performance of 802.16d system considering different types of channel coding rate for QPSK and 16-QAM. This figure can be summarized as comparison performance of PAPR reduction of original OFDM signal and OFDM with GPW-PTS as shown in table 4. From this table, it shows that with the increasing of channel coding rate, GPW-PTS also gives higher PAPR reduction.

TABLE II.   SIMULATION PARAMETERS

Parameters	Value
Number of OFDM symbols	1000
Number of subcarriers (N)	256
Modulation scheme	QPSK, 16-QAM, 64-QAM
Number of subblocks used in PTS method (V)	4
Oversampling factor	4
PTS partition method	adjacent

Fig 4. Comparison of PAPR performance with various modulation types in 802.16d system.

TABLE III.   COMPARISON OF GPW-PTS PERFORMANCE OF OFDM SIGNAL WITH VARIOUS MODULATION TYPES

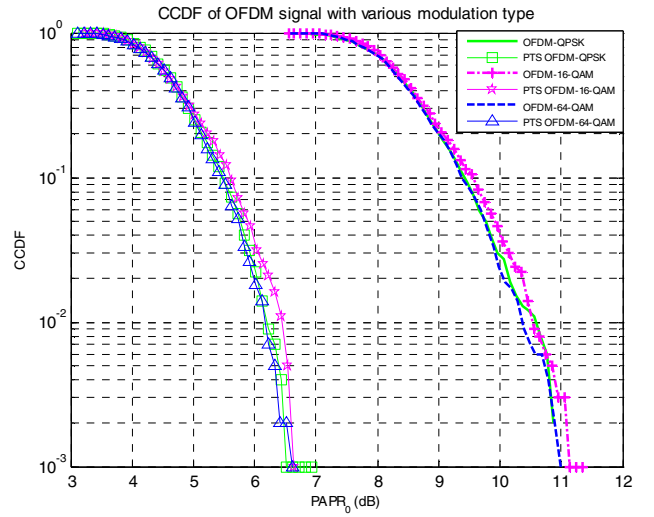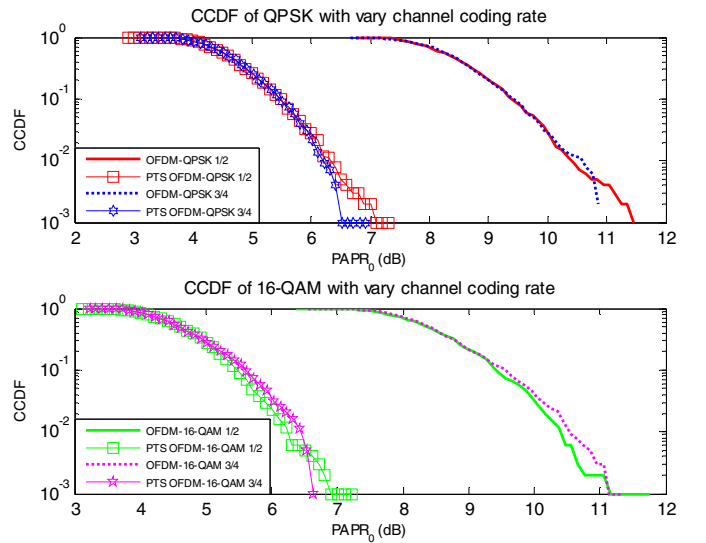| No	Modulation Type	PAPR of original OFDM (dB)	PAPR of PTS-OFDM (dB)	PAPR Reduction (dB)
1	QPSK	10,9414	5,9728	4,9686
2	16-QAM	11,4176	6,4974	4,9202
3	64-QAM	11,0673	6,5593	4,508

Fig 5. Comparison of PAPR performance with various channel coding rates in 802.16d system.

TABLE IV.   COMPARISON OF GPW-PTS PERFORMANCE OF OFDM SIGNAL WITH VARIOUS CHANNEL CODING RATE

No	Modulation Type	Channel Coding Rate	PAPR of original OFDM (dB)	PAPR of PTS-OFDM (dB)	PAPR Reduction (dB) c = a - b
			(a)	(b)	(c)
1	QPSK	1/2	11,4643	6,6327	4,8316
		3/4	10,9414	5,9728	4,9686
2	16-QAM	1/2	11,8504	7,3148	4,5356
		3/4	11,4176	6,4974	4,9202

V.   CONCLUSIONS

PAPR reduction technique applied to fixed WiMAX (IEEE 802.16d) system using GPW-PTS technique has been studied. GPW-PTS is used due to its less computational complexity then C-PTS. The derived results show that GPW-PTS can reduce PAPR effectively. Furthermore, the choice of modulation type does not give significant effect on the PAPR value. Even though, for QAM modulation, the higher order of modulation type gives less PAPR reduction. The use of GPW-PTS in 802.16d system with various channel coding rate shows that higher channel coding rate gives higher PAPR reduction.

REFERENCES

[1] A.N Naqvi, A.M Abbas, T.A Chouhan, "Performance Evaluation of Fixed and Mobile WiMAX Networks for UDP Traffic," *International Journal of Advanced Research in Computer and Communication Engineering (IJARCCE),* vol. 1, Issue 8, pp. 563-569, Oct. 2012.

[2] B.S.K Reddy and B. Lakshmi, "Channel Coding and Clipping in OFDM for WiMAX using SDR," *International Journal on Recent Trends in Engineering and Technology (IJRTET),* vol. 9, no. 1, pp. 66-74, July 2013.

[3] S.H. Han, J.H. Lee, "An Overview of Peak-to-Average Power Ratio Reduction Techniques for Multicarrier Transmission," *IEEE Wireless Communications*, vol. 12, no. 2, pp. 56–65, April 2005.

[4] T. Jiang and Y. Wu, "An Overview : Peak-to-Average Power Ratio Reduction Techniques for OFDM Signals," *IEEE Transactions on Broadcasting*, vol 54, no. 2, pp. 257-268, June 2008.

[5] D.W. Lim, S.J. Hoe, J.S No, "An Overview of Peak-to-Average Power Ratio Reduction Schemes for OFDM Signals," *IEEE Journal of Communications and Networks*, vol. 11, no. 3, pp. 229-239, June 2009.

[6] P. Manhas and M.K. Soni, "A Review of PAPR Reduction Techniques for OFDM System," *MR International Journal of Engineering and Technology*, vol. 6, no. 2, pp. 49-53, Dec. 2014.

[7] S. H. Muller and J. B. Huber, "OFDM with Reduced Peak-to-Average Power Ratio by Optimum Combination of Partial Transmit Sequences," *IEEE Electronics Letters*, vol. 33, no. 5, pp. 368-369, Feb. 1997.

[8] L.J. Cimini and N.R. Sollenberger, "Peak-to-Average Power Ratio Reduction of An OFDM Signal Using Partial Transmit Sequences". *IEEE Communications Letters*, vol. 4, no. 3, pp. 86-88, March 2000.

[9] L. Wang and J. Liu, "PAPR Reduction of OFDM Signals by PTS With Grouping and Recursive Phase Weighting Methods," *IEEE Transactions on Broadcasting*, vol. 57, no. 2, pp. 299-306, March 2011.

[10] P. Pandey and R. Tripathi, "Computational Complexity Reduction of OFDM Signals by PTS with Alternate Optimised Grouping Phase Weighting Method," *International Journal of Computer Applications*, vol. 78, no. 1, pp. 1-7, Sept. 2013.

[11] P. Pandey and R. Tripathi, "Computational Complexity and Peak-to-Average Power Reduction of OFDM signals by PTS with Sub-optimum Grouping Phase Weighting Method," *International Journal of Computer Applications*, vol. 79, no. 11, pp. 6-11, Oct. 2013.

[12] A.B. Narasimhamurthy, M.K. Banavar, C. Tepedelenlioglu, *OFDM System for Wireless Communications*, Morgan Claypool Publishers, 2010, pp. 31-32.

EEG Data Transmission Over Speech Channel in The Telephony System

Hendra Setiawan[1] Yusuf Aziz Amrulloh[1] and Erlina Marfianti[2]
[1]Electrical Engineering Department, University Islam Indonesia, Yogyakarta, Indonesia
(Tel : +62-274-895-287; E-mail: hendra.setiawan@uii.ac.id, yusuf.amrulloh@uii.ac.id)
[2]Internal Medicine Department, University Islam Indonesia, Yogyakarta, Indonesia
(Tel : +62-22-898-444; E-mail: erlyna_marf@yahoo.com)

Abstract-In this paper we present the most implementable scheme for transmitting 19 channels electroencephalography (EEG) and speech signals simultaneously using a speech channel of telephony system. The proposed system works based on re-sampling, multiplexing and filtering concepts. Re-sampling is applied to adjust EEG sampling frequency such that appropriate with speech signal sampling frequency. The 19 channels are time multiplexed then mixed with the speech to produce a transmitting signal. In the receiver side, speech and EEG are separated by filtering. Based on simulation result in the noise environment, the proposed system has successfully separated the speech and the EEG signals. The correlation coefficient between the received signals after separation and the original ones are more than 0.8 for EEG and more than 0.7 for speech in 30 dB SNR. Moreover, the proposed system has high possibility to be implemented with low computational complexity.
Keyword: data over speech, electroencephalography, filter, signal separation, patient telemonitoring.

I. INTRODUCTION

Telemonitoring is the remote monitoring of patients, including the use of audio, video, telecommunications and electronic information processing technologies to monitor patient status at a distance [1]. It consists of the transmission of patient data from a remote location to another location for data interpretation and decision-making. Based on [2] report, telemonitoring are effective in reducing the risk of all-cause mortality, improve health care dramatically, and reduce costs, that improves quality of life. The telemonitoring development is supported by advanced technology in miniaturization and nanotechnology, wireless communication, and computational algorithms [3].

An electroencephalography (EEG) is one of the main diagnostic tests for some cases related to brain and nerves. At least 19 electrodes put on around scalp to get 19 channels EEG. Online monitoring system requires those signals to be transmitted to another location for interpretation and decision-making by a medical specialist. However, a power consumption and bandwidth limitation are current issues in order to implement it. To address this problem, some methodologies are proposed, such as compressed sensing (CS) [4,5], discrete wavelet transform (DWT)-based encoding system, and a power-distortion-compression ratio (P-D-CR) framework [6]. However, implementation of those methodologies require additional computation that cause

impractical. Therefore, we introduce implementable EEG data transmission via speech that has low computational complexity. In practical, EEG signals send simultaneously with speech when patient makes his consultation with the physician.

The rest of this paper is organized as follows. In section II, the system model is briefly introduced, and is followed by EEG-speech signals mixing schemes in section III. The EEG-speech signals separation scheme is discussed in section IV. Finally, section V summarizes the paper.

II. TELEMONITORING SYSTEM MODEL

The system model consists of two inputs in the transmitter side, and two outputs in the receiver side as shown in the Fig.1. Transmitter and receiver is connected via a wire or wireless channel with a fix bandwidth that enough for speech only. EEG data and speech are combined in a mixer then transmitted by a telephony system. In the receiver, an additional computation is inserted to separate the received signal after the general process in telephony system.
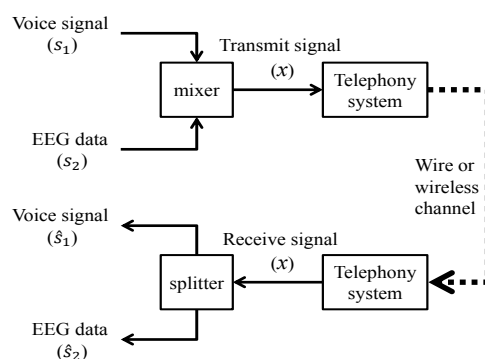
Fig. 1. EEG data over speech system model

Here, we do not make any modification in the general process inside of the telephony system and assume the overall process in telephony system has been perfectly done in the both side transmitter and receiver. Thus our concern is how to mix the signals in the transmitter and split it in the receiver.

There are five major brain waves distinguished by their different frequency range [7]. These frequency bands from low to high frequencies respectively are called delta (δ), theta (θ),

alpha (α), beta (β), and gamma (γ). Delta waves lie within the range of 0.1-4Hz, while theta waves lie within the range 4-8Hz. Alpha, beta, and gamma waves lie within the range 8-14Hz, 14-40Hz, 40-300Hz respectively.

In the telephony system, the usable speech frequency band ranges from approximately 300Hz to 3400Hz. The bandwidth allocated for a single speech-frequency transmission channel is usually 4kHz, including guard bands, allowing a sampling rate of 8 kHz to be used as the basis of the pulse code modulation system. Based on the Nyquist - Shannon sampling theorem, the sampling frequency (8kHz) must be at least twice the speech frequency (4kHz) for effective reconstruction of the speech signal. Thus, 8kHz is also the sampling frequency of EEG telemonitoring system.

In practical, the recording bandwidth of the routine clinical EEG is typically around 0.5-50 Hz [8, 9]. At least 12 bit A/D converter with accuracy lower than overall noise (0.3-2 μV pp.) is involved. Moreover, the sampling frequency is usually between 128 – 1024 Hz [8].

In this research, the EEG signals are obtained from 19 channels EEG. Fig.2 shows a snippet of EEG signals for channel 1, 5, 9 and 17 using 128Hz sampling frequency.

III. EEG AND SPEECH MIXING SCHEMES

The main task in order to develop data over speech is how to mix and separate data source from the speech source. The similar example is the "cocktail party problem", where a number of people are talking simultaneously in a room (for example, at a cocktail party), and a listener is trying to follow
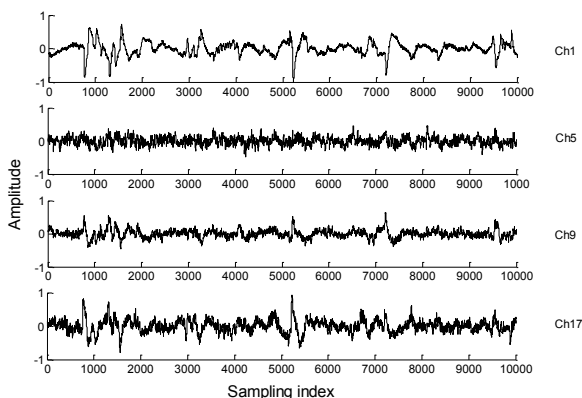

Fig. 2. A time domain snippet of EEG signals

one of the discussions. The human brain can handle this sort of auditory source separation problem, but it is a difficult problem in digital signal processing.

Several approaches have been proposed for the solution of this problem such as blind signal separation (BSS) [10] and beamforming technique [11]. However, there are some difficulties when they are implemented in the real system.

Second problem is related to the computation requirement. BSS computation requirement is proportional to the number of signal that needs to be split. High computation resources make

the duration of battery life is shorter than before. Thus, the computation load for signal separating should have a low computation when implemented in the mobile devices.

Here, we propose a separation scheme, especially for 19 channels EEG mixed with human speech signal, that implementable and has low computational requirement. The proposed technique is detailed below.

A. Human Speech Spectrum Occupancy

The range of human pitch depends on age and sex where is the child has the highest than the adults [12]. Typically, the range the is 50Hz to 3kHz. However, the power distribution is not uniform within the frequency range. In the normal condition, the spectrum is mostly between 500Hz to 2000Hz.
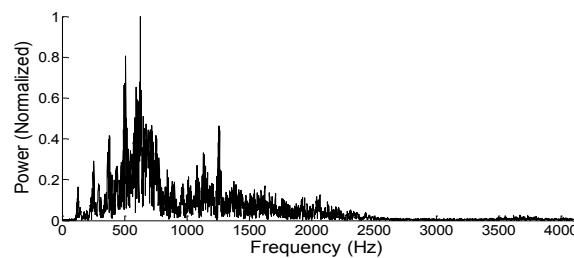
(a) Example of human speech in the frequency domain
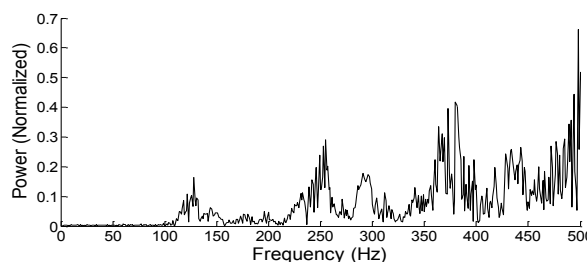
(b) Zoom in of (a) within 0 to 500Hz

Fig. 3. A human speech in the telephony system using 8kHz sampling frequency.

In the telephony system, human speech is converted to digital signal using 8kHz sampling frequency. Fig.3 shows an example of human speech spectrum in telephony system using 8kHz sampling frequency. The speech occupies in the range 100Hz to 2500Hz. The maximum power appears around 600Hz where the most part of information are contained.

There are unused bands i.e. lower band (<100Hz) and upper band (>3000Hz). Even though there is possibility for the speech to fill those bands, the probability is very small and therefore can be neglected. Therefore, any others information can be inserted in those bands. Since EEG signals have frequency that no more than 100Hz, they occupy in the lower band. Of course, there is a certain procedure to put EEG data in this limited band as detailed below.

B. Mixing EEG and Speech

The proposed system to mix EEG and speech as shown in Fig.4 consists of buffers, 16/5 up-sampler, a multiplexer 20 to 1, and an adder. The number of EEG sample after multiplexing

every n second/s is 8192n. This signal is added to human speech before send to voice line of transmitter telephony system.
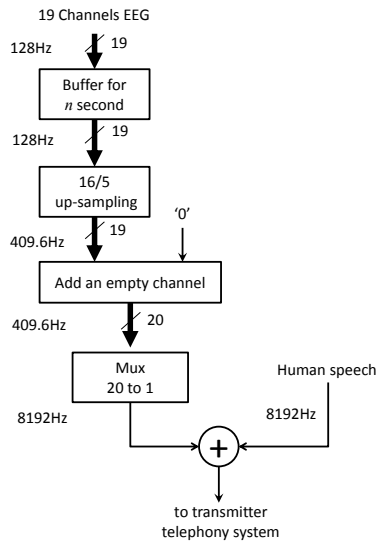

19 Channels EEG

128Hz / 19

Buffer for *n* second

128Hz / 19

16/5 up-sampling

409.6Hz / 19   '0'

Add an empty channel

409.6Hz / 20

Mux 20 to 1   Human speech

8192Hz   8192Hz

+

to transmitter telephony system

Fig. 4. Block diagram of EEG-speech mixing

(a) EEG channel 1

(b) Time multiplexing of EEG signals

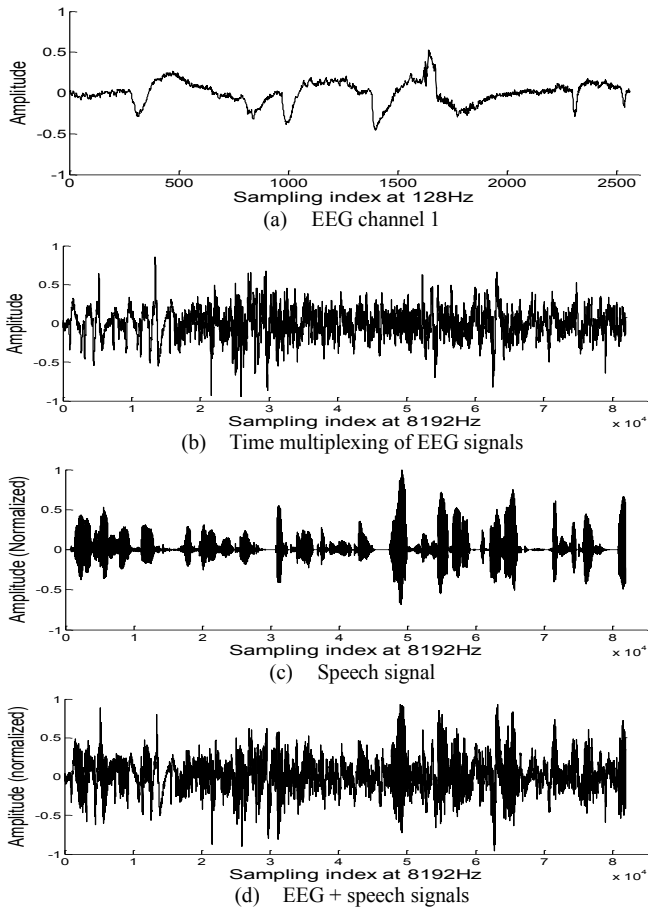

(c) Speech signal

(d) EEG + speech signals

Fig. 5. Snapshot of step by step mixing process in the transmitter side

As illustration, Fig.5(a) shows the EEG signal (channel 1) with 128 sampling frequency for n = 20 second. The output signal of mux 20 to 1 is shown in Fig.5 (b). Human speech and

transmitted signal to telephony system within 20 second are drawn in Fig.5(c) and Fig.5(d) respectively. The total latency in the transmitter side depends on how long the EEG is buffered (n).

IV. EEG-SPECH SIGNALS SEPARATION

A. Proposed Separation Scheme

In the receiver side, the proposed scheme to separate EEG and speech consist of a low pass filter (LPF), buffer, de-multiplexer 1 to 20, 16/5 down-sampler, and a subtraction as shown in Fig.6. The LPF is introduced to extract EEG signal from the mixed signal, while the subtraction is used to get speech signal by subtracting the mixed signal from the extracted EEG. De-multiplexer and down-sampler are included to bring back the EEG signals to the original form i.e. 19 channels with 128 sampling frequency.

The LPF is realized using average computation. In order to minimize the complexity, the average computation is realized using an architecture given in Fig.7. Here we propose the average computation done within 16 sample length. The multiplication by 1/16 is implemented by 4 point right-shifting. Thus, an average computation consists of two adders and a shifter. Due to the averaging process, the signal will be delayed by 16 sampling period. The total latency in the receiver is sum of latency in the LPF and de-multiplexing.

Received signal

8192Hz

Low pass filter   Buffer

8192Hz   8192Hz

−

8192Hz

Demux 1 to 20

Empty channel   409.6Hz / 19

16/5 Down-sampling   Speech signal

/ 19

128Hz

EEG signals
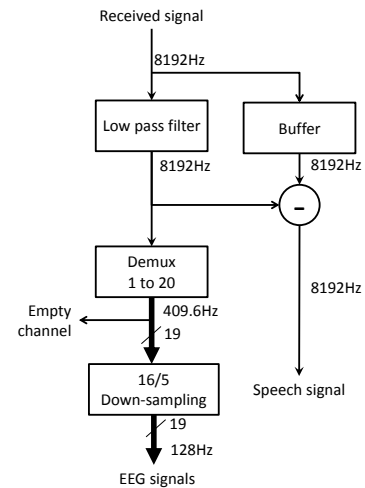
Fig. 6. Proposed system to separate EEG and speech

received signal z^{-1} 1/16   extracted signal (EEG)
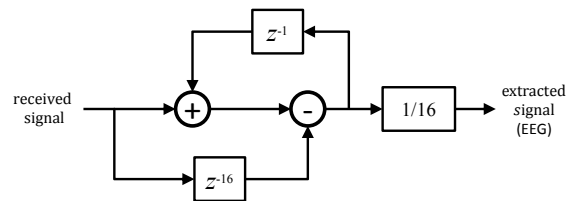
+   −

z^{-16}

Fig. 7. Low pass filter implementation

B. Simulation Result

In order to verify the functionality of proposed system, we perform simulation with some given parameters mentioned in Table 1. A part of input mixed signal is shown in Fig.5(d),

while a part of signal before and after separation are depicted in Fig.8 and Fig.9 for speech and EEG respectively. Note that those figures are obtained in the simulation for SNR = 60dB.

Parameters	Value
Speech bandwidth	4096Hz
Sampling frequency	8192Hz
Simulation duration	20 seconds
Noise type	White noise
Signal to noise ratio (S/N)	5-60dB

From Fig.8 and Fig.9, there are some deformations of speech and EEG signals after separation process. For speech, these signals are still acceptable for human hearing. For EEG,

(a) Original speech

(b) Estimated speech after separation
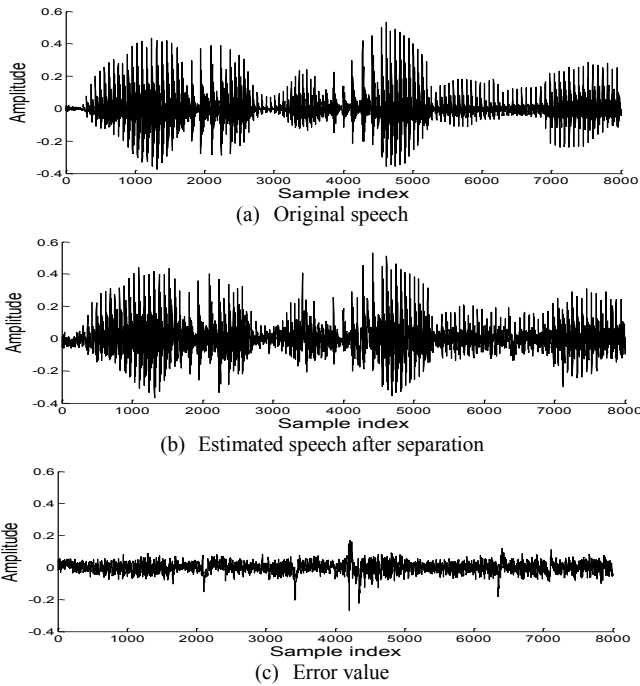

(c) Error value

Fig. 8. Comparison of the original speech signal and the estimated speech signal after separation.

however, an assessment from the specialist is necessary. Based on consultation to the specialist, the EEG signals after separation get the approval.

In order to check the similarity of the signal before (x) and after ($\hat{x}$) separation process, we calculate the correlation coefficient (ρ) as given below:

$$\rho = \frac{\frac{1}{N}\sum\left[(x-\bar{x})\cdot(\hat{x}-\bar{\hat{x}})\right]}{\sqrt{\frac{1}{N}\sum(x-\bar{x})^2}\cdot\sqrt{\frac{1}{N}\sum(\hat{x}-\bar{\hat{x}})^2}} \qquad (1)$$

where $\bar{x}$ is an expected value of signal x, and N is the length of signal. The correlation coefficient is in the range from -1 to 1. Two signals are exactly same if $\rho = 1$, independent if $\rho = 0$, and opposite polarity if $\rho = -1$.

(a) Original EEG channel 1

(b) Extracted EEG channel 1 after separation

(c) Error value
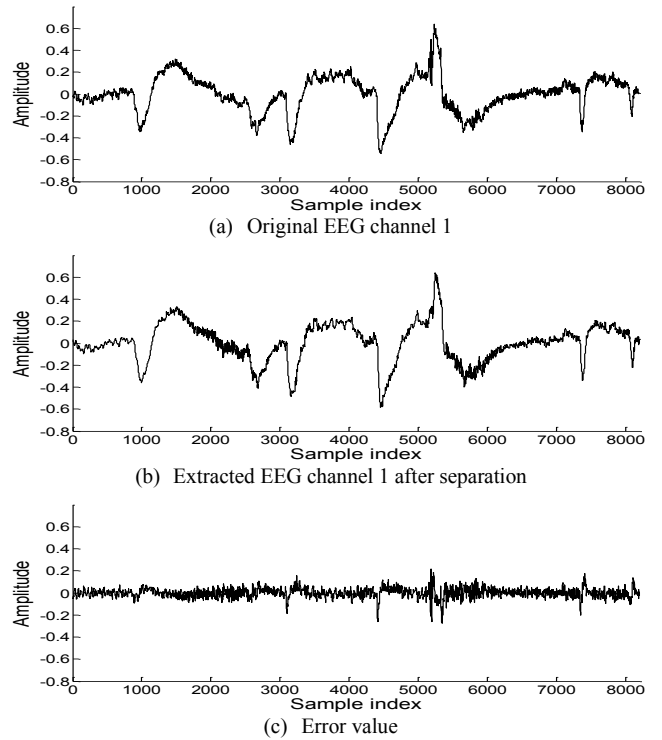
Fig. 9. Comparison of the original EEG signals and the extracted signals after separation, case for channel 1.

The impact of ρ for signals in each EEG channel under the noisy environment is shown in Fig.10. For the SNR higher than 10dB, the ρ is bigger than 0.8, even for some channels it is more than 0.9. Thus, the EEG signals after separation process is very similar with the original EEG signals.
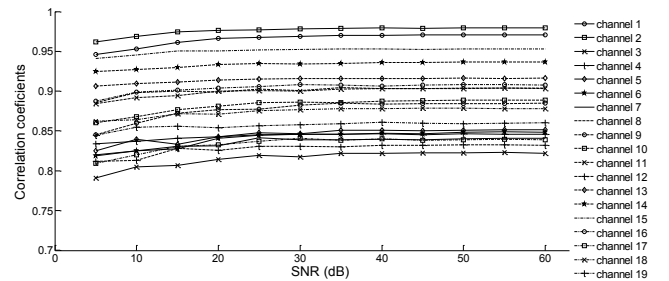
Fig. 10. Correlation coefficients of all channel EEG for n = 20s in the various SNR of AWGN channel.

In order to make comparison with the ρ for speech, we take the average of ρ for EEG, and then presented in Fig.11. It is clear that the similarity of EEG signal is higher than speech in whole channel conditions.

The buffer length n as mentioned in section III.B has influence in the performance as shown in Fig.12. The highest ρ for EEG occur when n = 20s, therefore longer n means better ρ. However, the opposite trend rises in the speech, where n is shorter, ρ is higher. Therefore there is a tread off between the performance of EEG and speech signals.
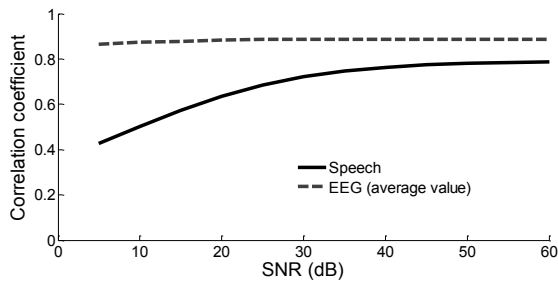
Fig. 11. Performance of EEG and speech separation for n = 20s in the various SNR of AWGN channel.

Fig. 12. Performance of EEG and speech separation for n = 5s, n = 10s, and n = 20s in the various SNR values

C. Computational Complexity and Latency

The proposed system consists of a mixing process in transmission and a separating process in the receiver side. The signal mixer actually requires buffers, up-sampler, a multiplexer 20 to 1, and an adder, and it is easy to be implemented in analog or digital circuit. This additional circuit put prior to the speech coding of the telephony system.

The signal separation in the receiver side as discussed in the previous subsection consists of buffers, two adders, a de-multiplexer 1 to 20, and a down-sampler. These requirements are also very easy to be realized into the hardware.
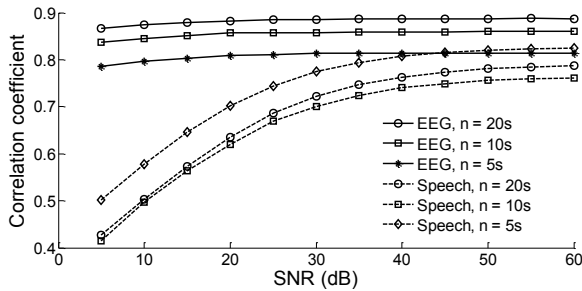
Regarding to latency, the mixing process in transmitter side needs n second latency, while separation process in the receiver side requires 16 clocks latency. Note that n second latency in the transmitter is applied for EEG only, so that the there is no significant delay for speech.

V. CONCLUSIONS

There is a big possibility for the patient to perform telemonitoring via speech line of telephony system. Patient clinical information is sent at the same time of consultation at a distance. In this paper, clinical information is represented by 19 channels EEG signals.

The proposed system consists of a mixing process in the transmitter (patient side) and a separation process in the receiver side (health care provider). The mixing process is built from buffers, an up-sampler, multiplexer 20 to 1, and an adder, while the separation process consists of LPF (implemented by averaging), buffers, de-multiplexer 1 to 20, and down-sampler.

Based on simulation result, the proposed system has successfully separated the speech and the all EEG signals. The correlation coefficient of EEG between before and after separation is in the range 0.8 up to 0.96 for SNR higher than 10dB. Correlation coefficient for speech can reach more than 0.75 when SNR is 30dB or higher. The separation performance for EEG is getting better if the buffer length is longer. However, a longer buffer length reduces the quality of speech.

Regarding the implementation, the mixing process in the transmitter side is put before speech coding, while separation process is done after speech decoding of a telephony system. Moreover, the proposed system has high possibility to be implemented with low complexity since it just involves three adders without any other complex computation

REFERENCES

[1] Institute of Medicine (U.S.) Committee on Evaluating Clinical Applications of Telemedicine and Field, "Telemedicine: a guide to assessing telecommunications in health care", Washington, D.C.: National Academy Press, xiv, 271, 1996.
[2] S.C. Inglis, R.A. Clark, F.A. McAlister, J. Ball, C. Lewinter, D. Cullington, S. Stewart, J.G.F. Cleland, "Structured telephone support or telemonitoring programmes for patients with chronic heart failure", Issue 8, John Wiley & Sons, Ltd., 2010.
[3] S. Meystre, "The Current State of Telemonitoring: A Comment on the Literature", Telemedicine and e-Health, vol.11, no.1, 2005.
[4] Z. Zhang, T.P. Jung, S. Makeig, B.D. Rao, "Compressed Sensing of EEG for Wireless Telemonitoring With Low Energy Consumption and Inexpensive Hardware", Biomedical Engineering, IEEE Transactions on, vol.60, no.1, pp.221-224, Jan. 2013.
[5] M. Mohsina, and A. Majumdar, "Gabor based analysis prior formulation for EEG signal reconstruction", Journal of Biomedical Signal Processing and Control 8, no.6, pp.951-955, 2013.
[6] R. Hussein, A. Awad, A. El-Sherif, A. Mohamed, and M. Alghoniemy, "Adaptive energy-aware encoding for DWT-based wireless EEG tele-monitoring system", in IEEE Digital Signal Processing and Signal Processing Education Meeting (DSP/SPE), pp. 245-250, 2013.
[7] G. Singh, V. Gupta, and D. Singh, "Coherence Analysis between ECG Signal and EEG Signal", International Journal of Electronics & Communication Technology, Vol. 1, Issue 1, pp. 25-28, 2010.
[8] M. Teplan, "Fundamentals of EEG measurement. Measurement science review", vol.2, section 2, pp.1-11, 2002.
[9] J.P. Lachaux, et al., "A quantitative study of gamma-band activity in human intracranial recordings triggered by visual stimuli". European Journal of Neuroscience, vol.12, no.7 pp.2608-2622, 2000.
[10] A. Mansour, A. K. Barros, N. Ohnishi, "Blind separation of sources: Methods, assumptions and applications", IEICE Trans. On Fundamental of Electronics, Communications and Computer Sciences, vol.E83-A, pp. 1498-1512, 2000.
[11] M. A. Dmour, M. Davies, "A New Framework for Underdetermined Speech Extraction Using Mixture of Beamformers", IEEE Trans. on Audio, Speech, and Language Processing, vol.19, no.3, pp.445-45, March 2011.
[12] L. R. Rabiner and R.W. Schafer, "Theory and Applications of Digital Speech Processing", 1st edition, Pearson, New Jersey, 2011.

High Performance CDR Processing with MapReduce

Mulya Agung, A. Imam Kistijantoro
School of Electrical Engineering and Informatics
Institut Teknologi Bandung, Indonesia
agung@tritronik.com, imam@informatika.org

Abstract— **A Call Detail Record (CDR) is a data record produced by telecommunication equipment consisting of detail of call transaction logs. It contains valuable information for many purposes of several domains such as billing, fraud detection and analytical purposes. However, in the real world, these needs face a big data challenge. Billions CDRs are generated every day and the processing systems are expected to deliver results in a timely manner. In our case, the system also has constraint that is running in limited computation resources. We found that our current production system was not enough to meet these needs. We had successfully analyzed the current system bottleneck and found the root cause. Based on this analysis, we designed and implemented a better performance system which is based on MapReduce and running on Hadoop cluster. This paper presents the analysis of previous system and the design and implementation of new system, called MS2. In this paper, we also provide empirical evidence demonstrating the efficiency and linearity of MS2. In a test case of telecommunication mediation system, our test has shown that MS2 reduces overhead by 44% and speedup performance by nearly twice compared to previous system. From benchmarking with several related technologies in large scale data processing, MS2 is also shown to perform better in case of CDR batch processing. Running on a cluster consists of eight core CPU and two conventional disks, MS2 is able to process 67,000 CDRs/second.**

Keywords— Call Detail Records, Telecommunication Mediation, MapReduce, Hadoop, Java EE, High Performance

I. INTRODUCTION

CDR generated by low-level telecommunication equipment must be prepared to be processed by other high-level applications. In telecommunication, the system which handles this preprocessing stage is called mediation system. Due to the large size of generated CDRs and need of fast processing result for various purposes, preprocessing stage in a mediation system become a big data challenge. As discussed in [2], to achieve acceptable performance, this kind of application needs different techniques than conventional computation.

For many years, a scalable mediation system called MS1 was used and running in production system to deliver CDR processing in one of the biggest telco provider in Indonesia. But, due to fast growth of subscribers, using it in current scale was becoming increasingly challenging. The biggest challenge comes from efficiency that is limited resources are demanded to process more data.

In this paper, we present the investigation and analysis of the current parallel system overhead due to I/O bottleneck. Then we present the design and implementation of new system which addressed the issues. This new system is called MS2. It runs on Hadoop cluster environment and uses MapReduce for parallel data processing. We also present results from empirical evaluation and COST analysis [7] to determine the system overhead compared to single-thread performance. We begin by briefly describing MS1 and motivation of MS2 in the next section. Then, in the section III, we describe alternative that we considered to address the problems describe above, and section IV presents the analysis, design and implementation of MS2. Results from empirical evaluation comparing MS1 and MS2 are presented in Section V. In section VI, We discuss related works and benchmark MS2 with several related technologies in large data processing. Finally, section VII contains our conclusion and points to some directions for future work.

II. MOTIVATION FOR MS2

MS1 has served the CDR processing needs at telecommunication billing system for the past several years. Based on our operation and maintenance experience at current scale, we need to improve the performance of current production system. Before that, we also needed to identify and analyze the possible bottlenecks or inefficiencies of MS1 that are highlighted in the following sections. These inefficiencies motivated us to develop MS2.

A. CDR Processing in Mediation System

Due to efficiency, CDR is generated by low-level telecommunication equipment in a compact binary format [8]. This binary format should be converted to a textual format so it can be processed by next steps or higher level application easier. Mediation is the first step in processing these CDRs, and involves capturing CDRs from upstream network systems and making them ready for processing by downstream applications (RA, BI, FM, warehousing). This complex task is composed of several steps that include functions of collection, validation, filtering, collating, correlation, aggregation, formatting, normalization and data transformation [15].

B. MS1 Architecture

MS1 splits one pipeline processing into three stages. Collection and decoding stage involves collecting CDR files from external input sources and decodes them to intermediary

format. Preprocessing stage evaluates rule against records' contents. Mediation function such as validation, aggregation, filtering and normalization are specified in this rule. Formatting and distribution stage convert and distribute processed data to destination-friendly format.

MS1 is designed and implemented with adopting Java Enterprise Integration Patterns architecture (EIP) [9] to integrate its components. It uses message-passing and shared memory model for data parallelism and achieved distributed processing by moving data to computation. Processing components are running in cluster nodes and data are distributed to computation node as needed (Fig. 1).

C. MS1 Performance Measurement and Analysis

Performance of existing system is measured and analyzed by conducting two test scenarios: the first test is performed in multi-thread configuration; and the second is performed in single-thread configuration. Both scenarios are tested on clustered nodes consisting two identical servers (i.e. Server1, Server2). The hardware specifications for each server are 2.66 GHz Intel Quad Cores CPU, 8 GB of DDR2 RAM, SATA 2 HDD 7200 RPM and one gigabit Ethernet. Servers run with Linux Operating System. Performance parameters used for analysis here are processing time and resources utilization.

1) Multi-thread configuration

Parallel performance is assessed using 1.6 GB data set consisting 100 of 16 MB batch CDRs files. The number of threads allocated for decoding, preprocessing and formatting is 1, 8, and 20 respectively. CPU utilization graphs (Fig. 2) shows pattern which gives a low CPU utilization in average. I/O utilization graphs show a similar pattern that Disk and Ethernet load has a high peak load and idle in several times. The investigation continues by increasing threads of preprocessing stages. Fig. 3a shows the performance of MS1 in several thread number configuration. The graph shows that increasing threads doesn't increase performance significantly. The result of thread analysis using JVisualVM shows that threads are using most of their time to wait others to finish. There is no indication of deadlock or blocked threads caused by thread synchronization.
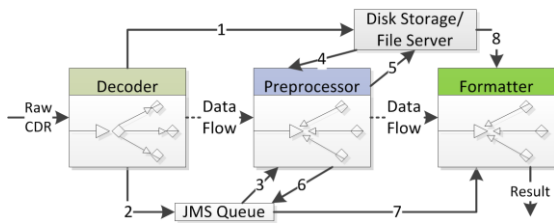

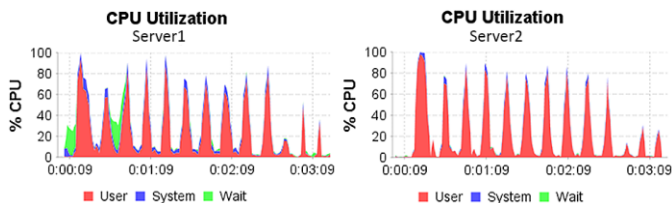Fig. 1. MS1 components and data flow
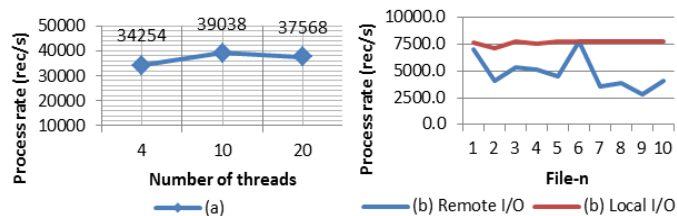

Fig. 2. CPU utilization in MS1

Fig. 3. MS1 Performance by (a) number of threads and (b) single-thread

2) Single-thread configuration

Many parallel systems have surprisingly large overhead [7]. The overhead is evaluated by benchmarking them against performance of single-thread system. With the same reason, this scenario is conducted for MS1. The single-thread configuration is tested on two types of I/O access that is local storage access and remote storage access. The analysis of both cases will give understanding of how both I/O type cause overhead to the overall performance. Test results shows that remote I/O gives more overhead than local I/O access. This overhead has reduced the overall performance of MS1 significantly in single-thread configuration and using remote access (Fig. 3b). Remote I/O overhead has decreased single-thread performance from 7658 record/s to 4427 record/s.

D. Efficiency Issues with MS1 Processing

Based on the performance assessment of parallel configuration and single-thread configuration, we may conclude that the overall performance of MS1 is not optimum due to inefficient resources utilization. The inefficiency comes from I/O overhead that caused by local disk access and network access. From single-thread configuration test, we found that the most significant reduction comes from network I/O. So by reducing these overheads, the overall performance of CDR processing should be increased significantly.

III. DESIGN ALTERNATIVE

As discussed in the previous section, the idea of increasing current performance is by reducing the I/O overheads. One principle that can be used to do this is locality [2, 10]. This principle can minimize network I/O overhead by ensuring that computation is always performed against data stored in local node. Technique known to use this principle is moving computation to data. This technique is used in MapReduce processing model to increase its batch processing performance [11]. Therefore, the analysis of MS1 brings us to current hypothesis that adopting MapReduce model to existing CDR processing system will reduce the overhead of distributed system and increase the overall performance.

IV. MS2

In this section, we briefly describe the analysis, design and implementation of MS2 components.

A. Analysis

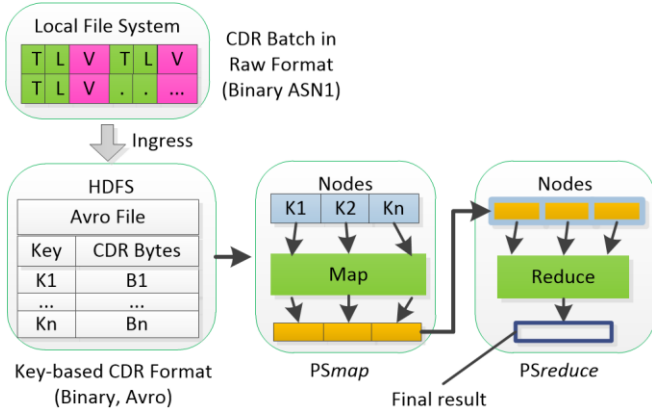Systems analysis of MS2 is broken down based on identified problem topics.
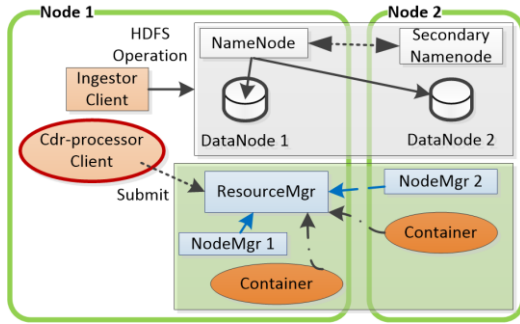
Fig. 4.   Data Parallelism in MS2.

Fig. 5.   MS2 Deployment in a Hadoop Cluster

1) Ingress & Egress Data

Ingress data is done by collection and decoding process, meanwhile egress data is done by formatting and distribution process. Several optimizations as explained in [12] are done in this step. Aggregation of many and small data elements to single and big file can optimize data migration to HDFS. Data format transformation is needed because in our case, CDR is not ideal to be directly processed by MapReduce. Based on works [2, 13, 25], in fixed disk, sequential access has much better performance than random access. So in our case of using conventional disk, sequential pattern implementation will improve ingress performance.

2) Mapping of MS1 Component to MapReduce

Mapping existing components to MapReduce model needs following considerations. Preprocessing stage is more optimal to be executed in mapper process because of the large input data. Mapper will process data with locality principle [1, 14] thus it will decrease network I/O access in large input CDR processing. Formatting stage is more optimal to be executed in reducer process because formatter component get intermediary data from preprocessing result, which is much smaller than ingress result. Reducer process uses intensive disk and network I/O, so to decrease the overhead, data and task amount has to be as small as possible [14, 23].

3) MapReduce and Java Enterprise Architecture

Transition from existing architecture meets its own challenge regarding MapReduce single fixed dataflow characteristic [17]. In MapReduce environment, Java Bean container that is initiated in one JVM cannot be accessed directly by Mapper and Reducer object in other JVM. But, patterns such as Data Access Object (DAO), Singleton and Dependency Injection (DI) depend on this container. Solution for this problem is reinitiating bean container when Mapper and Reducer object is executed. Consequently, time and resource needed in initiation process can impact the overall performance. The alternative and better solution is running Java Bean Container outside of MapReduce, and using stateless remote procedure call to access the container [18].

4) Hadoop Deployment

Deployment strategy is important to the overall performance because it determines total resources that will be utilized. To maximize resource utilization in existing nodes, HDFS and YARN should be deployed and running on all nodes. NameNode, DataNode, and NodeManager should run on all nodes and replication level is set to number of nodes. Since there is only one global ResourceManager, its deployment can be chosen in one of the server [1, 19].

B. Design

This chapter presents the design of MS2 components, parallelism and deployment.

1) Ingestor

This component moves CDR file to HDFS. It aggregates data by multiplexing. It is also designed to run sequentially to improve disk access performance. To store the result of this aggregation process in a compressed big file, a new data structure is designed using Avro serialization framework [1, 12, 14, and 31].

2) Mapper & Reducer

To maximize parallelism, mapper component bundle a partial decoding and preprocessing into one process. Mapper will take ingested file based on batch key and decode binary contents to intermediary data. Then it will call RecordProcessor to evaluate processing rules and generate array of CdrData as its results. Mapper will access RefData service for every database lookup. There will be additional I/O from HTTP and database access, but this can be reduced by placing database in the same host with service. With this locality, mapper only needs network I/O to access the service. Database access performance is also improved with data caching [21]. Reducer executes formatting and serialization by generating records in destination-friendly format. Serialization is needed to change intermediary format to text file format that conforms by upstream node. Reducer component is designed similar with external output pattern as explained in [22].

3) Data Parallelism

Before processing and formatting, CDRs generated by sources are loaded to MS2 by ingestion process and stored in key-value based data (Fig. 4). Under the Map-Reduce model, processing and formatting are expressed in terms of two processing stages (PS) – the PS_{map} and the PS_{reduce}. The same PS_{map} is running at all participating Mapper, and the same PS_{reduce} is running at all participating Reducer in parallel, such that each PS_{map} is applied to a set of key-value tuples (k,v) and transform it into a set of tuples of different type (k',v'); then all the values v' are re-partitioned by k' and each PS_{reduce}

aggregates the set of values v' with the same k', as expressed below.

$$PS_{map}: (k, v) => (k', v')*$$

$$PS_{reduce}: (k', v')* => (k', v'*)$$

4) Hadoop Cluster Deployment

Hadoop components are deployed to existing servers with the following structure. Node 1 and Node 2 is deployed in Server1 and Server2 respectively. Both HDFS and YARN components are deployed on both nodes. Primary NameNode and DataNode 1 of HDFS are deployed in Node 1. ResourcesManager and NodeManager 1 of YARN are also deployed in Node 1. Secondary NameNode, DataNode 2 and NodeManager 2 are deployed in Node 2. Fig. 5 shows MS2 deployment in Hadoop cluster and the execution of ingestion and MapReduce process.

C. Implementation

The implementation involves tasks that needed to ensures that system will be running with designed performance.

1) Components and Platform

The new components implemented are Ingestor, Cdr-processor and intermediary data structure. Cdr-processor is a MapReduce driver consisting Mapper and Reducer classes. MapReduce platform used in this implementation is Hadoop 2.6.0 and it is deployed and running with the same operating system used in MS1. Besides the components written in Java, Hadoop is providing components written in native C. These native components are needed to improve Hadoop performance by accessing resources directly [1]. Additional REST service component is implemented for reference database lookup. The initiation of shared object which doesn't need I/O is implemented in setup() method which is derived from Hadoop Mapper and Reducer interface. By overriding this method, the initiation will be ensured to run once in object lifetime [1].

2) Compression & Operating System Tuning

Compression is used to improve ingestion performance. Based on results in [16, 20, 23], snappy compression is chosen to give better performance than built-in method. Some useful OS tunings recommended in [16, 23] are applied in deployed system. These include using EXT4 file system and noatime option set in mount parameters for mount point used by HDFS. Noatime option is useful to reduce disk read overhead by disabling access log updates. Number of file descriptor allowed for Hadoop process is also increased. This tuning is useful to prevent possible exception triggered on high load which cause MapReduce jobs fail.
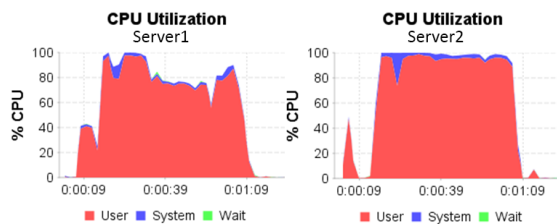

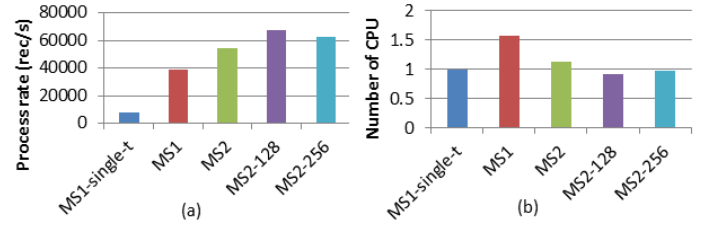Fig. 6. CPU utilization of 128 MB block size tuning

Fig. 7. Comparison of (a) throughput (b) CPU to achieve single-t throughput
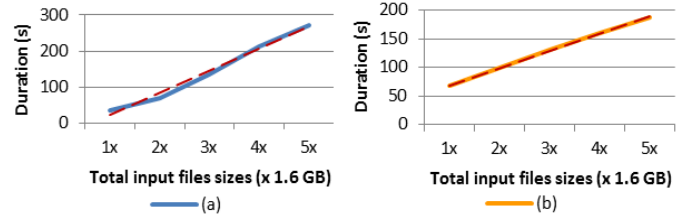

Fig. 8. Performance linearity of (a) ingestion and (b) processing

TABLE I.   TUNING CONFIGURATION OF 128 MB BLOCK SIZE

Configuration	Value
mapreduce.input.fileinputformat.split.minsize	224000000
mapreduce.task.io.sort.mb	500
mapreduce.map.java.opts	-Xmx1024m
mapreduce.map.memory.mb	1280

V.   EXPERIMENTS AND RESULTS

Experiments were carried out to evaluate the MS2 performance over the test cluster.

A. Ingestion experiment

Ingestion is performed to process the same data set used in MS1 performance assessment. To give more accurate results, this process is repeated in several iterations. This stage is running in Node 1 and the duration is measured after iteration finished. Ingestion needs 36.8 seconds in average to collect 1.6 GB data set and results in 1.43 GB compressed file stored in HDFS.

B. Cdr-processor Experiments

Configurations tested to evaluate processing performance are Hadoop default configuration, tuning for 128 MB block size and tuning for 256 MB block size. From the test results, configuration for 128 MB block size (Table I) is the highest performer with highest CPU utilization (Fig. 6). This configuration is set based on recommended calculation in [16, 23]. Input.fileinputformat.split.minsize property set the split size allocated to mapper process. It is set to 224MB so if the input file resulted from ingestion has size 1.43 GB then the minimal number of splitted tasks will be 1.43 GB/224 MB = 6.38 ≈ 7 tasks. This number of task is enough for total of 8 core CPU resources which cluster has. If each core executes one mapper task, then in overall, system still have one spare core for managing resources. Properties such as task.io.sort.mb, map.java.opts and map.memory.mb are set according to number of split tasks and total RAM available in the cluster. If one mapper task is allocated with 1280 MB heap, then one node will allocate (1280x4) MB = 5120 MB of memory. This

number is still below total RAM capacity of each node. This configuration ensures that mapper will not use swap memory to perform its tasks.

C. Overall Performance

Total performance is calculated from ingestion and Cdr-processor throughput. The performance of tested configurations is compared with MS1 and single-thread performance (Fig. 7a). MS2 with 128 block size tuning configuration (MS2-128) has the highest performance among them. Performance of evaluated systems and CPU allocated for each configuration is shown in Table II.

Compared to single threaded MS1 (MS1-single-t), MS2 with allocated 8 cores results in 8.7x performance speed up. Overheads of compared systems are also measured. Fig. 7b shows that MS1 system has the highest overhead between all evaluated systems. To achieve 7658 rec/s performance, parallel MS1 needs 1.6 cores but MS2-128 needs only 0.9 cores. This CPU cost reduction proves MS2-128 had successfully reduced 44% of overhead introduced by MS1. This result also shows that with the correct tuning, MS2 is able to achieve performance that is more efficient than MS1, even compared with single-thread performance.

D. Linearity

Experiments were carried out to see MS2 performance while load increases. The best performer configuration is used to process higher number of input files. Sample data with total files sizes increased from 1.6 GB to 3.2 GB, 4.8 GB, 6.4 GB and 8 GB are used as input. Fig. 8a shows the ingestion process time increases almost linearly from 1.6 GB to 8 GB input files sizes in 36.8 seconds to 272 seconds (slope=61.29). The increase of duration in processing stage is consistent as input files sizes increasing. Fig. 8b shows how the duration line of processing stage compared to its linear line. From these experiments results, we may have conclusion that the performance of MS2 is linear as total input files size increases.

TABLE II.   PERFORMANCE OF MS1 AND MS2 BY CPU

System and configuration	Performance (rec/s)	CPU core
MS1 (10 preprocessing thread)	39037.57	8
MS2 (default Hadoop configuration)	54719.85	8
MS2-128 (block size=128, split task=7)	67060.70	8
MS2-256 (block size=256, split task=6)	62839.25	8
MS1 Single-thread	7658.73	1

TABLE III.   PERFORMANCE OF MS2 AND RELATED TECHNOLOGIES

System	Rec size (B)	Performance (rec/s)	MB/s	CPU (core @ 2.xGHz)	RAM (GB)
MS2	200	67,060	13.4	8	16
Kafka Producer (Batch size=1)	200	50,000	10	16	32
Kafka Producer (Batch size-50)	200	400,000	80	16	32
Kafka Consumer	200	22,000	4.4	16	32
iMR (MR Jobs)	7	13,000,000	91	80	960

VI.   RELATED WORK

As the time of writing, publications specific to CDR preprocessing are still limited. Some works on CDR analysis techniques had been proposed [3, 4, 5] but these techniques are designed for analytical processing after CDR has been preprocessed by mediation. Work on middleware based mediation system has been reported by Bouilett et.al [15]. This system runs on IBM InfoSphere middleware and uses region based parallelism to improve its performance. Instead of using the same approach, MS2 uses record and locality based parallelism because region based parallelism give no benefit when CDRs are batched across different regions. They reported that the resulted performance which is 70,000 CDRs/second was not adequate to deliver business constraint at that time which is 220,000 CDRs/second. Unfortunately, we cannot compare this performance to MS2 because hardware configuration was not specified on their paper.

Pipeline based parallel framework for mass file processing [6] can be used to process file based CDRs and it is similar with technique used in MS1. However, this technique is not optimal enough for CDR processing because it uses file based decomposition instead of record based decomposition. A scalable and distributed system of CDR stream analytics was proposed in [26]. The solution is optimized for stream where CDR is received in much smaller chunks continuously. MapReduce is used to parallelize analytic processing after stream CDRs are previously merged and stored in a data warehouse. While there are additional costs for merging and storing in data warehouse, it will reduce performance when CDRs are ingested already in batches. Due to lack of performance evaluation in the paper, we cannot compare its performance to MS2.

Another class of related technologies comes from large-scale log processing such as iMR [27], Kafka [28], and Flume [29]. iMR increases performance by moving analytics on to the log servers themselves. By transforming data in place, it can increase locality and reduce volume of data crossing the network. But unlike batch oriented workloads (case of MS2), iMR take as input small and continuous input streams and can take benefit in performance by only processing subset of data and decreasing result fidelity (lossy). In many cases of CDR preprocessing, completeness is mandatory because unprocessed record may lead to missing transactions.

Both Kafka and Flume are focused on data loading such as log aggregation and message feeds. They lacks of parallelism model support for processing but often combined with other platform to deliver full real-time data analytic and processing [29, 30]. We found that in our case, both Kafka and Flume can be used to load CDRs to processing nodes but as they are optimized for stream, it may introduce overhead to split larger size of batched CDRs to smaller chunks.

To give a view of how is the efficiency of MS2 compared with other related technologies, we also compared the performance based on resources used (i.e. CPU and RAM). We choose Kafka and iMR since hardware configurations used in experiments are published on respective papers [27, 28]. From Table III, we can see Kafka producer is more efficient than

MS2 with larger batch size but it performs no data processing which is needed in case of MS2. The throughput of iMR on its test environment is higher than MS2 but the resources used are also higher than we used in MS2 evaluation. If we adjust the resources based on ratio, MS2 has higher performance than iMR. MS2 performs better because it doesn't need to do aggregation phase for continuous streams which is needed to be done in iMR.

VII. Conclusion and Future Work

The need of CDR processing at a telecommunication provider continues to grow, and in our production has pushed the limit of existing system can deliver in term of performance. To meet this need, we have designed and implemented a new CDR processing system called MS2 based on a deep analysis on existing system, which we have presented in this paper. We have also presented results from empirical evaluation of MS2 that demonstrates significant reductions in I/O overhead when using MS2, while delivering nearly 2 times improvements in throughput which are linear to number of input CDRs. The performance of CDR ingestion process has been increased by using multiplexing technique and sequential access. The performance of CDR preprocessing and formatting process has been increased by optimizing MapReduce process and applying the correct tuning. Correct tuning here means that system is configured to make optimum use of available CPU and memory resources.

However, the performance evaluated in this paper is based on one case scenario of CDR processing in telecommunication mediation system. The performance result can be possibly varied with different rules of CDR processing. Next research could be evaluating performance of proposed system for several patterns of CDR processing rules. This evaluation can be also helpful for system improvement and optimization in the future.

References

[1] Apache hadoop. http://hadoop.apache.org.

[2] Jacobs, Adam. "The pathologies of big data." Communications of the ACM 52.8 (2009): 36-44.

[3] Teng, Wei-Guang, and Ming-Chia Chou. "Mining communities of acquainted mobile users on call detail records." Proceedings of the 2007 ACM symposium on Applied computing. ACM, 2007.

[4] Ding, L., Gu, J., Wang, Y., & Wu, J, "Analysis of Telephone Call Detail Records Based on Fuzzy Decision Tree," Forensics in Telecommunications, Information, and Multimedia (pp. 301-311), 2011.

[5] Lin, Q., & Wan, Y., "Mobile customer clustering based on call detail records for marketing campaigns," Management and Service Science, 2009. MASS'09. International Conference on, 1-4.

[6] Liu, T., Liu, Y., Wang, Q., Wang, X., Gao, F., & Qian, D., "Pipeline-Based Parallel Framework for Mass File Processing," Cloud and Service Computing (CSC), 2013 International Conference on (pp. 42-48).

[7] McSherry, Frank, Michael Isard, and Derek G. Murray. "Scalability! But at what COST." 15th Workshop on Hot Topics in Operating Systems (HotOS XV). USENIX Association, 2015.

[8] ITU-T, X.690 Information Technology - ASN.1 Encoding Rules, ITU-T X-Series. International Telecommunication Union, 2002.

[9] Hohpe, G., Bobby W., Enterprise Integration Patterns, Addison-Wesley Professional, Addison-Wesley, 2003.

[10] Bell, Gordon, Jim Gray, and Alex Szalay. "Petascale computational systems." Computer 39.1, 2006, pp. 110-112.

[11] Dean, Jeffrey, and Sanjay Ghemawat. "MapReduce: simplified data processing on large clusters." Communications of the ACM 51.1 (2008): 107-113.

[12] Holmes, Alex. Hadoop in practice. Manning Publications Co., 2012.

[13] Gray, Jim, and Prashant Shenoy, "Rules of thumb in data engineering." Data Engineering, 2000. Proceedings. 16th International Conference on. IEEE, 2000.

[14] White, Tom. Hadoop: The definitive guide. " O'Reilly Media, Inc.", 2012.

[15] Bouillet, Eric, et al. "Processing 6 billion CDRs/day: from research to production (experience report)." Proceedings of the 6th ACM International Conference on Distributed Event-Based Systems. ACM, 2012.

[16] Joshi, Shrinivas B. "Apache hadoop performance-tuning methodologies and best practices," In Proceedings of the 3rd ACM/SPEC International Conference on Performance Engineering, pp. 241-242. ACM, 2012.

[17] Lee, Kyong-Ha, et al. "Parallel data processing with MapReduce: a survey." AcM sIGMoD Record 40.4 (2012): 11-20.

[18] Feng, Xinyang, Jianjing Shen, and Ying Fan. "REST: An alternative to RPC for Web services architecture." Future Information Networks, 2009. ICFIN 2009. First International Conference on. IEEE, 2009.

[19] Vavilapalli, Vinod Kumar, et al., "Apache hadoop yarn: Yet another resource negotiator," Proceedings of the 4th annual Symposium on Cloud Computing. ACM, 2013.

[20] Chang, J., Lim, K. T., Byrne, J., Ramirez, L., & Ranganathan, P., "Workload diversity and dynamics in big data analytics: implications to system designers," In Proceedings of the 2nd Workshop on Architectures and Systems for Big Data (pp. 21-26). ACM, 2012.

[21] Gadkari, Abhijit. "Caching in the distributed environment." Advances in Computer Science: an International Journal 2.1, 2013, pp. 9-16.

[22] Miner, Donald, and Adam Shook. MapReduce Design Patterns: Building Effective Algorithms and Analytics for Hadoop and Other Systems. " O'Reilly Media, Inc.", p189-195, 2012.

[23] Heger, Dominique. "Hadoop performance tuning-a pragmatic & iterative approach." Computer Measurement Group Journal 4 97-113, 2013.

[24] Hapner, Mark, et al. "Java message service." Sun Microsystems Inc., Santa Clara, CA (2002).

[25] Frank, Richard, et al. "High-speed database checkpointing through sequential I/O to disk." U.S. Patent No. 5,996,088. 30 Nov. 1999.

[26] Chen, Q., & Hsu, M, "Scale out parallel and distributed CDR stream analytics," In Data Management in Grid and Peer-to-Peer Systems (pp. 124-136). Springer Berlin Heidelberg.

[27] Logothetis, D., Trezzo, C., Webb, K. C., & Yocum, K., "In-situ MapReduce for log processing," In 2011 USENIX Annual Technical Conference (USENIX ATC'11), pp. 115, 2011.

[28] Kreps, Jay, Neha Narkhede, and Jun Rao, "Kafka: A distributed messaging system for log processing," Proceedings of the NetDB, 2011.

[29] Liu, X., Iftikhar, N., & Xie, X., "Survey of real-time processing systems for big data," In Proceedings of the 18th International Database Engineering & Applications Symposium (pp. 356-361). ACM, 2014.

[30] Sumbaly, R., Kreps, J., & Shah, S., "The big data ecosystem at linkedin," In Proceedings of the 2013 ACM SIGMOD International Conference on Management of Data (pp. 1125-1134). ACM, 2013.

[31] Floratou, A., Patel, J. M., Shekita, E. J., & Tata, S., "Column-oriented storage techniques for MapReduce," Proceedings of the VLDB Endowment, pp. 419-429, 2011.

Accelerating Internet Penetration to Rural Areas : A Government-Sponsored Internet-Kiosks Deployment Project in Garut Regency, West Java of Indonesia

A. Kurniawan[1], I. Zakia[1], E. Wartika[2], and A.G. Austin[3]

[1]*School of Electrical Engineering and Informatics*
Institut Teknologi Bandung
Jalan Ganeca 10, Bandung, 40132, Indonesia
[1]adit@stei.itb.ac.id

[2]*Study Program of Film and Television*
Institut Seni Budaya Bandung
Jalan Buahbatu 212, Bandung, 40265, Indonesia
[2]enok_wartika@yahoo.com

[3]*Faculty of Civil Engineering and Environment*
Institut Teknologi Bandung
Jalan Ganeca 10, Bandung, 40132, Indonesia
[3]azmighalib@yahoo.co.id

Abstract— **Internet penetration in developing countries depend on a variety of factors, including the Gross Domestic Product (GDP), the density of telephone connections, and the density of personal computer users. Internet kiosks have been deployed in 21 rural ditrict areas of Garut Regency to facilitate internet access for local/district government as well as for the community who have no access to internet. Each district was equiped with 10 PCs, a printer, a scanner, and an internet connection either using DSL or cellular access technology. The program was government sponsored through the Ministry of Communications and Information of the Republic of Indonesia. This program was also designed to provide education and training for the district internet kiosks operator as well as for the staffs of information technology at Garut Regency, on understanding, efficient use, management, maintenance, as well as the ethical/professional use of information to upgrade their skills. This study was then conducted to evaluate factors affecting internet penetration in rural areas of Garut Regency, West Java of Indonesia.**

Keywords—Demography; DSL; GDP per capita; internet kiosk; internet penetration; rural areas; TV.

I. INTRODUCTION

Internet penetration into remote areas would have positive impact on Gross Domestic Product (GDP) and the growth of the market [1]. The estimated impact will be greater in developing countries. Higher internet penetration growth will accelerate development of the economic potential in the region. But the challenge that needs to be solved is the difficulty and prohibitively expensive infrastructure for providing network access to remote areas, requiring high investment. The low rate of penetration of fixed wire telephone network also occurred in almost all parts of the world. This is due to the high cost of investment, while the development of wireless telecommunications with mobile technology continue to grow gradually and have been able to provide value added services to the people who live in rural areas [2].

The evaluation in [3] concluded that economic growth will develop faster in the higher income population compared to poorer regions. It is very important to be taken into consideration in building a strong telecommunications infrastructure to facilitate the rural population in order to adopt the internet. Based on the argument in [4], a hypothesis can be made that a region with a GDP per capita which is higher tend to have a faster internet adoption. Statement in [5] argued that the government's role in supporting the development of online services can increase internet penetration. The author argues that the government's role is very important to promote the involvement of all stakeholders' to develop IT in remote areas. However, to achieve that, not only the government officials involved, but also business organizations, civil society and consumer participation would have to play important roles. This confirms that the information economy will not take off without the init\iative of the business community [6]. In other words, the government alone can lead the adoption of e-government, and the private sector will follow government policy, especially in rural areas after the penetration of information began to rise and rolling. Thus, it can be said that the region with the availability of e-government information will have higher internet adoption rates. TV penetration in rural areas is also a factor that affects the penetration of the internet [7]-[8]. This network is generally used for multimedia content and entertainment purposes. All of these factors can affect the birth of interactive TV community. Thus, regions with higher ratio of televisions in households tend to have higher levels of Internet adoption.

On the other hand, provision of mobile phone services which prompted the creation of innovative communications services to individuals and businesses [9]-[11] are starting to get into remote areas that were previously not covered by the fixed telephone network. Service content available through the mobile phone network is also increasingly diverse and innovative, so it will encourage the rural population to enjoy a variety of useful services. Therefore, region areas with higher penetration rates of mobile phone networks tend to have higher Internet adoption rate as well.

Kim [12] showed that GDP willbe the significant variable that explains the variance in costs incurred by residents for communication needs. This study will also propose to make the policy and strategy, so that penetration of the Internet into remote areas can be faster to encourage the development of the economic potential of rural areas itself. It's been widely believed that information and communication technology (ICT) is one of the key factors for economic growth and the internet is a key component of ICT, the internet connection is necessary beforehand to serve people in rural areas [16]-[17]. To that end, this article will try to propose a techno-economic solution for accelerating penetration of ICT in areas that are economically potential but access to internet remains low. As a case study, the research carried out in this study is inline with the government program supported by the World Bank grant project through the Ministry of Communications and Information to deploy internet kiosks in 21 districts that have no internet access in Regency of Garut, West Java of Indonesia. The Regency of Garut, is representative to model rural areas of Indonesia with high enough of population density and economicallypotential. The map of Garut Regency is shown in Fig. 1.
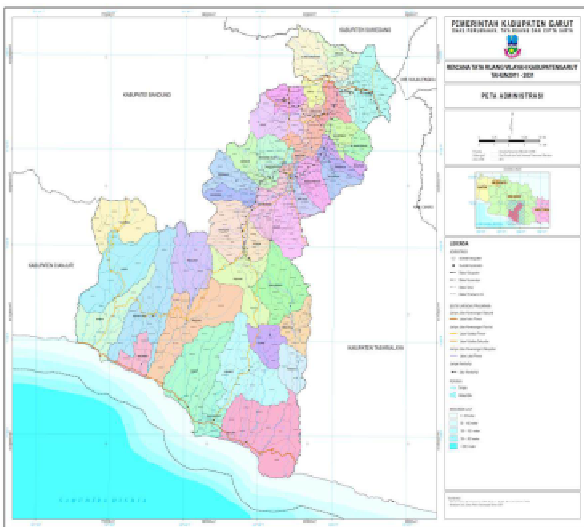

Fig. 1 Geographic Map of Garut Regency

The paper is organized as follows. Section II describes the pilot project to provide infrasructure and internet connection to rural areas in the Regency of Garut, West Java of Indonesia, Section III presents the strategic policy and techno-economy to accelerate rural internet penetration. Section IV evaluates the impact of internet penetration in rural areas on development and economy, and Section V concludes the paper.

II. PILOT PROJECT OF INTERNET CONNECTION AND INFRASTRUCTURES IN RURAL AREAS

A. Internet Kiosks and Connection

The use of VSAT for connectivity of rural areas has been used as an alternative technology for telephone connection. VSAT technology uses satellites for access to connect various remote areas easily because the problem of distance as well as difficult and expensive wiring on rough rural surface areas would no longer a constraint. However, access to the VSAT technology is still relatively expensive for wide bandwidth. As a result VSAT technology will only survive for data communications at low speed, which is currently widely used to interconnect the ATM network by the Bank.

The use of backhaul connection using WiFi technology for point to point application has already practiced widely by many operators. The use of this technology for data access is already quite good in a limited range, but become expensive for long and scattered area over vast rural environments. Another drawback of this technology is because this technology uses no license or permit to operate, then at one time it will quickly reach the saturation level after users began to grow.

Another alternative of backhaul technology using broadband access using DSL, which has also commercially available under the brand name of SPEEDY services provided by PT. Telkom in some remote areas. Technology can provide better connectivity to the internet service. However, growth is very slow, especially in rural areas because the cost is very high. Therefore, in the short term, technology selection based on availability and affordability in rural areas.

In this project, we adopt a combination of DSL using SPEEDY, cellular wireless modems, and point-to-point WiFi backbone technologies. DSL/SPEEDY technology was used for regions that already have telephone lines, cellular access technology using wireless modem for regions that have no telephone lines but have been covered by public cellular networks, and WiFi backbone technology was applied in regions that neither have telephone lines nor celluler networks coverage. Garut Regency government has launched a free internet program to 42 districts in Garut started in 2011 using the scheme of Universal Service Obligation (USO) program. This program also provides free internet connections for 48 months, for those using services at the District Information Service Center (internet kiosk) placed at the community district office. At the end of year 2012, 21 of the total of 42 districts have been facilitated by the Internet kiosk equipped with 10-12 PC connected to a DSL telephone line or a cellular modem for Internet connection. To provide skills for operators of internet kiosks, information technology and management training has been carried out. Every district sends two delegates representing each district as local partner to join in the training together. The training provides the background knowledge and skills to local partners, so that they would

understand that the Information and Communication Technology (ICT) in the era of globalization plays an important role as one of the pillars of development.

B. Access Tehnology

Access technology in rural areas is a challenge that needs to be addressed. Access solution using cable network is almost impossible because it would require prohibitively very high costs. The coverage of cellular mobile operators in remote areas is still limited because of the operator reluctance to deploy services in remote areas using standard technology with medium to high base stations capacity that requires a long enough period of time for investment return. Mobile data technologies such as GPRS, EDGE, WCDMA, HSPA, or a combination thereof, which is already commercially available in rural areas is considered as one alternative for rural internet connectivity. GPRS technology is quite interesting for data access in rural areas so that many operators in rural areas operate with 2G and 2.5G technologies. This is mainly due to the lack of 3G licenses and the reluctance to invest newer technologies in remote areas. EDGE, WCDMA and HSDPA technologies are still operating in dense residential areas because of the potential revenue for operators is still concentrated in the cities.

Another access technology that would be more suitable for rural environment at this time is to use the open BTS technology. Open BTS technology is a small base stations to cover certain areas not yet covered by the public operators. However there is no regulatory basis available of the use for frequency band to operate the open BTS. The limitations of the spectrum, therefore remains an obstacle for the presence time. This situation also detered new operators who want to take part in the telecommunications industry, without necessitating the new spectrum, called Mobile Virtual Network Operator (MVNO) to operate in Indonesia. If the regulatory can support, we can propose a new scheme that allows the operators in rural areas to provide services as franchise operator under the cooperation between the existing operators (in order to interconnect services) and the new franchise operators (specifically to serve rural areas) in the use of frequency spectrum that already licensed to the existing operators.

Access technologies can also use WiFi or WiMax technologies that already practiced by many users. The use of this technologies for data access is already good in a limited range, but to use them for voice access they require communication protocol modifications, such as using VoIP that require modifications to the phone being used. To implenent the access network deployment in rural areas, in addition to ree internet kiosk and connection, several districts in Garut Regency have been deployed with 149 new telephone line connection to serve for those who have not been touched by fixed telephone lines or cellular signals. The program was implemented to reduce the gap of access to information for people living in rural and remote areas.

III. STRATEGY TO SPEED UP INTERNET PENETRATION

A. Strategy on the Policy

This study was conducted in collaboration with local government of Garut Regency, under the scheeme project grant funded by the World Bank to deploy internet kiosks for rural areas, called the Community Access Point (CAP) to increase internet penetration. This program is to evaluate, whether internet penetration can boost the economic potential in rural areas, or the GDP that boost the internet penetration. In this study, the local governments take measures to use the penetration of internet as a driving force of the increase in GDP, i.e the economic potential of the region.

The strategic objective in the use of ICT is focussed on efficiency and effectiveness of public services, a paradigm shift of bureaucracy and encouragement of social transformation correctly. The expected results is that it will eventually overcome the digital divide, in an effort to alleviate poverty and improve people's welfare. In addition, the program of internet kiosks deployment in Garut Regency can be used to promote a variety of potential economic, social and cultural development in the future.

Based on these efforts, it is believed that the necessary increase of internet penetration indicates the government's commitment in the short term. While in the long term it is intended to promote the integration of isolated groups and bring traditional society to an information society. In addition , the government should develop online services to foster the effective use of the internet through education and skills training. Adoption of the internet can help rural areas get a competitive advantage toward achieving economic development . It also can increase social interaction between users and get them to engage in digital commerce as a viable method for developing a new economy.

B. Strategy on Techno-Economy

To support the government policy, which is necessary for the early stage, is the government commitment to allocate the initial cost as wel as an integrated government policy. This has been implemented through the government sponsored internet kiosk program described above. Techno-economic analysis for the connectivity needs to be carefully evaluated to be effective and sustainable. VSAT technology has been used for many years for long distance backhaul connection in this country, but for affordable internet access needs to be combined with other more affordable technologies.

Broadband internet access via fixed access using DSL technology is still very limited, although it has been available commercially in several districts under the brand name of SPEEDY services provided by PT. Telkom. Therefore, in the short term, technology selection should be based on the availability and affordability of the area. Additional provision in the telephone access connection internet kiosk program is also intended to increase connectivity of backhaul connections to several districts that have not been connected.

C. Model of Affordabel Internet Kiosk

Despite the initial and short term government sponsored internet kiosk program, for the long term we need to evaluate the market penetration of the Internet that would be commercially viable. When GDP and other economic factors have been able to take advantage of their internet connection, the results of previous studies show that internet penetration will drive GDP per capita. That is, in the long term, the internet penetration willcontinue to grow in rural areas without government supports. To evaluate that, we need to look at the following business model. We assume a medium-size kiosk internet terminal with 10 PCs, 1 printer, 1 scanner and connected via fixed data services or cellular data services using cellular modems. Capital investment for this model can be in the range of below IDR 50 million. Operational costs would consist of the kiosk rental fee of IDR 1 million per month, electricity consumption for this assumption may need about 4000 watts including air conditioning and lighting, which cost approximately IDR. 0.5 million per month. Cost of Internet connection using DSL/Speedy or cellular modem for maximum data rate of 2 Mbps would approximate IDR.0.5 million per month. Salary for kiosk operator assuming 1 person is IDR. 3 million every month. With this assumption the total monthly cost of operation will be around IDR. 5 million. Furthermore, revenue assumptionsfor a kiosk with each user pays IDR. 4,000 per hour of use of the PC, the operating time of 8 hours per day on average (although the stall is open 24 hours a day), and 70 % utilisation of kiosk occupancy and usage, generating a monthly income of IDR. 6.72 million. Using a simple calculation of the business plan, the payback period would be less than 3 years, which is very feasible to run.

IV. IMPACT OF INTERNET PENETRATION

A. Impact on GDP per Capita

This project can help solve the problem in remote areas to accelerate the penetration of the internet (information technology) to areas that are still poor but have high economic potential. This study indicate that the GDP per capita has a correlation with the internet penetration rate. We can see the GPD per capita for Garut Regency for the last 5 years from 2009 to 2013 in Fig.1
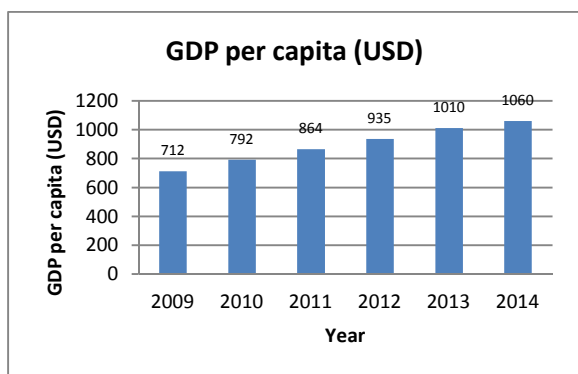

Fig. 1 Effect of Internet penetration on GDP per capita

Fig. 1 shows the average GDP for 21 district areas in Garut Regency from 2009 to 2014. It indicates that with the increasing penetration of internet in the area, the GDP per capita also increases. Data for each district shows different rates of GDP, and we also find that the area with higher internet penetration has higher GDP per capita.

B. Growth of Internet Kiosk

The driving factor of this project has encouraged the society. Villagers had no problem with the use of internet-related devices, such as PCs, modems, etc. DSL technology that has introduced the use of shared data and voice simultaneously using the same phone line, do not pose a problem for them. Figure 2 shows the effect of the penetration of personal computers (PCs) to the skills of the communities, which in turn encourages the penetration rate of the Internet kiosks.
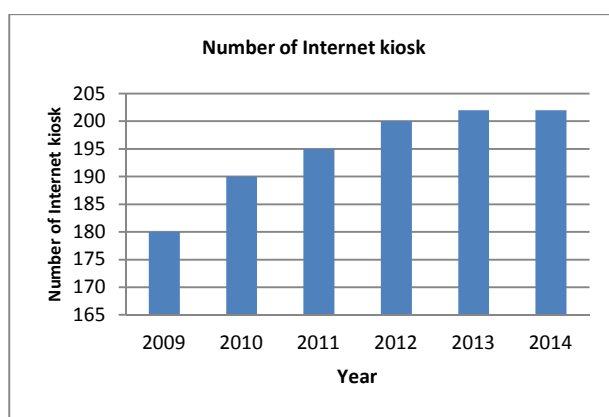

Fig. 2 Effect on internet kiosks growth

The level of motivation of new Internet users in rural areas will increase significantly with access to affordable and relevant content and technology support to increase economic opportunities and quality of life of their users. The Internet has played an important role not only in economic development through the sharing of knowledge, but also in providing equal and universal access to information. Many people consider the internet as a primary source of information to help make better decisions and share knowledge. In order to build the information society in countries where the Internet is not widely accessible, access to information resources should be increased.

C. Competition and Tarrif

Since 2002, the mobile sector in Indonesia has resulted in revenues that exceed fixed lines sector revenue. The dominance of the mobile sector is expected to rise further as voice conversations rates down and use the phone for data continues to increase. Currently, Indonesia has 11 mobile network operators and two operators of fixed phone line, which is also dominated by the PT. Telkom as the incumbent operator. Indonesian telecommunications market is very much alive and growing has had more than 180 million mobile

subscribers by the end of 2011 (subscription penetration is 70%) and approximately 10.7 million fixed-line subscribers are connected (subscription penetration of 5%). The driving forces on the growth of the market liberalization have been carried out by the regulator. The existence of 11 mobile network operators since 2002 has been able to lower telecommunications tariffs. This has resulted in a wave of mobile services, which in turn builds up mobile penetration continues.

Fixed telephone sector in Indonesia is now evolving toward broadband data services (broadband). Penetration of Public Switched Telephone Network (PSTN) is relatively constant at 5-7% until year 2011 and become stagnant after year 2012 as shown in Fig.3.
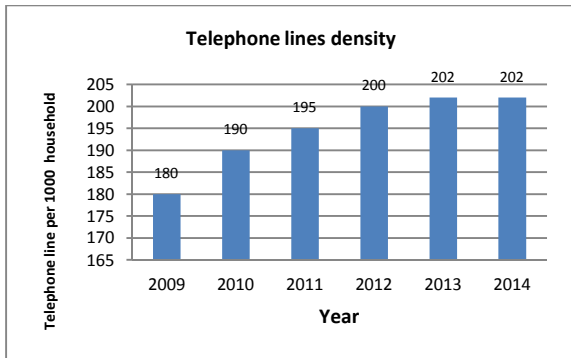

Fig. 3 Telephone density in Garut Regency

However, the penetration of fixed broadband connections is expected to increase, partly due to the inclusion of fixed broadband access. Digital Subscriber Line revenue potential offer (DSL) connections that rely on already installed will continue to increase, since PT. Telkom continues to offer data connections via a fixed connection is more reliable and faster, which is called "SPEEDY" as an attempt to maintain the fixed-line subscriptions.

V. CONCLUSION

This study identified several macro-techno-economic factors that affect the level of Internet penetration in rural areas of Indonesia. Garut has been as a case study, because it can be considered to represent a rural area in general with a fairly high population density in Indonesia. Arrowroot district is also one of the district that receives a grant project of the World Bank's Community Access Point (CAP) under the Rural internet kiosk project through the Ministry of Communications and Information Technology to accelerate the penetration of the Internet into rural and remote areas in Indonesia.

For the short term, government intervention to speed up the rate of penetration of the Internet into rural areas is still needed. However, in the long term, the model village cafe business plan or cafe districts shows can provide a rapid return on investment and costs affordable for small businesses. Because of cost efficiency is a primary factor for the development of rural ICT implementation, the analysis in this study shows that the technology selection should be based on the availability and affordability. Alternative technologies are fixed line or fixed data for areas already covered by fixed telephone connections, and using mobile data technology for areas already covered by the system pants. Wireless broadband technologies, such as WiFi and WiMax may be used as alternative access technology and backhaul technologies.

For the long term, rural communities can benefit from the low cost of internet access, because the technology is constantly evolving, and the impact of Internet penetration has been able to increase the purchasing power of people, the Internet penetration will grow just as has occurred in urban areas/cities. To achieve that, the village internet kiosks that at the moment is driven by government intervention needs to be well managed to generate growth business model towards independence. Management of village internet kiosks not only to meet the needs of internet connection, but also the associated components, such as the selection of technology, user management, skills training, and dissemination to the public. Obstacles that may occur need to be assessed carefuly, and the measures taken should be comprehensive and integrated.

Further research is needed to see the impact of the internet kiosks on socio-economic and socio-cultural for the countryside society. Operational local partners in running internet kiosks need to be monitored on how they obtain maximum benefits, as well as to avoid negative impacts that may occur.

REFERENCES

[1]. Leroux, C.G., Hangjung Zo, Jae Jeung Rho, "Factor Affecting Internet Adoption in Latin America," in Proc. Of Third International Conference on Convergence and Hybrid Information Technology, vol. 2, 2008. ICCIT '08, pp. 947-951.

[2]. Kilenga, A.I., Mneney, S.H. 2002, "Flexible network for Internet access in rural areas," The 6th IEEE Africon Conference in Africa, 2002. Volume: 1, pp. 211 – 216

[3]. K. Toyama, "Review of Research on Rural PC Kiosks," http://research.microsoft.com/research/tem/kiosks/, 2007. Bank Dunia. 2005. *Sistem Informasi Pedesaan*. Bank Dunia, Unit Sektor Pengembangan Pedesaan dan Sumberdaya Alam. Wilayah Asia dan Pasifik.

[4]. Kim, C., "A Study of Internet Penetration Percents of Africa Using Digital Divide Models," in Proc. of Technology Management for Global Economic Growth (PICMET), 2010, pp. 1-11

[5]. Kementerian Telekomunikasi dan Informatika RI. 2010. Penyediaan Infrastruktur Telekomunikasi dan Informatika - Kewajiban Pelayanan Universal (KPU)/ Universal Service Obligation (USO). Balai Penyedia dan Pengelola Pembiayaan Telekomunikasi dan Informatika, Kementerian Telekomunikasi dan Informatika RI.

[6]. A. Seth, D. Kroeker, M. Zaharia, S. Guo, and S. Keshav, "Low-cost communication for rural internet kiosks using mechanical backhaul," in Proc. ACM MOBICOM, 2006.

[7]. U. Ismail, and S. Keshav, "Design and Implementation of the KioskNet System," University of Waterloo Technical Report, CS200740, 2007.

[8]. L. Press, "The Internet and Interactive Television", Communications of the ACM, Vol. 36, No. 12, December 1993, pp. 19-23.

[9]. A. Pentland, R. Fletcher, and A. Hasson, "Daknet: rethinking connectivity in developing nations," Computer, vol. 37, no. 1, pp. 78–83, 2004. [Online]. Available: http://ieeexplore.ieee.org/xpls/abs all. jsp?arnumber=1260729

[10]. Glennan, T. K., and A. Melmed, "Fostering the Use of Educational Technology: Elements of a National Strategy," National Book Network, Lanham, MD, 1996.

[11]. Beilock, Richard and Daniela V Dimitrova, "An Exploratory Model of Inter-Country Internet Diffusion", *Telecommunication and Informatics*, vol. 19, 117-137, 2003.A. Seth, M. Zaharia, S. Keshav, and S. Bhattacharyya, "A Policy - Oriented Architecture for Opportunistic Communication on Multiple Wireless Networks," http://tinyurl.com/2j9ewt, 2006.

[12]. Kim, Chaiho, "Internet Penetration Rates of Countries by Geographical Regions Some Examples of Regional Digital Divides", *AMCIS 2009 Proceedings.* Paper 583, http://aisel.aisnet.org/amcis2009/583, 2009.

[13]. S. Ur Rahman, U. Hengartner, U. Ismail, and S. Keshav, "Securing kiosknet: A systems approach," University of Waterloo Technical Report, CS200743, 2007.

[14]. M. Tan, and T. S. H. Teo, "Factors Influencing the Adoption of Internet Banking", Journal of the AIS, Vol. 1, No. 1es, March 2000.

[15]. Chinn, M. D. and R. W Fairlie, "The Determinants of the Global Digital Divide: A Cross-Country Analysis Computer and Internet Penetration", Economic Growth Center, Yale University. Center Discussion Paper881, March 2004.

[16]. Y. Otero, M. Herrera, W. Maehr, and M. I. Castillo, "Mobile Internet User Experience in Latin America", Workshop on Mobile Internet User Experience, Singapore, September 9th, 2007.

10dB Planar Directional Coupler on FR4 Substrate for Automatic Gain Control

Arie Setiawan, Taufiqqurrachman, Y.N. Wijayanto
Research Center for Electronics and Telecommunication
Indonesian Institute of Sciences (LIPI)
Bandung, Indonesia
arie.setiawan@lipi.go.id

Abstract—**This paper presents 10dB planar directional coupler on FR4 substrate for Automatic Gain Control (AGC) system. The proposed design uses single section coupled line method that simulated using simulation software ADS 2011.10 and fabricated on FR4 substrate. The proposed design exhibits a return loss of -22dB, isolation of -26dB, a coupling level accuracy of 9.4dB and insertion loss of -0.7dB at 600MHz. The proposed design can be applied to translate the maximum Variable Gain Amplifier (VGA) output power level to a value lower than the highest detectable log detector power level in AGC system.**

Keywords—directional coupler; microstrip; AGC

I. INTRODUCTION

The HMC992LP5E is a complete high performance Automatic Gain Controller (AGC) solution, it can be configure as an AGC amplifier by using Variable Gain Amplifier (VGA) core and the built in log detector. In AGC amplifier configuration, the input signal is amplified by the HMC992LP5E's VGA. The output of the HMC992LP5E's VGA core is fed back to the input of the HMC992LP5E's log detector through an external coupler or attenuator to drop the maximum and minimum output level of the HMC992LP5E's VGA to within the dynamic range of the HMC992LP5E's log detector [1].

Directional couplers are one of most important passive microwave devices with a wide range of application [2], which is used for power meters, source leveling, automatic gain control loops, and test system. It's basic function to sample the forwards and reverse travelling waves through transmission line or waveguide. The common use of this coupler is to measure the power level of a transmitted or received signal [3]. Commonly directional coupler made in microstrip form such a coupled transmission line. Directional couplers with parallel microstrip coupled transmission line are widely utilized for various RF and microwave applications because they can be easily incorporated into and implemented with others circuits [4]. They are simple in structure, easy to analyze and design and can be implemented in many different transmission line media. Smaller structure, easier processing and manufacturing, low cost and portability, make its application to power measurement system more convenient [5]. However, the quarter wavelength size is sometimes too long for practical purposes such as low frequency applications and it lacks the design flexibility in that the design parameter is uniquely determined by the required coupling level [6]. Thus, size reduction is becoming major design considerations for practical applications [7].

In this paper, a structure of planar directional coupler for automatic gain control application is presented, which has coupling level accuracy 10dB at 600MHz, 10dB coupler ratio was chosen to translate the maximum VGA output power level to a value lower than the highest detectable log detector power level. Design uses single section coupler method which derived in approach analysis through the even-odd analysis. The presented structure was achieved by optimize the physical dimension length of the patch and gap between the two patch. The designed and fabricated coupler were used to eliminate any limitations that can arise due to highest detectable log detector in AGC system.

II. DESIGN METHODOLOGY

The coupler was designed using the coupled line method. When two unshielded transmission line are in close proximity, power can be coupled from one line to the other due to the interaction of the electromagnetic fields. Such lines are referred to as *coupled transmission lines*, and they usually consist of three conductors in close proximity, although more conductors can be used [8].

Basic configuration of directional coupler shown in Fig. 1, directional couplers usually have 4 ports: input, through/direct, coupled and isolation. Ideally power put into port 1 (input) only appears port 2 (through) and port 4 (coupled), no power on port 3 (isolation), but in realization there are still a leak power on the port 3 [9]. The characteristics from a directional coupler can be describe by its coupling factor, directivity, reflection loss, and the impedance matching of port. Important parameter in designing the coupler is patch width (W), gap or distance between the two patches (S), length of the patch (L), and other parameter which affect are height (H) and Thick (T) used substrate [10].
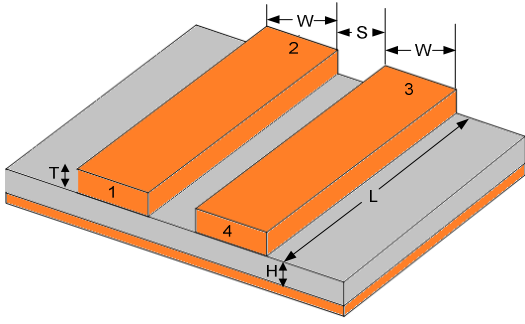
Fig. 1. A directional coupler model.

In [8] coupler design has two approach analysis that is odd mode (Zo_o) and even mode (Zo_e), for the odd and even mode characteristics impedances can be found using the equation (1) and (2),

$$Zo_o = Zo\sqrt{\frac{1-C}{1+C}} \tag{1}$$

$$Zo_e = Zo\sqrt{\frac{1+C}{1-C}} \tag{2}$$

Where Z0 are the normal impedance (50 Ohm) and for the coupling factor is define as :

$$C = 10^{\frac{coupling\ value(dB)}{20}} \tag{3}$$

and for the directivity is define as :

$$Directivity\ (D) = Isolation\text{-}Coupling \tag{4}$$

In this research a directional coupler the FR4 substrate (ε_r = 4.6, h = 1.5mm) is used in simulation and construction of the design. By using software ADS 2011.10, then design of directional coupled line method produced symmetrical dimension. By using parameter 1, 2, and 3 with LineCalc tools, the physical dimension of microstrip coupled line (MCLIN) and microstrip line for the proposed design was presented in Table I.

III.   SIMULATION & MEASUREMENT RESULT

Result by simulation and measurement of the design directional coupler are described in this section. By using ADS 2011.10, the result of simulation shows that s-parameter is close to design. Due to size from calculation, the physical dimension was optimized to get proportional size. The proposed design schematic of directional coupler is shown in Fig. 2. The values of parameters in the microstrip coupled line which were designed are W = 2.25462 mm, S = 0.15 mm, L= 50mm, and for a 50ohm impedance. The 50ohm impedance consist of one structure MLIN (W = 2.25462mm, L = 2mm) and MCurve (W = 2.25462mm, Angle = 90, and Radius = 1.1273mm). For this design, we must consider the width or length of the microstrip line is ease to fabricate. Fig. 3 shows the layout of optimized directional coupler.

TABLE I.   THE PHYSICAL DIMENSION OF DIRECTIONAL COUPLER

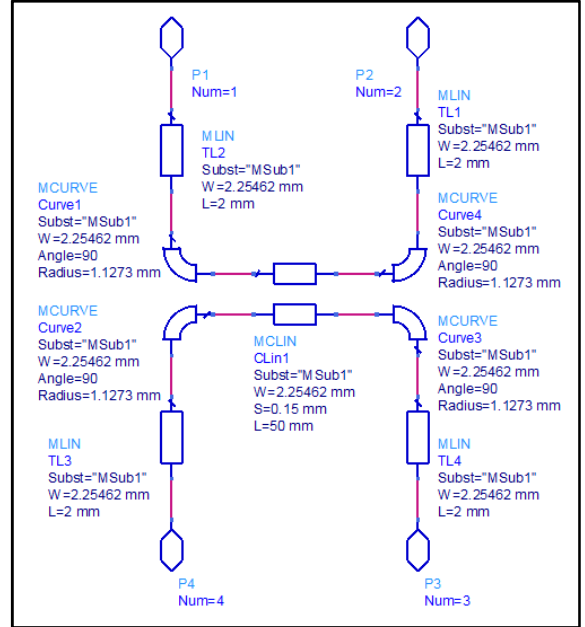| Impedance Value (Ohm)	W (mm)	L (mm)	S (mm)
Z0 = 50	2.730	67.424	-
Z0o = 36.047 Z0e = 69.334	2.255	69.376	0.335

Fig. 2. The proposed schematic design of directional coupler.

Fig. 3. The proposed design layout of directional coupler.

The results of simulation which have been done using ADS 2011.10 are shown below. Fig. 4 represent the simulation result of the proposed design that shows in S-parameter graph. The return loss of the input port denoted by S(1,1) achieve -27.224dB and its indicates that only 0.19% reflected power, its means the device has a good Voltage Standing Wave Ratio (VSWR) about 1.09 and reflection coefficient 0.043. For both ideal – forward and backward – couplers the reflection coefficients are zero[11]. The proposed design has only attenuation of 0.590dB that denoted by S(1,2). The isolation port showed by S(1,3) of this design attains -25.205dB and The S(1,4) represents coefficient coupling from this design that achieves -10.045dB. A directional device should, therefore, have a directivity of at least 15dB to make it suitable for forward power measurements [12], because directivity enhancement becomes extremely difficult especially for weak coupling levels [13], by using (4), the value of directivity (D) is 15.16dB.
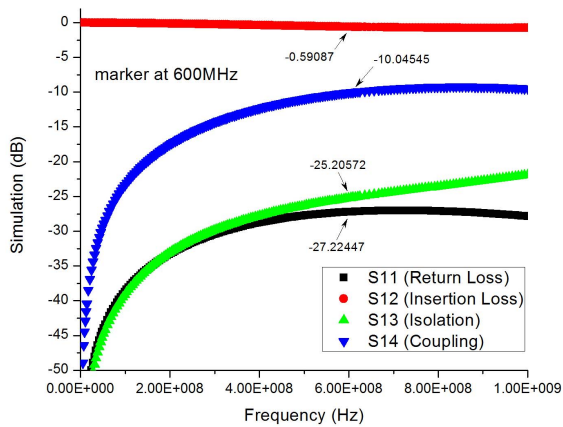
Fig. 4.   Simulation Parameter result of directional coupler.

The simulation result shows that the proposed directional coupler has good isolation effect and directivity. For the coupler construction, FR4 substrate using the SMA connector was used. The values of $\varepsilon_r = 4.6$ and losses tangent (tan δ) = 0.01. The thickness of the substrate is 1.5mm and the thickness of copper cladding is 35μm. The photograph of the constructed directional coupler is shown in Fig. 5. The constructed directional coupler have dimension about 62x9.5mm.

The measurement results were taken using an Advantest vector network analyzer. For the measurement, a termination 50ohm was added at both open ports. Performance of the directional coupled that proposed can be analyzed from the value of return loss for reflect port (S11), insertion loss of direct/through port (S12), coupled port (S14) and isolation port (S13). Based on Fig. 6a, results of the proposed design presenting a good results where the return loss for input port and the isolation are -22.462dB and -26.045dB and also coupling is -9.448dB at the center frequency 600MHz. The measurement result of coupling port are not accurate -10dB because the insertion loss at direct port (S12) value are -0.749dB which it should be around 0dB [9]. The value are not different significantly which is expected from the design, as shown in Fig. 6b, the measured coupling different about 0.597dB from the simulation. The difference between the simulation result and measurement result are due to problem on soldering at the SMA connector and uncertainty the value of the substrate permittivity that used in this design. Overall measured performance shows good agreement with simulation result.
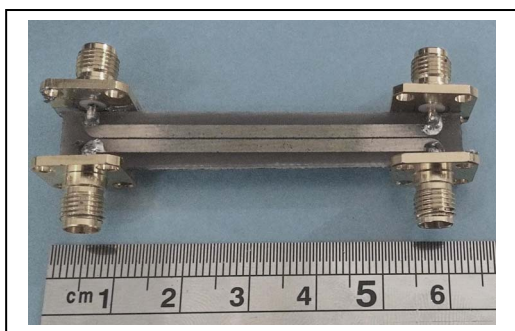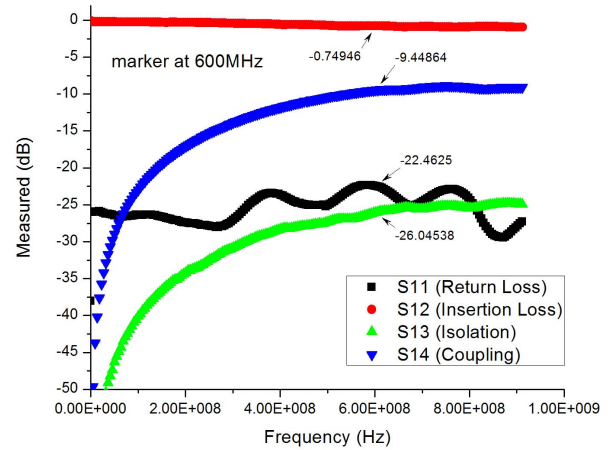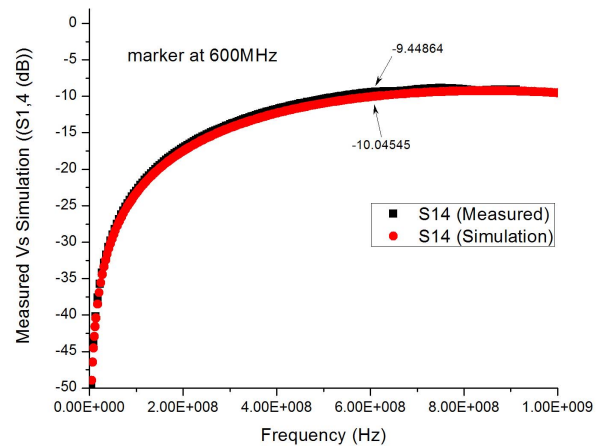

Fig. 5.   The photograph of the constructed directional coupler.

(a)

(c)

Fig. 6.   Measurement result of the proposed design. (a) Measured result parameter. (b) Comparison coupling measured and simulation result.

IV.   CONCLUSION

The planar directional coupler with 10dB coupling for center frequency 600MHz has been designed, simulated and fabricated. The measurement and simulation result show a good coupling performance, although there are little difference between the simulation and measurement results. The planar directional coupler can be applied to translate the maximum VGA output power level to a value lower than the highest detectable log detector power level in AGC system.

REFERENCES

[1]   Hittite microwave. Datasheet of HMC992LP5E. 2011

[2]   Ibrahim KM, El-Rabaie E-SM, Shalaby A-AT, Elkorany AS. Enhancement The Performance Of Coupled Line Couplers Based On Both Crlh- And High-Tc Superconducting Microstrip Lines. *Circuits Syst An Int J*. 2014;1(3):43-53.

[3]   Matzner H, Levy S, Ackerman D. Experiment 5 — Coupler Design . 2009;(June).

[4]   Kim CS, Kim YT, Song SH, et al. A design of microstrip directional coupler for high directivity and tight coupling. *2001 31st Eur Microw Conf EuMC 2001*. 2001:1-4. doi:10.1109/EUMA.2001.339173.

[5]   Chen ZL, Tong L, Tian Y, Gao B. Directional Coupler Using Multi-Stage Coupled Structure Theory. *Prog Electromagn Res C.* 2013;45(October):113-123.

[6]   Park M-J, Lee B. Analysis and Design of Three Section Coupled Line Couplers. *IEICE Trans Electron*. 2005;E88-C(2):279-281. doi:10.1093/ietele/E88-C.2.279.

[7]   Sung YJ, Ahn CS, Kim YS. Size Reduction and Harmonic Suppression of Rat-Race Hybrid Coupler Using Defected Ground Structure. *IEEE Microw Wirel Components Lett*. 2004;14(1):7-9. doi:10.1109/LMWC.2003.821499.

[8]   Pozar D. *Microwave Engineering.*; 2005.

[9]   Hardiati S, Arisesa H. Directional Coupler Frekuensi Radio Menggunakan Dua Jalur Asimetris Mikrostrip untuk Sistem Radar X - Band. *J Elektron dan Telekomun*. 2014;No.2/Vol.1.

[10]   Arisesa H, Wahab M, Hardiati S. Desain dan Simulasi 20dB Directional Coupler Untuk Aplikasi Radar. *Proceeding 5th IMEN-LIPI Jt Semin Microelectron Devices, Syst Instrumentations*. 2011:68-71.

[11]   Jahn S. A Tutorial 10dB Directional Coupler Design. 2005.

[12]   Jorgesen D, Marki C. Directivity and VSWR Measurements. 2012.

[13]   Lee S, Lee Y. A design method for microstrip directional couplers loaded with shunt inductors for directivity enhancement. *IEEE Trans Microw Theory Tech*. 2010; 58(4): 994-1002.doi: 10.1109/ TMTT.2010.2042544.

Performance Evaluation of Inter-cell Interference of LTE-A System Using Carrier Aggregation and CoMP Techniques

Desiana Ginting
School of Electrical Engineering
Telkom University
Indonesia
d3514n4_ginting@yahoo.com

Arfianto Fahmi
School of Electrical Engineering
Telkom University
Indonesia
arfianto.fahmi@gmail.com

Abstract—**Long Term Evolution Advanced (LTE-A) is a promising technology to achieve peak data rate up to 1Gbit/s in downlink and 500Mbit/s in uplink. As adjacent cells use the same frequency, interference between adjacent cells may degrade the bit rate at cell edges. Inter-Cell Interference Coordination based on carrier aggregation as well as Coordinated Multipoint (CoMP) transmission and reception is seen as promising technology for alleviating this degradation and improving the bit rate at cell edges.**

ICI can be mitigated with the help of different arrangements of frequency bands allocations and possibly with different transmission power distinguishing between the cell centre users and cell edge users.

In this paper different inter-cell interference mitigation and coordination are analyzed with different frequency allocation schemes, fractional frequency reuse, transmission power, and also different radio resource scheduling algorithms are evaluated to enhance cell edge performance, bandwidth efficiency and throughput.

Performance is evaluated in terms of SINR versus femtocell users, separation on distance from interfering cell. Performance is compared between conventional technique, CA technique and combined CA and CoMP.

Keywords— ICIC; LTE-A; CoMP; Carrier Aggregation

I. INTRODUCTION

Technology is moving so fast. From first generation (1G) to fourth generation (4G), from analogue to digital. Long Term Evolution (LTE) is the name given to a 3GPP project to evolve UTRAN to meet the needs of future broadband cellular communications.

With the standards definitions now available for LTE, the Long Term Evolution of the 3G services, eyes are now turning towards the next development, that of the truly 4G technology named IMT Advanced. The new technology being developed under the auspices of 3GPP to meet these requirements is often termed LTE Advanced.

3GPP's targets for LTE-Advanced were set independently from the IMT-Advanced requirements; it can be seen that some of the 3GPP targets exceed the IMT-Advanced requirements, such as the peak spectral efficiency and the control plane latency targets [1] [3].

These are many of the development aims for LTE Advanced. Their actual figures and the actual implementation of them will need to be worked out during the specification stage of the system.

LTE CoMP or Coordinated Multipoint is a facility that is

being developed for LTE Advanced many of the facilities are still under development and may change as the standards define the different elements of CoMP more specifically.

LTE Coordinated Multipoint is essentially a range of different techniques that enable the dynamic coordination of transmission and reception over a variety of different base stations. The aim is to improve overall quality for the user as well as improving the utilisation of the network.

Essentially, LTE Advanced CoMP turns the inter-cell interference, ICI, into useful signal, especially at the cell borders where performance may be degraded.

Over the years the importance of inter-cell interference, ICI has been recognized, and various techniques used from the days of GSM to mitigate its effects. Here interference averaging techniques such as frequency hopping were utilized. However, as technology has advanced, much tighter and more effective methods of combating and utilizing the interference have gained support.

The rest of the paper is organized as follow: Section 2 discusses related work on ICI mitigation schemes in CoMP and Carrier Aggregation (CA). Section 3 presents inter-cell interference (ICI) problem formulation. Section 4 shows simulation result for ICI problem mentioned in Section 3 and 4. Finally, the conclusion is drawn in Section 5.

II. RELATED WORK

The goal of ICIC scheme is to apply certain restrictions on the resources used in different cells in a co-ordinated way. From literature, we identified some ICIC schemes recently used to mitigate ICI in CoMP systems [3], [4], [5], [7], [8], [9] and those schemes classified into three main categories in [2].

2.1 Coordinated Multipoint (CoMP)

Coordinated Multi-Point (CoMP) transmission/reception, also known as Cooperative MIMO is a main element on the LTE roadmap beyond Release 9. CoMP is considered by 3GPP as a tool to improve coverage, cell-edge throughput, and system efficiency. It was introduced in the LTE-A technology to relax performance limitations. Many of the facilities are still under development and may change as the standards define the different elements of CoMP more specifically.

This technology is essentially a range of different techniques that enable the dynamic coordination of transmission and reception over a variety of different base stations. The aim is to improve the overall quality for the user as well as improve the utilization of the network. Essentially,

LTE Advanced CoMP turns the inter-cell interference (ICI) into useful signal, especially at the borders where performance may be degraded

The main purpose of CoMP is solving the interference problem at the edge area of cells. The interference is decreased on edge users of cells by jointly scheduling several cells with rather strong edge interference, or by joint transmission, so that the reception power and service experience of a cell's edge users can be improved. CoMP can be applied both in the uplink and downlink [2], [3]. The concept of LTE Advanced CoMP can be seen in Figure 2.1
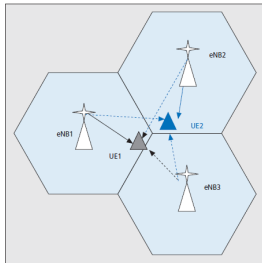

Figure 2.1: A CoMP framework for DL transmission where eNB1, eNB2, and eNB3 can coordinate and create a multipoint transmission to UE1 and UE2 [1].

The main idea of CoMP is when a UE is in the cell edge region, it may be able to receive signals from multiple cell sites and the UE's transmission may be received at multiple cell sites regardless of the system load. Given that, if the signaling transmitted from the multiple cell sites is coordinated, the DL performance can be increased significantly. This coordination can be simple as in the techniques that focus on interference avoidance or more complex as in the case where the same data is transmitted from multiple cell sites. For the UL, since the signal can be received by multiple cell sites, if the scheduling is coordinated from the different cell sites, the system can take advantage of this multiple reception to significantly improve the link performance.

In figure 2.1 the framework is depicted, where three eNBs may coordinate to create a multipoint transmission to UE1 which is served by eNB1 and UE2 which is served by eNB2. The objective of CoMP is to reduce interference for a UE set in the network that is close to multiple eNBs and therefore experiences an interference-limited environment. The interference to these UE sets may be reduced and can be predicted if there is some coordination between the interfering eNBs and the serving eNB.

2.2   Carrier Aggregation

LTE-Advanced had the target figures for data throughput in the downlink is 1 Gbps and 500 Mbps in the uplink. In order to achieve up to 1 Gbps peak data rate in the fourth generation (4G) mobile systems, carrier aggregation technology is introduced by the 3rd generation partnership project 3GPP to support wider transmission bandwidths (e.g., up to 100 MHz) in its new LTE-A standards [10]. By using carrier aggregation technology, it is possible to schedule a user on continuous or non-continuous component carriers (CCs). Carrier aggregation is used in frequency domain multiplexing inter-cell interference coordination scheme which is one of the most important features of LTE-A. This scheme allows LTE-A user to connect to several carriers at the same time. It also allows resource allocation across the carriers as well as fast switching between carriers without time consuming handovers, which means a node can schedule its control and data information on separate carriers. Main principle in HetNet scenario is to

partition the available spectrum into two separate component carriers and assign the primary component carriers (PCC) to different network layers as shown in figure 2.2.

Figure 2.2: Illustration of Carrier Aggregation based ICIC [6].

PCC is the cell that provides the control information to the UEs, by assigning this different frequencies interference on control channels between network layer can avoided. By means of so called cross carrier scheduling each network layer can still schedule UEs on other CCs called secondary component carriers (SCC) [6].

In the figure 2.2, f1 and f2 are PCC and SCC separately where 5 sub-frames are shown in each carrier. These carrier's components are used by both Macro and Femto layer. The sub-frames contain PDCCH, PCFICH, and PHICH in the beginning the blue part which is control signal and green part is data signal.

As shown in figure 2.2 above Macro layer can schedule its control signal on f1 but can still schedule its users on both f1 and f2, so by scheduling control and data information for both Macro Layer and Femto layer on different component carriers, interference on control and data can be avoided.

III.   ANALYSIS AND MODELING

3.1   Path Loss Model

In order to estimate the SINR, first we need to calculate the path loss between a macro eNB and an UE that are in the same apartment stripe and a femto eNB and an UE. The path loss for the first case and for a macro user roaming outdoor in the urban area, can be expressed as [11]:

$$PL \ (dB) = 15.3 + 37.6 \log_{10}R \qquad (3.1)$$

Whereas, for the case of an indoor macro user the path loss is given by:

$$PL \ (dB) = 15.3 + 37.6 \log_{10}R + L_{ow} \qquad (3.2)$$

Where R is the distance between the transmitter (Tx) and the receiver (Rx) in meters and L_{ow} is the penetration loss of an outdoor wall. The path loss between a femto base station and an UE is calculated by the following equation [11]:

$$PL \ (dB) = 38.46 + 20 \log_{10}R + 0.7d_{2D}, \text{ indoor} + q*L_{iw} + 18.3n^{((n+2)/(n+1)-0.46)} \qquad (3.3)$$

Where, n is the number of penetrated loors, q is the number of walls separating the apartments between femto BS and the UE, and L_{iw} is the penetration loss of the wall separating apartments. Also the term $0,7d_{2D}$, indoor takes account of penetration loss due to walls inside an apartment and is expressed in m.

Finally, the case of an outdoor femto user associated to an indoor femto eNB. In this case the outdoor wall loss is also considered as [11]:

$$PL(dB) = \max(15.3 + 37.6 \log_{10}R, 38.46 + 20\log_{10}R) + 0,7d_{2D}, \text{ indoor} + q*L_{iw} + L_{ow} + 18.3n^{((n+2)/(n+1) - 0,46)} \qquad (3.4)$$

3.2   SINR Estimation

The estimation of the received SINR of a macro user m on subcarrier k, when the macro user is interfered from

neighboring macrocells an all the adjacent femtocells, can be expressed as [12]:

$$SINR_{m,k} = \frac{P_{M,k}G_{m,M,k}}{N_o\Delta f + \sum_{M'}P_{M',k}G_{m,M',k} + \sum_{F}P_{F,k}G_{m,F,k}}$$ (3.5)

where $P_{M,k}$ and $P_{M',k}$ is transmit power of serving macrocell M and neighboring macrocell M' on subcarrier k, respectively. $G_{m,M,k}$ is channel gain between macro user m and serving macrocell M on subcarrier k. Channel gain from neighboring femtocell are denoted as $G_{m,M',k}$. Similary, $P_{F,k}$ is transmit power of neighboring femtocell F on subcarrier k. No is white noise power spectral density, and Δf is the subcarrier spacing.

In case of a femto user f on subcarrier k interfered by all macrocells and adjacent femtocell, the received SINR can be written as:

$$SINR_{f,k} = \frac{P_{f,k}G_{f,F,k}}{N_o\Delta f + \sum_{F'}P_{F',k}G_{f,F',k} + \sum_{M}P_{M,k}G_{f,M,k}}$$ (3.6)

The channel gain G is dominantly affected by path loss, which is different for outdoor and indoor scenarios (3.1), (3.2), (3.3), and (3.4). So, it can be written as [12]:

$$G = 10^{-PL/10}$$ (3.7)

3.3 Throughput Calculation

The throughput can be calculated after we had obtaining the SINR. The practical capacity of macro user m on subcarrier k can be written as [12]:

$$C_{m,k} = \Delta f * \log_2(1 + \alpha SINR_{m,k})$$ (3.8)

Where α is a constant for target Bit Error Rate (BER), and defined by $\alpha = -1.5/\ln(5BER)$. In this analysis BER is set to 10^{-6}. Finally, the throughput of serving marcocell M can be expressed as [12]:

$$T_M = \sum_{m}\sum_{k}\beta_{m,k}C_{m,k}$$ (3.9)

Where, m,k is represents the subcarrier assignment for macro users. When $m,k = 1$ means that the subcarrier k is assigned to macro user m. Otherwise, $m,k = 0$. In a macrocell, in every time slot, each subcarrier is allocated to only one macro user, this is known from the characteristics of the Orthogonal Frecuency Division Multiple Access (OFDMA) system. So this implies that [12]:

$$\sum_{m=1}^{Nm}\beta_{m,k} = 1$$ (3.10)

Where $_{Nm}$ is the number of macro users in a macrocell.

IV. SIMULATION RESULTS

4.1 Conventional Scheme

In conventional scheme SINR for each user j attached to cell i is calculated as [12]:

$$SINR_{j,i} = \frac{P_iG_iPL_{j,i}}{\sum_{k=0(\neq i)}^{N}(P_kG_kPL_{j,k})}$$ (4.1)

Where $PL_{j,k}$ is the path loss between user j and femtocell k. The capacity is calculated as:

$$C_{j,k} = BW.(1 + \alpha.BER)SINR_{j,I}$$ (4.2)

4.2 Proposed Scheme

A. Carrier Aggregation (CA)

Step 1: Initialization:
Each femtocell is assigned 1 sub-band (out of 10). If all the sub-bands are already taken, then the one with least interference is selected, based on measurement of total capacity from the neighboring cells.
Step 2:
After the initial sub-band has been assigned to the user by the serving femtocell, a check is then performed to find out whether 1 more sub-band can be allocated. This procedure is being repeated for all sub-bands. Parallel to that, check is performed to determine whether the capacity within the 3 neighboring cells has increased or not.
Step 3:
Step 2 is repeated until there is no more change in the capacity across any femtocell neighborhood, or until the iteration limit is reached. The iteration limit of 15 is used.
Thus, the SINR for each user j attached to cell i can be written as [12]:

$$SINR_{j,i} = \frac{P_iG_iPL_{j,i}}{P_i(IM_j x SB) x SB_i^T}$$ (4.3)

where SB is the sub-band matrix. The SB value 1 when a specific sub-band is used by a particular femtocell. It is equal to 0 when the given femtocell is not using the corresponding band. The sub-band matrix can be shown as:

$$SB = \begin{bmatrix} 1 & \cdots & 0 \\ \vdots & \ddots & \vdots \\ 0 & \cdots & 0 \end{bmatrix}$$

The number of rows represents femtocell IDs (1…Number of femtocells) and the number of columns represent band IDs (1…Number of bands).
IM is an interference matrix defined as:

$$IM = \begin{bmatrix} G,PL & \cdots & \\ \vdots & \ddots & \vdots \\ & \cdots & \end{bmatrix}$$

The number of row represent femtocell user IDs (1…Number of femtocell users) and the number of columns represent femtocell IDs (1…Number of femtocells).
In $(IM_j x SB) x SB_i^T$ the first multiplication produces a vector of sums over all interfering femtocells at user j as:

[[G1 * PL1 *SB(1,1) + G2 * PL2 * SB(2,1) + …], [G1 * PL1 * SB(1,2) + G2 * PL2 * SB(2,2) + …]]

Thus every element in the array produced by the first multiplication is a summation of interferences at particular band. This is multiplied by a transposed band vector at the present femtocell i, producing sum of only those interferences which are using the same band as the present femtocell i. The capacity can be written as [12]:

$C_{j,i} = BW (1 + \alpha SINR_{j,i})$, where $\alpha = -1.5/\log(5*BER)$ and BER is 10^{-6}.

B. CA along with CoMP

To model CoMP, the most interfering components of the Interference Matrix (IM) are removed. One value is removed for each femtocell, so that each femtocell supports 1 CoMP user. In reality more CoMP users per femtocell can be supported, but for the simplicity case 1 CoMP user per femtocell is considered. For each femtocell, a maximum value of interference is found across all the users. This femtocell and

the user form a CoMP pair, which adds to the throughput of that user, only at those points where the sub-bands coincide. SINR for each user j attached to cell i is calculated as [12]:

$$SINR_{j,t} = \frac{P_i G_i PL_{j,i}}{IM_j \times SB_j^i} + \sum_{c=1}^{Nc(j)} \frac{P_0 G_0 PL}{(IM_j \times SB)} \quad (4.4)$$

Where c is index represent those femtocells that provide CoMP to the user j. Nc(j) represents the number of femtocells that provide CoMP to user *j*. Nc(j) is found by counting elements of another matrix, called CoMP matrix, which is same dimension as the Interefence Matrix, but has a value of either 1 or 0, representing yes or no scenario for particular user-femtocell combination if they form CoMP pair.

The Interference Matrix (IM) is modified from the one used in CA by zeroing the elements which is correspond to the CoMP user-femtocell pair. The zeroed elements are chosen based on maximum value on interference as calculated along all the users per each femtocell i.e. one zero for each femto cell, at the place of worst interference. Capacity is later calculated in the same way as for CA.

4.3 Topology Used

The topology used in the simulation, we assumed there are 30 femtocells deployed in random spot, along with 55 femtocell user and 10 macrocell users. There are 30 buildings, with 5 along the x axis and 6 along the y axis. The road width is taken approximately as 10 m. The modulation scheme is 64 QAM and the bandwidth is 20MHz/100MHz. Figure 4.1 represent scenario with 30 Femtocells. The result is shown in figure 4.3 and 4.4.
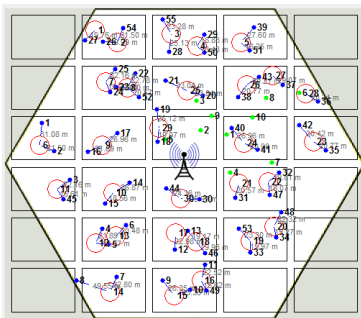

Figure 4.1: Topology with 30 Femtocells

Figure 4.2 represent when we assumed there are 50 femtocells deployed in random spot, along with 55 femtocell user and 10 macrocell users. There are 30 buildings, with 5 along the x axis and 6 along the y axis. The road width is taken approximately as 10 m. The modulation scheme is 64 QAM and the bandwidth is 20MHz/100MHz. The result is shown in figure 4.5 and 4.6.
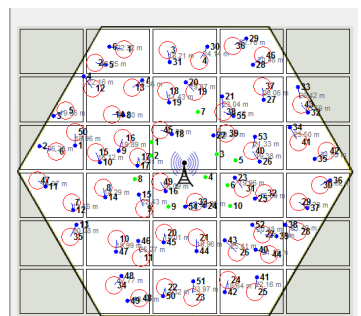

Figure 4.2: Topology with 50 Femtocells

4.4 Results

Figure 4.3 & 4.4 are the results from first scenario. In these figure we depict the throughput vs average distance of femto users
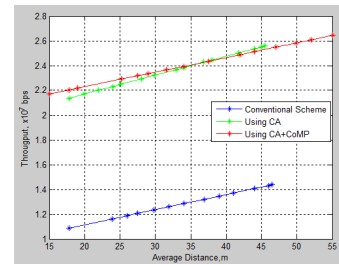

Figure 4.3: Throughput vs Average Distance Femto User with BW 20 MHz, Femtocells-30

The plot in the result (Fig. 4.3) is shown that using CA combined with CoMP is provided higher throughput than using only CA and conventional scheme. With CA alone the throughput value at some point higher than using CA combined with CoMP. The throughput performance increases when average distance of femto users increases. The use of CA and CoMP methods almost double the throughput compared to that for conventional scheme.
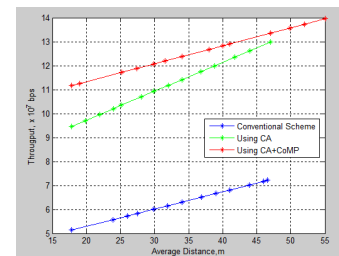

Figure 4.4: Throughput vs Average Distance Femto Users with BW 100 MHz, Femtocells-30

Figure 4.4 depict the throughput vs average distance of femto users with bandwidth 100 MHz and number of femtocells are 30. With conventional scheme throughput is lower than when only CA is employed, as well as, when CA combined with CoMP techniques are employed. The higher throughput we get when using CA combined with CoMP.
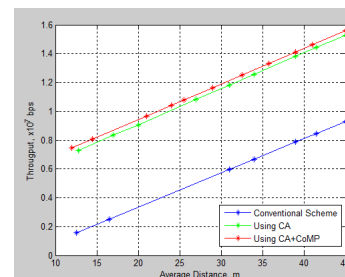
Figure 4.5: Throughput vs Average Distance Femto User with BW 20 MHz, Femtocells-50

As we can see in figure 4.5 and 4.6, the throughput increases when the average distance of femto users increases. The throughput is also higher for a wider bandwidth. When using CA combined with CoMP at average distance of 10-15 m the throughput increases effectively. However, at the distance of 15-20 m it has one slot delay. At an average distance of 20-45 m, the throughput increases effectively again. When using only CA method, at an average distance of 10-20 m the throughput increases effectively, but at a distance of 20-25 m it has one slot delay. At an average distance of 25-

45 m, the throughput increases effectively again. The use of CA and CoMP methods almost double the throughput compared to that for conventional scheme.
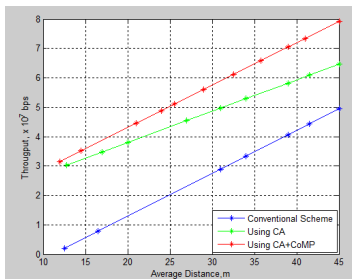

Figure 4.6: Throughput vs Average Distance Femto user with BW-100 MHz, Femtocells-50

Figure 4.7 depict SINR vs number of femto users. The SINR performance decreases when number of femto user increases. In other hand, the interference increases when we increasing number of femto user. The use of CA and CoMP provide higher SINR compared to that for CA as well as conventional scheme.
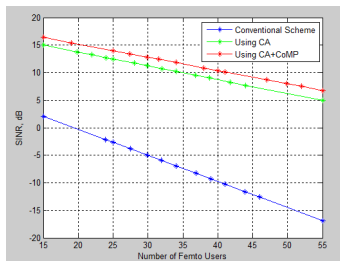

Figure 4.7: SINR vs Number of Femto Users

As we can see in figure 4.8, the effect of adding femtocells is causing a degradation of the SINR. Using CA combined with CoMP provids higher SINR than using CA method alone and the conventional scheme
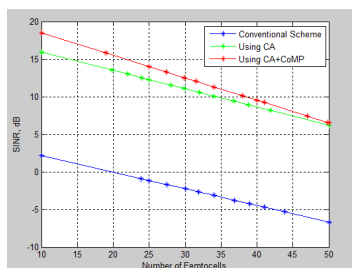

Figure 4.8: SINR vs Number of Femtocells

V. CONCLUSION

In paper performance of inter-cell interference of LTE-A system that employs Carrier Aggregation (CA) and Coordinated Multipoint (CoMP) techniques has been evaluated. The performance was evaluated in term of throughput and SINR as a function of average distance from femtocell user, and also as a function of the number of user, for different bandwidth.

The results show that throughput increases when average distance of femtocell increases. Throughput is also higher for smaller number of femto user. The use of CA and CoMP methods almost double the throughput compared to that for conventional scheme.

The throughput is also higher when CA and CoMP are employed simultaneously compared to that when CA only is

employed. This shows that CA and CoMP methods can reduce the inter-cell interference effectively.

The SINR performance decreases with increasing number of femto users, as well as, with increasing number of femto cells. However the SINR improves by approximately 12-20 dB when CA and CoMP techniques are employed. When CA and CoMP are used together the SINR performance is about 2-4 dB higher compared to that when only CA is employed. This indicates that CoMP and CA methods are effectively mitigate the inter-cell interference.

REFERENCES

[1] A. Ghos, R. Ratasuk, B. Mondal, N. Mangalvedhe, "LTE-Advanced: Next Generation Wireless Broadband Technology." Wireless Communication, IEEE (Volume 17, Issue 3) June 2010

[2] Norshidah Katiran, Norsheila Fisal, Sharifah Kamilah Syed Yusof, Siti Marwangi Mohamad Maharum, Aimi Syamimi Ab Ghafar, Faiz Asraf Saparudin, : Inter-cell Interference Mitigation and Coordination in CoMP Systems. International Conference, ICIEIS 2011, Part III, CCIS 253, pp. 654–665 (2011), Springer-Verlag Berlin Heidelberg 2011

[3] Wiley,: LTE-The UMTS Long Term Evolution From Theory to Practice, 2nd Edition.

[4] Immer, R., Droste, H., Marsh, P., Brueck, S., Mayer, H., Thiele, L., Jungnickel, V.: Coordinated Multipoint: Concepts, Performance and Field Trial Results. IEEE Communications Magazine, 102–111 (2011)

[5] Ghaffar, R., Knopp, R.: Fractional Frequency Reuse and Interference Suppression for OFDMA Networks. In: Proceedings of the 8th International Symposium on Modeling and Optimization in Mobile, Ad Hoc and Wireless Networks (2010)

[6] V. Pauli, E. Seidel: Inter-cell Interference Coordination for LTE-A. Nomor Research GmbH, Munich, Germany, September, 2011

[7] Tosin, O., Diyana, K.: Coordinated Multipoint Transmission/Reception, 2011

[8] Xiao Xue, Ji-hong Zhao, Hua Qu,: Inter-cell Interference Coordination Scheme Based on CoMP. International Conference on Advanced Communication Technology (ICACT), Feb. 2012 IEEE page 19-22.

[9] Liu, L.; Zhang, J.; Inter-cell Interference Coordination through Limited Feedback. International Journal of Digital Multimedia Broadcasting, November 2009.

[10] LIN Le-Xiang, LIU Yuan-an, LIU Fang, XIE Gang, LIU Kai-ming, GE Xin-yang.: Resource scheduling in downlink LTE-Advanced system with carrier aggregation. The Journal of China Universities of Posts and Telecommunications, February 2012, 19(1): 44-49

[11] www.3GPP.org.

[12] LTE-A Femto-Macro Throughput Simulator.
http://ru6.cti.gr/ru6/femtomacro_throughput_simulator.zip

Improving Bio-Cryptography Authentication Protocol

Irfan Fadil
School of Computing
Telkom University
Bandung
Email: i.fadil88@gmail.com

Ari Moesriami Barmawi
School of Computing
Telkom University
Bandung
Email: mbarmawi@melsa.net.id

Abstract—User authentication is a method for authenticating a user. Recently there were some authentication method proposed by researchers, such as a method proposed by Seung .et.al where the user authentication process was done using biometric (fingerprint) and password. However, this method has weaknesses such as weak against fake user attack, high time complexity, and it is possible for fake device to obtain the fingerprint of the user. In this work, Elliptic Curve and Keccak Hash Function were proposed to solve the problem. The Elliptic Curve is used for conducting device authentication such that there is no possibility for obtaining user fingerprint by unlegitimate device, while Keccak Hash Function is used for improving the user authentication process, such that the authentication process can be succeeded only if both password and fingerprint is authenticated. The result of experiment shows that the user authentication processing time decreased 35.06 ms - 41.6 ms compared with the method proposed by Seung .et.al, while the probability of obtaining the fingerprint and password using the proposed method is less than the previous method of 2^{-57}. It is proven that the proposed method is strong against fake device attack for stealing the biometric information and password.*

Keywords—Authentication, Bio Key, Elliptic Curve, Keccak Hash

I. Introduction

Recently, authentication becomes indispensable in daily life, because of the increasing number of fraudulent transactions through cyberspace (such as in banking transaction, e-commerce, etc). Authentication is needed for authenticating one party by the communicating parties and it is usually implemented in client-server system where the server needs to know who is accessing their information or between the clients to authenticate each other.

There are many methods for user authentication such as fingerprint authentication [1], a fingerprint based bio-cryptography security protocol design for client/server authentication in mobile environment [2], and efficient authentication protocol based on Elliptic Curve for mobile network [3].Most of those proposed methods used password or biometrics (fingerprint) as their identity. However, there was a method proposed by Sung-hyu Han et al [4] which used biometrics and password, but this proposed authentication method was done using only one of them. It can be concluded that the authentication will be succeeded if the password or the fingerprint is valid. Thus, there is still opportunities for an attacker to succeed the authentication process even his

fingerprint is not valid. In the previous method it was assumed that the fingerprint scanner is a device that can be trusted, or in other words, the scanner is a legitimate device (not a cheater). Furthermore, nowadays there are many detractors who disguise as a fingerprint scanner for stealing fingerprint feature. Therefore, a method for authenticating the fingerprint scanner is necessary.

II. Related Works

User authentication method proposed by [4] uses RSA Method. In this method, the communicating parties were assumed to be Alice and Bob. Alice use fingerprint information by extracting fingerprint feature and password as 4 digit number in authenticating process and Bob use public key parameter to authenticate Alice. The authenticating procedure is shown as follows :
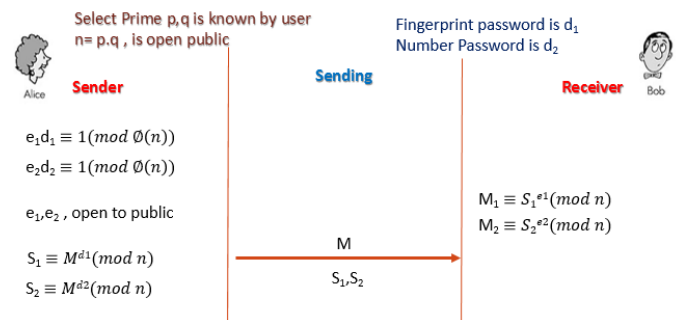
Fig. 1: The Scheme of Previous Method [4]

Notes that e_1 and e_2 is a public key. The authentication process begins with Bob compares the result of M_1 and M_2 with the message M. If $M_1 = M$ and $M_2 = M$ then Bob authenticates Alice as the legitimate user. But if $M1 \neq M$ or $M2 \neq M$ then Bob is doubtful to authenticate Alice as the legitimate user.

III. Modified Bio-cryptography Authentication Protocol

This proposed method involves three parties : authentication device consist of fingerprint reader or scanner, keyboard and a processor, user with printed bio key that has computing capability, and secure server that stores the public key (called public server). For authenticating user, this method needs two

devices that is bio key generator and bio key authenticator. Bio key generator device has a function to generate printed user bio key while bio key authenticator device has a function to generate and compare with printed user bio key.

The authentication method consists of two processes and use wireless media to communicate each other. The first process is device authentication and the second process is the user authentication. The basic idea of user authentication process was matching the user printed bio key with the original bio key. The original bio key was obtained by hashing the real user fingerprint feature and password. This process was conducted using authentication device to ensure that the authentication device is legitimate then the authentication device should be authenticated by the user. For authenticating the device, Elliptic curve based authentication is proposed the device authentication process consists of user and device registration as well as the user and device authentication. Figure 2 shows the registration of user and device, while Figure 3 shows user and device authentication.
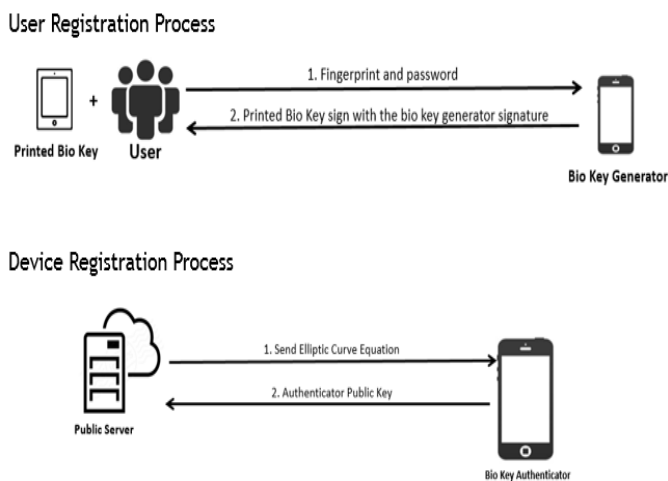

Fig. 2: Architecture System for Preprocessing Authentication

In Figure 2, it is shown that three parties are involved. The user registration process in step 1 and 2 were conducted to generate the bio key by processing the user fingerprint feature and password. The bio key generator sent the printed bio key to the related user. The user stored the bio key into his device. In device registration process, the bio key authenticator registered its public key to public server, by assuming that the public server was a legitimate device owned by the government/related company.

For conducting user and device authentication, public server and bio key authenticator is necessary as shown in Figure 3. Reffering to Figure 3, step 1,2,3,4,5 is a procedure of device authentication while step 6,7 is a procedure of user authentication. Device registration begins by sending authenticator public key and elliptic curve equation which is used in the authentication process. After receiving the authenticator public key and elliptic curve equation, the user compares the bio key authenticator public key stored in the public server with the one sent by the bio key authenticator. The device authentication starts by sending user random number to the bio

key authenticator. Furthermore the bio key authenticator sends the function of user random number, device random number and device secret key. The user compare the function result sent by the bio key authenticator and the one that is calculated by the user. If they are equal then the user decide that the bio key authenticator device is the legitimate one and the user authentication is conducted. The bio key authenticator verifies the bio key generator signature. If the bio key authenticator verified the bio key signature as the legitimate bio key generator signature, then the user authentication is conducted. The user authentication is conducted by comparing the printed bio key and the bio key generated by the bio key authenticator.
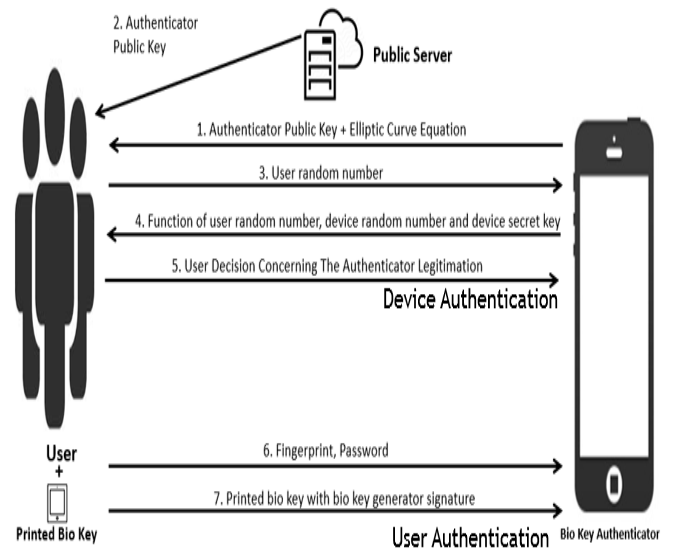
Fig. 3: Architecture System for Device and User Authentication

A. Generating Bio Key

The beginning phase of authentication process was generating bio key using bio key generator. The input of this process required user fingerprint feature and password. The extracted feature of fingerprint (original extracted feature) and password (original password) were concatenated and processed with Keccak hash function for generating bio key.

Each one of original extracted feature has 9 bits length. The password consists of 8 characters or in other word has 64 bits length. Original extracted feature and original password were processed using Keccak hash function to get a single arbitrary value. In this method we select 224 bits output as the maximum number of bits used in device authentication process. The set parameter which used were 1152 bit rate, 448 bit security and 224 bits as output of this process.

For example, the original extracted feature represented by hexa is 290485604374d02af50e189d8545c81c24631198ed612 178ca and the password of user is 'Indra123'. The result output of extracted feature and password using Keccak hash function is D91371BD564F1A464833E7E25789E2C434BEDAAC7B DA45444FE9E791. The diagram block of bio key generator is shown in Figure 4.

Fig. 4: Bio Key Generator

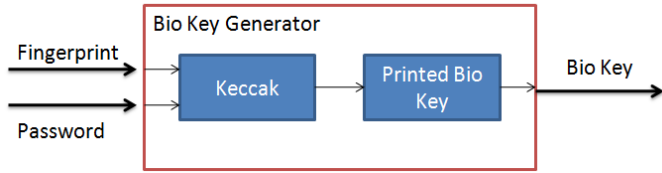## B. Device Authentication

This authentication was conducted using Elliptic Curve. Elliptic curve was chosen because it required only a small number of bits as the same minimum security with the authentication methods used in previous studies [4]. A small number of bits is required because proposed methods is intended to be used in mobile environment. In order to determine the validity of legitimate device, the mutual authentication process was carried out based on elliptic curve. Elliptic curve has the following equation:

$$E : y^2 = x^3 + ax + b \; ; with \; finite \; field \; F = c \quad (1)$$

A seed value was needed to be taken to obtain the value of a and b. The procedure to obtain the equation of elliptic curve was described in [5]. The value of a and b should met the security criteria of elliptic curve [5]. The Elliptic curve equation is called Bada55 as follows:

$$E : y^2 = x^3 - 3x + (b' mod \; c) \quad (2)$$

where b' is a value that generated in procedure [5]. So that a and b has the following values: a=2695994666715063979466 7015087019630673557916260026308143510066298878; b=2 670845009189460221458901418547329584336822224994 16 2716450205986542;

The point on the elliptic curve is selected as the base point and a chosen integer number as secret key. Furthermore, the secret key selected by user is a prime number in the range of $[1...2^{224}]$ because we used 224 bits key. After determining the secret key, a number is generated which is relatively prime to the secret key. After obtaining the secret key and numbers which are relatively prime to the secret key then compute the public key. For example, let the selected number as follows:

modulus number n =2695994666715063979466670150870 19630673557916260026308143510066298881;

secret key K = 18224309726210493156569408788499200 4445083412208348056192210840974;

then the number which is relatively prime to the secret key K is R =25797063021564030386152390239990089764947 12 53553872997093245377660382; If the elliptic curve equation used is accordance with the equation 1 and Point $P = (x_1, y_1)$ at a value of x_1 and y_1 as follows:

x_1=2647098374834734005492096092466021773423709291 0257058601256000081095;

y_1=82262022224192067510761655470735694927717345 2535374663742208522819;

then public key $K_p = (x_2, y_2)$ is obtained from

$$K_p = (secret \; key \; K * point \; P) \quad (3)$$

=(18224309726210493156569408788499200444508341220 83480561922108409774)*(2647098374834734005492096092 466021773423709291025705860125600081095,822620222241 920675107616554707356949277173452535374662220 85228219)

=(27420517932060606282027405322883885598762300338 654597672358766610394,26807552064050540194948639331 939790822085463699519283621960128869599)

so the value of K_p produce x_2 and y_2 values as follows :

x_2=27420517932060606282027405322883885598762300 33865459767235876610394;

y_2=26807552064050540194948639331939790822085463 6995192836219601286959;

In the device authentication process it is assumed that the device must have K_s which can produce K_p. K_p is sent to Public Server. Besides K_s and K_p, the device and user have an ID. The device authentication process is done by the following order:

1) Public server sends elliptic curve equation E to legitimate device
2) The legitimate device registers a valid K_{pP} and ID_P to public server.
3) The legitimate device sends E and base point P to user.
4) Furthermore, the legitimate device sends K_{pP}, ID_P and R_c to user. Where R_c is the multiplication point of P and R_1. R_1 is relatively prime to K_{sP}.
5) Users sends ID_P which is received from device to public server.
6) The public server sends K_{pS} in accordance with ID_P which is received from user. The user checks whether K_{pS} which is received from public server have the same value with K_{pP} which is received from device. If both of value are equal, then the process is continued but if not equal the process of device authentication is terminated and user declares that the device is not valid (adversary).
7) The user sends R2 to the device where R2 is a number that is relatively prime to K_{sU}.
8) The legitimate device computes and sends AVC to user where AVC is built by formula :

$$AVC = R_1 + (R_2 * K_{sP}) \quad (4)$$

the user check using the following formula:

$$(AVC * P) - (R_2 * K_{pP}) = R_c \quad (5)$$

If AVC is equal to R_c, then the user declares that the device is legitimate device and the process is continued. But if not equal then the process of device authentication is terminated and the user declares that the device is not valid (adversary).
9) Furthermore, the user sends R_3 and ID_U where ID_U is used by device to identify which user is communicating with it and R_3 is the result of point multiplication

of R_2 and R_c. The device checks whether R_3 is equal with formula :

$$R_1 * R_2 * R_c = R_3 \quad (6)$$

If the formula is true, then the process of device authentication is terminated and the system declared that device and user are legitimate. But if the formula is not true then the process is terminated and the system states that the device and user are not legitimate.

The device authentication is successful if step 7, 9 and 11 both device and user declare that the device or the user is legitimate. Step 7 is to ensure that the device is registered. Step 9 is to determine whether the device is legitimate or not and step 11 is to ensure that user is legitimate user to scan a fingerprint and password into system. All procedures in device authentication scheme is shown in Figure 5, 6 and 7 .
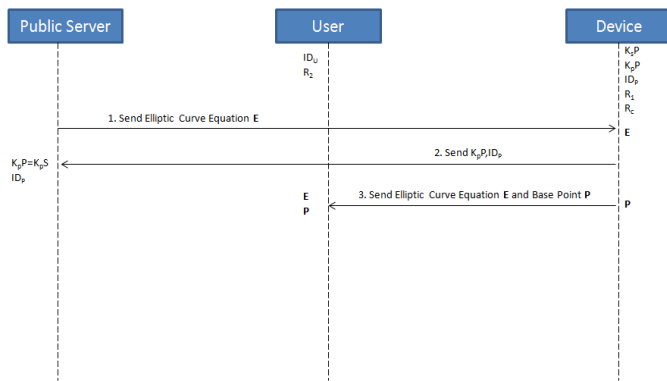

Fig. 7: User Authentication Scheme

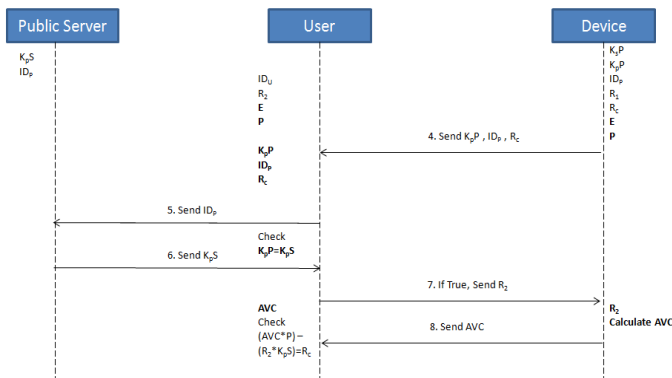Fig. 5: Preprocessing of Device Authentication

Fig. 6: Device Authentication Scheme

C. User Authentication

User authentication process is a process for verifying whether the user is the owner of the printed bio key or not. This process is similar with process of bio key generator. The user authentication process have three inputs which are bio key user, fingerprint and password user.

User scans his/her fingerprint and input the password to bio key authenticator device and sends the user bio key to bio key authenticator device. Furthermore, the bio key is
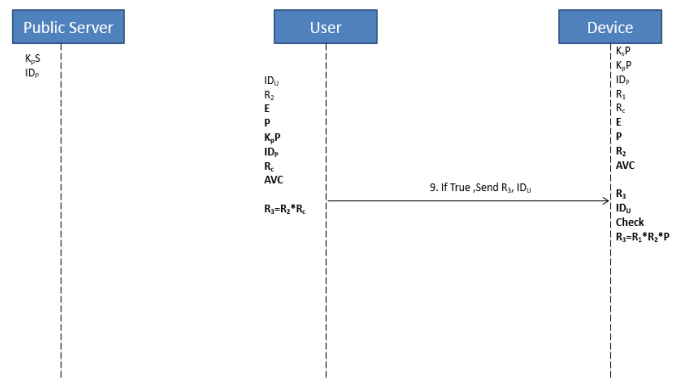
stored temporarily in memory of bio key authenticator. At first, the bio key authenticator device compared the fingerprint with the template of extracted user fingerprint feature for a matching process used algorithm by [6] which is modified in the matching by using algorithm. This process used a threshold tolerance for accepting extracted user fingerprint feature. If the process of fingerprint feature extraction match more than 89,7 % then the result is accepted and continued with Kecccak process with a password user, else a user authentication process was terminated.

A bio key is the combination of the password and the extracted feature of original user. The value of original bio key was compared with printed bio key signed by signature of legitimate device. If the values were equal then the user who carried the printed bio key was a legitimate person. If the value was not equal then the user was unauthorized person. Figure 8 shows the block diagram of user authentication process. For
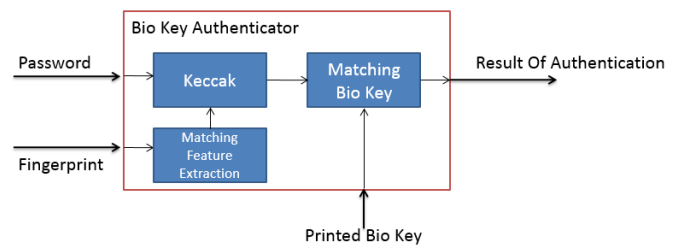
Fig. 8: User Authentication Process

example, the original extracted feature represented by hexa is 290485604374d02af50e189d8545c81c24631198ed61217 8ca and the password of user is 'Indra123'. The result of fingerprint and password by Keccak hash function is D913 71BD564F1A464833E7E25789E2C434BEDAAC7BDA4544 4FE9E791(called printed bio key). If the password of user was set different such as '12345678', then the result of bio key was 8F38DD16D139969DA30FE6A8EC7FD3AE507F79 0A52179C82DFC05EEE (called original bio key). Thus, the comparison of value between printed bio key and original bio key are not equal then the user was unauthorized person.

IV. RESULT OF EXPERIMENTS

The result of experiments consists of user authentication performance experiment, device authentication performance experiment , guessing fingerprint and password and probability of attack on device authentication scheme.

A. User Authentication Performance Experiment

For user authentication, the performance is measured in processing time. The time performance of user authentication process is shown in table I. The proposed method has maxi-

TABLE I: User Authentication Performance

No	User	Result	Proposed Times	Previous Times
1	Trial 1	Authenticated	2.38 ms	94.9 ms
2	Trial 2	Authenticated	2.11 ms	148 ms
3	Trial 3	Authenticated	2.12 ms	111 ms
4	Trial 4	Authenticated	2.14 ms	155 ms
5	Trial 5	Authenticated	2.15 ms	151 ms

mum processing time of 3,8 ms and minimum processing time of 2,06 ms while the previous method has maximum processing time of 168 ms and minimum processing time of 78,3 ms. Meanwhile, the average of authentication processing time of the proposed method is 2,317 ms and the previous method is 128,32 ms. This condition is occurred because the proposed method only uses one function (ie. Keccak Hash Function) with complexity of $O(N)$ while the previous one uses RSA encryption method, where RSA needs more complexity for finding the large primes which is $O(NlogN)$. Furthermore, the time complexity of RSA cryptosystem is $O(2(NlogN))$ while the time complexity of Keccak hash functions is $O(N)$.

B. Device Authentication Performance Experiment

In this experiment, the performance of device authentication was measured in processing time. Furthermore, the device has device parameters such as device public key, device secret key , random number($R1$), a function of secret key and point elliptic curve(Rc). The other parameter $R2$ is owned by user which is a random number and unique for each user. The processing time of device authentication is shown in table II. The maximum processing time is 37,8 ms and the

TABLE II: Device Authentication Performance

No	User	Result	Times
1	Trial 1	Legitimate Device	34.5 ms
2	Trial 2	Legitimate Device	33.4 ms
3	Trial 3	Legitimate Device	37.8 ms
4	Trial 4	Legitimate Device	33 ms
5	Trial 5	Legitimate Device	36.1 ms

minimum processing time is 33 ms. The average time of device authentication process is 34,48 ms. Thus, the proposed method only needs about 35,06 ms to 41,6 ms for user authentication process including device authentication. It means that even the proposed method includes the device authentication process, the whole authentication process (user and device authentication) needs less time than the authentication processing time of the previous method.

C. Guessing Fingerprint and Password Complexity

The authentication key which is used in the proposed method is generated by fingerprint and user password using keccak hash Function. Suppose that the adversary knows the authentication key. Suppose that the adversary tries to guess the fingerprint and user password based on the authentication key.

The authentication key which is generated by the proposed method have a length of 224 bits. To guess user fingerprint and password, the adversary uses attack on which is proposed in [7]. However this attack didn't produce an original fingerprint and user password. Since this attack is based on collision, it means that the probability of two original fingerprint and user password has similar authentication key is 2^{-57}.

Furthermore, to guess user fingerprint and password, if the same bio key is implemented in the previous method, then the probablitiy of guessing the bio key is similar to the complexity of factoring the modulus number. Based on [8], the probability of finding the factor of the modulus number is equal to $\sqrt{N}^{-1}$ where N is the bio key length. Thus, if N=224, then the probability of finding the user password and finger print is equal to $(2^{112})^{-1}$. The result of authentication key is shown in Table III and IV.

D. Security Against Fake Device Attack

Since there was possibility to impersonate the device in order to obtain the user fingerprint and password, the attack on device authentication had to be observed. Several fake device wanted to communicate with the original to obtain user fingerprint and password directly. The proposed scheme could avoid the fake device by conducting the device authentication scheme.The scenario of the attack is shown in Figure 9 and 10. In Figure 9, fake device uses public key and its identity of the original device. The other parameter such as R_1 and R_c were generated by fake device. Furthermore, Figure 10 shows the fake device with fake parameters.
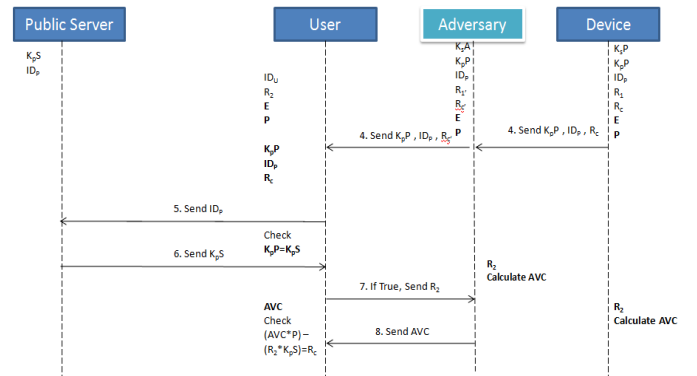

Fig. 9: Attack using the public key original device

If the fake device an outsider of the system, the fake device uses its own of device public key and the other parameter (see Figure 10) then send it to the user. In this case the fake device is considered as an unauthorized device. This condition happened because the device public key and identity were not

TABLE III: The Proposed Method Authentication Key

No	Fingerprint	Password	Bio Key
1	290485604374d02af50e189d8545c81c2463 1198ed612178ca	Indra123	8C294F4859E9D163B74F529D573FECCB E1B4F62B8DCC230AD7E00EF8
2	1a9b4343e01844fc6823030cc359117c0a2c0 21fc484e048bcae1a34188a01a0e0104c7e0b 130	Paheri12	C5212A3F7F2F08433CD54F92E68588B05 C26FA97B4DADFD018C03BF9
3	222008785079051b0583e130f8ec763c11c9e 330b0e8	Sambath1	9C0BB1960338C88494F7DE776C5CF5273 B345C787C22C69DD97B4690

TABLE IV: The Previous Method Authentication Key

| No	Encrypted Fingerprint	Encrypted Password
1	39b99b79ae114decc39be72678361758b97b43aae3477f57887351f 9d2b54f8348d9c78251fd8774709a0eac5b0ad1b6d707cfaf6ecbc8fc	552bee26c87110480ec343d80113caf42c07d0ce0e79371bbf4dd9ca 1bcc57065c29445f53664a46d1fe875677f4e7547d07078e1caf93
2	8b615c8bf679f4534cd5d121cf9c1dbe7d8c94f511214d4ba6320330 4595f2c4a26ac02134070dd403d7a9de3eac0b72637fa167c1818c03	1e0c78b846afa1f83eaa204edd746c0a12206e440fc7a1302d0b24c1 42b34c74f5007ed1e345185411d8814d8790fac3645181a4f912e0b 9
3	3a28ac0747b52b5f103e00a19e956778dd4296a909fabe64c2db642 de432538ae5eda7fcfaff86301d8abdf7d77e38a8aaaa04ca0bcd2e1f	54151afdd351f0a6ad788abbb7d81ca033ea26cf3ec20743335e89ee 7f56faf6867b902915cdb85a7db4cf805297996c15f6a2359be0d0a3
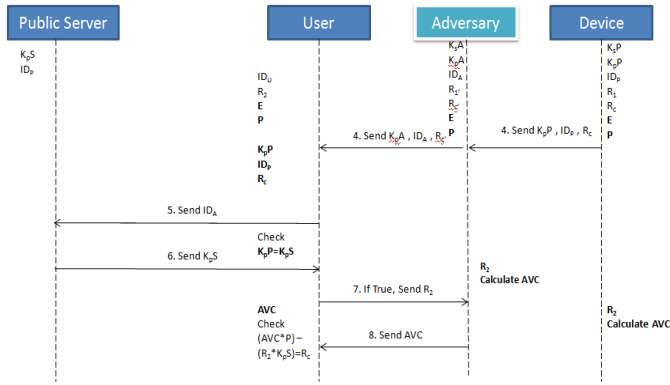
Fig. 10: Attack using fake device public key

registered in the public server. If the fake device uses the identity of original device and public key, the authentication will be failed because the user found that the parameter which is related to the device secret key is not true.

The other attack scenario is that the fake device in insider of system (see Figure 9). The fake device only knows the public parameter of the legitimate device. The fake uses this public parameter to authenticate the process and sends it to user. The user receives a public parameter from the fake device and sends the identity of device to public server. The public server sends back a device public key with the related identity of the device to the user. The user compares the device public key sent by the fake device and the device public key sent by the public server. If they were equal then the device is legitimate. Furthermore, the user sends a random number parameter to the fake device. The fake device sends back the number which is computed by the function of the user random number parameter, the fake device random number and the secret key of fake device (called AVC). The user computes a function AVC using the device public key and compares it with a point which has been sent previously. In this step the user detects that the device is an unauthorized device. This condition happened because the device public key is not

corresponding with the secret key.

V. CONCLUSION

It has been proven that using the proposed method, the authentication processing time is reduced to 65.23 % compared with the previous one. Moreover, the security strength is increased as the impact of Keccak hash function security.

The proposed method introduces the device authentication process for securing against the fingerprint and password stolen by fake device. It has been proven that the device authentication can prevent the fingerprint and password stealing using elliptic curve based authentication.

REFERENCES

[1] Wuzhili. Fingerprint recognition. Master's thesis, Hongkong Baptist University, 2002.

[2] Fengling Han Kai Xi, Tohari Ahmad and Jiankun Hu. A Fingerprint based bio-cryptographic security protocol designed for client/server authentication in mobile computing environment. SECURITY AND COMMUNICATION NETWORKS, 2010.

[3] Ms.P.G.Rajeswari et.al. An efficient authentication protocol based on elliptic curve cryptography for mobile networks. IJCSNS International Journal of Computer Science and Network Security, 2009.

[4] Sung-hyu Han Jae-cheol Ryou Seung-hwan Ju, Hee-suk Seo and Jin Kwak. A study on user authentication methodology using numeric password and fingerprint biometric information. Hindawi Publishing Corporation BioMed Research International, 2013.

[5] Daniel J. Bernstein et.al. How to manipulate curve standards: a white paper for the black hat, July 2014.

[6] Sharat S. Chikkerur. Online fingerprint verification system. Master's thesis, State University of New York at Buffalo, 2005.

[7] Orr Dunkelman Itai Dinur and Adi Shamir. New attacks on keccak-224 and keccak-256. 2011.

[8] Thorsten Kleinjung et al. Factorization of a 768-bit rsa modulus. 2010.

[9] J. M. DeLaurentis. A further weakness in the common modulus protocol for the rsa cryptoalgorithm. Cryptologia, 1984.

[10] M J Wiener. Cryptanalysis of short RSA secret exponents. IEEE Transactions on Information Theory, 1990.

Spectrum Sensing of OFDM Signals using GLRT Detector with Bootstrap Approach

Fajar Nugraha
School of Electrical Engineering
Telkom University
Bandung, Indonesia
fajar.nugraha.02@gmail.com

Suhartono Tjondronegoro
School of Electrical Engineering and Informatics
Institut Teknologi Bandung
Bandung, Indonesia
shtntjnegoro@stei.itb.ac.id

Fiky Y. Suratman
School of Electrical Engineering
Telkom University
Bandung, Indonesia
fysuratman@gmail.com

Abstract—**Among some of its duties, the cognitive radio's main role is to do spectrum sensing in the surrounding radio environment. In order to do mapping and can determine the frequency of use vacant frequencies which can be optimized for the use of cognitive radio communication. Even to the worst conditions in which the detector system has no knowledge of the signal and noise. There are several techniques that can be used to perform spectrum sensing in this condition, among these techniques are simpler implementation of energy detection techniques. This technique has a weakness at noise conditions are unknown and uncertainty. In this condition, a technique that can be used and better than energy detection is GLRT detector. However, this detector requires choose threshold with empirically. This process has a problem when we move from one location to another, it is necessary to conduct empirical calculations again. And would face difficulties if we do detect a signal that is already active in a new place. so it is necessary to know the exact time the signal was not active. In this condition the bootstrap approach can help determine the threshold detector directly from the active signal is received. So the detector can gain threshold which is always updated with any condition, anytime and anywhere.**

The simulation result show that GLRT detector with bootstrap approach has a toughness in the face of uncertainty noise. Even able to exceed the performance of which is owned by the energy detector and GLRT. At condition SNR -5 dB and uncertainty noise 1 dB, GLRT with bootstrap approach improve probability of miss detection almost 0.030 than ordinary GLRT and 0.094 than energy detector.

Keywords—spectrum sensing, OFDM, GLRT, Bootstrap, cyclic prefix, second-order statistic

I. INTRODUCTION

The use of frequencies is still considered optimal. Such as the data submitted by the FCC, that the radio frequency is still below 20% of its course [1]. And so we need a technology that is able to maximize or improve the effectiveness of the use of the frequency band. Therefore made Cognitive radio, as a technology that is expected to overcome these problems. Cognitive radio originally introduced by J. Mitolla [2]. The most important characteristics in Cognitive radio is its ability to sense the environment, making decisions based on observations and mission objectives, and learn from past experience for future decision-making.

According to Simon Haykin [3], cognitive radio has three main tasks, namely radio-scene analysis or spectrum sensing, the estimated channel status and predictive models, transmit power control and dynamic spectrum management. Among the three tasks of cognitive radio, spectrum sensing is the main task before the next task. Because if we make mistakes in the detection of the spectrum where the detector should have detected the presence of primary signal but decided no signal, it will lead to disruption or interference to the primary user communication

Simple spectrum detection could use energy detector on condition unknown signal conditions but known noise variance. However, detection capability have weaknesses in detecting the low SNR condition. So that the detection capabilities should be able to detect low SNR conditions. Moreover, the condition of the realities faced in the detection process is unknown noise parameters. During simulation modeling research many of these parameters with previous knowledge. In fact, when we did not have prior knowledge of the condition of the noise, it will make the design of different detector.

Spectrum detection process can be done by observing the characteristics of the signal parameter affected user. Detection of the OFDM signals can be done by taking into account the parameters used in the system. OFDM modulation can be used in the detection process, in which OFDM has the property repeated in each symbol, ie, cyclic prefix (CP). And its used for detection using calculation of autocorrelation coefficient. In this study, conducted in conditions when the noise is unknown and a maximum length of data known [4]. This technic have improved when length of cyclic prefix known. This technique is based on autocorrelation can not be used when the noise condition is unknown. Because the detection system will be different in different conditions. So that detection research using GLRT detector on conditions noise and signal are unknown [5]. This is best detector when condition are unknown and uncertainty noise. To get a good GLRT detector,

we need data that is very long to get to the threshold conditions there is only noise alone which means that the condition is offline. And we will have difficulties when we move from one location to another places, it is necessary to conduct empirical calculation again on condition there is only noise. In the study [7], that spectrum sensing using the bootstrap can determined the distribution of test statistic with small size sample. This allows detection calculation process performed GLRT detector to determined threshold on condition only noise from received signal.

II. MODEL

Model for the OFDM signal spectrum sensing system requires the ability to detect in low SNR conditions and unknown parameters of noise variance and resistant to changing environmental conditions. Spectrum sensing system is made to detect the presence of the primary users so they can determine whether the frequency spectrum is being used or not. Sensing is done by the system by processing the signal transmitted from the transmitter block and added noise. In studying the spectrum sensing for OFDM signals, it can be generally described as follows:
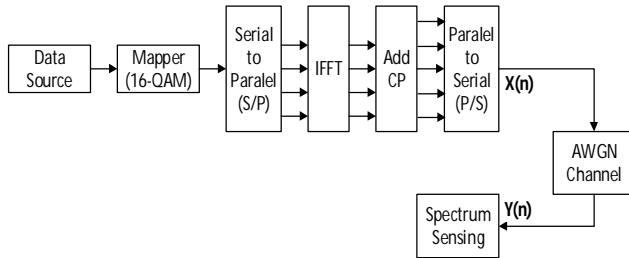

Fig. 1. Common block of OFDM spectrum sensing

Overall system blocks can be divided into 3 parts, namely OFDM transmitter block, transmission channel block, and spectrum sensing system block. The spectrum sensing block uses GLRT detector with bootstrap approach.

OFDM signals have specific properties cyclic prefix that can be used to perform on signal detection. In the presence of these cyclic prefix, autocorrelation can be done to determine whether there is a signal or not. There is some paper that examines the OFDM signal correlation structure such in [4][5]. Below is figure of the OFDM signal with cyclic prefix:
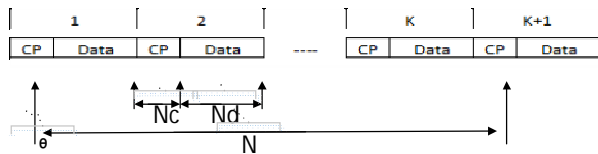

Fig. 2. Model N samples of the received OFDM signal [8]

Nd data length which is the number one symbol of the block size of the inverse fast Fourier transform (IFFT) used in the transmitter and is equivalent to the number of subcarriers. Nc cyclic prefix length and a repetition of the last data sample along Nc. Symbol assumed transmitted data is distributed

Identics and independent (IID), a zero average and has a signal variance σ_s^2, then the auto-correlation function (ACF) is

$$r_x[n,\tau] \triangleq E\left[x(n)x*(n+\tau)\right] \qquad (1)$$

OFDM signal being nonstationer by adding a cyclic prefix and therefore the auto-correlation function $r_x[n,\tau]$ is changing with time. Where specifically, the value is not zero when the lag time τ = Nd to time instant n, and zero for the other. The value is not zero auto-correlation function occurs along the repetition symbol on the cyclic prefix.

III. SPECTRUM SENSING METHOD

In the cognitive radio, the detection of the use of the frequency spectrum can be done by the detect primary user signal, if the signal active users means that the frequency spectrum is being used. So that a simple problem encountered in the detection process decides that this is how it was with the noise signal or just noise was present. Where if there is only noise was present means being in a state of frequency spectrum unused or empty. So there are two possible hypotheses on the simple detection of this, namely:

    1.The presence of signal and noise or
    2.The presence of noise only.

In the detection process that requires a fast time, we need to collect data as efficiently as possible in decision-making with the hope can decide right all the time. And because the data collected in the form of a random signal the arrival of the necessary statistical approaches [10].

If we have common communication system by the following figure:
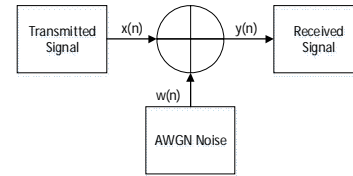

Fig. 3. Block of common communication system

So we can have two hypothesis from that figure as below:

• Noise Only $\rightarrow H_0 : y[n] = w[n], \quad n = 1,...,N$

• Signal Present $\rightarrow H_1 : y[n] = x[n] + w[n], \quad n = 1,...,N$ (2)

Where y[n] is the received signal, x[n] represents the primary user of the transmitted signal and w[n] represents of the noise added to the signal and n represents the time. With the development of the telecommunications system in terms of the techniques that emerged with a new method of signal transmission making structure has diversified mixed signal. Like the example above signal x[n] is the primary user signal which has a specific signal structures. This spesifically can be found both in terms of coding techniques, modulation techniques, as well as certain other signal properties. One property that is the cyclic prefix signal contained in the OFDM modulation is almost used throughout the telecommunications system of the present. This typical of the signal structure could be an opportunity to create an efficient detector design.

A. Basic Signal Detection

In the signal detection we will process the received signal y along a certain time. And the main task of detection signals in this case is to determine whether the observed signal y derived from H_0 atau H_1. So as to decide the detector needs to have a statistical test form Λ(y) of the received data and predetermined threshold η for later comparison. So that the general shape of the detector design formula is

$$\Lambda(y) \underset{H_o}{\overset{H_1}{\underset{<}{\overset{>}{}}}} \eta \tag{3}$$

From the formula above, the presence of a signal can be determined if the test statistic is greater than a predetermined threshold, which means the main user of the frequency band being used and can not be disturbed by the secondary users. Applies vice versa, whereby if the test statistic is smaller than a predetermined threshold then the frequency band is empty and can be used by secondary users cognitive radio.

B. Matched Filter

If we consider the equation 2.5 and are perfectly aware of the probability distribution y was observed under both hypotheses then we can get a good performance of the detector.. This means that the detector should be aware of all the parameters, such as noise variance, the variance of the signal, and the channel coefficients. If a signal is detected x known perfectly then the received signal is $y \sim N(x, \sigma^2 I)$ under H_1. So it will easily show that the optimal statistical test was matched filter output [9].

$$\mathrm{Re}(x^H y) \underset{H_o}{\overset{H_1}{\underset{<}{\overset{>}{}}}} \eta \tag{4}$$

But the reality is very difficult for us to know perfectly all the parameters of the signal and noise.

C. Energy Detector

Energy detector measures the energy received during a limited time interval and compared with a predetermined threshold. This detector assumes that the detected signal does not have the knowledge structures that can be exploited and model it through Zero-mean circularly symmetric complex Gaussian $x \sim N(0, \sigma_S^2 I)$. Then $y \mid H_0 \sim (0, \sigma_n^2 I)$ and $y \mid H_1 \sim (0, (\sigma_n^2 + \sigma_n^2)I)$. So after eliminating unrelated constants obtained test is written as follows [8][5]:

$$\Lambda(y) = \frac{\|y\|^2}{\sigma^2} = \frac{\sum_{i=1}^{LN} \|yi\|^2}{\sigma^2} \underset{H_o}{\overset{H_1}{\underset{<}{\overset{>}{}}}} \eta \tag{5}$$

Operations of the detector is to compare the received signal energy to the threshold. Can be known with good performance as shown in the following detection probability:

$$P_D = P_r\left(\Lambda(y) > \eta \mid H_1\right) = 1 - F_{X_{2NL}^2}\left(\frac{2\eta}{\sigma_s^2 + \sigma_n^2}\right)$$

$$P_D = 1 - F_{X_{2NL}^2}\left(\frac{F_{X_{2NL}^2}^{-1}(1 - P_{FA})}{1 + \frac{\sigma_s^2}{\sigma_n^2}} \right) \tag{6}$$

For OFDM signal detection using energy detector will be close to optimal if perfect knowledge of the noise is known. Conversely, if the knowledge of unknown noise variance then the energy detector can not be used because the noise variance is used to determine the threshold. If the threshold value is determined by the value of the variance that does not comply will result in detector with low performance [5].

D. Detector based on autocorrelation coefficient

At [4] design detector utilizing auto-correlation coefficient OFDM signal or perform the calculation of average of the normalized auto-correlation of the received power as a statistical test.

$$\frac{\sum_{n=1}^{N-Nd} \mathrm{Re}(\hat{r}[n])}{\sum_{n=1}^{N} |y[n]|^2} \underset{H_o}{\overset{H_1}{\underset{<}{\overset{>}{}}}} \eta \tag{7}$$

Advantages of this statistical test is only necessary to know the length of data Nd and do not need knowledge cyclic prefix length Nc. This is very useful when we do not know the length Nc. But the shortcomings of this detector is not exploiting the fact that the OFDM signal nonstationer. This can be seen from all the samples r[n] measured the same when forming the statistical test, so the variation of time is not visible on the detection criteria. And not surprisingly, the variation-time can be exploited and result in better performance [12].

E. GLRT Detector

On [5], proposes using GLRT approach and handle the synchronization mismatch between the transmitter and receiver. Detector is also designed to condition the signal and noise variance is unknown. In contrast to [sachin], this detector to enter characters in the calculation of non-stationary. So that it can produce a better detector of [4].

$$\max_{\tau} \frac{\sum_{i=1}^{Nc+Nd-1} |R_i|^2}{\sum_{k \in S_\tau} \left|R_k - \frac{1}{N_c}\sum_{i \in S_\tau} \overline{R}_i\right|^2 + \sum_{j \notin S_\tau} |R_j|^2} \underset{H_o}{\overset{H_1}{\underset{<}{\overset{>}{}}}} \eta \tag{8}$$

Where

$$R_i \triangleq \frac{1}{K} \sum_{k=0}^{K-1} r_{i+k(N_c+N_d)}, \quad i = 0, ..., N_c + N_d - 1$$

The price paid for performance improvement in this detector is requires knowledge cyclic prefix length Nc. And disadvantages that this detector is in terms of determining the threshold is done empirically. So that at different times and location allows the threshold is not updated according to changes in environmental conditions surrounding noise at any time.
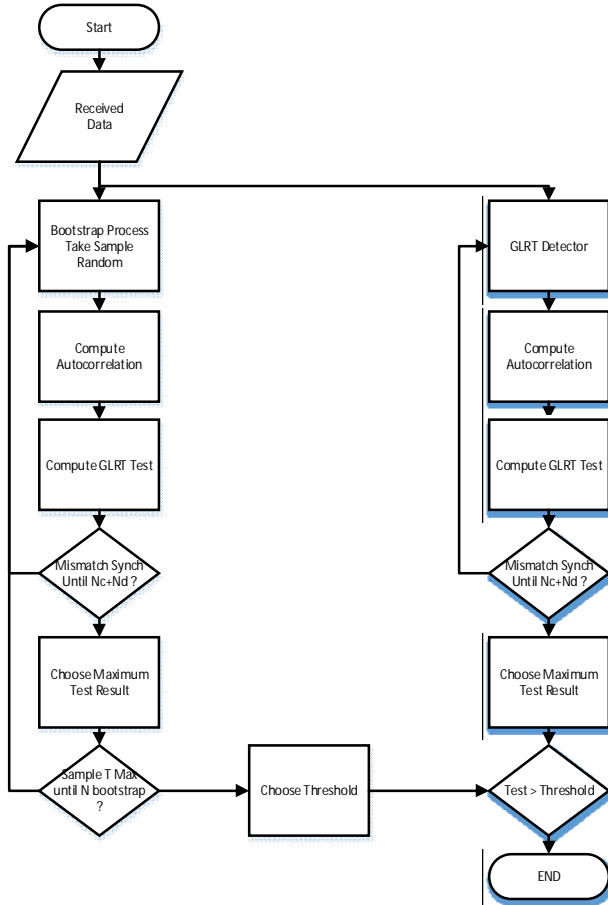

Fig. 4. GLRT detector with bootstrap approach Flowchart

F. GLRT Detector with bootstrap approach

Block of spectrum sensing using a GLRT detector with bootstrap approach where sensing process is done after getting the signal that has been added noise. GLRT algorithm used to perform calculations with unknown parameters such as signal variance and noise variance. While bootstrap test is used to obtain the distribution at the time of H_0 or when there is only noise. Bootstrap process uses input data signal received and carried as many as the number of bootstrap resample desired. Resample process will perform data collection at random on the data signal is received. Resample result data allows repetition of data. After that, then processed using statistical tests GLRT detector. Resample process made possible by the structure and sequence generates a random signal as well, making it possible to produce signals that are not correlated.

And can be regarded just as a noise by the detector. Flow diagram of GLRT detection using the bootstrap process can be seen at fig 4.

IV. SIMULATION

To measure the performance of the proposed detector then there are some simulations carried out that, to measure the effects of cyclic prefix length and gauge the effect of the number of bootstrap resample. Then perform measurements to compare the proposed detector with other detector like Autocorrelation Function, GLRT, and energy. Comparisons were made with a view "Probability of miss detection versus SNR" and "Probability of detection vs Probability of false alarm". In all scenario of simulation running on standar parameters length of OFDM symbol K=10, length of data Nd=32, length of cyclic prefix Nc=1/4Nd, monte carlo number =1000, at probability of false alarm Pfa=0.1 and bootstrap resample number 50.

Result 1 : Effect of Cyclic Prefix length
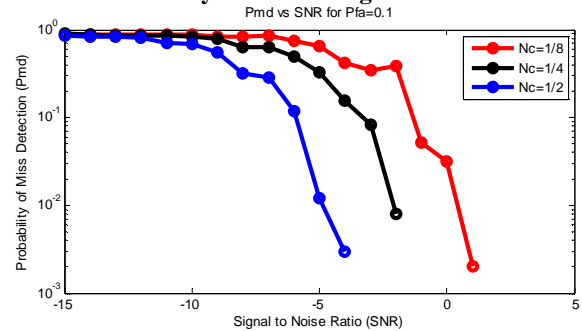
Fig. 5. Comparison effect of Cyclic Prefix length

From the figure 5, we can see at SNR is -4 dB sequentially with cyclic prefix length Nc 1/8, 1/4, and 1/2, resulting in a miss detection probability for 0.418, 0.157, and 0.003. It shows the longer cyclic prefix specified then it will affect the detection of the spectrum is the smaller the probability of miss detection value. If we want to get probability of miss detection around 0.003, there is an improvement from Nc 1/8 to 1/4 is about 3 dB and from Nc 1/4 to 1/2 is about 2 dB and from Nc 1/8 to 1/2 is about 5 dB.

Result 2 : Effect of OFDM symbol number

Fig. 6. Comparison effect of OFDM symbol number

From figure 6 we can see at -2 dB SNR with regard OFDM symbol length K frames 10, 30, and 50. So the probability of miss detection will result in a sequence are 0.498, 0.022, and 0.002. This indicates that the longer frame K OFDM symbol will yield the probability of miss detection are getting smaller and result in an increased probability of detection. And if we w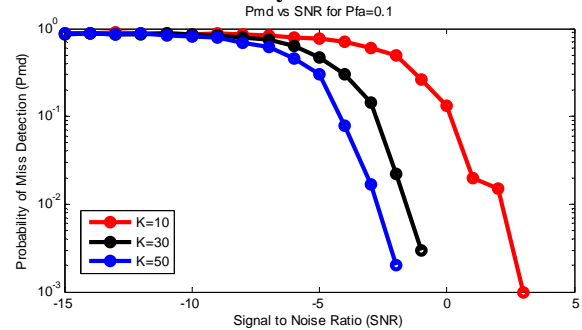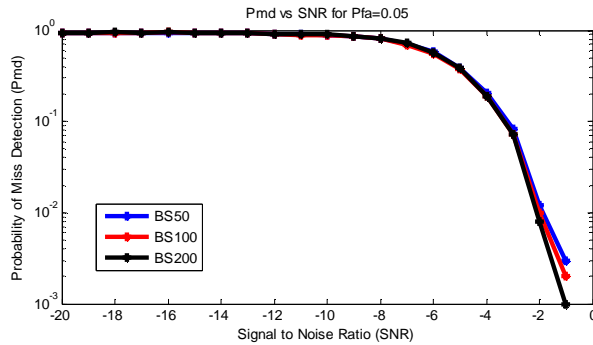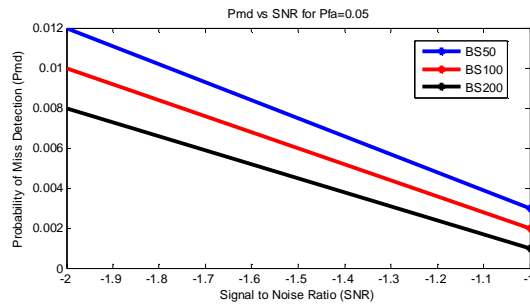ant to get probability of miss detection around 0.002, there is an improvement from K 10 to 30 is about 4 dB and from K 30 to 50 is about 1 dB and from K 10 to 50 is about 5 dB.

Result 3 : Effect of bootstrap resample number

**Fig. 7.** Comparison effect of bootstrap resample number

Fig. 8. Zoom-in from comparison effect of bootstrap resample number between SNR -2 to -1 dB

From the graph in figure 8 we can see that the greater number of bootstrap resample it will make the better performance of the detector. Although influence the number of bootstrap resample hardly noticeable until the value of -4 dB SNR, and visible effect on the -2 dB SNR. It looks at which time -2 dB SNR conditions, probability of miss detection value for the number of bootstrap resample 50, 100, 200 respectively are 0.012, 0.010, 0.008. And as -1 dB SNR conditions, probability of miss detection value for the number of bootstrap resample 50, 100, 200 respectively are 0.003, 0.002, 0.001. Where the greater number of resample number will result in a probability of miss detection is getting smaller. Which means that the detector can produce a greater probability of detection. Differences in performance resulting change in the number of bootstrap resample system shows the results are not too significant on improving the probability of miss detection, wherein a difference for every 50 bootstrap

resample able to provide repair the probability of miss detection 0.001 at SNR -1 dB and 0.002 at SNR -2 dB.
.

Result 4 : Comparison detector

From the graph in figure 9 we can see that the energy detector has the best performance. This is caused by the noise variance conditions that are well known by the detector and the environmental situation has not changed. And GLRT with the proposed bootstrap approach is able to provide almost same performance to the ordinary GLRT.
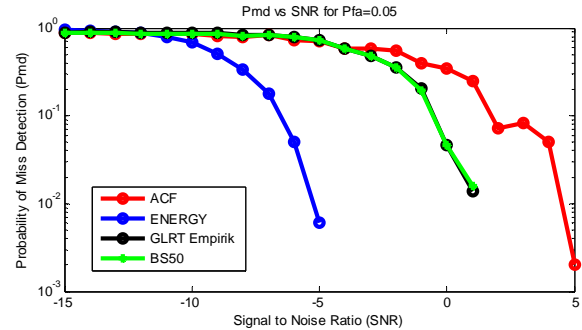
Fig. 9. Comparison of detector on certain noise

Result 5 : uncertainty noise

We can see in figure 10 that GLRT and GLRT with bootstrap approach can exceed the performance of which is owned by the energy detector to -4 dB SNR. And we can see the comparison of the current detector before -4 dB SNR that is at -5 dB SNR, where the energy detector produces the probability of miss detection 0.188, usual GLRT produces 0.123, and GLRT with bootstrap approach produces 0.094. We can see that the ordinary GLRT and GLRT with bootstrap approach could be better than energy detector. At condition SNR -5 dB, GLRT with bootstrap approach improve probability of miss detection almost 0.030 than ordinary GLRT and 0.094 than energy detector.
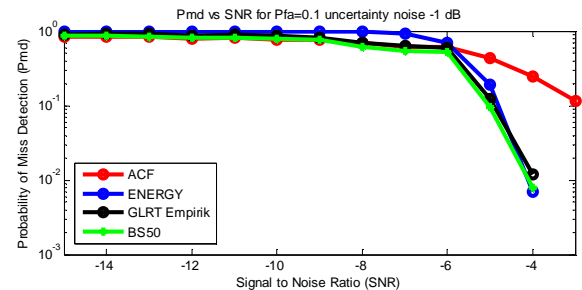
Fig. 10. Comparison of detector on uncertainty noise -1 dB

Result 6 : ROC of Detector

In this scenario, we want to show the comparison energy detector and detector based second-order on ROC graphic. In this simulation running on length of OFDM symbol K=10, montecarlo number=1000, resampling number until 50, and SNR= -5 dB. And from figure 11 show every

detector with receiver operating curve. And show that GLRT with bootstrap approach has almost same curve with ordinary GLRT.

Fig. 11. Comparison of ROC detector based on second order

V. CONCLUSION
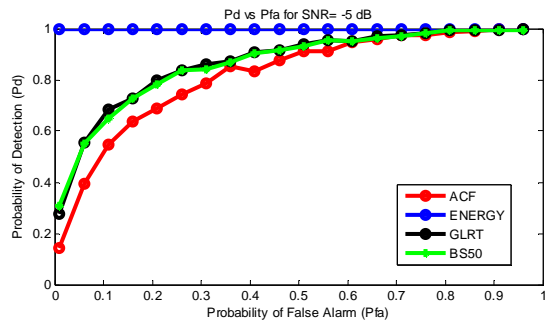
The energy detector has the best performance because the noise variance conditions that are well known by the detector and the environmental situation has not changed. And GLRT with the proposed bootstrap approach is able to provide almost same performance to the ordinary GLRT.

The ordinary GLRT and GLRT with bootstrap approach can exceed the performance of which is owned by the energy detector to -4 dB SNR. GLRT with bootstrap approach even better than ordinary GLRT at the SNR condition -5 dB and uncertainty noise 1 dB, GLRT with bootstrap approach improve probability of miss detection almost 0.030 than ordinary GLRT and 0.094 than energy detector. The GLRT with bootstrap approach has almost same curve with ordinary GLRT.

REFERENCES

[1] FCC, "Spectrum policy task force report," Tech. Rep. 02-135, Federal Communications Commission, November 2002.

[2] J. Mitola et al., "Cognitive radio: Making software more personal,"*IEEE Pers. Commun.,* vol. 6, no. 4, pp. 13–18, Aug. 1999.

[3] S. Haykin, "Cognitive radio: brain-empowered wireless communications , "*IEEE Journal on Selected Areas in Communications*, vol. 23, no. 2, pp. 201–220, Feb. 2005.

[4] S. Chaudhari, V. Koivunen, and H. V. Poor, "Autocorrelation-based decentralized sequential detection of OFDM signals in cognitive radios," *IEEE Transactions on Signal Processing*, vol. 57, no. 7, pp. 2690–2700, July 2009.

[5] E. Axell and E. G. Larsson, "Optimal and suboptimal spectrum sensing of OFDM signals in known and unknown noise variance," *IEEE Journal on selected areas in communication, vol.29, No.2, February 2011*

[6] Manish B. Dave, "Spectrum sensing in cognitive radio : use of cyclo-stationary detector," Thesis, May 2012.

[7] Fiky Y. Suratman, "Spectrum Sensing in Cognitive Radio: Bootstrap and sequential detection approaches," Dissertation, February 2014.

[8] H. Urkowitz, "Energy detection of unknown deterministic signals, "*Proceedings of the IEEE*, vol. 55, no. 4, pp. 523–531, April 1967.

[9] H. V. Poor, *An Introduction to Signal Detection and Estimation*. New York: Springer-Verlag, 1994.

[10] Steven M. Kay, "Fundamentals of Statistical Signal Processing: Detection Theory", Vol.II, Prentice-Hall, Inc., 1998

[11] B Efron, RJ Tibshirani, An Introduction to the Bootstrap, CRC Press, 1994

[12] E.Axell, Geurt Leus, E. G. Larsson, H. V. Poor, "Spectrum Sensing for Cognitive Radio," IEEE Signal Processing Magazine, May 2012

[13] Cho, Y. S., Kim, J., Yang, W. Y. and Kang, C. G. References, in MIMO-OFDM Wireless Communications with MATLAB®, John Wiley & Sons, Ltd, Chichester, UK, 2010.

The Effects of Apodization profile on uniform Fiber Bragg Gratings

Rumadi

Department of Electrical Engineering, Faculty of Science
and Technology
University of Al Azhar Indonesia
Jakarta, Indonesia
ary@uai.ac.id

Ary Syahriar, Dwi Astharini, Ahmad H. Lubis

Department of Electrical Engineering, Faculty of Science
and Technology
University of Al Azhar Indonesia
Jakarta, Indonesia
rumadi13@hotmail.com

Abstract— the sensing applications of fiber Bragg gratings (FBGs) offer a high sensitivity, as well as other important advantages, such as real-time processing, long-term stability, immunity to electromagnetic interference, and convenient multiplexing capabilities. The reflection spectrum of fiber Bragg gratings with a uniform modulation of the refractive index is accompanied by series of sidelobes at the adjacent wavelength. It is very important to minimize and, if possible, eliminate the reflectivity of these sidelobes. The design of fiber Bragg gratings used Coupled Mode Theory. The coupled mode equations were solved by the Transfer Matrix Method since it was considered as good approximation to calculate the spectral response of fiber Bragg gratings. Apodization techniques are used to get optimized reflection spectrum. . The uniform FBGs with several types of apodization were modeled in this project. It was proven that apodization profile could be reduced the sidelobes. In addition, each profile also has the bandwidth and the maximum reflectivity better than others.

Keywords— *maximum reflectivity; fiber Bragg gratings; coupled mode equation; transfer matrix method; apodization*

I. INTRODUCTION

Fiber Bragg gratings are important component in fiber communication and fiber sensing fields. The FBGs are used extensively in telecommunication industry for dense wavelength division multiplexing (DWDM), dispersion compensation, laser stabilization, and Erbium amplifier gain flattening [1-2]

The apodization is a well known technique used in many FBG application, few literature review deal with optimizing sensor performance using apodized FBGs [3-4]. In this final project, we introduce a comprehensive study on the impact of using different apodization profile (Blackman, Hamming and Raised sine) on the performance of uniform FBGs. The performance evaluation parameters tested in this study are uniform FBGs the reflectivity, sidelobes and full width half maximum (FWHM).

II. BASICS THEORY

A. The Uniform Fiber Bragg Gratings

A uniform Fiber Bragg Grating is simple FBG where the period and amplitude modulation index change remains constant for the entire gratings length. In common optical fiber, the UV-induced refractive index changes are uniform or non-uniform inside the fiber core and negligible in the cladding. With this assumption, a perturbation to the effective refractive index n_{eff} of the guided mode of interest, expressed as equation (1) [6].

$$\delta n_{eff}(z) = \overline{\delta n_{eff}(z)}\left[1 + s\cos\left(\frac{2\pi}{\Lambda}z + \phi(z)\right)\right] \quad (1)$$

For a uniform, $\overline{\delta n_{eff}}$ is a constant and $\phi(z) = 0$. A typical schematic of uniform fiber Bragg gratings with input and output signal indicated is shown on Figure 4.1
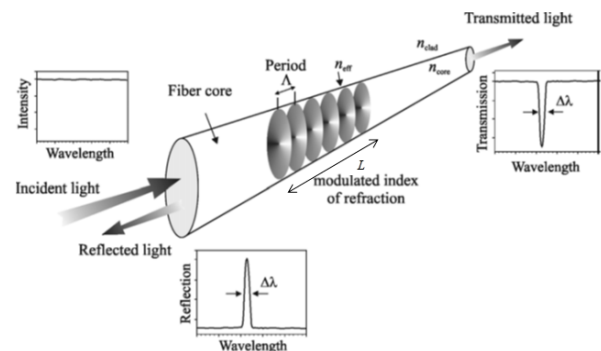

Fig. 1. Illustrating the change induced in the refractive index to create an FBGs in the fiber core [5]

B. Coupled-mode Theory

In this section, we follow the development presented by Gopakumar Sethuraman [7]. The characteristic of the Fiber Bragg Gratings can be understood and modelled by several approach. The most widely used theory is the coupled mode

theory[8-9]. The coupled-mode theory is a suitable to describe the propagation of the optical waves in a waveguide with a slowly varying index along the length of the waveguide [10]. The basic idea of coupled mode theory in fiber Bragg gratings (FBGs) is that the grating serves as a perturbation that electrical field of the waveguide with a perturbation can be represented power between the forward and backward moving modes. The transverse component of the electric field at position in the perturbed fiber can be described by a linear superposition of the ideal guided modes of the unperturbed fiber.

. In a uniform Fiber Bragg Gratings having a constant grating period, forward and backward propagating fields are given by coupled mode equation [6-7]:

$$\frac{d}{dz}R(z) = i\hat{\sigma}R(z) + i\kappa S(z) \qquad (2a)$$

$$\frac{d}{dz}S(z) = -i\hat{\sigma}S(z) - \kappa R(z) \qquad (2b)$$

where, $R(z)$ and $S(z)$ are amplitude of forward wave and amplitude of backward wave.

The general "dc" self-coupling coefficient $\hat{\sigma}$ can be presented by[6][11],

$$\hat{\sigma} = \delta + \sigma - \frac{1}{2}\frac{d\phi}{dz} \qquad (3)$$

where $\frac{1}{2}\frac{d\phi}{dz}$ is describe possible chirp of grating period and ϕ is the grating phase. The detuning can be presented [6-7][11]:

$$\delta = \beta - \frac{\pi}{\Lambda} = \beta - \beta_D = 2\pi n_{eff}\left(\frac{1}{\lambda} - \frac{1}{\lambda_B}\right) \qquad (4)$$

where $\lambda_B = 2n_{eff}\Lambda$ is the design peak reflection wavelength for a very weak grating, $\delta n_{eff} \rightarrow 0$ with a period Λ . For a single-mode Bragg reflection grating, we find the following simple relation [6]:

$$\sigma = \frac{2\pi}{\lambda}\overline{\delta n_{eff}} \qquad (5)$$

$$\kappa = \frac{\pi}{\lambda}s\overline{\delta n_{eff}} \qquad (6)$$

C. Transfer Matrix Method

The transfer matrix method was first used by Yamada [12] to analysis optical waveguides. This method can also be used to analysis the fiber Bragg problem. The coupled-mode equation (2a) and (2b) can be solved by the transfer matrix method for uniform gratings. Solving coupled mode equation for transfer matrix method (TMM) is found. We can get amplitude reflection ρ of the grating is given by [6-7]

$$\rho(\lambda) = \frac{-\kappa\sinh(\gamma_B L)}{\hat{\sigma}\sinh(\gamma_B L) + j\gamma_B\cosh(\gamma_B L)} \qquad (8)$$

where,

$$\gamma_B = \sqrt{\kappa^2 - \hat{\sigma}^2} \qquad (9)$$

The power reflection coefficient $R(\lambda)$ can be written by [6-7]:

$$R(\lambda) = |\rho|^2 = \frac{\sinh^2(\gamma_B L)}{\cosh^2(\gamma_B L) - \dfrac{\hat{\sigma}^2}{\kappa^2}} \qquad (10)$$

At the center wavelength of the Fiber Bragg Gratings the wave vector detuning is $\hat{\sigma} = 0$, power reflection becomes [6]:

$$R(\lambda) = \frac{\sinh^2(\kappa L)}{\cosh^2(\kappa L)} = \tanh^2(\kappa L) \qquad (11)$$

D. Apodization Function

Apodization is a variation of modulation depth along the grating length and is used to reduce the side lobes [13]. The apodized fiber grating can be modelled by the coupled mode theory and then using transfer matrix method is used to solve the coupled mode equation.

Several apodization functions was chosen in this thesis. We will choose the best three of the profiles (Blackman, Hamming and Raised sine profile) that are applicable to references that have been done by Ashry [3]. Although apodization is well-known technique used in many applications FBG, this method is expected to optimize the

performance of FBG Bandpass Filter. There are examples of several samples apodization profile [5]:

Sinc Profile

$$s(z) = \frac{\sin\left(\dfrac{2\pi(z - \dfrac{L}{2})}{L}\right)}{\dfrac{2\pi(z - \dfrac{L}{2})}{L}} \tag{12}$$

Blackman Profile

$$s(z) = \left[\frac{1 + 1.19\cos\left(\dfrac{2\pi(z - \dfrac{L}{2})}{L}\right) + 0.19\cos\left(\dfrac{4\pi(z - \dfrac{L}{2})}{L}\right)}{2.38}\right] \tag{13}$$

Sine Profile

$$s(z) = \sin\left(\frac{\pi z}{L}\right) \tag{14}$$

Raised sine Profile

$$s(z) = \sin^2(\frac{\pi z}{L}) \tag{15}$$

Hamming Profile

$$s(z) = \frac{1 + 0.9\cos\left(\dfrac{2\pi(z - \dfrac{L}{2})}{L}\right)}{1 + 0.9} \tag{16}$$

Positive-tanh profile ($a = 4$)

$$s(z) = \tanh(\frac{2az}{L}) \tag{17}$$

where,

$$0 \leq z \leq L \tag{18}$$

The various apodization profiles are plotted in Figure 3. From the various functions, there are some function whose slope is higher. When we look at the existing references, a function that has a greater slope is able to reduce the sidelobes of the FBG. Figure 3 show that the Blackman profile has the greatest slope. Further, we will optimize the function of the best three from several functions.
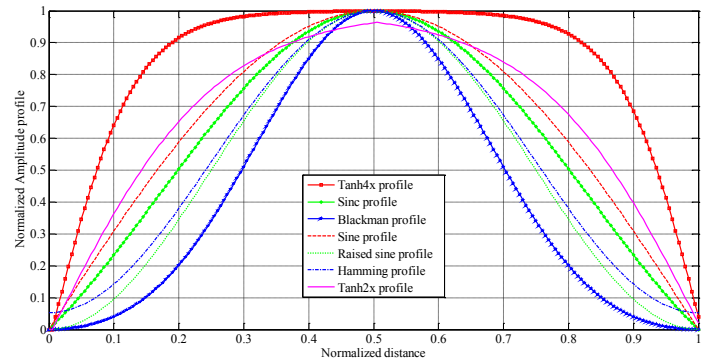
Fig. 2. Several Apodization function

The effect of the apodization in the models of the Bragg gratings can be represented by using z-dependent function $s(z)$ in refractive index. If apodization function is substituted into equation (6), the spectral response of the apodized gratings can be obtained by solving these equations.

III. SIMULATION RESULT

In this paper, the simulation will be limited to single-mode silica-based fiber operating at wavelength of 1550 nm. The grating length (L) is within range 1 mm to 16 mm and index change ($\overline{\delta n_{eff}}$) is 0.0004. And then analysis of the different three apodization profile to see in terms of the maximum reflectivity, sidelobes and FWHM.

A. Uniform FBGs with and without Apodized

Based on the equation (11), Fig. 4 show the reflection spectrum on uniform FBGs with and without apodization. The maximum reflectivity apodized grating is reduced slightly (1→0.99), but the sidelobes are suppressed and the ripple is reduced. This is caused by the reduction in the index change on both sides of the gratings.

Fig. 3. Reflection spectrum of a uniform FBGs (red solid line) and uniform apodized FBGs (blue solid line).

Fig. 4. Reflection spectrum of a uniform FBGs (red solid line) and uniform apodized FBGs (blue dashed line) with power reflection in dB)

B. Apodized Gratings

Based on several reflection spectrum at yield equation (11), we can create a plot of the relationship between the index 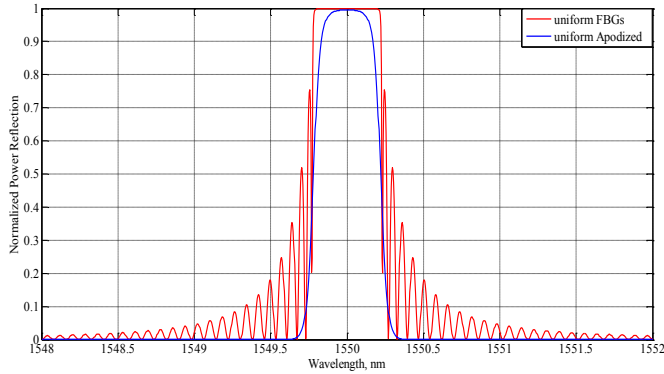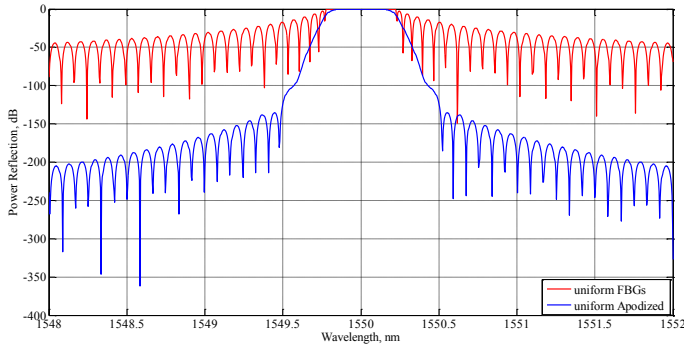change versus maximum reflectivity and grating length on several apodized on uniform FBGs. It shows that the maximum reflectivity is increased if the grating length is increased, until it reaches saturation.

Blackman apodized on uniform FBGs

When $L = 9$ mm, the maximum reflectivity reaches 0.9913. This value has been able to meet the specifications when used for bandpass filters. If we look at the value of FWHM in Fig. 7, the smallest bandwidth is when $L \geq 13$ mm. Because the consideration is FWHM and maximum reflectivity, the best option is when $L = 13$. Where the value of the FWHM is 0.428 nm and maximum reflectivity is 0.9994.

Fig. 5. The maximum reflectivity on Blackman apodized uniform gratings versus length with the index change value is 0.0004.

Fig. 6. The FWHM on apodized Blackman uniform gratings versus length with the index change value is 0.0004.

Hamming Apodized on uniform FBGs

When $L = 8$ mm, the maximum reflectivity reaches 0.9957. This value has been able to meet the specifications when used for bandpass filters. Compared to Blackman apodized, Hamming apodized has bigger maximum reflectivity at the same length.

Figure 10 is a plot of the relationship between the full wave at half maximum (FWHM) and grating length on Hamming apodized uniform grating. At the grating length equal to 11 mm, the value of FWHM been constant with a value of 0.428 nm. Because the consideration is the FWHM and the maximum reflectivity, the best option is when L = 11 mm. Where the value of the FWHM is 0.428 nm and maximum reflectivity is 0.9997.
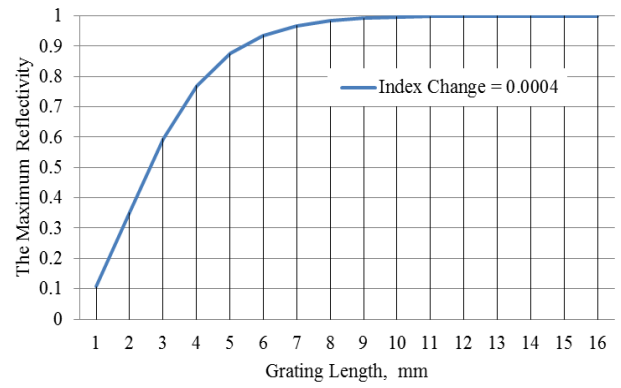
Fig. 7. The maximum reflectivity on Hamming apodized uniform gratings versus length with the index change value is 0.0004.
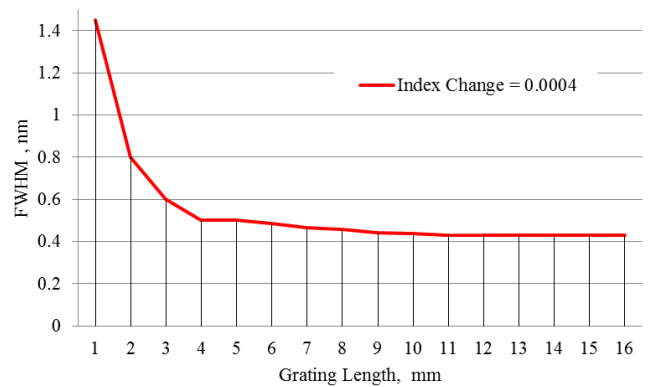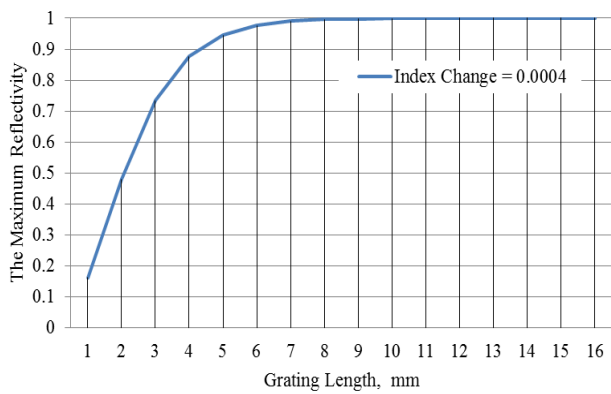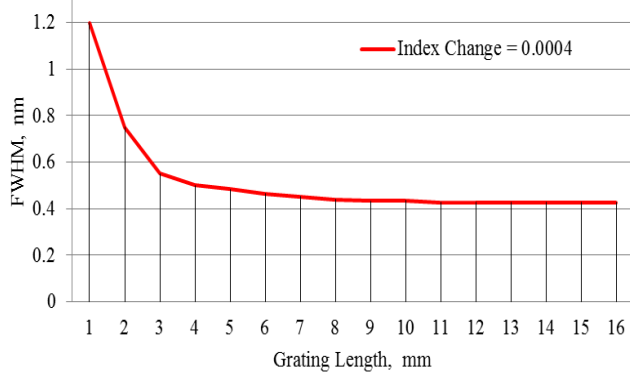

Fig. 8. The FWHM on apodized Hamming uniform gratings versus length with the index change value is 0.0004.

Raised sine Apodized on uniform FBGs

When L = 8 mm, the maximum reflectivity reaches 0.9939. This value has been able to meet the specifications when used for bandpass filters. Compared with Blackman apodized, Raised sine apodized has bigger the maximum reflectivity at the same length but smaller than Hamming apodized.
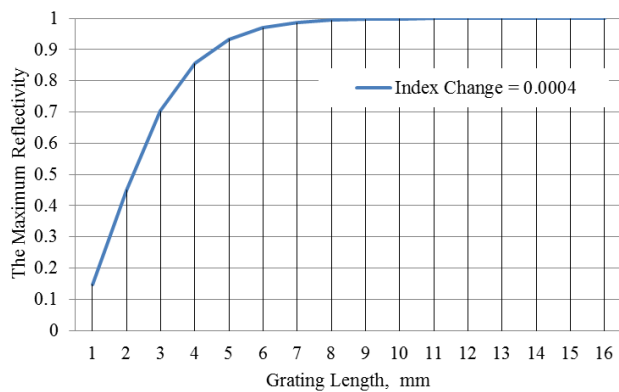
Fig. 9. The maximum reflectivity on Raised sine apodized uniform gratings versus length with the index change value is 0.0004.

Figure 13 is a plot of the relationship between the FWHM and grating length on Hamming apodized uniform grating. At the grating length equal to 13 mm, the value of FWHM been constant with a value of 0.428 nm. Because the consideration is the FWHM and the maximum reflectivity, the best option is when L = 13 mm. Where the value of the FWHM is 0.425 mm and mximum reflectivity is 0.9999.
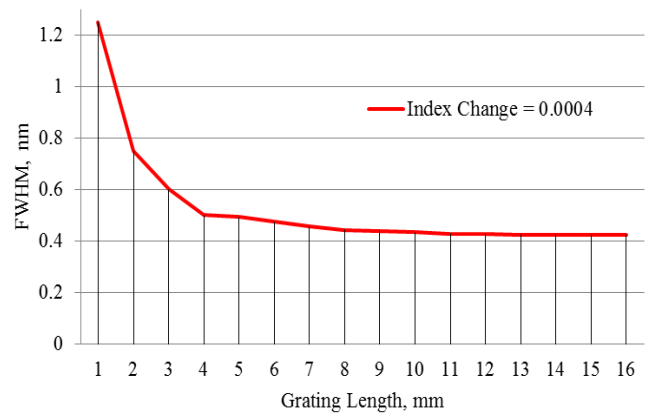
Fig. 10. The FWHM on Raised sine apodized uniform gratings versus length with the index change value is 0.0004.

C. Comparison of three apodization profile

The maximum reflectivity of different apodization profile is compared to use a constant grating length, L and index change, $\overline{\delta n_{eff}}$. By using Transfer Matrix Method, we can obtain the reflectivity of each apodized FBG. Result of comparing apodized uniform FBG and uniform FBG, the peak value slightly down and then sidelobes smaller. Based figure 15 and 16, the maximm reflectivity of each apodized profile is summarized in Table I.

FBG is used for sensing applications must have a high reflectivity, low-level sidelobes and narrow FWHM. The results obtained in the two previous sections showed that the Blackman apodized profile has a minimum level of sidelobes but the peak value is lower than the other.

The apodization has a significant impact on reducing the sidelobes found in uniform FBG. The sidelobes level reductions caused by different apodization profile are illustrated in Fig. 13, when the reflectivity is represented on logarithmic scale.

TABLE I.   COMPARISON APODIZED UNIFORM FBGS

Apodization Profile	Parameter		
	Maximum Reflectivity	*Sidelobes*	*FWHM*
Uniform	1	-3.483dB	0.467 nm
Blackman	0.9956	-136.6 dB	0.437 nm
Hamming	0.9992	-77.95 dB	0.435 nm
Raised sine	0.9988	-95.6 dB	0.434
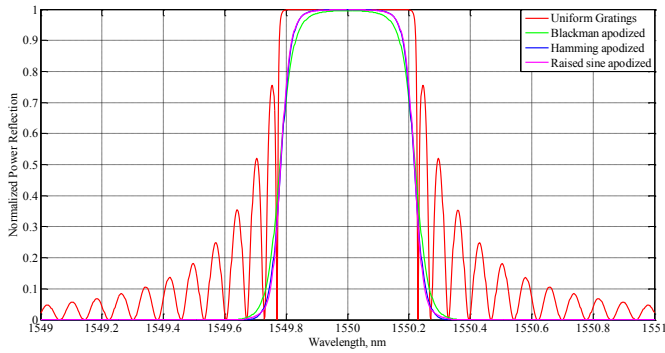
Fig. 11. The reflection spectrum of different apodized uniform FBGs at *L* = 10 mm and index change = 0.0004.
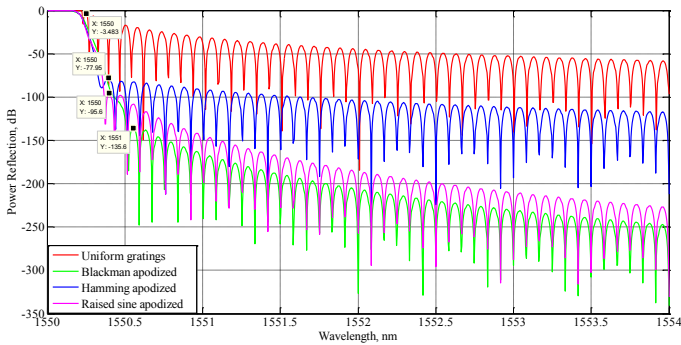
Fig. 12. The reflection spectrum in dB of different apodized uniform FBGs at L = 10 mm and index change = 0.0004.

IV. CONCLUSION

The evaluation parameter used for comparing apodization profile on uniform FBGs are maximum reflectivity, sidelobes level and FWHM. The maximum reflectivity and FWHM are relatively similar, but sidelobes are suppressed and the ripple is reduced.

For Blackman apodized profile with index change ($\overline{\delta n_{eff}}$) equal to 0.0004, the results of the optimization at *L* = 13 mm, has a maximum reflectivity = 0.9994, the FWHM = 0.428 nm and sidelobes = -131.4 dB. For Hamming apodized profile with index change ($\overline{\delta n_{eff}}$) equal to 0.0004, the results of the optimization at *L* = 11 mm, has a maximum reflectivity = 0.9997, the FWHM = 0.428 nm and sidelobes = -80.15 dB. For Raised sine apodized profile with index change ($\overline{\delta n_{eff}}$) equal to 0.0004, the results of the optimization at L = 13 mm,

has a maximum reflectivity = 0.9999, the FWHM = 0.425 nm and sidelobes = -90.28 dB

As sensing application, when viewed in terms of the sidelobes, the Blackman apodized profile is the best than Hamming and Raised apodized profile. In terms of FWHM, the Raised sine apodized profile is the best than Blackman and Hamming apodized profile. In terms of the maximum reflectivity, the Hamming apodized profile has the best result.

Acknowledgment

References

[1] O. Ozolin and G. Ivanovs "Realization of optimal FBG Band–Pass Filters for High Speed DWDM*",* Journal of Electronics and Electrical Engineering, 2009, No. 4(92) ISSN 1392 – 1215.

[2] R. Dongre, A. Sharma, S. Changlani, "Comparatively analysis of without and single & double FBG optical filter in 75 Gbps Optical DCDM based communication system", IJIREEICE, Vol. 2, Issue 1, January 2014.

[3] I. Ashry, A. Elrashidi, A. Mahros, M.Alhaddad, K. Elleithy, "Investigating the Performance of Apodized Fiber Bragg Gratings for Sensing Applications", IEEE Transaction on Magnetic, April 2014.

[4] N. A. Mohammed, T. A. Ali, and M. H. Aly , "Evaluation and performance enhancement for accurate FBG temperature sensor measurement with different apodization profiles in single and quasi-distributed DWDM systems," Opt. and lasers in Engineering, vol. 58, pp. 22–34, Jan. 2014.

[5] A. Othonos, K. Kali, "Fiber Bragg gratings : fundamental and application in telecommunications and sensing", Artech House, 1999

[6] Erdogan *T, "Fiber Grating Spectra"*, Journal of Lightwave Technology, vol. 15, no. 8, 1997, pp. 1277 – 1294

[7] Sethuraman, Gopakumar, "*Fiber Bragg Grating (FBG) Based Chemical Sensor*" (2008), VCU Theses and Dissertations, Paper 1575.

[8] Yariv A., "*Coupled-mode Theory for Guided-wave Optics"*, IEEE Journal of Quantum Electronics, vol. QE-9, 1973, pp. 919 – 933.

[9] Kogelnik H. and Shank C.W., "*Coupled wave theory of distributed feedback lasers",* Journal of Applied Physics, vol. 43, 1972, pp. 2327 – 2335.

[10] Jianfeng Zhao, " An Object-oriented Simulation Program for Fiber Bragg Gratings", Thesis Master of Engineering of Electrical and Electronic Engineering, University Johannesburg : Republic of South Africa, 2001

[11] D.K. Mahanta, "Design of Uniform Fiber Bragg gratings using Transfer Matrix method", IJCER, Vol. 03, Issue 5, 2013

[12] Yamada M. And Sakuda K., "Analysis of almost-periodic distributed fedback slab waveguide via a fundamental matrix approach", Applied Optics, Vol. 26, No. 16, 1987, pp. 3474-3478.

[13] K. Ennser, Mikhail N. Zervas, and R. I. Laming, "*Optimization of Apodized Linearly Chirped Fiber Bragg Gratings for Optical Communications*", IEEE Journal of Quantum Electronics, Vol. 34, No. 5, May 1998.

A Conceptual Framework of Engaged Digital Workplace Diffusion

Dinda Lestarini, Sarifah Putri Raflesia, Kridanto Surendro
School of Electrical Engineering and Informatics
Bandung Institute of Technology
dinda.lestarini@gmail.com, syarifahpr@gmail.com, surendro@gmail.com

Abstract---**Digital workplace creates challenges to improve the way people do their business. By using it, the organization is able to collect, process, and provide data faster, share knowledge, enforce their employee to communicate and collaborate with any devices. Digital workplace can be enabled by implementing many recent technologies such as big data, cloud computing, search-based application, and internet connection. But in this paper, we argue that technology is not enough to help the organization to do its business and reach its goal. According to these arguments, we propose the conceptual framework of digital workplace diffusion. This conceptual framework integrates diffusion theory, user's engagement, and controls. Controls are contained IT governance, risk management, compliance. We believe that user engagement and control are one of the keys for successful digital workplace diffusion. User engagement measurement is able to show the degree of employees' understanding and acceptance to the digital workplace. Meanwhile, control is used to help the organization in managing, monitoring, ensuring the digital workplace is aligned to the requirements and regulations.**

Keywords--- *digital workplace; digital workplace diffusion; user engagement; technologies.*

I. INTRODUCTION

In information age, technology changes rapidly. It affects the way people work which becomes new challenge to begin improvement.The digital workplace is meant to be a virtual equivalent to the physical workplace[1] where employees can work anywhere by using any devices, share knowledge, and browse data faster. This idea is based on the used of several recent trends, Bring Your Own Devices (BYOD), Internet of Things (IoT), people-centric work methods, and analytics [2] which help employees to collaborate, do tasks, and activities effectively.

In this paper, we propose a conceptual framework to digital workplace diffusion. Beside adding the technologies and diffusion theory, we include user engagement-centric and controls in order to succeed well transformation

According to previous research, there is a positive correlation between full user involvement and participation with system success [3]. It becomes the reason for us to consider and focus on user engagement, we believe that the

more users engage, the more chance for digital workplace diffusion to be success.

II. LITERATURE REVIEW

In this section, we will describe and discuss about related theories towards digital workplace diffusion.

A. Digital workplace

Digital workplace is a coordination between technology, process and people [1]. Digital workplace enables employees to work effectively from anywhere, at any time, on any device, and it provides an internet-like participative mode and user experience no matter where their location [4].

Digital workplace creates employees' ability to do their job by collaborating, communicating and connecting with others [5]. To achieve this goal, we need technologies as support. Digital workplace is focused on developing an application for mobile environment. The integration of four technologies; mobile, big data, cloud computing, and search-based application enable us to achieve the desirable feature of digital workplace [6].

B. Diffusion

Technological diffusion is defined as multi-stage process comprised of adoption which uses and widespread in corporation or society [7]. Roger describes diffusion as the process by which an innovation is communicated through certain channel over time among the members of a social system. Diffussion has four elements, (1) innovation, (2) communication, (3) time, (4) social system.

Innovation is as an idea, practice, or object that is perceived as new by an individual or other unit of adoption [8]. Innovation is about figuring out how to add value for an organization. Innovation is the act with idea and successfully bringing them to life to solve problem and create opportunities [9].

In order to introduce the innovation, we need communication channels. It defines as which media to transfer the messages from one individual to another in social system[8].

COMMUNICATION CHANNEL

PRIOR CONDITION :
1. Previous practice
2. Feel needs/problems
3. Innovativeness
4. Norms of social system

KNOWLEDGE → PERSUASION → DECISION → IMPLEMENTATION → CONFIRMATION

Characteristics of The
Decision-Making Unit :
1. Socioeconomic
   characteristics
2. Personality variables
3. Communication
   behavior

Perceived characteristics
of the Innovation :
1. Relative advantage
2. Compatibility
3. Complexity
4. trialibility
5. Observability

Adoption → Continued Adoption
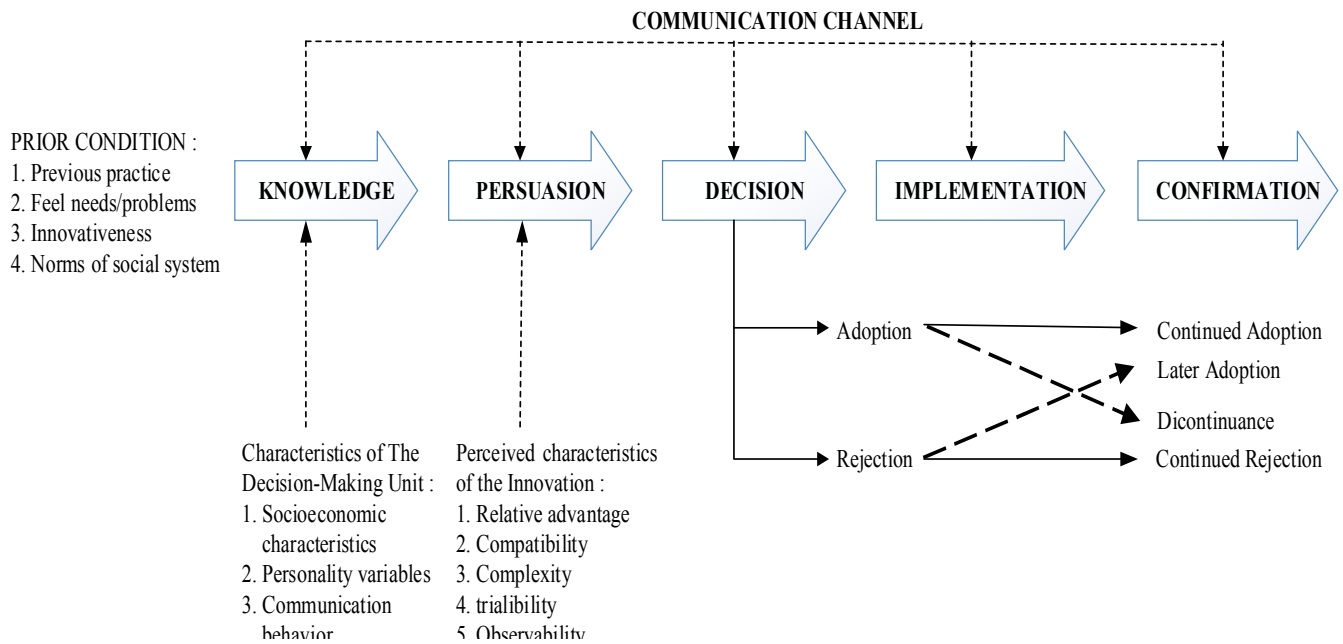Later Adoption
Dicontinuance
Rejection → Continued Rejection

Fig. Innovation Decision Process [8]

The third element of diffusion is time. We can find time dimension of diffusion in the innovation-decision process. The innovation-decision process is essentially an information-seeking and information-processing activity in which the individual is motivated to reduce uncertainty about the advantages and the disadvantages of the innovation. Fig.1 shows five stages of innovation decision process[8].

The last element of diffusion is social system which defines as the environment where the diffusion occurs. The members or units of a social system maybe individuals, informal groups, organizations, and/or subsystems. Diffusion is a kind of social change because the decision to adopt or reject an innovation will lead to changes in structure and function of social system[8].

C. User engagement

In order to engage digital workplace, we need to ensure that users are involved and participated. These are compressed as user engagement. User engagement is defined as the quality of the user experience that emphasizes the positive aspects of the interaction. It is not just about usability, but it also contains how users invest time, attention, and emotion when they are connected to the system [10]. It matters because it is related to the confirmation of adoption status. When a user is engaged, it means they will more understand about what they should do and they will admit the value of the whole system and there will be a chance to the innovation to be well adopted. User engagement has become an issue in the implementation of

IT. It is a cognitive aspect which represents of positive emotion like enjoy and willingness [11]. It will suddenly cause the internal satisfaction. According to previous research, user engagement has 6 attributes, focused attention, aesthetic, novelty, perceived usability, endurability, felt involvement [12]. Table 1 shows the list of engagement attribute and description. This attributes will be used to measure user engagement of digital workplace.

TABLE I. DESCRIPTION OF USER ENGAGEMENT ATTRIBUTES

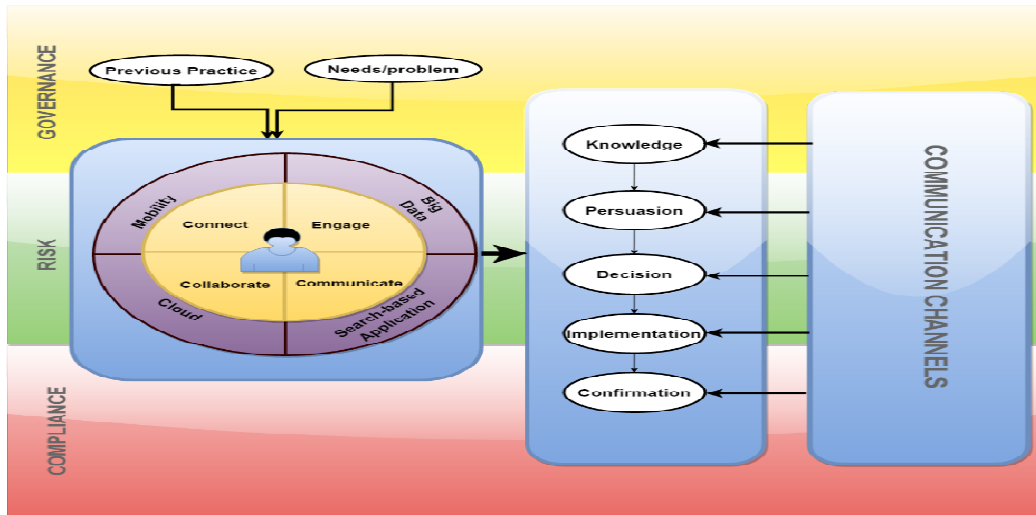| Attributes	Description
Focused attention	The state of total absorption in situation, and full attention [13]
Aesthetics	Aesthetic is defined as the feeling of beauty when a user interact to the system[14].
Novelty	The feeling of surprise and excitement when interacting to interface [12]
Perceived usability	It is defined as the perception when system is not beautiful means the system is not usable. [15]
Endurability	This attribute is defined as the state when the system is worth to try again in the future [16]
Felt involvement	The feeling of self-relevance which affects attention [17]

Fig.2. Conceptual framework of digital workplace Diffusion

III. DESIGN OF CONCEPTUAL FRAMEWORK FOR DIGITAL WORKPLACE DIFFUSION

In this part, we will introduce the conceptual framework for digital workplace diffusion. As we can see fig.2, this model contains integration between diffusion theory, digital workplace concept, and user engagement. These two concepts lie on control which responsible to manage risks, compliance, run good IT governance along digital workplace diffusion.

A. Initial Stage

Before we decide to use the innovation, we have to identify where we are now. This activity enables us to define current status, future target, and how digital workplace helps the organization to reach its goal. The common reasons of digital workplace diffusion are awareness and organization needs. It is an awareness if the organization becomes more active in improving and monitoring the IT trends. In this state, the organization is more open to the digital workplace because it has advanced understanding to the advantage of implementing digital workplace.

Organization needs are caused by dissatisfaction to current practice. In this state, the organization will examine a new technology to fulfill its needs. Digital workplace diffusion enables the organization to improve the used of technology from a previous state to the desired state. It involves new technologies and employees' habits which are enable the core competencies of the digital workplace.

B. Digital Workplace Technology

Nowadays, many new technologies emerged to support business. Those technologies, such as cloud computing, big data, mobile, and search-based application, create an opportunity for organization to create a digital workplace.

Along with those technologies, we also need to consider business goal and capability of organization in order to build a digital workplace that can be accepted by employees and give a positive impact for organization.

Digital workplace is focused on developing applications in mobile environment. Cloud computing enables people to access data or application by using any devices which are already used by employee, such as PC, tablet or smart phone. It also enables people to connect and work together no matter where they are.

Organization also needs many data to support its business. These data comes from many different sources and in different formats. Big data helps employee to collect, process and visualize data faster. Given the amount of data involved, we need to develop search-based application in order to help employee access those data faster.Integration of those technologies will make a big improvement to organization's performance.

C. Innovation Decision Process

In this part, we will discuss about innovation-decision process. It contains knowledge, persuasion, decision, implementation, and confirmation. In every activity, there will be a communication channel to facilitate us to introduce and give an understanding about the digital workplace to employees as adopters.

1. Knowledge

In this stage, we will introduce the idea of digital workplace to the decision-making unit. The decision-making unit is represented as IT manager or IT supervisor. This stage is an important state because it determines how the process will proceed and it matters because if decision-making unit is failed to receive the basic understanding about benefits and business impact of digital workplace,

they will reject to use it. According to this issue, we have to focus on how we present the idea. Moreover, we have to take concern at socioeconomics, personality variables, and communication behavior in order to identify the type of adopters. It matters to help us in choosing suitable communication channels.

Socioeconomics is about how to identify education level, income, and occupation. Moreover, personality variables are used to find personality type. At this activity, we can use five-factor model (FFM). FFM is widely known as psychology model to identify human personality. This model contains openness to experience, conscientiousness, extraversion, agreeableness, neuroticism.

After we identify employees' personality type, we can continue to check on communication behavior. It contains three characteristics; communication quality, the extent of information sharing between employees, and participation in planning and goal settings [18]. After we analyze three characteristics of decision-making unit, we can find the type of digital workplace adopter.

According to the type of adopters, we may choose communication channels to present the digital workplace. Earlier adopter will more interest in a cosmopolite mass media channel. Meanwhile, later adopter will more interest in cosmopolite interpersonal channel.

2. Persuasion

Persuasion stage aims to form the attitude of decision-making units toward digital workplace. After they gain some understanding about digital workplace through knowledge stage, they will more involve with the idea of the digital workplace. They will find more information about digital workplace. Table 2 shows the characteristics of the digital workplace which have to be covered. Finding the characteristics of the digital workplace as innovation is important to decrease the degree of uncertainty for individual. In this stage, we can use interpersonal channel to communicate with decision-making unit.

TABLE 2. CHARACTERISTICS OF DIGITAL WORKPLACE

Characteristics	Description
Relative Advantage	How digital workplace increasing user engagement and job satisfaction which can lead to productivity and profit organization
Compatibility	Digital workplace meets organization needs and must be compatible with existing value and system
Complexity	Digital workplace must be easy to be understood and used. Additionally, along the implementation and use, there will be many changes which come from business and technical, so digital workplace must be easy to customizable
Trialability	At the persuasion stage, the idea of digital workplace

	seems to be uncertain, to minimize the risk which will lead to rejection, we must add prototype. By using prototype, we can present and demonstrate digital workplace. Moreover, we must enable the users to try or even use it to prove the list of advantages.
Observability	As we discuss at trialability section, we enable the organization to try the prototype and understand the mechanism. It will ensure that organization are able to check on what digital workplace can do for the organization.

3. Decision

Organization will decide to adopt or reject the implementation of the digital workplace for their organization at decision stage. In this stage, we will use interpersonal communication channel. If the organization decides to adopt, we may prepare the requirements to implement the suggested innovation. In contrary, the rejection can be a passive and active rejection. Passive rejection is the state when the organization refuses to adopt an innovation at the first presentation of innovation. Meanwhile, the active rejection is defined as the state when the organization considers adopting the innovation but at the end organization decides to not implementing the innovation [8].

4. Implementation

When the organization decides to adopt digital workplace, the next step is to implement it in organization. The organization and developer must discuss IT infrastructure, configuration, standard operations, and set up a support system to ensure the digital workplace runs properly. We also need to communicate the changes which are caused by implementation of digital workplace to all employees. In this stage, we can combine interpersonal and mass media communication channel.

5. Confirmation

After implementing digital workplace in organization, we have to review and monitor the impact of digital workplace implementation. It will ensure that organization make a right decision. Organization can reverse the decision if they find the implementation of digital workplace has failed to boost the desired performance.

In this stage, we also propose user engagement measurement. Implementation of IT, including digital workplace, needs full participation of employees as users. We propose the use of user engagement measurement which is formulated by Heather O'Brien. Using this measurement, we will measure every attribute of user engagement.

D. Control

This part describes about control as the element to help organization in managing, controlling, and ensuring the digital workplace diffusion is aligned to the internal and external standard. The internal standard can be

organizational standards policies and procedures while external standard can be a government's regulation.

1. IT Governance

We need IT governance along the implementation of the digital workplace as an innovation. IT governance helps organization to ensure the use of IT is effective, efficient, and meet its goals. IT governance enables the organization to fix organization's culture issue along with digital workplace as IT product implementation and measure IT and business performance. Digital workplace as IT product requires an enterprise-wide focus, by implementing digital workplace organization must have solution for issues which are related to business and strategic. There are many frameworks which are related to IT governance, such as COBIT, ITIL, etc. Every organization is unique, so we can discuss with the board about what kind of IT Governance that might be suitable.

2. Risk Management

Every project has risks and if it is being left uncertainty and ignored, it will become seeds of failures for organization. Digital workplace diffusion is a big project with high level of cost, risk management must be run to help the organization in identifying, monitoring, prioritizing, minimizing risk, formulating guide, strategy, and policy, and more important is providing a solution of risks using technology, human and organization resources. There are many frameworks for IT risk management, such as Cobit, Coso's Enterprise Risk Management (ERM), Risk Management Framework (RMF), etc.

3. Compliance

The implementation and operation of the digital workplace must comply to organization policy and regulation in which it is implemented. When we decided to use digital workplace, we must define all the relevant rules and regulations, such as privacy law, Data Protection Act (DPA) etc. Thereafter, those rules and regulations along with organization policy will serve as guidelines for developer to develop the digital workplace. In operation of digital workplace, we also need to monitor employee's compliance to organization policy and regulation to avoid misuse of the digital workplace.

IV. CONCLUSION

In this proposal, diffusion theory is suggested as an approach in introducing and implementing digital workplace. We also propose the use of user engagement-centric and control. User engagement-centric helps organization to measure the degree of user involvement and acceptance to the digital workplace. Meanwhile, control which contains IT governance, risk management, and compliance help organization to align digital workplace and its business, evaluate, and monitor the activities in the digital workplace. Further research of this proposal is the

validation of the model and the impact of digital workplace to organization culture.

REFERENCES

[1]   N.Dotson, Building a Better Digital Workplace., San Fransisco, CA, CMSWire.

[2]   D.Lavenda, "What Gartner Wants You to Know About the New Digital Workplace." Internet : http://www.cmswire.com/social-business/what-gartner-wants-you-to-know-about-the-new-digital-workplace/, May 28, 2015 [Sep. 5, 2015].

[3]   M.I.Hwang and R.G.Thorn, "The effect of user engagement on system success: a meta-analytical integration of research findings." *Information and Management Journal*, vol.35, pp.229-336, Apr.1999.

[4]   J. Mcconnell, "Digital Workplace - Trends and Transformation," Washington D.C, 2013.

[5]   F. Herrera et al, "The digital workplace: Think, share, do,"Deloitte, Canada, 2011.

[6]   M.White."Digital workplaces: Vision and Reality".*Business Information Review,* vol.29, 205-214, Des.2012

[7]   M.S. Elliott and K.L. Kraemer. Computerization Movements and Technology Diffusion: From Mainframes to Ubiquitous Computing. New Jersey: American society for Information Science and Technology. 2008.

[8]   E.M.Rogers. *Diffusion of Innovations*. New York: Free Press, 2003.

[9]   R.B. Tucker. Innovation is Everybody's Business: How to Make Yourself Indispensable in Today's Hypercompetitive World.Hoboken, NJ: John Wiley & Sons, 2011, pp.12-13.

[10]   J.Lehmann, M.Lalmas, E. Yom-Tov, G.Dupret,"Model of User Engagement," in *UMAP'12 Proceedings of the 20th international conference on User Modeling, Adaptation, and Personalization*, Montreal, CA, 2012, pp.164-175.

[11]   B.Laurel, *Computer as Theater*. Boston, MA: Addison-Wesley Longman, 1993.

[12]   H.L.O'Brien and E.G.Toms,"The Development and Evaluation of a Survey to Measure User Engagement," *Journal of the American Society for Information Science and Technology*, vol.61, pp. 50-69, Jan 2010.

[13]   M.Jennings, "Theory and models for creating engaging and immersive e- commerce websites," in *SIGCPR '00 Proceedings of the 2000 ACM SIGCPR conference on Computer Personnel Research*, New York, USA, 2000, pp. 77-85.

[14]   R.Hunicke, M. LeBlanc, R.Zubek, "MDA: A Formal Approach to Game Design and Game Research," in *Proceedings of the 2004 AAAI Workshop on Challenges in Game Artificial Intelligence*, San Jose, USA, 2004.

[15]   O.Eliav and T. Sharon, "Usability in Israel," in *Global Usability*, I.Douglas and L.Zhengjie, Eds.London: Springer, 2011, pp.169-194.

[16]   Y.Hung, W.Li, Y.S Goh,"Integration of Characteristics of Culture into Product Design: A Perspective from Symbolic Interactions,"in*Cross-Cultural Design, Methods, Practice, and Case Studies*, vol. 8023.P.L.P.Rau, Ed. Berlin: Springer,2013,pp.208-217.

[17]   R.L.Celsi and J.C.Olson."The Role of Involvement in Attention and Comprehension Processes."*Journal of Consumer Research*, vol.15, pp.210-224, Sep.1988.

[18]   J. J.Mohr and R.E.Spekman, "Characteristics of Partnership Success : Partnership Attributes, Communication Behavior, and Conflict Resolution Techniques." *Strategic Management Journal*, vol.15,pp.135-152, Feb.1994

An Emulation of Transparent Interface Design Based on TCP/IP Implemented onto FPGA of an Altera Nios® Board

Arthur Silitonga[1,2], and Mervin Hutabarat[2]
1) Study Program of Electrical Engineering - President University, Bekasi 17550, Indonesia
2) School of Electrical Engineering and Informatics – Institut Teknologi Bandung, Bandung 40132, Indonesia
arthur@president.ac.id

Abstract—**A TCP/IP-based interface design has been designed, and the interface can process data based on the Ethernet IEEE 802.3 Standard. This interface is able to identify Ethernet Frame IEEE 802.3, Header of LLC 802.2, Header and the Packet Data of IP Datagram. In addition, the interface can perform simple encryption process, and renew FCS (Frame Check Sequence) data of an ethernet frame. After the interface design had been simulated, it was implemented onto Altera Stratix EP1S10F780C6ES FPGA of an Altera Nios® Board. The interface's synthesis result shows that the interface's internal frequency is up to 78.01 MHz. Moreover, the implementation result was verified using SignalTap II Logic Analyzer. The interface functions as an emulator properly which can operate in half duplex mode.**

Keywords—**Altera Nios® Board, TCP/IP, FPGA, Ethernet, and Encryption.**

I. INTRODUCTION

The advance of information technology including the improvement of data communications is rapidly increasing. This opportunity influences the development of other life aspects. Indeed, the advance of the information technology itself impacts also on technology developments of designing and implementing electronics-based system.

Usage of internet, considered as one medium or system of data communications, results many advantages, such as high speed of data transmission, data security, widespread connectivity, and reliable data exchange mechanism. However, when the data which will be exchanged are confidential, a reliable secure transmission process from data theft is extremely needed.

Within its implementation, the performance of internet network which will be used is definitely influenced by devices or equipment used within the network. The equipment which will be used can be viewed as from the physical aspect, i.e. the hardware aspect. Protocols which will be used for data communications are also considered as important part of implementing the internet network.

The facility of applying data encryption generally can be performed by involving the usage of a terminal, for instance, PC (*personal computer*) equipped with adequate software applications or programs. Indeed, if we would like to create a transparent module which can be used as a combination between hardware unit and software application applying the facility of simple data encryption.

Creating the transparent module considers to many limitations, and the module will reduce some design constraints, such as cost, space, and complexity when we implement embedded system of the transparent module.

The designed module will be an hardware-based integrated system designed using VHDL which may perform data encryption of user data together with handling the information relating communication protocols or standards which are used. Furthermore, the module is implemented on an Altera Nios® Board shown in Fig. 1.1.

The main aim of designing the module is an interface module used to separate and remerge Header + Trailer of TCP/IP-based ethernet frame. After the part of the frame has been separated, a certain data processing, i.e. simple encryption to user data has to be performed. This interface will be implemented onto FPGA.
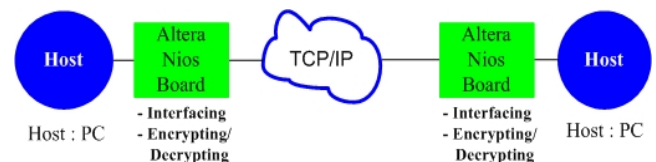
Fig. 1.1 Concept of Interfacing and Encrypting/Decrypting

The interfacing process of the module will be focused on the interfacing of Layer 2 (*Data-link layer*) and several parts of Layer 1 (*Physical layer*) based on the Ethernet protocol IEEE 802.3 for the chosen connectivity of Ethernet 100 Mbps. The encryption process is performed by using a FPGA where the process sketched in Fig. 1.2. However, the encryption is only a simple encryption process applied to *User Data* using a hardware description language, i.e. VHDL.

Fig. 1.2 Method of Encrypting User Data

II. TCP/IP AND ETHERNET

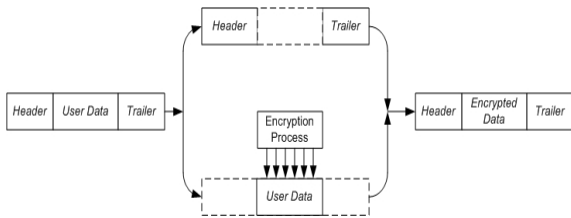In this transparent interface design, there are several parts or aspects of communication protocols. The protocols are focused to fundamental concept of TCP/IP and Ethernet IEEE 802.3.

A. TCP/IP and OSI

A certain system which is occupied in the process of data communication may vary and be complex depending on hardware and software aspects.

ISO (International Standard Organization) divides data communication system into seven layers modeled as stacked layers from the highest one (application layer) to the lowest one (physical layer) called as Open System Interconnection (OSI). Every layer does its own functionality or role in the communication process. Every single layer of the OSI works based a specific type of protocol to interact to peer layer of another node or system.

Instead of the ISO-OSI standard introduced to data communications, The U. S. Department of Defense (DoD) through a Defense Advanced Research Project Agency (DARPA) developed already a type of communication network called as ARPANET which then merged to other standards of communication network issued by other organizations. The merged system became a wide scope of computer networks called as internet [6].

The protocol mainly used in internet is called Transmission Control Protocol/Internet Protocol (TCP/IP). With the wide usage of internet, a lot of protocols in terms of TCP/IP used as the fundamental procotols for ISO-OSI. There are actually no interrelations between TCP/IP and standards issued by ISO. However, we can highlight the levels of TCP/IP to the equivalent levels of ISO-OSI shown in Fig. 2.1.
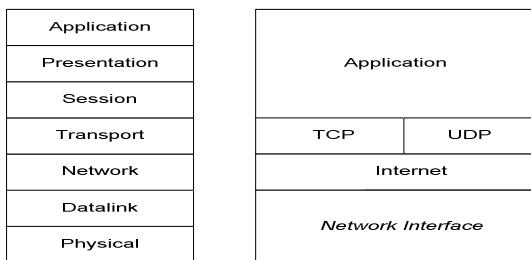
OSI Layer   TCP/IP Protocol

Fig. 2.1 Layers of Communication Systems
based on two different standards/protocols[1]

B. Ethernet

The TCP/IP protocol is one of transparent protocols to in respect to data-link layer existed on a communication network, for instance a LAN (local area network). Concept of transparent protocol means that TCP/IP protocol is able to be operated together with any type of protocol used on the data-link layer. Several types or standards used for data-link layer can be mentioned as follow as : ISO HDLC, X.25, IEEE 802.X, etc.

Within this design, standard or protocol used for the data-link and physical layers defined in the form of Ethernet 100baseT stated in the standard of IEEE 802.2 and IEEE 802.3. Functionally, the data-link layer of Ethernet LAN can be handliand Medium Access Control (MAC). LLC functions as controller of data flow between two LAN stations logically, and MAC keeps the addressing between two LANs and adaption of the network based on the characteristics of the physical medium.

Examples of canonical frame format of Ethernet data-link layer according to IEEE 802.3 can be expressed in the Fig. 2.2 and Fig. 2.3 [2][4][5].
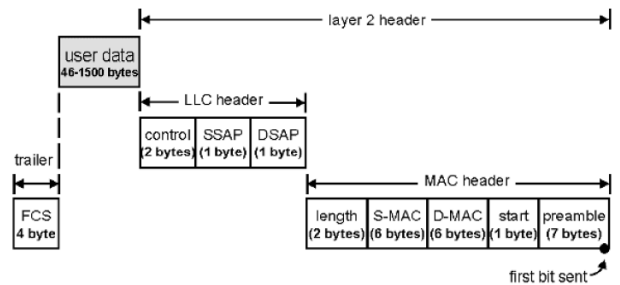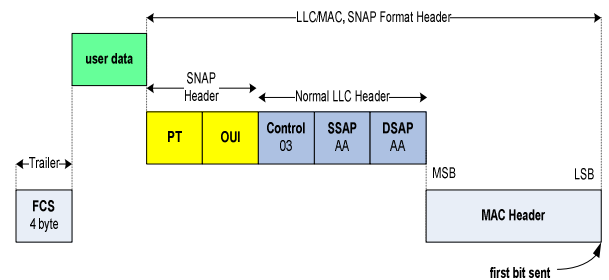

Fig. 2.2 Frame Format of Ethernet (Data-link Layer)

Legends :
D-MAC   : Destination Address MAC
DSAP   : Destination Service Access Point
FCS   : Frame Check Sequence
LLC   : Logical Link Control
MAC   : Medium Access Control
S-MAC   : Source Address MAC
SSAP   : Source Service Access Point
SNAP   : Sub-network Access Protocol

Fig. 2.3 SNAP Format of Ethernet IEEE 802.3

III. THE DESIGN & ITS SIMULATION

For our interface design and development, the concept of work flow can be expressed as follows as: the first step of our concept design is started with defining specification of our system design. The work flow of our design and development has been ended as the system fulfilled already important criterias seen from the verification process of the hardware implementation using FPGA of a Altera Nios® Board.

A. Design Specification

The first design step is begun with defining design specification. The design definitely concerns on data interfacing resulted from ethernet controller of an Altera Nios® Board. Data resulted from the controller are 4 bit – data which will then be encrypted on specific parts of the data frame.

Data handling of this design is not focused on the data resulted from the Ethernet PHY. The data are actual data conforming to the IEEE 802.3 Ethernet Standard. These actual data will be stored into ROM (Read Only Memory) of FPGA. The content of the ROM (LPM_ROM) is the data conforming to the IEEE 802.3 Ethernet Standard, and the ROM needs to be initialized with the standardized data.

The encryption process of the data is not the main focus of this design and implementation. Moreover, this design is not implemented for 10 Mbps of Ethernet connectivity. However, the design will be implemented based on the method of 100 Mbps Fast Ethernet.
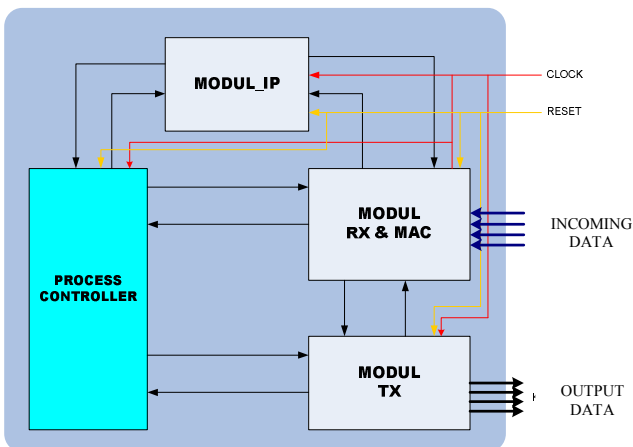

Fig. 3.2 Main Modules of Interfacing System Implemented onto Altera Nios® Board

B. Functionality of the Designed Interface

The designed system consists of two main units. The first unit is located at the host/computer of the transmitter (TX), and the second unit is located at the host/computer of the receiver (RX). The first unit and the second unit are reversible.

The system diagram of the interface can be depicted in Fig. 3.2.

Generally, modules which construct the interfacing system consist of four important modules. The modules are Process Controller, RX-MAC, IP, and TX.

Every module has its own specific functionality. The functionality of each module can be defined as :

- *Process Controller*, functions as controller of signal usage which is not related to data of the RX-MAC Module, IP Module, and TX Module.
- *Modul RX-MAC*, is a module which processes input data, which will then identify the existence of Ethernet Frame conforming to the MAC IEEE 802.3 protocol within the data flowing through the system.
- *Modul IP (Internet Protocol)*, is the module which functions as the regulator and identifer of data which may load IP datagram packet, and the Header of LLC IEEE 802.2.
- *Module TX*, is a module which functions to regulate the data transmission out from the interfacing system. The data transmission is related to bits of MAC (four bits), and physical data relating to 4B5B code.

Process Controller module is composed of several submodules which control signals activating and deactivating submodules of RX-MAC module, IP Module, and TX Module.

RX-MAC module is composed of several submodules such as STP8, CHECKFRAME, ADDMATCH, COUNTERSAMA, COUNTDATA, COUNTERDATAFR, CRCSTANDARLSB, CHIPER_ENKRIPSI, and BUFFER_RESTART.

IP module consists of some significant submodules, i.e. the modules of INDI_SSAP_DSAP, INDI_SNAP, CHECK_SUM, CK_HEADER_LENGTH_IP, COUNT_HEADER_LENGTH, and COUNT_DATA_IP. TX module consists of the selector submodule, and 4B5B encoder submodule.

C. Identification Process

Identification process of our interface design is the process occured whenever data inserted to the interfacing system.

The identification process is based on several steps which can be mentioned as follows as :
- *Preamble identification*. This type of identification will consider to detect first seven bytes of an Ethernet frame, and to detect the byte of Start Frame Delimiter (SFD).
- Whenever the process of preamble identification has been done, the identification of Destination Address, and Source Address of Ethernet frame shall be performed. The destination address and source address occupy six bytes for each type of the address.
- The next step is related to identification the information of the frame length, status of DSAP-SSAP and SNAP used for the header of LLC, counting the

length of IP header, identification of IP header, and encryption of IP datagram packet.

- FCS checking has to be performed, as the process of encryption has been done. New FCS has to be created whenever the old FCS is not error.
- The last step relates to the encoding from four bits to five bits following the 4B5B encoding protocol.

IV. SIMULATION, IMPLEMENTATION, AND VERIFICATION

A. Simulation

Simulation of the design was performed using ModelSim SE 6.0 Mentor Graphics. The ModelSim SE 6.0 was used to simulate the VHDL-based interface design. Within the simulation, every submodule of the integrated system will be accessed based on the functionality and time constraint.

In the Fig. 4.1, detection of valid IP Packet is shown, and the yellow circle indicates the length of IP header which is 0x14. This result is compared with the data stream used for the verification of this simulation. The comparison shows that the detection of IP packet can be made correctly based on the standard, i.e. RFC-1042 [3][5].
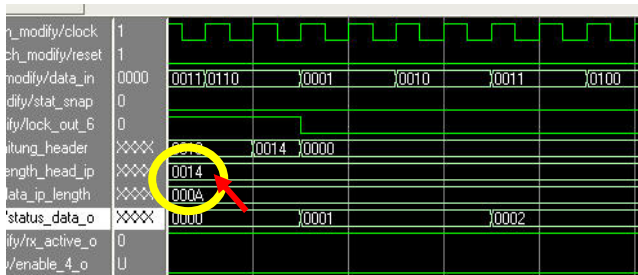

Fig. 4.1 Detection of Header Length of IP Packet

For the simulation verification of Ethernet Frame, one instance of a frame was sent to the receiver, and checked. According to the Fig. 4.2, whenever the FCS sent to the receiver, the RX-MAC module of Process Controller compares the FCS to the other FCS resulted by checking Ethernet Frame from the SYN to the data section of the Ethernet Frame. It is indicated by the red ellipse below that the compare signal will be equal to logic "1" whenever the FCS from the Ethernet Frame is equal to the FCS processed by the Process Controller. Compare signal will be equal to logic "0" if the FCS from the Ethernet Frame is not match to the FCS generated by Process Controller.
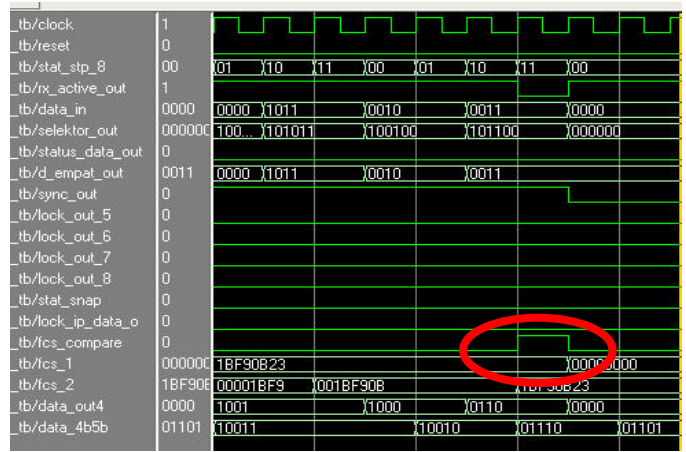
Fig. 4.2 No Error FCS Detection of Ethernet Frame

In case there is a difference or with an error, i.e. the FCS from the Ethernet Frame differs than the FCS generated by the Process Controller, the compare signal will be equal to logic "0". FCS Detection of Ethernet Frame With Error can be seen in Fig. 4.3 marked by the red ellipse below.
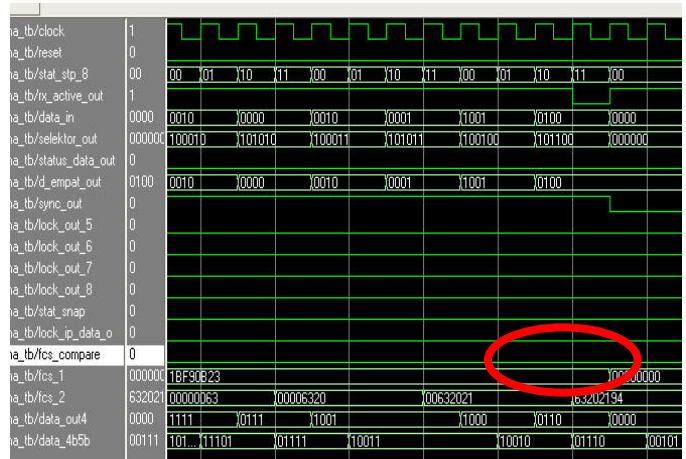
Fig. 4.3. FCS Detection of Ethernet Frame With Error

A certain encryption process can be also made and verified as shown as in Fig. 4. 4. In this figure, it is shown that the data_in as the input is encrypted, and the data_out as the output. To simplify the concept of interfacing and encryption, the method of the encryption is based on a XOR operation.

Fig. 4. 4. Simulation of Encryption Chiper

B. Implementation

The implementation of this interface design will be done onto the *FPGA Altera Stratix EP1S10F780C6ES* of an Altera Nios® Board. The real-time implementation was verified by using in-system verification with the *SignalTap II Logic Analyzer*.

Fig. 4.4 Altera Nios® Board

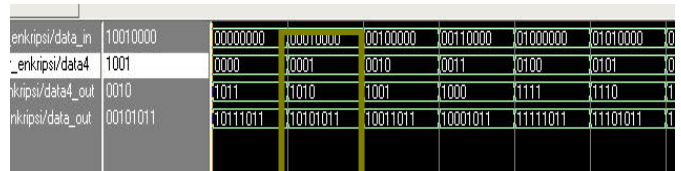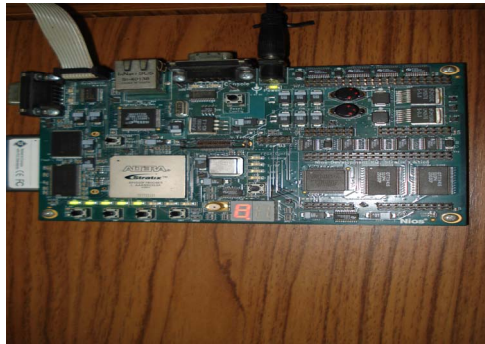Synthesis of the TX-RX at one side and TX-RX at another side was performed using Altera Quartus Version 5.0 Web Edition. It was assumed that the cloud of TCP/IP shown in Fig. 1.1. was implemented as a direct connection in FPGA between the TX of the left side and the RX of the right side and vice versa.

The synthesis result can be shown below, i.e.

Quartus II Version	5.0 Build 148 04/26/2005 SJ Web Edition
Revision Name	modul_akhir
Top-level Entity Name	modul_akhir
Family	Stratix
Device	EP1S10F780C6ES
Timing Models	Final
Met timing requirements	Yes
Total logic elements	1,048 / 10,570 (9 %)
Total pins	40 / 427 (9 %)
Total virtual pins	0
Total memory bits	38,912 / 920,448 (4 %)
DSP block 9-bit elements	0 / 48 (0 %)
Total PLLs	0 / 6 (0 %)
Total DLLs	0 / 2 (0 %)

Maximum frequency which can be achieved by this interface to operate is 78,01 MHz which is more than the minimum frequency, i.e. 50 MHz.

C. Verification

To verify whether the system functions as it is expected, we occupied the SignalTap II Logic Analyzer. This analyzer captured the result of implementation when it was running into operation.

The file processing in SignalTap II Logic Analyzer can be shown in Fig. 4.5. The process in the Altera Stratix (FPGA) consists of the TCP/IP interface module, FIFO modules, ROM, and multiplexers. Based on the same figure, datastream of Ethernet Frames will be stored in one ROM, and the process will be started by passing all data from the ROM to the TCP/IP interface, and the result will be stored in the RAM. The process of verification can be done by examining the data as results of passing data via TCP/IP interface from ROM to RAM. The result of operation of the TCP/IP interface can be shown based on the result captured by SignalTap II Logic Analyzer. The SignalTap II Logic Analyzer will display the process result to the monitor of the Host PC.
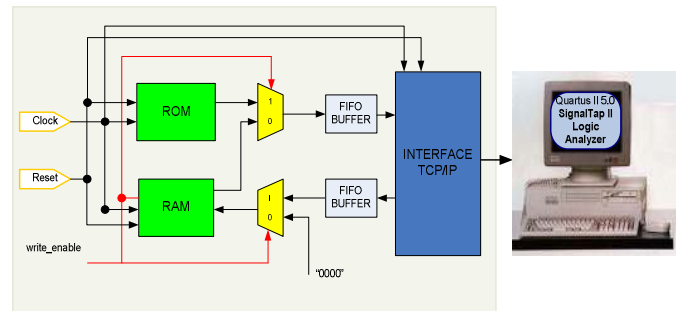
Fig. 4. 5. Communication between FPGA and Host PC with SignalTap II Logic Analyzer

Two examples of implementation result's verification are shown in Fig. 4.6. and Fig. 4.7. The beginning of an Ethernet Frame sent from TX and received by RX can be shown in the Fig. 4.6. The output data ot TX, data_out shown in Fig. 4.6, are compared to the data_bg which are the processed data at RX, after the RX received data_out as its input data.
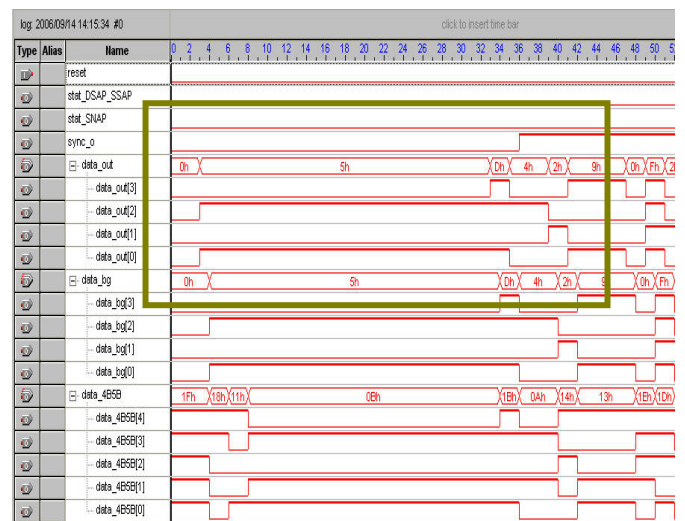
Fig. 4.6. Capturing the Implementation Result in the Beginning of several Ethernet Frames

Moreover, another example of verification result of the TCP/IP interface when it was in the operation mode can be depicted in Fig. 4.7. After the data 0x6h, user data were

encrypted and the encryption process was performed correctly. Every byte of user data were encrypted with a certain key by performing a XOR operation with 0x4.

Fig. 4.7. Encryption Result

Indeed, other important implementation results have been checked and verified, such as detection of ethernet frame, LLC 802.2, IP packet, TCP packet.

Hence, based on the verification result, it can be concluded that the transparent TCP/IP interface works properly in half duplex mode. This interface is open or transparent to any type of media used for data communications.

V. CONCLUSION

In summary, a transparent interface design based on TCP/IP protocol via Ethernet has been done. The type of this interface design can be categorized as an emulation. It is called as an emulatio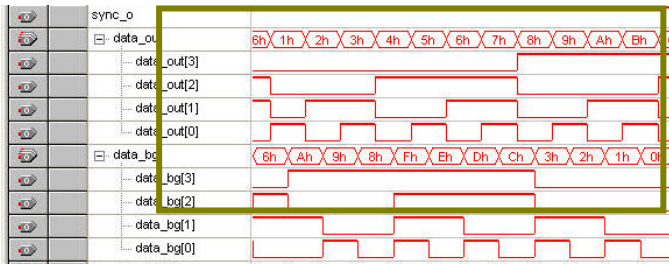n as the interface design imitates a real TX-RX to another TX-RX module communication using TCP/IP protocol via ethernet. This emulator does half-duplex communication between one TX-RX module and another TX-RX module.

This interface, which consists of TX module and RX module, is able to identify Ethernet Frame conforming to IEEE 802.3, and TCP/IP datagram/packet referring to the RFC-793 & RFC-1042.

To design this interface, it is needed 1048 logic elements, and based on the synthesis result, the interface is able to operate at frequency of more than 50 MHz. Verification process of the interface's functionality was performed using SignalTap II Logic Analyzer. It has been verified that the interface works properly as it can detect 802.3 ethernet frame, and TCP/IP datagram/packet.

REFERENCES

[1] C. P. Martin, "Data Networks, IP and the Internet: Networks, Protocols, Design, and Operation". West Sussex, UK : John Wiley & Sons, Ltd., 2003.

[2] A. Leon-Garcia, and I. Widjaja, "Communication Networks : Fundamental Concepts and Key Architectures". New York, USA : McGraw-Hill, 2001.

[3] J. Postel, and J. Reynolds, *RFC-1042 Standard for the Transmission of IP Datagrams over IEEE 802 Networks*. 1988.

[4] SMSC Co., LAN91C111 – 10/100 Non PCI Ethernet Single Chip MAC + PHY Datasheet. July 2005, http://smsc.com.

[5] C. E. Spurgeon, "Ethernet The Definitive Guide". California, USA : O'Reilly & Assocciates, Inc. 2000.

[6] W. R. Stevens, "TCP/IP Illustrated, Volume 1 The Protocols". 2001.

Design of Wireless Battery Charger Using Near-field Induction Method

Firdaus, Tyo Fabian Fadel and Wahyudi Budi Pramono
Department of Electrical Engineering, Universitas Islam Indonesia, Yogyakarta, Indonesia
(Tel : +62-274-895287; E-mail: firdaus@uii.ac.id)

Abstract- Wireless power transfer system allows electric current to flow from one device to another without intermediate copper wire. This technology facilitates the battery charging process on electronic tools that have relatively little power. Wireless power transfer technology utilizes properties of magnetic induction between transmitter and receiver coils. The efficiency of wireless energy transfer depends on the distance between the coils and their frequency. In this paper successfully designed wireless power charging that work at a frequency of 60.606 kHz using near-field method and flat pancake wheeler coil types. Optimal efficiency of 41.06% was obtained when the distance between the coils is 2cm.

Keyword: wireless power transfer, battery charging, near-field, flat pancake wheeler coil, induction.

I. INTRODUCTION

Wireless technology is not only used for data transmission, but is also used to transmit electricity. Wireless energy transfer is a process of energy transmission electricity from a power source to an electrical device without interconnecting wires[1]. There are several currently used schemes, which rely on non-radiative modes (magnetic induction), but they are restricted to very close-range or very low-power (mW) energy transfers [2,3]. There are two different basic methods for wireless energy transfer. The first method is a far-field method using power shots, laser, radio transmission, and microwave [4]. The second method is a method using a near-field induction [5]. One type of this method is loosely-coupled WPT that offers unique advantages, principally, freedom of device placement on the x-y plane of the charging source, and the ability to charge multiple devices simultaneously, among many other features [6]. Both methods use the same electromagnetic fields and magnetic fields.

The aim of this research is to design a device that can be used to transfer power wirelessly by utilizing near-field method using the principle of induction. The profit of making battery charger using near-field method is a loss that resulted from the induction smaller than the far-field method due to the induction of a closer distance. Circuit and component support for near-field method is relatively easy to make and obtained.

II. WIRELESS POWER TRANSFER

The initial research at MIT led by Marin Soljacic in 2007 [7,8]. Researchers at MIT managed to light the lamp with a 60 watt power without wires, using two types of 5-turn coils of copper with a diameter of 60 cm. Distance shipping 2 meters with efficiency of 45%. [9]

A. The magnetic field

The magnetic field is the area where the magnetic force will still affect the surrounding objects. So if we bring certain metal objects in the area of the magnetic field, then the metal will be attracted by a magnet. The magnetic field is strongest at the poles of a magnet. Magnet has two poles, the north (N) and south (S). A magnetic field can be described with the magnetic lines of force called magnetic spectrum. Lines of magnetic force are defined as an imaginary line emanating from the north pole to the south pole and they never cut each other.
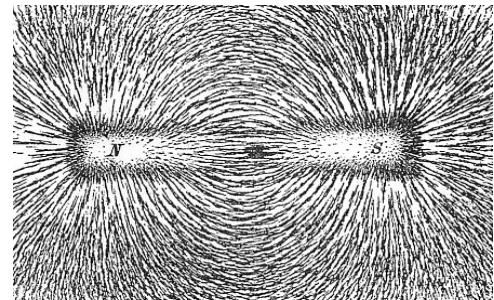
Fig. 1. Illustration of magnetic force line with iron powder

B. Electromagnetic induction

Electromagnetic induction is an electromotive force across a conductor when it is exposed to a time varying magnetic field. The interaction of magnetic force lines can be illustrated in the figure 2.
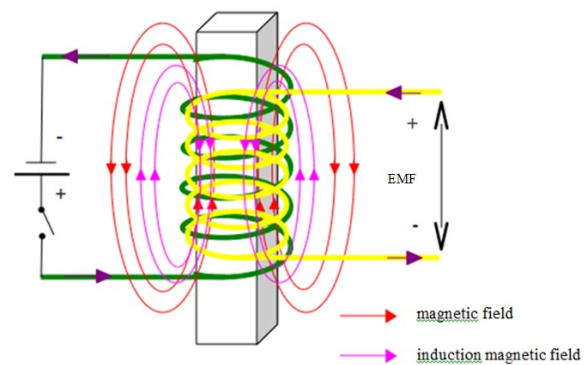
Fig. 2. Magnetic induction in transformer with iron core

Magnetic induction equation is the change of force to the moving charges. Magnetic induction β, normal velocity V sin ϕ and magnetic force F that perpendicular to each other.

Magnetic induction is actually derived from the electromagnet law discovered by Faraday. Faraday discovered that an electric current can be generated from the changes of magnetic field. The generating of electric current due to the changes of magnetic field is called electromagnetic induction [10].

$$B = \frac{F}{qv \sin\varphi} \qquad (1)$$

EMF equation that satisfies Faraday induction is as follows.

$$\varepsilon_{ind} = -N\frac{\Delta\varphi}{\Delta t} \qquad (2)$$

N is the number of windings and $\Delta\varphi/\Delta t$ is the rate of change of the magnetic flux (wb/s)

C. Inductive charging

Inductive charging (also known as "Wireless Charging") uses an electromagnetic field to transfer energy between two objects. This is usually done at the filling station. Energy is sent through inductive coupling to the electrical devices, where energy can be used to charge or run the device. Induction chargers typically use an induction coil to create an alternating electromagnetic field at the base station charging, a second induction coil adjacent to form an electrical transformer [11,12]. Greater distance between sender and receiver coils can be achieved when the inductive charging system using resonant inductive coupling.

D. Resonance

Tuning Circuit is a circuit that serves to tune the signal with a certain frequency at one frequency band. Doing tuning means the series 'resonate' with the signal. In the tuned state, the respective signal selected to be forwarded to the next stage. Tuning circuit is basically composed of a capacitor and inductor that connected series or parallel. In a state of resonance, impedance has imaginary part equal to zero [13].

III. SYSTEM DESIGN

Flowchart of design and block diagram of the system can be seen in Figure 3 and Figure 4.
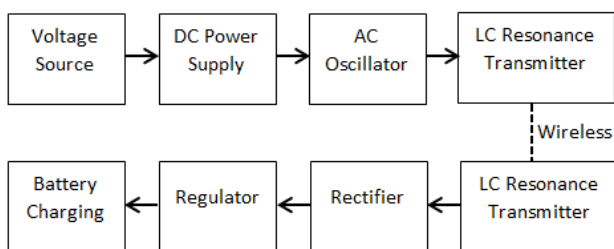

Figure 3. Block diagram of system

System block diagram explains the device workflow. The first step, a source of AC voltage is converted into DC voltage. Then the DC voltage is converted into a high frequency AC voltage using the oscillator, afterward it propagate through the transmitter coils. The voltage of the transmitter coils are transmitted through the air and received by the receiver coils in the form of an AC voltage. AC voltage received by the receiver coils converted back into a DC voltage using wave rectifier. After becoming a DC voltage, the voltage is regulated using the voltage regulator to be accepted by the load.
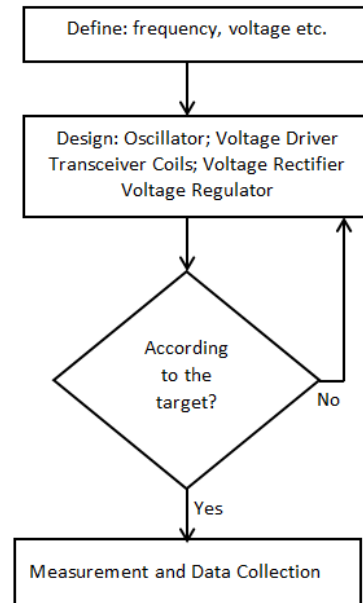
Figure 4. Flowchart of design process

A. Oscillator Design

Oscillator circuit use TL494 IC. It provides a positive sawtooth wave on a dead-time setting and a PWM comparator (pulse width modulation), this parameters can be used as a comparison to various control signals.

The frequency range for WPT from several kHz to several MHz, but generally below 10 MHz[14]. Oscillator frequency is generated by determining the value of resistors (RT) and capacitor (CT). The desired frequency is 60.606 KHz. However for the next stage of this frequency should be adjusted to the rules of regulatory agencies. The formula to determine the frequency obtained from the datasheet IC-TL494, this circuit used a series of push-pull with MOSFET IRFZ44N. The capacitor value is 1 nanofarad, so the oscillation frequency of the push-pull is:

$$
\begin{aligned}
f &= 1/(2R_T \times C_T) \qquad (3)\\
60606 &= 1/(2R_T \times 10^{-9})\\
R_T &= 8250\,\Omega
\end{aligned}
$$

f is frequency (Hz), C_T is timing eksternal capacitor (Farad), and R_T is timing eksternal resistor (ohm).

B. Push-Pull Amplifier

A push pull amplifier is an amplifier which has an output stage that can drive a current in either direction through through the load. The output stage of a typical push pull amplifier consists of of two identical BJTs or MOSFETs one sourcing current through the load while the other one sinking the current from the load. Push pull amplifiers are superior

over single ended amplifiers (using a single transistor at the output for driving the load) in terms of distortion and performance.[15]

The advantages of the push-pull amplifier are a low distortion, no magnetic saturation in the core of the coupling transformer and power supply ripple cancellation that can eliminate noise. While the disadvantage is the need of two or more identical transistors and a large coupling on the transformer.
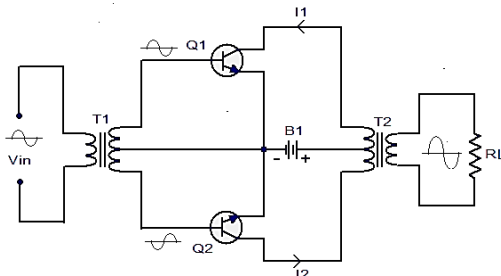

Fig. 5. Illustration of Signal Output in Push-pull amplifier

C. Design of transmitter and receiver coil

The changes of electric current in the transmitter coil causes the magnetic field. The magnetic field will induce the receiver coil, so that the receiver coil will appear electric current. The coils that is used is flat pancake wheeler models. Coil shape can be seen in the image below.
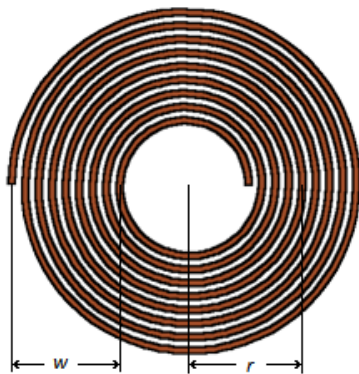

Figure 6. Flat pancake wheeler coils

Transmitter and receiver coils have the same inductance value. Transmitter coil connected to the resonant capacitor in parallel, while the receiver coil is fitted with a resonant capacitor in series. Parameters used include coil radius 4.3cm, a width of coil 2.3cm, and the number of windings 20 rolls.

The value of the radius and width of the coil must be changed to inches to get the results in microHenry. The formula to calculate the inductance in the flat pancake coil wheeler models are:

$$L = \frac{r^2 \times N^2}{8 \times r + 11 \times w} \qquad (4)$$
$$L = \frac{1.692^2 \times 20^2}{8 \times 1.692 + 11 \times 0.905}$$
$$L = 48.73 \text{ uH}$$

L is the inductance (μH), r is the radius of the coil (inches), N is the number of windings, and w is the width (inches).

TABLE I
Transmitter coil characteristics

Parameters	Symbol	Value
Radius	r	1.692 inci
Number of windings	w	0.905 inci
Width of windings	N	20 rolls

Figure 7. Design of coil

Based on the value of L that has been acquired then it can be searched value of C resonant. To get value of C in nanofarad, L and f need to be converted into the miliHenry and Megahertz. L is 0.04873 mH and f is 0.060606 MHz.

$$f = \frac{1}{2 \times \pi \times \sqrt{L \times C}} \qquad (5)$$
$$2\pi f = \frac{1}{\sqrt{L \times C}}$$
$$\sqrt{LxC} = \frac{1}{2 \times \pi \times f}$$
$$LC = \left(\frac{1}{2 \times \pi \times f}\right)^2$$
$$0.04873 \times C = \left(\frac{1}{2 \times 3.14 \times 0.060606}\right)^2$$
$$0.04873 \times C = 6.903$$
$$C = \frac{6.903}{0.04873}$$
$$C = 141.65 \text{ nF}$$

Then 3 pieces of 47 nF capacitors are arranged in parallel, so the total is 141 nF.

D. Transmitter and Receiver Resonant

Once the value of L and C is obtained, then the value of the inductive reactance (X_L) and inductive reactance (X_C) in ohms can be calculated.

$$X_L = 2 \times \pi \times f \times L \qquad (6)$$
$$X_L = 2 \times 3.14 \times 0.060606 \times 48.73$$
$$X_L = 18.3 \text{ ohm}$$

$$X_C = \frac{1}{2 \times \pi \times f \times C} \qquad (7)$$
$$X_C = \frac{1}{2 \times 3.14 \times 60.606 \times 147 \times 10^{-6}}$$
$$X_C = 18 \text{ ohm}$$

IV. RESULT AND DISCUSSION

Testing is done to get the data from the tool. Parameters measured include distance, voltage, current, power, and the efficiency.

$$P = V \times I \tag{8}$$

$$n = \frac{Pout}{Pin} \times 100\% \tag{9}$$

V is the voltage (volts), I is the current (amperes), n is the efficiency (%), P is the power (watts), Pout is the power output (watts), and Pin is the input power (watts)

A. Testing on Transmitter

Tests performed at the output of the power supply. Testing is done to see the effect of the load on the receiver to the power supply output. The voltage measured at the positive and negative point of the device, while the current measurement is done at the series point of equipment that has been provided. Parameters measured were distance, voltage, current, and power. Measuring instruments used is voltmeter and ampermeter.

Measurement results on transmitter when it is affected by lamp load at receiver can be seen at table 2 and figure 8, this test is done to see if the voltage at the transmitter may be affected by the load on the receiver.

TABLE II
Result of testing on transmitter with lights load in receiver
(V = 15.3Volts)

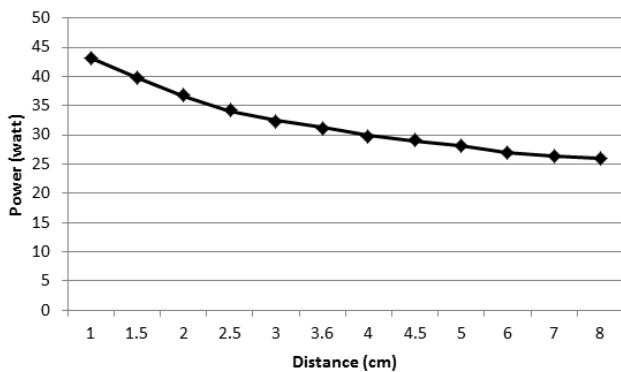| Distance (cm)	Current (A)	Power (watt)
1	2.82	43.146
1.5	2.6	39.781
2	2.4	36.721
2.5	2.23	34.119
3	2.12	32.436
3.6	2.04	31.212
4	1.95	29.835
4.5	1.89	28.917
5	1.84	28.152
6	1.76	26.928
7	1.72	26.316
8	1.7	26.011

Fig 8. Relationship between distance and power at transmitter with lights load in receiver

Testing on transmitter with battery charging in receiver. The measurements made when the transmitter is affected by the charging of mobile phone batteries in the receiver. This test is done to see if the voltage at the transmitter may be affected by the load on the receiver.

TABLE III
Result of testing on transmitter with battery charging in receiver
(V=15.3 volt)

Distance (cm)	Current (A)	Power (watt)
1	2.5	38.25
2	2.31	35.343
3	1.88	28.764
4	1.62	24.786
5	1.61	24.633
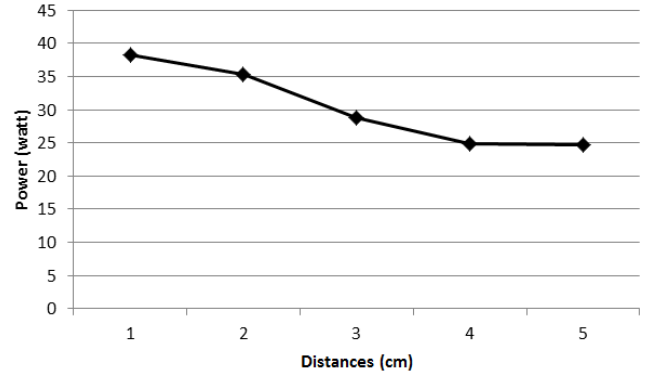
Fig 9. Relationship between distance and power at transmitter with battery charging in receiver

B. Testing on Receiver

Tests performed at the receiver output. Tests conducted on two types of load, ie lights and cell phone batteries. Testing is done to obtain and ascertain whether the receiver can work properly. Testing on receiver with lamp load. The measurement is done when the receiver is affected by the light load, test is done to see if the receiver is able to receive the voltage of the transmitter at a certain distance.

TABLE IV
Testing on receiver with lamp load

Distance (cm)	Voltage (V)	Current (A)	Power (watt)
1	3.1	1.05	3.255
1.5	7.5	1.25	9.375
2	11.6	1.3	15.08
2.5	9.7	1.27	12.319
3	5.2	1.17	6.084
3.5	2.6	1.05	2.73
4	1.4	0.97	1.358
4.5	1	0.75	0.75
5	0.6	0.73	0.438
6	0.2	0.5	0.1
7	0.1	0.35	0.035
8	0.08	0.25	0.02

Testing on Receiver with battery load. Receiver parameters measurement is done when the receiver is affected by the charging of cell phone battery. Testing is done to see if the receiver is able to receive the voltage from the transmitter at a certain distance.

TABLE V
Result of testing on receiver with battery load

Distance (cm)	Voltage (V)	Current (A)	Power (watt)
1	5.2	0.47	2.444
2	5.2	0.47	2.444
3	5.2	0.47	2.444
4	4.3	0.03	0.129
5	3.3	0	0

C. The system efficiency

The system efficiency can be calculated if the output power has been measured. The output power can only be measured when the system has been loaded, the load on the receiver is lamp. System efficiency gained from comparing the power generated by the transmitter and the received power on receiver. P_{TX} is the transmitter power and the P_{RX} is receiver power. Maximum efficiency is obtained when the distance is 2 cm, which amounted to 41.06%. The value approach the efficiency produced by previous research.[16]

TABLE VI
The system efficiency

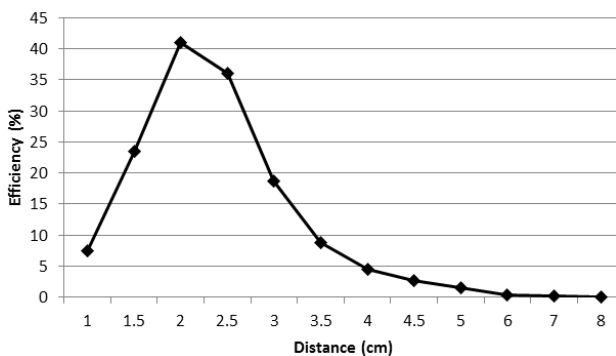| Distance (cm)	P_{Tx} (watt)	P_{Rx} (watt)	Efficiency (%)
1	43.146	3.255	7.54
1.5	39.78	9.375	23.56
2	36.72	15.08	41.06
2.5	34.119	12.319	36.11
3	32.436	6.084	18.75
3.5	31.212	2.73	8.74
4	29.835	1.358	4.55
4.5	28.917	0.75	2.59
5	28.152	0.438	1.55
6	26.928	0.1	0.37
7	26.316	0.035	0.13
8	26.01	0.02	0.076

Fig 10. Relationship between distance and system efficiency

V. CONCLUSSION

Wireless battery chargers using near-field induction method has been successfully designed and tested. The distance between the transmitter and receiver influence on system efficiency, maximum efficiency is obtained when the distance is 2 cm, which amounted to 41.06%. The farther the distance between transmitter and receiver, the smaller the received power. Wireless energy transfer has the potential to be developed, as long as there are components, design, and precise calculations.

REFERENCES

[1] N. Tesla, Apparatus for transmitting electrical energy, US patent number 1,119,732, issued in December 1914
[2] Karalis, A., Joannopoulos, J. & Soljacic, M. (2008). Efficient wireless non-radiative mid-range energy transfer, Elsevier Annals of Physics (323): 34–48.
[3] L. Ka-Lai, J.W. Hay, and P.G.W. Beart, Contact-less power transfer, US patent number 7,042,196, issued in May 2006
[4] Low, Z. N., Chinga, R. A., Tseng, R. & Lin, J. (2009). Design and test of a high-power high-efficiency loosely coupled planar wireless power transfer system, IEEE Transactions on Industrial Electronics 56(5).
[5] Mingbo Yang; Guodong Yang; En Li; Zize Liang; Bo Zhai, "Topology and inductance analysis for wireless power transmission system," in Control and Decision Conference (CCDC), 2013 25th Chinese , vol., no., pp.2052-2056, 25-27 May 2013
[6] Grajski, K.A.; Tseng, R.; Wheatley, C., "Loosely-coupled wireless power transfer: Physics, circuits, standards," in Microwave Workshop Series on Innovative Wireless Power Transmission: Technologies, Systems, and Applications (IMWS), 2012 IEEE MTT-S International , vol., no., pp.9-14, 10-11 May 2012
[7] Castelvecchi, Davide,"Wireless Electricity could power consumer, industrial electronics" MIT News, 2006
[8] Hadley, Franklin, "Goodbye Wires". MIT News, 2007
[9] J. Gozalvez, WiTricity-The Wireless Power Transfer, IEEE Vehicular Technology Magazine, 2007
[10] Koenraad van Schuylenbergh, Robert Puers, Inductive Powering: Basic Theory and Application to Biomedical Systems, Springer Science & Business Media, 2009
[11] Wu, H.H, Gilchrist, A, Sealy, K, Israelsen, P, Muhs, J., "A review on inductive charging for electric vehicles," in Electric Machines & Drives Conference (IEMDC), 2011 IEEE International , vol., no., pp.143-147, 15-18 May 2011
[12] Wells, Brannon P, "Series resonant inductive charging circuit." Patent - US6972543 (B1), 2003
[13] Teck Chuan Beh; Imura, T.; Kato, M.; Hori, Y., "Basic study of improving efficiency of wireless power transfer via magnetic resonance coupling based on impedance matching," in Industrial Electronics (ISIE), 2010 IEEE International Symposium on , vol., no., pp.2011-2016, 4-7 July 2010
[14] J. Nadakuduti, L. Lu, and P. Guckian, "Operating frequency selection for loosely coupled wireless power transfer systems with respect to RF emissions and RF exposure requirements," in Wireless Power Transfer (WPT), 2013 IEEE, 2013, pp. 234–237
[15] Bogart, Theodore F., Jeffrey S. Beasley, and Guillermo Rico. Electronic devices and circuits. Pearson/Prentice Hall, 2004
[16] H.V Leal, A.G Angel, The Phenomenon of Wireless Energy Transfer: Experiments and Philosophy, InTech Croatia, 2012

Wireless Sensor Network Application for Carbon Monoxide Monitoring

Firdaus[1], Nur Ahriman[1], Andik Yulianto[2], Medilla Kusriyanto[1]
[1]Department of Electrical Engineering
[2]Department of Environmental Engineering
Universitas Islam Indonesia, Yogyakarta, Indonesia
(Tel : +62-274-895287; E-mail: firdaus@uii.ac.id)

Abstract-Carbon monoxide (CO) is an odorless, tasteless and colorless gas in which it is difficult to be recognized by human beings. CO gas that enters the human body at a certain concentration has negative impact on health. A monitoring system which can recognize the amount of CO gas concentration, especially for the indoor is needed to cope with this problem. In this paper, monitoring system is designed using XBee as a data transmission medium. Three XBee are integrated with the sensor node circuits, microcontroller as a data processor and one XBee as a data collector. The sensor nodes consist of an LM35DZ temperature sensor, a humidity sensor HSM 20-G and a CO sensor TGS 2600. The data are read by sensor nodes and then they are transmitted wirelessly using XBee. The data collector functions as the receiver, processor and data viewer in the form of tables and graphs using Visual Basic 6.0. From this design, the results of data transmission can be displayed in the form of graphs and tables which are then stored into the database. The data transmission range is ± 53 meters indoor, where the average error TGS 2600 sensor reading is 4.414 %.

Keyword: monitoring; carbonmonoxide; wireless sensor network; zigbee; TGS2600.

I. INTRODUCTION

Sources of air pollution can come from a variety of activities, such as: industries, transportations, offices and housings. One of the parameters of air pollution is carbon monoxide (CO) contained in the air [1]. The Scottish Pollutant Release Inventory (SPRI) reports that the main source of carbon monoxide is from petrol vehicles which are not fitted with a catalytic convertor. Carbon monoxide levels in urban areas closely reflect traffic density (in combination with weather conditions). Natural processes produce relatively small amounts. As it is odorless and colorless, it is very difficult for human beings to detect CO in the air. Therefore, a system that can monitor the level of CO gas in the air is strongly needed. Wireless sensor network has been applied in many systems, among others, for the detection of hydrogen gas leak at a hydrogen fueling station.[2] It has also made the development of wireless networks and characterization of gas sensors to detect flammable or explosive gases.[3] Research has also developed with a focus on saving power consumption in sensor networks.[4] One of the reliable communication protocol used is Zigbee (IEEE 802.15)[5].

Previous research conducted by Anggit[6] which explained that TGS 2442 gas sensor is used as detector for carbon monoxide (CO) level and the results are then displayed on the LCD. Subsequent research conducted by Adhi[7], parameters of vehicle exhaust emissions (CO) are measured using MQ-7 gas sensor, data from the sensor are processed using microcontroller and then it is displayed on the LCD. From the two previous researches, it can be concluded that the detection of CO gas can only be done at single point and data from sensor readings are only displayed on the LCD. Hendhi [8] found that the data acquisition system consists of several parts, namely general sensor nodes, gateways, and servers. Sensor nodes consist of RCM4510w based system are equipped with temperature sensors, humidity, and gas sensors (CO_2).

This research design carbon monoxide monitoring system used wireless sensor networks. This system consist of multi node, its mean that this system can monitored several points or place. The network used bus topology, where it allowed the data transmission over longer distances due to the addition of a repeater.

II. SYSTEM DESIGN

The design of a wireless sensor network application system for monitoring the CO gas included hardware and software design. The hardware consisted of a series of sensors, XBee transmitter[10], ATMega8 microcontroller and receiver circuit The component diagram and phisycal form of sensor node can be seen at Figure 1 and Figure 2.

The sensors are TGS 2600[11] as CO gas reader, HSM20-G[12] as a humidity reader, and LM35DZ[13] as temperature readers. XBee transmitter uses 2.4 Ghz, because it is ISM (Industrial-Scintific-Medical) frequency or unlicenced frequency. Block diagram of the overall system design can be seen in Figure 3.
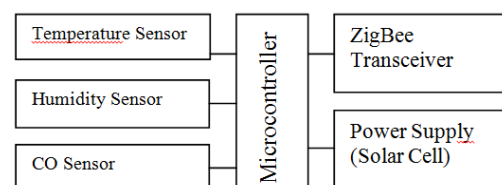
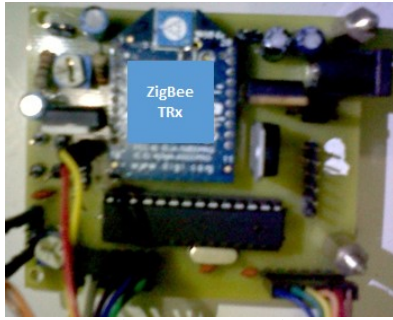

Figure 1. Components of sensor node
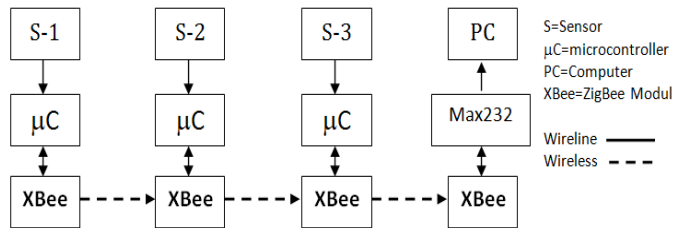
Figure 2. Sensor node

Figure 3. Block diagram of system

S=Sensor
μC=microcontroller
PC=Computer
XBee=ZigBee Modul

Wireline ———
Wireless - - - -

This system consist of 3 pieces of sensor nodes, they are connected to form a bus network topology. The first node read the data from sensor then sent them to the second node. The second node sent the data read from sensor 2 and 1 to the third node. The third node read the data from sensor 3 then sent all the data to the last XBee nodes, then the data are displayed on a computer.

III. RESULT AND DISCUSSION

Before measuring the CO gas concentration using a sensor TGS 2600, there are several steps to do. Fisrtly, the relationship between Rs/Ro with CO gas concentration using polynomial regression should be found. We have two equations to determine the value of the concentration of CO gas[11].

$$ppm = 56{,}69x2 - 133x + 77{,}76 \; ; for \; 1 \geq x \geq 0{,}75 \qquad (1)$$
$$ppm = 322{,}3x2 - 573{,}1x + 256{,}7 \; ; for \; 0{,}75 > x \geq 0{,}36 \qquad (2)$$

Where x is Rs/Ro. Then the value of Rs and Ro of the sensor is determined. Rs is the resistance values change when the sensor detected the presence of CO gas exposure, whereas Ro is a barrier whose value is fixed. Ro is a constant divider in the calculation to obtain the value of ppm. Ro values obtained by conditioning the sensor at a temperature of 20 ± 2°C and humidity of 65 ± 5 %. After a conditioning upon the certain temperature and humidity, the value of the sensor output voltage is determined. Temperature sensors in this test is 21°C and humidity is 62%. The average percentage error of sensor readings is 4.414%.

LM35DZ temperature sensor has the characteristic whereby every degree displayed is represented by the value of the output voltage of 10mV. The average of percentage error is 1.91% at node 1 and node 2, 2.01% at node 3. The test results can be seen in Table 1.

TABLE I
Results of temperature sensor testing

Temperature by Sensor (°C)			Thermometer (°C)
Node 1	Node 2	Node 3	
21.23	20.66	20.76	21
22.48	21.14	21.70	22
23.46	22.58	22.65	23
25.90	25.46	25.48	25
27.37	26.42	26.89	27
28.35	27.38	27.60	28

Humidity sensor (HSM 20-G) test is done by comparing the value of the humidity sensor readings with hygrometer readings. To get the value of different humidity, the test is done at different times and locations.

TABLE II
Results of humidity sensor testing

Humidity by Sensor (%)			Higrometer (%)
Node 1	Node 2	Node 3	
61.63	55.89	60.76	58
63.76	59.42	62.52	60
66.78	61.93	64.80	62
71.18	67.67	69.11	66
74.44	71.60	73.54	70
76.62	72.33	74.52	72

Tests are carried out since noon, night and early morning, while test locations are indoor and outdoor areas. The average error percentage of sensor readings are 6.5%, at node 1, 1.54% at node 2 and 3.53% at node 3. The test results of humidity sensor can be seen in Table 2. System test is done to get the performance of data transmission and reception. This test used node 3 and node 2. Node 3 functioned as a transmitter and node 2 functioned as a receiver. Based on the test above, the maximum data transmission distance is 53 m in condition that there are 3cm thick doors barrier and a 27cm thick wall.

Location test map can be seen in Figure 4a. Scenario 1, three nodes are placed in 3 different rooms with a floor of the same building. Location test map can be seen in Figure 4b. Between node 3 and node 2 there is a 27cm wall as barrier and the distance of the two nodes is 11.87m. While, the placement of node 2 and node 1 is restricted by a barrier in the form of room and the 2 pieces of walls of 27 cm thick, and the distance between node 2 and node 1 is 19.94m. All data readings of sensor nodes can be well received by the receiver. Scenario 1 test results can be seen in Table 3.

TABLE III
Results of test in scenario 1 to scenario 5

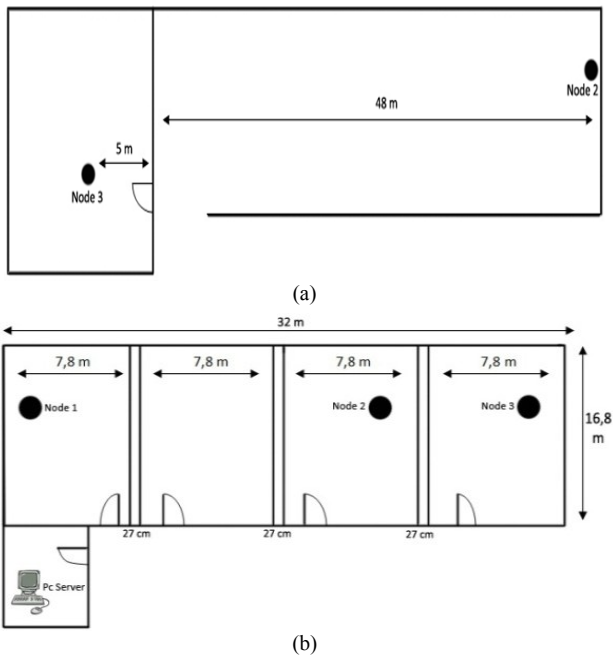| Transmission	Result of scenario				
	1	2	3	4	5
Node 3 to node 2	Sent	Sent	Sent	Sent	Sent
Node 2 to node 1	Sent	Sent	Sent	Not Sent	Sent
Node 1 to *receiver*	Sent	Sent	Sent	Not Sent	Sent

(a)

(b)

Figure 4. Plan testing area distance (a) and location plan scenario 1 (b)

Location test map for scenario 2 can be seen in Figure 5. In test scenario 2, the position of the node 3 to node 2 is limited by 3 cm thick wooden doors. The door is closed when the test is conducted to determine the ability of the XBee PRO to delivery data with a barrier in the form of the door. Between node 2 to node 1 is limited by a room with a width of 7.8 m and 2 pieces walls with the thickness of 27 cm in each room, the distance between two nodes 28.74 m. Test result data with scenario 2 can be seen in Table 3.
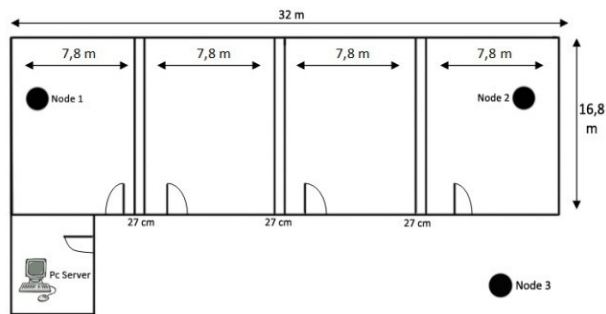

Figure 5. Location of the test for scenario 2

In scenario 3, three sensor nodes are installed in 3 rooms on different floors (Figure 6). Node 3 on the 2nd floor, node 2 on the 3rd floor, node 1 and the receiver on the 4th floor. The test is conducted to determine the ability of XBee PRO in data delivery on the vertical room with a concrete barrier. Each node is placed on the table, 1m from the floor, 3.5m high of room, media thickness of the concrete barriers is about 30 cm and the distance between each node from the window is 2m. Table 3 shows the results of the test that had been done.
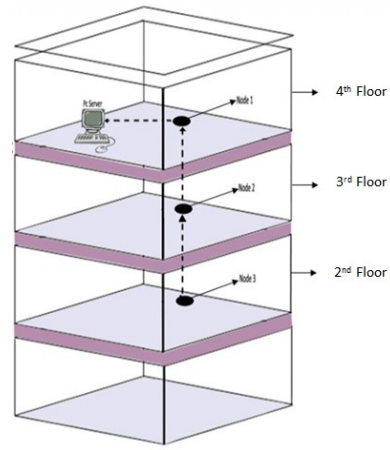
Figure 6. Location of the test for scenario 3

In scenario 4, node 3 is placed in the hallway on the 2nd floor of the building, node 2 in one of the rooms on the 2nd floor , node 1 and receiver on 4th floor (Figure 7). The distance between node 3 to node 2 is 15m with a medium barrier wall 27cm thick. The distance between the node 2 with node 1 is as far as 7.6m with 2 pieces of media in the form of a concrete barrier with a thickness of 30cm each. Node 3 sent data to node 2, then node 2 sent to node 1 and is transmitted to the receiver. The results of the test can be seen in Table 3. Node 1 did not receive the data from node 2, this is due to the ability of the radio waves emitted by XBee PRO is not able to penetrate the barrier in the form of two pieces of 30cm concrete thickness. Receiver did not receive the data from node 1 because node 1 in the standby state and waited for data from node 2. One of the weaknesses of the system that had been made that if one node got error, all of the data readings from the sensor nodes would not be accepted by the receiver.
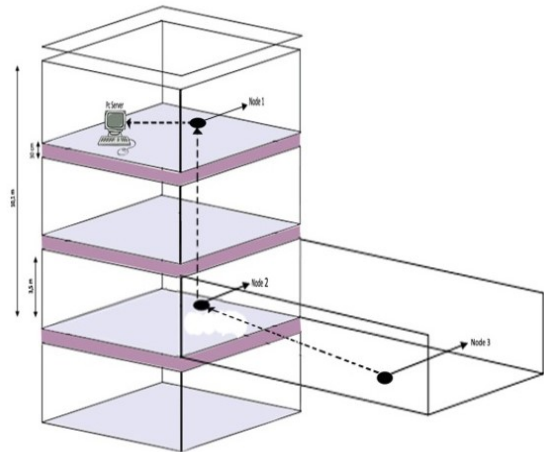
Figure 7. Location of the test for scenario 4

In testing of scenario 5, each node is installed in the same room with the floor, location test map can be seen in Figure 8. At this test, all three nodes would transmit the data directly to the receiver without passing through repeaters. The results of the test can be seen in Table 3. By using multipoint-to-point topology, all of the data the sensor readings are well received by the receiver for the receiver is within the range of the radio

waves emitted by each node. One of the advantages of using this topology is if one node got error then it would not affect the work of other nodes. One disadvantage of this topology is the use of the data transmission distance is limited. If monitoring is done in indoor area with the distance between the rooms are not so far away, multipoint-to-point topology should be used. But, if the distance between the rooms to be monitored is far enough, bus topology is better to use.
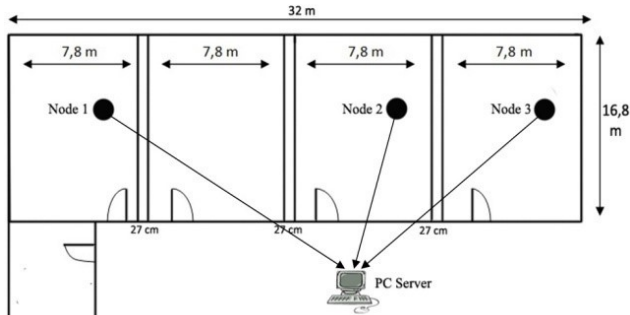
Figure 8. Location of the test for scenario 5

Finally, all data will display and storage at server (PC). The interface can be seen at Figure 9.
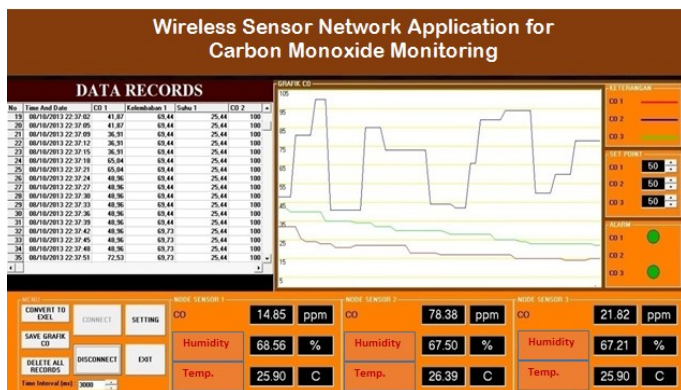
Figure 9. Interface at server

IV. CONCLUSSION

From the tests, it can be concluded as follows: HSM 20-G sensors have different sensitivity to moisture measurement. Percentage of the average value of the sensor reading error is 6.50% at node 1, 1.54% at node 2 and 3.53% at node 3. Percentage of the average value of the temperature sensor readings LM35DZ error is 1.91% at node 1 and node 2, and 2.01% at node 3. By using a second order polynomial regression model for sensor readings TGS 2600, it is obtained that an average error value when compared to the datasheet of 4.414% (if using all the data) and 2.12% (if the data outliers eliminates 3). The maximum distance for data transmission between nodes in an indoor area with a barrier condition 3cm thick door and a wall thickness of 27cm is 53m. Network which had been designed to work well over the nodes could receive the radio waves emitted. The data received by the receiver is compatible with the data transmitted by the transmitter. When using bus topology, if one node got error,

the system would not work, there is no incoming data to the receiver. When using multipoint to point topology, if one node error, it would not affect the work of other nodes.

REFERENCES

[1] Homan, C.S., Brogan, G.X., *Carbon Monoxide Poisoning in Handbook of Medical Toxicology*, 1st ed., Little Brown and Co, Boston, 1993.
[2] Nakano, S., Goto, Y., Yokosawa, K., Tsukada, K., *Hydrogen Gas Detection System Prototype with Wireless Sensor Networks*, The 4th IEEE Conference on Sensors, Oct. 31 – Nov. 3, Irvine, CA, USA, 2005.
[3] Somov, A., Baranov, A., Savkin, A., Ivanov, M, Calliari, L., Passerone, R., Karpov, E., and Suchkov, A., *Energy-Aware Gas Sensing Using Wireless Sensor Networks*, Proceedings of Wireless Sensor Networks: 9th European Conference, EWSN 2012, Trento, Italy, February 15-17, Springer , 2012.
[4] Somova, A., Baranovb, A., Savkinb, A., Spirjakinb, D., Spirjakinb, A., Passeronec, R., *Development of wireless sensor network for combustible gas monitoring*, Journal of Sensors and Actuators A: Physical vol. 171 page 398-405, Elsevier, 2011
[5] IEEE Computer Society, *IEEE 802.15.1 Wireless medium access control (MAC) and physical layer (PHY) specifications for wireless personal area networks (WPAN)*, 2005.
[6] Perdana, A., *Prototype of Monitoring and Warning System Gas Levels of Carbon Monoxide (CO) at Cars Cabin Based Microcontroller ATMega8*, Undergraduate theses, Universitas Diponegoro, Semarang, 2011.
[7] Adhi, E., *Design of Exhaust Emission Measurement, Case Study: Measurement of Gas Carbon Monoxide (CO)*, Undergraduate theses, Institut Teknologi Sepuluh November, Surabaya, 2011.
[8] Hermawan, H., *Design of Network-Based Sensor Module RCM4510w On Weather Data Acquisition System*, Undergraduate theses, Politeknik Elektronika Negeri Surabaya, 2012.
[9] Digi International, *Datasheet XBee PRO 802.15.4*, www.digi.com (Januari 2013)
[10] Figaro, *Datasheet Sensor TGS 2600*, www.figarosensor.com (Januari 2013)
[11] Cytron, *Datasheet Sensor HSM 20-G*, www.cytron.com.my (Januari 2013)
[12] Texas Instruments, *Datasheet Sensor LM35DZ*, www.ti.com (Januari 2013)

Early Warning System for Infectious Diseases

Inayatulloh
School of Information Systems
Bina Nusantara University
KH. Syahdan 9 Kebonjeruk, Jakarta, Indonesia
inay@binus.ac.id

Selvyna Theresia
School of Information Systems
Bina Nusantara University
KH. Syahdan 9 Kebonjeruk, Jakarta, Indonesia
selvyna.theresia@binus.ac.id

Abstract— **Infectious diseases are among the most serious health issues in the world. The emergence of these diseases affected by various factors such as multiple human, biological, climate, and ecological determinants. Within the last decade, the world has witnessed the global outbreak of infectious diseases. This situation highlights the need for an early warning disease detection system that would be able to detect, identify, and contain pathogens with epidemic potential. This article presents how Early Warning System (EWS) could be a proactive system that would be able to predict infectious disease outbreaks and detect the sudden increase of any livestock disease with the potentials to become epidemic before spreading.**

Keywords—Infectious diseases; infectious disease outbreak; livestock disease; pathogen; epidemic; early warning system

I. INTRODUCTION

The United Nations (UN) predicted that in the next 25 years, Asian countries would be the world's center of economic growth. The increase of economic activities in the cities would lure people from rural areas to migrate to big cities as well as prompting the rise of domestic and international harvests and livestock trade. The surge in the movement of people and goods will increase the risk of epidemic transmission not only domestically, but also internationally.

Within the last decade, the world has witnessed the global outbreak of infectious diseases such as severe acute respiratory syndrome (SARS) and swine flu (H1N1). The spread of these diseases underlined the need for better global outbreak surveillance, particularly through the increasingly improving Internet. The Internet can help develop a better global-scale communication as well as surveillance and reporting frameworks following the implementation of World Health Organization's (WHO) International Health Regulations (IHR 2005) in 2007 [3]. It is important to have a proactive early warning disease detection system that would be able to detect, identify, and contain pathogens with epidemic potential before spreading.

The emergence and reemergence of infectious diseases is affected by various factors such as multiple human, biological, and ecological determinants. Another important factor is the climate, particularly due to the changes that have happened and will continue to happen in the future, such as the rising global temperatures—estimated to rise by as much as 2.0° Celsius by the year 2100. The changes may trigger the introduction and dissemination of many serious infectious diseases that are sensitive to climate, such as mosquito-borne diseases like malaria, dengue, and viral encephalitis. Climate change would directly affect disease transmission by shifting the vector's geographic range and increasing reproductive and biting rates and by shortening the pathogen incubation period.

When the climate-related change occur in sea surface temperatures and sea level, it may cause an increase in the occurence of water-borne infectious and toxin-related illnesses, such as cholera and shellfish poisoning. Human migration may also contribute to the spread of diseases, although in a more indirect way. Moreover, climate change may affect agricultural products—which then cause malnutrition—and the increased influx of ultraviolet radiation may disturb human immune system. These will make humans more prone to infections. In order to determine the multi-faceted impact of climate change in the occurence of infectious diseases, there should be an interdisciplinary cooperation among physicians, climatologists, biologists, and social scientists. Furthermore, to ensure public health authorities and medical staff can implement better measures to anticipate the occurence and outbreak of infectious diseases, there should be an increase in disease surveillance, integrated modeling, and the use of geographical-based data systems. Understanding the linkages between climatological and ecological change as determinants of disease emergence and redistribution will ultimately help optimize preventive strategies [2].

II. LITERATURE REVIEW

A. Infectious Disease

One of the ways to detect infectious diseases as a part of the early warning system in determining infectious disease outbreaks is by observing friends and colleagues. By looking at a group of closely connected people who are likely to catch infectious diseases such as flu early on, epidemiologists can observe outbreaks and can warn authorities earlier than other methods.

Nicholas Christakis from Harvard University and James Fowler from the University of California, San Diego conducted a research using the friendship paradox to monitor the spread of both seasonal flu and swine flu (H1N1) through students and their friends at Harvard University. According to the paper they submitted to the Proceedings of the National Academy of Sciences and online repository of research papers arXiv, they randomly selected 319 undergraduates and asked them to

nominate up to three friends. The nomination was then used to collect another group of 425 friends. In line with the friendship paradox, the second group was more popular and more central to the connections among Harvard students. Christakis and Fowler monitored the group for flu infections from September 1, 2009 to December 31, 2009 through the university's health services and the students' responses to health surveys sent by email twice a week.

The study found that around 8% of the students were diagnosed with the flu by the health services and another 32% were self-diagnosed. The infection rate among the group of more-connected friends peaked two weeks earlier compared to those who were less-connected, showing that their connectedness caused them to get infected earlier than others.

Based on the findings of the study, the two researchers tried to find ways to provide real time early warning signs of an outbreak that is about to happen. They started comparing the daily diagnoses of the two groups (the friend group and the random group) for every day of the four-month study. There was a notable difference between the two groups regarding the timeframe of the outbreaks. The friend group that was diagnosed by a medical staff peaked 46 days earlier from the estimated peak visit to the university's health services. On the other hand, the friend group that self-diagnosed peaked 83 days earlier than the estimated peak of daily incidence in the self-reporting system.

The early results of the study showed that it might be able to report a possible outbreak much sooner than the current methods used to assess an infection by the U.S.' Centers for Disease Control and Prevention which lag an outbreak by around 1-2 weeks. Google's Flu Trends monitors millions of queries to Google for flu-related keywords can only show the outbreak as it happens, not beforehand. Christakis and Fowler suggested combining the methods so that the search queries of popular and well-connected individuals could be monitored closely for signs of the flu.

In spite of the small-scale research that they performed, both researchers think that the research findings could help predict other infectious diseases on a larger scale, whether in cities or regions. Public health officials have already been conducting random samplings for years and they could ask the subjects to provide several friends' names to test this theory.

B. *Early Warning System*

Early warning systems (EWS) are essentially management tools to predict infectious diseases outbreaks as well as to detect the sudden increase of any livestock disease with the potentials to become epidemic, for example the climate-based EWS for malaria [1]. It is mainly based on disease surveillance, reporting, and epidemiological analysis. Information systems is the pillar of EWS because it enables integration, analysis, and sharing of animal health data combined with relevant layers of information such as socioeconomic, production, and climatic data. The outcome will enable researchers and public health officials to understand the underlying ecological and epidemiological mechanisms responsible for the maintenance and spread of a disease, which would help to define and implement cost-effective control strategies.

The importance of EWS has not been fully understood and developed, indicated by the lack of protocol to evaluate and compare EWS as well as specific EWS for various diseases. For example, there has not been any development of EWS for tropical diseases whose transmission is sensitive to environmental conditions, even though they caused havoc for the affected society. Among the few systems in place is the FAO Early Warning System to monitor worldwide avian influenza occurrences, which provides better understanding of the disease and shows the potential for better integration and exchange of information among key stakeholders [10].

EWS is critical to prepare for potential biological attacks that have an incubation period, providing time to respond effectively. There are two reasons why early recognition and detection of infectious diseases is important. First, it allows medical staff to administer effective prophylactic treatment in a timely manner [10]. Second, it minimizes the opportunity for transmission of the agent [9]. If a terrorist group attacks using biological weapon, they may launch an announced attack—in which they publicly discloses the agent that was used—or an unannounced attack. If it is the former, public health officials may be more aware of the particular agent and therefore can detect and diagnose cases better. If it is the latter, the detection and identification of the agent will not happen until after patients seek medical help, which resulted in time lost that could have been used to locate and treat new cases. There is also a possibility that the terrorist used an unknown agent or even various agents, resulting in patients presenting similar symptoms but different illnesses [9].

III. DISCUSSIONS

EWS developments that have already been conducted are as follows:

- Early Warning System *In Indonesia and many other Southeast Asian countries,* dengue and dengue hemorrhagic fever (DF and DHF) are very common. This study used analytic cross sectional study with Epi.yr as the dependent variable, aimed to predict the occurrence of dengue virus infection using weather data. Epi.yr is dichotomous, which indicates whether an epidemic occurred during a particular year. The monthly number of cases of DF and DHF in Yogyakarta, Indonesia and Greater Bangkok area, Thailand were relatively high. Cases in Yogyakarta have often been very near the epidemic threshold of 278 cases but only in 1992 with 237 cases they were incorrectly labeled. Only a simple calculator or a computer to calculate the derived equation is needed for this method [7].

- An EWS for upcoming DHF epidemics was developed using a simple predictive regression model based on past and present DHF cases, climate and meteorological observations as inputs to make future prediction. This system was expected to give a warning three months in advance of a predicted outbreak. The model, which

used Peirce score as a measure of prediction skill, has only successfully predicted a moderately severe epidemic at lead time of up to 6 months. Another model, which used discriminant method, was also developed and gave much higher score and longer lead times than the regression model. The study also showed that families who implemented the prediction into their decision making process obtained more benefit than those who had to make uninformed decision [4].

- On the other part of the world, a research was conducted for a Malaria EWS (MEWS) in Africa by relying on the access to rainfall information with the integrated early warning systems for malaria and other climate sensitive diseases. Rainfall anomalies are usually the main determinant of epidemic outbreaks in warm semi-arid regions and can be an important information source for the highland-fringe; therefore, the operational rainfall monitoring tools were developed for the MEWS. This system may be modified in future with further evaluation and user feedback. Meanwhile, email has become easier to access in Africa, which prompted information sharing between regional support centers. For example, WHO-Intercountry Programme for Malaria Control in Southern Africa prepare bulletins with malaria relevant climate data to be distributed both through email and courier to district health teams in epidemic prone areas as part of an overall MEWS [2].

- EWS is also developed by considering several factors such as climate and living environment that may cause the spread of infectious diseases as depicted in the diagram below [8].
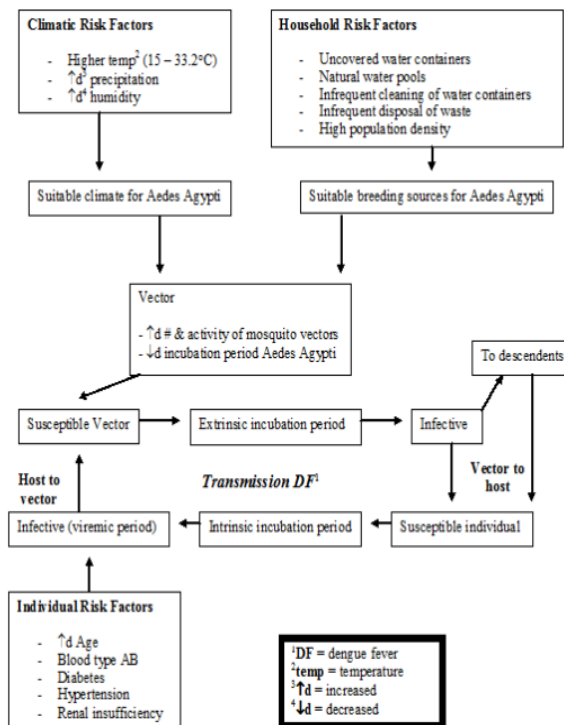
Fig. 1. Living Environment Factors

Various research have been conducted to develop EWS for some infectious diseases such as dengue, malaria and SARS. This system will detect the spread of infectious diseases using mobile technology by receiving information from various sources in the neighborhood, which would be important indicators regarding the spread of infectious diseases.

Below is the data obtained from observation and survey in some parts of DKI Jakarta by gathering samples from health institutions such as hospitals, labor and delivery hospitals, and polyclinics.
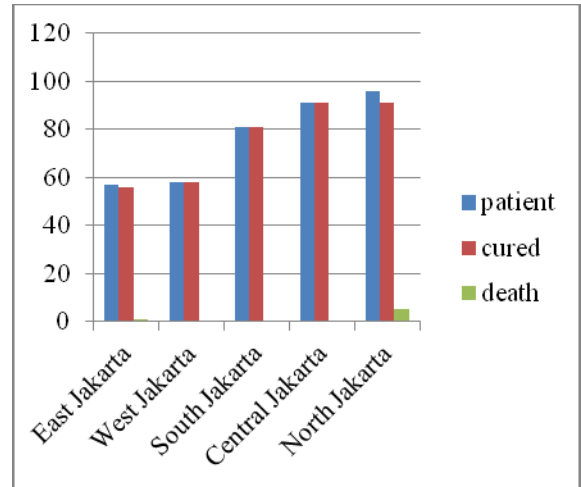
Fig. 2. The Amount of Infectious Diseases Patients in 2010-2015

The figure above shows the amount of infectious diseases spread in different regions. The graph indicates the relatively high number of both infectious diseases and cure rates. Only two regions recorded deaths.
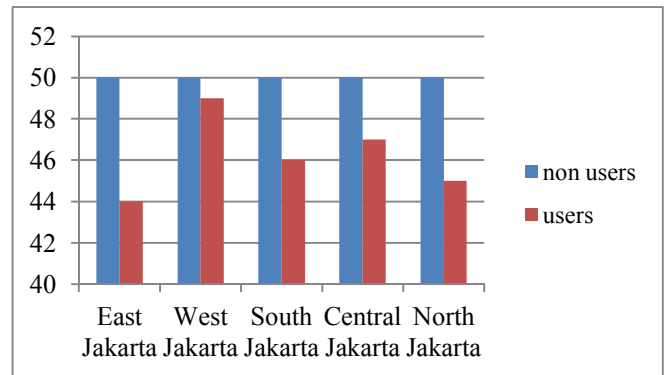
Fig. 3. Mobile Device Users

The figure above shows the number of mobile device used by health care professionals such as medical doctors, nurses, and midwives in several different regions. In general, almost all health care professionals use mobile device except in one region, where the ratio between the number of mobile device users and non-users is relatively equal.
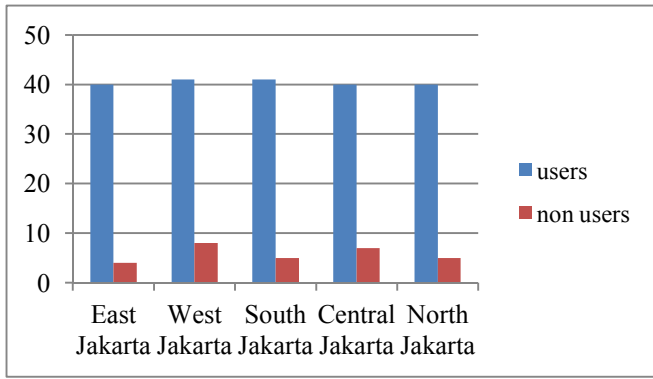
Fig. 4. Mobile-Based Health Software Application (Apps) Users

The figure above shows the number of health care professionals using their mobile device to get health-related information from the health apps. The number shows great potentials to develop other health apps.
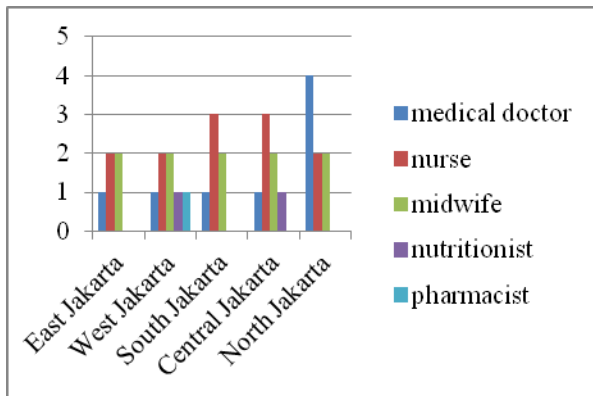
Fig. 5. Mobile Device Users and The Potentials in Developing Apps That Can Detect Early Infectious Disease Outbreak

Nurses and medical doctors are the most potential users of the apps due to their gadget availability and their access to informational health apps.

Based on the surveys conducted to some health care professionals, a model of early warning infectious disease apps has been designed as follow:
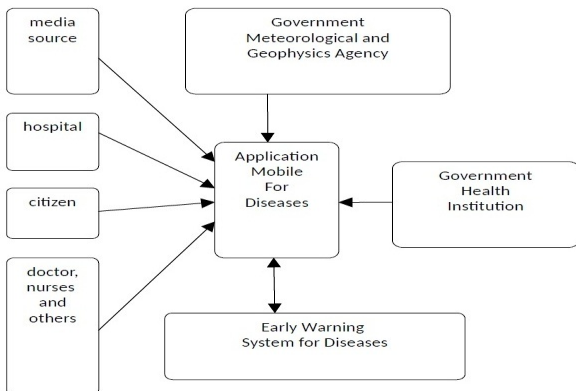
Fig. 6. Information Sources of Infectious Diseases

Information regarding infectious diseases that emerged in the society can come from various sources such as individual, society, and institution. One of the institutions that would provide information regarding infectious diseases is the hospital where they will report and continuously update the number of infectious diseases occurences. Meteorogical and geophysical institution would regularly provide reports of climate change in the region. The information would be used by EWS to find the correlation between the climate change and the spread of infectious diseases.

The system would verify and validate the continuously updated information on the spread of infectious diseases gathered from all the sources which would then be processed by the system to generate the final report on the spread of infectious diseases.

The simulation of EWS for Infectious Diseases using mobile device is as follows:

- First time users have to register themselves.

Fig. 7. Registration Page for New User

- Once the users registered, they can log in to the system, which then would direct them to the page displaying a form to be filled with the disease category and the amount of each disease as shown below.
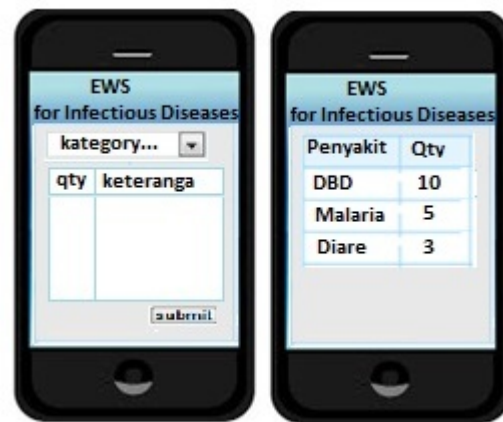
Fig. 8. Disease Category Page

Based on observations in 5 regions of DKI Jakarta for the cases of dengue fever and other diseases, the results are as follows:
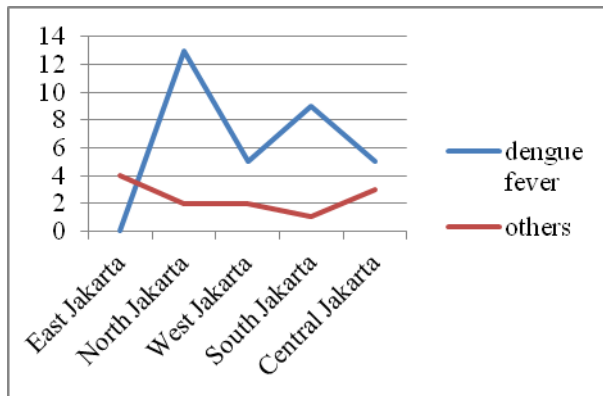
Fig. 9.   Result of Observations in 5 Regions of DKI Jakarta

IV. CONCLUSION

This system still needs to be improved in several areas such as disease category, sources of information, and the supporting tools. Moreover, the results generated by this system regarding the spread of infectious diseases should be better distributed so that this system can give more valuable benefits.

Early detection for diseases can help medical authorities in taking pre-emptive measures to avoid bringing about more victims.

REFERENCES

[1] L.F Caves, M. Pascual M, "Comparing Models for Early Warning Systems of Neglected Tropical Diseases," PLoS Negl Trop Dis 1(1):e33, DOI:10.1371/ journal.pntd.0000033. Retrieved on June 8, 2015.

[2] E.G. Kopec, M. Kawano, R.W. Klaver, B. Blumenthal, P. Ceccato, S.J. Connor, "An Online Operational Rainfall-Monitoring Resource for Epidemic Malaria Early Warning Systems in Africa," Malaria Journal, 2005, 4:6, DOI:10.1186/1475-2875-4-6. Retrieved on June 15, 2015.

[3] Emily H. Chan (2010), Global Capacity for Emerging Infectious Disease Detection," Proceding Of The National Academy Of Science Of United State of America, vol. 107, no. 50, 2010.

[4] H. Halide, Rais, Peter Ridd, "Early Warning System for Dengue Hemorrhagic Fever (DHF) Epidemics in Makassar", Jurnal Matematika & Sains, vol. 16, no. 1, pp. 26-34, 2011.

[5] J.E. Quansah, B. Engel, G.L. Rochon, "Early Warning Systems: A Review", Journal of Terrestrial Observation, vol. 2, issue 2, article 5, pp. 24–44, 2010.

[6] L. Racel, T.C. Bailey, D.B. Stephenson, R.J. Graham, C.A.S. Coelho, M.S. Carvalho, C. Barcellos, "Spatio-Temporal Modelling of Climate-Sensitive Disease Risk: Towards an Early Warning System for Dengue in Brazil," Computers & Geosciences Journal, vol. 37, issue 3, pp. 371-381, 2011.

[7] M. Juffrie, D.A. Focks, "Early Warning System (EWS) For Dengue In Indonesia And Thailand," Jurnal Berkala Ilmu Kedokteran, vol. 41, no. 3, pp. 134-142, 2009.

[8] V. Racloz, R. Ramsey, S. Tong, W. Hu, "Surveillance of Dengue Fever Virus: A Review of Epidemiological Models and Early Warning Systems," PLoS Negl Trop Dis 6(5): e1648, DOI:10.1371/journal.pntd.0001648. Retrieved on June 15, 2015.

[9] T.G. Veenema, J. Tõke, "Early Detection and Surveillance for Biopreparedness and Emerging Infectious Diseases," Nursing Online Journal, DOI:10.3912/OJIN.Vol11No01Man02. Retrieved on August 10, 2015.

[10] V. Martin, S. Dobschuetz, A. Lemenach, N. Rass, W. Schoustra, "Early Warning, Database, and Information Systems for Avian Influenza Surveillance", Journal of Wildlife Diseases, 43(3), pp. S71-S76, 2007.

Outage Probability Analysis for Optical Inter-platform HAPS-Link over Log Normal Turbulence Channels

H. Akbar and Iskandar
School of Electrical Engineering and Informatics, Bandung Institute of Technology
Jl. Ganesha No.10 Bandung 40132 Indonesia
E-mail: ahasbi81@gmail.com, iskandar@stei.itb.itb.ac.id

Abstract—**In this paper, the outage probability performance of optical inter-platform link is analyzed. Atmospheric turbulence is one of the main impairment affecting the operation of optical inter platform link. An inter-HAP channel was modeled as a random process with log normal distribution. The outage probability expression is theoretically derived and numerical results are presented. The results illustrate the outage probability dependence on the power margin, turbulence strength, and propagation path length.**

Keywords—component; optical interplatform link, outage probability, power margin, log normal distribution.

I. INTRODUCTION

Optical wireless communication or free space space optical communication is an emerging technology that offer several advantages, such as high data rates (several in regime gigabits per second), small antena (telescope) sizes with high antenna gain, tap-proofness, and free license near-infrared spectrum bands [1]-[2]. Some applications of FSO links have various scenarios from short-distance, mid-range, and long-rang links such as between satellites, High Altitude Platforms (HAPs), Unmanned Aerial Vehicles (UAVs), aircrafts and soon.

High Altitude Platform Stations (HAPs) are quasi-stationary vehicles in the stratosphere at an altitude of 20 to 50 km above the Earth's surface [3]-[7], where the atmospheric impact on a laser beam is less severe than directly above ground [8]. Optical Inter Platrform Links (OIPLs) is a term for optical link that connects two HAPS (High Altitude Platform Stations). The potetial utility of such links is that they can make up for the terestrial bone network in case of emergency [9]-[10]. Ilustration of optical interplatform link can be seen in figure 1.

The major problem of free space optical communications links is the atmospheric turbulence, which results in fluctuations at the received signal, severely degrading the link performance [11]. Atmospheric turbulence is the result of in-homogenities in the index of refraction known as scintillation, which leads to stochastics amplitude (and power) fluctuations [12]. This phenomenon is called fading or scintillation. Various models describing the probability density function (PDF) of the irradiance fluctuation have been developed. For weak turbulence regime, lognormal statistics can be used as turbulence model. Beyond weak regime, where multiple scattering exists, the gamma-gamma anda negative exponential

Fig. 1. Ilustration of Optical Interplatform Link[4]

models corresponding to the weak-to-strong and saturation regimes, respectively.

In this paper, outage probability has been chosen as performance parameter of optical inter platform link in the presence of atmospheric turbulence. For inter-HAPS link, because of lower density of particles and gas, the random attenuation due to atmospheric turbulence is weak [13]. The log-normal distribution can be used to model atmospheric fading in weak turbulence regimes. In weak to moderate turbulence regime, aperture averaging has been recomended as an effective way to mitigate turbulence [14]-[15]. We presented the extra power margin that required to achieve a certain outage probability using aperture averaging.

II. CHANNEL MODEL

A. Structure Parameter Index Refractive (C_n^2)

In atmospeheric turbulence, the structure parameter, $C_n^2(h)$, represents the total amount of energy contained in the stochastic field of the refractive index fluctuations [2]. It is a measure of optical turbulence strength and required for the calculation of important fading related parameters like the scintillation. In this paper, the altitude profile for the parameter C_n^2 is generated using the Hufnagel-Valley (H-V) model. The H-V model is expressed as a function of height as follows [2]:

$$C_n^2(h) = 5.94 \times 10^{-3} \times (v_{rms}/27)^2 \times (h/10^5) \times \exp(-h/1000)$$
$$+ 2.7 \times 10^{-16} \times \exp(-h/1500) + C_n^2(0)\exp(-h/100) \quad (1)$$

where h is the altitude in meters, v_{rms} is the rms wind speed in m/s and $C_n^2(0)$ is the structure constant at level ground.

B. Scintillation Index

The intensity Scintillation Index (SI) is defined as the normalized variance of irradiance fluctuations. For such a high divergence and a long propagation paths, the Gaussian beam wave is close to a speherical wave in terms of scintillation [16]. Scintilattion index is expressed as:

$$\sigma_I^2 = \exp\left[\frac{0.49\sigma_{I,sp(0)}^2}{(1+0.18d^2+0.56\sigma_{I,sp(0)}^{12/5})^{7/6}} + \frac{0.51\sigma_{I,sp(0)}^2(1+0.69\sigma_{I,sp(0)}^{12/5})^{-5/6}}{1+0.9d^2+0.62d^2\sigma_{I,sp(0)}^{12/5}}\right] - 1 \quad (2)$$

where $d = \sqrt{\frac{kD^2}{4L}}$ and $\sigma_{I,sp(0)}^2 = 0.4\sigma_R^2 = 0.492 C_n^2 k^{7/6} L^{11/6}$ ($k = \frac{2\pi}{\lambda}$ is the oprical wave number; L is the length of optical link; D is the receiver's aperture diameter).

C. Turbulence Model

An inter-HAP channel, under the influence of IRT, can be modellede as a scintillation channel with fades and surges. In case of weak turbulence, generally the influence of turbulence is modelled as a random process with log normal distribution [15]. The probability density function (PDF) of the log normal model is given by [16],

$$p(I) = \frac{1}{I\sqrt{2\pi\sigma_I^2}} \exp\left\{-\frac{\left(\ln(I)+\frac{\sigma_I^2}{2}\right)}{2\sigma_I^2}\right\} \quad (3)$$

where is the scintillation index defined in (2).

III. INTER HAPS SCENARIOS

In this paper several optical inter platform link scenarios are examined. The various scenarios are based on a system consisted of two HAPs, both are placed at altitude 20 km in a graze height 13km. Graze height is the minimum of the optical link above the surface of the earth [17]. In this paper, two scenarios are defined. The first one is turbulence strength varying with constant link distance, and the second one is the link distance varying with constant turbulence strength.

A. Scenario 1

In scenario I, parameter link distance is 600km, receiver's aperture diameter is 0.2 with various turbulence strength. Table 1 shows various turbulence strength in three conditions. Scintillation Index (SI) is calculated with expression (2).

TABLE I VARIOUS TURBULENCE STRENGTH IN SCENARIO 1.

Cn 2 [m-2/3]	SI	Turbulence
3x10^-19	0,4701	Weak
7x10^-19	0,641	Moderate
2x10^-18	0,8798	Strong
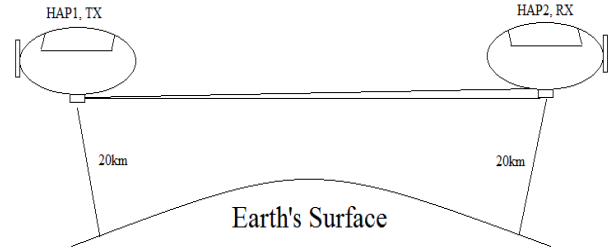
Fig. 2. Ilustration of scenario optical link inter platform

B. Scenario 2

In scenario II, parameter system turbulence strength is 7×10^{-19}, receiver's aperture diameter is 0.2 with various link distance from 400km, 450km, 500km, 550km, and 600km. Figure 2 ilustrate scenario of optical link inter platform in this paper.

IV. OUTAGE PROBABILITY

Outage probability is one of metric for quantifying the performance of communication systems in fading channels. A system with an adequate average BER can temporarily suffer from increases in errorr rate due to deep fades and this 'short outages' is not adequately modelled by the average BER [16]. The probability of outage due to the presence of optical turbulence is defined as probability that the instantaneous SNR falls below a predetermide SNR threshold due to the presence of atmospheric turbulence. If a parameter m represent power margin that is intoduced to account for the extra power needed to cater for turbulence-induced signal fading, then the outage probability for inter-HAP channel modelled as a random process with log normal distribution, given by [18],

$$P_{out} = \Pr(m\gamma(I) \leq \gamma^*) = \int_0^{I_0/m} \frac{1}{I\sqrt{2\pi\sigma_I^2}} \exp\left\{-\frac{\left(\ln I/I_0 + \sigma_I^2/2\right)}{2\sigma_I^2}\right\} dI \quad (4)$$

$$= Q\left(\frac{1}{\sigma_I}\ln m - \frac{\sigma_I}{2}\right)$$

where σ_I^2 is scintillation index expressed in (2).
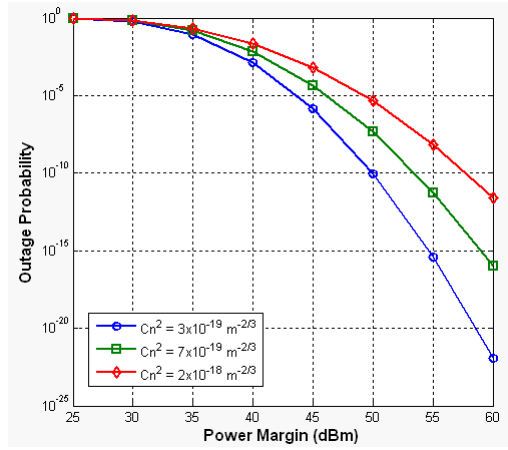
Fig. 3. Outage Probability vs power margin for various turbulence strength $C_n^2 = [3x10^{-19}, 7x10^{-19}, 2x10^{-18}]$ with L = 600 km and D = 0.2 m.

Fig. 4. Outage probability vs power margin for various link distance L=[400km, 450km, 500km, 550km, 600km] with turbulence strength C_n^2= 7x10D = 0.2 m.

V. NUMERICAL RESULTS AND DISCUSSION

Using the above-derived closed form for the outage probability (4), we investigate the required power margin to achieve a certain value of outage probability. The parameters under consideration that affect the system are the link distance (L), receiver's aperture diameter (D), and atmospheric turbulence streng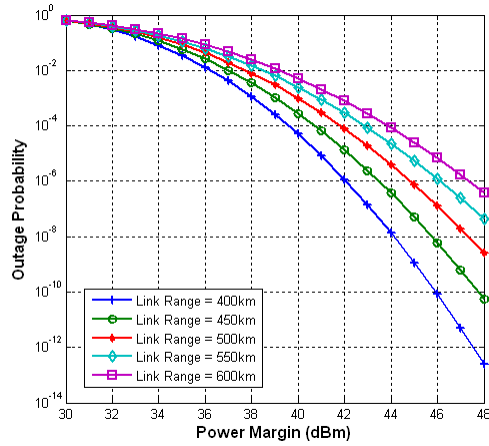th (C_n^2). The value of link distance varies beetween 400 – 600 km, and D = 0.2 m, and three different atmospheric turbulence conditions as defined in Tabel I.

In fig.3,. we present the outage probability of the optical inter platform link as a function of power margin for three conditions of turbulence strength (weak, moderate, and strong

turbulence strength). In this case, the link distance is 600 km and the receiver's diameter aperture is 0.2 m. It shows that the

TABLE II REQUIRED POWER MARGIN (SCENARIO I).

Cn2 (m^-2/3)	Outage Probability				
	10^-2	10^-3	10^-4	10^-5	10^-6
3x10^-19	38 dBm	40dBm	41.8dBm	43.6dBm	44.4dBm
7x10^-19	38.6dBm	41.8dBm	43.9dBm	45.6dBm	47.7dBm
2x10^-18	41.3dBm	44.2dBm	47.1dBm	49.4dBm	51.3dBm

TABLE III REQUIRED POWER MARGIN (SCENARIO II).

Link Distance	Outage Probability				
	10^-2	10^-3	10^-4	10^-5	10^-6
400 km	36.2dBm	38.2dBm	39.4dBm	40.6dBm	42.3dBm
450 km	37dBm	38.8dBm	40.8dBm	42.3dBm	43.7dBm
500 km	37.8dBm	40.2dBm	41.9dBm	43.7dBm	44.6dBm
550 km	38.4dBm	40.9dBm	42.7dBm	44.6dBm	46.3dBm
600 km	39.3dBm	41.4dBm	43.7dBm	45.5dBm	47.4dBm

atmospheric conditions affect the outage probability of link. Tabel II shows the required power margin to achieve a certain value of outage probability for scenario I (with various conditions of turbulence strength). Based on table II, we can conclude that, power margin above 40dBm can guarantee the outage probability smaller than 10^{-3} for all three conditions of turbulence strength.

Outage probability dependence on the power margin for different link distance is shown in fig. 4. By increasing the link distance, the required power margin becomes larger to achieve certain value of outage probability. Figure 4 and tabel III use parameter system in scenario II. From table III, we can conclude that, power margin above 40dBm can also guarantee the outage probability smaller than 10^{-3} for all various link distance.

VI. CONCLUSION

In this paper, we have theoretically analyzed outage probability of optical interplatform link under turbulence atmospheric conditions modelled by the log normal distribution. We studied the dependence of the outage probability of optical interplatform link through turbulent atmosphere as a function of principal paramaters of such a link, link distance, power margin, atmospheric turbulence conditions between the transmitter and the receiver. The numerical result show that power margin that required to achieve certain target outage probability.

REFERENCES

[1] J Ramírez, A Shrestha, S Parthasarathy, D Giggenbach, "Gigabit Laser Ethernet Transceiver for Free-Space Optical

Communication Systems", Applications of Lasers for Sensing and Free Space Communications 2013. 2013

[2] L. C. Andrews and R. L. Phillips, Laser Beam Propagation through Random Media, 2nd ed. Bellingham, WA: SPIE, 2005.

[3] Iskandar and S. Shimamoto, "Prediction of propagation path loss for stratospheric platforms mobile communications in urban site LOS/NLOS environment," in Proceedings IEEE International Conference on Communication (ICC), vol. 12, pp. 5643 - 5648, June 2006.

[4] Iskandar and S. Shimamoto, "Channel characterization and performance evaluation of mobile communication employing stratospheric platform," IEICE Transactions on Communications, vol. E89-B, no. 3, pp. 937-944, March 2006.

[5] Iskandar, A. Kurniawan, E. B. Sitanggang, and S. Shimamoto, "Step Size Optimization for Fixed Step Closed Loop Power Control on WCDMA High Altitude Platforms (HAPs) Channel," in Proceedings of IEEE Global Telecommunication Conference (GLOBECOM), vol. 1, pp. 1-5, Dec. 2008.

[6] Iskandar and S. Shimamoto, "On the downlink performance of stratospheric platform mobile communications channel," in Proceedings of IEEE Global Telecommunication Conference (GLOBECOM), vol. 1, pp. 1-5, Dec. 2006.

[7] Iskandar, A.Kurniawan, and M.E. Ernawan, "Closed Loop Power Control with Space Diversity to Improve Performance of Low Elevation Angle Users in HAPs-CDMA Communication Channel," in Proceeding of The 8th International Conference on Telecommunication Systems, Services, and Applications (TSSA 2014), vol 1, pp. 1-5, Oct. 2014.

[8] E. Katimertzoglou, D. Vouyioukas, P. Veltsistas, and P. Constantinou, "Optical Interplatform Links Scenarios for 20 km Altitude , 16th IST Mobile and Wireless Communications Summit", p. 1-5, Budapest, Hungary, 2007

[9] Fidler, F., Knapek, M., Horwath, J., Leeb, W., "Optical Communications for High-Altitude Platforms," Selected Topics in Quantum Electronics IEEE Journal of, 16, 1058-1070. 2010.

[10] X. Zhu and J. M. Khan, "Free-space optical communication through atmospheric turbulence channels," IEEE Trans. Commun., vol. 50, pp.1293–1300, Aug. 2002.

[11] Andrews L.C., Phillips R.L., HOPEN C.Y.: „Laser beam scintillation with applications (SPIE Press, Bellingham, WA, 2001)

[12] C.Robert, J.M.Conan, V.Michau and et., "Retrieving Parameters of the Anisotropic Refractive Index Fluctuations Spectrum in The Stratosphere from Balloon-Borne Observations of Stellar Scintillation", in Remote Sensing of Clouds and the Atmosphere Conf., Jan 2008, vol.6745, pp.379-393.

[13] M. A., Khalighi, N. Aitamer , N. Schwartz, and S Bourennane. "Turbulence mitigation by aperture averaging in wireless optical systems." In 10th International Conference on Telecommunications, 2009. ConTel 2009,pp59-66, 2009.

[14] J. Horwath, N. Perlot, D. Giggenbach, and R. Jüngling, "Numerical simulations of beam propagation through optical turbulence for high-altitude platform crosslinks", Proceedings of the SPIE 2004, vol. 5338B, 2004.

[15] Parthasarathy, Swaminathan and Giggenbach, Dirk and Kirstädter, Andreas, "Simulative Performance Analysis of ARQ Schemes for Free-Space Optical Inter-HAP Channel Model ".Proceedings of Photonic Networks.Photonic Networks;16 ITG Symposium 2014, 7-8May 2015, Leipzig,German.ISBN:9783800739387

[16] Majumdar A.K.: 'Free-space laser communication performance in the atmospheric channel', Journal of Optical and Fiber Communications Research,2005,2,pp.345–396

[17] V. W. S.Chan, Free-space optical communications, IEEE Journal of LightwaveTechnology, 24, 4750–4762, 2006

[18] Z. Ghassemlooy, W. Popoola, S. Rajbhandari., Optical wireless communications : system and channel modelling with MATLAB, CRC PRESS, 2012

Telemetry, Tracking and Command Subsystem for LibyaSat-1

Faisel EM M Tubbal, Akram Alkaseh and Asem Elarabi

Technological Projects Department

The Libyan Center for Remote Sensing and Space Science

Tripoli, Libya

femt848@uowmail.edu.au,   elkaseh1972@gmail.com,   asemelarabi@sk.kuee.kyoto-u.ac.jp

Abstract— In this paper we present the design and the analysis of Telemetry, Tracking and Command Subsystem (TT&CS) for Libyan imaging microsatellite (LibyaSat-1). This subsystem is the brain and the operating system of any satellite or spacecraft as it performs three important functions; tracking microsatellite position, monitoring microsatellite health and status and processing received and transmitted data. Moreover, the uplink and downlink budgets for s-band and x-band antennas are presented. We also designed s-band C-shaped patch antenna for command receiver (2.039 GHz). Electromagnetic simulation was performed to this antenna High Frequency Structure Simulator (HFSS). Our results show that the s-band C-shaped patch antenna achieves high gain of 6.45 dB and wide bandwidth; i.e., 1500 MHz. The achieved simulated return loss is -19.6 dB at a resonant frequency of 2.039 GHz.

Keywords—microsatellite; TT&C; transponder; telemetry

I. INTRODUCTION

Polar orbiting microsatellites have a wet mass ranging from 10 to 100 kg and are sun-synchronous. They operate at Low Earth Orbit (LEO) at altitudes of 700 to 1000 km [1]. Compared to conventional, medium and mini sized satellites, as set out in Table I, they have lower mass, cost less, and consume less power. Microsatellites are used for (i) remote-sensing; e.g., land imaging and weather forecasting, (ii) scientific research; e.g., ocean color and communication experiments, or (iii) telecommunications; e.g., rescue in ocean and for general purpose [2].

An example of a microsatellite is the SATEX I project [3]. It is a Mexican experimental microsatellite used for electronic telecommunications research at universities and multi-institutional environment. Another example is the SPOT satellites; i.e., SPOT 1, SPOT 2, SPOT 3, SPOT 4, and SPOT 5. They are French microsatellites and their primary mission is obtaining earth's imagery for land-use, agriculture, forestry, geology, cartography, regional planning, and water resources. For example, SPOT 5 is a sun-synchronous imaginary microsatellite that orbits at altitude 832 km. This satellite provides high resolution images for Libyan Centre for Remote Sensing and Space Science (LCRSSS) as part of commercial operations between France and Libya. Fig. 1 shows an image of Tripoli international airport in the capital of Libya with a resolution of 2.5 m. This image was captured by SPOT 5 in 2012 and it has been processed at LCRSSS.

TABLE I. COMPARISON BETWEEN SATELLITES

Types	Mass (kg)	Cost (US $)	Power Consumption
Conventional	>1000	0.1-2 B	0.1-2 B
Medium	500-1000	50-100 M	50-100 M
Mini	100-500	10-50 M	10-50 M
Micro	10-100	2-10 M	2-10 M
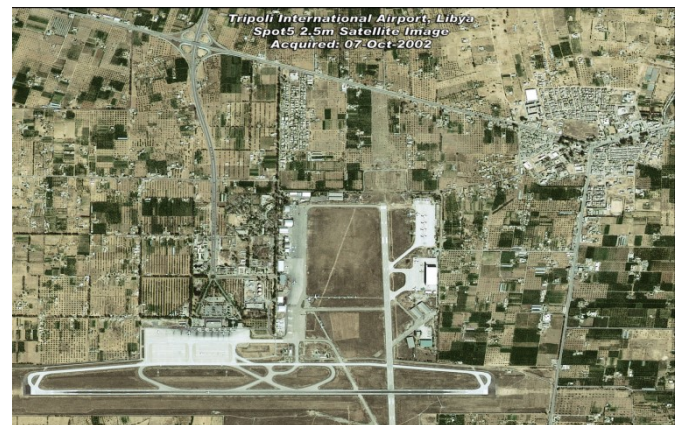
Fig. 1.   An image of Tripoli international airport

Libyan national agency for scientific research is planning to have its own remote sensing satellite [4]. Therefore, Libyan Satellite project (LibyaSat-1) is planning to develop a micro-satellite program to meet the requirements of LCRSSS. The main aim of this project is to be the first earth observation microsatellite to serve the needs of Libya and African countries, in the fields of natural resources management and agriculture. Moreover, the main mission of the LibyaSat-1 under the remote sensing program is to monitor terrestrial, marine environment, desertification and resources throughout Libyan landscape and its surrounding waters and possibly over other regions of the world for international cooperation. It is also recognized as an opportunity to validate new technologies in telecommunications, space science and allows achieving skilled human resources for all microsatellite subsystems.

A critical subsystem of microsatellite that provides a communication link with the ground stations is Telemetry, Tracking and Command (TTC) Subsystem. It also allows gathering and sending information to help in determining the satellite's orbit and to download images from payloads to control center [5]. An example of a ground station in Libya is Murezeq ground station which receives images and information from SPOT 5; see Fig. 2. In this paper, we focus on the design and requirements of telemetry, tracking and command subsystem for LibyaSat-1. We will present and discuss all

key requirements for T&C subsystem and image date downlink. These requirements include T&CS architecture, X-band subsystem architecture conceptual design, hardware components, operation requirements, components requirements and link analysis. We also present s-band patch antennas design for up and downlink communications. The LibyaSat-1 characteristics shown in Table II are considered when designing T&CS requirements.
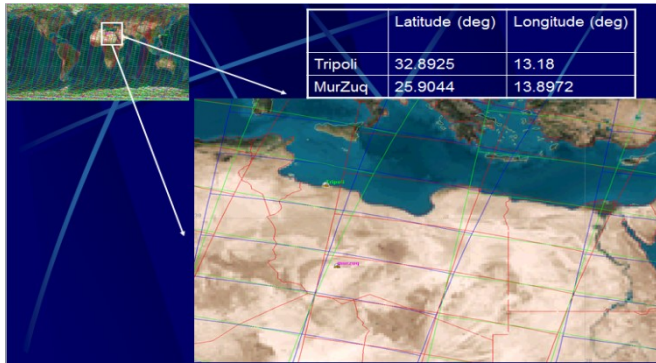

Fig. 2.   The geographical locations of Tripoli and Murezeq

II.   TELEMETRY, TRACKING AND COMMAND SUBSYSTEM

The aim of this project is to design, construct, implement and test of a RF subsystem to be used on a digital communication link at 2.039 GHz (s-band uplink) and 2.215 GHz (S-band, downlink), for the LibyaSat-1 microsatellite.   The system consists of transmitters, receivers, transponders and antennas. We present and analyse the link budget and the T&C architecture. Hardwar components with their characteristics and performance are also presented. LibyaSat-1 characteristics shown in Table II are considered when designing T&CS requirements.

TABLE II.   LIBYASAT-1 CHARACTERISTICS

Mission Orbit	775 km circular, sun synchronous orbit.
Satellite lift-off (Wet) weight	no more than 500 kg.
Mission life	5 years minimum.
Resource of power	solar sell and battery.
Launcher	Falcon 1e.
Data storage volume	no less than 80Gbits.
Satellite reliability	0.6 at the end of the 5-year mission
Swath:30km GSD : 2.5m (PAN) , 10m(MS).	Swath:30km GSD : 2.5m (PAN) , 10m(MS).
Satellite power	3% margin at the end of the 5-year mission.
Downlink rate (x-band	no more than 150 Mbps.
Downlink rate (s-band)	no more than 2.0 Mbps (State-of-Health and Scientific Data).
Attitude control	3-Axis Stabilization.

A. An Overview

TT&C subsystem receives commands from Command and Data Handling subsystem (CD&H) and provides health and status of the satellite to CD&H. It also performs antenna pointing and mission sequence operations for each stored software. All these operations are done through communications between the satellite and ground station using telemetry, command and tracking signals.

1) Telemetry.

As shown in Fig. 3 telemetry is a set of signals that have one-way direction from satellite to ground station. These signals are the taken measurements on board the micro satellite of the status of the spacecraft resources, health; i.e., temperatures, voltages, and currents. It also measures the attitude, scientific data, images, spacecraft orbit and timing data for ground navigation etc. Then all these measurements are sent to the control Centre through the ground station by RF system.

2)   Command

A set of one-way signals that are sent from ground station to the micro satellite in space. This links is used either for controlling the payload or for sending commands to control the satellite and its attitude at the critical phase.   When the solar cells is deployed, commends are then sent to turn on equipment that was off during launching phase; i.e., records and payloads. After the deployment of the solar cells, the micro satellite should operate automatically and less command will be sent.

3)   Tracking

For tracking the satellite to accurately locate its orbit, the same link is used to receive different measurements. These measurements include the time taken by RF signals for trip; i.e., station – satellite – station, frequency shift because of the satellite velocity, and the antenna orientation with respect to azimuth and elevation. By using all the aforementioned measurements, the accurate location of the satellite can be determined.

Fig. 3.   Communication links between satellite and ground station

B. TT&C Architecture

As shown in Fig. 4, S-band TT&C subsystem consists of two TT&C s-band antennas, RF Distribution Unit (RFDU) and two transponders. Each transponder has a receiver, transmitter and duplexer. These two transponders are used to backup each other and to provide RF channels for micro satellite tracking, telemetry, ranging and command. The duplexer at each transponder is used to switch between receiver and transmitter.

Fig. 4.   Micro satellite TT&C subsystem block diagram

1) Transponder

Two transponders in TT&C subsystem are used to backup each other and to provide RF channels for micro satellite tracking, telemetry, ranging and command. This redundancy ensures that the TT&C subsystem has reliability should one of transponders fail. In addition, the duplexer at each transponder is used to switch between receiver and transmitter. The requirements and parameters of TT&C transponder (s-band command receiver and s-band telemetry transmitter) of the LibyaSat-1 are shown in Table III. The command receiving sensitivity is −110dBm, noise figure is less than 6 dB and the output power of the s-band telemetry transmitter is about 5 W. Transponders are connected to both antennas via hybrid coupler which distributes signals in both directions; see Fig.4. The polarization of these antennas should be Circular Polarization (CP). This is important as it achieves the best signal strength and mitigates multipath fading.

TABLE III.   PARAMETERS OF S-BAND COMMAND RECEIVER AND TELEMETRY TRANSMITTER FOR LIBYASAT-1

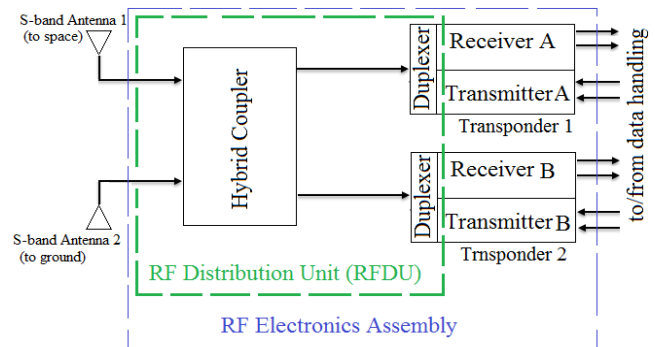| S-band Command Receiver	
Frequency	2.039 GHz
Sensitivity threshold for <10-6 bit error rate	-110 dBm
Receiver noise figure, maximum over temperature	< 6 dB
Signal modulation	BPSK +PM
Data Rate	32 kbps
S-band Telemetry Transmitter	
Frequency	2.215 GHz
Output power	5 W
Transmitter error vector magnitude	<10 %
Signal modulation	BPSK
Maximum transmit data rate	2Mbps

2) S-band antennas

As mentioned earlier, s-band command receiver and telemetry transmitter antennas should have resonant frequencies of 2.039 and 2.215 GHz respectively. To this end, we have designed s-band C-shaped patch antenna using the High Frequency Structure Simulator (HFSS) [6-8]. This antenna for s-band command receiver and operates at resonant frequency of 2.039 and meet all aforementioned requirements. For telemetry transmitter, we will purchase s-band antenna that provides the specifications mentioned in Table III above.

a) 2.039 GHz C-shaped patch antenna

Fig. 5 shows the 3D model of s-band C-shaped antenna for command receiver. The dimensions of the upper and lower patches are 69.2×24.4 and 46.8×7.3 mm^2 respectively. Three shorting pins are connected at the edges of the upper patch and are located between the upper patch and 122×122 mm^2 ground plane. Their main purpose is to achieve a wide impedance bandwidth at small antenna size.

Fig. 5.   Geometry of 2.039 GHz C-shped patch antenna

Fig. 6 presents the 3D gains of the s-band C-shaped patch antenna at 2.039 GHz. We see that the antenna has a high gain of 6.4 dB and a uniform radiation pattern. Fig. 7 shows the return losses over varying frequencies for s-band C-shaped antenna. The antenna has a wide -10 dB bandwidth; i.e., 1500 MHz (1.8-3.3 GHz). The return loss at resonant frequency of 2.039 GHz is about -19.6 dB.

Fig. 6.   3D gain of C-shaped patch antenna at 2.039 GHz

Fig. 7.   Simulated return losses (S$_{11}$) of C-shaped patch antenna

3) Passive components

Passive components that are used in TT&C subsystems are filters, hybrids, diplexers, and transmission lines. A band pass filter with 2.215 GHz center frequency and bandwidth of 50 MHz is used for a telemetry transmitter. The same band pass filter is used by the command receiver but at center frequency of 2.039 GHz. The coupler or divider provides a frequency range that covers 2.039 and 2.215 GHz at coupling rate of 3dB and a maximum insertion loss of 0.4. Another passive component is diplexer which has a maximum insertion loss of 0.5, minimum isolation of 30 dB and frequency range covers 2.039 and 2.215 GHz. Moreover, low loss cables and waveguides are used as transmission lines.

III. IMAGE DATA DOWNLINK

We now study the key requirements of image data downlink for LibyaSat-1. These requirements include real time transmission, store and dump transmission, the center frequency of x-band transmission, data rate, and type of coding scheme. Fig. 8 shows the architecture design of x-band subsystem for LibyaSat-1 including the x-band antenna and its pointing mechanism. Moreover, the downlink budget of x-band subsystem is presented in Table VI.

Fig. 8. X-band subsystem architecture

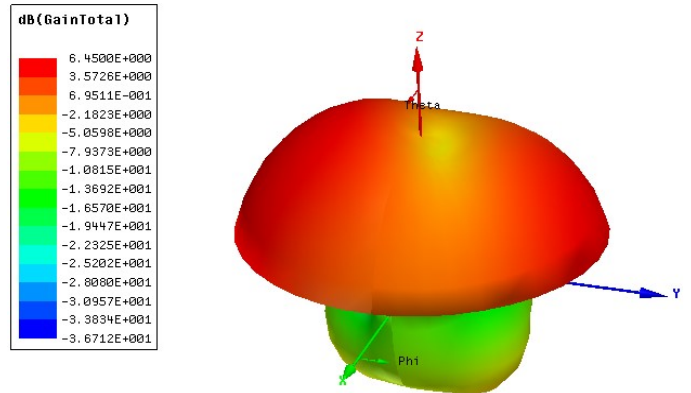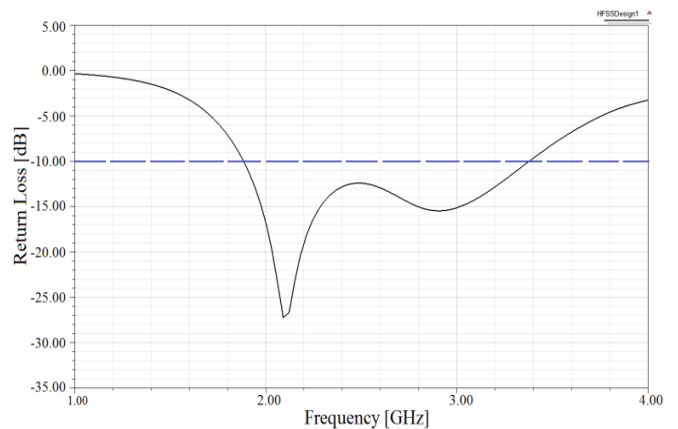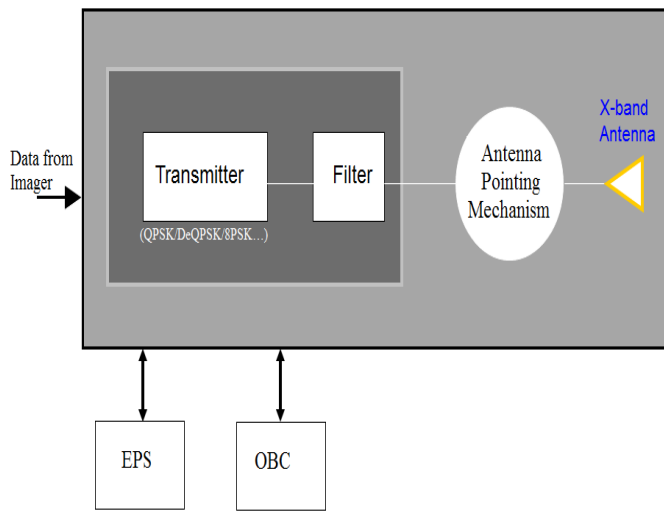### A. Real Time Transmission

The x-band communication link shall be with at least 6 dB link margin in clear sky with a cross-track viewing angle $< \pm30$ degrees toward the ground station. Moreover, the ground station elevation angle should be >20 degrees and passes where maximum elevation angle of $\geq$30 degrees.

B. Store and Dump Transmission

The store-and-dump transmission capability shall be provided to process the data that is not dumped in real-time downlink.

C. Resonant Frequency of X-band Antenna

The centre frequency of the x-band transmission antenna shall be 8.150 GHz with a minimum gain of 10 dB. The bandwidth of this antenna must be about 150 MHz and should provide right hand circular polarization (RHCP). Next we provide more details about this antenna.

D. Data Rate and Coding Scheme

The data rate shall be 150 Mbps for the operation in QPSK/DeQPSK/8PSK/ mode. The proposed coding scheme is Reed-Solomon (255,223) that implemented in the imager.

IV. MUREZEQ GROUND STATION

This ground station is a multi-mission ground station which was installed by LCRSSS in 2007. The main aim of this station is to send commands to satellites in space and receive images back from these remote sensing satellites; i.e., SPOT 5 and ENVISAT. It uses 5.4 m x-band sub-system dish antenna a diameter of 5.4 m; see Fig. 9. It features an innovative Cassegrain feed and sub-reflector design which leads to high gain, low noise and high antenna efficiency. It feeds with LNA, mono-pulse tracking, and equipment to receive remote sensing data, including a GPS location and timing system. The characteristics of this x-band antenna are set out in Table IV.

Murezeg ground station has five sub-systems as following:

- Antenna sub-system: dish, feed and LNA, pedestal X\Y, control unit, wind gauge, and GPS antenna.

- RF sub-system: fixed frequency conversion from X-band to S-band, RF splitters, and programmable frequency conversion from S-band to FI 720MHz.

- Base band sub-system: demodulation, auto-tracking, time reference, test and measure equipment.

- Supervision sub-system: monitor and control of all equipment, management of tracking sequences, and interface with orbital data source.

- Infrastructure sub-system: radome, temperature and humidity control equipment, and UPS.

Fig. 9. X-band dish antenna at Murezeq station

All the functions of Murezeq ground station are performed by the RF sub-system, baseband sub-system, and supervision sub-system. It is main objective is to receive data directly from French satellites; i.e., SPOT 5, 6 and 7, at frequency of 8.15 GHz with the occupied bandwidth of $\leq$ 250 MHz, the bit data rate of 310 Mbps (Reed Solomon coding included), the EIRP of 26 dBW, a minimum flux density of -123 dB/m^2, and the modulation used is D-QPSK. Nevertheless, it has the ability to receive from other satellites such as Envisat ASAR, GPS, and Vsat. Moreover, the system can automatically track the satellites, acquire, demodulate and archive the telemetry from remote sensing satellites.

TABLE IV. CHARACTERISTICS OF X-BAND DISH ANTENNA

Parameter	Specification
Diameter of dish	5.4 m
Frequency	8000 – 8500 MHz
LNA gain	≥ 40 dB
Polarization	R/L HCS selectable
G/T at 5^0 elevation	30.5 dB/K
Side lobes	< 14 dB

A. Link Budget Analysis

We now provide a link analysis for x-band downlink and s-band up and downlinks. As mentioned above, the C-shaped patch antenna is proposed to be used for s-band uplink for command receiver. Currently the LCRSSS is using a parabolic antenna for uplink communication with SPOT 5 as command transmitter. This antenna operates at a resonant frequency of 2.039 GHz and provides high directivity. Moreover, it has a diameter of 2.4 m and an aperture efficiency of 0.65%. Although the designed C-shaped patch antenna provides a gain of 6.45 dBi, we have used a gain of 5 dB in the link budget calculation as a worst case scenario. The link budgets for s-band up and down links and x-band image downlink are presented in Table V and VI. Fig. 10 shows the key parameters of the link analysis. These parameters are calculated using the equations in [9] as following,

Fig. 10. Key parameters of a link analysis

Ls = free space loss
L0 = Other losses: atmospheric losses, transmitting and receiving losses, equipment losses, de-pointing losses and polarization mismatch losses

$$G_t = 10 \times \log(e_A \left(\pi D / \lambda\right)^2) = 32.3 \ dBi.$$

With a maximum transmitted power of 100W and feeder loss of 1dB, the EIRP is:

$$EIRP = G_t + P_T - L_{co} = 32.3 + 10 \times \log(100) - 1 = 51.3 \ dBW.$$

At satellite altitude of 775 km and elevation angel of 10°, the slant range is equal to:

$$= \sqrt{r^2 - (R_e \ \cos\emptyset)^2} - R_e \sin\emptyset = 2315 \ km$$

The power flux density radiated from the ground station to the satellite can be calculated as following:

$$\beta = \frac{P_t G_t}{4\pi d^2} = EIRP - 10 \times \log(4\pi d^2) = 51.3 - 138.$$
$$= -86.98 \ dBW/m^2$$

The uplink space loss is equal to:

$$L_s = \left(\frac{c}{4\pi df}\right)^2 = 147.55 - 20\log(d) - 20\log(f) = -165.93 dB$$

The received power at the satellite:

$$P_r = EIRP + G_r + L_a + L_s = 51.3 + 5 - 11.5 - 165.93 = -121.13 dBW$$

The system noise temperature (T_s) of the satellite communication link is the sum of the antenna noise (290K), line loss noise (35K) and receiver noise (289K).

The noise power at the receiver can be calculated to be:

$$N_o = kT_s = -228.6 + 27.9 = -200.7 \ dB/Hz$$

The carrier to noise density ratio is equal to:

$$\frac{C}{N_o} = -121.13 + 200.7 = 79.57 \ dB - Hz$$

The receiver figure of merit (G/T)= 5-27.88 = -22.88 dB/K.

At uplink data rate of R=32 kbps, the ratio of received energy per bit (Eb) to noise density (No) is equal to:

$$\frac{E_b}{N_o} = P_r + 228.6 - 10\log(T_s) - 10\log(R) = 34.52 \ dB.$$

Modulation and coding techniques are very important for link budget calculation, satellite system with BPSK/PM technique and bit error rates (BER) of <10^{-6}, the required Eb/N_0 can reach to 15.8 dB.

TABLE V. S-BAND UP AND DOWNLINK BUDGETS

Feature	Uplink	Downlink
Frequency	2.039 GHz	2.215 GHz
Satellite Altitude	775 km	775 km
Elevation Angel (deg)	10^0	10^0
Transmitter Power(Pt)	20 dBW	7 dBW
Ground Sation Antenna Gain (Gt)	32.3 dB	6.4 dB
EIRP Power	51.3 dBW	13.4 dBW
Space Loss	-165.93 dB	-166.63 dB
Atmospheric Losses	-0.5 dB	-0.5 dB
Rain Loss	-0.5 dB	-0.5 dB
Polarization Loss	-0.3 dB	-0.3 dB
Pointing Loss	-0.2 dB	-0.2 dB
On-Board Losses	-10 dB	-4.5 dB
System Noise Temperature(Ts)	27.9 dB/k	24.6 dB/k
Satellite Antenna Gain	5 dB	5 dB
Figure of Merit (G/T)	-22.88 dB/k	-18.2 dB/k
Bite rates	32 Kbps	2000 Kbps
C/No Received	79.57 dB-Hz	77.07 dB-Hz
Eb /No Received	34.52 dB	14 dB

Bit Error Rate (BER)	10^{-5}	10^{-5}
Required Eb /No	11.8 dB	9.6 dB
Implementation Loss	-2.5 dB	-1 dB
Margin	20.72 dB	3.4 dB

TABLE VI.   X-BAND DOWNLINK BUDGET

Link Parameters	Data
Frequency	8.1 GHz
Elevation Angle	20^0
Satellite Altitude	775 – 800 km
Satellite slant range	1723 km
Bit rate	150 MHz
Transmitter power	6 W
Transmitter imperfection losses	-2.5 dB
Transmitter feed losses	-0.5 dB
Antenna gain	15 dBi
EIRP	19.7 dBW
Propagation loss	-175.4 dB
Atmospheric losses	-1.5 dB
Rain losses	-0.5 dB
Polarization losses	-0.2 dB
Pointing losses	-0.3 dB
G/T ground station	32 dB/k
Eb/N0 received	20.7 dB
GS implementation losses	-2.0 dB
Eb/N0 achieved	18.7 dB
Eb/N0 required	6.5 dB
TM margin	12.23 dB

V. CONCLUSION

We have presented a conceptual design of telemetry, tracking and command subsystem for LibyaSat-1. The most important characteristics of TT&C subsystem were presented in this paper, explaining the uplink and downlink budgets. We also presented the design of s-band C-shaped patch antenna for command receiver. Simulation results show that the C-shaped patch antenna has a return loss that is well below -10 dB at the operational frequency of 2.039 GHz, and achieves an impedance bandwidth of 1500 MHz. The achieved simulated 3D gain is 6.4 dB at 2.039 GHz. We have obtained a margin > 3 dB, which means the calculation of link budget is good and within the range. In addition, the calculated and estimated values for budget links are acceptable and within the range for a real current model satellite.

REFERENCES

[1] C. Underwood, V. Lappas, A. D. S. Curiel, M. Unwin, A. Baker, and M. Sweeting, "Science Mission Scenarios Using "PALMSAT" Pico-Satellite Technology," presented at the 18th Annual AIAA/USU Conference on Small Satellites, Logan, Utah, 2004.

[2] F. EM. M. Tubbal, R. Raad, and K-W. Chin, "A Survey and Study on the Suitability of Planar Antennas for Pico Satellite Communications " unpublished.

[3] E. Pacheco, J. L. Medina, R. Conte, and J. Mendieta, "Telemetry and command subsystem for a Mexican experimental microsatellite," IEEE Conference on Aerospace Big Sky, MT, United State pp. 3/1159-3/1165 vol.3, 2001.

[4] A. Elarabi, A. Elkaseh, A. Abughufa, S. Ben Rabha, A. Turkman, and M. Alayeb, "Libyan CubeSat for monitoring desertification and deforestation," 5th Nano-Satellite Symposium University of Tokyo, Japan, pp. 1-4, November. 2013.

[5] D. Cinarelli and P. Tortora, "TT&C system for the ALMASat-EO microsatellite platform," IEEE First AESS European Conference on Satellite Telecommunications (ESTEL) Rome, Italy, pp. 1-6, October 2012.

[6] High Frequency Structure Simulator (HFSS) [online] available: http://www.ansys.com/.

[7] F. EM. Tubbal, R. Raad, K-W. Chin, and B. Butter, "S-band Shorted Patch Antenna for Inter Pico Satellite Communications," IEEE 8th International Conference on Telecommunication System, Services and Application, Bali, Indonesia, pp. 1-4, October, 2014.

[8] F. EM. Tubbal, R. Raad, K-W. Chin, and B. Butters, "S-band Planar Antennas for a CubeSat," International Journal on Electrical Engineering and Informatics, vol. 7, December 2015.

[9] W. J. Larson and J. R. Wertz, Space Mission Analysis and Design: Microcosm Press, California, USA   1999.

Utilizing Mean Greedy Algorithm using User Grouping for Chunk Allocation in OFDMA Systems with Carrier Aggregation

Arfianto Fahmi[1], Rina Pudji Astuti[2], Linda Meylani[3], Vinsensius Sigit Widhi Prabowo[4]

[1-4]Telecommunication Engineering Study Program
School of Electrical Engineering
Telkom University, Bandung, Indonesia
arfiantof@telkomuniversity.ac.id[1], rinapudjiastuti@telkomuniversity.ac.id[2], lindameylani@telkomuniversity.ac.id[3],
vinsensigitwp@gmail.com[4]

Abstract— **In this paper, utilizing user-order chunk allocation algorithm for OFDMA systems using carrier aggregation environment is proposed and evaluated. Chunk allocation algorithm is performed based on mean greedy algorithm which has low complexity. In order to adopt this algorithm to those system, all users are divided into a certain group in accordance with the number of available aggregated carriers. The simulation results are shown that the performance and time complexity of the proposed scheme is same with the system without user grouping. Therefore, the proposed scheme could be considered to realize in LTE-advanced platform.**

Keywords—Mean Greedy; User Grouping; Chunk Allocation; OFDMA; Carrier Aggregation

I. INTRODUCTION

In wireless multiuser systems, the phenomena of time varying frequency selective channels occur on different users at different time [1] [2]. Multiuser diversity is a result from independent fading channels across different users [1] [2]. In order to improve system performance over wireless channels, the multiuser diversity should be exploited by allocating the radio resources to users properly according to the instantaneous channel conditions of active users [1] [2]. These phenomena are overcomed in LTE system which uses OFDMA systems by dynamically allocating radio resources such as subcarrier to different users every time transmission interval (TTI) [2].

The latest works of radio resource allocations for OFDMA systems are developed based on mean greedy-based algorithms since they have low time complexity. Mean greedy (MEG) [3], single mean greedy(SMEG) [3] and multi-criteria ranking based greedy (MCRG) [4]are proposed by performing a user-order allocation based on the user's utility performance. Combined-order algorithm based on mean greedy-based algorithm [2] is also investigated to balance between spectral efficiency and fairness by determining a certain decision weighting factor. In above allocation schemes, all available chunks are allocated to all users on user by user basis.

Spectrum aggregation (or carrier aggregation) was introduced by 3GPP in its new LTE-Advanced standards, which is a candidate radio interface technology for IMT-Advanced systems. Carrier aggregation in LTE-A has extended the concept to introduce aggregation of non contiguous spectrums in different spectrum bands. Two or more component carriers (CCs) of different bandwidths in different bands can be aggregated to support wider transmission bandwidth between the E-UTRAN NodeB (eNB) and the user equipment (UE) [5]. The illustration of carrier aggregation schemes can be described in figure 1.
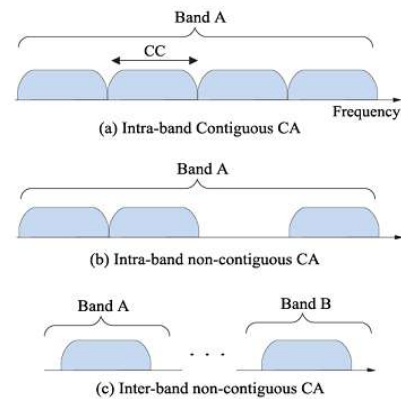
Figure 1. The illustration of carrier aggregation (CA) [5]

Since chunk by chunk-based using mean greedy algorithms are emerging subcarrier allocation on previous works, in this paper user-order mean greedy allocation is adopted to LTE-Advanced (LTE-A) systems which use aggregation scheme in OFDMA-based technology. In order to adopt its allocation in LTE-A systems, user grouping is proposed by partitioning all users into some group according to the number of carrier that they can be scheduled on. A group is contain some users who have the similar characteristic of pathloss propagation. The user grouping used

in this paper is based on the Pathloss (PL) value suffered by all users on the number of aggregated carriers. The PL value suffered by each user on all aggregated carriers are diverse due to the location different of all user. In [6], user grouping process only done by grouping the users according to the PL of each user to all component carriers. In this paper, its user grouping process is modified by distributing chunk from each component carrier to each group of user before chunk allocation is performed. The proposed user grouping could be realized on LTE-A platform which aggregates two or more carrier components belonging to a single or different frequency bands.

We organize this paper into five sections. After introducing the background in section 1, we describe the model and formulation in section 2. In section 3, the proposed algorithms and their time computational complexities are determined and compared with the previous works. The simulations of the proposed algorithms are described in section 4 and followed by conclusions in section 5.

II. Model and formulation

Considering a single cell using non adjacent inter band aggregation scenario. There are 3 component carriers which are f_1, f_2 and f_3, where $f_1 < f_2 < f_3$. Each carrier has transmitted power P_T. Since the impact of fading on high frequency is bigger than the lower ones, it causes the coverage of f_2 is smaller than f_1 and the coverage of f_3 is smaller than f_2. The cell structure model is shown in figure 1. User 1 is out of coverage of f_2 and f_3, so it only could be scheduled on f_1. While user 2 is inside the coverage of f_1 and f_2. User 3 could be scheduled on all carriers.
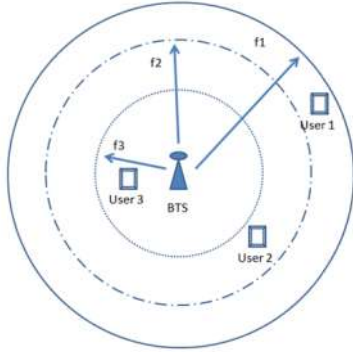

Figure 2. Cell Structure Model

A cell consist of a base station with N users. L is the number of component carrier which could be aggregated. Each component carrier has the same bandwidth. V is the total of chunk on each carrier. With equal power allocation (EPA), each chunk z has transmitted power $p(z) = P_T / V$. A group which consist of aggregated carrier could be defined by :

$$F = \{f_1, f_2, \dots, f_L\}, f_1 < f_2 < \dots < f_L \qquad (1)$$

A grouping is done by calculating the maximum value of path loss *(PL)* of all users on each component carrier. A user who has the *PL* value is less then the threshold path loss (PL) could be included into a certain group. The *PL* suffered by user i from each component carrier can be obtained using [6] :

$$\Omega_i = \{PL_i^k | PL_i^k < PL_{th}, 1 \le k \le L\}, 1 \le i \le N \ (2)$$

Where PL_i^k is the *PL* value from user i on carrier f_k. The element for group Ω_i denoted by N_i. If $N_i = j$, it means total number of carrier that can be scheduled on user i is j. So user could be divided into several groups [6] :

$$M_j = \{i | N_i = j, 1 \le i \le N\}, 1 \le j \le L \qquad (3)$$

The pathloss model used in this work is based on the Spatial Channel Model and PL_i^k could be determined as [6]:

$$PL_i^k = 58.83 + 37.6 log10\,(d_i) + 21 log10(f_k) \qquad (4)$$

Where d_i is the distance from user i to the base station. The coverage radius of f_k denoted by R_k could be calculated by [6]:

$$PL_{th} = 58.83 + 37.6 log10\,(R_k) + 21 log10(f_k) \quad (5)$$

It can be obtained that :

$$R_1 > R_2 > \dots > R_L \qquad (6)$$

In [6], user grouping process only done by grouping the user according to the PL of each user to all component carriers. In this paper, its user grouping process is modified so that the user-order chunk allocation based on mean greedy [2] [3] could be conducted. Before this algorithm is performed, the chunk distribution is done to distribute chunk from each component carrier to each group of user.

The total value of PL from all user in group M_j on carrier f_k can be defined as :

$$TM_j^k = \sum_{i=0}^{N_j} PL_i^k \qquad (7)$$

Where N_j is the number of total member group M_j. Since the number of chunk from each carrier is V, it means that the number of chunk divided from carrier f_k on each group must not greater than V. The number of chunk obtained by group M_j from carrier f_k could be calculated by :

$$RM_j^k = \left\lfloor \frac{TM_j^k}{\sum_{l=j}^{L} TM_l^k} \cdot V \right\rfloor \qquad (8)$$

$$\sum_{l=j}^{L} RM_l^k \le V \qquad (9)$$

The total number of chunk obtained by group M_j from all carrier that can be scheduled is defined by :

$$XM_j = \sum_{m=j}^{L} RM_j^k \qquad (10)$$

The chunk allocation is performed on each RM_j^k. In this state, each user group has specific number of chunk of carrier that can be scheduled based on equation (8) and (10). The group of chunk on each user group is introduced in this paper where it is called Group-Chunk-User (GCU). Each GCU contain the signal to noise ratio (SNR) of user - i on chunk - z which is given by :

$$r_i(z,s) = p(z)xH_i(z,s) \quad (11)$$

$H_i(z,s)$ is the total loss propagation and s is the scheduling slot which is slot within one time transmission interval (TTI). After all SNR of all users on all chunks have been known, chunk allocation is conducted on each GCU. SNR of all chunks on each user are averaged and sort them from the lowest. A user on each GCU who has the lowest SNR choose the best chunk. The algorithm of the proposed allocation is called UG-MG algorithm.

III. THE PROPOSED ALGORITHM

The UG-MG algorithm consist of 2 step, the first step is user grouping process and followed by chunk allocation process. The steps of the proposed algoritm could be described as follow :

1. For all users, calculate the PL_i^k of all aggregated component carriers according to (4).

2. All users are divided into specific group using (2) and (3).

3. Determining GCU by distributing all chunks on each carrier into related user group based on (8), (9) and (10). Each user group has specific number of chunk from the carrier that can be scheduled on.

4. On each GCU :

i. Calculate SNR of all users on each chunk.

ii. Calculate the average of chunk's SNR on each user.

iii. Choose one user who has the lowest chunk's SNR. This user can selects a chunk which has the best SNR.

iv. Repeat step iii to iv until all chunks have allocated.

5. Calculate average throughput and fairness of all users. Where throughput system could be defined as [7]:

$$R_T = \frac{B}{N}\sum_{i=1}^{N}\sum_{z=1}^{V} S_{i,z} log_2(1 + SNR_{i,z}) \quad (10)$$

R_T is the throughput system and $S_{i,z}$ is chunk assignment index. B is bandwidth system and $SNR_{i,z}$ is SNR of user-i on chunk-z.

The fairness is based on [8] :

$$F = \frac{(\sum_{i\in N} R_i)^2}{N \sum_{i\in N} R_i^2} \quad (11)$$

Where F is fairness index and R_i is throughput of user-i.

An algorithm complexity of the proposed algorithm is investigated using asymptotic approach in [9] to quantify its time complexity. Investigating of time complexity is as follow:

1. Step one need $O(LN)$, since number of aggregated carrier is less than the user number, step one would be $O(N)$

2. Step two need $O(LN)+O(LN) = O(LN)$ since number of aggregated carrier is less than the user number, step two would be $O(N)$

3. Step three need $O(L^2)+O(L^2)=O(L^2)$. Due to the number of aggregated carrier is less than the user number, it means that this step is constant and it could be ignored.

4. Step four need $O(NV)+O(1)+O(V)+O(V)=O(NV)$.

The tota time complexity of the proposed allocation is then $O(N)+O(N)+O(NV) = O(NV)$. The time complexity of mean greedy in [2] [3] are given by $O(NV)$. It means that the proposed algorithm has the same time complexity with the previous mean greedy algorithms however user grouping step is performed before chunk allocation process.

IV. SIMULATIONS AND RESULTS

In order to evaluate the proposed scheme, the computer simulation is performed using montecarlo method. The number of simulation trial is equal to the number of time transmission interval.

TABLE I.   SIMULATION PARAMETERS [6]

Parameter	Value
Bandwitdh per carrier	5 Mhz
Number of chunk per carrier	25 chunk
TTI	200 TTI
Cell radius	250 meter
Cell Layout	Single cell
Component carrier frequency	700 Mhz, 800 Mhz, 1800 Mhz
Chunk bandwith	180 kHz
Propagation Model	Spatial Model Channel, Rayleigh channel
Gain eNB	18 dBi
Gain UE	0 dBi
Noise Figure	7 dB
eNB transmitted power	40 Watt (46 dBm)
Penetration Loss	20 dB
Number of user	5 - 80

The simulation is conducted for downlink path of LTE-Advanced with non-contiguous interband carrier aggregation. The simulation is done by varying the number of users from 5 to 80 users within a cell. The performances of the proposed schemes is compared with mean greedy algorithm (MG) [3] which does not conduct the user grouping before chunk allocation. The average throughput and fairness index of both schemes are compared and evaluated. The simulation parameters are listed in Table I.
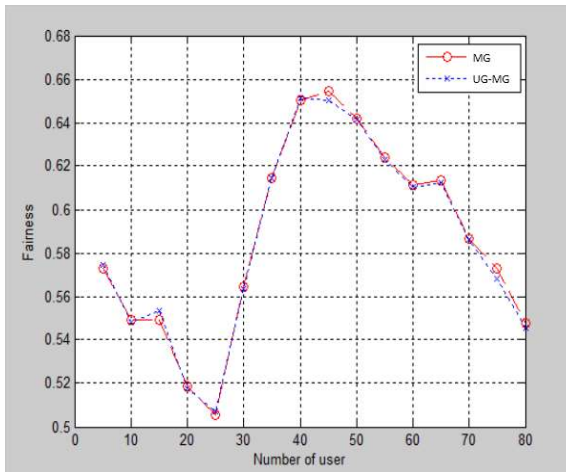
Figure 3. The fairness comparison

could be considered to be applied in LTE-Advanced system which apply carrier aggregation.

V. CONCLUSIONS

In this work, a utilizing mean greedy algorithm which combined with user-grouping is proposed and evaluated. This scheme is applied on LTE-A system which conduct carrier aggregation in OFDMA-based technology. Its scheme is called UG-MG algorithm. Varying the number of of users, the proposed scheme gives the same performances and time complexity. Therefore, it could be considered to apply in LTE-A platform.

As the results of simulations, they are shown in figure 3 and figure 4 that the proposed scheme has the same performances in term of fairness and average of throughput as well. In figure 3, it is shown that there are a little bit difference of fairness between MG and UG-MG algorithms for all users. The differences among them are in the range between 0% until 0.05%. It could be concluded that there are no the difference fairness value between MG and UG-MG.

In figure 4 it is also shown that there are a slightly difference average of throughput occurred among MG and UG-MG for all users. The difference range is between 0 until 3.3 kbps. It could be concluded that both schemes have almost the same fairness.

References

[1] Huiling Zhu and Jiangzhou Wang, "Chunk-Based Resource Allocation in OFDMA Systems - Part 1 : Chunk Allocation," *IEEE Transactions on Communications*, vol. 57, no. 9, pp. 2734-2744, September 2009.

[2] Arfianto Fahmi, Muhamad Asvial, and Dadang Gunawan, "Combined-order Algorithm using Promethee Mrthod Approach and Analytic Hierarchy Decision for Chunk Allocation in LTE Uplink Systems," *International Journal of Communication Networks and Information Security (IJCNIS)*, vol. 5, no. 1, pp. 39-47, April 2013.

[3] Obilor Nwamadi, Xu Zhu, and Asoke K Nandi, "Dynamic Physical Resource Block Allocation Algorithm for Uplink Long Term Evolution," *IET Communications*, vol. 5, no. 7, pp. 1020 - 1027, 2011.

[4] Obilor Nwamadi, Xu Zhu, and Asoke K. Nandi, "Multicriteria ranking based greedy algorithm for Physical Resource Block Allocation in Multicarrier Wireless Communications," *Elsevier Signal Processing*, vol. 92, pp. 2706-2717, 2012.

[5] Haeyoung Lee, Seiamak Vahid, and Klaus Moessner, "A Survey of Radio Resource Management for Spectrum Aggregation in LTE-Advanced," *IEEE Communications Surveys and Tutorials*, vol. 16, no. 2, pp. 745 - 760, 2014.

[6] Shi Songsong, Feng Chunyan, and Caili Guo, "A Resource Scheduling Algorithm Based on User Grouping for LTE-Advanced System with Carrier Aggregation," *IEEE 2009 International Symposium on Computer Network and Multimedia Technology*, 2009.

[7] Sanam Sadr, A Anpalagan, and K Raahemifar, "Radio Resource Allocation for the Downlink of Multiuser OFDM Communication Systems," *IEEE Communication Surveys & Tutorials*, vol. 11, no. 3, pp. 92-106, 2009.

[8] R Jain, M Chiu, and W Have, "A Quantitative Masure of Fairness and Discrimination for Resource Allocation in Shared Systems," Eastern Research Lab, DEC Research Report TR 301 1984.

[9] Kennet H Rosen, *Discrete Mathematics and Its Applications*.: Mc Graw Hill, 2007.
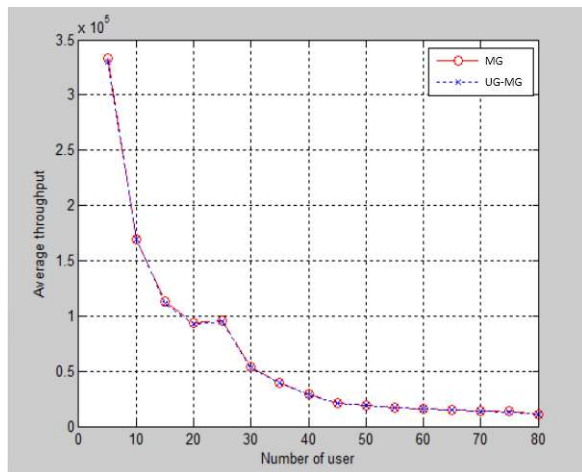
Figure 4. The average user throughput comparison

Considering the results altogether, it can be concluded that the proposed scheme have the same performances and time complexity as well with previous scheme in [*3*] however user grouping is performed. Hence, the proposed scheme

Designing Gamified-Service Towards User Engagement and Service Quality Improvement

Sarifah Putri Raflesia
School of Electrical Engineering and Informatics
Bandung Institute of Technology
Bandung, Indonesia
syarifahpr@gmail.com

Kridanto Surendro
School of Electrical Engineering and Informatics
Bandung Institute of Technology
Bandung, Indonesia
surendro@gmail.com

Abstract--- **Organizations find new challenge which is related to employees' engagement along service desk implementation. Gamified-service is defined as service desk which integrated Information Technology Infrastructure Library (ITIL) and gamification model. This integration enables fun, challenge, and reward to boost employees' motivation. Pressure in the workplace and employees' personal issues become the main trigger to decrease productivity. According to this reason, we need to add persuasive approach along implementation of ITIL best practices. This research focused on designing gamified-service prototype in order to help organization build game-like workplace environment. We believe that gamified-service will help employees do their job with fun way.**

Keyword---gamification;ITIL;service desk;user engagement;web-based application

I. INTRODUCTION

Nowadays there are a lot of organizations use information technology (IT) to support their business. It makes the organizations spend big amount of investment for IT. But, even they pay expensive cost for IT, it can help them to avoid them from incident of IT. Incident IT is able to slow the business operation. When business operation is corrupted, there will be delayed activities. It will cause negative impacts for organizations. According to this matters, organizations which operate and demand on IT need a function that enables communication line to report incident IT and give solution.

Service desk is well known function which acts as first communication point between user and IT department. It handles incident, request, event, and problem of IT. This function will be required to be implemented at every organization which runs IT as tool to help their business [1].

Along the implementation of service desk, organization need to follow best practices. Information Technology Infrastructure Library (ITIL) is the most popular best practices to implement good service desk as ITSM feature. According to ITIL, service desk runs processes. These processes are important because they are directly connected to customers' needs.

Along the implementation of ITIL, there is new challenge which is related to engagement of service desk staffs. According to previous research, there is positive correlation between user engagement and successful IT implementation [2]. It is supported by other research which says that effective ITIL implementation is related to user engagement [3]. Therefore, we need other approach to boost service desk staffs' motivation.

In this research, we use gamification model as persuasive approach. We believe that gamification model will help service desk to do their task with fun way and ITIL as best practices will ensure that service desk staffs follow well documented and standard procedures.

II. LITERATURE REVIEW

A. ITIL

ITIL is document that presents best practices to manage the implementation of IT service. ITIL explains the detail of management and IT operations such as incident management, problem management, change management, configuration management, and availability management. The latest version of ITIL is ITIL 3.0 which has been published in 2007 by Office of Government (OGC). It contains 5 phases of service lifecycle.
1) Service strategy
2) Service design
3) Service transition
4) Service operation
5) Continual service improvement

B. Service desk

To run ITIL processes, we need a function. Service desk is a function to provide communication between users and IT employees. Service desk roles and responsibilities are senior service desk manager, service desk manager, service desk supervisor, and service desk analyst [4]. Service desk primary tasks are providing solution of IT infrastructure incident, request, problem,etc. Moreover, service desk is a single and first line which communicate with users in order to information about status of incident, request, problem, etc.

C. Incident management

Process is defined as a set of structured activities and tasks that produce a specific goal [5]. ITIL processes have been specified. Such as incident management, it has been specialized to manage incident. Incident management is often the first process when introducing the ITIL framework to a service desk, and offers the most immediate and highly cost reduction and quality gains [6]. Below are activities which are operated by incident management [7][8]:

1) Incident identification
2) Incident logging
3) Categorization incident
4) Prioritization incident
5) Diagnostic
6) Escalation
7) Further diagnostic
8) Resolution
9) Close incident

D. Gamification

Many organizations have implemented gamification model in order to motivate their employees while doing their tasks. Last four years, gamification has been discussed. In 2011, for the first time gamification is defined by Deterding, it is defined as the used of game design elements in non-game context [9].

Gamification is triggered by research about human's brain by scientists around the world. They agree that challenge – achievement - reward loop promotes production of dopamine. It can create satisfaction and reinforce desire to play [10].

Many applications have been using gamification, like Nike+ Running, GoJek, and Foursquare. Gamification helps the organization to gain customer 's satisfaction. It is not a user interface design, it is about how to reach the goal with fun way. Gamification enables win – win solution between organization and employee [11]. Organization can reach their goal, and employees are able to get the internal satisfaction, like fully engaged system.

Based on research, job satisfaction, high loyalty, and productivity of employees are stimulated by good internal service and organization policy [12]. It means issues which are related to employees satisfaction is critical in helping organizations reach their goals and business such as satisfying their customers.

E. User Engagement Measurement

User engagement is defined as the quality of the user experience that emphasizes the positive aspects of the interaction. It is not just about usability, but it also contains how users invest time, attention, and emotion when they are connected to the system [11]. We can identify each attributes of user engagement degree by using user engagement measurement. According to the previous research, user engagement attributes are focused attention, aesthetic, novelty, perceived usability, endurability, felt involvement[13].

III. DESIGNING GAMIFIED-SERVICE

Gamified- service is web-based service desk system that gamifying the processes which are mentioned in ITIL service operation documents. In this paper, we will introduce the prototype of gamified – service which runs function service desk and process incident management. Based on ITIL, there are 3 main roles of service desk, service desk analyst (SDA), service desk supervisor (SDS), service desk manager (SDM).

First, SDA acts as the first level of service desk. It responsibles to provide quick solution for reported incidents, entry all details about incident, do basic analyze, and deliver solution from upper level to customer if the incident report is escalated.

Second, SDS as second level who ensures the skill levels of staffs are maintained and representing SDAs at meetings, SDS becomes the escalation point when SDA finds difficulties or controversial calls.

Third, SDM as escalation point from SDS level. SDM provides solution for incidents which can not be handled by first and second level. Moreover, he responsibles to do advance analyze of business impact which caused by incidents and report it to the board. Fig 1 shows the use case diagram for service desk roles.

Fig.1 Use Case Diagram of Service Desk Roles

There are seven main features of gamified- service prototype, namely, (1) record customer, (2) record incident, (3) solution database (4) known error database (KEDB), (5) escalation, (6) close incident, (7) leaderboard.
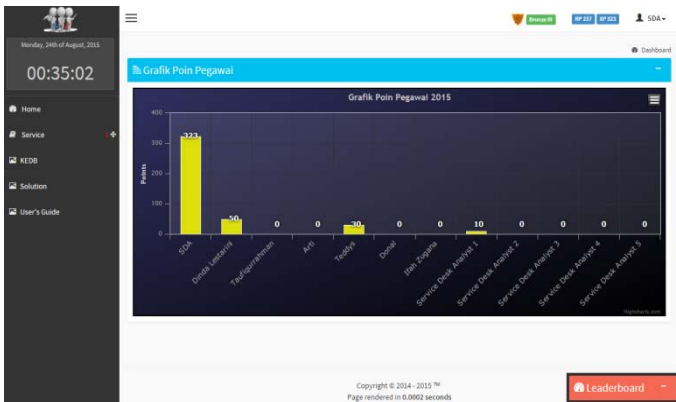
Fig.2. Gamified- Service Home Page

First, customer will report the incident to SDA and he will create a new data customer if customer does not exist in database.

Second, when the record of customer is already saved, SDA entries the details of incident such as category of incident, description of incident, time and date of incident, level of urgency, etc.

Third, SDA checks solution database to find solution. If expected solution can not be found in solution database, he will provide solution based on his skills and knowledge. This activity is also the mechanism of input solution. When solution of incident is first time recorded to database, it is not directly inserted to solution database. It needs supervisor to review the solution. Once it is accepted, it will be recorded as solution.

Fourth, incidents which are reported more than once will be recorded on KEDB. This features will help organization to find the weakness of IT Service and enable the opportunity to evaluation and improvement. In this feature, we will see incident records, their solutions, and how many times they reported.

Fifth, SDA can use solution database to deliver the solution and his own skills and knowledge, if customer is satisfied, SDA is able to close the incident. In contrary, if SDA finds the customer doubts, it means SDA has to provide more information and find suitable solution. In order to get support and help, SDA can run escalation feature. This feature enables SDA to create incident ticket and forward it to upper level, SDS and SDM. SDS and SDM are responsible for opening the escalated ticket. Previous research finds that the key success of ITIL implementation is user engagement with good support from upper level [3]. It means SDS and SDM are able to work together with SDA and direct them if they find problem to solve incident. If SDS can not fix incident, SDS escalated incident ticket to SDM. If SDM finds difficulties and he needs more time to fix they will forward the incident ticket to problem management, which means the incident ticket is failed. Moreover, incident ticket will fail if the incident ticket is not open, and it causes SDA loses RP. But, the gamified-service does not include the punishment for irresponsible SDS and SDM. This matters will be charged to upper level of organization.

Sixth, when solution for incident is delivered, SDA close the incident management process. If the incident management is closed before time ends, SDA will get points. and in contrary if it is closed after time has ended, SDA will lose points. In this system, points are categorized by two types, redeemable points, and experience point (XP). Service is failed if the incident ticket is not opened and solution is not delivered to customer until the time ends. Table 1 shows description about urgency level and estimated time to solve the incident.

TABLE 1 URGENCY LEVEL AND TIME TO SOLVE

Urgency level	Estimated time to solve incident
1 = Low	12– 23 hours 59 minutes 59 seconds
2 = Middle	6 – 11 hours 59 minutes 59 seconds
3 = High	0 – 5 hours 59 minutes 59 seconds

When the time ends, incident ticket is failed and SDA will lose promised RP. In contrary, even the incident ticket is failed, XP keeps gaining because even incident ticket is failed, SDA gets experience. In other case, when SDA delivers the solution to customer on scheduled time, RP and XP will gain. RP can be exchanged to desirable contents, such as bonus, shopping voucher, etc. While XP represents SDA real experience. Table 1 shows the XP rules and table 2 shows RP rules.

TABLE 2 RULES FOR XP

Condition	Urgency	XP gains when incident ticket is success	XP gains when incident ticket is failed
XP current = 0-750	1	+10	+1
	2	+12	
	3	+20	
XP current = >751	1	+5	
	2	+10	
	3	+15	

TABLE 2 RULES FOR RP

Condition	Urgency	RP gains when incident ticket is success	RP gains when incident ticket is failed
RP current = 0-500	1	+10	-5
	2	+12	-6
	3	+20	-10
RP current	1	+5	-3

= >751	2	+10	-5
	3	+15	-8

Seventh, leaderboard shows SDAs with highest XP and RP. It helps organization to create competition environment in workplace. There are many game elements that can be used, in this prototype we use points as core element. Points are able to be converted to other game elements, when SDA has points, then organization can add other elements such as avatar, badges, exclusive contents, virtual contents, etc. These elements depend on points, system needs points to upgrade badges, so does when system needs to give exclusive contents to SDA.

Along the implementation of gamified-service, we need to identify what are indicators of success. It also helps organizations to get information about how far they have gone. Tabel 4 shows the basic evaluation indicators for service desk [13]. In order to find if users are engaged with gamified-service, we need to use User Engagement Scale (UES) [12].

We suggest a gap analysis between pre-implementation of gamified-service and post implementation. After do a gap analysis, organizations are able to discover if the gamified-service reaches the target. Additionally, gap analysis enables organization to find new challenge in IT service improvement.

TABLE 4 BASIC EVALUATION INDICATORS FOR SERVICE DESK

Indicators	Explanation
Response time	Response user's calls as soon as possible
Call rate	Rate of request for help (RFH) that comes from service desk
Records of request call	Numbers of the events and incidents recorded by service desk
Rate of complaints	Assessing the service desk whether handling incident
Accuracy of incident classification	Assessing the service desk whether handling accidents by the defined categories
Growth rate of desk incident	The rate that incidents could not be processed
Rate of incident handling	Remote processing rate when service desk recieves the RFH
First call completion rate	Connected rate when user first calls

IV CONCLUSION

Service desk employees must be fully engaged to the system because they responsible to communicate with users in order to help users fix incidents, problem, etc. If they can not engage to the system, then it will cause slow response to the request, event-handling, incident, etc. Engagement deals with employees' motivation, involvement, and participation. According to this matter, we propose a design of gamified-service which integrate ITIL best practices and gamification model. By using gamification in service desk, the engagement

will be increased and may return benefits to organization such as internal satisfaction, customer trust, etc. This design can be used to do some future research in gamified- service, like implementing mobile gamified-service, gamification system for customer, and finding what are the most influence user engagement attributes for gamified service.

REFERENCES

[1] G. K. Kundu, B. M. Manohar, and J. Bairi, "Incident Management Process Capability: A Simulation Study," Communications in Computer and Information Science Global Trends in Information Systems and Software Applications, pp. 243–255.

[2] M.I.Hwang and R.G.Thorn, "The effect of user engagement on system success: a meta-analytical integration of research findings." Information and Management Journal, vol.35, pp.229-336, Apr.1999.

[3] A. Cater-Steel and W. Tan, 'Transforming IT Service Management – the ITIL Impact', vol. 17, 2006.

[4] D. Knapp, A guide to service desk concepts, 3rd ed. Boston, MA: Course Technology, Cengage Learning, 2010.

[5] T. H. Davenport, Process innovation: reengineering work through information technology. Boston, Mass.: Harvard Business School Press, 1993.

[6] Q. Wang, J. Song, L. Liu, X. Luo, and E. Xinhua, "Building IT-based incident management platform," 5th International Conference on Pervasive Computing and Applications, 2010.

[7] J. Bon, Foundations of IT service management based on ITIL, 2nd ed. Holland: Van Haren Publishing, 2005.

[8] _____, OGC, (2007), ITIL V.3 ITSM Library, London.

[9] S. Deterding, D. Dixon, R. Khaled, L. Nacke, "From Game Design Elements to Gamefulness: Defining "Gamification" ," , 2011.

[10] G. Zichermann and C. Cunningham, Gamification by design: implementing game mechanics in web and mobile apps. Sebastopol, Calif.: O'Reilly Media, 2011.

[11] A.Narayanan, Gamification for Employee Engagement, UK : Impackt Publishing, 2014.

[12] J.K.Heskett, J.O.Jones, et.al., Putting the Service-Profit Chain to Work, USA :Harvard Business Review, 1994.

[13] J.Lehmann, M.Lalmas, E. Yom-Tov, G.Dupret,"Model of User Engagement," in UMAP'12 Proceedings of the 20th international conference on User Modeling, Adaptation, and Personalization, Montreal, CA, 2012, pp.164-175.

[14] H.L.O'Brien and E.G.Toms,"The Development and Evaluation of a Survey to Measure User Engagement," Journal of the American Society for Information Science and Technology, vol.61, pp. 50-69, Jan 2010.

[15] Z. Yao and X. Wang, "An ITIL based ITSM practice: A case study of steel manufacturing enterprise," 2010 7th International Conference on Service Systems and Service Management, 2010.

A Conceptual Framework for Implementing Gamified-Service to Improve User Engagement by Using ITIL

Sarifah Putri Raflesia
School of Electrical Engineering and Informatics
Bandung Institute of Technology
Bandung, Indonesia
syarifahpr@gmail.com

Kridanto Surendro
School of Electrical Engineering and Informatics
Bandung Institute of Technology
Bandung, Indonesia
surendro@gmail.com

Abstract--- Gamified- Service is defined as a service desk which uses ITIL and gamification model to boost the motivation of service desk employees. Along the implementation of service desk, organizations find the challenge which is related to the human resource who deliver the service. Pressure at workplace and personal issues become trigger to decrease their productivity. According to this fact, standard service desk is not enough. We need persuasive approach to guarantee that employees are totally engaged. Moreover, we are challenged to ensure that good service desk is implemented, we need best practices of IT Service Management, it is Information Technology Infrastructure Library (ITIL). This research is focused on creating a framework to build, implement, and maintain good service desk with fully engaged employees.

Keyword---gamification;ITIL;service desk;user engagement

I. INTRODUCTION

Most of organizations in this era implement information technology (IT) to help their activities run more effective and efficient. But, there are always unexpected incidents and problems during the use of IT. Those unexpected situation can slow the activities down. So that, there will be delay time which will cause disappointment of end users as stakeholder. It is why we need service desk to solve the IT incident and problem.

The implementation of service desk needs best practice which is able to ensure that standardized service desk is well designed and implemented. In this research, we use Information Technology Infrastructure Library (ITIL). But, we argue that best practice is not enough because it just handles the mechanism of how to deliver good service desk, it can not handle the motivation of service desk employees. Moreover, it can not ensure the engagement between employees and the system they use. Base on this finding, we need other persuasive approach.

Gamification model is the use of game design in non-game context[1]. This model is used as persuasive approach to motivate users of system in order to reach the system owner's

goals. By using gamification, we can increase productivity of service desk employees.

Naturally, human like challenges, games appeal to the players because there are challenges and uncertainties. Scientists who research about human's brain around the world agree that challenge – achievement - reward loop promotes production of dopamine. It can create satisfaction and reinforce desire to play [2].

This research focuses on the integration of ITIL and gamification model. The representation of the integration is a conceptual framework to build, implement, and monitor gamified- service. We believe that full engagement of employees will increase the productivity.

II. LITERATURE REVIEW

A. ITIL

ITIL is document that presents best practices to manage the implementation of IT service. ITIL explains the detail of management and IT operations such as incident management, problem management, change management, configuration management, and availability management. The latest version of ITIL is ITIL 3.0 which has been published in 2007 by Office of Government (OGC). It contains 5 phases of service lifecycle.
1) Service strategy
2) Service design
3) Service transition
4) Service operation
5) Continual service improvement

B. Service desk

To run ITIL processes, we need a function. Service desk is function to provide communication between users and IT employees. It is discussed in service support section for ITIL 2.0 while in ITIL 3.0 it is discussed in service operation document.

Service desk becomes first point for users to report incident, request, problem of IT, etc. It responsibles to provide feedback, guidance, and solution for every reports. The roles and responsibilities of service desk are senior service desk

manager, service desk manager, service desk supervisor, and service desk analyst [3].

C. Service desk Processes

1) Incident management

Process defines as a set of structured activities and tasks that produce a specific goal [4]. ITIL processes have been specified. Such as incident management, it has been specialized to manage incident. Incident management is often the first process when introducing the ITIL framework, and this process offers the most immediate, highly cost reduction, quality gains [5].

2) Event management

Event is an observable and measurable occurrence which affects the IT infrastructure management or provision of IT service [6]. It involves activities from detecting event, filtering, categorizing, classifying, correlating, triggers, reaction of possibilities, assessment, and closing.

3) Request fulfillment

This process handles all request activities which are requested by IT users through service desk. The request can be small changes with low risk and cost or it can be the request for big changes, high risk, and expensive.

4) Access management

Every request for access is handled by access management. It ensures all authorized users are able to access the system.

5) Problem management

This process contains activities to diagnose the root cause of incident. It also responsible to maintain problem information and resolution. So that organization is able to minimize incident. Moreover, this process aims to prevent the incident and problem happen again and help organization to minimize the impact of unprevented incidents [7].

D. Gamification

Many organizations have been implementing gamification model in order to motivate their employees while doing their tasks. Last four years, it has been discussed and proposed the new idea to boost productivity of employees. It enables win – win solution between organization and employees [8]. Organization can reach their goal, and employees are able to get the internal satisfaction, like fully engaged system, reward, and reputation.

There are several success applications which use gamification such as Nike+ Running, GoJek, and Foursquare. It helps the organization to gain employees' satisfaction and costumers' satisfaction by giving more attractive system.

Based on research, job satisfaction, high loyalty, and productivity of employees are stimulated by good internal services and organization policy [9]. It means issues which are related to employees satisfaction is critical in helping

organizations reach their goals and business such as satisfying their customers.

E. User Engagement Measurement

User engagement is defined as the quality of the user experience that emphasizes the positive aspects of the interaction. It is not just about usability, it also contains how users invest time, attention, and emotion when they are connected to the system [10].

According to the previous research, user engagement attributes are focused attention, aesthetic, novelty, perceived usability, endurability, felt involvement[11]. By using user engagement scale (UES), we can get the score of each attributes. While, the accumulation of every score is the degree of user engagement. But, it is also available for us to present the result as the score of each attributes in order to simply identify which attribute is being a focus to evaluation.

E. Service Life Cycle Development

In Application Management document which is one of ITIL product shows SDLC as an approach to manage service application[12]. The steps of SDLC are :

1) Feasibility study

In this first step, we will do a set of practices to ensure that service is feasible to be implemented.

2) Analysis

Implementation of service desk needs the analysis about what is the current and desired state of selected process or function, and how do we reach the desired state. Moreover, we have to do some research and observe about stakeholder's needs and system requirements.

3) Design

After we gather the stakeholder's needs and system requirements, we will create desired process business scheme. In this step, it is possible for us to build prototype in order to give better understanding to stakeholders about the system which will be deployed.

4) Testing

The prototype or design that have been created in previous step will be tested. In this step, we will ensure that design is well designed and meet the stakeholder's needs and system requirements.

5) Implementation

In this step, the design which has been created will be transformed to application. After the application is coded, we need to test and if the application has been agreed by stakeholder, we will set up the infrastructures to support the application.

6) Evaluate

After the application has been set up, we need to evaluate the system periodically in order to find bugs and errors.

7) Maintenance

When the bugs and errors have been listed, we need to fix the system. In this step, we must ensure that system run properly. Moreover, along the maintenance, we have

opportunities to gather information and monitor the system in order to find a challenge for improvement.

III. FRAMEWORK DESIGN

A. Gamification Framework Design

From literature study [13] [14], we design gamification framework that will be used to develop game mechanics on service system. Figure 1 shows the presentation of model.
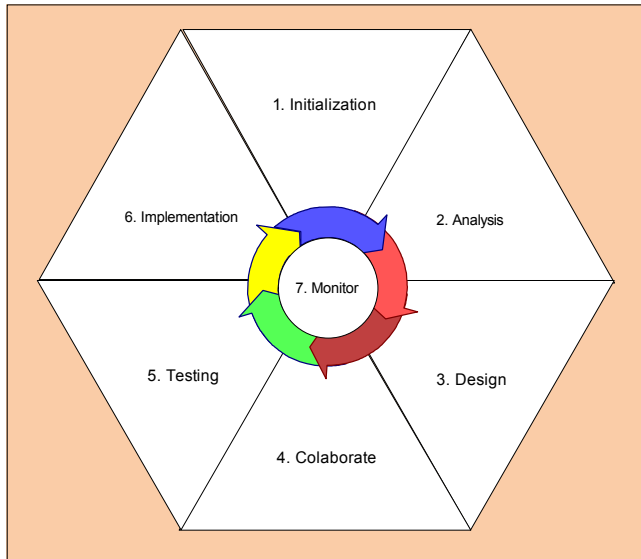

Fig. 1. Gamification framework design

The steps of gamification framework are :

1) Initialization
   In this step, we need to know which part of process that must be gamified. Moreover, we need to identify who will join the project and form teams.

2) Analysis
   After we identify what process that will be improved or built, we need more detail and deeper analysis about current state of process and what is the desired state, after that we need to identify who are the users of system. Identifying users is needed because we need to choose game elements. Moreover, in this steps we have to discover what kind of technology that will be used.

3) Design
   In the analysis step, we have identified who are the users. In this design step we will design game element that will be used. Such as designing badges, virtual contents, etc.

4) Collaborate
   After the elements are ready, we will integrate the element to the system and create game mechanics. Game mechanics is about how a game operate, what are applied rules, and how the players interact to the game[15]. In gamified- service perspective, this component defines tasks and actions that user can do to system.

5) Testing
   In this step, we will test the design or prototype. We will present the design and let the system owner to fully check the correctness.

6) Implementation
   If the design is accepted and the tests are success. We will continue to implementation step. In this step, the full gamification model will be deployed. After the deployment, the second tests will be held. It includes functional and non-functional tests. Additionally, this step will engage the end users to try the system.

7) Monitor
   In this step, we need to ensure that gamification elements and mechanics work properly and meet the agreements.

B. Proposed Conceptual Framework for Building Gamified-Service

The conceptual framework gamified- service is deal with two frameworks which have been explained and created at previous section. Fig 2. We can see the combination of SDLC and gamification model design
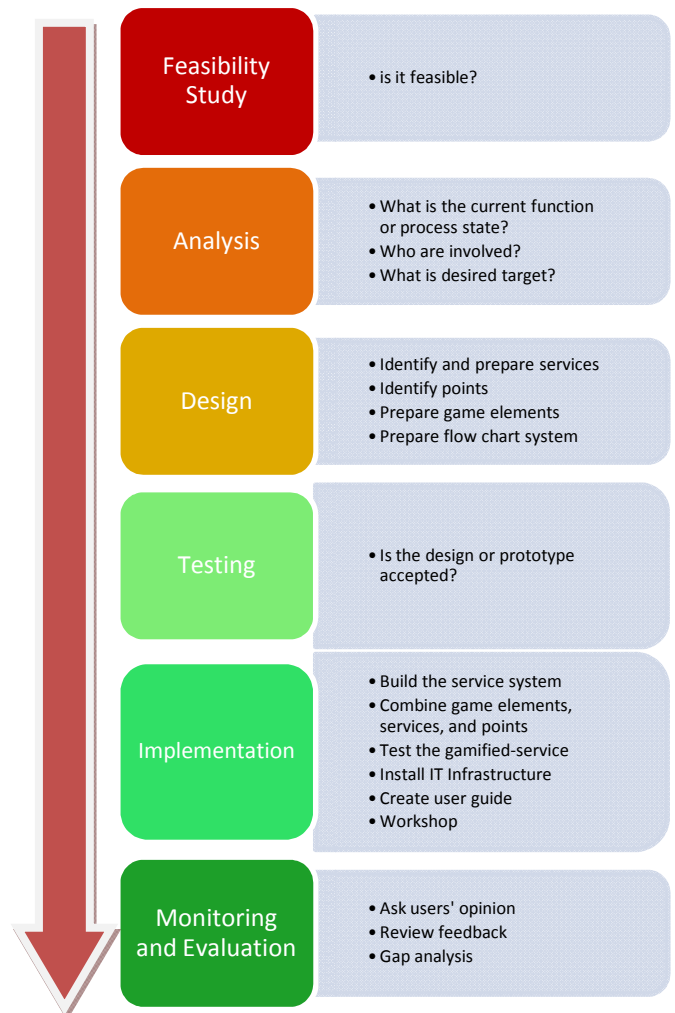

Fig. 2. Conceptual framework for Implementing Gamified-Service

The steps of conceptual framework for gamified-service are:

1) **Feasibility Study**
   This step deals with the study to identify feasibility status of implementation gamified service. We need to identify the benefits of implementing gamified-service.
2) **Analysis**
   If we find that gamified- service is feasible to be implemented, we can continue to analysis step. This step is focused on what is the current state of process or function that will be integrated with gamification model. We need to identify indicators in Table 1to simply assess current state of service desk[16] :

<div align="center">TABLE 1 BASIC EVALUATION INDICATORS FOR SERVICE DESK</div>

Indicators	Explanation
Response time	Response user's calls as soon as possible
Call rate	Rate of request for help (RFH) that comes from service desk
Records of request call	Numbers of the events and incidents recorded by service desk
Rate of complaints	Assessing the service desk whether handling incident
Accuracy of incident classification	Assessing the service desk whether handling accidents by the defined categories
Growth rate of desk incident	The rate that incidents could not be processed
Rate of incident handling	Remote processing rate when service desk receives the RFH
First call completion rate	Connected rate when user first calls

Moreover, we have to identify who are the users and then we identify user engagements, motivation, opinions and stakeholder's needs which are related to their view about the system. After gathering the stakeholder's needs and user's opinions, we need to identify their desired target.

3) **Design**
   In this step, we prepare service and gamification contents. We also need to design rules for every actions. Below are activities of design:
   - Identify and prepare service
     This part deals with identification service features which are based on ITIL concept.
   - Identify Points
     In this activity, points are identified. Points are used to get contents and stimulate elements

   - Prepare game elements
     After identifying the service and points we will prepare what are game elements that will be integrated to the service system.
   - Create flow chart system
     After preparing all requirements, we need to create a process business of gamified- service. If needed, we can create prototype to deliver the design and gamified- service mechanism to system owner.
4) **Testing**
   The design has been created and we can continue to the testing step. In this step, we need to present our design to system owner to ensure the design meets their requirements.
5) **Implementation**
   The design that has been created and accepted will be transformed to service application. In this step, we will also do activities below :
   - Combine game elements, service, and points
     In this activity, every elements which has been chosen will be combined with rules.
   - Testing gamified- services
     In this activity, we have to complete functional test, non-functional test, user acceptance test (UAT). The goal of functional test is ensuring the gamified- service runs properly without errors. Based on ITIL, we may use diagnostic hooks which provide information to fix errors. While, non-functional testing is more advance. It will test the degree of security, performance, usability, etc. When functional and non-functional test are done, we may engage the users to run UAT. This final test will direct to approval or rejection.
   - Set up IT infrastructure
     To run gamified- service we need other support technologies such as hardware and network. In this activity, we will engage IT Technical Expert.
   - Create user guide
     User guide is needed to provide guidance to users. It helps users to understand and operate the gamified-service.
   - Giving workshop and training
     This activity is important because it is the best way to help user to operate and understand system.
6) **Monitor and Evaluate**
   We need to monitor system activity to ensure that system run properly. The other activities that we should do in this step are :
   - Asking user's opinion
     In order to gather information about user engagement, we need to interview system users. Their opinions are needed to identify what should be fixed and improved.
   - Review feedback
     After gathering the information from users, we can set up solution to fix or improve the system.

- Gap analysis

  First, we need to review the degree of user engagement. We can use user engagement measurement to ensure that we reach one of gamified-service goals. In order to assess the quality of service desk, we can do assessment based on table 1. In the analysis step, we have the information about the state before the implementation. To ensure that we meet the goals, we can compare the state before and after implementation.

IV CONCLUSION

Service desk employees must be fully engaged to the system because they responsible to communicate with users in order to help users fix incidents, problem, etc. If they can not engage to the system, then it will cause slow response to the request, event-handling, incident, etc. Engagement deals with employees' motivation, involvement, and participation. So, we propose conceptual framework which integrate ITIL and gamification model. By using gamification in service desk, the engagement will be increased and may return benefits to organization such as internal satisfaction, customers' trust, etc. This framework can be used to do some future research in gamified- service, like implementing mobile gamified-service or gamification system for customers.

REFERENCES

[1] S.Deterding, D. Dixon, R. Khaled, L. Nacke, "From Game Design Elements to Gamefulness: Defining "Gamification" ," , 2011.

[2] G. Zichermann and C. Cunningham, *Gamification by design: implementing game mechanics in web and mobile apps*. Sebastopol, Calif.: O'Reilly Media, 2011.

[3] D. Knapp, *A guide to service desk concepts*, 3rd ed. Boston, MA: Course Technology, Cengage Learning, 2010.

[4] T. H. Davenport, *Process innovation: reengineering work through information technology*. Boston, Mass.: Harvard Business School Press, 1993.

[5] Q. Wang, J. Song, L. Liu, X. Luo, and E. Xinhua, "Building IT-based incident management platform," *5th International Conference on Pervasive Computing and Applications*, 2010.

[6] J. Bon, *Foundations of IT service management based on ITIL*, 2nd ed. Holland: Van Haren Publishing, 2005.

[7] Office of Government Commerce OGC, Service Operation, UK : The Stationary, 2007.

[8] A.Narayanan, *Gamification for Employee Engagement*, UK : Impackt Publishing, 2014.

[9] J.K.Heskett, J.O.Jones, et.al., *Putting the Service-Profit Chain to Work*, USA :Harvard Business Review, 1994.

[10] J.Lehmann, M.Lalmas, E. Yom-Tov, G.Dupret,"Model of User Engagement," in *UMAP'12 Proceedings of the 20th international conference on User Modeling, Adaptation, and Personalization*, Montreal, CA, 2012, pp.164-175.

[11] H.L.O'Brien and E.G.Toms,"The Development and Evaluation of a Survey to Measure User Engagement," *Journal of the American Society for Information Science and Technology*, vol.61, pp. 50-69, Jan 2010.

[12] Office of Government Commerce OGC, Application Management, UK : The Stationary, 2002.

[13] P.Herzigg, M.Ameling, et.al. " *Gamification in Education and Business*. Springer International Publishing, 2015.

[14] S. Harris and K. O'Gorman, *Mastering Gamification : Customer Engagement in 30 days : the Revolutionary way to Attract Customers,*

Keep Them Coming Back for More, and take Your Business to the Next Level, UK : Impackt Publishing, 2014.

[15] A.Ernest and A.Rollings, *Fundamentals of Game* Design, USA : Prentice Hall,2006..

[16] Z. Yao and X. Wang, "An ITIL based ITSM practice: A case study of steel manufacturing enterprise," *2010 7th International Conference on Service Systems and Service Management*, 2010.

Smart Home Platform Based on Optimized Wireless Sensor Network Protocol and Scalable Architecture

Trio Adiono[1], Rachmad Vidya Wicaksana Putra[2], Maulana Yusuf Fathany[3],
Muhammad Ammar Wibisono[4], Waskita Adijarto[5]
Microelectronics Center
Institut Teknologi Bandung, Indonesia
[1]tadiono@stei.itb.ac.id, [2]rachmad@pme.itb.ac.id, {[3]myfathany,[4]ammarwibisono}@gmail.com, [5]waskita@ee.itb.ac.id

Abstract—In this paper, we propose a smart home platform based on optimized wireless sensor network (WSN) protocol and scalable architecture. In this platform, system environment is divided into two main environments, indoor and outdoor. Outdoor environment uses internet-cloud system, while indoor environment uses WSN system. This scheme is also well known as Internet-of-Things (IoT) concept. Those two environments are connected to each other by using access point bridge. WSN system is established from efficient and scalable WSN components. Each component of WSN is designed to use an optimized protocol. WSN components are connected to each other in mesh topology in order to provide scalable architecture for further extension and changes. For outdoor environment, the existing internet-cloud system is used as infrastructure. Thus, this smart home platform can be monitored and controlled from smart phone, anytime and anywhere, as long as mobile data access is provided. For databasing implementation, SQLite database system is chosen because of its low cost and easy configuration. For system evaluation, several tests have been conducted to deliver the profile of proposed system.

Keywords—*Internet-of-Things; smart home platform; wireless sensor network; mesh topology.*

I. INTRODUCTION

Internet-based information system is a fundamental study in the Internet-of-Things (IoT) concept. Various research scenarios in this topic have been published, starting from physical to application layer. This condition leads to rapid development of the IoT concept into the Internet-of-Everything (IoE) concept. Because, IoE concept is not only about connecting something based on its function, but also build a system configuration that supports smart applications (e.g. user monitoring status, log of the user activities and behavior, doctor treatment's plan, etc). This is more complex scheme from basic communication of Machine to Machine (M2M).

Issues on IoT topics are usually about power consumption, system flexibility, smart self-configurable system, and level of security. Regarding those issues, a small operating system (OS) can be a solution to ease the application development and system implementation [1]. Because, a small OS will consume less power than the complex ones and it is easy to be configured anytime. Hence, power consumption and system flexibilties issues can be solved partially with this technique. Several studies on the integration of small OS in Wireless Sensor Network (WSN) have been reported. For examples, Harri Pensas *et.al* proposed integration EPIS with TinyOS 2.0 [2]. In 2012,

Chunlong Zhang *et.al* also reported WSN integration with μC / OS-II [3]. Besides small OS-based approach, some protocols have been proposed to solve these IoT issues (i.e efficient power consumption, easy configuration system, and secure system). For examples, Yuanbo Xu *et.al* proposed WZ-lcp by using authentication and keys updating as solution for security problem [4]. Another solution is the mesh network topology. Mesh topology has greater flexibility against interference and allows multiple paths to a destination [5].

Actually, IoT study is not only focused on WSN, but conncetion to internet-cloud is also compulsory. A device which serves as a bridge between outdoor environment (internet-cloud) with indoor environment (WSN) has important role. Because, this bridge has responsibilities to convert the data protocol and store any important data. For examples, paper [6] proposed using MySQL database engine for data storing. By using the existing databasing system, information management will be easily conducted. Thus, if we can choose low-cost (open-source and light-weight) database system, it will be better.

In this paper, we try to complete the story of smart home concept by using an efficient and scalable platform for smart home system. The efficient term is based on the optimization of WSN protocol which has been proposed in our previous research [5]. Meanwhile, scalable term is based on mesh architecture and its software program design. In WSN connection, we use three kinds of connection (i.e ZigBee, bluetooth, and WiFi). Each kind of connection can be a complement to the others, thus the disadvantages of each connection can be covered with others. For databasing system, we use SQLite system because its low-cost and light-weight implementation. In this databasing system, we store an update any important informations regarding the status of connected devices.

This paper is organized in several sections. First section is an introduction about research backgrounds and several related researches. Second section explains about proposed system architecture. Third section is about experimental evaluations. It is followed by conclusion and future works. The last two sections are acknowledgment and references respectively.

II. PROPOSED ARCHITECTURE

In the proposed smart-home concept, system environment is divided into two main environments, indoor and outdoor, which represent internet-cloud system and WSN system respectively.

Those two environments are connected to each other by using access point bridge, thus this indoor-outdoor connection can be seen as internet-of-things (IoT) concept. But, our vision for smart home concept is not only about connecting devices to internet but also establishing a smart environment to increase the quality of user experiences. Indoor environment will be established from WSN system based on a particular protocol which will be discussed later. Meanwhile, outdoor environment will use the existing internet-cloud scheme.

A. The Environments

Indoor environment has four main parts based on the functionality: access point, WSN host, WSN nodes, and WSN end-point devices. Access point is responsible to connect the internet outside the house with WSN system inside the house. Hence, it will distribute the internet protocol (IP) address to devices which are supposed to connect to internet (i.e smart phone, computer, WSN host). WSN host is responsible to be a coordinator for WSN. It is the center of WSN activities. It has to be able to understand all of the connected protocols. WSN host has to know all informations (identification number, status, configuration, etc) from all connected devices (i.e WSN nodes and end-devices). In contrast, WSN nodes has the simplest responsibility in WSN system. It only needs to broadcast any received data without bother to know where to transmit. With this scenario, we can add nodes as many as we need without worry about the addressing. For WSN end-point devices, design is related to the application. Important things for end-point devices are status informations. They have to be monitored and updated regularly into the WSN host database system. Because, from this database, user can access all information and monitor the status of all devices.

In WSN system, we use three communication protocols: ZigBee, bluetooth, and IEEE 802.11b (WiFi). Because, each protocol has its own advantages and disadvantages, combining all together into a single system can eliminate the disadvantages. Comparison of those three protocols can be seen in Table I. ZigBee has positive points on its simplicity data structure and range, but it lacks on data rate. Hence, ZigBee is suitable for backbone of nodes and end-point devices connection which only needs low data rate and low power consumption. Meanwhile, bluetooth has strong points on medium data rate communication and compatibility to connect to smart phone. Hence, bluetooth is suitable for user smart phone applications which need low or medium data rate (e.g controller app). Lastly, WiFi has strong points on high data rate communication and compatibility to connect to smart phone. Hence, WiFi is suitable for user smart phone applications which need high data rate (e.g video stream). WiFi connection can also establish a communication between WSN with internet-cloud. Hence, WSN system can obtain an IP address which will be managed by access point bridge for outdoor controlling purpose.

TABLE I. COMPARISON OF BLUETOOTH, ZIGBEE, AND WIFI [7]

Features	ZigBee	Bluetooth	IEEE 802.11b
Complexity	Simple	Complex	Very Complex
Typical Range	70-300 m	10 m	100 m
Data rate	250 kbps	1 Mbps	11 Mbps

For main architectural connection in WSN, we choose mesh topology, because it has advantages in the scalability. If we want to extend the WSN, we only need to add nodes or end-point devices in the range of another nodes or end-devices.

Outdoor environment is designed for mobility purpose. User needs to monitor any devices in the house which are connected to WSN system, anytime and anywhere. Hence, user of smart phone or gadget needs to connect internet-cloud. Access point bridge will manage any devices in WSN system which are supposed to be connected to internet-cloud, with particular IP addresses. With this scheme, user can monitor and control any devices inside the smart home WSN system, anytime and anywhere. Illustration of the complete proposed architecture is presented in Fig. 1.
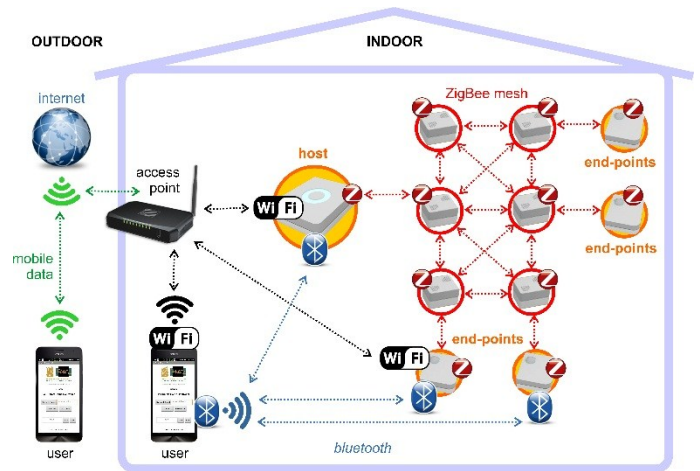

Fig. 1. Proposed system architecture

B. Data Protocol

In this WSN system, we use data protocol design as shown in Table II, which has been proposed in our previous research [5]. By using this optimized data protocol, we can design an efficient packet data for each application. Features of the proposed protocol will cover many informations, such as: devices availility, status, information type, data continuity, and payload data length.

TABLE II. DEVICE ADDRESSING REGISTER [5]

header	address	packet init	data payload	checksum
3-byte	2-byte	1-byte	n-byte	1-byte

C. Databasing System

Proposed databasing system is designed by using SQLite. SQLite databasing system is choosen because its low-cost and light-weight characteristics, which are compatible for smart home implementation. In order to use SQLite system, we need to define the devices addresses register. In this research, we still use addressing register scheme from our previous work [5]. Devices addresses register are presented in Table III and implemented into SQLite system by using Python programming. Implementation example of SQLite database system is shown in Fig. 2. It contains primary number, actual device identification number, device status, and processing date and time. By using

this format, we only need to define name of device with its identification number and status definition.

TABLE III. DEVICE ADDRESSING REGISTER [5]

Category	End-Point App	Address	n-Byte
Monitoring	Temperature	0x01	2
	Humidity	0x02	2
	Others	… - 0x3F	…
Controlling	Lamp	0x30	1
	Switch	0x31	1
	Curtain Mechanic	0x32	2
	IrDA	0x33	78
	VLC	0x34	32
	Others	… - 0xBF	…
Combination	Keypad	0xC0	2
	Lock	0xC1	1
	Others	… - 0xFF	…


```
id|equipment_id|status|processed|updated_at
1|2|0|0|2015-08-28 00:00:00.000000
2|3|0|0|2015-08-28 00:00:00.000000
3|2|8|0|2015-08-28 00:00:00.000000
4|3|7|0|2015-08-28 00:00:00.000000
5|1|500|0|2015-10-05 00:00:00.000000
6|2|313|0|2015-10-05 00:00:00.000000
sqlite>
```

Fig. 2. Example of SQLite database structure format

III. EXPERIMENTAL EVALUATION AND ANALYSIS

In order to conduct experimental evaluations, we need to define the test locations. Fig. 3 illustrates host and eight test locations in our laboratory building.
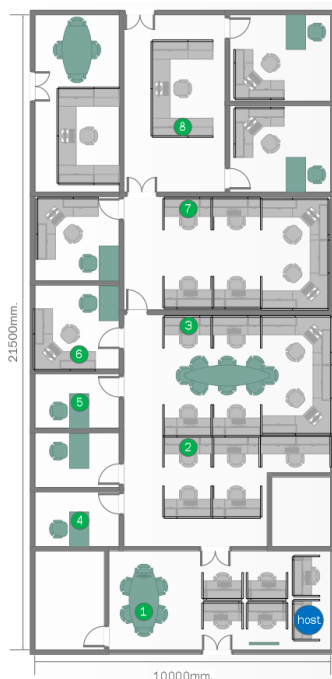
Fig. 3. Experimental test locations scenario

Loc1 is located in the same room with host and only separated with two tiny cubicles. Loc2 and Loc3 are located in the different room with host and separated only with wall and

door. Loc4, Loc5, Loc6, and Loc7 are located in different room with previous spot, where they are separated by a big single room from host. Last, Loc8 is located in a room which is separated by two big rooms from host.

D. Received Signal Strength Indicator (RSSI) for ZigBee

First experimental test is about RSSI measurements for ZigBee protocol with various transmitted power and locations. Fig. 4, Fig. 5, and Fig. 6 present the measured RSSI data for different transmitted power. Lowest transmitted power is defined equal to 5mW (+7dBm), while medium and highest transmitted powers are defined equal to 63mW (+18dBm) and 250mW (+24dBm) respectively.
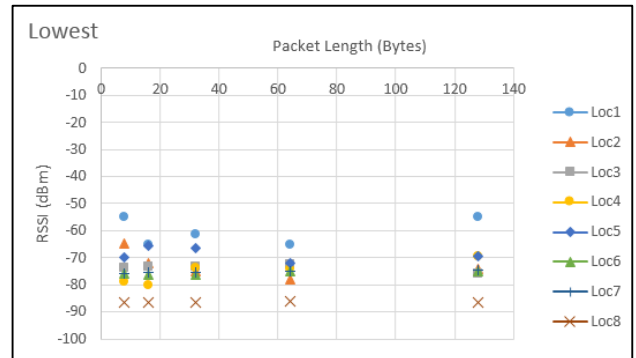

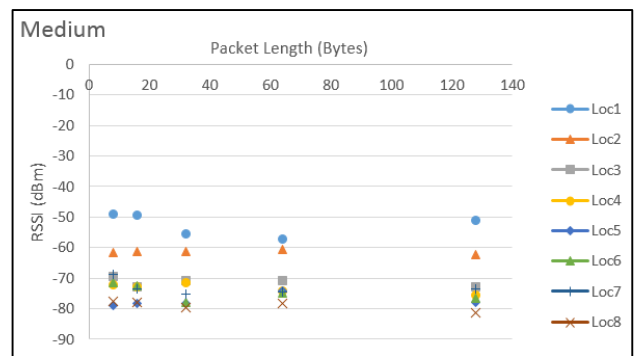Fig. 4. RSSI data for lowest transmitted power
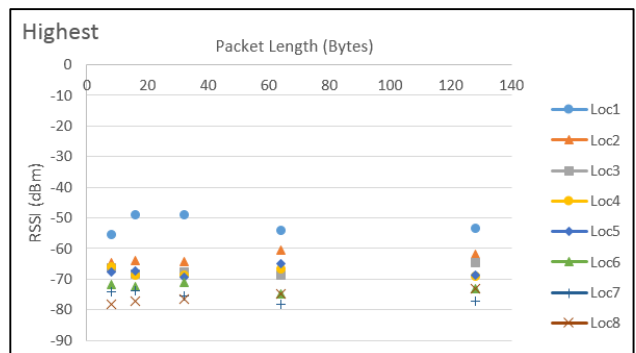

Fig. 5. RSSI data for medium transmitted power

Fig. 6. RSSI data for highest transmitted power

If we observe these charts, we will find that from the nearest location (Loc1) and the farthest location (Loc8), received RSSI data which have around 30dBm difference. Measured RSSI data

show that distance and obstacles in transmission medium will affect to signal strength. Significant decreases are found when there are obstacles that covers the signal spectrum. For example, RSSI data difference in Loc-1 to Loc-2 are significantly decreasing. Hence, if we want to optimize the distance of ZigBee signal, we need to consider the structure and composition of the obstacles.

E. Data Throughput for ZigBee Connection

Data throughput is the number of data which can be received and processed perfectly by the receiver. For this evaluation, we use STM32L1 microprocessor and XBee 900HP (ZigBee) as end-point receiver device. This receiver is placed in Loc-1. As transmitter, we used Raspberry Pi which is configured with XBee 900HP (ZigBee). This transmitter is placed in Host-spot. Hence, receiver and transmitter are separated around 5 meters. Transmitter is programmed to send characters continuously, while receiver is programmed to receive and count the received data. For each second, STM32L1 microprocessor will send its counting result to LCD for display purpose.

Results of this throughput test are presented in Fig. 6 as a single chart. It shows that baudrate number will affect the throughput performance. It is logically accepted, because with higher value of baudrate, sampling performance will be higher too. Highest value from throughput test reach almost 45000 bit/second.
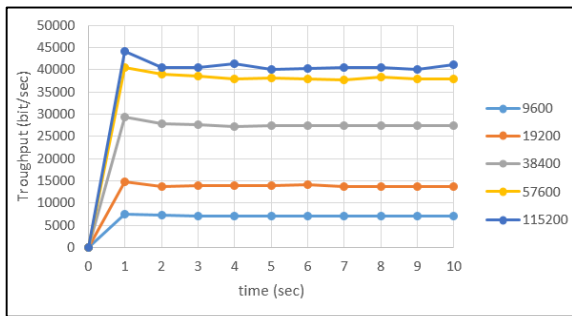

Fig. 7.   Throughput chart based on various baudrates

F. Bluetooth Communication

Bluetooth communication test is eshtablished by sending data from smart phone to WSN host via bluetooth. We can see in Fig. 8, when we send four characters from smart phone, WSN host will receive every single character independently in the different time and store them one-by-one.
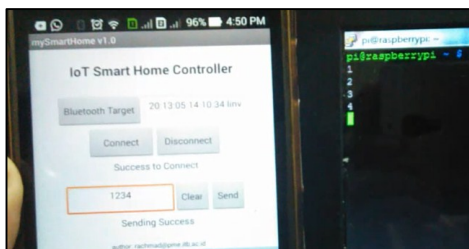

Fig. 8.   Smart phone - bluetooth - WSN host connectivity test

It shows that our smart home application program in smart phone can work properly and build a bluetooth connection with bluetooth module in WSN host. It is a fundamental test to ensure that user can send a command via wireless from smart phone to WSN host.

G. Switching and Relay Functions

For switching and relay function, we set up the test by using LED lamps and monitor as end-point devices. We control them by using smart phone. Smart phone is connected to WSN host by using bluetooth protocol. When we send command data, smart phone will send them to WSN host via bluetooth. Then, received data in WSN host are processed and sent to end-devices by using ZigBee protocol. Hence, in this scenario, there is data protocol conversion that is processed by WSN host. Those transmitted data from WSN host via ZigBee will be received by end-point devices and translated become physical command representation. LED lamps respond by illuminating and monitor respond with a clear display as shown in Fig. 9. This test shows that proposed architecture with optimized data protocol can work properly.

Fig. 9.   Test for lamp controller and power relay

IV. CONCLUSION AND FUTURE WORKS

In this research, we propose smart home platform based on optimized WSN protocol and scalable architecture. In this smart home concept, system environment is divided into two main environments, indoor and outdoor. Outdoor environment uses internet-cloud based system, while indoor environment uses WSN system. Those two environments are connected to each other by using access point bridge. WSN components are connected to each other in mesh topology in order to provide scalable architecture. There are three communication protocols in WSN system: ZigBee, bluetooth, and IEEE 802.11b (WiFi). Each protocol has its own advantages and disadvantages, combining all together into a single system can eliminate the disadvantages. For databasing implementation, SQLite database system is chosen because of its low-cost and easy configuration. For system evaluation, the proposed protocol and architecture can work properly.

For future research, we will add smart behavioral learning in the system. This smart learning will lead smart home system to

understand user regular habit and needs. It can also improve the quality of user experiences and productivities.

REFERENCES

[1] T. Adiono, "Challenges and opportunities in designing internet of things," Proc. of Int. Conf. on Information Technology, Computer and Electrical Engineering, pp.11-12, November 2014.

[2] H. Pensas, H. Raula, and J. Vanhala, "Energy efficient sensor network with service discovery for smart home environments", Proc. of Int. Conf. on Sensor Technologies and Application, pp.399-404, June 2009.

[3] C. Zhang, M. Zhang, Y. Su, and W. Wang, "Smart home design based on ZigBee wireless sensor network", Proc. of Int. ICST Conference on Communications and Networking in China, pp.463-466, August 2012.

[4] Y. Xu, Y. Jiang, C. Hu, H. Chen, L. He, and Y. Cao, "A balanced security protocol of wireless sensor network for smart home", Proc. of Int. Conf. on Signal Processing, pp.2324-2327, October 2014.

[5] M. Y. Fathany and T. Adiono, "Wireless protocol design for smart home on mesh wireless sensor network", Int. Symp. on Intelligent Signal Processing and Communication System, unpublished.

[6] S. Sankaranarayanan and A. T. Wan, "ABASH – android based smart home monitoring using wireless sensors", Proc. of IEEE Conf. on Clean Energy and Technology, pp.494-499, November 2013.

[7] V. Abinayaa and A. Jayan, "Case study on comparison of wireless technologies in industrial applications", Int. J. of Scientific and Research Publications, Vol. 4, Issue 2, February 2014.

Analysis of Camera Array On Board Data Handling using FPGA for Nano-Satellite Application

[1]Whildan Pakartipangi, [2]Denny Darlis, [3]Budi Syihabuddin, [4]Heroe Wijanto, [5]Agus Dwi Prasetyo

[1, 3, 4, 5]School of Electrical Engineering, Telkom University, Bandung, Indonesia

[2]School of Applied Science, Telkom University, Bandung, Indonesia

Email : whildanpakar@gmail.com, {dennydarlis, budisyihab, heroewijanto, adprasetyo}@telkomuniversity.ac.id

Abstract— **Nanosatellite has limited functions because of the mass constraint from 1 to 10 kg. Therefore, the requirement of low cost, low mass, low dimension, and low power consumption must be fulfilled in designing and choosing the component of nanosatellite. To obtain wider coverage area while maintaining the low dimension, camera array was used to produce image with wider area. In this research, On Board Data Handling (OBDH) implemented in FPGA used below 100% of the total FPGA resource. LUT-FF pairs was the most used resource with 75% of usage. OBDH also combined the image from each camera to get image with wider area. The FPGA and 4 cameras used 2264.44 milliwatt of power consumption, higher than the remote sensing system of SNAP-1 nanosatellite which used 1 milliwatt of power consumption.**

Keywords—Array Camera, On Board Data Handling, FPGA, Nanosatellite

I. INTRODUCTION

Nanosatellite with capturing image ability is one of the research developed at Nanosatellite Laboratory of Telkom University. From research [1], image with 305,38 km x 240,81 km of coverage area was obtained by using CAM130 camera. The image resolution can be increased by lengthening focal length of camera lens. However, by using that method, coverage area of the image will be smaller [2]. To get the wider image coverage area, technique in research [3] was used by utilizing array of camera. Wider and more detailed image was expected to be achieved by using this technique.

In this research, the performance of On Board Data Handling (OBDH) using FPGA XuLA2 LX9 Spartan 6 as the processor was analyzed. This research was developed from the previous research, [4] and [5]. Both research used the same FPGA series. Research [5] only utilized a camera while research [4] has designed 4 cameras integrated with XuLA2 LX9 Spartan 6. Four images from 2x2 camera matrix were produced but the image processing done at PC has not combined 4 images into larger image. This research was the development of the research [4] by combining 4 images into image with wider coverage area.

FPGA was chosen in this research because it is easy for user to configure without using fabrication by remaking the logic circuit to get the expected output. FPGA also has a low cost production [6] and can resist the radiation [7]. Therefore, FPGA can be used for nanosatellite application. FPGA XuLA2

LX9 Spartan 6 [8] has dimension of 51 mm x 25 mm with 1.2 volt or 3.3 volt of voltage input and 65 mA – 6A of current consumption. It has 12 MHz of frequency that can be overclocked to 384 MHz. Based on those reason, XuLA2 LX9 can be applied at nanosatellite.

This paper consists of introduction in first section, FPGA system design and data fetching flow in second section, and analysis of On Board Data Handling (OBDH) and the result of image fetching and image combining in third section. The conclusion is in the fourth section.

II. SYSTEM DESIGN

The system design followed the research [4] with system block diagram as shown in Fig. 1 and Fig. 2. The system consisted of processor using FPGA as OBDH and 4 cameras arranged into 2 x 2 array. FPGA controlled the image fetching and sending the image to the PC, the PC then arranged the image according to the camera array. System blocks designed in FPGA were UART PC Controller, UART Camera Controller, Clock Generator, Baud rate Generator, Bridge, and Baud rate and Camera Switch.
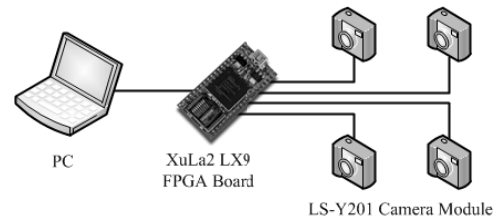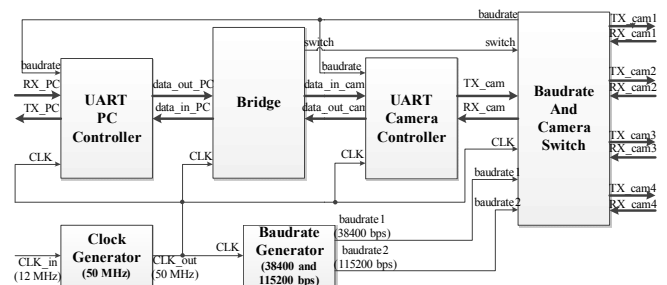

Fig. 1. System Configuration

Fig. 2. Schematic data of camera array interface

A. Clock Generator

This block was used to increase the default clock frequency of XuLA2, from 12 MHz to 50 MHz. This block provided clock for another blocks in the system. This block used Xilinx Digital Clock Manager (DCM) which could overclock the clock frequency [9]. Digital Frequency Synthesizer (DFS) in DCM produced output signal CLKFX by multiplying the input clock signal CLKIN with the integer ranging from 2 to 32 and then dividing it with integer ranging from 1 to 32. Fig. 3 shows the process of overclocking 12 MHz clock to 50 MHz. To produce 50 MHz of clock frequency, 12 MHz of default clock frequency was multiplied by 25 and then divided by 6.

B. Baud Rate Generator

This block had a function to produce the desired baud rate by activating enable pulse 16 times from the desired baud rate [10]. The enable pulse was derived from system clock. This block produced 2 baud rates, 38400 and 115200 baud. To produce 115200 of baud rate, the number of enable pulse activated was 16 x 115200 = 1,843,200 pulse per second. By using 50 MHz of clock frequency, one enable pulse was excited every 50,000,000/1,843,200 = 27.1267 clock cycle or rounded down to 27 clock cycle. To produce 38400 of baud rate, the number of enable pulse activated was 16 x 38400 = 614,400 pulse per second. By using 50 MHz of clock frequency, one enable pulse was excited every 50,000,000/614,400 = 81.38 clock cycle or rounded down to 81 clock cycle.

C. UART PC Controller

This block is used as communication channel between FPGA and PC. UART PC Controller was built using UART Macros made by Xilinx for PicoBlaze KCPSM6 on Spartan-6 [10]. This UART Macros was suitable for use in this research because it is designed with low level definition. Therefore, it efficiently used the FPGA resource gate. UART PC Controller consisted of UART_TX and UART_RX combined into one block which worked using 50 MHz of clock frequency.

UART Controller sent the data by assigning 8 bits of data into uart_tx_data_in. The sending data request signal then excited by changing the state of write_to_uart_tx into active high (1). When detected the sending data request, uart_tx_data_present changed its state into active high (a). This state was maintained during the excitation of data bits which would be sent through uart_tx. As long as the state uart_tx_data_present was low (0), uart_tx was in idle condition (constantly in active high (1) state). When the state of uart_tx_data_present was active high (1), start bit (0) was excited at uart_tx, followed by bits which would be sent (LSB first), and ended by stop bit (1). After the sending data process ended, uart_tx was back into idle condition and uart_tx_data_present was back into low (0) state.

UART Controller received the data when uart_rx detected the start bit. Then, uart_rx started to read the data bits (LSB first) and stopped when detected the stop bit. After data reading stopped, uart_rx_data_present changed its state into active high (1), indicating the received data was available in uart_rx_data_out. Data was available in uart_rx_data_out as long as the state of uart_rx_data_present was active high (1). If received data was successfully processed, read_from_uart_rx changed its state into active high (1) and uart_rx_data_present was back into its low state (0), indicating uart_rx_data_out was cleared and ready to received new data.

D. UART Camera Controller

UART Camera Controller is used as communication channel between FPGA and camera modules. UART Camera Controller also used UART Macros like UART PC Controller. Therefore, UART Camera Controller worked the same as the way UART PC Controller worked. The only difference was UART Camera Controller was only able to communicate (transmit-receive) with one camera module at a time, but it was able to send the data to all camera modules simultaneously. The communication channel between FPGA and camera modules was controlled by Switch block. Switch block decided which camera that can communicate using UART Camera Controller. UART Camera Controller also worked with 50 MHz of clock frequency.

E. Bridge

Bridge block connected the UART PC Controller with UART Camera Controller. This block forwarded the data received from PC to be sent to camera module, as well as the opposite way. Besides that, this block also had a function to forward the UART Camera Controller communication channel setting command and baud rate switch command to Switch block. Switch command (swc) was indicated by the header AA_{16}.

There were 2 scenarios in this block, data flow from PC to camera module and data flow from camera module to PC. The data flow from PC to camera module was done by checking uart_rx_data_out_pc, if it contained the AA_{16} data, then the next data was switch command (swc) and sent the swc data to Switch block. If it contained the data other than AA_{16}, then forwarded the data to uart_tx_data_in_cam and sent the data to camera module using UART Camera Controller. The data flow from camera module to PC was done by forwarding all data contained in uart_rx_data_out_cam to uart_tx_data_in and sending the data to PC by using UART PC Controller.

F. Baudrate and Camera Switch

Switch block is used as multiplexer, deciding which camera module that can communicate using UART Camera Controller. Besides that, this block also controlled the baud rate changing of UART Controller from 38400 to 115200 and vice versa. This block worked by the switch command (swc) forwarded by Bridge block.

III. ANALYSIS

A. Analysis of Clock Generator Block

Clock Generator block worked well. Input clock (clk) had 12 MHz of frequency. Therefore, one clock cycle had 1/12.000.000 = 83,3333 ns or rounded down to 83 ns of period. The output was clko which had 19,920 of one cycle period so it had 1/(19,920 x 10-9) = 50,2008 MHz or rounded down to 50 MHz of frequency.

B. Analysis of Baud Rate Generator Block

Fig. 4 shows that Baud Rate Generator worked as expected. This block worked according to the counter. One cycle clock of enable pulse was excited every time the counter went back to zero. This block excited 2 baud rate, baud_1 38400 and baud_2 115200. Baud_1 counter counted 81 clock cycles (0000000_2 to 1010000_2) while baud_2 counter counted 27 clock cycles (00000_2 to 11010_2).

C. Analysis of UART Controller TX

Based on the simulation, UART Controller TX could excite the data bits at uart_tx pin according to the specification. In the simulation, the data which would be sent were 10101011_2 or AB_{16}. From bits excited by uart_tx, start bit (0) is seen, followed by data bits with LSB first (11010101_2), and ended by stop bit (1). During the process of bits excitation at uart_tx, uart_tx_data_present is seen in active high (1) condition. When the process ended, uart_tx_data_present went back into low (0) state. The excitation of 1 bit data needed 16 enable pulses. Therefore, the transmission of 1 byte (8 bits) data needed 160 enable pulses (start bit and stop bit were also counted).

D. Analysis UART Controller RX

UART Controller RX worked according to specification. At first, uart_rx_data_out was still empty, indicated by 00000000_2 in Fig. 6. After stop bit detected by uart_rx, uart_rx_data_out was contained with data received by uart_rx, 10101011_2 or AB_{16}. When uart_rx_data_out was contained with data, uart_rx_data_present changed its state into active high (1). When read_from_uart_rx changed its state into active high (1) as long as one clock cycle, uart_rx_data_present went back into low (0) state, indicating uart_rx_data_out was cleared and ready to received new data. In the next data receiving, the data at uart_rx_data_out changed into new received data 00001010_2.

E. Analysis of Baud Rate Changing

In simulation, system baud rate changed according to the given command. Baud rate changing command ($AA39_{16}$ and $AA30_{16}$) is seen at uart_rx_data_out_pc where the data from PC received by FPGA. When detecting the AA_{16} data, Bridge block forwarded the next data which was the baud rate changing command to Switch block using swc signal. Switch block then changed the baud rate according to the command, the data 39_{16} to change the system baud rate from 115200 to 38400 and the data 30_{16} to change the system baud rate from 38400 to 115200.

F. Analysis of Choosing the Communication Channel

Simulation of choosing the communication channel was done for sending data to all camera modules and sending data only to one camera module, camera 1. Fig. 8 shows the sending data to all camera modules. The sending data to all camera modules was done by sending the $AA35_{16}$ command. Fig. 8 shows that PC sent the $AA3563_{16}$ data to uart_rx_data_out_PC. The data which would be sent to uart_camera_controller was 63_{16}. When Switch block received the 35_{16} command, Switch block set the bits excited by uart_camera_controller at uart_tx_cam to be forwarded to

uart_tx_1, uart_tx_2, uart_tx_3, and uart_tx_4. Fig. 8 shows the signal excited at uart_tx_cam was also excited at uart_tx_1, uart_tx_2, uart_tx_3, and uart_tx_4.

Fig. 9 shows the simulation of sending data from PC to camera 1. Communication mode to camera 1 was done by sending the $AA31_{16}$ command. In this simulation, PC wanted to send the 64_{16} data to camera 1, shown by the 31_{16} data after AA_{16} at uart_rx_data_out_pc. Switch block set the bits excited at uart_tx_cam were only forwarded to uart_tx_1. It can be seen in Fig. 9 where the waveform of uart_tx_cam is the same as waveform of uart_tx_1.
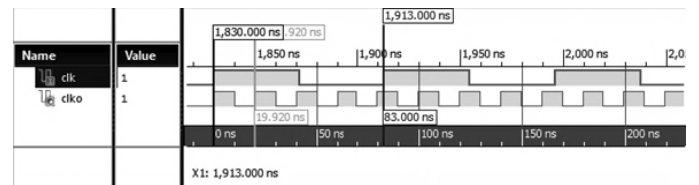

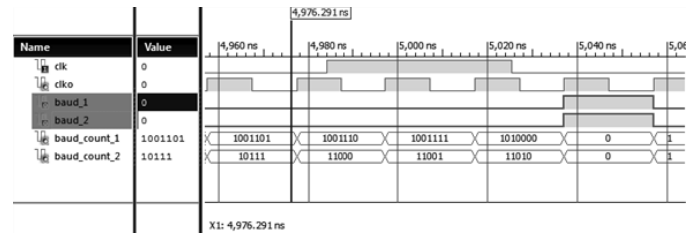Fig. 3. Simulation of clock generator

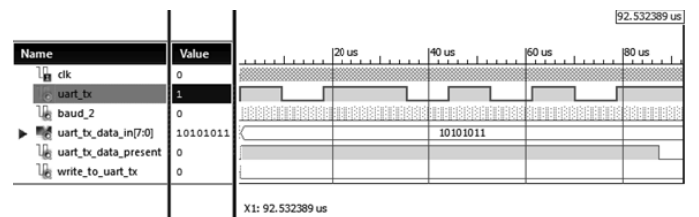Fig. 4. Simulation of baud rate generator

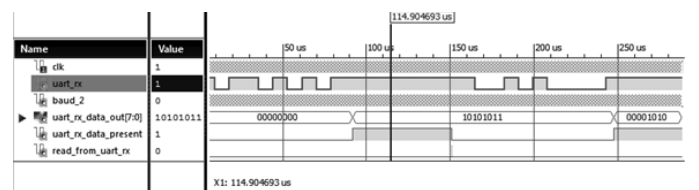Fig. 5. Simulation of UART Controller TX
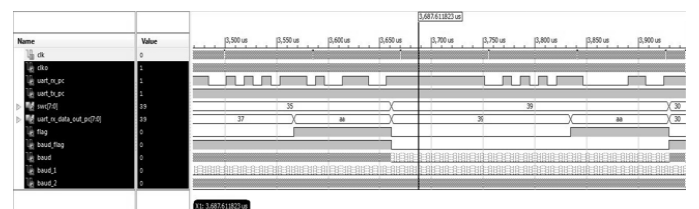

Fig. 6. Simulation of UART Controller RX

Fig. 7. Simulation of baud rate changing

Switch block also set the sending data from camera 1 to PC. Data received through uart_rx_1 were forwarded to uart_rx_cam. Then, uart_rx_cam forwarded the data to uart_pc_controller so that the data transmitted through uart_tx_pc. Fig. 10 shows the simulation of sending data from camera 1 to PC.

G. FPGA Resource Utilization

System design which had been made in this research was possible to be implemented in FPGA because the FPGA resource needed were below the available FPGA resource. Table I shows the utilization percentage of FPGA resource used in this research.

TABLE I.   UTILIZATION OF FPGA RESOURCE

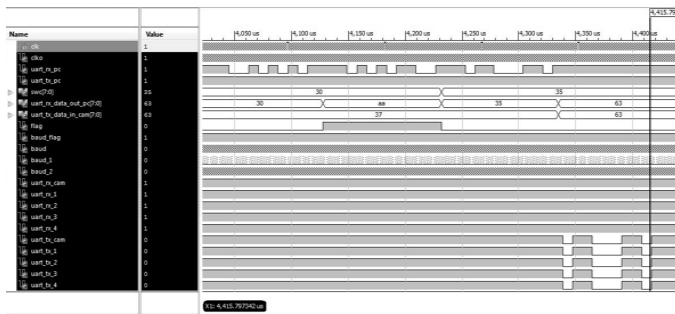| Slice Logic Utilization	Used	Available	Utilization
Number of Slice Registers	144	11.440	1%
Number of Slice LUTs	125	5.720	2%
Number of fully used LUT-FF pairs	97	130	74%
Number of bonded IOBs	11	186	5%
Number of BUFG/BUFGMUXs	1	16	6%
Number of DCM/DCM_CLKGENs	1	4	25%

Fig. 8.   Simulation of sending data to all camera modules

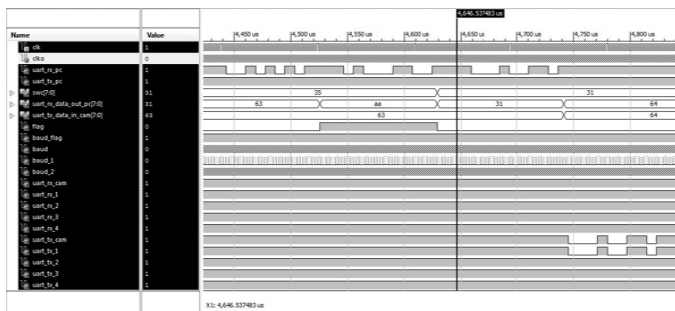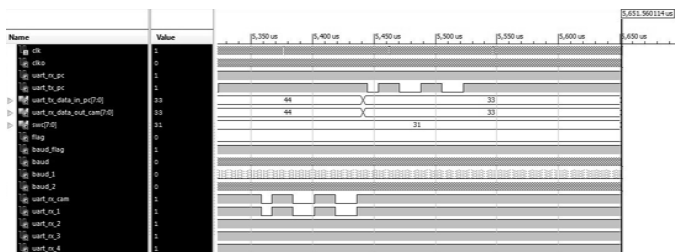
Fig. 9.   Simulation of sending data to camera 1

Fig. 10. Simulation of sending data from camera 1 to PC

H. Design Verification Using USB to UART

To verify the design, 5 USB to UART was used in this research, 1 USB to UART was used to observe the TX-RX pins of PC while the rest were used to observe TX-RX pins of camera 1, 2, 3, and 4. TX pin of USB to UART was connected to RX pin of FPGA. RX pin of USB to UART was connected to TX pin of FPGA. Then, USB to UART was connected to USB Hub that connected to USB port of PC.

The next step was opening the hyperterminal program at PC. In this research, X-CTU was used as hyperterminal program. Because there was 5 ports to be observed (1 uart_pc and 4 uart_cam), 5 windows of X-CTU were needed. COM1 port was assigned for uart_pc while the other ports were assigned for uart_cam (COM41 for uart_cam1, COM42 for uart_cam2, COM43 for uart_cam3, and COM44 for uart_cam4). Before serial port opened, each port was set with 38400 of baud rate, without flow control, 8 bit of data, without parity, and 1 stop bit.

Fig. 11 and Fig. 12 show the interface worked according to design and simulation. Switch command also worked as expected. When PC sent the $AA31_{16}$ command, PC could communicate (transmit-receive) with uart_cam1. Another ports also worked that way. When PC sent $AA35_{16}$ command, PC could send data to all ports simultaneously. Baud rate changing command also worked well. When PC sent $AA30_{16}$ command, PC could communicate to each port after the baud rate setting at each port had been changed into 115200.
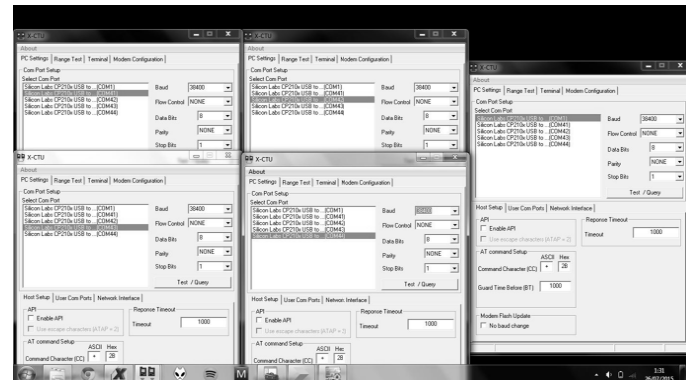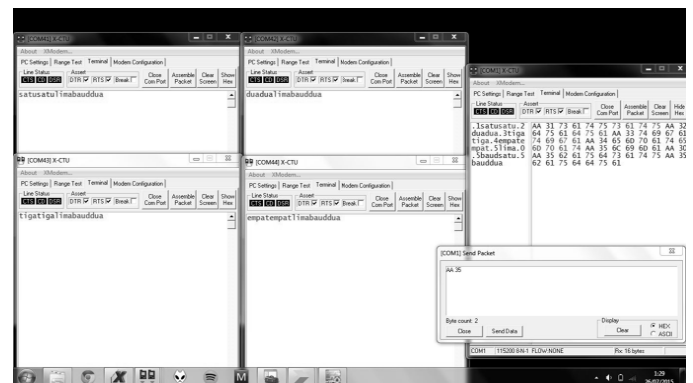

Fig. 11. Serial port setting at each port

Fig. 12. Verification of interface implementation in FPGA using USB to UART

I. Analysis of System Power Consumption

Analysis of system power consumption was done to observe how much power needed by the system. Power consumption also determined whether the system built in this research could be implemented in nanosatellite. Measurement was done by measuring the current and voltage of each component three times. Power consumption was obtained by multiplying the mean of current with the mean of voltage of each component. Power consumption is shown by Table II.

Based on Table II, system of 4 cameras interface based on FPGA built in this research needed 2265.4 milliwatt or 2.26544 watt of power consumption. Power needed by this system is relatively high if it is compared with the power consumption of remote sensing payload of SNAP-1 nanosatellite which only needs 1 watt of power consumption [11]. This was caused by the system built in this research using 4 cameras. Therefore, the power consumption needed was higher than remote sensing system using only 1 camera. Voltage needed by camera module in this system also relatively high which used 5 V. To decrease the power consumption of system in this research, camera module can be given 3,3 V of voltage.

J. Analysis of Image Stitching

Each camera produces RGB image in JPEG format with resolution of 640 x 480 pixels. Because 4 cameras were used, the combined image has resolution of 1280 x 960 pixels. Fig 13 shows the image produced from previous research [4]. The image was captured with 0º of angle between cameras and 1 m of capturing distance. This image has not perfectly combined. The edge of image from each camera can still be seen. The brightness of image was also different with each other. At some cameras, image produced seemed blurry or unfocused. This was caused by the very small distance between camera and the object. Overlapping area also can be seen at some images. To produce perfectly combined image, image enhancement was needed to crop the overlapping area and to match the brightness of image elements.

In this research, image stitching process was performed at PC. Image stitching process combined the image by matching the features at each image as interest points. Each image then was transformed based on the transformation matrix made by those interest points. Fig. 15 shows the result of stitching the image elements shown by Fig 14, which was captured with 0º of angle between cameras and 1 m of capturing distance.

The image taken with 0º of angle between cameras as shown by Fig 14 has overlapping area, causing smaller coverage area. The farther the capturing distance, the coverage area of image taken with 0º of angle between cameras will be smaller. This is caused by the distance between camera and the object. The farther the distance of camera from the object, the overlapping area will be larger, decreasing the image coverage area, according to Fig 18. To get the optimum coverage area of the image, the angle between cameras must be set to minimize the overlapping area according to Fig 18. Fig 16 shows the image taken with 52º of angle between cameras and 1 m of capturing distance. Fig 16 has larger coverage area (226 cm x 210 cm) than Fig 15 (125 cm x 120

cm), but the image could not be stitched because the image elements of Fig 16 did not have overlapping area.

Fig. 17 shows the image of map 1 : 4,750,000 scale that taken using 4 cameras with distance of 14.7 cm, or 700 km according to map scale (LEO height), depicting the Borneo Island. The image was taken with certain angle to minimize the overlapping area (30º of angle). Image produced from each camera has resolution of 640 x 480 pixels. Therefore, the combined image has resolution of 1280 x 960 pixels. Based on the measurement on the map, the map area captured by the cameras has 30 cm of length and 21 cm of width. According to map scale, the image coverage area at real distance has 1,425 km of length and 997.5 km of width.

TABLE II.   SYSTEM POWER CONSUMPTION

Component	Current Mean (mA)	Voltage Mean (V)	Power Consumption (mW)
XuLa2 LX9	148.43	3.28	487.356
LS-Y201 (cam1)	108.07	4.80	518.72
LS-Y201 (cam2)	108.63	4.66	506.593
LS-Y201 (cam3)	78.50	4.73	371.305
LS-Y201 (cam4)	79.03	4.83	381.468
Total of System Power Consumption			2265.44

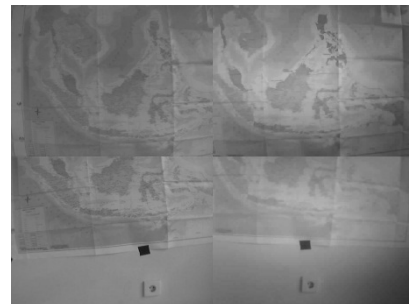Fig. 13. Image produced from previous research [4]

Fig. 14. Image captured from distance of 1 meter with 0º of angle between cameras before being stitched

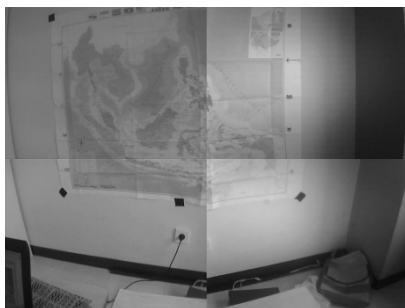Fig. 15. Image captured from distance of 1 meter with 0º of angle between cameras after being stitched

Fig. 16. Image captured from distance of 1 meter with angle setting between cameras

Fig. 17. Map with 1:4,750,000 scale captured with 4 cameras from distance of 14.7 cm and 30º of angle between cameras.

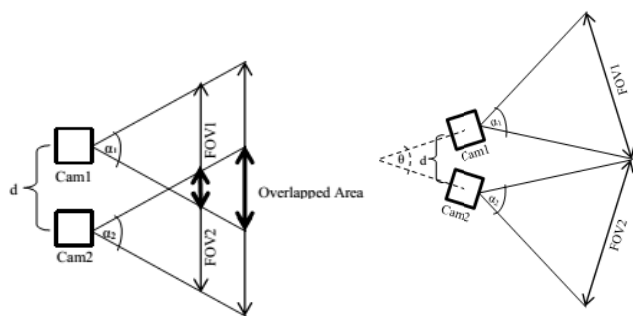Fig. 18. Field of View of capturing image without angle setting (0º) between cameras and with angle setting between cameras

IV. CONCLUSION

In this research, On Board Data Handling (OBDH) by using FPGA and array of camera was designed and analyzed. Image was produced by 4 cameras which captured image one by one. Image stitching was performed in this research to combine the image taken by each camera. The FPGA resources used by the design were 144 slice registers, 125 slice LUTs, 97 LUT-FF pairs, and 11 IOBs. All resources used were below 100%. This system using 4 cameras needed 2265.44 milliwatt of power consumption, relatively higher than power consumption of SNAP-1 nanosatellite remote sensing system which uses 1000 milliwatt of power.

REFERENCES

[1] Edwar and M. A. Murti, "Implementation and Analysis of Remote Sensing Payload Nanosatellite for Deforestation Monitoring in Indonesian Forest," in *Recent Advances in Space Technologies (RAST), 2013 6th International Conference on*, Istanbul, 2013.

[2] J. C. Leachtenauer and R. G. Driggers, *Surveillance and Reconnaissance Imaging Systems: Modeling and Performance Prediction*. Norwood: Artech House, Inc, 2001.

[3] V. Vaish, "Synthetic Aperture Imaging Using Dense Camera Arrays," Department of Computer Science, Stanford University, Stanford, Disertasi 2007.

[4] W. Pakartipangi, B. Syihabuddin, and D. Darlis, "Design of Camera Array Interface Using FPGA for Nanosatellite Remote Sensing Payload," in *The 2015 International Conference on Radar, Antenna, Microwave, Electronics and Telecommunications*, Bandung, 2015.

[5] D. Cahyono and A. Nugroho, "Design and Realization Camera Controller for a Remote Sensing Payload of Nanosatellite FPGA (Field Programmable Gate Array) System Based," in *Recent Advances in Space Technologies (RAST), 2013 6th International Conference on*, Istanbul, 2013.

[6] F. W. Wibowo, *FPGA DAN VHDL: Teori, Antarmuka dan Aplikasi*. Sleman: Penerbit Deepublish (CV Budi Utama), 2014.

[7] H. D. Schmitz, "Application Examples: How to Use FPGA's In Satellite Systems," Actel Corporation, Sunnyvale, 2010.

[8] XESS. (2012) XESS. [Online]. HYPERLINK "http://www.xess.com/static/media/manuals/XuLA2-manual.pdf" http://www.xess.com/static/media/manuals/XuLA2-manual.pdf

[9] Xilinx. (2015) Xilinx. [Online]. HYPERLINK "http://www.xilinx.com/support/documentation/user_guides/ug382.pdf" http://www.xilinx.com/support/documentation/user_guides/ug382.pdf

[10] K. Chapman, "Ultra-Compact UART Macros for Spartan-6, Virtex-6 and 7-Series with PicoBlaze (KCPSM6) Reference Designs," California, 2014.

[11] R. Lancaster, "An Optical Remote Inspection System for the Surrey Nanosatellite Applications Program," Surrey Space Centre, University of Surrey, Guildford, Tesis 2001.

Use of Clustering Concept for Chunk Forming based on Constellation Signals on OFDMA Resource Allocation Systems

Budi Prasetya[1,2], Adit Kurniawan[1], Iskandar[1]
[1]School of Electrical Engineering and Informatics
Institut Teknologi Bandung
Bandung, Indonesia

Arfianto Fahmi[2]
[2]School of Electrical Engineering
Telkom University
Bandung, Indonesia

Abstract—In OFDMA (Orthogonal Frequency Division Multiple Access) wireless system, environmental conditions and mobility of all users make the conditions of propagation of each user on all subcarriers changed at different times. Required radio resource allocation scheme that works with accurate, has a fairly low complexity and it is able to adapt to changing conditions. This research is to answer these issues by developing a new resource allocation scheme that is adaptive to changes in the channel, with the classification of some subcarriers into one chunk is based on the analysis of the constellation signal received on each subcarrier. We propose grouping some subcarriers into one chunk by using clustering concept, the algorithm chosen for the simplicity of the computing process is a K-Mean Clustering. The simulation results indicate that the resource allocation scheme that we have proposed give SSE (Sum Squared Error) improvement and can improve throughput when compared to the conventional scheme which uses clustering on the received signal level.

Keywords—OFDMA, resource allocation, clustering, chunk forming

I. INTRODUCTION

Currently, the needs of mobile data services are increasing. At the end of 2015, the International Telecommunication Union (ITU) predicts there are about 7.085 billion mobile cellular subscribers with 96.8 per 100 inhabitants. ITU also reported an increase number of mobile broadband cellular subscribers of 11.5 per 100 inhabitants in 2010 to 47.2 per 100 inhabitants at the end of 2015 [1], or increased to more than four times.

On the other hand, wireless access network as a leader in expanding the infrastructure to provide services, have limited resources such as frequency, power and timing. So, we need a method of resource sharing by implementing resource allocation in order to remain efficient resource and have the quality of service is maintained. Standard Third-Generation Partnership Project-Long Term Evolution (3GPP-LTE) capable of providing data rates up to 100 Mbps at the user level that are vehicular mobility.

In order to achieve high speed data transmission through wireless channels, a novel resource sharing methods continue to be discovered and developed in OFDMA systems and SC-FDMA (Single Carrier-Frequency Division Multiple Access) systems. One is the radio resource allocation technique that allocates radio resources such as frequency, power and bits to the many users. In the study [2] - [5] proposed resource allocation scheme by dividing into power allocation and subcarrier allocation. Water filling power allocation using power allocation and subcarrier allocation is done per unit of the subcarrier. In [3] and [5], the objective of the allocation is to maximize the amount of spectral efficiency while [3] and [4] is to maximize fairness.

To reduce complexity, In studies [6] - [10] simplify the allocation subcarrier be allocated per unit chunk, with the allocation of power and a bit in the downlink direction and allocation of power using equal power allocation in the uplink direction. Chunk is a set of combined subcarrier based on quality criteria. In [6] - [10] still using classification / grouping multiple subcarriers into one chunk by SNR (signal to noise ratio) or BER (bit error rate), so it can still be developed alternate methods of classification of some subcarriers into one chunk especially those that can improve accuracy.

This proposed study is also in the area, with emphasis on classification / grouping multiple subcarriers into one chunk is based on the concept of clustering. Clustering here is grouping constellation signaling signal after passing through the downlink wireless channel, signal constellation which has a similar Euclidean distance will grouped into a subcarrier group called chunk.

The contents of this paper consist of the following sections: explanatory summary of research on resource sharing in chapter 1, the discussion of system OFDM (Orthogonal Frequency Division Multiplexing), OFDMA and SC-FDMA and radio resource allocation described in section 2, OFDMA system resource allocation model, chunk forming with the clustering concepts, wireless channel model discussed in section 3, the simulation results presented in section 4, while conclusions and discussions presented in section 5.

II. COMMUNICATION SYSTEMS OFDM, OFDMA, RESOURCE ALLOCATION

A. OFDM Communication Systems

The basic concept OFDM is to divide the high-speed serial data into low-speed parallel data that is transmitted with multiple subcarriers. Each subcarrier made mutually orthogonal that allows spectral overlap to improve bandwidth

efficiency. Another advantage of OFDM systems is the ability to reduce the effects of multipath channel, since channel with frequency selective fading properties of the OFDM signal will be considered to be flat fading on each subcarrier.
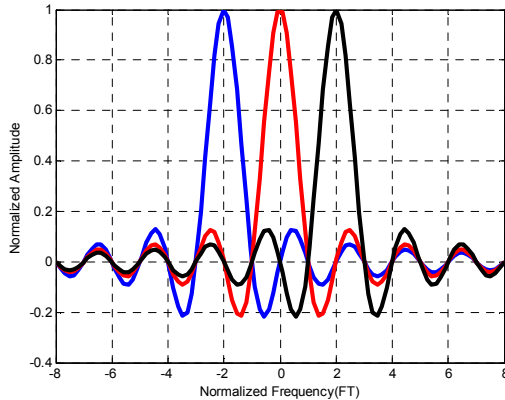

Figure 1. Spectrum of OFDM signals for three subcarrier [11]

The use of discrete Fourier transforms (DFT) on the OFDM system will reduce the level of complexity of the transmitter and receiver system. DFT is used in order to generate subcarriers that is orthogonal, each other, to shorten the computing time can be implemented algorithms of Fast Fourier Transform (FFT). But the FFT process is still done at the baseband level.

To generate baseband OFDM symbol, the first serial data sequence modulated using a modulation scheme such as Phase Shift Keying (PSK) or Quadrature Amplitude Modulation (QAM). This data Symbols are then converted into a sequence of parallel data by using a serial to parallel before multicarrier modulation. Each subcarrier sampled with a sampling rate N/T_s, where N is the number of subcarriers and T_s is the OFDM symbol duration. The frequency separation between the adjacent subcarrier is $2\pi / N$. OFDM symbol is the sum of each subcarrier expressed by the following equation [11]:

$$x_m = \frac{1}{N} \sum_{n=0}^{N-1} X_n \exp\left\{ j\frac{2\pi mn}{N} \right\}, \quad 0 \le m \le N-1 \quad (1)$$

Where:
N = number of point IDFT (subcarrier total) used
X_n = the symbol data transmitted on the nth subcarrier (frequency region)
x_m = OFDM symbol output in IDFT process

The purpose of this process is to ensure orthogonality between subcarrier, although the spectrum can be made to overlap each other. IDFT can be implemented using Inverse Fast Fourier Transform (IFFT). With the IFFT, computation process has also become faster.

B. *OFDMA and SC-FDMA*

Third Generation Partnership Project (3GPP) has introduced LTE (Long Term Evolution) as the standard of 4th Generation (4G), which has adopted as a standard OFDMA multiple access technology in the downlink direction to accommodate a wide variety of broadband services based Internet protocol. In the OFDMA system each user occupies a different frequency, each user occupies a space between the subcarrier with subcarrier designed by *Rs* (symbol rate of each subcarrier). As for the direction uplink, systems use SC-FDMA as a multiple access technology standard that uses a single carrier for each user [12]. Illustrations difference OFDMA and SC-FDMA can be described as Figure 2.
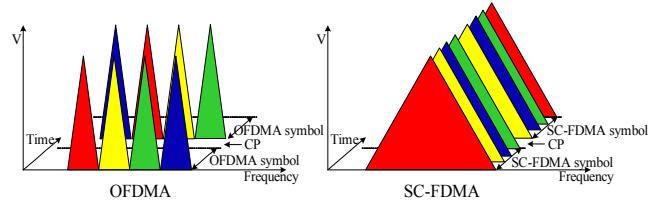

Figure 2. Differences OFDMA and SCFDMA [13]

C. *Problems in systems OFDMA and SC-FDMA*

After passing through the propagation channels which are frequency selective fading and time varying channel, so each different user will have different responses as well as shown in Figure 3. To achieve better communication quality, maximum throughput, spectral efficiency and energy are needed solution resource allocation scheme that can adapt to changes in channel conditions.
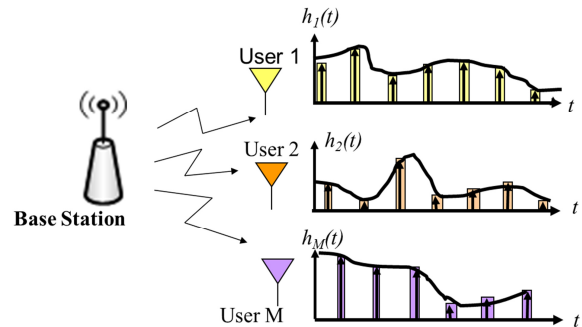

Figure 3. Each user goes through different responses

Figure 3 illustrates the communications downlink direction. User 1 passes through the different propagation channel with other users, so it had a different response.

D. *Radio Resource Allocation*

The idea of the use of channel state information (CSI) at the transmitter to increase the performance of the communication system was first conceived in [14]. The basic idea is the use of the knowledge of the transmission channel to set the parameters in order to maximize communication performance. The concept was first known as the concept of adaptive modulation and coding. The use of adaptive modulation and coding developed further in the case of a single user at [15] - [16].

The development of the concept of adaptive modulation to schedule users on a multiuser wireless system evolve since introduced the term multiuser diversity [17] and the proportional fair scheduling [18]. In both of these studies, the

wireless channel affected by fading can be seen as a means to improve system performance when it is used for multiuser applications.

In a system of OFDMA and SC-FDMA does not occur multiple access interference (MAI) phenomenon for each user using a set of subcarriers or chunk which differ from one another in one TTI (time transmission interval) when the session traffic exchange. The division of use subcarrier every user is done through the process of resource allocation. The process is carried out at the beginning of each TTI by allocating all N available subcarriers to a number of such K-user that in one TTI does not happen multiple access interference.

Resource allocation utilizing the diversity of instantaneous channel state information conditions in the duration of one TTI. As a result of the mobility of the user, the propagation channel changes in the frequency and time domain. Subcarriers experiencing fading at a particular user can be viewed as a subcarriers that are not experiencing fading by another user. So it can be done available subcarrier allocation and power of each subcarrier to all users individually by the scheduler. The scheduler can view this condition as a condition of multiuser diversity because there are variations of propagation conditions on all the subcarriers available for all users.

III. OFDMA RESOURCE ALLOCATION SYSTEM MODEL

Model of resource allocation in OFDMA system for single cell is shown as in Figure 4, where there are M active users and N chunk. The total system bandwidth available is B and the bandwidth of each subcarrier is b_s. In the model, at the beginning of a transmission time interval, the base station sends the same symbol mapping/modulation signal to M-user using signaling channel. At the receiver in each user, OFDM demodulation process is carried out using the FFT process. The output of the FFT is the symbol with the constellation same as on the transmitter, the difference is that the symbol on the receiver already passed the downlink wireless channel. Constellation these signals are fed back to the base station,

assuming the feedback works perfectly. By utilizing the signal constellation information of each user, then grouping subcarriers that have quality similar / almost equal to one chunk commonly referred to as a chunk forming. Furthermore, the base station allocates power and bit into each chunk, and allocate an available chunk of all users.

A. Use of Clustering for Chunk Forming

Cluster analysis is an attempt to find a group of objects that represent a character of the same or similar between one object to another object in a group and have differentiated or not similar to the objects in other groups. Clustering algorithms trying to find a group of natural objects, based on some similarities [19].

The most important concept to realize is that the clustering process that will result in clusters with high quality if it has a high degree of similarity in one class (high intra-class similarity) and a low level of similarity between the classes (low inter-class similarity). Similarity is a numerical measurement of the two objects. In measuring the value of similarity has often used methods of Euclidian Distance.

Euclidean distance between two objects or signal $c(t)$ and $y_i(t)$ is [20] :

$$dist(y_i, c) = \|y_i(t) - c(t)\| = \sqrt{(a_{i1} - c_1)^2 + (a_{i2} - c_2)^2} \quad (2)$$
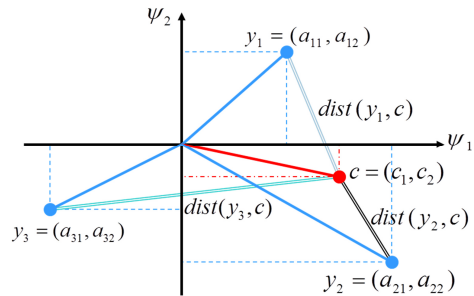$$i = 1, 2, 3$$

Figure 5. Euclidean distance in the signal space analysis [20]
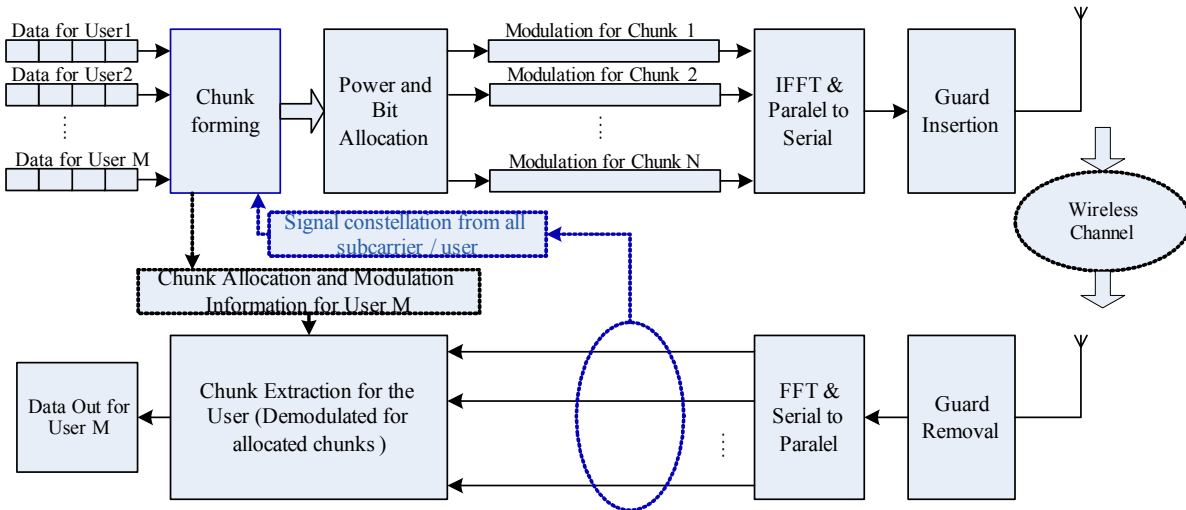

Figure 4. The proposed model of resource allocation in OFDMA systems with chunk allocation, power and bit, modified from [7].

Where $c(t)$ is the central point of a cluster (centroid), while c_1 is a projection of $c(t)$ to the first base function or Ψ_1 and c_2 is the projection of $c(t)$ to the second base function or Ψ_2. Symbol $y_i(t)$ is the data or object will be done grouping or clustering, a_{i1} is projected $y_i(t)$ to the first base function or Ψ_1 and a_{i2} is projected $y_i(t)$ to the second base function or Ψ_2.

In the study of resource allocation, the clustering algorithm will be used in the process of forming chunk as shown in Figure 4 above. Object or data $y_i(t)$ will be clustering is signaling signal constellation received from each user or subcarrier after the FFT process, where there are M-user or subcarrier of FFT output. FFT output signal constellation can indicate the condition of the channel passed by each user or subcarrier, so by clustering this constellation signal means also group some subcarriers that have similar quality / almost equal to one chunk.

B. K-Means clustering Algorithm

The K-means clustering algorithm is one of the top ten clustering algorithms, it is simple algorithm [21]. In this study, we use this algorithm because the process is simple. The purpose of this algorithm is to split the data into several groups or K-group. This algorithm accepts input in the form of data without a label. Input received is a data or object and k-groups (clusters) as desired. This algorithm will classify data or objects into K-group. At each cluster there is a central point (centroid) which represents the cluster.

Basic K-Means clustering algorithm is as follows [22]:
1. Select K points as initial centroid randomly.
2. Categorize the data, thus forming K-clusters with each cluster centroid point is the centroid point that has been previously selected.
3. Update centroid point value.
4. Repeat steps 2 and 3 until the value of the centroid point are no longer changed.

The process of grouping data into a cluster can be done by calculating the distance (Euclidean distance) of a data closest to a centroid point.

C. SSE (Sum Squared Error)

SSE is used to determine the better clustering results, if the centroid of its initialization is different. SSE calculates the error of each data point, its Euclidean distance to the closest centroid, and then compute the total sum of the squared errors. Given two different sets of clusters that are produced by two different runs of K-mean, we prefer the one with the smallest squared error since this means that the prototypes (centroids) of this clustering are a better representation of the points in their cluster. SSE is formally defined as follows [22]:

$$SSE = \sum_{i=1}^{K} \sum_{y \in C_i} dist(c_i, y)^2$$

(3)

Where c_i is the centroid of cluster C_i, C_i is the ith cluster and y is an object or data.

D. Wireless Channel Model

We model the OFDMA downlink network with one transmitter (base station) and M-receiver (user), as shown in figure 6(a) below. The complex baseband representation of the impulse response of wireless channel for user i can be describe by [23] :

$$h_i(t, \tau) = \sum_l \alpha_{l,i}(t) . \delta(\tau - \tau_{l,i})$$

(4)

Where $\tau_{l,i}$ is the delay of the lth path and $\alpha_{l,i}(t)$ is the corresponding complex amplitude. The $\alpha_{l,i}(t)$'s are assumed to be wide-sense stationary, narrow band, complex Gaussian process, which are independent for differents paths or users. The frequency response of the channel impulse response can be expressed as [23] :

$$H_i(f, t) = \int_{-\infty}^{+\infty} h_i(t, \tau) e^{-j2\pi f\tau} d\tau = \sum_l \alpha_{l,i}(t) e^{-j2\pi f\tau_{l,i}}$$

(5)

If only instantaneous channel conditions are considered, the channel frequency response corresponding to user i is denote by $H_i(f)$. Consequently, the M-user wireless channel can be represented as in figure 6(b).
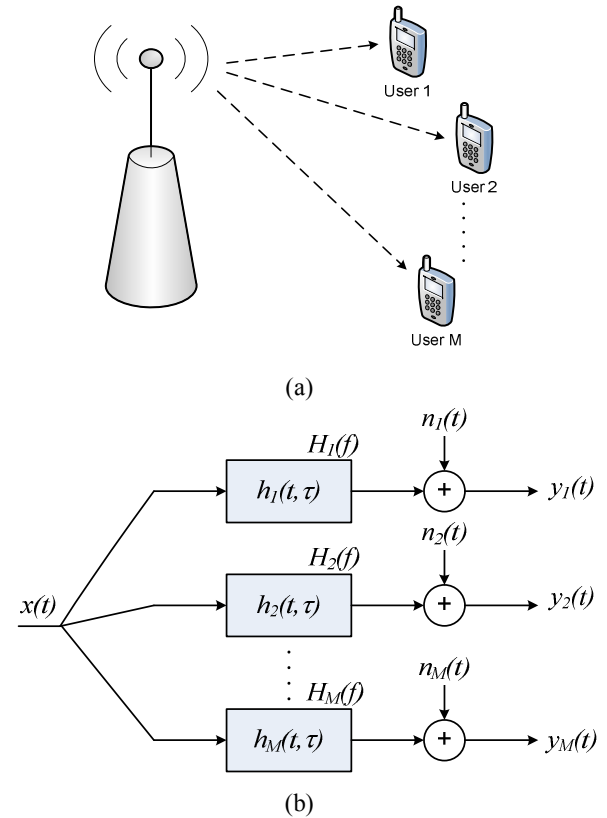

(a)

(b)

Figure 6. (a) OFDMA downlink network. (b) Channel model [23]

IV. SIMULATION RESULTS

In this section, we present simulation results to illustrate the performance of the proposed chunk forming in resource allocation. Channel model as shown in Figure 6 (b), with transmitted signaling signal $x(t)$ is a BPSK modulated signal with the symbol '1' and the transmit power of 1 watt, emitted by the IFFT 64 subcarriers or 64 users. Whereas $y_i(t)$ is the received signaling signal for each user after passing through the wireless channel.

Wireless channels that are used in the simulation $h_i(t,\tau)$ is a large scale propagation model combined with small scale fading. The large scale propagation model is a function of distance and frequency. The distance in this simulation is made randomly from 100 m until 3 km distributed uniformly. The frequency used from 2100 MHz, using 64 subcarriers at 15 kHz spacing. Small scale fading (due to multipath fading and movement of the user) are using the jakes method with the movement speed of the user is made randomly from 3 km/h until 100 km/h.
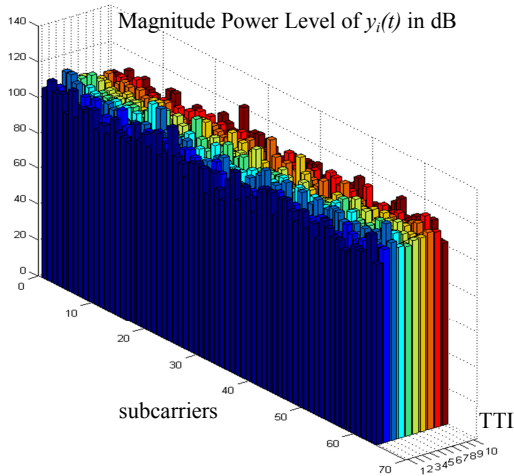
In Figure 7, we show the difference in the Magnitude Received Power Level of $y_i(t)$ for 10 TTI of each subcarrier. The differences caused by differences in random distances, multipath fading and random movement speed of each user.

Figure 8 shows the results of clustering using K-means clustering algorithm on 64 subcarriers to 5 chunks on each subcarrier / user after passing through the wireless channel. There are differences in the clustering results based on received signal level (conventional) and constellation signals (proposed method), but the proposed method show more accurate results because the signal is grouped actual signal that has real and imaginary parts.

Figure 9 shows the curve of SSE of the clusters as a function of SNR. From low SNR to high SNR, K-mean clustering algorithm if applied to signal constellation for chunk forming (proposed method) indicate the smaller value of SSE (average 1.239×10^{-18}) if compared with Clustering the received signal level (conventional).

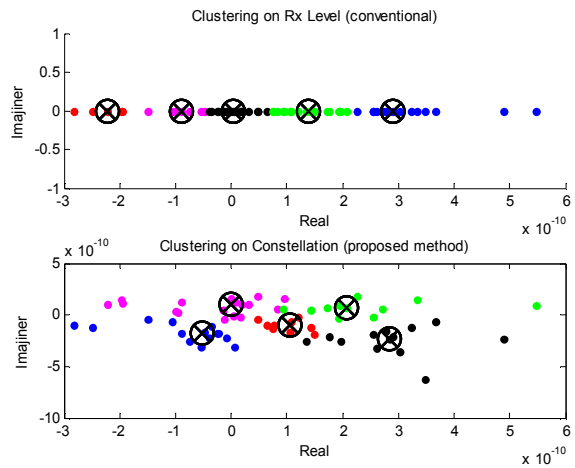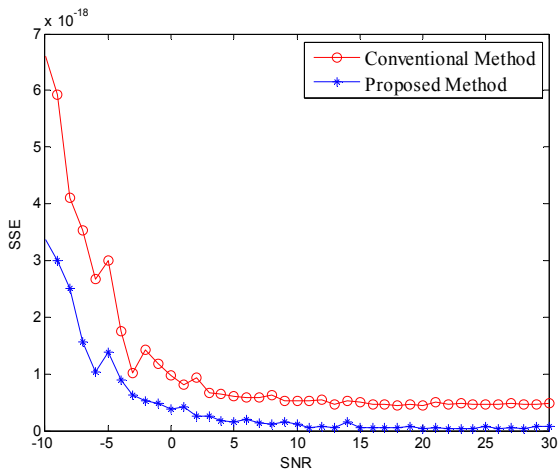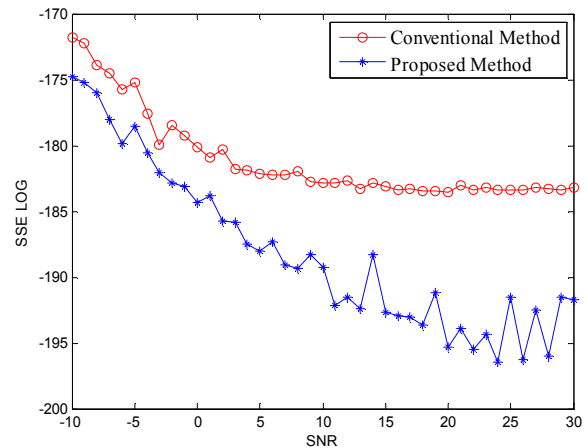Figure 7. Magnitude Received Power Level

Figure 8. Clustering using K-means clustering algorithm

(a)

(b)

Figure 9. Sum Squared Error of the clusters. (a) In numeric, (b) in decibels
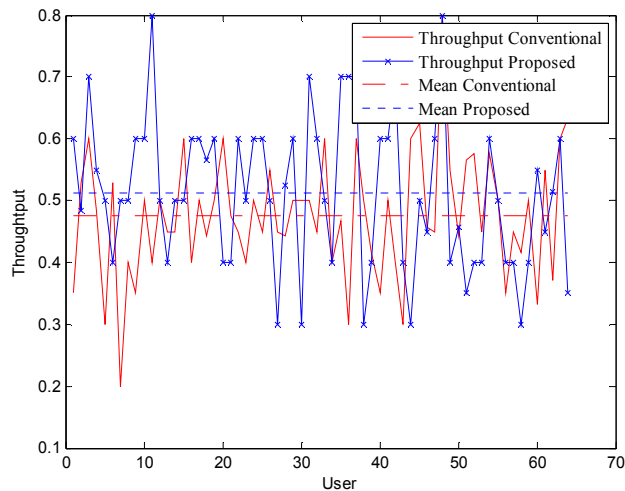
Figure 10. Throughput versus the number of users

Figure 10 shows the throughput curves as a function of the number of users. Throughput value will fluctuate if the number of active users is also different. However, the average throughput with a chunk forming using the proposed methods increase (0.05) when compared to conventional methods.

V. CONCLUTIONS

In this paper, we have presented a novel chunk forming using the clustering concept for resource allocation in OFDMA systems. The proposed method utilizes feedback constellation signal from each user / subcarrier. We proposed clustering process using K-means clustering because it is simple and fast computation process. Simulation results show that using K-means clustering algorithm on the process of chunk forming provide lower SSE compared with clustering using received signal level. Using K-means clustering algorithm on a chunk forming process can also increase the average throughput compared with clustering using received signal level (conventional).

In our study, we use K-means clustering and the maximum number of subcarrier/users by 64. In future studies may use others algorithm and a larger number of subcarriers.

REFERENCES

[1] ICT Data and Statistics Division of International Telecommunication Union ITU (2015), "ICT Facts and Figures, the world in 2015," Mei 2015.

[2] K. Kim, Y. Han, and S. L. Kim, "Joint Subcarrier and Power Allocation in Uplink OFDMA Systems," IEEE Communications Letter, vol. 9, no. 6, pp. 526-528, June 2005.

[3] L. Gao and S. Cui, "Efficient Subcarrier, Power and Rate Allocation with Fairness Consideration for OFDMA Uplink," IEEE Transactions on Wireless Communications, vol. 7, no. 5, pp. 1507-1511, May 2008.

[4] C.Y. Ng and C. W .Sung, "Low Complexity Subcarrier and Power Allocation for Utility Maximization in Uplink OFDMA Systems," IEEE Transactions on Wireless Communications, vol. 7, no. 5, pp. 1667-1675, May 2008.

[5] J. Huang, V. G. Subramanian, R. Agrawal, and R. Berry, "Joint Scheduling and Resource Allocation in Uplink OFDMA Systems for Broadband Wireless Access Networks," IEEE Journal on Selected Area in Communications, vol. 27, no. 2, pp. 226-234, February 2009.

[6] H. Zhu, J. Zou, "Chunk-Based Resource allocation in OFDMA Systems—Part I: Chunk Allocation.Transactions on Communications," Vol. 57, No. 9, September 2009. 2734-2744.

[7] H. Zhu, J. Zou, "Chunk-Based Resource Allocation in OFDMA Systems–Part II: Joint Chunk, Power and Bit Allocation," IEEE Transactions On Communications, Vol. 60, No. 2, February 2012. 499-509.

[8] A. Fahmi, M. Asvial, D. Gunawan, "Improved Performance of Mean Greedy Algorithm for Chunk Allocation in SC-FDMA Uplink Systems using Joint-User and Chunk-Based Allocation," Journal of ICT Research And Applications. vol. 7C, no. 1, pp. 59-81. 2013.

[9] A. Fahmi, M. Asvial, D. Gunawan, "Combined-order Algorithm using PrometheemMethod Approach and Analytic Hierarchy Decision for Chunk Allocation in LTE Uplink Systems," International Journal of Communication Network and Information Security (IJCNIS). vol. 5, no. 1, pp. 39-47. April 2013.

[10] H. Zhu, J. Zou, "Performance Analysis of Chunk-Based Resource Allocation in Multi-Cell OFDMA Systems," IEEE Journal on Selected Areas In Communications, Vol. 32, No. 2, February 2014. 367-375.

[11] B. Prasetya, S. Tjondronegoro, "Kinerja Sistem MIMO-OFDM dengan Beamforming pada Kanal Rayleigh," Jurnal Telekomunikasi, STT Telkom, Desember 2006.

[12] 3rd Generation Partnership Project, "Technical Specification Group Radio Access Network," Physical Layer Aspect for Evolved UTRA (Release 7).

[13] M. Rumney, "3GPP LTE: Introduction Single-Carrier FDMA," Agilent Measurement Journal, Januari 1, 2008.

[14] J. Hayes, "Adaptive feedback communications," IEEE Transaction on Communications, vol. 16, pp. 29-34, February 1968.

[15] A. J. Gold and S. G. Chua, "Variable Rate Variable Power M-QAM for Fading Channels'," IEEE Transactions on Communications, vol. 45, no. 10, pp. 1218-1230, 1997.

[16] T. Chung and A. Goldsmith, "Degrees of freedom in adaptive modulation: a unified view," IEEE Transactions on Communications, vol. 49, no. 9, pp. 1561-1571, September 2001.

[17] R. Knopp and P. Humblet, "Information capacity and power control in single cell multiuser communications," in IEEE International Conference on Communications, 1995.

[18] P. Viswanath, D. Tse, and R. Laroia, "Opportunistic beamforming using dumb antennas," IEEE Transactions on Information Theory, vol. 48, no. 6, pp. 1277-1294, 2002.

[19] M. W. Berry, "Survey of Text Mining: Clustering Classification and Retrieval" Springer; 2004 edition.

[20] B. Sklar, " Digital Communications : Fundamentals & Applications," 2nd Edition, Prentice Hall, 2009.

[21] X. Wu and V. Kumar, eds., The Top Ten Algorithms in Data Mining. Chapman and Hall, 2009.

[22] P.N. Tan, M. Steinbach, and V. Kumar, "Introduction to Data Mining," First Edition. Boston, MA, USA: Addison-Wesley Longman Publishing Co., Inc., 2005.

[23] G. Song and Y. Li, "Cross-Layer Optimization for OFDM Wireless Networks-Part I: Theoretical Framework," IEEE Transactions on Wireless Communications, vol. 4, no. 2, pp. 614-624, March 2005

Comparison Performance Analysis of OWDM and OFDM System on Multipath Fading Rayleigh Channel

Yuyun Siti Rohmah, Aly Muayyadi, Rina Pudji Astuti

Telkom University
Bandung, Indonesia
yuyunsr@tass.telkomuniversity.ac.id; alimuayyadi@telkomuniversity.ac.id; rinapudjiastuti@telkomuniversity.ac.id

Abstract— **Improvement of information technology especially in telecommunication system support wireless communication system must provide high data rate service. OFDM is the system that have high data rate and had been used as the method to overcome multiple channel effect. But the weakness of OFDM system is PAPR. Large PAPR causes non linear distortion of signal and non orthogonal of sub carrier that caused performance of OFDM system will decrease. Recently, it has been developed a system as an alternative to OFDM system called OWDM (Orthogonal wavelet division multiplex). Basic idea of OWDM is replaced Inverse Discrete Fourier Transform (IDFT) with the Inverse Discrete Wavelet Transform (IDWT) for generating orthogonal sub-carrier. Like IDFT on OFDM systems, function of IDWT on OWDM system is modulator, while demodulator process used DFT (Discrete Fourier Transform) on OFDM and DWT (Discrete Wavelet Transform) on OWDM. This paper will compare the performance between OWDM and OFDM system on fading Rayleigh channel. Simulation both of system resulted same performance on multipath Rayleigh fading channel but different PAPR value PAPR of OWDM system is smaller than OFDM system. Thus OWDM techniques can be chosen as an alternative method to overcome the problems of the high PAPR value in OFDM techniques.**

Keywords—owdm; ofdm; papr; dwt; idwt ;rayleigh fading

I. INTRODUCTION

Today's mobile wireless communications system are required to provide high speed data service. One technique that can provide high speed data services is OFDM (Orthogonal frequency-division multiplexing). OFDM is multicarrier technique that has long been used as an efficient method to counteract the effect s of multipath channel on a system that has a high data rate. However, one drawback of this system is the high value of Peak to Average Power Ratio (PAPR). PAPR is the ratio of peak power of the signal with average power. Large PAPR causes non linear distortion of signal and non orthogonality of sub carrier and produce peak value of signal so performance of OFDM system will decrease. Large PAPR value also causes the difficulty of implementation of power amplifier device and higher cost of implementation. Nowadays, multicarrier systems have been proposed based on wavelet transform that called as Orthogonal Wavelet Division Multiplexing (OWDM). Wavelet theory has been predicted by some experts as a good platform for building-based

multicarrier waveform. Akansu et.al.emphasizes the relationship between filter bank and predicts theory about OWDM multiplexers that has the ability to play in the upcoming communication systems [2]. In this study, Performance on fading Rayleigh and Peak to Average Power Ratio (PAPR) of both systems will be compared.

II. OVERVIEW OF OWDM AND OFDM SYSTEM

A. OWDM (Orthogonal Wavelet Divison Multiplexing)

OWDM in a communication system consists of processes such as signal synthesis filter bank with multiple inputs and one output in transmitter. OWDM synthesis process generates a signal as a combination of weighted pulses OWDM. Each pulse OWDM weight is representation of the symbol. In the receiver, signal is analyzed by using the filter bank with single input and multiple output[1].

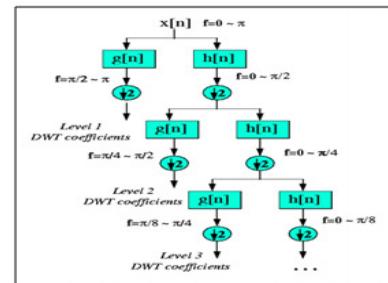- Discrete Wavelet Transformations (DWT) [5] [10]

Fig. 1. Signal decomposition procedure with Discrete Wavelet Transform

In discrete wavelet transform, digital signal representation is obtained by using digital filtering techniques. Filter with different cut off frequency is used to analyze signals at different scales. The signal is passed to the circuit High Pass Filter (HPF) for analyzing high frequency, and also passed to the Low Pass Filter (LPF) to analyze the low frequency. Signal resolution is a representation of amount signal detailed information that is converted by filtering operation, while the scale is converted by down-sampling and up-sampling operations (sub-sampling). Down-sampling process means lowering the sampling rate or throw some signal samples, while up-sampling process means

raising the sampling rate of a signal by adding new samples to the signal.

Fig. 1 explains the procedure of the Discrete Wavelet Transform:

➢ The signal is passed to the HPF and LPF to analyze high frequency and low frequency signals. Filtering process is the convolution operation between signals and response impulse of filter. Mathematically filtering process can be written as:

$$x[n] * h[n] = \sum_{-\infty}^{\infty} x[k].h[n-k] \qquad (1)$$

➢ After the signal through the LPF and HPF, conducted subsampling by a factor of2. Mathematically it can be written as:

$$y[n] = \sum_{-\infty}^{\infty} h[k].x[2n-k] \qquad (2)$$

➢ DWT analyze the signal at different frequency bands by means of the decomposition of the signal into detail coefficients and approximation coefficients. DWT consists of two sets of functions, namely the scaling function and wavelet function. Decomposition of the signal into different frequency bands obtained by high pass and lowpass filtering. After filtering process, output of each filter is done subsampling by a factor of 2. The output signal for each level of decomposition process can be written mathematically as:

$$y_{high}[k] = \sum_{-\infty}^{\infty} x[n].g[2k-n] \qquad (3)$$

$$y_{low}[k] = \sum_{-\infty}^{\infty} x[n].h[2k-n] \qquad (4)$$

Where $y_{high}[k]$ and $y_{low}[k]$ are the output of the HPF and LPF after subsampling by a factor of 2

➢ The most important properties of the transformation wavelet is the relationship between the impulse response of the HPF and LPF that can be seen from the equation:

$$g[L-1-n] = (-1)^n.h[n] \qquad (5)$$

Where L is the length of the filter

• Inverse Discrete Wavelet Transform (IDWT) [5][10]

IDWT is used to reconstruct process that consists of up sampling and filtering. The procedures of IDWT are:

➢ Each signal level consists of up sampling process by a factor of 2and then passed to the synthesis high pass filter g'[n] and a low pass h' [n] which is summed finally. Up sampling is the restore and combine process of signals with insert in a column of zeros between each column and perform convolution on each line with a filter.

➢ Reconstruction equation can be written:

$$x[n] = \sum_{-\infty}^{\infty}(y_{high}[k].g[2k-n]) + \sum_{-\infty}^{\infty}(y_{high}[k].g[2k-n]) \qquad (6)$$

➢ If the filters are not ideal, the perfect reconstruction cannot be achieved. It is impossible to achieve the ideal filter, but it is possible to find filters that provide perfect reconstruction.That is called Daubechies wavelets which developed by Ingrid Daubechies.

B. OFDM (Orthogonal Frequency Divison Multiplexing)[12]

OFDM is a multicarrier modulation technique using mutually orthogonal frequency .The basic concept of OFDM is to split a high-speed serial data into a low-speed parallel data transmitted by multiple sub-carriers. In OFDM systems, each sub-carrier spacing is set to overlap but do not cause interference between adjacent sub-carriers. OFDM signal generation process can be done at the base band level by using Inverse Discrete Fourier Transform (IDFT) as a modulator and Discrete Fourier Transform (DFT) as a demodulator. OFDM symbol generated from the following equation:

$$s(k) = \frac{1}{N}\sum_{n=0}^{N-1} S(n)e^{j[2\pi nk/N]};0 \le k \le N-1 \qquad (7)$$

where:

N   = Number of IDFT point (sub-carriers total)

S(n) = Symbol of transmitted data on k[th] sub-carriers
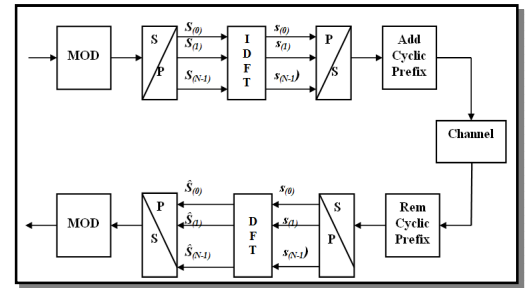
s(k) = Output of IDFT

Fig. 2. OFDM Transceiver system

III.   SYSTEM MODEL

A. OWDM System Model

System model of OWDM consists of the reconstruction process of transmitter that is done with IDWT (Inverse DWT) and while decomposition at the receiver uses DWT. The numbers of sub-bands that used in system model are 4, 8 and 16. OWDM is illustrated in the following blocks [2] [3]:

• IDWT (Inverse Discrete Wavelet Transform)

The results of QPSK encoding are transformed with IDWT from frequency domain to the time domain. Conversion process is performed by using the 2-band wavelet transform. Sub-symbols output of S/P converter at each level is passed to up sampling process with a factor of 2. The sub-symbols of the upper sub-band to the one sub-band before lower sub-band is set as the detail coefficients (Cd) entered into a high pass filter (HPF) while for the lower sub-band symbol is set as an approximation coefficient (Ca) entered into

the low pass filter (LPF). All sub symbols of HPF and LPF output are summed at each level use (6).

- DWT (Discrete Wavelet Transform)

Wavelet modulated signal x [n], which has passed through the channel will have additional noise from the result as y[n]. To get back sub symbols, the transformation process using Discrete Wavelet Transform (DWT) is performed. This signal is obtained by extracting the signal y[n] to approximation coefficients and detail coefficients. Each level of decomposition is done by using (3) and (4).
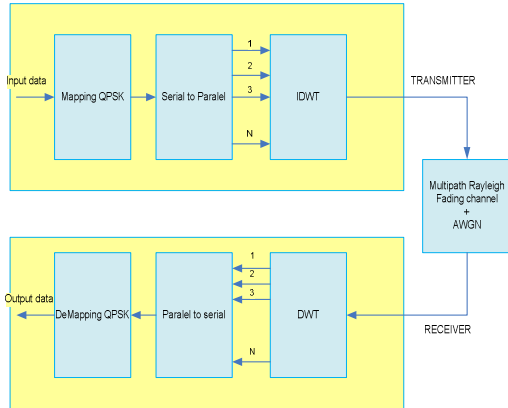

Fig. 3.   OWDM Transceiver system
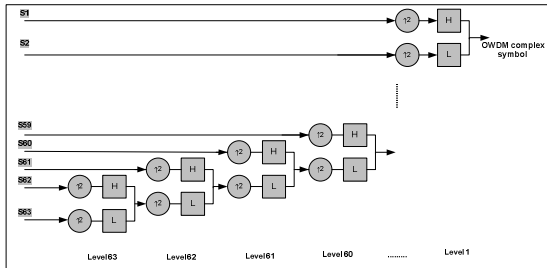

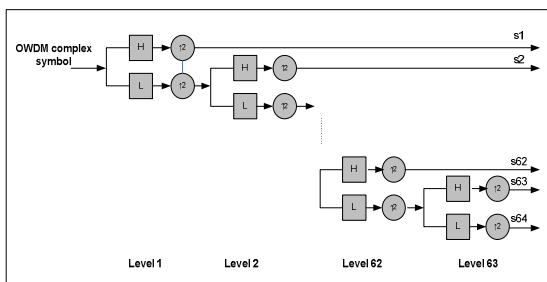Fig. 4.   IDWT (synthesis filter bank) with N level[10]

Fig. 5.   DWT (analysis filter bank) with N level[10]

B. *Simulation Parameter*

- *OWDM and OFDM Parameter*

TABLE I.   PARAMETER OF OWDM AND OFDM SYSTEM

PARAMETER	UNIT and VALUE
Type of Modulation	BPSK, QPSK
Number of *sub-band/sub-carrier* (N)	4, 8, 16
Channel model	AWGN + Multipath Rayleigh Fading
Bandwidth (BW)	2 MHz
Bit rate (R_b)	2 Mbps
Frekuensi *Carrier* (F_c)	2 GHz
Delay spread (σ_τ)	200 ns
User velocity (v)	0,3,75,100 km/jam
Number of bit	262144
Filter Wavelet	db1, db2,db4,db8

- *Channel Parameter*

   a) *Delay Spread and Coherence Bandwidth*

The value of delay spread determine condition of fading channel. It will be flat fading or frequency selective fading. On simulation, value of rms delay spread is 200 ns for suburban area [11]. This value was chosen to reach the characteristics of fading channel in the simulation who want assumed as frequency selective fading . Coherence bandwidth value is 1 Mhz. Because B_s > B_c the transmission channel is frequency selective fading. For OFDM system , the distribution of the signal bandwidth be seen from the following table:

TABLE II.   BANDWIDTH OF EACH SUB-CARRIER OF OFDM SYSTEM

Sequence of Sub-carriers	Bandwidth of sub-carrier (MHz)
4	0.5
8	0.25
16	0.125

It appears that after using multicarrier OFDM technique of each sub -carrier will be felt flat fading. The table shows that for each sub - band bandwidth is smaller than the coherent bandwidth so each sub - band feels flat fading.

For OWDM , Distribution of bandwidth of each signal can be seen from the following table :

TABLE III.   BANDWIDTH OF *OWDM WITH 4 SUB-BANDS*

Sequence of sub-band	Bandwidth of sub-band (MHz)
1	0.25
2	0.25
3	0.5

4	1

From the table it is seen that after use OWDM techniques, each sub - band bandwidth value is smaller than a coherent bandwidth channel . So that each sub - band feels flat fading .

b) *Doppler Spread* and *Coherence Time*

TABLE IV. DOPPLER FREQUENCY VALUE AND COHERENCE TIME

User velocity (km/h)	Doppler Shift	Coherence Time	
0	0 Hz	∞	$(T_c \gg T_s)$
3	5.56 Hz	0.076 s	$(T_c \gg T_s)$
75	138.88 Hz	0.003045 s	$(T_c \gg T_s)$
100	185.185 Hz	0.00228 s	$(T_c \gg T_s)$

Based on calculation results obtained (Tc >> Ts) , so the transmission channel is a slow fading .

IV. SIMULATION RESULT

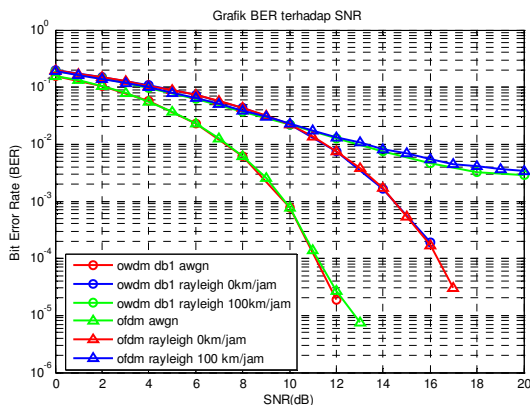*A. Comparative Performance Analysis OWDM and OFDM on AWGN channel and rayleigh Multipath Fading*

Fig. 6. Graph of comparison OWDM and OFDM system on AWGN and Multipath Rayleigh Fading

Fig.6 shows comparisons OWDM system and OFDM in AWGN channel and Multipath Rayleigh Fading, OFDM and OWDM system with 16 sub-band/ sub-carrier. In OWDM system uses *wavelet Daubechies* 1 (db1). Both system provide the same performance. This is because the orthogonality between sub - band / sub - carrier and OFDM systems OWDM same.SNR value for each system can be seen in Table below.

TABLE V. SNR REQUIRED FOR BER 10-3 ON AWGN AND RAYLEIGH FADING CHANNEL

B. Comparison Performance Analysis of OWDM and OFDM with variation of user velocity
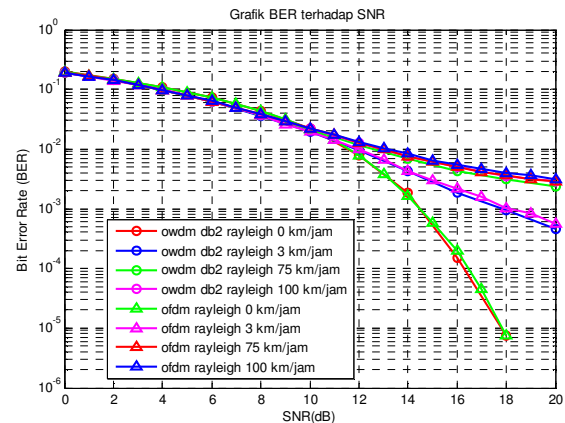
Fig. 7. Graph of comparison OWDM and OFDM system with variation of user velocity

In this simulation used QPSK modulation number of sub-carrier is 16 for OFDM system. OWDM system used daubechies wavelet second order (db2). Figure. describe that the greater the speed of the user make higher Doppler frequency which will affect degrade system performance. OWDM and OFDM system at variation condition user velocity give same performance.

TABLE VI. SNR REQUIRED FOR BER 10-3 WITH VARIATION OF USER VELOCITY

User Velocity	SNR for BER 10⁻³(dB)
OWDM 0 km/h	$\pm$ 14.5
OWDM 3 km/h	$\pm$ 18
OWDM 75 km/h	$\pm$20
OWDM 100 km/h	$\gg \pm$20
OFDM 0 km/h	$\pm$ 14.5
OFDM 3 km/h	$\pm$ 18
OFDM 75 km/h	$\gg \pm$20
OFDM 100 km/h	$\gg \pm$20

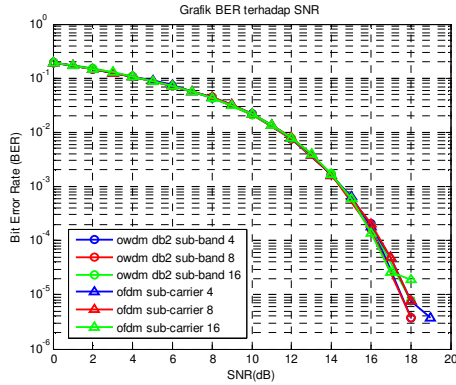## C. Comparison Performance Analysis of OWDM and OFDM with variation of number of sub-band/sub-carrier.

Fig. 8. **C**omparison Graph OWDM and OFDM system in Rayleigh Multipath Fading Channels with variation number of su-band/sub-carrier

In this simulation used QPSK modulation number of sub-carrier is 16 for OFDM system. OWDM system used daubechies wavelet second order (db2). Fig.8 describe that performance of both system is same in this condition. Figure also describe that number of sub-band did not affected performance of system. This is caused by flat fading occurs at each bandwidth sub-band/sub-carrier of OWDM for 4 sub-bands, 8 sub-band and 16 sub-band. Where for every sub-bands have signal bandwidth that more less than coherence bandwidth.

TABLE VII.   SNR REQUIRED FOR BER 10-3 WITH VARIATION OF NUMBER OF SUB-BAND/SUB-CARRIER

Number of Sub-band/sub-carrier	SNR for BER 10^{-3}(dB)
OWDM 4 sub-bands	$\pm$ 14.5
OWDM 8 sub-bands	$\pm$ 14.5
OWDM 16 sub-bands	$\pm$ 14.5
OFDM 4 sub-carriers	$\pm$ 14.5
OFDM 8 sub-carriers	$\pm$ 14.5
OFDM 16 sub-carriers	$\pm$ 14.5

D. Comparison Performance Analysis of OWDM and OFDM with variation of modulation technique.

In this simulation, OWDM and OFDM system uses BPSK and QPSK modulation. OWDM uses wavelet Daubechies second order (db2). The picture shows that the performance OWDM and OFDM system has the same performance for each type of modulation. Additionally seen also for both of system, BPSK modulation types provide better performance compared with QPSK modulation types. This is because the BPSK 1 bit = 1 symbol on the receiver side so that the chances of error is less than QPSK where one symbol = 2 bits . in BPSK modulation space between symbols have more tenuous than other modulation types . So that the current

through the transmission channel that is lossy and occur shifting the phase , the signal with large value of M (number of symbols) will be more cause error. So that, a decrease in power level and phase change is able to 1 changes in the symbol so that the decision circuit will be wrong in decision process accordance point constellation at the transmitter .
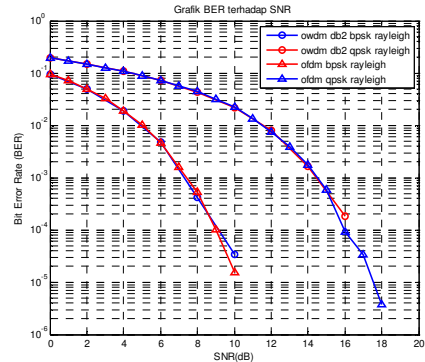
Fig. 9. **C**omparison Graph OWDM and OFDM system in Rayleigh Multipath Fading Channels with variation number of modulation technique

TABLE VIII.   SNR REQUIRED FOR BER 10-3 WITH VARIATION MODULATION TECHNIQUE

Type of Modulation	SNR for BER 10^{-3}(dB)
OWDM with BPSK	$\pm$ 7.5
OWDM with QPSK	$\pm$ 14.8
OFDM with BPSK	$\pm$ 7.6
OFDM with QPSK	$\pm$ 14.8

E. Comparison Performance Analysis of OWDM and OFDM with variation order of Daubechies wavelet for OWDM system.
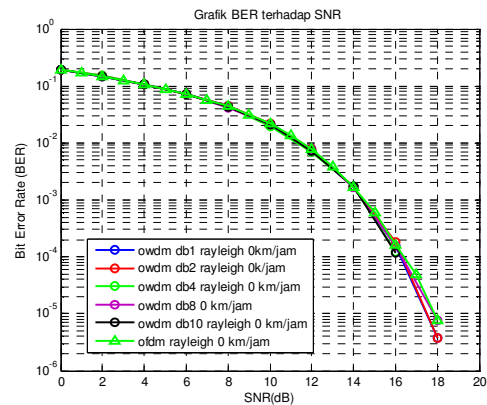

Fig. 10. **C**omparison Graph OWDM and OFDM system in Rayleigh Multipath Fading Channels with variation order of Daubechies wavelet for OWDM system

In Fig.10 ,simulation performed on QPSK modulation , number of sub - band / sub – carrier is 16. It shows that

OFDM and OWDM system performance resulted the same performance . Where the order does not affect the Daubechies wavelet to system performance OWDM .

TABLE IX. SNR REQUIRED FOR BER 10-3 WITH VARIATION ORDER OF DAUBECHIES WAVELET FOR OWDM SYSTEM

Wavelet daubechies order	SNR for BER 10^{-3}(dB)
OWDM with db1	$\pm$ 14.5
OWDM with db2	$\pm$ 14.5
OWDM with db4	$\pm$ 14.5
OWDM with db8	$\pm$ 14.5

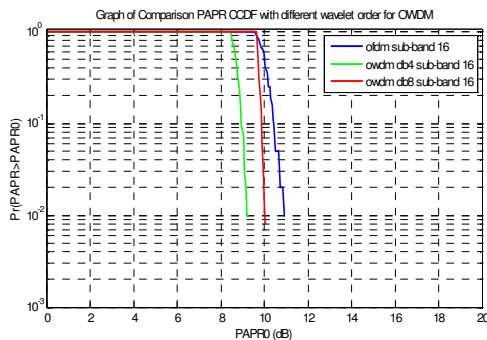*F. Comparison PAPR of OWDM and OFDM system.*

Fig. 11. Comparison PAPR CCDF Graph of OWDM and OFDM System

TABLE X. VALUE OF $PAPR_0$, PR (PAPR>PAPR0) = 10^{-2} FOR OWDM AND OFDM SYSTEM

Type of Modulation	$Pr(PAPR>PAPR_0)$	$PAPR_0$(dB)
OWDM db4	10^{-2}	9.35
OWDM db8	10^{-2}	10
OFDM	10^{-2}	10.8

Each sub-band of OWDM in this simulation used Daubechies filter 4th order (db4) and Daubechies filter 8th order (db8) with 16 sub-band. While OFDM system use QPSK mapping and 16 sub-carrier. Fig 11 describes that OWDM system give reduction of PAPR value about ± 1.45 dB for OWDM with db4 and ± 0.8 dB for OWDM with db8.

The PAPR value of OWDM system is smaller than OFDM system. In OFDM system, IFFT process produces signal that has variation of power. This condition causes PAPR value will be enlarged. The power variation caused by modulating each sub-carrier is performed by different frequencies so that if output signal of multiple sub-carrier has a phase coherent amplitude, it will appear with a much greater level of average power. In contrast to OWDM, because each sub-bands of each level IDWT has 2 different frequency bands where the scale and the shift have been set before, from the 1st sub-bands to-Nth sub-band, so that when signal with phase coherence from

each sub-band is summed, it does not cause high value of PAPR. Thus OWDM techniques can be chosen as an alternative method to overcome the problems of the high PAPR value in OFDM techniques.

V. CONCLUSION

1. Simulation of OFDM and OWDM system resulted the same performance . In the AWGN channel for both system, BER 10^{-3} For SNR required ± 9.8 dB . While the multipath rayleigh fading channel with user velocity 0 km / h required SNR of ± 14.6 dB.

2. The result show that a greater number of sub-bands result in a higher PAPR value for OWDM and OFDM system. This allows the growing number of sub-bands which means that the probability summation of coherent symbols is also getting bigger.

3. Simulation of (PAPR) in OWDM and OFDM system shows that PAPR of OWDM is smaller than OFDM system about ± 1.45 dB for OWDM with db4 and ± 0.8 dB for OWDM with db8.

4. OWDM techniques can be chosen as an alternative method to overcome the problems of the high PAPR value in OFDM techniques.

REFERENCES

[1] "Communication System Using Orthogonal Wavelet Division Multiplexing (OWDM) and OWDM-Spread Spectrum(OWSS) Signaling". US patent Issued on June 6 2006.

[2] Hassen, S.Fadel., "The Performance of Orthogonal wavelet Division Multiplexing (OWDM) in Flat Rayleigh Fading Channel". Journal of Engineering and Development, Vol .12, No.1, March 2008.

[3] Nerma, Mohamed,H.M., Kamel, Nidal.S and Jeoti, Varun, "An OFDM System Based on Dual Tree Complex Wavelet Transform (DT-CWT)". Signal Processing: An International Journal (SPIJ), Volume(3) : Issue(2).

[4] Silanders, Anders., " On Wavelet for Digital Communication". Thesis for The Degree of Licentiate of Philosophy. Sweden. 1999.

[5] Polikar, R. "The Wavelet Tutorial". Department of Electrical and Computer Engineering, Rowan University. 1995.

[6] Ahmed, Nadeem.,"Joint Detection Strategies for Ortoghonal Division Multiplexing". Thesis Master of Science. Texas. April 2000.

[7] Ramchandran, Kannan., Vetterli, Martin., Fellow., IEEE and Herley,Cormac., "Wavelet, Subband Coding and Best Bases". Proceeding of The IEEE, Vol.84.no.4, April 1996.

[8] Jamin, Antony., Mahonen, Petri., "Wavelet Packet Modulation for Wireless Communication". Publshed in Wireless communication & Mobile Computing Journal, March 2005, Vol.5, Issue 2.

[9] Strang, Gilbert., Nguyen, Truong., "Wavelet and Filter banks". Wellesley. Cambridge Press.

[10] Burrus, C. Sidney.,Gopinath, Ramesh A and Guo, Haitao.,"Introduction to Wavelet and Wavelet Transform A Primer". Prentice-Hall, Inc.1998.

[11] Rappaport,Theodore.S.,"Wireless Communications Principle and Practice".

[12] Prasetya, Budi., "Performance of MIMO-OFDM system with Beamforming over Rayleigh channel". Thesis, STEI ITB. Bandung. 2006.

[13] Akansu, Ali.N., "Orthogonal Transmultiflexer in Communication : A Review". IEEE Transaction on Signal Processing, Vol.46,no.4, April 1998.

[14] Lawrey, E. Phillip, "Adaptive Techniques for Multiuser OFDM", Electrical and Computer Engineering School of Engineering, James Cook University, 2001.

[15] The MathWorks, "Image Processing Toolbox User's Guide", 2008.

[16] Karina, Adela., "Simulation and Analisys of Power Loading Effect to PAPR OFDM system". Final Project Jurusan teknik Elektro Sekolah Tinggi Teknologi Telkom. Bandung. 2007.

[17] Li Lin, Yu, "Performance Analysis in the PAPR of OFDM Systemvia SLM Scheme", Department of Electrical Engineering, National Cheng Kung University. Taiwan. 2003.

On Comparison of Multigrid Cycles for Poisson Solver in Polar Plane Coordinates

Nurhayati Masthurah, Iftitahu Ni'mah, Furqon Hensan Muttaqien, Rifki Sadikin
Research Centre for Informatics - Indonesian Institute of Sciences, Indonesia
Email: masthurah@informatika.lipi.go.id, iftitahu.nimah@lipi.go.id, furq001@lipi.go.id, rifki.sadikin@lipi.go.id

Abstract—**Fast Multigrid Poisson solvers have been considered essential for developing efficient numerical method solutions in diverse fields. In this paper, we compare fast and simple multigrid methods: V-Cycle, W-Cycle, and F-Cycle to solve Poisson Equation (PE) in polar plane coordinates. The solver is analysed toward different $2^n + 1$ grid sizes to evaluate its convergence properties, i.e. precision and accuracy, as compared to reference problem of cylindrical annulus. Each multigrid cycle is evaluated based on computation time, convergence error, and relative error. The results show that W-Cycle ($\gamma = 4$) gives more optimized solution as Poisson solver in comparison with the other multigrid methods.**

Index Terms—**Multigrid cycles, poisson solver, polar coordinates**

I. INTRODUCTION

Several works are motivated by the need for applying fast PE solver, including research in plasma physics and engineering [1], [2], computational fluid dynamics [3], galactic dynamics [4], electromagnetism [5], and computer vision [6]. In the telecommunication field, multi-purpose Poisson solvers are used for numerous applications and technological innovations, such as for investigating Resonant Tunnelling Diodes (RTDs) [7]–[9]. The RTD has been increasingly studied over the years due to its basic characteristic as a primary nanoelectronic device for analog and digital applications. Aforementioned works in Quantum modelling of RTDs involving space charge effects simulation by PE, for instance, provide useful insights for building desirable devices with fast switching operation.

As versatile approaches of computational problems, multigrid methods have been applied to improve PE solvers in diverse domains. The specific use of multigrid methods in boundary value problems and its discretization is to solve PE in square domain and other boundary conditions (i.e. Dirichlet, Neumann, mixed, and periodic) [10]. Early study in this field [11] works on improving the performance of Multigrid Poisson solver. Analysing Full-Multigrid (FMG) on 2D PE with Dirichlet boundary condition, the authors [11] highlight several problems for building Multigrid Poisson solver: (1) the performance dependency upon vector lengths (i.e. different grid sizes); (2) Computational cost on finer and coarser grids, which is related to the presence of data-motion operations in interpolations and residual calculation stage.

More recent study on 3D Poisson solver for space charge simulation in cylindrical coordinates [12] compares the Cartesian and Cylindrical Poisson solvers to simulate the beam dynamics. The authors [12] emphasize the low accuracy of Cartesian coordinate system in large transverse of beam size due to different boundary condition used, as compared to solver in cylindrical coordinate for the same problem domain. Concerning the slow convergence and computational bottlenecks, the advantages of multigrid algorithm are then used in particle accelerator [13] to boost up the calculation of space-charge effects.

Following these findings, our study focuses on the comparison of different multigrid cycles for solving PE in a 2D vertical slice of cylindrical region. The classical Gauss-Seidel and Jacobi relaxation methods are used as smoothing iterations of multigrid V-cycle, W-cycle, and F-cycle. The evaluation covers computation time (i.e. CPU and wall time) for running different cycles on different grid sizes, convergence error, and relative error metrics. The relative error observes discrepancies between analytical (i.e. exact solution of chosen reference problem) and numerical solutions (i.e. the approximation result of the solver) as an indication of how good the approximation relative to the true value. Whereas, the convergence measures how fast the solvers converge to the solution.

This paper is organized on several sections as follows. Section 2 summarizes preliminary studies on Poisson solver in polar plane coordinates and multigrid cycles. Section 3 explains the numerical derivation and implementation of Multigrid Poisson equation solver in this study, including a brief explanation about multigrid V-cycle, W-cycle, and F-cycle. Section 4 presents analysis and comparison results. Finally, section 5 concludes the paper.

II. RELATED STUDY

Preliminary study on numerical analysis of boundary value discretization [14] points out the efficiency of multigrid approaches as they solve finite-difference equation by taking advantages of finer-coarser grids interactions. As the authors [14] also state, this efficiency is independent from different types of boundary and robust enough toward the choice of parameters.

With regard to the geometrical coordinate system, a study on Poisson solver in polar and cylindrical coordinates [15] presents a spectral collocation method to overcome pole coordinate singularity problem when transforming Polar to Cartesian domain. We adopt the authors' idea in combining radius (r) and length (z) directions, along with the simplification of PE calculations by Eigen-value and the use of exact solution of PE reference problem [16], [17] in evaluation stage.

On comparison of different multigrid cycles (i.e. V-cycle, W-cycle, F-cycle), an exhaustive study on multigrid methods and applications [18] assesses the numerical efficiency of multigrid solvers by observing their convergence behaviours and the computational work per iteration step (cycle), resulting: (1) the convergence speed and numerical efficiency of the algorithm are influenced by the number of relaxations, i.e. pre- and post-smoothing steps, and the cycle type; (2) the convergence of multigrid is independent of the size of the finest grid; (3) the choice of restriction matrix, i.e. either *full weighting (FW)* or *half weighting (HW)*, can affect the convergence speed and costs. As such, processing the coarse grid level and applying sufficient smoothing steps more frequently can result in a better convergence. For instance, F-cycle and W-cycle with pre- and post-smoothing converge better than V-cycle with similar smoothing. Based on these theoretical and numerical results, we design our multigrid experiment.

III. MULTIGRID POISSON SOLVER

A. Multigrid Components and Procedures

Multigrid solvers generally consist of 4 main components: (1) choice of coarse grids; (2) choice of coarse grid operators; (3) restriction matrix; (4) interpolation matrix. Utilizing these components, the multigrid methods have to approximate problems on fine grid by a coarser grid and solve the corresponding coarse grid's problems. Then, the methods need to interpolate coarse grid solution onto the fine grid and recursively solve coarse grid problem [18].

As such, two major issues of multigrid algorithm are the smoothing and coarse grid error corrections. The smoothing properties consist of relaxation methods, namely Gauss-Seidel and the Jacobi-Type Iterations. Whilst, the concept of coarse grid correction is based on the formula $A^h u^h = f^h$ on (Ω_h) [19]. Coarse grid correction scheme $v^h \leftarrow CG(v^h, f^h, \alpha_1, \alpha_2)$ is illustrated in Fig. 1, as follows: (1) Relax α_1 times on $A_h u_h = f_h$ on (Ω_h) with arbitrary initial guess v^h; (2) Compute $r^h = f^h - A^h v^h$; (3) Compute $r^{2h} = I_h^{2h} r^h$; (4) Solve $A^{2h} e^{2h} = r^{2h}$ on Ω^{2h}; (5) Correct fine grid solution $v_h \leftarrow v_h + I_{2h}^h e^{2h}$; (6) Relax α_2 times on $A_h u_h = f_h$ with initial guess v^h.

Fine grid

Relax on $A^h u^h = f^h$
Compute $r^h = f^h - A^h u^h$
Correct $u^h \leftarrow u^h + e^h$

Restrict $r^{2h} = I_h^{2h} r^h$
Interpolate $e^h \approx I_{2h}^h e^{2h}$

Solve $A^{2h} e^{2h} = r^{2h}$ $e^{2h} = (A^{2h})^{-1} r^{2h}$
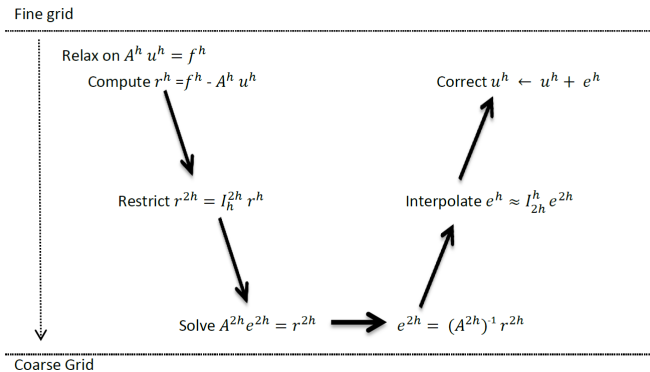
Coarse Grid

Fig. 1: Coarse Grid Correction Scheme

B. Multigrid Cycles

Multigrid methods are basically the recursive use of two-grids method that combines a simple iterative method and coarse grid correction. One iteration of a multigrid method from the finest grid to the coarser grid and back to the finest grid again is called a *cycle*. The number of cycles is represented by γ. When $\gamma = 1$, the multigrid is called V-cycle. $\gamma = 2$ results in W-cycle. $\gamma > 2$ forms the concatenated multigrid between V-cycle and W-cycle, which is called F-cycle. Fig. 2 illustrates the structure of these multigrid cycles.
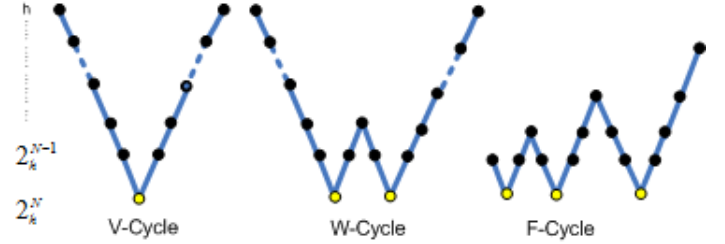

Fig. 2: The structures of Multigrid Cycles used in this study, from finer-to-coarser grid depth, and vice versa

1) V-Cycle: Coarse grid correction solve coarse grid system, the resulting recursive algorithmic scheme is called a multigrid V-Cycle. The algorithm of V-Cycle is given in Algorithm 1.

Algorithm 1 V-Cycle Algorithm

1: perform smoothing on the fine level system $\Rightarrow$ solution α_1
2: compute the residual $r^h = f^h - A^h v^h$
3: perform restriction of $r^{2h} = I_h^{2h} r^h$ to the coarse grid Ω^{2h}
4: solve coarse grid system $A^{2h} e^{2h} = r^{2h}$ by recursive call to the V-cycle algorithm
5: interpolate the coarse grid solution e^{2h} to the grid Ω^h
6: add the resulting correction to v^h
7: perform post-smoothing on the fine grid (if necessary)

---

2) W-Cycle: Cycles that perform two or more coarse grid correction steps.

3) F-Cycle: Perform more multigrid cycles scheme on the next coarser grid, interpolate initial guess to the current grid and perform V-cycle to improve the solution. The algorithm of F-Cycle is given in Algorithm 2.

Algorithm 2 F-Cycle Algorithm

1: Initialize $f^h, f^{2h}, f^{4h}, ..., f^H$
2: Solve a coarsest grid $e^H = (A^H)^{-1} f^H$
3: Interpolate initial guess v^{2h}
4: Perform V-Cycle v^{2h}
5: Interpolate initial guess v^h
6: Perform V-Cycle v^h

C. Numerical Calculations and Experimental Design

In this study, the solver is applied to PE for cylindrical domain, i.e. a vertical slice of cylindrical region as shown in Fig. 3. The numerical methods of Multigrid Poisson solver are implemented in GNU C++ and ROOT system, an object oriented framework for large scale data analysis [20]. The specification of computing environment is i7-4500U CPU with 8 cores and 4GB RAM. We use $2^n + 1$ grid sizes ($0 < n < 11$) to analyse the performance of each multigrid cycle. The parameters under observation are relative error, convergence, and computational time.
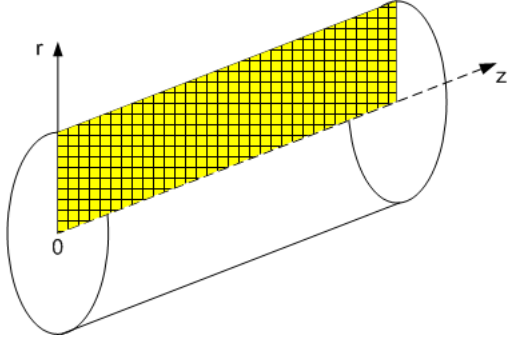

Fig. 3: Polar Plane Coordinates illustrated in yellow shading

The 2D PE in this polar coordinates can be written as

$$\nabla^2 \Phi(r, z) = \rho(r, z) \tag{1}$$

$$\frac{\partial^2 \Phi}{\partial r^2} + \frac{1}{r} \frac{\partial \Phi}{\partial r} + \frac{\partial^2 \Phi}{\partial z^2} = \rho(r, z) \tag{2}$$

where Eq. 1 shows the original PE solver with radius r as height and z as length of a polar plane region. To evaluate this Poisson solver, we adopt an available reference problem for cylindrical annulus [16], [17], as follows.

$$
\begin{aligned}
\Phi_{exact}(r, z) &= [r^4 - (r_0 + r_1)r^3 + r_0 r_1 r^2]e^{-bz^2}, \\
&\quad z \in [-1, 1] \quad r \in [r_0, r_1] \\
&\quad r_0 = 0.0 \\
&\quad r_1 = 1.0
\end{aligned} \tag{3}
$$

$$
\begin{aligned}
\rho(r, z) &= (16r^2 - 9(r_0 + r_1)r + 4(r_0 r_1))e^{-bz^2} + \\
&\quad (r^4 - (r_0 + r_1)r^3 + r_0 r_1 r^2)(4b^2 z^2 - 2b)e^{-bz^2}
\end{aligned} \tag{4}
$$

Then, we use Eq. 5 to compute relative error ($e_{relative}$) between numerical and exact solutions, as follows.

$$e_{relative} = \left\| \frac{\Phi_{num} - \Phi_{exact}}{max(\Phi_{exact})} \right\| \tag{5}$$

Whilst, in order to compute the convergence error (e_{conv}), we use Eq. 6.

$$
\begin{aligned}
e_{conv} &= \| \Phi_{num,i} - \Phi_{num,i-1} \| \\
&\quad i > 0, \text{ where } i = \text{iterative step}
\end{aligned} \tag{6}
$$

IV. ANALYSIS

Figure 4 shows $e_{relative}$ of different multigrid cycles in log domain. Both V-cycle and W-cycle have the same $e_{relative}$ values at around 10^6 in the beginning of the iteration. In contrast, F-cycle has much lower error value at 10^{-2}. This large difference indicates the initial guest of F-cycle is already fit and the numerical assumption is satisfied before the first iteration.
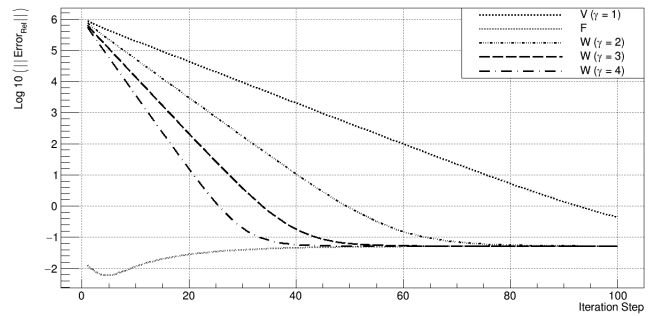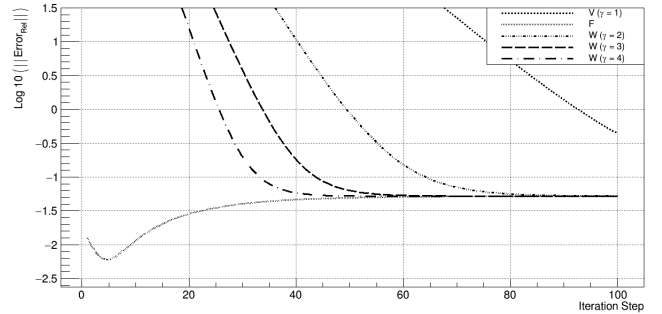

Fig. 4: Relative Error for Each Multigrid Cycle Type

Fig. 5: Relative Error for Each Cycle Multigrid Type after 20 Iteration Steps

However, while in the beginning F-cycle has the lowest $e_{relative}$, the error value increases gradually after approximately 10 iteration steps. This increasing behaviour, i.e. a case when the numerical operations on each step add more error to the result, needs further investigation with regard to the construction of the most optimum multigrid F-cycle. In addition, the result also shows that the higher γ value, the faster its relative error value to converge and become stable, as shown in Figure 5. The relative error of W-cycle ($\gamma = 4$)

converges after 40 iteration steps at $10^{-1.5}$, which is the same number of iteration step needed by F-cycle to produce convergent relative error.
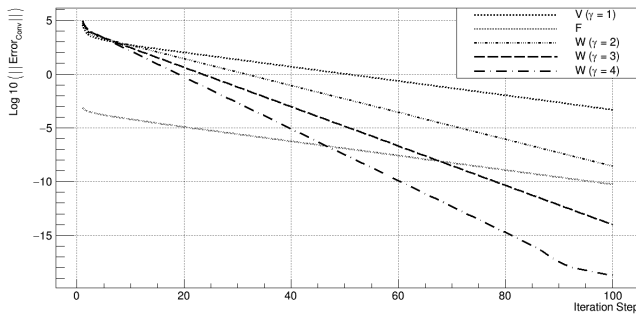

Fig. 6: Convergence Error for Each Multigrid Cycle Type

Another parameter used to evaluate the type of multigrid cycle is the convergence error as described in Figure 6. Overall, all cycle types needs more than 100 iteration steps to converge to the solution. The line graph shows that W-cycle ($\gamma = 4$) is the fastest multigrid method, which converges after 90 iteration steps. While theoretically F-cycle has properties to be the most efficient multigrid solver in term of convergence speed and computational cost, in this experiment the method is outperformed by W-cycle ($\gamma = 4$) after 40 iterations. With regard to the number of cycles (γ) in our multigrid experiment, the increase of γ value affects the convergence speed of the multigrid cycles. Corresponding to this convergence speed, W-cycle ($\gamma = 4$) generally shows a superior performance in term of CPU execution time (Figure 7), i.e. by slow exponential time growth as compared to the other multigrid cycles. This speed performance of W-cycle ($\gamma = 4$) also outperforms F-cycle for more complex grid, i.e. above $1024x1024$ grid size.
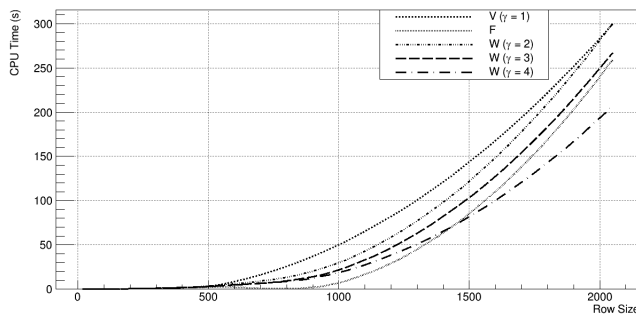

Fig. 7: CPU Time of Multigrid cycles

V. CONCLUSION

Based on three parameters used to analyse each multigrid cycle, the experimental results suggest that the bigger number of cycle in multigrid method, which is represented by γ, the faster its relative error to converge. The γ value also affect

the convergence parameters in the same way as it affects the relative error metrics. To sum up, W-cycle ($\gamma = 4$) gives more optimized solution as Multigrid Poisson solver especially in more complicated grids. Further numerical study is needed for investigating the performance of W-cycle ($\gamma = 4$) and F-cycle toward the choice of multigrid components and structures, specifically the evaluation of F-cycle with and without restriction to the coarsest grid.

REFERENCES

[1] Charles K Birdsall and A Bruce Langdon. *Plasma physics via computer simulation*. CRC Press, 2004.
[2] JR Roth. *Industrial Plasma Engineering Volume 1 Principles. Bristol and Philadelphia*. 1995.
[3] M Yousuff Hussaini and Thomas A Zang. "Spectral methods in fluid dynamics". In: *Annual review of fluid mechanics* 19.1 (1987), pp. 339–367.
[4] James Binney and Scott Tremaine. *Galactic dynamics*. Princeton university press, 2011.
[5] T Bui, M Read, and L Ives. "Temporal particle-in-cell in Beam Optics Analyzer". In: *Plasma Science (ICOPS), 2011 Abstracts IEEE International Conference on*. IEEE. 2011, pp. 1–1.
[6] Atul K Chhabra, Timothy Grogan, et al. "On Poisson solvers and semi-direct methods for computing area based optical flow". In: *Pattern Analysis and Machine Intelligence, IEEE Transactions on* 16.11 (1994), pp. 1133–1138.
[7] Markus Karner, Andreas Gehring, Stefan Holzer, et al. "A multi-purpose Schrödinger-Poisson solver for TCAD applications". In: *Journal of Computational Electronics* 6.1-3 (2007), pp. 179–182.
[8] L Shifren, C Ringhofer, and DK Ferry. "A Wigner function-based quantum ensemble Monte Carlo study of a resonant tunneling diode". In: *Electron Devices, IEEE Transactions on* 50.3 (2003), pp. 769–773.
[9] Qingmin Liu, Alan Seabaugh, Prem Chahal, et al. "Unified AC model for the resonant tunneling diode". In: *Electron Devices, IEEE Transactions on* 51.5 (2004), pp. 653–657.
[10] W. Hackbusch. *Multi-grid methods and applications*. Vol. 4. Springer Science & Business Media, 2013.
[11] D. Barkai and A Brandt. "Vectorized multigrid Poisson solver for the CDC Cyber 205". In: *Applied Mathematics and Computation* 13.3 (1983), pp. 215–227.
[12] Jin Xu, Peter N Ostroumov, and Jerry Nolen. "A parallel 3D Poisson solver for space charge simulation in cylindrical coordinates". In: *Computer Physics Communications* 178.4 (2008), pp. 290–300.
[13] Gisela Pöplau, Ursula Van Rienen, Bas Van der Geer, et al. "Multigrid algorithms for the fast calculation of space-charge effects in accelerator design". In: *Magnetics, IEEE Transactions on* 40.2 (2004), pp. 714–717.
[14] Achi Brandt. "Multi-level adaptive solutions to boundary-value problems". In: *Mathematics of computation* 31.138 (1977), pp. 333–390.

[15] Heli Chen, Yuhong Su, and Bernie D Shizgal. "A direct spectral collocation Poisson solver in polar and cylindrical coordinates". In: *Journal of Computational Physics* 160.2 (2000), pp. 453–469.

[16] Ivar Christopher, George Knorr, Magdi Shoucri, et al. "Solution of the Poisson Equation in an Annulus". In: *Journal of Computational Physics* 131.2 (1997), pp. 323–326.

[17] Henner Eisen, Wilhelm Heinrichs, and Kristian Witsch. "Spectral collocation methods and polar coordinate sin-gularities". In: *Journal of Computational Physics* 96.2 (1991), pp. 241–257.

[18] Ulrich Trottenberg, Cornelius W Oosterlee, and Anton Schuller. "Multigrid". In: (2000).

[19] William L Briggs, Steve F McCormick, et al. *A multi-grid tutorial*. Siam, 2000.

[20] Rene Brun and Fons Rademakers. "ROOT - An object oriented data analysis framework". In: *Nuclear Instruments and Methods in Physics Research* 389.1-2 (1997), pp. 81–86.

Efficient Implementation of EC based Key Management Scheme on FPGA for WSN

Priya Mathew, Jilna P., Deepthi P. P

Department of Electronics and Communication Engineering
National Institute of Technology Calicut, India
E-mail: priyamathew.kpm@gmail.com

Abstract—Communication driven era demands the use of new cryptographic protocols and hardware with reduced computational and structural complexity for resource constrained applications. This paper presents the hardware implementation of a key management scheme based on Elliptic Curve Cryptography (ECC) for applications in wireless sensor networks. Security-critical applications in WSNs rely on ECC for the key management since it offers increased security per bit of the key. This paper proposes efficient hardware architecture for the implementation of EC based key exchange in such a way that number of pre-stored values for key exchange and overall hardware complexity of the system are optimised without affecting security level. Algorithms for pseudo random sequence generation and message authentication code based on cryptographic one way function of elliptic curve point multiplication are developed. A single point multiplication unit based on Lopez-Dahab algorithm is time shared for pseudo random sequence generation and authentication to reduce the overall hardware complexity. Thus the proposed implementation scheme supports increased number of node addition phases. Evaluation of the design is done in terms of storage and hardware complexity. Proposed system gives 23.76% hardware efficiency over the existing EC based system. The design for $GF(2^{163})$ has been simulated in ModelSim PE 10.4, synthesized in Xilinx ISE 14.7 and successfully implemented on Kintex-7 KC705 Evaluation Board.

Keywords—*Elliptic Curve Cryptography; MAC; PRSG; wireless sensor network; key exchange; FPGA; VHDL*

I. INTRODUCTION

Wireless sensor networks (WSNs) are easily attacked compared to wired networks due to their wireless and dynamic nature. Hence there is a great need that data being transferred from node to node must be secured properly. A main challenge of large scale sensor networks is the employment of a practical and robust security mechanism to mitigate the security risks on the resource constrained sensor devices [1].

While symmetric key cryptography offers low complexity solutions for data confidentiality, it has a much complicated key exchange as compared to public key cryptosystem [2]. Hence present day energy efficient secure systems are hybrid in the sense that they depend upon public key schemes for key exchange and private key schemes for data confidentiality. In public key cryptography, ECC is one of the domain where intensive researches are being carried out. For a properly chosen elliptic curve, no known sub-exponential algorithm can be used to break the system through the solution of the discrete logarithm problem (DLP). Significantly smaller parameters can be used in ECC than in other competitive system such as

RSA with equivalent levels of security. Since the use of smaller key size helps to reduce processing power and bandwidth, it is used in wireless sensor networks for secure key management especially in health care applications where the data is private and critical.

Many light-weight key distribution schemes are proposed in the literature for WSN and are evaluated based on suitable metrics namely Security metric, Efficiency metric and Flexibility metric [3]. Majority of the key distribution schemes are based on key pre-deployment. One method in the key pre-deployment approach is the use of network-wide keys or global keys. A single master key is loaded in all sensor nodes in this scheme. But under security metric this scheme is worst since the compromise of any one node reveals the secret key of the entire network. In full pair wise key (FPWK) scheme, each node receives (n-1) pair wise keys to communicate with every other node in the network of n nodes. But FPWK lack scalability due to the fact that storage requirement increases drastically with increase in network size. In key derivation information pre-deployment, the amount of pre-distributed information is reduced. Here each pair of neighbouring sensor nodes after deployment computes a shared secret key using the key derivation information.

Many proposals for EC based authentication and data aggregation are available [1], [5], [6]. The effect of a compromised node in a network is negligible for EC based approaches compared to other schemes. But the major disadvantage of existing EC based schemes is that of increased storage requirement which imposes a great restriction on the number of links that can be formed. In this work, an efficient hardware architecture for the implementation of EC asymmetric key exchange protocol narrated in [6] is proposed. Required modifications are incorporated into the algorithm to optimize the storage requirement and there by facilitating more node additions.

The rest of the paper is organized as follows: Section II briefs the related works. Section III presents the proposed key establishment scheme for secure communication system. The FSM (finite state machine) and hardware architectures are described in section IV. Implementation details are specified in section V. In section VI results are summarized and conclusion is drawn in section VII.

II. RELATED WORKS

ECC based cryptography is an emerging field and many efforts have been made on implementation of key management

systems. A survey on the key management schemes available for WSN is discussed in [3]. This section summarizes some of the state-of-the-art protocols highlighting their benefits and drawbacks. MAKM, EG, LEAP+ and RSDTMK schemes were discussed in [4], [7], [8], [9]. In LEAP+ [8], a master key is employed to generate the secret pair wise keys. Once the master key (MK) is compromised, then the whole network is compromised. There is trade-off between security and connectivity of the network based on the time-out period. In random key pre-distribution and transitory MK based schemes [8], [9] security is dependent on the secrecy of the keying material and the invertibility of pseudo random function. If a node is compromised in the initialization phase, a major part of the network is compromised. The schemes based on hard mathematical problems offers high security even if nodes are compromised in the initialization phase but with increased storage requirement and hardware complexity. For the key establishment scheme in [5], a unique seed key and a pre-computed key pool are stored as pre-distributed values. The scheme is not efficient in terms of memory usage.

In [6] authors have presented two protocols for key establishment in WSN based on EC cryptography. The first scheme is the hybrid (EC-H) that combines both symmetric and asymmetric key techniques. The pre-loaded secret material consists of a private key, an implicit certificate and the symmetric keys for mutual authentication. The second method in [6] is purely asymmetric (EC-A). Here multiple independent EC key pairs which consist of a private key and an implicit certificate are pre-loaded into each sensor. In both schemes, pair wise secret key is generated by executing a key derivation function with EC point and the random nonces as inputs. As the number of pre-loaded keys are more, the storage requirement is high and the scheme can support only limited number of node addition phases. A comparison study shows that the computational cost of this method is much less compared to other EC based methods in the literature. Also, the resilience provided by the key exchange method in [6] is very high when compared with other light weight schemes (Random key pre-distribution, LEAP etc.). Hence the key exchange method in [6] is used for implementation in this proposal. This work attempts to develop a simple hardware structure for key management technique by mitigating the storage requirement and hardware complexity of original scheme without affecting the security.

III. PROPOSED KEY ESTABLISHMENT SYSTEM

This paper proposes FPGA implementation of a modified version of key management system based on asymmetric protocol (EC-A) specified in [6]. The main drawbacks of the EC-A algorithm are its high storage requirement and the limitation in the number of node addition phases it can support. In the proposed scheme the number of pre-stored values is minimized without affecting the security thus reducing the storage requirement at the node. A hardware efficient secure PRSG based on EC [10] is used to provide various random numbers used in key exchange to effect the reduction in storage requirement. Also, an efficient non-iterative EC

based MAC is used as the authentication function as well as the key derivation function. This avoids the need for other standalone functions like SHA and AES for authentication and key derivation in original scheme. Moreover, this MAC and PRSG are designed by time-sharing the ECPM unit used for key exchange. Thus the hardware complexity is reduced much through reuse of hardware modules.

For implementations in $GF(2^{163})$, the values to be stored in EC-A algorithm [6] during pre-deployment are point P (40 bytes), Network wide Symmetric key K (20 bytes), Implicit certificate of the node IC_x (44 bytes), Public key of Certification Authority (40 bytes) and Secret EC key of the node q_x (20 bytes). Also the scheme demands that each node should store EC key (20 bytes) and Implicit Certificate (44 bytes) for any new node added in the node addition phase. Thus the total storage requirement is 164 + 64 N bytes for implementation in $GF(2^{163})$ where N is the number of node addition phases. As can be seen, this storage requirement puts a great limitation on the number of node addition phases that can be supported in a network where nodes are constrained in resources. In order to overcome these drawbacks of EC-A algorithm, the proposed system limits the stored values to point P (40 bytes), network wide symmetric key K (20 bytes), secret key of certification authority q_{CA} (20 bytes) and makes use of a PRSG to generate other random numbers. The PRSG is chosen in such a way that it reuses the resources already available and doesnt add much to the structural complexity of the system.

Also, original version of EC-A uses SHA-1 as key derivation function (kdf) and for hashing while AES is used to provide authentication. Usage of these independent stand alone units cause increase in structural complexity of the system. Hence this work makes use of a non-iterative EC based MAC for hashing, authentication and key derivation. This MAC is chosen because the hardware complexity of this scheme is very low. It needs only a few shift registers in addition to EC point multiplication unit. Since operations of random number generation, authentication and key derivation are done sequentially, the hardware design is efficiently developed in the proposed work in such a way that a single EC point multiplication unit is time shared. Thus the proposed design optimizes the hardware design by removing redundancy in various phases.

Communication flow and algorithms involved in the modified version of basic EC-Asymmetric algorithm [6] implemented in this work are detailed below:

A. Proposed Key Establishment Scheme

WSN is assumed to be static and homogeneous with all sensor nodes having the same memory, computational power, except the sink node. Proposed key establishment scheme is the modified version of EC-A symmetric algorithm specified in [6]. Here the pre-deployed values are changed in order to minimize the storage. Point P, network wide symmetric key K and secret key of certification authority q_{CA} are loaded into the sensor nodes prior to deployment. Elliptic curve based MAC unit is used as the hash function and kdf function and

thus the MAC unit is effectively utilized. Various stages in key establishment between two nodes is described in Fig 1.
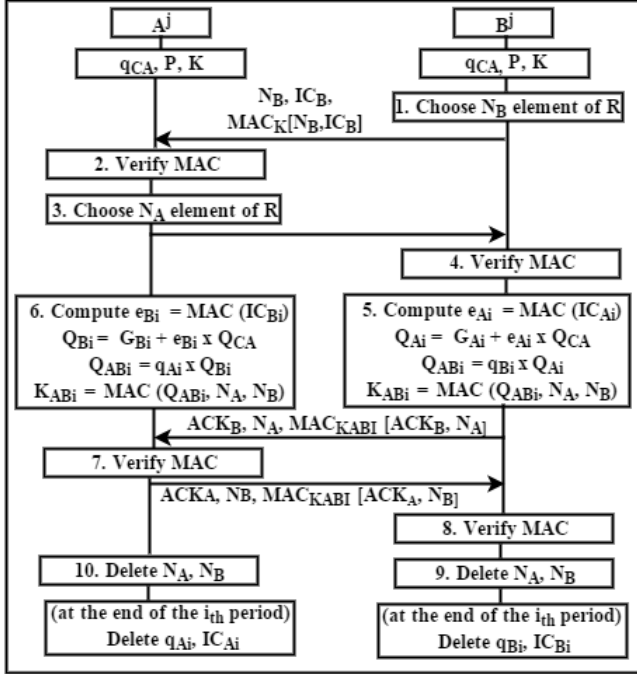

Fig. 1: Key Establishment Process

The steps in key establishment are detailed below:

- Pre-Deployment Phase
  Step 1 : Pre-deploy each node with the values point P, network wide symmetric key K and secret key of certification authority q_{CA}.

- Initialization Phase
  Step 2 : Node B initiates the link establishment by broadcasting a random nonce N_B and the implicit certificate IC_B along with the MAC of the above for initial authentication. IC_B is computed as follows: Take a random value g_B element of $GF(2^{163})$. Compute $G_B = g_B \times P$ and then IC_B is $\{G_B, M\}$ with $M = (i, ID_x, t_x)$ where i is the generation, ID_x is unique identifier of the node and t_x is the expiration time.
  Step 3 : The neighboring node A receives the MAC and verifies it. If the verification succeeds, it chooses a random nonce N_A, which will be used in the randomization of the ECDH key exchange.
  Step 4 : The node A broadcasts the values N_A, N_B, IC_A along with the MAC computed on these. The Node B receives the values and verifies the MAC value.

- Establishment of Pairwise keys
  Step 5-6 : If both the verification succeed Node A and B computes the static public key Q_{AB_i} using the Implicit certificate, the public key of CA and the current secret keys as $Q_{AB_i} = q_{B_i} \times Q_{A_i} = q_{A_i} \times Q_{B_i}$. Then the final pairwise key K_{AB} is computed by applying kdf function. The function kdf is implemented through a one-way cryptographic hash function MAC over the K_{AB} value.
  Step 7-10 : Both nodes use MAC computed on the derived key for the confirmation. If confirmation succeeds then both node accepts the key as pairwise key and the N_A, N_B values are deleted immediately.

IV. FSM AND HARDWARE ARCHITECTURE OF THE PROPOSED SYSTEM

A. Finite State Machine of the Proposed System

In the proposed system, a network of n sensor nodes is considered where each node is initialized with different time delay. The sequence of operations in a single node is shown in the FSM. The values to be pre-deployed into the nodes are stored in the memory. Initially all the nodes will be in idle state. Once initialized, the nodes in WSN will be pre-deployed with point P, the network wide symmetric key K and the secret key of certification authority. When the node powers up, each node will broadcast their details. Once the random nonces, implicit certificate and MAC value received from the other node are loaded into FIFO, the FSM will start to process the received data.
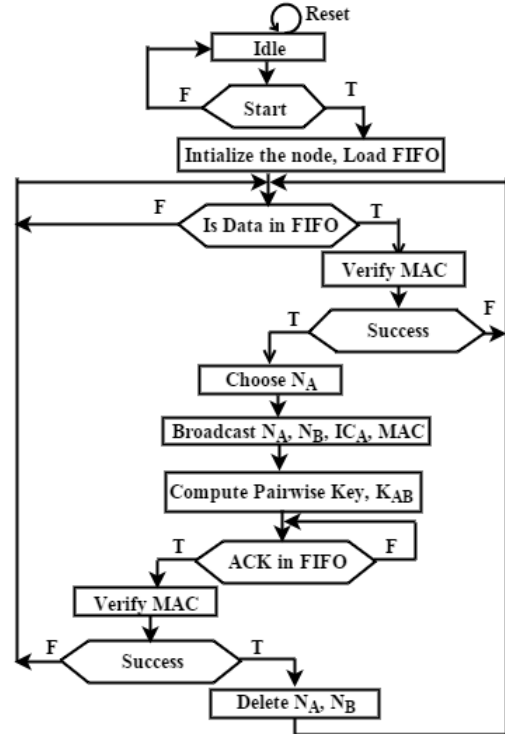

Fig. 2: FSM of Key Establishment System

The main states of FSM are idle, MAC verification, Pairwise key computation and Deletion. Idle state indicates that the PHY module does not transmit or receive any data to or from any of the neighbouring nodes in the network and all registers will be initialized with the predefined values. During the MAC verification state, FSM verifies the MAC received with the calculated MAC value. Once validated, it broadcasts the random nonces, implicit certificate and MAC value to the neighbouring nodes. During pairwise key computation, the FSM computes secret EC key of node and generates the pairwise key. The key calculation involves computation using PRSG, point multiplication and field multiplication. Upon receiving the acknowledgement signal, it further computes and

verifies the MAC with newly generated pairwise key as input. Once succeeded, it establishes the communication link and deletes the implicit certificate and other stored random nonces in the deletion state. Once the link is established, the FSM will go back to the initial state and checks for data in buffer. PHY module is ready for the processing of next data from other neighbouring nodes.

B. Hardware Architecture for implementation

Fig. 3 shows the architecture of the key exchange system in hardware platform. The PHY module can interact with the higher layer via FIFO. PRSG unit and MAC unit are the basic blocks of the system. The controller generates the control signals for the ECPM unit and multiplexes the inputs from different modules namely PRSG and MAC.
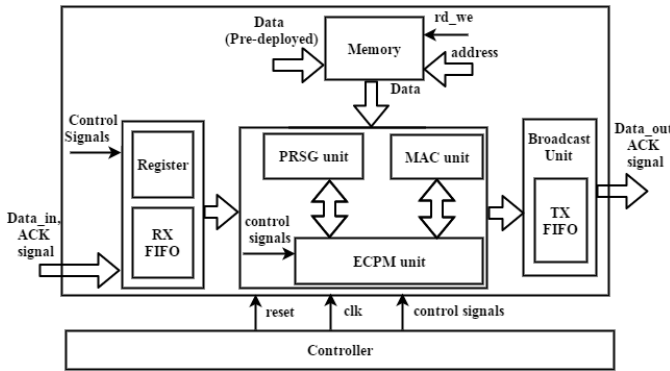

Fig. 3: Block Diagram of Integrated Key Exchange System

Initially in the network all the nodes are in idle state. Once the network comes into communication mode, all the nodes in the WSN gets powered up. The initial values P, K and q_{CA} are stored in memory of individual nodes. All the nodes broadcast their information to the neighbouring nodes. At the receiving node, it buffers the data like Implicit certificate of the node, and random nonces upon reception. Once the data of one node is received and stored in RX FIFO it is given to the MAC unit for verification and is then authenticated. Pairwise key is computed using the MAC which in turn is based on point multiplication. Random element is generated using the PRSG module.Further MAC is computed over the generated pairwise key and verified with the received MAC value. MAC value, ACK signals and random nonces are stored in the TX FIFO. Once the MAC is verified, it exchanges the handshaking signals and establishes the link. The pairwise key is stored back into the memory.The algorithms and hardware design of various individual blocks in the complete unit are detailed below:

1) ECPM Unit: ECPM unit is the basic building block for PRSG and MAC modules and hence its efficient implementation is an important prerequisite. The algorithm used for implementing point multiplication unit is Lopez-Dahab (LD) algorithm [11]. LD algorithm is based on standard projective co-ordinates and is derived from montgomery ladder algorithm. Since number of field operations in the algorithm is independent of the key bits, it resists side channel attack.Two main advantages of LD algorithm are (1) number of inversions

are minimized due to use of projective co-ordinate representation. (2) faster implementation with resistance to timing attacks is possible since the same operations are performed in every iteration of the main loop.
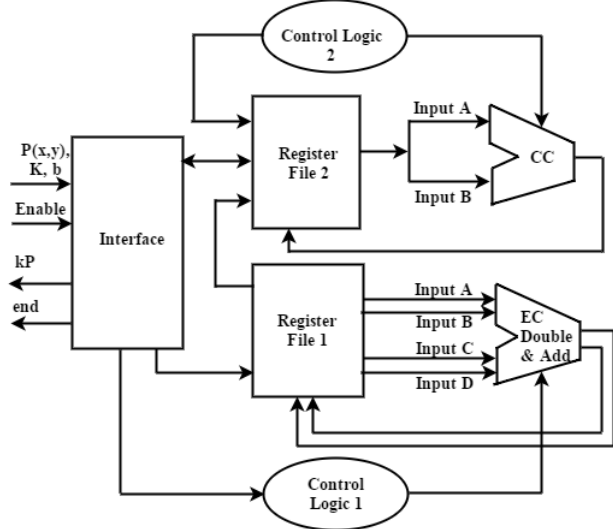

Fig. 4: Block Diagram of ECPM unit

As shown in the Fig. 4 [11], the ECPM unit consists of interface (which is the host interface HI), register file1, register file 2, control logic1, control logic 2, EC doubling and addition unit and co-ordinate conversion (CC) unit. The HI communicates with the top module. The initialization unit is used to convert the affine co-ordinate values into projective co-ordinate values x1, x2, z1and z2. Initialization unit takes values from the register file 1, which receives data from HI. The inputs are multiplexed and given to the addition and doubling unit. For each iteration, the control logic generates the select signals of the multiplexer depending on the key bits. The final output values x1; x2; z1; z2 and y co-ordinate are given to the co-ordinate conversion (CC) unit to generate the affine co-ordinate representation of the elliptic curve point. HI receives kP results from register file 2. The co-ordinate conversion unit consists of a field inversion module. The ECPM unit is designed as an FSM. Architectural design of various basic modules in ECPM unit is detailed below:

a) GF Multiplier unit: The finite field elements are represented using GNB to reduce the complexity of field operations. In this paper the conventional GNB field multiplier algorithm is implemented [12]. The implemented system employs a serial multiplier to suit the use in resource constrained applications.

b) GF inversion unit: The final output values of LD algorithm are in projective co-ordinates. In the proposed system since point multiplication is used repetitively, the values are to be converted into an affine co-ordinate system. The outputs of LD algorithm along with y co-ordinate of elliptic curve point are given to the co-ordinate conversion unit, which is the most complex unit in the design. Inversion unit is implemented using the Itoh-Tsuji algorithm [13]. From the known algorithms in literature, IT algorithm is the best for GNB with less number of multiplications. The algorithm is

implemented using GF multipler unit which is time shared among other modules.

c) GF Squaring unit: Polynomial basis and normal basis are the two typical basis representations of field elements. Since squaring operation is a simple shifting operation in normal basis, this basis representation is adopted in this work.

2) PRSG Unit: Implementation of PRSG in this paper is based on algorithm described in [14]. Pseudo random sequence generation based on elliptic curves requires the point multiplication unit, GF addition unit and LFSR and the block diagram is shown in Fig. 5.
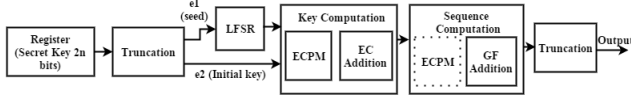

Fig. 5: Block Diagram of PRSG

Initially the secret key of length 2n bits is stored in the register. Secret key is truncated to get e_1 and e_2 of required number of bits. Here it is truncated to two 163 bits e_1 and e_2.The LFSRs loaded with initial keys e_1. e_2 are given to key computation block. In the key computation block, the initially stored key is multiplied with the elliptic curve point P and then GF addition is performed over LFSR value and the result. In the sequence computation block, EC addition is done over the K_iP, generated by the key computation block and e_1P. Generated output sequence is truncated to required number of bits. In the current implementation number of output bits is 50 bits. The key generated in the current iteration is used as the key input to sequence generation block and for key computation in the next iteration and same operations will be repeated.

3) MAC Unit: The message authentication code (MAC), is the basic unit of every key establishment technique. Hardware complexity can be reduced by using a single MAC unit as the hashing and key derived functions instead of standalone modules. MAC implementation time shares the point multiplication unit used for key exchange. The algorithm presented in [14] is used for implementing the MAC function.
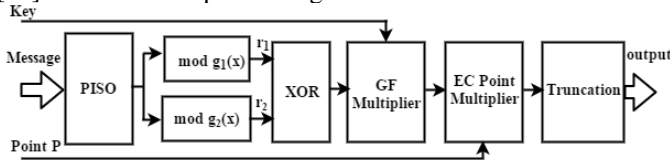

Fig. 6: Block Diagram of MAC Unit

Fig. 6 shows the block diagram of MAC unit. The message input is given serially to the modular division unit via parallel-in-serial-out register. Modular division of message is performed with two generator polynomials $g_1(x)$ and $g_2(x)$ and in hardware it is implemented using LFSR. The residues r_1 and r_2) are stored in registers and xor operation is performed. The xored value ($R = r_1 + r_2$) is given to the GF multiplier along with the secret key. EC point multiplication is performed on the result and it is then truncated to the required number.

4) FIFO: The Synchronous FIFO, a First-In-First-Out memory queue with control logic, is employed in this design which manages the read and write pointers, generates status flags and provides optional handshake signals for interfacing with the user logic. When a request/ACK signal is received, data presented at the modules data-input port is written into the next available empty memory location on a rising clock edge when the write-enable input is high. The memory full status output indicates that no more empty locations remain in the modules internal memory. Data can be read out of the FIFO via the module's data-output port in the order in which it was written by asserting read-enable prior to a rising clock edge. FIFO width and depth can be set as per the number of neighbouring nodes in the network. There is one transmitter and receiver FIFO to store the data. The values received from neighbouring nodes are stored in receiver FIFO and processed. The values ACK signals, Implicit certificate and MAC of corresponding node to be broadcasted to all neighbouring nodes are stored in the transmitter FIFO. Once the key establishment process is completed, the data from the next node stored in the FIFO is popped out and processed.

V. IMPLEMENTATION DETAILS

This work includes the design and simulation of the key establishment system using an HDL and its validation using Kintex-7 KC705 evaluation board. The security of all EC based algorithms used in this work is determined by the size of the field over which the elliptic curve is defined. According to NIST standard, the size of n, where n is the order of the base point P for various algorithms, should be at least 163 for 80 bit security. Therefore elliptic curve defined over GF (2^{163}) is used for implementation.

Various random numbers for key exchange are generated by PRSG. PRSG module outputs a 50 bit sequence in one run. It is then iterated 4 times to generate 200 bits which can be customized to 163 bits by truncating. The outputted 163 bit sequence is used in the key exchange scheme. The implementation is strictly based on NIST standard [16] to ensure security and the elliptic curve chosen is E: $y^2+xy = x^3+ax^2+b$ with a = 0 and b = 1 over a field GF (2^{163}). The primitive polynomial used for the construction of finite field GF (2^{163}) is NIST standard polynomial: $x^{163}+x^7+x^6+x^3+1$. NIST standard recommends use of type 4 GNB for the above specified field. The type of GNB specifies its complexity. Field addition is simple bitwise xor operation and squaring is a single cyclic shift in shift registers. The squaring unit in normal basis requires only 1 clock cycle to produce the result. To reduce the complexity, a serial Galois field multiplier is used. GF multiplier over (2^{163}) requires 163 clock cycles for finite field multiplication. Inversion unit designed for the point multiplication is at cost of 9 field multiplications.

The MAC module is for message authentication and is used as both key derivation function and authentication function thus reducing redundant hardware. In the key exchange process, MAC is used four times, twice for verification and then once as hash and kdf functions. MAC implementation makes use of modular division and point multiplication unit. $x^{163}+x^{131}+x^{129}+x^{115}+1$ and $x^{163}+x^{99}+x^{97}+x^3+1$ are the generator polynomials used for modular division which is

realized in hardware using LFSR. LFSR base systems have simple hardware structure. MAC module is designed for a message input of 480 bit sequence. When the input sequence is less than the required field size standard pattern is appended at the end of the string. Output bit sequence can be a multiplexed for 50 or 163 bits. The MAC and PRSG units have used a single ECPM module on time shared basis in the key exchange process. The entire system works on a single clock.

For comparison, implementation of the existing system in [6] is done. Here SHA-1 is implemented as the hashing and key-derivation functions and AES is implemented as authentication function. SHA-1 takes 512 bits as inputs and produces a 160 bit hash value. AES uses 128 bit key and generates a 128 bit MAC value. Both existing and proposed systems are designed as FSM and implemented on Kintex-7 FPGA. The resource utilization of both systems was compared.

VI. RESULT AND DISCUSSION

Design, development and evaluation of a secured communication system for WSN are done. Function of major building blocks like PRSG, MAC and ECPM were verified in MATLAB 2012b. Then, the IP was written in register transfer level VHDL. The VHDL implementation was simulated using ModelSim and implementation was done on Xilinx XC7K325T-2FFG900 FPGA. Resource utilization of integrated system is minimized by reusing and time-sharing of GF multiplier, GF squaring and LD multiplier modules for both PRSG and MAC units. The synthesis tool reports a maximum clock frequency of 318.193 MHz for the implemented IP. Resource utilization of the existing system is compared with that of the proposed system and is shown in Table I.

TABLE I: Hardware Utilization Summary

Logic Utilization	Proposed work	Existing work [6]
Number of Slice Registers	17576	18012
Number of Slice LUTs	14170	25175
Number of fully used LUT-FF pairs	12267	14546

The proposed system gives 23.76% reduction in hardware utilization compared to the existing system. This results in reduced power consumption and hence increased life time when interfaced with a sensor node. In the existing work, the memory required prior to deployment in order to support at least 10 node addition phases is 804 bytes whereas in the proposed scheme, the storage requirement is independent of the node addition phases and requires only 82 bytes which is much less compared to 4 KB RAM available in sensor nodes such as Micaz and Firefly. Thus the proposed implementation has both storage and energy efficieny in comparison with the existing scheme.

VII. CONCLUSION AND FUTURE WORK

An efficient hardware design and implementation of secure key management scheme for resource constrained WSN has been presented in this paper. Various modules in the overall system are carefully chosen and the hardware architecture for their implementation is developed in such a way that the available resources are fully and efficiently utilized and

hardware redundancy is totally mitigated. The proposed system offers much reduction in storage space compared to original version and thereby support greater number of node addition phases. Design was synthesized using Xilinx ISE 14.7 and successfully implemented on Kintex-7 FPGA. The implementation results show that the proposed architecture gives 23.76% improvement in hardware efficiency over the existing EC based system. Thus the proposed hardware is highly suitable for implementation of secure key exchange in wireless sensor networks with limited hardware resources and battery power. As a future work, the implementation can be extended for ensuring confidentiality and can be integrated with sensor nodes to prototype the complete cryptosystem as a SoC.

REFERENCES

[1] H. Wang, B. Sheng, C. C. Tan, and Q. Li, "Public-key based access control in sensornet," Wirel. Netw., vol. 17, no. 5, pp. 1217−1234, 2011.

[2] Rahman M, Sampalli S, "An efficient pairwise and group key management protocol for wireless sensor network," Wirel Person Commun,, vol. 84, no. 3, pp. 2035−2053, 2015.

[3] M.A. Simplcio Jr., P.S.L.M. Barreto, C.B. Margia, T.C. Carvalho, "A survey on key management mechanisms for distributed Wireless Sensor Networks," Computer Networks, Vol. 54, no. 15, pp. 2591−2612, 2010.

[4] D. Du, H.G. Xiong, H.L. Wang, "An efficient key management scheme for wireless sensor networks," International Journal of Distributed Sensor Networks, Vol.2012, 2012, doi:10.1155/2012/406254.

[5] Kishore Rajendiran, Radha Sankararajan and Ramasamy Palaniappan, "A secure key predistribution scheme for WSN using elliptic curve cryptography," ETRI Journal, vol. 33, no. 5, pp. 791−801, 2011.

[6] P. Kotzanikolaou, E. Magkos, D. Vergados, and M. Stefanidakis, "Secure and practical key establishment for distributed sensor networks," Security and Communication Networks,vol. 2, no. 6, pp. 595−610, 2009.

[7] L. Eschenauer and V. D. Gligor, "A key management scheme for distributed sensor networks," in Proc. 9th ACM Conf. Comput. Commun. Security, pp. 41−47, 2002.

[8] S. Zhu, S. Setia, and S. Jajodia, "Leap+: Efficient security mechanisms for large-scale distributed sensor networks," ACM Transactions on Sensor Networks (TOSN), vol. 2, no. 4, pp. 500−528, 2006.

[9] F. Gandino, B. Montrucchio, and M. Rebaudengo, "Key management for static wireless sensor networks with node adding," IEEE Trans. Ind. Informat., vol. 10, no. 2, pp. 1133−1143, 2014.

[10] Jilna Payingat and Deepthi P. Pattathil, "Pseudorandom Bit Sequence Generator for Stream Cipher Based on Elliptic Curves," Mathematical Problems in Engineering, vol. 2015, Article ID 257904, 16 pages, 2015.

[11] C. H. Kim, S. Kwon, and C. P. Hong, "FPGA implementation of high performance elliptic curve cryptographic processor over GF(2^{163})," J. Syst. Archit., vol. 54, no. 10, pp. 893−900, 2008.

[12] B. Ansari and M. Hasan, "High-performance architecture of elliptic curve scalar multiplication," IEEE Trans. Comput., vol. 57, no. 11, pp. 1443−1453, 2008.

[13] R. Azarderakhsh and A. Reyhani-Masoleh, "Low-complexity multiplier architectures for single and hybrid-double multiplications in gaussian normal bases," IEEE Trans. Comput., vol. 62, no. 4, pp. 744−757, 2013.

[14] Jilna P, Deepthi P. P., Sameer S.M., Sathidevi P.S. and Vijitha A. P., "FPGA implementation of an elliptic curve based integrated system for encryption and authentication," IEEE International Conference on Signal Processing, Informatics, Communication and Energy Systems (SPICES), pp. 1−6, 2015.

[15] NIST−National Institute of Standards and Technology, Recommended Elliptic Curves for Federal Government Use, Jul. 1999 [Online].

An Agent-Based Approach for Resource Allocation in the Cloud Computing Environment

Mohamed El-kabir Fareh*, Okba Kazar†, Manel Femmam†, and Samir Bourekkache†
*Computer Science Department, Biskra University, Biskra, Algeria
fareh.medelkebir@yahoo.fr
†LINFI Laboratory, Computer Science Department, Biskra University, Biskra, Algeria
kazarokba@yahoo.fr, fmanel@hotmail.fr, s.bourekkache@gmail.com

Abstract—One of the major challenges in cloud computing is Resources´ allocation. In such environment, the providers and the users have different objectives; providers aim to maximize the revenue by increasing the use of resources, while users want to reduce expenditures and, in the same time, to meet their performance requirements. However, it is very difficult to allocate the resources mutually and to use the optimal manner due to the lack of sharing information between the two partners. Using the agent paradigm and inspiring the model ¨call for bids¨, we propose an approach based agent to connect the different heterogeneous cloud providers with the cloud users. The objective of our system is to allow users to choose the appropriate resources that can meet their needs. In addition, it enables cloud providers to efficiently allocate their resources. For the results validation of our system, we explore the JADE environment and the simulator CloudSim.

Index Terms—cloud computing, resource allocation, agent, MAS, UML.

I. INTRODUCTION

In recent years, cloud computing has known an important interest as a main paradigm for the use of resources. It provides these resources on the market as a service that can be consumed in a flexible and transparent manner. In such environment, there are two main actors: users and cloud providers. In the first hand, the user aims to get the resource allocation that is associated with the pay as you go model of use, which reduces the waste payment of unused resources. In the other hand, the main interest of cloud provider lies in the scale factor that introduces the creation of large sets of resources. In this paper, we propose a new architecture that contains a set of layers in order to connect various heterogeneous cloud providers with cloud users. This architecture is oriented agents, so we are particularly interested in the design and development of a multi-agent system, which allows the consumers to choose the appropriate resources that can meet their needs. In addition, it allows cloud providers to efficiently allocate these resources. The use of agents improves the interaction of clouds with users and makes the resources allocation more efficient to different applications.

The paper is organized as follows: section 2 presents the system of resources allocation in cloud computing. Some related works, that are close to our work, are described in the section 3. In section 4, we present and explain our proposed approach

and architecture. Section 5 shows the method of resources mapping. Then, our simulation results are expressed in the section 6. Section 7 is the conclusion and the perspectives of this work.

II. RESOURCE ALLOCATION SYSTEM IN THE CLOUD

The resource allocation system (RAS) may be considered as all mechanisms designed to ensure that applications´ requirements are taken into account correctly by the provider's infrastructure. These mechanisms of resource allocation should also review the current status of each resource in the cloud environment to apply algorithms in order to better allocate the physical and/or the logical resources for user applications. It is important to note that cloud users can see the limited resources as unlimited thanks to RAS [1].

Resource management in Clouds is at several levels, from a finer granularity to the top level. At the lowest level, VMM (Virtual Machine Monitor) built on physical machine allocates fractions of CPU, memory, disk and network to the different VMs, that are installed upon the VMM. At the middle level, VMs are managed by the Cluster Manager: using different management strategies, VMs are allocated to different applications, and VM can be migrated among different physical machine to achieve workload balanced. Whereas at the top level, Clouds Manager have to determine the manner of selecting appropriate cluster or PC in order to run different applications of Cloud Clients with their QoS met [3].

III. RELATED WORKS

In the literature, resource allocation in cloud platforms is treated by several works. While allocating resources in cloud, we must consider numerous parameters such as high throughput, maximum efficiency, SLA aware, QoS aware, maximum energy and power consumption etc. In this section, we present some works that are close to our approach.

a) Based economics and market approaches: In the work [2] the authors applied the methods of auction model, neural network and intelligent optimization according to the features of cloud resource allocation; The authors proposed a double multi-attribute auction based cloud resource allocation mechanism. For aim of improving resource utilization of large Data Centers while delivering services with higher QoS to

Cloud Clients, an automatic resource allocation strategy based on market Mechanism (ARAS-M) is proposed in [3].

b) Based workload and geographical location of Data Center: In [4], the authors proposed an adaptive resource allocation model that allocates the consumer's job to an appropriate data center. In order to find a proper data center, they used two evaluations: the geographical distance between a consumer and data centers, and the workload of each data center. The authors of [6] presented an SLA-based cloud computing framework for facilitating resource allocation. This approach takes into account some features such as: the workload and geographical location of distributed data centres.

c) Based intelligent decision: The work proposed in [5], presents an Intelligent Cloud Resource Allocation Service (ICRAS). This service maintains an overview of current CSP resources offerings and evaluates them for the purpose of finding the most appropriate configuration to meet the consumers preferences. In the work [7], the authors presented a resource allocation algorithm based on game theory for multi-resource environment; They modelled the problem as a finite extensive game; the set of physical servers, that provide resources, are modelled as game players and each player has the knowledge about the utility information of other players.

d) Based quality of service: Generally, the goal satisfying the QoS of both cloud providers and consumers is considered a main task. In [8], in order to perform the best matching of resources supply and resources consumption, the authors used a kind of resources configuration optimization scheme based on the structure supportiveness. A strategy of resource allocation and price adjustment based on particle swarm algorithm is proposed in [9], According to the workload characteristics, a utility function is designed to evaluate QoS. However, in the presented works above, the researches neglected how to optimize resource allocation scheme from the consumers point of view to obtain the best service at a lower price. In this paper we will treat this problem taking into account the optimal use of resources from the point of view of the cloud provider.

IV. PROPOSED APPROACH

A. Conceptual modeling of cloud computing environment for resource allocation

The two main actors in the cloud environment are the cloud users and the cloud providers:

- From the point of view of cloud users (CUs), users are directed economy entities when making the decision to use cloud services [10]. The cloud users are modeled as a set $CU = \{CU_1, CU_2, ..., CU_m\}$, where m is the number of users who request resources at a given moment.
- From the point of view of cloud providers (CPs), a large number of resources must be allocated to thousands of distributed user, in a profitable, fair and dynamic way [10]. The cloud providers are modeled as a set: $CP = \{CP_1, CP_2, ..., CP_n\}$, where n is the number of the providers in the cloud at a given moment.
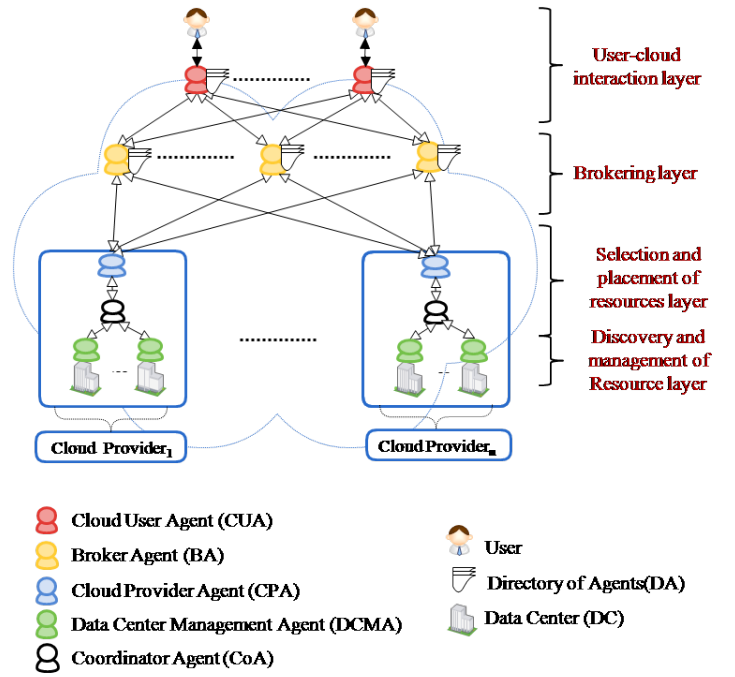

Fig. 1. Layered architecture for resources allocation in the cloud computing.

- Each cloud provider $CP_{i=1..n}$ has several datacenters modeled as a set: $DC = \{DC_1^{CP_i}, ..., DC_j^{CP_i}, ..., DC_d^{CP_i}\}$; where d means the number of data centers provided by the CP_i at a given moment.
- Each datacenter $DC_{j=1..d}$ is generally composed of a large number of physical nodes modeled as a set $PN = \{PN_1^{DC_j}, ..., PN_k^{DC_j}, ..., PN_p^{DC_j}\}$; where p means the number of physical nodes in DC_j at a given moment.
- Each physical node$PN_{k=1..P}$ in the cloud can run multiple virtual machines (VM) modeled as a set $VM = \{VM_1^{PN_k}, ..., VM_l^{PN_k}, ..., VM_w^{PN_k}\}$; where w means the number virtual machines running on PN_k at a given moment. Each VM is called a resource and it can be assigned to a part of users demand.

B. General Architecture

The general hierarchical architecture of our system contains four main layers that interact with each other (Fig. 1):

1) User-cloud interaction layer: It is the intermediate layer between cloud computing system and the cloud user. It allows users to interrogate the cloud system. This layer provides a graphical user interface (GUI) (to introduce the user's needs, display the results of resource allocation ... etc.). To specify these requirements, the user should interact with this GUI. As a result of this interaction, the Cloud User Agent (CUA) forms a description of the user request, which must be forwarded to broker agents (BAs). CUAs help users to find the appropriate resources for their needs and they act on behalf of each user in the phase of definition of required QoS and the formalization of the agreement negotiated between the both parts (cloud user

and cloud provider).

At this level we suppose that the service requested by the user is composed of a set of application $(a_1, a_2, ..., a_v)$; the execution of every application requires multidimensional resources that must be virtualized in the form of virtual machines hosted on a physical node. Let R the user request:

- v is the number of VMs needed to satisfy the user request.
- w is the dimension of the resource of every VM.
- R_{ij} is the capacity of the resource i of the virtual machine j where $1 \leq i \leq v$ and $1 \leq j \leq w$.

$$R = \begin{array}{cc} \begin{array}{cc} R_1 & \cdots & R_w \end{array} & \\ \begin{pmatrix} r_{1,1} & \cdots & r_{1,w} \\ \vdots & \ddots & \vdots \\ r_{v,1} & \cdots & r_{v,w} \end{pmatrix} & \begin{array}{c} VM_1 \\ \vdots \\ VM_v \end{array} \end{array}$$

2) Brokering layer: It is the intermediate layer between the first layer and the cloud providers; it includes brokers agents (BAs) which perform the discovery of the most appropriate offer to the user request from the provider offers. Broker agents are led by negotiation activities of the mutually acceptable conditions to establish the SLA between the cloud providers and the cloud users, to satisfy the cloud users requirements.

3) Selection and placement of resources layer: This layer contains the set of cloud providers agents (CPAs) and coordinators agents (CoAs). At this level, and for each user request, the CPA communicates with the CoA to select the appropriate resources for each received request. the CoA coordinates between agents of the lower layer, more specifically with the data center management agents to acquire the resource capacities of each physical node. C_{CP} is the state of resources of the cloud provider ($C_{CP} = \cup C_{DC}$) where C_{DC} is the state of resources in the data center.

- q is the number of the physical nodes of the CP.
- w is the dimension in resource of every physical node.
- C_{ij} is the capacity of the resource i of the physical node j where $1 \leq i \leq q$ and $1 \leq j \leq w$.

$$C_{CP} = \begin{array}{cc} \begin{array}{cc} C_1 & \cdots & C_w \end{array} & \\ \begin{pmatrix} c_{1,1} & \cdots & c_{1,w} \\ \vdots & \ddots & \vdots \\ c_{q,1} & \cdots & c_{q,w} \end{pmatrix} & \begin{array}{c} PN_1 \\ \vdots \\ PN_q \end{array} \end{array}$$

4) Discovery and management of Resource layer: This is the lowest layer in our system, it includes a set of data center management agents (DCMAs), each DCMA is responsible for managing the resources of a data center, and it discovers the capacity resource of each physical node at a given moment. C_{DC} is the state of resources in the data center:

- p is the number of the physical nodes in a data center.
- w is the dimension in resource of each physical node.
- C_{ij} is the capacity of the resource i of the physical node j where $1 \leq i \leq p$ and $1 \leq j \leq w$.

$$C_{DC} = \begin{array}{cc} \begin{array}{cc} C_1 & \cdots & C_w \end{array} & \\ \begin{pmatrix} c_{1,1} & \cdots & c_{1,w} \\ \vdots & \ddots & \vdots \\ c_{p,1} & \cdots & c_{p,w} \end{pmatrix} & \begin{array}{c} PN_1 \\ \vdots \\ PN_p \end{array} \end{array}$$

C. The used economic model

A large number existing of economic models. Some models use simple interactions, whereas others involve more or less mechanisms of negotiation. In our case we use the model of call for bids. Inspiring from the call for bids model, we will use a directory of agents that contains a list of contacts (agents) that will be contacted by an agent to accomplish these tasks, each agent can develop its own directory (add, delete, or update contacts) according to its skills. In our system we have two agents that need this type of directory:

- Cloud user agent (CUA): each CUA holds a directory of broker´s agents that will be contacted to find the appropriate resources to a cloud user request. The CUA executes the same process as the process of call for bids.
- Broker agent (BA): each BA has a directory of cloud provider´s agents that will be contacted to find the appropriate resources to a cloud user re-quest. The BA executes the same process as the process of call for bids.

D. Detailed architecture

1) Generic internal Architecture of the agents: According to Wooldridge [11], the internal architecture of an agent is a map of its internal modules, its data and the operations that can be applied to these data. The different agents of our MAS are distinguished by the nature of the internal modules that compose them; also by the way these modules are imbricated some in the others. The generic internal architecture of each agent consists of three modules:

- Knowledge module:
  - Individual knowledge: reflect the view of the agent on himself, in particular its: name, address, individual objectives, various possible states.
  - Social knowledge: reflect the knowledge of the agent on the representation of its social environment.
- Communications module: this module manages the communications with other agents. On the one hand, this module receives from the treatment module requests of transmission of message to one or several agents. On the other hand, it is responsible of the reception of the messages sent by other agents.
- Treatment module: this module is based on a set of knowledge acquired by the agent and the messages coming from other agents to develop or select, according to the case, either an answer to a request or performing a precise task.

a) Internal architecture of CUA: It represents the user in the cloud environment; it participates in the system and aims to bring a maximal profit for the user. In addition to the modules of the generic internal architecture, the internal architecture of the CUA includes an interface module that provides basic methods to support the interaction human/agent and a data structure to represent the directory of broker agents.

b) Internal Architecture of CPA: It represents the provider in the cloud environment; it participates in the system and aims at obtaining a maximum benefit for the provider. In

addition to the internal modules of the generic architecture, the internal architecture of CPA has an establishment of offers module based on the response of the coordinator agent concerning a cloud user request, it adds the economics attributes.

c) Internal Architecture of BA: The main role of the broker agent is to find the best offer which satisfies the request of the user in the cloud. In addition to the modules of the generic internal archi-tecture, the internal architecture of the BA contains a negotiation module and a data structure to represent the directory of the cloud provider´s agents.

d) Internal architecture of a CoA: It coordinates between DCMAs to manage and control the physical/virtual resources of a cloud provider; in addition to the modules of the generic internal architecture, the internal architecture of CoA, includes a consolidation and selection module to consolidate the current states of different resources in different data centers and select the available resources that can satisfy the demand of the user.

e) Internal Architecture of DCMA: Its main task is to discover the capacity of resources on the physical nodes and manages the virtual machines in the data center. A virtual machine management module that contains virtual machines management mechanisms (creation, suspends, resume recording, catering, shutdown, restart ...).

2) Interaction between agents: We chose the use of UML for the modeling of the interactions between agents in our MAS (Fig. 2).

V. RESOURCES MAPPING

This is the main task of the coordinator agent; it will find the right selection that satisfies the user request. For this aim, the method uses a multidimensional comparison of each resource requested by the user and the available resources of provider. The physical node PN_k can host a virtual machine VM_l if and only if: $R_{li} \leq C_{ki} / \forall i \in \{1..w\}$. To facilitate the modeling of the problem, we have adopted a binary vector $V(0/1)$ for each physical node; it takes the value 1 if the physical node PN_k can host the virtual machine VM_l. So this vector dimension is equal to the number of virtual machines.What gives us afterward a binary matrix $P(0/1)$ of dimension (qxv); $P_{kl} = 1$ If the physical node PN_k can host a virtual machin VM_l and $P_{kl} = 0$ Otherwise.

For a correct allocation of the resources, the following formula must be verified:

$$\sum_{l=1}^{v} R_{lz}.P_{kl} \leq C_{kz} \left\{ \begin{array}{l} 1 \leq k \leq q \\ 1 \leq z \leq w \end{array} \right.$$

VI. IMPLEMENTATION AND SIMULATION

A. Implementation

The proposed approach is experimentally validated thanks to the exploitation of the JADE environment and the CloudSim simulator. JADE is an observation and visualization tool of MAS, and CloudSim is a utility primarily intended for research in the design and evaluation of the underlying architecture of IT services demand platforms [12]. These tools are integrated in ECLIPSE and we have used the Java language.
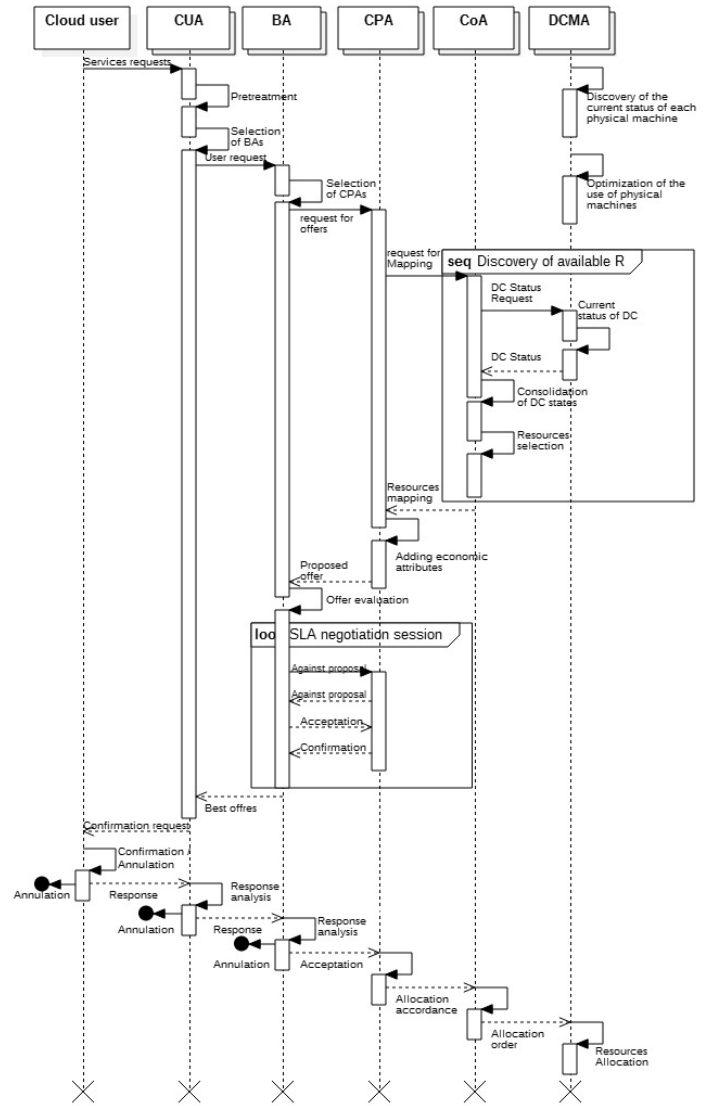

Fig. 2. Sequence diagram (Global Interaction)

B. Description of Application

We created an interface that facilitates the user access and manipulation of CloudSim simulator, because CloudSim does not offer a graphical interface that allows the user to take full advantage of the simulator (change simulation parameters, the graphical display of the results, view the unfolding of a simulation). Using the JADE platform, we can follow all the actions of agents and their interactions of our system. Also, JADE provides the use of the Sniffer agent that can be launched automatically with the application in order to capture and display all the exchanged messages between the agents. Primarily a simulation takes place in three steps: setting simulation, launching of a simulation, displaying results. Setting the simulation is performed by the user using three parts:

- Global Settings: This part is used to initialize the number of CPs, the number of users, the number of BAs in the brokerage layer and initializing the directory of CUAs and BAs.

- Cloud Computing: This part allows the introduction of cloud computing parameters: number of DCs, number of PNs in each DC, configuration of each PN...etc.
- Users requests: This part determines user requests including: number of services or applications, his resource requirements, and the budget of each user.

C. Simulation

1) Metric used: The cloud user wants to treat all of its services or applications at the lowest cost. In our simulation, we assume that the service cost or application equals to the sum of consumption costs of each resource used in the treatment:

$$Cost_{Sce/App} = \sum consumption\ cost\ of\ each\ resource$$

2) Example of simulation: We will present in this part an example of simulation of resources allocation approach based agents in cloud computing that we have proposed:

- Global parameters: number of CPs is three, number of users is five, number of brokers is four, and we initialized the directories of CUAs and directories of BAs as followings (Table I).

TABLE I
INITIALIZATION OF DIRECTORIES OF CUAS AND BAS

ID_CUA	1	2	3	4	5	ID_BA	1	2	3	4
Nbr BAs	3	2	4	1	4	Nbr CPAs	3	1	2	3

- The configuration of the parameters of the cloud computing environment is presented in Table II.

- User requests: R = (PE in MIPS, Memory in MB, storage in GO and Bandwidth in MB/S) is the resource description used to describe the user requests. We assume a request user = R (450, 4, 200, 128) with a budget = 100U.

After the launch of the simulation: The second BA (ID_ BA=2) proposes an allocation of a VM hosted on the PN1 in DC3, owned by the CP1 with a cost= 107.3775 U. The fourth BA (ID_ BA=4) proposes an allocation of a VM hosted on the PN1 in DC1, owned by the CP3 with a cost = 30.93 U. The example presented shows that the fourth broker agent directory

TABLE II
EXAMPLE OF C.C ENVIRONMENT SETTINGS

		Capacities of physical nodes								
		Number of physical nodes	Number of PE	Power of each PE (MIPS)	Memory (MB)	Storage(GO)	Bandwidth (MB/S)	Cost of processing element (U)	Cost of memory (U)	Cost of storage (U)	Cost of bandwidth (U)
CP1	DC1	2	2	1000	2	500	128	3.0	0.5	0.1	0.01
	DC2	1	4	400	1	250	256	4.0	1.2	0.3	0.01
	DC3	4	3	2000	4	750	1024	1.5	0.8	0.5	0.03
CP2	DC1	1	5	5000	8	750	512	2.0	0.5	0.4	0.05
CP3	DC1	4	4	2500	4	750	512	2.5	0.7	0.1	0.06
	DC2	3	2	3200	4	500	2048	1.0	1.1	0.8	0.02

size (contains all the cloud providers) is greater than the size of the second broker agent (contains a single cloud provider), which affects the resource allocation.

VII. CONCLUSION AND PERSPECTIVES

In this paper, we presented an agent-based approach for resource allocation in the cloud; the proposed approach is based on: a layered architecture to connect the cloud providers of different heterogeneous cloud with the cloud users. The multi-agent system is used to model the process of allocating of cloud resources. Several experiments show that autonomous agents make the clouds smarter in their interactions with users and more efficient in resources allocation. The only metric used in the validation phase is the cost of services or applications, while studying the performance of a system is usually measured by the speed of sending the response to a user. Thus, we will propose in future a new work to measure the elapsed time of each cloud user agent to meet the demand of the user. Moreover, we need to perform a study of the influence of directories of CUAs and BAs on the response time flow to satisfy a request of a user.

REFERENCES

[1] G. Estcio et al, Resource Allocation in Clouds: Concepts, Tools and Research Challenges, 29th Brazilian Symposium on Computer Networks and Distributed Systems - XXIX Simpsio Brasileiro de Redes de Computadores e Sistemas Distribudos - (SBRC), pp. 197-240, 2011.
[2] S. Jiajia et al, A Cloud Resource Allocation Scheme Based on Microeconomics and Wind Driven Optimization, 8th ChinaGrid Annual Conference (ChinaGrid), pp. 34 39, August 2013.
[3] Y. Xindong et al, ARAS-M: Automatic Resource Allocation Strategy based on Market Mechanism in Cloud Computing, Journal of Computers, Vol. 6, No. 7, pp. 1287-1296, July 2011.
[4] J. Gihun, S. Kwang Mong, Agent-based Adaptive Resource Allocation on the Cloud Computing Environment, 40th International Conference on Parallel Processing Workshops (ICPPW), pp. 345 351, September 2011.
[5] K. Clark et al, An intelligent cloud resource allocation service -Agent based automated Cloud resource allocation using micro-agreements, the proceedings of the 2nd International Conference on Cloud Computing and Services Science (CLOSER 2012), pp. 37-45, 2012.
[6] Seokho Son et al, An SLA-based cloud computing that facilitates resource allocation in the distributed data centers of a cloud provider, The Journal of Supercomputing, Volume 64, Issue 2, pp 606-637, May 2013.
[7] X. Xin and Y. Huiqun, A Game Theory Approach to Fair and Efficient Resource Allocation in Cloud Computing, Mathematical Problems in Engineering, Volume 2014, 14 pages, 2014.
[8] W. Yuan et al, Research on Optimization of Resources Allocation in Cloud Computing Based on Structure Supportiveness, Frontier and Future Development of Information Technology in Medicine and Education, Volume 269 of the series Lecture Notes in Electrical Engineering (ITME), pp 849-858, December 2013.
[9] F. Xie et al, A Resource Allocation Strategy Based on Particle Swarm Algorithm in Cloud Computing Environment, Fourth International Conference on Digital Manufacturing and Automation (ICDMA), pp. 69-72, June 2013.
[10] V. Krishna Reddy, Meta-heuristic based multi objective task scheduling for managing the cost in cloud computing environment [Online], doctoral thesis, chapter 2, Department of Computer Science & Engineering, Acharya Nagarjuna University, 2012, Available: http://hdl.handle.net/10603/8273.
[11] M. Wooldridge, Multi-agent systems: A modern approach to distributed artificial intelligence, Edited by G. Weiss, pp. 27-78, MIT Press, London, England, 1999.
[12] L. Sylvain, Load balancing services for the cloud: Application to multimedia data processing [Online], doctoral thesis, Doctoral Informatics, Telecommunications and Electronics (Paris), Sep 2014. Available: https://tel.archives-ouvertes.fr/tel-01062823.

Application-state Aware Scheduling for Video Delivery over LTE Network

[1]Farhan Pervez, [2]Muhammad Salman Raheel

[1]COMSATS Institute of Information Technology, Lahore, Pakistan
[2]University of Wollongong, New South Wales, Australia
Email: farhanpervez@ciitlahore.edu.pk; msr949@uowmail.edu.au

Abstract— **With the evolution in mobile systems technology it is possible to provide high data rate applications to the end user. Apart from the bottleneck problem in the core network, efficient utilization of the air interface remains a big challenge. Therefore, it is necessary to have intelligent resource management mechanisms in order to provide precise quality to the end users who have high expectation about the quality of service they receive. Here we propose a QoE based approach in order to improve the playback of a YouTube video in LTE network. The effectiveness and setbacks of our approach when put into practice on a running network will also be analyzed.**

Keywords— QoE (Quality of Experience), resource management, LTE (Long Term Evolution)

I. INTRODUCTION

4th generation (4G) mobile networks based on 3GPP LTE [1] provide high data rates across mobile users in order to enable the usage of high quality Internet services such as multimedia communication. According to traffic and services forecasts, it is estimated that the total mobile videos traffic will exceed 66% by 2017 of all generated traffic which will increase 26-fold compared to 2012 [2]. Moreover, with the deployment of LTE-Advanced and small cell networks, in the same time frame will increase the growth of mobile capacity by10 folds.

In the past, a number of approaches have been discussed to improve the quality of the video in wired networks as discussed in [3-4]. However, it is always considered to be a challenging task to improve video quality in wireless or mobile networks. Apart from the problem of limited capacity, the mobile operators also face the challenge of user satisfaction [5]. Customers have high expectations on the delivered quality of the services. The delivery is largely based on the Internet, and not under the control of the operator, which can have congestions and delays.

The quality requirements of applications to be delivered to the users vary. The depend on multiple diverse parameters such as screen size of the device, the used coding technique, or the previous usage history of the user. For these different user based quality requirements, ITU defines Quality of Experience (QoE) to quantify the delivered application quality.

QoE is the overall acceptability of an application or service as perceived by the end user [6,7]. Compared to QoS, which considers only network parameters, QoE includes any subjective and objective parameters such as video content, encoding parameters, usage scenario, network performance, and application state.

Figure 1 shows the hard and soft influence factors by which QoE is determined. The factors can be divided in three different categories namely technical system, usage context or the user itself [7].

For applications such as YouTube video delivery with time-dynamic bandwidth requirements due to encoding, download patterns, or user behavior, QoS based resource management is often not sufficient to provide an acceptable QoE. A simple mapping of a QoS parameter, such as throughput in case of YouTube, is difficult since it also depends on the user perceived quality of the application. The paper proposes a specific scheduling scheme which is based on application parameters instead of QoS network parameters.
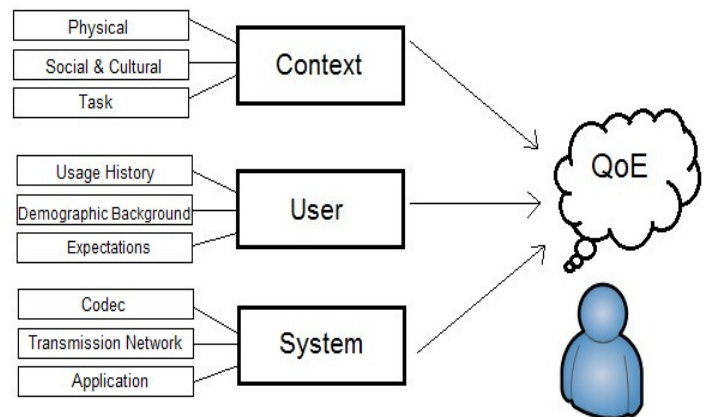

Fig. 1. Factors affecting the viewers QoE

II. QoE-BASED YOUTUBE VIDEO DELIVERY

A. YouTube Video Streaming

A YouTube video stream uses H.264/MPEG-4 Advanced Video Coding (AVC) as the default compression format of the video content [8]. The encoded data is transmitted over HTTP and buffered at the YouTube client buffer. The buffering is a two phase process. Firstly, there is an initial buffering of a

fixed length of the YouTube video. After that periodic refilling of the buffer is done that is controlled by the YouTube server. The periodic refilling is adapted for every video according to the total video rate [9][10]. The buffering process helps in sustaining bad network conditions or large delays and so therefore prevents playback stalling. Figure 2 presents analysis and modeling of YouTube traffic presented in [11].
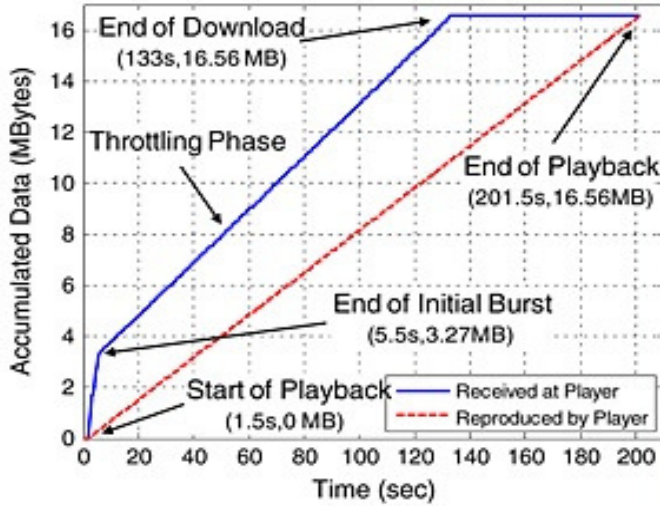

Fig.2. Analysis and Modeling of YouTube traffic

B. Application-state Aware Scheduling

Some previous studies [12][13] have indicated that the status of the user buffer is the most influencing parameter on the user QoE. Here we propose a scheduler called buffered video scheduler (BVS). The application-aware scheduler is based on the buffer state that is continually sent by the user. The algorithm provides two thresholds. The buffer state can have a minimum and a maximum threshold represented by α and β respectively. The scheduler tags a flow as being critical if feedback is received indicating that the buffered playtime is below α. A flow is tagged as normal if feedback is received indicating that the threshold β is exceeded. If the scheduler receives a YouTube video packet, it checks whether the packet belongs to a video flow in a critical state or not. If the state of the video is critical then the scheduler prefers this packet and allocates it to the transmission frame, otherwise the packet is passed to the resource allocator and scheduling is done according to QoS parameters like channel quality or service-level.

C. Simulation and Scenario

A single mobile cell is simulated. The users move around within the cell with a speed of 1m/s. Each user may watch a YouTube video, download a file, or browse the Internet. A single YouTube video is simulated for 20sec. The average video rate is 454 kbps.

For web browsing users, a web server is simulated that is answering HTTP requests and TCP connection handling is done according to Apache web server default configuration. The TCP implementation runs TCP New Reno. A web page containing objects for example images, JavaScript code and CSS style sheets is used to load the system.

At the link layer signaling and control channels are simulated as error free. The channel model includes path loss, shadow fading (zero-mean Gaussian distribution with standard deviation of 2dB and with de-correlation distance of 50m) and multipath fading (according to ITU Pedestrian B profile). A single input single output antenna is used and simulated bandwidth of 1.4MHz is set. At the application layer, the YouTube download server and a YouTube Flash Player is simulated that processes HTTP data to display the YouTube video. The buffered video playtime is given in seconds. The initial pre-buffering and the periodic buffer refill both depend on block size (b = 64kB) and inter-block arrival time [9] as mentioned using equation (1) and (2).

$$f_{ibr} = min\,(\alpha_{th},\,px^q + r) \qquad (1)$$

Inter-block arrival time with an upper threshold at $\alpha_{th} = 2096$, x as the total data rate, and $p = 400000$, $q = -1$, $r = -5.71$

$$Initial\ Buffering\ Period\ f_{ibs} = 32.\,b.\frac{1000}{f_{ibr}} \qquad (2)$$

### D. Analyzing the Results of BVS with State of the Art Round Robin Scheduling

We evaluate the proposed BVS with a classical state of the art round robin scheduler (RRS). A round robin scheduler assigns time slices to each user in equal portions and in circular order handling them without any priority. In this section two different scenarios are analyzed. The first scenario contains a YouTube user with three download users. The second scenario contains a YouTube user with different numbers of web browsing users.
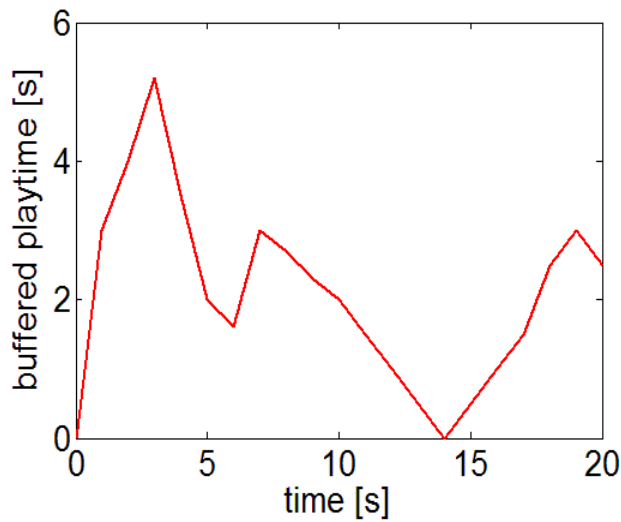
a) HTTP Downloads and YouTube

In this scenario the main performance metric is the buffered playtime of the YouTube video. The three best effort download users generate heavy load in the cell so that the buffered playtime is affected. Figure 3 gives the results for RRS. Figure 3(a) shows the throughput that is almost equal for all users and will only be influenced by the transmission channel conditions of moving users. Figure 3(b) shows the buffered playtime of the YouTube video over the simulation time. It can be seen that there is an initial buffering and a stalling at 14s.
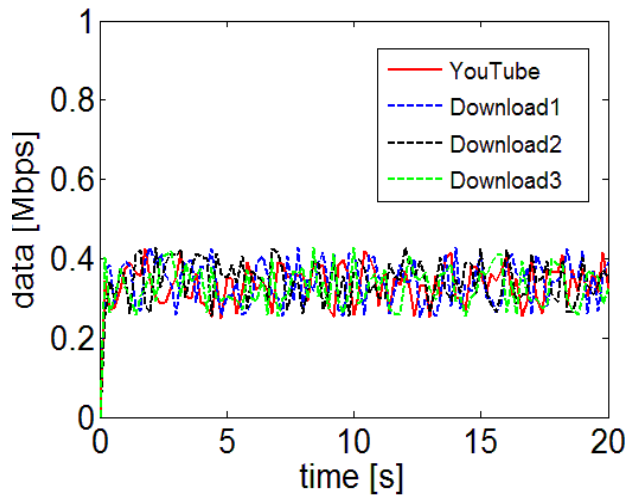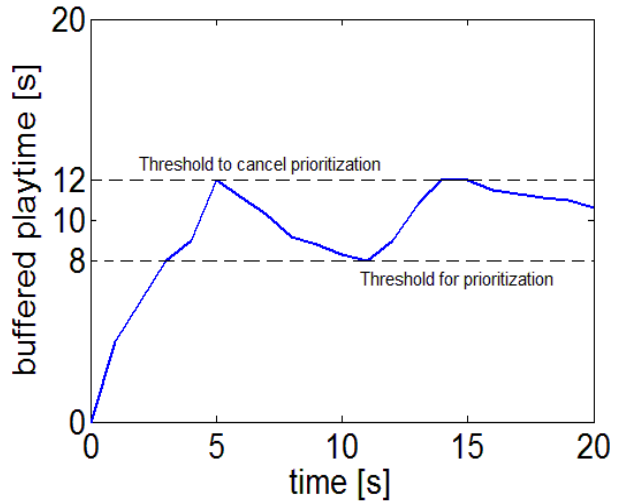
a) Throughput
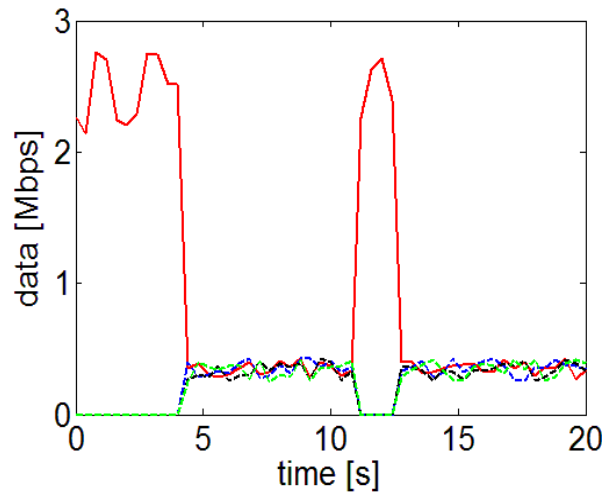
a) Throughput

b) Buffered Playtime of YouTube video

Fig. 3. RRS with 3 download users and one YouTube user
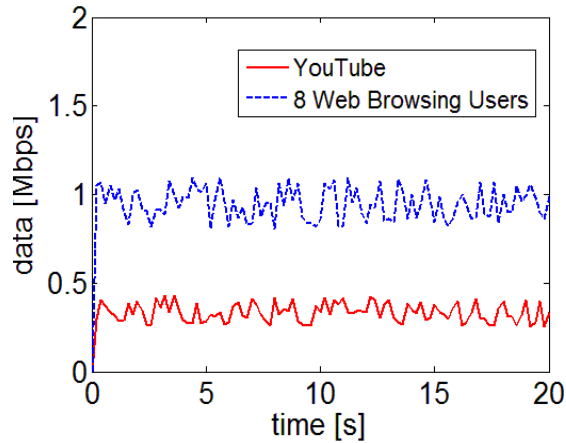

b) Buffered Playtime of YouTube video

Fig. 4. Buffered playtime scheduler with three download users and one YouTube user
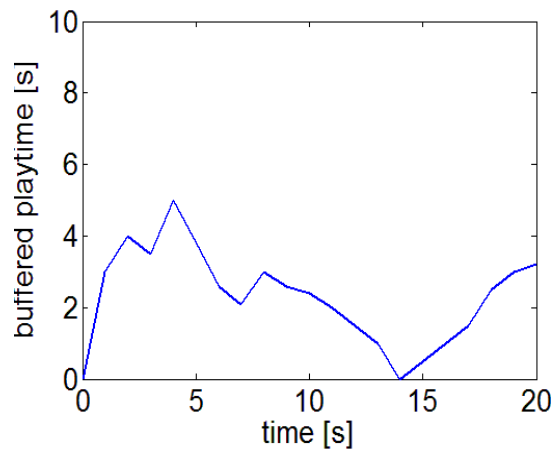
b)   Web Browsing and YouTube

Figure 4(a) shows the throughput when BVS is used. The red curve shows the YouTube flow that is prioritized in the beginning and for 1.5 s at about 11s due to the scheduling strategy. Almost no data of the download users is transferred at these time periods. Outside these periods scheduling is done as in RRS strategy. For the download users the download time increases from 4s to 5s However, the YouTube user does not experience any stalling. This is showed in Figure 4(b). It can also be seen that if the buffer level is higher than β (12s), round robin scheduling is used. If the buffer level falls below α (8s), YouTube video is prioritized again.

This section shows the results of a simulation for a YouTube user and a different number of web browsing users. The results show similar benefit of using BVS over RRS, as in the previous case of HTTP downloads. It is also analyzed that the knowledge of the exact buffer level (α and β) of the YouTube video helps to keep the impact on the web browsing users at minimum.

Figure 5(a) shows the throughput when a RRS is used with 8 web browsing users and one YouTube user. The figure shows very low throughput for the YouTube user. This results in a stalling at 14s that can be seen in Figure 5(b).

(a) Throughput round robin scheduler, 8 web users

(b) Buffered playtime of YouTube video

Fig. 5. Web browsing with one YouTube video

Figure 6 shows three curves that represents the buffered playtime of different schedulers (RRS, BVS with α of 8s and β of 12s, BVS with α of 9s and β of 10s) for 7 web users. It can be seen that for BVS (β=12s) there is no significant decrease in the buffer when it reaches 12s. This effect is due to the initial buffer level which is able to compensate the variable encoding of the video for the whole simulation time. On the other hand, although the buffered playtime is lower for BVS (β=10s), it has an advantage that the data transmission of web browsing users is delayed for a shorter time period in comparison to BVS (β=12s).

We conclude that preventing the YouTube video from stalling is achieved by delaying the web pages in favor of the YouTube flows.

III. ANALYSIS OF THE PROPOSED BVS

In this section we analyze our BVS for a real LTE network. First, here we have assumed that the YouTube server is present at the cell base station and the scheduler always has the video data available to schedule. Whereas in a real network YouTube

server has to be accessed by the base station through the core network in order to schedule the video flow to the end user. The core network comprises of Internet as well that can have packet drop and delays due to congestion. This may result in affecting the periodic buffer refilling of YouTube video. This does not deny the advantage which our BVS scheme provides.

Second, we assume a logical feedback channel for getting the buffer threshold (α and β) values at the scheduler. In a real network this requires signaling. Here we do not analyze how much this extra signaling is beneficial in terms of enhancing user perceived quality of the YouTube video and the cost it takes to perform this signaling.

Third, signaling and control channels are simulated as error free. Whereas in a real wireless environment there can be channel quality issues. Furthermore, we consider a single cell environment. Therefore, the effect of cell handoff on TCP, and hence on the buffered playtime, is not analyzed.

Moreover, we have although taken care of stalling of the YouTube video by using BVS, but if the YouTube user decides to stop watching the video or switch to another video, then the progressive download, which is the buffered playtime, would be waste of resources. This problem can be addressed by the HTTP based adaptive streaming [14].
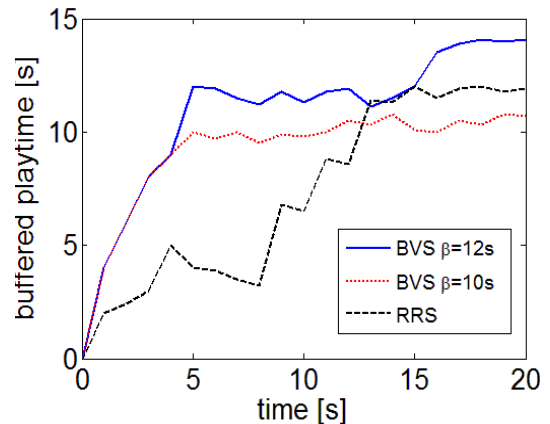

Fig. 6. Web browsing with one YouTube video

IV. CONCLUSION

In this paper we proposed an application-state aware QoE oriented scheduling, BVS. First, a YouTube video together with best-effort downloads is simulated. It shows that overall QoE of the YouTube user can be improved at expense of increased download time. Second, BVS is evaluated by simulating HTTP web browsing users along with a YouTube video. The impact on web browsing users is presented that shows that they are only affected if the YouTube player runs out of buffered video data.

After analyzing our scheme, the suggested future work can be to do an economic analysis of the extra signaling required for buffer feedback and consider other applications for the concept of QoE-oriented and application aware scheduling. In case of more than one YouTube users the effect of prioritizing one YouTube video flow over another YouTube user can also be investigated. Furthermore, a YouTube user has an option to change the video quality, so the effectiveness of BVS can also be analyzed in case the user often varies the video quality. The comparison of BVS with proportional fair scheduler or maximum rate algorithm can also be examined.

REFERENCES

[1] 3GPP, TS 36.300 V10.5.0; Evolved Universal Terrestrial Radio Access (E-UTRA) and Evolved Universal Terrestrial Radio Access Network (EUTRAN); Overall description, 3GPP Std., Sep. 2011.

[2] Cisco, "Cisco Visual Networking Index: Global Mobile Data Traffic Forecast Update, 2012-2017," Feb. 2013.

[3] Raheel, M.S.; Raad, R.; Ritz, C., "Efficient utilization of peer's upload capacity in P2P networks using SVC," in *Communications and Information Technologies (ISCIT), 2014 14th International Symposium on* , vol., no., pp.66-70, 24-26 Sept. 2014

[4] M. S. Raheel, R. Raad, and C. Ritz, (2015) "Achieving maximum utilization of peer's upload capacity in p2p networks using SVC," Peer-to-Peer Netw. Appl. pp. 1-15

[5] Pervez, F.; Raheel, M.S., "QoE-based network-centric resource allocation for on-demand uplink adaptive HTTP streaming over LTE network," in *Application of Information and Communication Technologies (AICT), 2014 IEEE 8th International Conference on* , vol., no., pp.1-5, 15-17 Oct. 2014

[6] Baraković, Sabina, and Lea Skorin-Kapov. "Survey and challenges of QoE management issues in wireless networks." Journal of Computer Networks and Communications 2013 (2013).

[7] Raimund Schatz, Tobias Hossfeld, Lucjan Janowski, and Sebastian Egger. From Packets to People, Quality of Experience as New Measurement Challenge. Springer's Computer Communications and Networks series, 2012.

[8] Apple Inc Press Information: http://www.apple.com/pr/library/2007/06/20YouTube-Live-on-Apple-TV-Today-Coming-to-iPhone-on-June-29.html

[9] Alcock, S. and Nelson, R., "Application flow control in YouTube video streams," ACM SIGCOMM Computer Communication Review, vol. 41, no. 2, pp. 24–30, 2011.

[10] Alcock, Shane, and Richard Nelson. "Application flow control in YouTube video streams." ACM SIGCOMM Computer Communication Review 41.2 (2011): 24-30.

[11] Pablo Ameigeiras, Juan J. Ramos-Munoz, Jorge Navarro-Ortiz and J. M. Lopez-Soler, ' Analysis and modelling of YouTube traffic", Transactions on Emerging Telecommunications Technologies, Trans. Emerging Tel. Tech. 2012; 23:360–377

[12] Schatz, Raimund, Tobias Hossfeld, and Pedro Casas. "Passive youtube QoE monitoring for ISPs." Innovative Mobile and Internet Services in Ubiquitous Computing (IMIS), 2012 Sixth International Conference on. IEEE, 2012.

[13] Cheng, Xu, Jiangchuan Liu, and Cameron Dale. "Understanding the characteristics of internet short video sharing: A YouTube-based measurement study." Multimedia, IEEE Transactions on 15.5 (2013): 1184-1194.

[14] Famaey, Jeroen, et al. "On the merits of SVC-based HTTP adaptive streaming."Integrated Network Management (IM 2013), 2013 IFIP/IEEE International Symposium on. IEEE, 2013.

Coverage and Capacity Trade-off Using Admission and Power Controlled CDMA System for Wireless Internet Services in Rural Environments

A. Kurniawan[1], I. Zakia[1], E. Wartika[2], and A.G. Austin[3]

[1]*School of Electrical Engineering and Informatics*
Institut Teknologi Bandung
Jalan Ganesa 10, Bandung, 40132, Indonesia
[1]adit@stei.itb.ac.id

[2]*Study Program of Film and Television*
Institut Seni Budaya Bandung
Jalan Buahbatu 212, Bandung, 40265, Indonesia
[2]enok_wartika@yahoo.com

[3]*Faculty of Civil Engineering and Environment*
Institut Teknologi Bandung
Jalan Ganesa 10, Bandung, 40132, Indonesia
[3]azmighalib@yahoo.co.id

Abstract— In this paper the coverage and capacity of CDMA system is evaluated using admission and power control to serve for low to medium speed internet services, such as digital TV or film/video streaming in rural areas. One of the unique characterstics of CDMA system is that it is possible to trade off between capacity and its coverage, called the cell-breathing. Open loop and closed loop power control can be used to increase the capacity of CDMA system; while admission control can be applied to trade-off between its capacity and the coverage. Computer simulation was conducted to evaluate the power control performance in Rayleigh fading channel. Then semi-analytical evaluation was performed to obtain the coverage-capacity trade-off. The result shows that the capacity of CDMA systems increases when power control was employed. Numerical and semi analytical evaluation show that CDMA coverage and capacity can be traded-off to meet various demand of traffic capacity and cell coverage in rural environments.

Keywords— *Capacity*; *CDMA*; *coverage*; *digital TV*; *film/video streaming*; *power control*; *rural area*.

I. INTRODUCTION

Direct Sequence Code Division Multiple Access (DS-CDMA) system requires a tight power control in order to overcome the near-far problem and to mitigate the effect of multiple access interference among CDMA users in cellular and mobile channel environments. The near-far problem can be solved by an open loop power control algorithm, but the effect of multiple access interference due to multipath fading requires a closed-loop algorithm when the uplink and downlink frequencies are not the same in a frequency duplexing (FDD) scheme [1]. Fading channel significantly degrades the performance of CDMA systems because communication over fading channels requires higher power

levels, and thus producing higher unwanted multiple access interference among CDMA users.

Uplink CDMA power control is more important compared to that on the downlink because uplink signals consist of all users from different locations (different path losses), while the downlink signals originate from the same base station and arrive at mobile stations with the same power level [1]. This paper shows that the use of power control is effective to produce reliable and high capacity of CDMA system. This paper also shows that when the capacity is reduced, then the CDMA system can provide wider area coverage. This unique characteristics of CDMA system is called the cell breathing capability of the CDMA systems [2].

The rest of the paper is organized as follows. Section II presents the CDMA signal and channel models. Section III describes the power controlled CDMA systems. Section IV presents the capacity-coverage trade-off in CDMA systems. Finally, Section V concludes the paper.

II. CDMA SIGNAL AND CHANNEL MODELS

A. CDMA Signal Model

DS-CDMA baseband signal model of system with *K*-users that employs shared frequency spectrum is shown in Fig. 1 [3]. Signaling interval for each user's data symbol is *T* seconds, and the input data symbols is a sequence of binary symbols {+1, -1}. Spreading codes are unique for each user with a chip rate higher than the rate of the symbol data rate belongs to each user, so each symbol will contain many spreading chips as shown in Fig. 1 (a). In the frequency domain the data symbols for each user before undergoing the process of spreading has a narrow spectrum, and after experiencing the process of spreading will have a wider frequency spectrum, as shown in Fig. 1 (b).
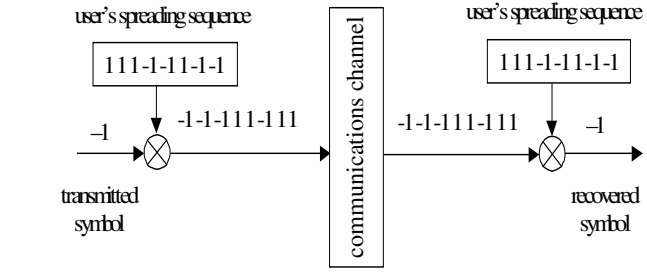
(a) Time domain
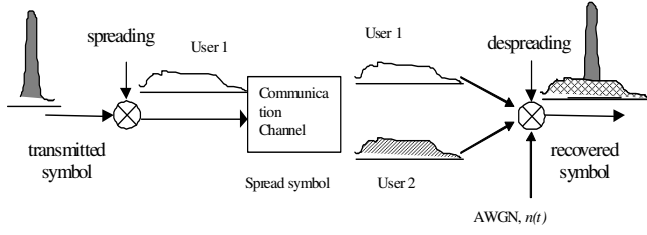
(b) Frequency domain

Fig. 1 CDMA signal model [4]

Each user CDMA signal is sent to the communication medium (channel), in that in the mobile wireless system it will experience multi-path propagation. At the receiver side, the single-user detection perform the reverse process of spreading (despreading) to recover the data symbols transmitted by each user. At the symbol signaling interval, the i-th input vector for the CDMA system is $x_i = (x_i^1, ..., x_i^k)^T$, with x_i^k is the i-th input symbol for the k-th user. The k-th user ($k = 1, ..., K$) will be allocated a spreading code $c_k(t)$ in the time interval $[0, T]$ which is normalized to [4]

$$\int_0^T c_k(t)^2 dt = 1 \qquad (1)$$

If the i-th symbol interval for the k-th user has a_i^k channel attenuation and transmission delay of τ_k, then the baseband signal of the k-th user using a single path ptropagation is

$$y^k(t) = \sum_{i=0}^{\infty} x_i^k a_i^k c_k(t - iT - \tau_k) \qquad (2)$$

The signal received by each user on the detector is the sum of signals from all users plus $n(t)$ as an additive white Gaussian noise noise (AWGN), written as follows:

$$y(t) = \sum_{k=1}^{K} y^k(t) + n(t) \qquad (3)$$

which will undergo a filtering process (matched filter) at the receiver to generate statistical variables for the detector/decorelator.

B. CDMA Channel Model

In wireless communication system, signal transmitted by each user will suffer from multipath propagation. Fig. 2 illustrates the uplink CDMA channels in a wireless communication system [4]. At the basestation, the kth user recovers the transmitted symbol by correlating the received signal with the kth user spreading sequence. Due to non-zero crosscorrelations between spreading sequences of different users, the kth user will observe multiple access interference from the other K-1 users.

If the received power levels at the basestation are not equal, the correlating receiver may not be able to detect the weak user's signal due to high interference from other users with higher power levels.
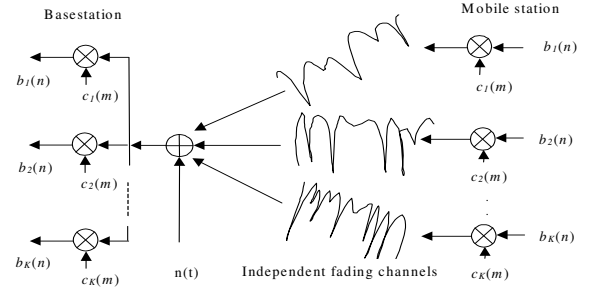

Fig. 2 CDMA uplink channel model [4].

Clearly, if a user signal is received with a weak power, it will suffer from the interference generated by stronger users' signals. Therefore power control in the uplink is very important to keep the interference acceptable to all users and to obtain a considerable channel-capacity improvement.

III. POWER CONTROL OF DS-CDMA SYSTEMS

A. Open LoopPower Control

An open loop power control algorithm can be used to overcome the near-far and shadowing problems on the reverse link of a CDMA system [3]. The open-loop power control is designed to ensure that the received powers from all users are equal in average at the basestation. In the open-loop algorithm, the mobile user can compute the required transmit power by using an estimate from the downlink signal (no feedback information is needed), because the large-scale propagation loss is reciprocal between uplink and downlink channels. Fig. 3 (a) shows how an open-loop power control algorithm solves the near far problem in the reverse link of a CDMA system.

In Fig. 3 (a), user 1 located at distance d1 from the basestation receives a power level P_{r1} [3]. This power level is higher than that received by user 2, P_{r2}, who is located at distance d2 from the base station because d1 < d2. Therefore to deliver an equal power received at the basestation, user 2 must transmit a higher power level than user 1 or $P_{t2} > P_{t1}$.

(a) Near-far distance problem

Delay spread

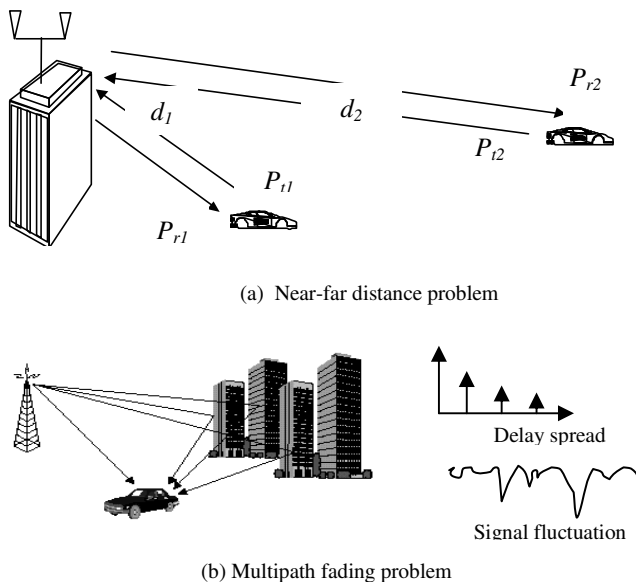Signal fluctuation

(b) Multipath fading problem

Fig. 3 Wireless Channel Model in Cellular Mobile Communications [3]

The procedure to determine the transmit power can be expressed as

$$P_t = -P_r + P_{off} + P_p, \qquad (4)$$

where P_t (dBm) is the required transmit power for a mobile user, P_r (dBm) is the received power at the mobile, P_{off} (dB) is the offset power parameter, and P_p (dB) is the power adjustment parameter. The power adjustment parameter is used to compensate for differences with regards to different cell sizes and shapes, basestation transmit power, and receiver sensitivities. The offset power parameter is also used to compensate for different frequency bands, i.e. $P_{off} = -76$ dB for the 1900 MHz and $P_{off} = -73$ dB for the 900 MHz frequency band [3].

We also need to consider the power control parameters, such as the dynamic range, power-update rate, and power-update step size. To illustrate the dynamic range, consider one user that is located at 100 m away from the basestation and another user is at 10 km from the same basestation. Using the path loss equation shown as [3]

$$L_p(d) = L_{d0} + 10\,n.\log\left(\frac{d}{d_0}\right). \qquad (5)$$

the received power of the first user is 80 dB higher than the second user if they are located in an environment that has a path loss exponent $n = 4$. Therefore, the dynamic range can be very large and requires large and fast power-update rate which depends on the measurement period of the downlink signal. A higher power-update rate will require a shorter measurement period [5]. If measurement period is too long it may average out the effect of shadowing and therefore open-loop power control may not compensate for the shadowing effect. On the other hand if the measurement period is too short, rapid fluctuation due to multipath may still exist and may not give an accurate result for the mean power measurement. The

method described in [6]-[7] can be referred to, to perform a good measurement method of the mean received power in a fading environment. In [8] an optimal technique for estimating a local mean signal is also presented.

B. Closed Loop Power Control

In CDMA systems, channel characteristics differs between the communication link from base station to mobile station (downlink) and the link from mobile station to base station (uplink). In the downlink, the spread signals for all users are transmitted synchronously by the base station because they originate from the same location (base station). These signals will go into the same multipath fading channel, experience the same propagation path loss, and fade simultaneously.

In the uplink, signals from different mobile users are subject to different propagation mechanisms, resulting in different propagation path losses and independent fading that lead to unequal received power levels at the base station. When non-orthogonal spreading sequence of unequal received power levels arrive at the base station, multiple access interference becomes a serious problem [9].

At the base station, the user despreads the transmitted symbol by correlating the received signal with the user spreading sequence. Due to non-zero cross correlation between spreading sequences of different users, the user will observe multiple access interference from the other users. If the received power levels at the base station are not equal, the correlating receiver may not be able to detect the weak user's signal due to high interference from other users with higher power levels.

Clearly, if a user is received with a weak power, it will suffer from the interference generated by stronger users' signals. Therefore power control in the uplink is very important to keep the interference acceptable to all users and to obtain a considerable channel-capacity [10]. In this paper power control is considered for the uplink CDMA channel based on SIR measurement as shown in Fig. 4.

For uplink power control, the mechanism of predictive power control algorithm proceeds as follows. First, the SIR for each user, $\gamma(i)$ is measured at the base station for the ith time slot. Due to the feedback delay introduced in the power control loop, the SIR for the ith time slot needs to be predicted D step ahead, where D is the total feedback delay introduced in the loop. Here the feedback loop delay is introduced in the power control algorithm due to measurement time, processing and propagation time of the command bits [10]. Therefore in Fig. 4, $\gamma(i)$ is predicted using the past SIR measurements to obtained the predicted value of SIR for the ith time slot, $\gamma_{pred}(i)$. We use the SIR predictor to obtain $\gamma_{pred}(i)$ using the past input samples [11]. The predicted SIR for the ith time slot $\gamma_{pred}(i)$ is then compared with the target SIR γ_t to produce the error signal $e(i)$. The error signal $e(i)$ is then quantized using a binary representation, so it can be transmitted via the downlink channel to instruct the mobile stations to increase or decrease their transmit power. The quantized form of error signal is called the power control command (PCC) bits, which can be implemented using a pulse code modulation (PCM)

realization of mode q, where q is the number of PCC bits required in each power control interval [9].

After the PCC bits are received by a mobile station, the mobile station computes the required power adjustment, Δp x PCC. The step size Δp is preset at 1 or 2 dB [7], while the PCC is either {+1, -1} in a fixed-step algorithm (q=1) or any integer between $-q$ and $+q$ in a variable-step algorithm.
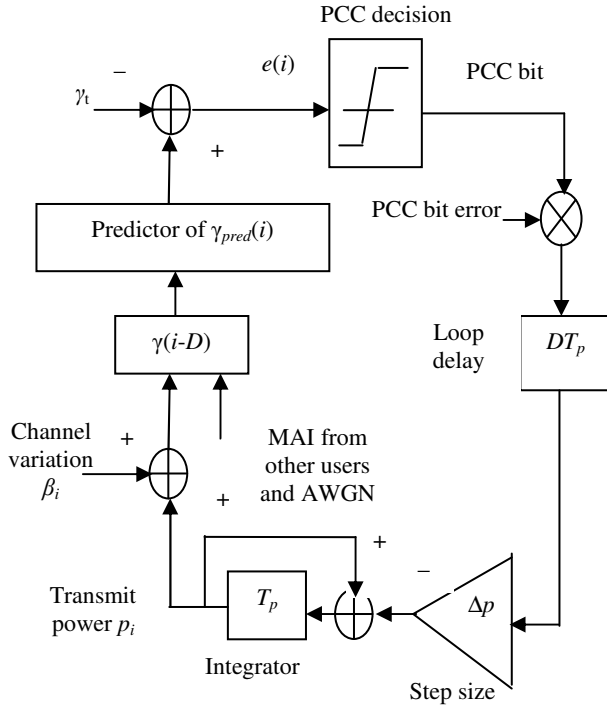

Fig. 4. Closed loop power control algorithm

The difference between the predicted and the desired *SIR* after quantization $e(i)_q$ is sent to the mobile to adjust the mobile's transmit power by Δp. $e(i)_q$ dB. Assuming the PCC bits are error free, in the absence of channel predictor, the transmit power at the next interval is

$$p(i+1) = p(i) - \Delta p \cdot e(i-D)_q. \tag{6}$$

For the fixed step algorithm (q=1) the PCC bit can be expressed as

$$\text{PCC bit} = sign[e(i-D)_{q=1}] = \begin{cases} +1 & e(i-D) < 0, \\ -1 & e(i\text{-}D) \geq 0 \end{cases} \tag{7}$$

where $e(i\text{-}D)$ is the power control error at the (i-D)th power control interval designating DT_p loop delay from the ith control interval.

IV. NUMERICAL SIMULATION AND RESULTS

A. Power Control Performance of DS-CDMA System

A single-cell CDMA system with the varying number of users K is assumed in the simulation, to see its effect on BER

performance is considered. To reflect a practical situation, all users are considered in motion with different vehicle's speeds and thus have different maximum Doppler spreads.

We model this situation by varying the users' vehicle speeds from 10 to 10 k km/h at 10 km/h interval (i.e., the speed of the kth user is $v_k = 10 k$ km/h for $k = 1, 2, ..., K$). Carrier frequency $f_c = 1.8$ GHz is used, so that the corresponding maximum Doppler spreads, f_D for the users are approximately ranging from 17 to 17 k Hz at 17 Hz interval [1]. The power-update rate of 1.5 kHz is considered, which corresponds to the power control interval $T_p = 0.667$ ms. SIR measurement is performed during a period of one time slot that corresponds to one power control interval $T_p = 0.667$ ms [12]. The DS-CDMA processing gain is $M = 128$ and the modulation scheme is QPSK with a data rate $R_b = 64$ kbps (symbol rate $R_s = 32$ ksps in QPSK scheme). The chip rate $R_c = 4.096$ Mcps is assumed in the simulation, resulting in each time slot to contain 2560 chips. Therefore, 20 binary symbols per time slot are available for SIR measurement. The simulation parameters is summarized in Table 1.

Table 1. Simulation parameters

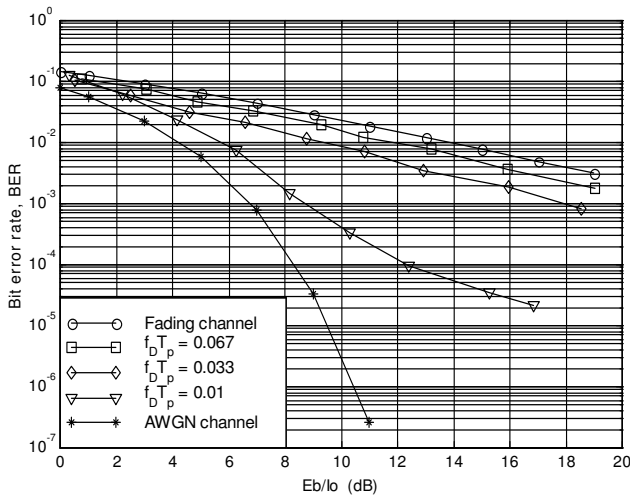| Parameter	Notation and value
Number of users	$K = 10$
Carrier frequency	$f_c = 1.8$ GHz
Vehicle's speed of the kth user	$v_k = 10.k$ km/h, $k = 1, 2, ..., K$
Maximum Doppler spread of the kth user	$f_{D,k} = 1.67 v_k$ Hz, $k = 1, 2, ..., K$
Processing gain	$M = 128$
Chip rate	$R_c = 4.096$ Mcps
Power control interval	$T_p = 0.667$ ms
Data rate	$R_b = 64$ kbps
Power update step size	$\Delta p = 1$ dB

The simulation is conducted for $f_D T_p = 0.01$, 0.033, and 0.067; then the performance is evaluated in terms of bit error rate (BER) as a function of bit energy-to-interference power density ratio (E_b/I_0). The simulation results for fixed step algorithm (q=1) and for variable step algorithm (with quantization level $q = 4$) are shown in Fig. 4 (a) and (b), respectively.

From Figure 4. (a) we can see that the fixed step power control is less effective at higher fading rates with $f_D T_p$ greater than 0.033. However it works effectively at slow fading channel, as it is shown by the BER performance at $f_D T_p = 0.01$. Similar behaviour is obtained with variable-step algorithm, i.e the performance improves with decreasing values of the parameter $f_D T_p$.
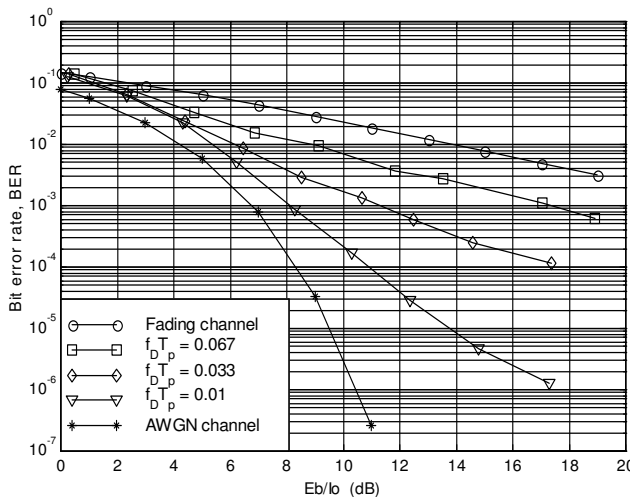
For the same value of $f_D T_p$, the variable step algorithm has a better performance than the fixed step size algorithm. We can see that to achieve BER = 10^{-3}, the required E_b/I_0 would be

approximately 7-18 dB, compared to that of fixed step algorith which requires E_b/I_0 of between 8 to more than 20 dB .

$$K = 1 + \frac{W}{R}\left[\frac{1}{E_b/I_0}\right] - \frac{1}{SNR} \qquad (9)$$
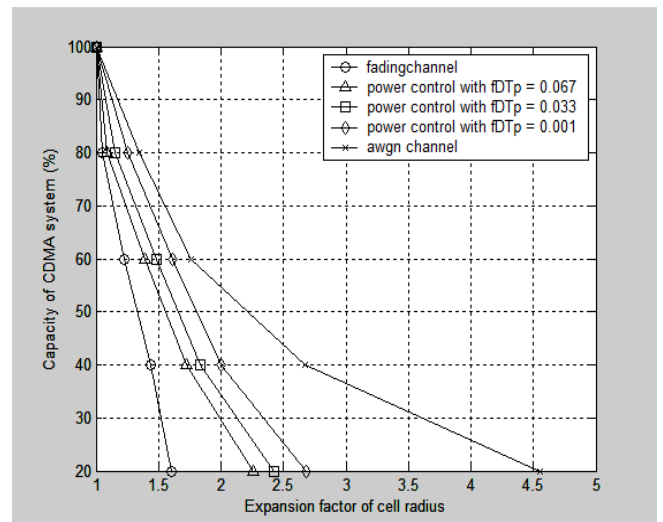
with SNR is the CDMA signal to AWGN noise ratio.

To evaluate the effect of the proposed method of power control on capacity of CDMA system, semi analytical evaluation was performed. As we can see that from Fig. 4 it can be seen that to achieve BER = 10^{-3} the required value of E_b/I_0 is between 7 to 18 dB, we can use this value to calculate the capacity of CDMA system based on (8) and (9).

We normalized the cell radius for the nominal capacity as 100 percent, based on the value of E_b/I_0 in (8) for BER = 10^{-3}, which is associated with the number of simultaneous user K in (9). The value of W/R remains the same of 128, and we assume thermal noise has 10 dB of SNR. Then we reduce the number of simultaneous user to 80, 60, 40, and 20 percent, respectively and its impact on the resulting value of E_b/I_0 is recalculated. Of course reduction of K will increase the value of E_b/I_0 for each user, resulting in link margin that can be transformed to the link budget. Using the well known propagation path loss as shown in (10), we can compute this.

$$L_{pu} \text{ [dB]} = \begin{array}{l} 69.55 + 26.16 \log f - 13.82 \log h_b \\ - a(h_m) + (44.9 - 6.55 \log h_b) \log d \end{array} \qquad (10)$$

where h_b is the antenna tower height, h_m is the receiver antenna height, d is the propagation distance, and L_{pu} is the propagation path loss. We can then use the slope of propagation power loss factor over distance of approximately 40 db/decade for antenna tower height of around 6-7 meters from the ground level.

The capacity-coverage trasformation or trade-off is shown in Fig. 5. This unique characteristics of CDMA system can be used to serve for wireless internet services, such as low to medium speed digital TV/video/film streaming in rural areas, where users are often scattered in small groups over a wide area. In other words, the CDMA system is flexible to serve various traffic capacity and/or coverage areas.

(a) fixed-step algorithm;

(b) variable-step algorithm (q=4).

Figure 4. BER performance of power control for different fading rates.

B. Coverage and Capacity Trade-off in CDMA System

The capacity of CDMA system can be perceived as the number of simultaneous users using the same CDMA carrier. When the number of user K each of which has a data rate of R shares the same CDMA carrier using a CDMA chip rate of W, then the resulting signal to interference ratio per bit E_b/I_0 can be expressed as

$$\frac{E_b}{I_0} = \frac{P/R}{[\sigma_n^2 + (K-1)P]/W} \qquad (8)$$

where P is the power level of each CDMA user, and σ^2 is the average power of thermal noise (AWGN). By eliminating K and dividing the numerator and denumerator by P, the number of users can then be written as

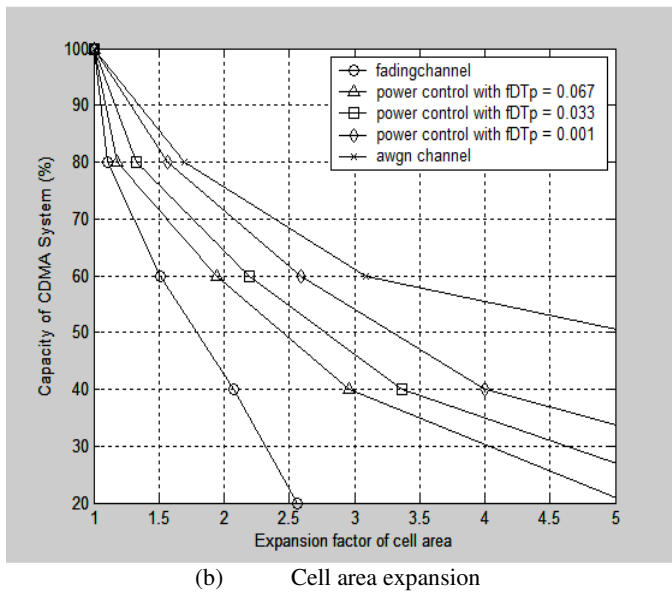(a)   Cell radius extention

(b)   Cell area expansion

Fig. 5 Coverage-capacity Trade-off in CDMA system

As we can see from Fig. 5 (a) that when the CDMA capacity is set to 80 % of its nominal load, it can strech up the cell radius by a factor of between 1.1 to 1.3, or expand the cell area by a factor of 1.2 to 1.7. If the CDMA capacity is set to 60 %, it can stretch up the cell radius by a factor of 1.2 to 1.8, or expand the cell area by a factor of 1.4 to 3.2.

V.   CONCLUSION

The need of power control to overcome multiple access interference of CDMA systems in fading channel environment has been presented. The performance of power control depends on fading rates. The variable-step algorithm is shown to outperform the fixed-step algorithm. Since power control updating rate is constant, the effect of higher fading rate degrade the performance of power control.

The capacity of CDMA system is higher for lower values of E_b/I_0 which can be obtained when power control can perform well. When the number of simultaneous active user or the CDMA capacity is reduced, higher figures of E_b/I_0 received by active users increases their link margin that can be transformed to strecht up the cell radius or to expand the cell coverage. This charactersitic is suitable to serve for wireless internet services, such as low-to-medium speed digital TV/video/film streaming in rural areas, where users are often scattered in small groups over a wide area.

ACKNOWLEDGEMENT

VI.   REFERENCES

[1] A. Kurniawan, Iskandar, and S. Machdar "Improved Predictive Power Control of CDMA System in Rayleigh Fading Channel," *Makara Journal of Technology*, Vol 13, No. 1, 2009.

[2] K.S. Gilhousen, et al., "On the Capacity of a Cellular CDMA System," IEEE Transaction on Vehicular Technology, vol. 40, pp. 303-312, May 1991.

[3] A. Kurniawan, *Predictive Power Control in CDMA Systems.* PhD dissertation, Institute for Telecommunications Research, University of South Australia, 2002

[4] A.Kurniawan, "Power-Controlled Multicarrier and Multiuser Detection Techniques in Wireless CDMA Systems, *International Journal on Electrical Engineering and Informatics,* Vol. 6, No. 3, Sept 2014 pp. 618-630

[5] A. Kurniawan, "Effect of feedback delay on fixed step and variable step power control algorithms in CDMA systems," in *Proceedings of the 8th International Conference on Communication Systems* (ICCS) 2002, Singapore, CD-ROM 3P-02-04, November 2002.

[6] F.C.M. Lau and W.M. Tam, "Novel SIR-estimation-based power control in a CDMA mobile radio system under multipath environment," *IEEE Transactions on Vehicular Technology*, vol. 50, no. 1, pp. 314-320, January 2001.

[7] K. S. Gilhousen, I. M. Jacobs, R. Padovani, and L. A. Weaver, Jr., "Increase capacity using CDMA for mobile satellite communications," *IEEE Journal on Selected Areas in Communications*, vol. 8, no. 4, pp. 503-513, May 1990.

[8] A. Chockalingam, P. Dietrich, L. B. Milstein, and R. R. Rao, "Performance of closed-loop power control in DS-CDMA cellular systems," *IEEE Transactions on Vehicular Technology*, vol. 47, no. 3, pp. 774-778, August 1998.

[9] C. J. Chung, J. H. Lee, and F. C. Ren, "Design of power control mechanisms with PCM realization for the uplink of a DS-CDMA cellular mobile radio system," *IEEE Transactions on Vehicular Technology*, vol. 45, no. 3, pp. 522-530, August 1996S.

[10] Ariyavisitakul, "SIR-based power control in a CDMA system," in *Proceedings of IEEE Global Telecommunications Conference*, Orlando, USA, December 1992, pp. 868-873.

[11] A. Kurniawan, Iskandar, and Sayid Mazdar, "Predictive power control of CDMA systems in Rayleigh Fading Channel," submitted to *International Conference on Telematic System, Services, and Applications (TSSA) 2008, Institut Teknologi Bandung*, Desember 2008.

[12] "Physical channels and mapping of transport channels onto physical channels (FDD)," *Third Generation Partnership Project (3GPP) Technical Specification TS 25.211*, v2.5.0, October 1999.

Development of AVR Microcontroller-based Antenna Measurement Tool for Student Experimentation

Muhammad Ammar Wibisono[1], Achmad Munir[2]

Radio Telecommunication and Microwave Laboratory
School of Electrical Engineering and Informatics, Institut Teknologi Bandung
Jalan Ganesha 10 Bandung 40132 - Indonesia
[1]`ammarwibisono@gmail.com`, [2]`munir@ieee.org`

Abstract—A development of antenna measurement tool for student experimentation is proposed based on AVR microcontroller as main controller unit (MCU). The system of antenna measurement tool is expected to be low-cost and easy-to-use to overcome the problem in cost and complexity of the commercial tool. The proposed system which uses an AVR ATMega8535 as an MCU controls the position of antenna under test (AUT) in spherical coordinate using elevation-over-azimuth configuration. Mechanically, the system is implemented by stepper motor, gear system and a turntable for positioning the AUT on azimuth and elevation angle. The user interface of system is realized by a keypad and LCD display. From the result, it shows that the realized antenna measurement tool can handle a patch antenna of 50gram weight with the deviation angle of 1°. Meanwhile for a patch antenna of 100gram weight, the deviation angle increases to be 2.5°. In addition, due to the torque of antenna, the deviation on elevation angle becomes larger for the elevation angle closer to 180°.

Keywords—*Antenna measurement tool; antenna under test; AVR microcontroller; elevation over azimuth.*

I. INTRODUCTION

Antenna measurement is required to obtain the parameters of the antenna, e.g. radiation pattern, directivity, gain, polarization, bandwidth, return loss, VSWR and the impedance [1]. These parameters are essential for understanding the properties and performance of an antenna, especially in the study of antenna and wave propagation for electrical and telecommunication engineering students. Students are expected to conduct antenna measurement experiment in the lab in addition to the course and literature study in the class [2]. Therefore, an antenna measurement tool for student's experimentation in the lab is needed.

Since the commercial antenna measurement tool are relatively expensive and requires additional instrumentation device and software, a low cost and easy-to-use antenna measurement device is needed for student's experiment in the study of antenna and wave propagation [2]. To reduce the complexity and cost, the control system is simplified using AVR microcontroller as the MCU [6].

In this paper, the system design and realization of antenna measurement tool including hardware, software, mechanical construction and its realization is described. The hardware system is developed based on AVR microcontroller. The design will be implemented for educational purpose in the study of antenna system.

II. SYSTEM DESCRIPTION

The overall system of the antenna measurement tool consists of AVR ATMega8535 microcontroller as the MCU, LCD display and keypad as the user interface, L298 driver and stepper motor as the azimuth controller, servo motor as the elevation controller and mechanical system which consists of gear system, turntable and an arm [6]. The block diagram of system is shown in Fig. 1.
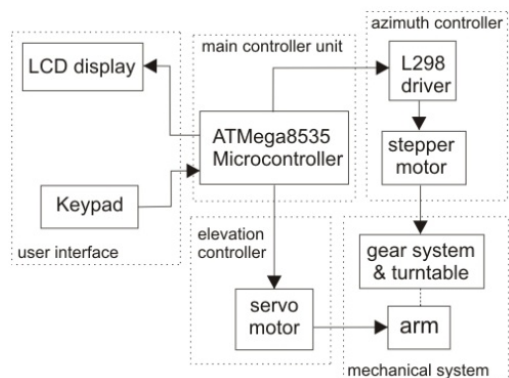

Fig. 1 Block diagram of system design

User enters the azimuth and elevation angle using the keypad, while the LCD displays the current angle. MCU produces pulse signals to drive the stepper motor via L298 dual H-Bridge IC [8][10], which moves the gear system and turntable to control the AUT at azimuth angle. To control the elevation angle of AUT, MCU directly sends PWM signal with certain pulse width to determine the angular position of servo motor's arm [4].

III. HARDWARE AND SOFTWARE SYSTEM DESIGN

A. MCU Module

AVR microcontroller provides some useful features as the MCU, e.g. basic I/O ports for interfacing with keypad, LCD, stepper motor, and 16-bits PWM channels for servo motor control [4], [9]. For further development, ADC on the MCU can be used to measure the field strength received by the AUT. USART and SPI interface on the MCU can also be used for communicating the system with other device, e.g. PC or data logger.

The MCU circuit shown in Fig. 2 uses 16 MHz crystal oscillator as the clock source. Pin PB0-PB7 are connected to keypad, PC0-PC7 to LCD display, PD0-PD3 to stepper motor, and PD4 (OC1B) to servo motor [6].
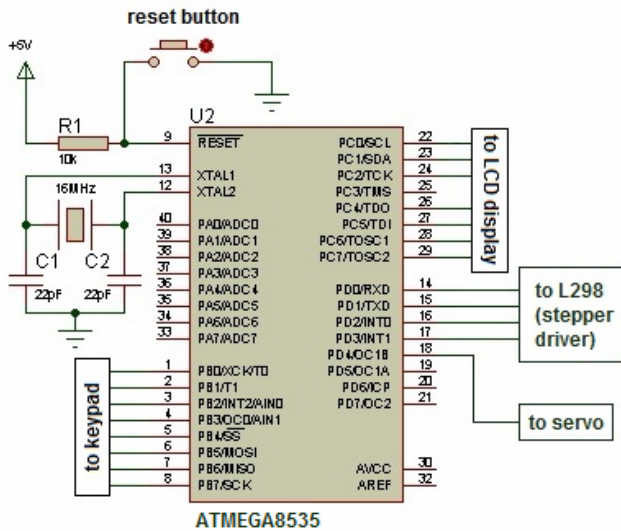

Fig. 2 MCU module circuit

B. Stepper and Servo Motor Module

MCU drives the stepper motor via L298 dual H-Bridge IC. The four input pins of L298 (IN1-IN4) are connected to pin PD0-PD4 of MCU, while its four output pins (OUT1-OUT4) are connected to the stepper motor. Two reverse-biased diodes are connected to each of the output pins of L298 for surpressing back e.m.f generated by the motor's coil when it undergoes transient state [3], [10].

On the other hand, MCU directly controls servo motor by giving PWM signals with 20 ms period from PD4/OC1B pin. The servo motor's angular position is proportional to the pulse width of the PWM signal. The range of the servo motor's angular position is 0^0 to 180^0. The circuit is shown in Fig. 3.
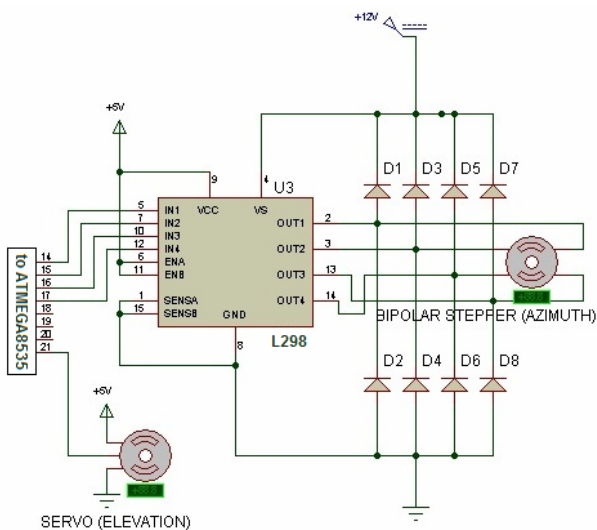

Fig. 3 Stepper and servo module circuit

Generally, the mechanical system consists of a turntable, gear system, and an arm. The system uses elevation-over-azimuth configuration [5], [7], in which the arm lies on the turntable. Majority of these parts are made from white acrylic, except the bearing, the rotator axis, and the horn gear which have to be made from metal. The gear ratio value is 5:9 (20 to 36 gears) to scale the stepper motor step angle from 0.9^0 to move the AUT at 0.5^0 step angle [6].

C. Keypad and LCD Module

User interface module is implemented using alphanumeric 16x2 characters LCD and 4x4 keypad. The LCD has 16 columns and 2 rows of character space, and the keypad has 16 buttons which include numbers, up/down button and some additional buttons for user interactions with the system. The circuit is shown in Fig.4.
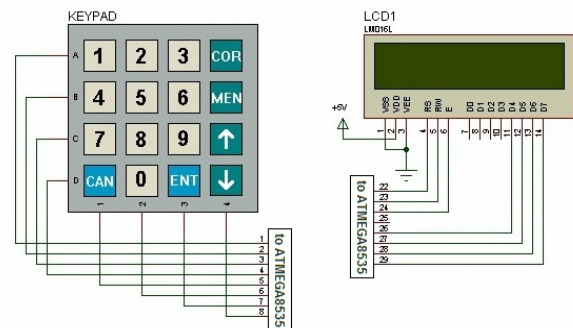

Fig. 4 LCD and keypad module

D. Software System Design

The software design for the MCU handles all of the input/output process in the system. Since there are no feedback, the only input process is keypad scanning. The output process, on the other hand, includes LCD displaying, servo and stepper motor control [6].

The working procedure of the software system can be described as follows. First, the MCU initialize the I/O ports, LCD and PWM channel. Then the user sets the initial elevation angle, calibrates azimuth angle, and sets the angle increment value for changing the azimuth/elevation angle. The user can change the azimuth and elevation angle while the MCU displays the current angle.

IV. HARDWARE REALIZATION AND CHARACTERIZATION
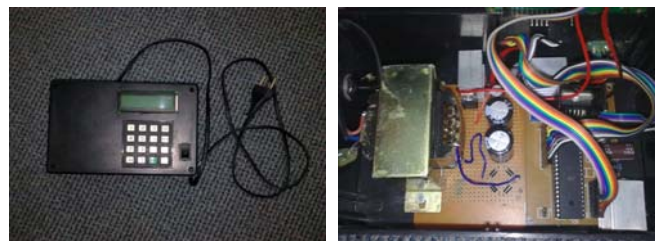
A. Realization of System

Fig. 5 Control module of the tool (left) and its inside part (right)

The mechanical system mostly made from 3mm thick acrylic, except for the axis and the bearing which have to be made from metal. Two SMA connectors are added for placing and connecting the AUT to the measurement devices like spectrum or vector network analyzer. A connector of DB9 is also used for connecting the mechanical system to the control module of the tool. The realized mechanical system of proposed antenna measurement tool is shown in Fig. 6.
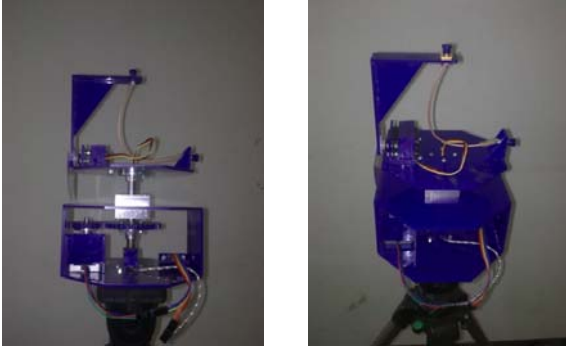

Fig. 6 The realized mechanical system

B. System Characterization

Characterization of system is performed to determine the accuracy of the tool at azimuth and elevation angle before load, i.e. AUT, is placed. Furthermore, accuracy testing of the tool at elevation angle is performed to obtain angle correction for the servo motor. Angle correction for the servo motor is done by updating the pulse width of the PWM signal from the microcontroller after the deviation angle of servo motor is obtained.

From the testing result, a maximum deviation angle of 1^0 is obtained. In this case, the correction for the azimuth angle can not be conducted because the stepper motor moves by a step angle of 0.9^0. For the elevation angle, the correction is carried out by updating the value of *OCR1B* register of the ATmega8535 microcontroller which determines the pulse width of PWM signal for controlling servo motor angular position or the elevation angle of AUT. The correlation between *OCR1B* register value and the angular position of servo motor is given by (1).

$$OCR1B = OCR1B_{\min} + k\theta \qquad (1)$$

where $OCR1B_{min}$ is the value of *OCR1B* register at 0^0 elevation angle and k is the servo motor constant. The accuracy testing result for elevation angle is shown at Fig. 7. After elevation angle correction, load test is performed to obtain maximum weight and dimension of AUT which yields maximum deviation angle of 1^0. The test is performed using 3 antennas with dimensions and weight as follows:

1. Patch antenna with dimensions of 61mm x 60mm and weight of 50gram.
2. Patch antenna with dimensions of 80mm x 80mm and weight of 100gram.
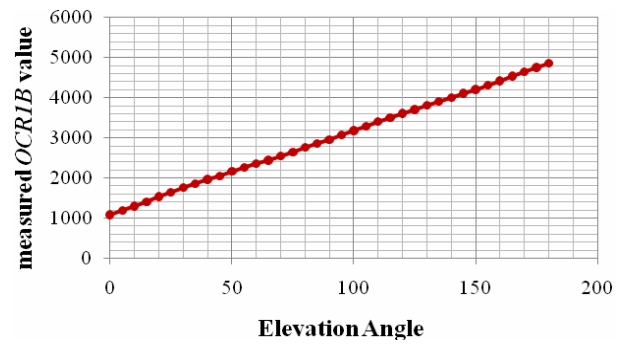3. Patch antenna with dimensions of 119mm x 75mm and weight of 100gram.

Fig. 7 Correlation between measured *OCR1B* value and the elevation angle

The load characterization of realized antenna measurement tool with 3 antennas is shown in Fig. 8. The result shows that antenna with weight of 50 grams gives a maximum deviation angle of 1^0, whereas another antenna with weight of 100 grams produce larger deviation angle of $2,5^0$. Deviation on elevation angle becomes larger when closer to 180^0 because of the torque from the antenna.

Fig. 8 The load test using patch antenna with dimensions of 61mm x 60mm and weight of 50grams (left), patch antenna with dimensions of 80mm x 80mm and weight of 100gram (center) and patch antenna with dimensions of 119mm x 75mm and weight of 100gram (right).

V. CONCLUSIONS

The development of antenna measurement tool for student experimentation using AVR ATMega8535 microcontroller have been successfully demonstrated. It has been shown that the proposed system of antenna measurement tool has provided some advantages such as reduction on complexity and cost and also makes the system more user-friendly. The realized system has been characterized to show the capability in handling the antenna with different dimension and weight. However, the system has had some limitations in which the maximum weight of AUT depends on the maximum torque of stepper motor. In addition, the precision of azimuth and elevation angle depends on the characteristic of the motors and the mechanical system fabrication.

REFERENCES

[1] J. D. Kraus, R. J. Marhefka, *Antennas for All Applications, 3rd edition,* New York: McGraw-Hill, 2002.
[2] C. A. Balanis, *Antenna Theory, Analysis and Design, 3rd ed.*, New Jersey: John Wiley & Sons Inc., 2005.
[3] G. C. Onwubolu, *Mechatronics Principles and Applications*, Oxford: Elsevier Butterworth-Heinemann, 2005
[4] D. V. Gadre, *Programming and Customizing AVR Microcontrollers*, New York: McGraw-Hill Companies Inc., 2001.

[5] Kummer, W. H. et al. *IEEE Standard Test Procedures for Antennas*, IEEE Std 149-1979 (R2008), New York. 2008.

[6] M. A. Wibisono and A. Munir, "Low Cost Small Antenna Measurement Tool Based on ATMega8535 Microcontroller," *International Conference on Electronics, Information and Communication (ICEIC)*, pp. 171-172, Jan.-Feb. 2013.

[7] G. F. Masters and S. F. Gregson, "Coordinate System Plotting for Antenna Measurements", *Antenna Measurement Techniques Association Conference*, 2007.

[8] I. A. Wibowo, M. Zarar, K. Al-Amin, and Fazliana, "Control Systems of a Turntable and Antenna Positioning Device in an Open Area Test Site", *International Conference on Intelligent and Advanced Systems (ICIAS)*, pp. 1-4, 2010.

[9] W. Weihong and X. Liegang, "Design and Implementation of a Control System using AVR Microcontroller," *International Conference on Image Analysis and Signal Processing*, pp. 320-323, 2009.

[10] Z. Yajun, C. Long, and F. Lingyan, "A Design of Elevator Control System Model", *IEEE International Conference on Neural Networks & Signal Processing*, pp. 535-538, 2008.

Analysis of Wave Characteristics between Cylindrical and Cartesian Coordinate System–based Structure Using FDTD Method

Nabila Husna Shabrina
Radio Telecommunication and Microwave Laboratory
School of Electrical Engineering and Informatics
Institut Teknologi Bandung
Bandung, Indonesia
nabila.husna@students.itb.ac.id

Achmad Munir
Radio Telecommunication and Microwave Laboratory
School of Electrical Engineering and Informatics
Institut Teknologi Bandung
Bandung, Indonesia
munir@ieee.org

Abstract—**Numerical computation is needed to solving the problem of electromagnetic waves. There are many methods that can be used to analyze electromagnetic waves like Method of Moment (MOM), Finite Element Method (FEM), Finite Volume Method, and also Finite Difference Time Domain (FDTD). FDTD is chosen because it has several advantages that are easy to understand has short development time and naturally explicit. In this work, FDTD will be used to modeling and comparing wave characteristic and propagation in 3D Cartesian and cylindrical coordinate. The size that used in 3D Cartesian structure is x = 60cm, y = 30cm, and z = 120cm whereas the dimension in cylindrical structure is r = 60cm, φ = 30 , and z = 120cm. The grid size of both structure is made equal so either Cartesian or cylindrical structure has identical Δt. TE mode is applied in this simulation with propagation along z-axis. The source for this simulation is sinusoidal wave modulated with Gaussian pulse with frequency 1GHz. The simulations are undertaken in some variations of condition. The first condition is for modeling free space in both Cartesian and cylindrical structure. The result is in the form of frequency cut-off for both structures. The second and the third are for modeling dielectric and conductive medium which objective is for observing the effect of adding these medium in wave propagation characteristic. The result from cylindrical structure will be analyzed and compared to the result of Cartesian structure.**

Keywords—*Cartesian coordinate; cylindrical coordinate; FDTD method; wave characteristics.*

I. INTRODUCTION

Electromagnetic energy has a very large applications ranging from communications, radar systems, electronics, and even medicine. However, the problem of electromagnetic wave is quite complex to be understood. Therefore, solving the problem of electromagnetic waves need numerical computation. With a fairly rapid growth in computing technology, numerical computation methods are becoming increasingly easy to do. There are many methods that can be used to analyze the electromagnetic waves such as the Method of Moment (MoM), Finite Element Method (FEM), Finite Volume Method and the Finite Difference Time Domain (FDTD) [1]. However, some of these methods have disadvantages which are requiring large memory. One method that is often used in analyzing the electromagnetic wave is the Finite Difference Time Domain (FDTD). Currently, the FDTD method is widely used in various applications because it has several advantages such as easy to understand, has short development time and naturally explicit. But there is also a disadvantage of FDTD method that is needs long computational time.

FDTD method is proposed by Kane Yee in 1966 [2]. This method is based on Maxwell Equation in differential form [3][4]. The fundamental algorithm of FDTD method is to updating magnetic and electrical field one after another using time leapfrog method [5]. The derivation of this algorithm is to discretize spatial and time components in Maxwell Equation. Implementation of the use of FDTD method in this work is to make the 3D modeling in Cartesian coordinates and cylindrical in some kind of wave propagation medium. The results of both these modeling will be analyzed and compared with each other.

II. 3D FDTD METHOD IN CARTESIAN AND CYLINDRICAL COORDINATE SYSTEM

A. Update Equation for 3D Cartesian Coordinate System

Placement of electric (E_x, E_y, E_z) and magnetic (H_x, H_y, H_z) field components on 3D Cartesian cell follows interleaving indexing system which placing the electric field on the center of the cube edge while the magnetic field is at the center of the cube surface, as shown in Fig. 1.
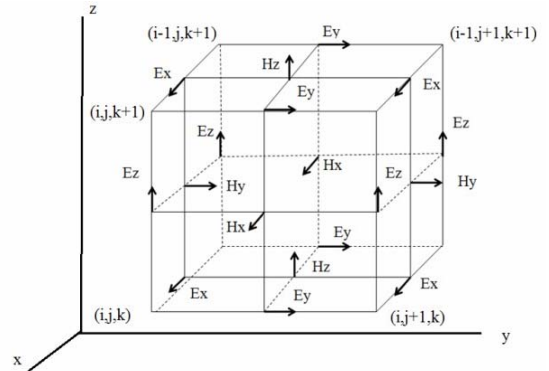

Fig. 1 Placement of electric and magnetic fields in a cell of 3D Cartesian coordinate system

Updating equation for 3D Cartesian coordinate system is obtained after deriving and discretizing differential form of Maxwell equation, as is given in (1)-(2).

$$E_x|_{i+1,j,k}^{n+1} = E_x|_{i+1,j,k}^{n} + \frac{\Delta t}{\varepsilon}\left[\frac{H_z|_{i,j+1,k}^{n+\frac{1}{2}}-H_z|_{i,j,k}^{n+\frac{1}{2}}}{\Delta y} - \right.$$

$$\left. \frac{H_y|_{i,j,k+1}^{n+\frac{1}{2}}-H_y|_{i,j,k}^{n+\frac{1}{2}}}{\Delta z}\right] \qquad (1.a)$$

$$E_y\big|_{i,j+1,k}^{n+1} = E_y\big|_{i,j+1,k}^{n} + \frac{\Delta t}{\varepsilon}\left[\frac{H_x\big|_{i,j,k+1}^{n+\frac{1}{2}}-H_x\big|_{i,j,k}^{n+\frac{1}{2}}}{\Delta z} - \right.$$

$$\left.\frac{H_z\big|_{i+1,j,k}^{n+\frac{1}{2}}-H_z\big|_{i,j,k}^{n+\frac{1}{2}}}{\Delta x}\right]$$

(1.b)

$$E_z\big|_{i,j,k+1}^{n+1} = E_z\big|_{i,j,k+1}^{n} + \frac{\Delta t}{\varepsilon}\left[\frac{H_y\big|_{i+1,j,k}^{n+\frac{1}{2}}-H_y\big|_{i,j,k}^{n+\frac{1}{2}}}{\Delta x} - \right.$$

$$\left.\frac{H_x\big|_{i,j+1,k}^{n+\frac{1}{2}}-H_x\big|_{i,j,k}^{n+\frac{1}{2}}}{\Delta y}\right]$$

(1.c)

$$H_x\big|_{i+1,j,k}^{n+\frac{1}{2}} = H_x\big|_{i+1,j,k}^{n-\frac{1}{2}} + \frac{\Delta t}{\mu}\left[\frac{E_y\big|_{i,j,k+1}^{n}-E_\emptyset\big|_{i,j,k}^{n}}{\Delta z} - \right.$$

$$\left.\frac{E_z\big|_{i,j+1,k}^{n}-E_z\big|_{i,j,k}^{n}}{\Delta y}\right]$$

(2.a)

$$H_y\big|_{i,j+1,k}^{n+\frac{1}{2}} = H_y\big|_{i,j+1,k}^{n-\frac{1}{2}} + \frac{\Delta t}{\mu}\left[\frac{E_z\big|_{i+1,j,k}^{n}-E_z\big|_{i,j,k}^{n}}{\Delta x} - \right.$$

$$\left.\frac{E_x\big|_{i,j,k+1}^{n}-E_x\big|_{i,j,k}^{n}}{\Delta z}\right]$$

(2.b)

$$H_z\big|_{i,j,k+1}^{n+\frac{1}{2}} = H_z\big|_{i,j,k+1}^{n-\frac{1}{2}} + \frac{\Delta t}{\mu}\left[\frac{E_x\big|_{i,j+1,k}^{n}-E_x\big|_{i,j,k}^{n}}{\Delta y} - \right.$$

$$\left.\frac{E_y\big|_{i+1,j,k}^{n}-E_y\big|_{i,j,k}^{n}}{\Delta x}\right]$$

(2.c)

B. *Update Equation for 3D Cylindrical Coordinate System*

In 3D cylindrical coordinate system, position of the electric (E_r, E_φ, E_z) and magnetic (H_r, H_φ, H_z) field in the cell is shown in Fig. 2.
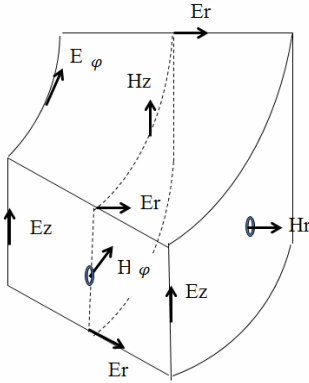

Fig. 2 Placement of electric and magnetic field in a cell of 3D cylindrical coordinate system

Updating equation for 3D cylindrical coordinate system is given in (3)-(4).

$$E_r\big|_{i+1,j,k}^{n+1} = E_r\big|_{i+1,j,k}^{n} + \frac{\Delta t}{\varepsilon}\left[\frac{1}{r}\frac{H_z\big|_{i,j+1,k}^{n+\frac{1}{2}}-H_z\big|_{i,j,k}^{n+\frac{1}{2}}}{\Delta\emptyset} - \right.$$

$$\left.\frac{H_\emptyset\big|_{i,j,k+1}^{n+\frac{1}{2}}-H_\emptyset\big|_{i,j,k}^{n+\frac{1}{2}}}{\Delta z}\right]$$

(3.a)

$$E_\emptyset\big|_{i,j+1,k}^{n+1} = E_\emptyset\big|_{i,j+1,k}^{n} + \frac{\Delta t}{\varepsilon}\left[\frac{H_r\big|_{i,j,k+1}^{n+\frac{1}{2}}-H_r\big|_{i,j,k}^{n+\frac{1}{2}}}{\Delta z} - \right.$$

$$\left.\frac{H_z\big|_{i+1,j,k}^{n+\frac{1}{2}}-H_z\big|_{i,j,k}^{n+\frac{1}{2}}}{\Delta r}\right]$$

(3.b)

$$E_z\big|_{i,j,k+1}^{n+1} = E_z\big|_{i,j,k+1}^{n} + \frac{\Delta t}{\varepsilon}\left[\frac{H_\emptyset\big|_{i+1,j,k}^{n+\frac{1}{2}}-H_\emptyset\big|_{i,j,k}^{n+\frac{1}{2}}}{\Delta r} - \right.$$

$$\left.\frac{H_r\big|_{i,j+1,k}^{n+\frac{1}{2}}-H_r\big|_{i,j,k}^{n+\frac{1}{2}}}{r\Delta\emptyset}\right]$$

(3.c)

$$H_r\big|_{i+1,j,k}^{n+\frac{1}{2}} = H_r\big|_{i+1,j,k}^{n-\frac{1}{2}} + \frac{\Delta t}{\mu}\left[\frac{E_\emptyset\big|_{i,j,k+1}^{n}-E_\emptyset\big|_{i,j,k}^{n}}{\Delta z} - \right.$$

$$\left.\frac{1}{r}\frac{E_z\big|_{i,j+1,k}^{n}-E_z\big|_{i,j,k}^{n}}{\Delta\emptyset}\right]$$

(4.a)

$$H_\emptyset\big|_{i,j+1,k}^{n+\frac{1}{2}} = H_\emptyset\big|_{i,j+1,k}^{n-\frac{1}{2}} + \frac{\Delta t}{\mu}\left[\frac{E_z\big|_{i+1,j,k}^{n}-E_z\big|_{i,j,k}^{n}}{\Delta r} - \right.$$

$$\left.\frac{E_r\big|_{i,j,k+1}^{n}-E_r\big|_{i,j,k}^{n}}{\Delta z}\right]$$

(4.b)

$$H_z\big|_{i,j,k+1}^{n+\frac{1}{2}} = H_z\big|_{i,j,k+1}^{n-\frac{1}{2}} + \frac{\Delta t}{\mu}\left[\frac{E_r\big|_{i,j+1,k}^{n}-E_r\big|_{i,j,k}^{n}}{r\Delta\emptyset} - \right.$$

$$\left.\frac{r_{i+1}E_\emptyset\big|_{i+1,j,k}^{n}-r_iE_\emptyset\big|_{i,j,k}^{n}}{r\Delta r}\right]$$

(4.c)

III. SIMULATION AND RESULT

Simulation is based on C language. The source for this simulation is plane source which is formed by sinusoidal wave modulated with Gaussian pulse with frequency 1 GHz. The boundary condition used in all simulation is PEC (Perfect Electric Conductor) which set the entire magnetic and electric component in the boundary as zero. The maximum time looping used in the program is 25000 iterations.
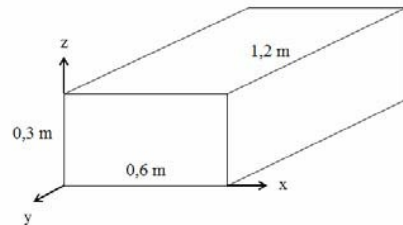
A. *3D Cartesian Coordinate System Simulation*

Fig. 3 3D Cartesian coordinate system structure

The dimensions used in modeling 3D FDTD based on Cartesian coordinate system are 0.6m x 0.3m x 1.2m, as given in Fig. 3. The grid $\Delta x, \Delta y$, and Δz are set as 0.01m. From that grid size we can calculate Δt value which indicates the amount of time required to execute one grid element. Δt Can be obtained from courant stability equation as shown below.

$$\Delta t = \frac{1}{3x10^8 \sqrt{\frac{1}{(0.01)^2} + \frac{1}{(0.01)^2} + \frac{1}{(0.01)^2}}}$$

$$\Delta t = 1.9285 \; x \; 10^{-11} \; s$$

Wave mode used in this simulation is TE mode with propagation along z-axis. The source uses electric component E_x to excite the wave. With the dimension mentioned before, we can calculate the cut-off frequency of the structure we made. Using the formula of waveguide's cut-off frequency, we obtain cut-off frequency TE_{01}= 500 MHz. Fig. 4 shows the result for modeling waveguide in free space medium. From the simulation we get first operating frequency of the structure 558,706 MHz.
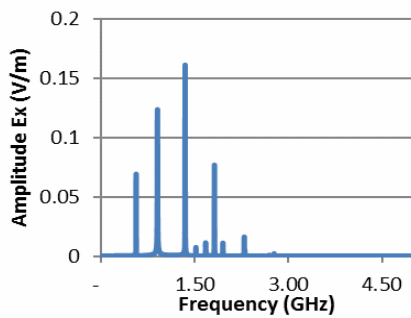

Fig. 4 Simulation result of 3D Cartesian coordinate system with free space medium

The second simulation is adding relative permittivity of the earth. First, the structure is used to modeling wet ground of the earth with ε_r 30. Second, the structure will be made as two layers, first layer for modeling wet ground while the second one is for modeling air. Third, the structure will be divided into three layers for modeling wet ground, water and air. The results can be seen in Figs. 5–7.
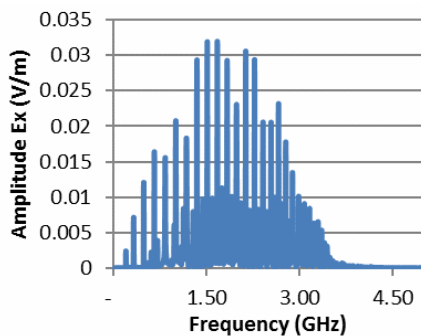

Fig. 5 Simulation results of 3D Cartesian coordinate system with one layer dielectric medium
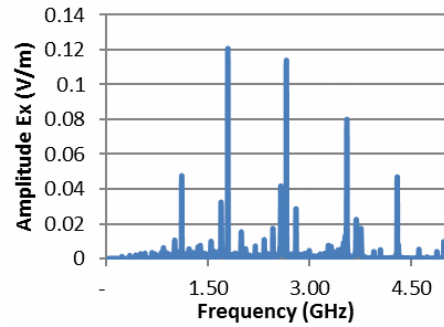

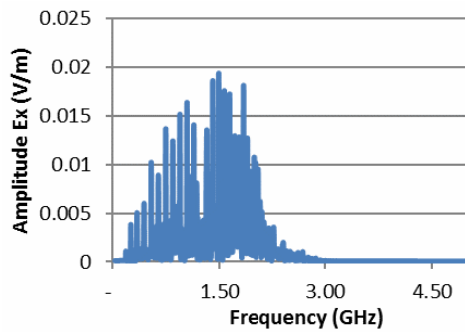Fig. 6 Simulation results of 3D Cartesian coordinate system with two layers dielectric medium

Fig. 7 Simulation results of 3D Cartesian coordinate system with three layers dielectric medium

For the first structure, calculation gives cut-off frequency 102.005 MHz while from the simulation we get 203.540MHz. In second structure, calculation gives result for the cut-off frequency 141.911MHz whereas from simulation the result is 224.309MHz. In the third structure, we get cut-off frequency 91.851MHz from the calculation and 178.617MHz from the simulation. The difference between the result from the calculation and simulation is because the first operating frequency which appeared in the structure is not at TE_{01} but TE_{20} mode. As state before, frequency input for the simulation is 1GHz so cut-off frequency that may be appear on the structure are TE_{01}, TE_{10}, TE_{11}, TE_{20}, TE_{21} and TE_{31}, so when the simulation give the result in TE_{20} mode is still correct theoretically.
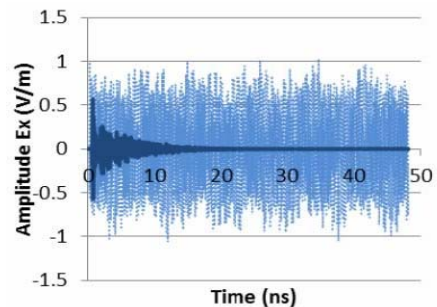

Fig. 8 Simulation results in the field of 3D Cartesian coordinate system with one layers conductive medium

The third simulation is to observe the effect of adding conductivity of the earth surface in the structure. Similar with the second simulation, the simulation will be divided into three parts. First, adding conductivity $\sigma = 0.01$ for modeling wet ground in the whole structure. Second, the structure will be divided into two layers first layer for modeling wet ground while the second one is for modeling air with $\sigma = 0$. Third, the structure will be made as three layers for modeling wet ground with $\sigma = 0.01$, water with $\sigma = 0.03$, and air with $\sigma = 0$. The results are shown in Figs. 8–10.
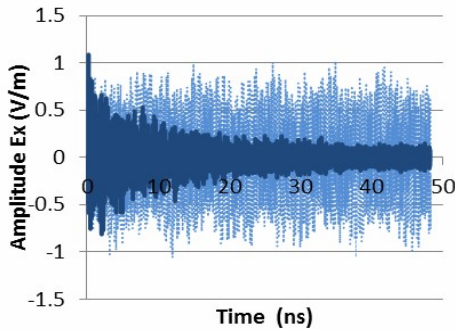

Fig. 9 Simulation results in the field of 3D Cartesian coordinate system with two layers conductive medium
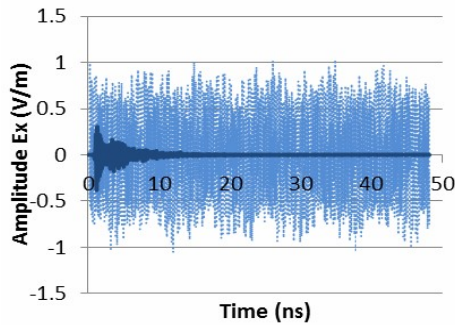

Fig. 10 Simulation results in the field of 3D Cartesian coordinate system with three layers conductive medium

Fig. 8 shows that as well as a lossy simulation have been included with $\sigma = 0.01$, the amplitude decay faster as the source goes away from the excitation point. The decay rate of the simulation is 0.3439Neper/m. The frequency we get from the simulation is 207.694 MHz. Similar with the result in Fig. 8, Fig. 9 shows that the amplitudes of lossy structure is fast decay, but the reduction of the amplitude is not as much as in Fig. 8. This is happened because the structure is built into two part, lossless in the half upper side and lossy for the rest so the σ_{eff} of the structure is lower than the one before. The decay rate of the simulation is 0.2392Neper/m. The frequency we get from the simulation is 228.463MHz.

Fig. 10 shows that amplitude reduction also occurred in this simulation with greater reduction compared with two previous simulations. This happens because of the magnitude of the effective conductivity is bigger as a result of adding a layer of water ($\sigma = 0.03$) in the middle of the structure. The decay rate of the simulation is 0.6194Neper/m. and the first

operating frequency from the simulation is 178.617MHz. All of the first operating frequencies we get from these simulations are close enough with the result in dielectric medium. Those show that the addition of conductive medium did not cause any change in the working frequency.

B. *3D Cylindrical Coordinate System Simulation*

The cylindrical coordinate system structure for simulation has size of $r = 0.6$ m, $\varphi = 30°$ and $z = 1.2$m. From this dimension, we get the same value of Δt as in Cartesian coordinate system which is 1.9285×10^{-11} s. The structure of cylindrical coordinate system shape is given in Fig. 11. To ensure comparability with 3D Cartesian structure, electric component Er is applied in the excitation source with wave mode used in modeling this structure is TE mode.
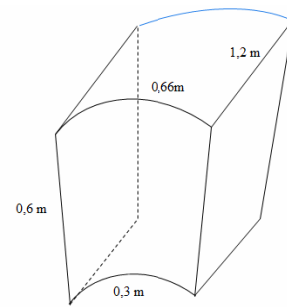

Fig. 11 3D cylindrical coordinate system structure

Fig. 12 shows result in cylindrical coordinate system structure with free space medium. Cut-off frequency attained from the simulation is 498.466MHz. This frequency has a big difference compared to the frequency obtained in Cartesian 3D. This is caused by the shape of a cylindrical structure that does not exactly same as the 3D Cartesian structure. In the Fig. 11 can be seen that the first arc length is 0.3m, but because of the influence of the angle φ, the greater the radius of the field, the circular arc will be enlarged so that the long arc of cylindrical at the top of the structure becomes 0.61m. Dimensions of the structure will affect the cut-off frequency of the structure. Thus, the existence of irregularities in the shape of cylindrical and Cartesian causes the first working frequency in the cylindrical does not exactly match with the Cartesian
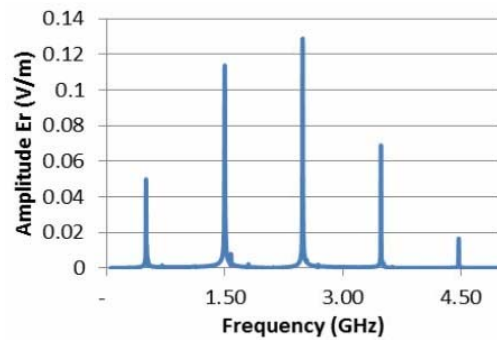

Fig. 12 Simulation result of 3D cylindrical coordinate system with free space medium

Following the simulation in 3D Cartesian coordinate system, the second simulation is to add relative permittivity of the earth surface to the structure with the same conditions which have already mentioned before. The simulation results are given in Figs. 13–15.
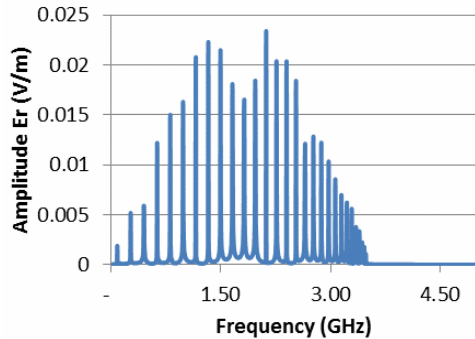

Fig. 13 Simulation results of 3D cylindrical coordinate system with one layer dielectric medium
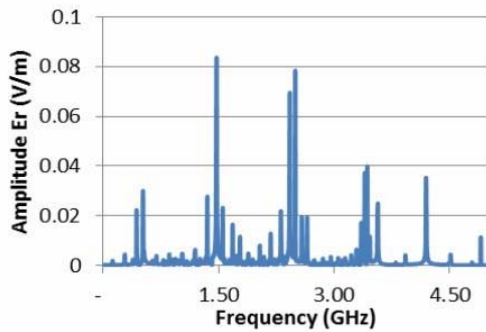

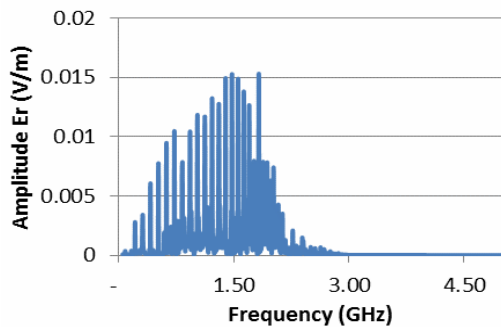Fig. 14 Simulation results of 3D cylindrical coordinate system with two layers dielectric medium

Fig. 15 Simulation results of 3D cylindrical coordinate system with three layers dielectric medium

For the first model, cut-off frequency obtained from calculation is 91.007MHz while from the simulation is 91.385MHz. In second structure, calculation gives result for the cut-off frequency as 138.24MHz whereas from simulation the result is 282.464MHz. In the third structure, we get cut-off frequency 91.851MHz from the calculation and 84.526MHz from the simulation. All of the results are correct theoretically which state that operating frequency will be bigger than cut-off frequency.

The third simulation is to adding conductivity of the earth surface in the simulation structure. The three conditions of simulation will be made exactly same with the 3D Cartesian coordinate system. The simulation results are shown in Figs. 16–18.
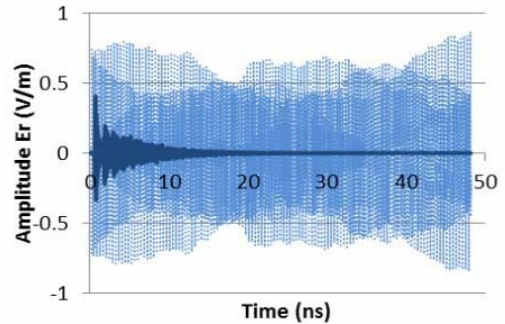

Fig. 16 Simulation results of 3D cylindrical coordinate system with one layer conductive medium
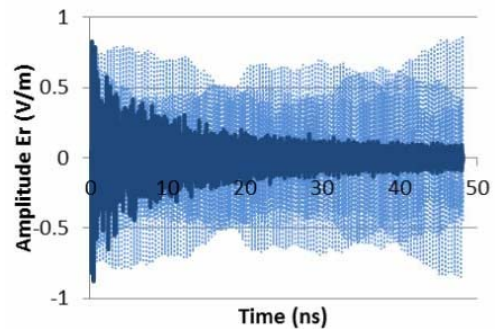
Fig. 17 Simulation results of 3D cylindrical coordinate system with two layers conductive medium
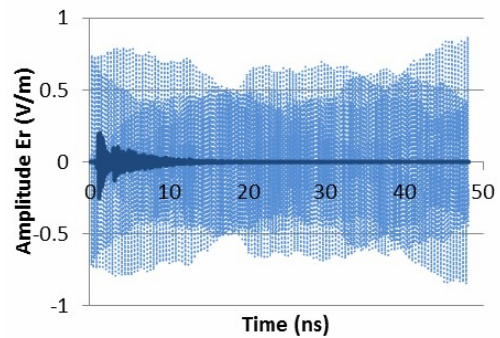
Fig. 18 Simulation results of 3D cylindrical coordinate system with three layers conductive medium

From Figure 16, it is shown that the amplitude for lossy condition decay as a consequence of adding σ=0.01 into the body of the shape. The decay rate of this structure is same with the Cartesian structure. Cut-off frequency we get from the simulation is 91.385MHz. Fig. 17 shows the result of the simulation when it is used as a model of the two earth layer. Comparing to the result Fig. 16, it provide us information that the reduction of amplitude in Fig. 17 is not as much as which happened in Fig. 16. This is the effect of divided the structure

into two condition so the σ_{eff} will be lower. σ_{eff} in this structure is 0.004 with decay rate 0.2089Neper/m. The first operating frequency obtained from this simulation is equal to 274.156MHz.

Furthermore, Fig. 18 shows that amplitude decay occur in this simulation is quite large due to of the effective conductivity in this structure is bigger than the two previous structure as shown in Figs. 16 and 17. The magnitude of the decay rate α in this area is 0.4025Neper/m while the first operating frequency obtained from this simulation is 91.385MHz. Similar with the 3D Cartesian coordinate system results, all of the first operating frequencies we get from adding conductive medium are close enough with the result in dielectric medium. It shows that the addition of conductive medium did not affect the operating frequency.

IV. CONCLUSION

FDTD Method is effective for solving electromagnetic wave. It can be used for modeling wave propagation both in 3D Cartesian and 3D cylindrical structure. In this paper, the dimension and the source for cylindrical structure is set similar with 3D Cartesian shape to perform comparison between the result in 3D Cylindrical and 3D Cartesian. The result shows that cut-off frequency as an outcome from 3D cylindrical structure has difference value compare with cut-off frequency produced in 3D Cartesian. The difference is caused by the shape of a cylindrical structure that does not exactly same as the 3D Cartesian structure. Additional dielectric medium   in the structure decreases cut-off frequency of as much as $1 \left/ \sqrt{\varepsilon_r} \right.$

While adding conductive medium will decay the amplitude of the waves that pass through the medium without changing the operating frequency. The magnitude of the decay rate is proportional to the conductivity of the medium.

REFERENCES

[1] S. Inan and A. Marshall, "Numerical Electromagnetics, the FDTD Method", Cambridge University Press, UK, 2011
[2] K. S. Yee, "Numerical Solution of Boundary Value Problems Involving Maxwell's Equation in Isotropic Media", IEEE Transaction on Antenna and Propagation,, vol. 14, pp. 302–30, May 1966.
[3] A. Taflove and S. C. Hagness, "Computational Electrodinamics, the Finite Difference Time Domain Method 3rd Edition", Artech House, Norwood, 2005.
[4] D. M. Sullivan,"Electromagnetic Simulation Using   The   FDTD Method", IEEE Press, 2000.
[5] K. S. Yee and J. S. Chen, "The Finite Difference Time-Domain (FDTD) and the Finite-Volume Time-Domain (FVTD) Methods in Solving Maxwell's Equations", IEEE Transaction on Antenna and Propagation, vol 45, no 3, March 1997.

Adult Image Classifiers Based On Face Detection Using Viola-Jones Method

M. Dwisnanto Putro
Informatic Engineering
Sam Ratulangi University
Manado, Indonesia
dwisnantoputro@unsrat.ac.id

Teguh Bharata Adji
Electrical Engineering
Gadjah Mada University
Yogyakarta, Indonesia
adji.tba@gmail.com

Bondhan Winduratna
Electrical Engineering
Gadjah Mada University
Yogyakarta, Indonesia
bondhan1510@yahoo.com

This research consists of a classification system to determine the adult and benign image. Adult image in this research was defined as image that is perceived as pornographic by Indonesian people. The method in this research combines face detection and HS skin color detection on an image. Face detection is done by using the Viola-Jones method. After face detection process, skin detection is performed on the image. Based on the results of face and skin detections, a set of features is extracted and inserted into the classifier. The classification used in determining adult or benign image will be based on the percentage of face area in the image, the position of face in the image, and the percentage of the skin color in the image. For each feature, the threshold value is defined in this research. The results of the classifier is whether an input image is benign or adult images. From 30 sample images, the classification process classifies 5 pieces of images as benign images and 25 images as adult images. False positive rate are 2 images and false negative rate is 1 image with the accuracy of 90%.

Keywords - Face detection, Viola-Jones method, Adult image.

I. INTRODUCTION

Image is a combination of points, lines, shapes, and colors to create and imitation or replica of a physical object or item (humans, animals, plants, ect) [19]. Along with the development of graphics technology, image are fully utilized for the welfare of mankind. However, on the other side, can also be a destructive force moral and human behavior, including a negative image as a pornographic image or adult image. Definition of pornographic images are very difficult to be interpreted because pornographic images that contain a lot of sense perception depends on each person. Indonesian Crime Law does not explain the definition of pornographic image clearly and detailed. In Major Indonesian Dictionary, pornography is defined as the depiction of erotic behavior with a painting or image to arouse desire. But the desire of stimulation can be very subjective, depending on the views of the beholder.

Pornographic image has penetrated the public, especially students. In general, students who are mostly young people have a tendency to try new things and his curiosity is very high. It is found in many cases that the pornographic images can lead to negative behavior and criminal sexuality, as well as to damage students' moral and mental. Therefore we need an action to restrict and inhibit the expansion of the pornographic or adult images in order not to be freely enjoyed

by the general public as well as to protect society from these images that can damage behavior, mental and moral society, especially of the youths/students. One of the actions is classifying the images that are accessed via the internet using digital image processing with human face and skin detection method. In the last few years, many image processing methods used to detect human face in a frame. The detection of human face is very important in the development of digital image processing. From a face image, many features can be obtained, such as eyes, nose, and mouth features. Even the number of faces in a frame can be calculated. These kind of researches have been carried out with the advantages and disadvantages.

Currently, applications that use the face detection has been developed. Face detection can be done in various methods, one of them is using the Viola-Jones method, which combines support vector machines, boosting algorithms and cascade classifier [17]. This method is applied to a digital image, to obtain position of the face in the image. These methods get results quickly, accurately, and efficiently than other face detection methods [Viola et al, 2004]. Viola-Jones method is the mostly used algorithms to detect faces recently.

This research designs classification system to determine the adult and benign image. This is performed using a combination of face detection using Viola-Jones method and skin color detection based on Hue and Saturation values (HS). Sample images from this research of 30 which taken from the internet. Sample images is limited to only have one face with the position of the face image is upright (frontal), not hindered in part by another object, not a lot of cut, and did not move.

II. THEORY AND BASIS LITERATURE REVIEW

A. *The Theory*

1. *Face detection*

Face detection is a problem of pattern classification where the input is images and the output is class label of those images. There are two class labels, face and non-face. Face recognition techniques is performed by the assumption that the face data possibly has the same size and background. In the real world, this assumption is not always valid because the face can appear in various sizes and positions with varied backgrounds [10]. Face detection is more important. This is why the face detection is put as the first step before face

recognition process. Research fields related to face processing are:

- Face recognition is to compare the input face image with a database face and find the face that best matches with the input image.
- Face authentication is testing the authenticity/similarity of a face with the face of data that has been entered previously.
- Face localization is the face detection but assuming there is only one face in the image
- Face tracking is approximate location of a face in the real time video.
- Facial expression recognition is recognize human emotions.

The challenges faced in the face detection problem caused by the following factors:

- Position the face. The position of the face in the image can vary is upright position, tilt, turn, or viewed from the side
- The components of the face such as mustache, beard, and glasses.
- Facial expressions. Facial appearance is influenced by facial expressions, such as smiling, laughing, sad, talk, and etc.
- Hindered other objects. A face image can be some hindered by other objects or faces, for example, the image contains a group of people.
- Condition of image acquisition. The image obtained is strongly influenced by factors such as room light intensity, direction of light sources, and characteristics of the sensor and the camera lens.

2. Skin Detection

Skin detection is a process of finding the pixel or part of an image or a digital video that has a color (similar) the skin. The appearance of the skin on the image is very dependent on the lighting conditions. Humans are very good in identifying the color of the object in good lighting. But not necessarily with a computer, a new problem is how to detect the appearance of the skin with a variety of skin colors and different lighting conditions. Another challenge is the number of objects that have similar color to the skin such as wood, sand, hair and even clothing that have the same color skin. This makes difficult the skin detection. These problems can be minimized if the skin detection method is most suitable by analyze the results of any existing methods, to can be conclude that the best method

The skin detection to filter content on the internet that image with image processing and deciding the feasibility of that image to be displayed after taking into account other considerations. If you are using a skin detection method based on color, skin detector must have a data form a variety of shades of color in various lighting conditions that can be used as a reference to decide the appearance of the skin. Them adaptive method of thresholds that do not require the data as a reference. Adaptive thresholds method work is to find the optimum threshold and then eliminate or remove the background.

III. METHODS

A. Overview

The data used in the form of a sample image taken from the internet as many as 30 images. This research uses MATLAB R2010a and OpenCV library version 2.2 for classifying and separating adult and benign images. In this research, Viola-Jones method is written as OpenCV library which is called by the developed program written in MATLAB R2010a. The Viola-Jones library also calls Haar library.

Based on Figure 1, image samples are the input of the developed system. Then face detection process is then carried out to determine whether each image is of a human image or not. After getting the results of face detection process, skin detection process is performed on the images to determine the human skin area. Based on the face and skin detection processes, facial features and skin regions are extracted and then inserted into a classifier. Finally, the system determines whether each image is of adult images or benign. The overall system flowchart of this research can be seen in Figure 1.
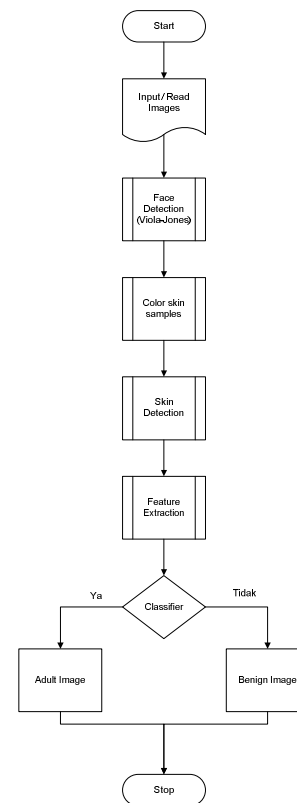

Fig. 1. Flowchart of research

B. Viola-Jones Face Detection

Face detection plays an important role in image classification in this research. Face detection process is carried out before the process of skin color detection. The face detection system uses Viola-Jones method, which has the advantages of fast and efficient in getting the facial region compared to previous methods of face detection [Viola et al, 2004]. The process is done by reading each sample image in JPEG using MATLAB R2010a. The image is then fetched into Haar feature classification. The classification read Haar

features written in XML and converts the XML file into Matlab file. After the conversion process, a Matlab file named **haarcascade_frontalface_alt** serves as a process to call and determine Haar features in each image to detect face. Haar features are the features used in Viola-Jones method which can also be called features of a square wave. To two dimensions is referred to as one bright and one dark. The existence of Haar features is determined by subtracting the average of pixels in dark areas of an average of pixels in the bright areas. If the value of the difference is above the threshold value, it can be said that the feature is there. Next to determine whether or not of hundreds of Haar features in an image at different scales and efficiently by using the Integral Image. Generally, the integration is to add small units simultaneously. The small units are pixel values. Integral value for each pixel is the sum of all the pixels from top to bottom. Starting from top left to bottom right, the whole image can be summed with some integer operations per pixel.

Then to select the specific Haar features and to adjust the threshold value, we used a machine learning AdaBoost. AdaBoost combines many of weak classifier to make a strong classifier. by combining some of the AdaBoost classifier as an efficient filter circuit to characterize the image. The next stage of the cascade classifier. Filter in the cascade sequence is determined by the weight given AdaBoost. Filter with the greatest weight is placed on the first time, to erase the not face image as fast. During the classifying process, if there is one filter fails to pass an image area, the area it directly classified as non-face. But when the filter is missing an image area up through all the filters, then the area is classified as a facial image. The last stage of the display object has been detected on the face or not face, with a square mark if the object is considered as the face.

C. *Skin Detection*

Skin detection took part in this research. Because of a feature in determining the classification of benign and adult image, there are elements of skin detection in the image area. The first step skin detection is to read the facial skin samples based on result face detection process in previously by MATLAB R2010a. Next the skin sample RGB images are converted to form the Hue and Saturation (HSV). From the HSV value is then separated between Hue and the Saturated value. So we get the values of the color distribution in the form of HS, which can then be plotted on the 3D and 2D graphics. Threshold value using to determine the skin area on an image from the distribution of the skin of HS. The threshold values of skin color in this research refers to previous research [Still.J, 2007] who has determined in HSV color value is 0-11 for the Hue value and 20-70 for the Saturation value. the scale of each Hue and Saturation value is 0-100. Then do the skin detection process in whole part image based on threshold values of Hue and Saturation.

In the sample image will do the skin detection process, the first step to do is read the sample image by MATLAB R2010a. Then convert the RGB values image into HSV values. After getting the value of HSV, separated between the Hue and Saturation value of the image. The next step is to determine

skin area by only selecting values within the rectangle skin range.

$$skin=(s>s\_range(1))\&(s<s\_range(2))\&(h>h\_range(1))\&(h<h\_range(2)) \quad (1)$$

Based on Equation 1, to determine the skin skin in an image is a combination of the S (saturation) value at the sample image is greater than the first threshold from saturation value and S (Saturation) value at the sample image is smaller than the second threshold from saturation value. The H (Hue) value at the sample image is greater than the first threshold value from Hue value and the H (Hue) value at the sample image is smaller than the second threshold from Hue value. Then the results of skin detection is displayed in the form of a binary image, a binary 1 for the skin area and binary 0 for non-skin area.

D. *Feature Classification*

Face detection is beginning process of the whole method of this research, because the face is the most distinctive part of humans body. Detection of faces can allow the observer to form a hypothesis about the presence of humans in the scene and other measures can be taken to verify whether or not they are nudes. Detection of skin area in image also affect the decision to determine the adult image and benign image.

We empirically choose three features for benign or adult image classification. These features are all related to face:

1. Face area: the area of face regions. Images in which face regions cover too much area may be full-face portraits. We define K1 in Equation 2:

$$K1 = \frac{number\ of\ pixel\ in\ face\ region}{number\ of\ pixel\ in\ whole\ image} \quad (2)$$

2. Face position: This feature classifies the image that displays in the middle of the face in general is benign image. We defined the value of x1 and x2 is the threshold distance of the center of image pixel x. The value of y1 and y2 is the distance threshold y pixel image center, then Equation 3 can be defined as follows:

$$x1<Distance\ center\ face\ x<x2, \quad (3)$$
$$y1<Distance\ center\ face\ y<y2$$

Equation 3 shows the face position is in the threshold area the center of image.

3. Comparison of skin: classification feature is the comparison between the number of skin area the image and the face area. So that in Equation 4 can be defined as the K3:

$$K3 = \frac{Number\ of\ Pixel\ Skin\ on\ the\ image}{number\ of\ pixel\ in\ face\ region} \quad (4)$$

Based on three features, can be made whole in the form of decision tree classification. Figure 2 shows the classification tree shape composed of nodes. Node in the tree involves testing each feature and compare with a constant threshold value. At first go through the first

classification feature is K1, if K1 is greater than the threshold value (T1) it was decided as a benign image, and if the result is smaller than the threshold value (T1) then passed to the classification second feature of K2. On the K2 if the center of the face is in the center of image area threshold (<T2) it was decided as a benign image. But if it is outside the threshold region (> T2) then continued to the classification feature of K3. This classification feature is a last classification decisions as adult or benign image. If the classification of K3 is smaller than the threshold value (T3) it was decided as a benign image, and if otherwise is classified as an adult image.
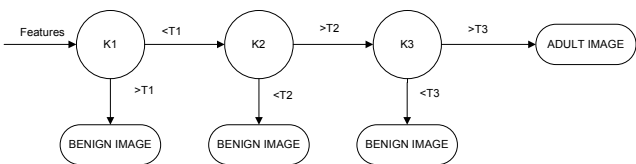

Fig. 2. Classification scheme for determining the image adult

IV. RESULTS AND DISCUSSION

In the classification process adult images and benign images, face detection is performed before the skin detection process on the image area. This section show the results of testing of face detection using the Viola-Jones method. The following are faces images that have been detected as a face.

Fig. 3. The results of face detection

The whole image is detected an face image. The first stage of classification system is adult image, it requires face detection on first stage, to determine whether there is a human image or not. If there is no face in that image, so not considered a human image, so the image is said to be the direct a benign image. Face detection process is the initial determination of the image adult or benign image. Image of the sample in general is image with upright or near-frontal face because some image are not upright or not frontal face can not be identified face in the image. Therefore, upright position of the face / frontal or not, very influence the face detection process.

The skin detection process becomes a role in the classification system of adult image and benign image. Skin detection is a factor in the classification of features that will determine the image adult or benign image. Image samples detected the existence of skin color on the overall image by giving binary classification of the image, and change to the

binary color. Skin color samples obtained from the previous face detection process produces color distributions in the form of Hue and Saturation. The whole image sample performed of skin detection for the classification of adult or benign image. Here are the results of the skin detection process.

Fig. 4. The results of skin detection in all areas of the image sample.

The results of skin detection in this research are shown in Figure 4. Skin detection performed on the whole sample image, the end result of skin detectin to change the sample image into a binary image, the skin color is assumed to be logic 1 and the non-skin color assumed a logic 0. At the beginning of the process of detection of the skin, change the pixel RGB (Red, Green and Blue) value the sample image into the HSV (Hue Saturation Value). Then separated between the Hue and Saturation value image. Next obtained the distribution of color images, which show in graphic form in 3D. Here is a 3D graphic color distribution on the sample 1.
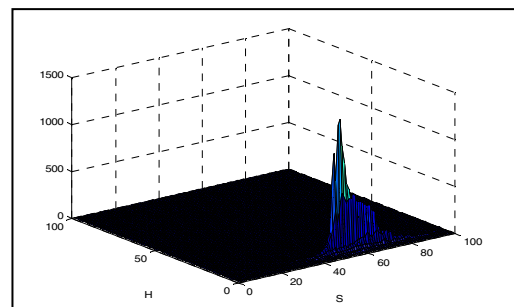

Fig. 5. 3D graphic color distribution on the sample 1.

Based on Figure 5, the color distribution can be seen from sample 1, has a variety of colors (in HSV). The spread of colors in this image, dominates the value of 0-20 for the Hue and value of 0-100 for the saturation. Based on the spread of the distribution of these colors, then determined the threshold value to specify the skin color. Color range for the skin detection on the whole image is set based on the color distribution obtained from a sample image of the face detection. Based on the research [Still.J, 2007], skin color on skin detection process takes a Hue value of 0-11 and the saturation value of 20-70 as the threshold value is considered the color of human skin.

The classification used in determining adult or benign image will be based on the percentage of face area in the

image, the position of face in the image and the percentage of the skin color in the image. With each of these classifications have value threshold. Each classification has a supporting components among which are size of the image, size of skin pixel image,size of the pixel face and the distance to the center of the face image. So it can be combined in the overall classification feature with a sequence K1-K2-K3 to determine adult images and benign images. Here is the result of cascade classification in this research.

TABLE I. Classification results

No. Image	Type of Image	Classify			Decision
		K1	K2	K3	
1	Adult	0.0174	> T2	38.1941	Adult image
2	Adult	0.1539	> T2	2.6988	Adult image
3	Adult	0.0377	> T2	6.0469	Adult image
4	Adult	0.1069	> T2	3.8318	Adult image
5	Adult	0.0534	> T2	7.0806	Adult image
6	Adult	0.0440	> T2	7.4390	Adult image
7	Benign	0.0368	> T2	4.4194	Adult image
8	Adult	0.0174	> T2	32.1055	Adult image
9	Adult	0.0372	> T2	4.2919	Adult image
10	Adult	0.0809	> T2	3.9610	Adult image
11	Adult	0.0200	> T2	16.8464	Adult image
12	Adult	0.1566	> T2	2.4969	Adult image
13	Adult	0.0151	> T2	29.8048	Adult image
14	Adult	0.0737	> T2	9.1284	Adult image
15	Adult	0.0793	> T2	4.4476	Adult image
16	Adult	0.0376	> T2	14.1911	Adult image
17	Adult	0.0247	> T2	22.1199	Adult image
18	Adult	0.1623	> T2	3.2340	Adult image
19	Adult	0.2216	> T2	1.9443	Benign Image
20	Adult	0.1107	> T2	3.9555	Adult image
21	Adult	0.0373	> T2	9.0514	Adult image
22	Adult	0.0188	> T2	10.4988	Adult image
23	Adult	0.1082	> T2	4.3571	Adult image
24	Adult	0.1539	> T2	2.7687	Adult image
25	Adult	0.1539	> T2	2.9751	Adult image
26	Benign	0.2226	< T2	2.8631	Benign Image
27	Benign	0.0226	> T2	8.0918	Adult image
28	Benign	0.5493	< T2	0.8902	Benign Image
29	Benign	0.1963	< T2	0.4960	Benign Image
30	Benign	0.2538	> T2	0.0950	Benign Image

TABLE I which is a False positive rate are 2 images and false negative rate is 1 image With the percentage of error classification system are the difference between the total number of sample images and the number of correctly classified images which compared with the total number of sample images are 10%. With the percentage accuracy of classification system are 90%.

V. CONCLUSION

This research designing a classification system to determine adult images and benign images. The face detection method in this study using the Viola-Jones, which has advantages in quickly and efficiently compare other face detection methods. The weakness of the face detection system with this method are not able to determine the face not upright or not frontal face. The upright position of the face or not upright determine the success of face detection. Face and skin detection plays a dominant role in this method, where the results of the face and skin detection is a key element for classifying the images an adult or not. The classification used in determining adult or benign image will be based on the percentage of face area in the image, the position of face in the image and the percentage of the skin color in the image. For each feature, the threshold value is defined in this research are T1 = 0:17, T2 = 30% of the center's image and T3 = 1. Percentage of accuracy system are 90%.

REFERENCES

[1] Chan.Y, Harvey. R, dan Smith. D, "Building systems to block pornography" Challenge of Image Retrieval, Newcastle, 1999.
[2] Viola, P., Jones, M. J.: Rapid Object Detection Using A Boosted Cascade of Simple Features. IEEE Conference on Computer Vision and Pattern Recognition, Jauai, Hawaii, 2001.
[3] Y. Wang and B. Yuan, "A novel approach for human face detection from color images under complex background," in Pattern Recognition, pp. 1983–1992, 2001.
[4] Ries Christian, and Lienhart. R , "A Survey On Visual and Adult Image Recognition" Multimedia Tools and Aplication. April 2014. Vol 69. Issue 3, pp 661-688, 2014.
[5] Wijaya. I. G. P. S , "Phonographic image recognition using fusion of scale invariant descriptor" Frontiers of Computer Vision (FCV) Korea-Japan. Page 1-5, 2015.
[6] Lin. Y. C , Tseng. H. W, and Fuh. C. S , "Pornography Detection Using Support Vector Machine" Conference on Computer Vision, Graphics dan Image Processing (CVGIP 2003), 2003.
[7] Viola, P., Jones, M. J.: Robust Real-Time Face Detection. International Journal of Computer Vision, Kluwer Academic, Netherlands, 2004.
[8] Zheng. Q. F, Zhang. M. J, and Wang . W. Q, " A Hybrid Approach to Detect Adult Web Images," Springer-Verlag Berlin Heidelberg. 2004.
[9] Zheng. H, Daoudi, and Jedynak. B, "Blocking Adult Images Based on Statistical Skin Detection" Universitat Aut_onoma de Barcelona, Barcelona, Spain, 2004.
[10] Nugroho, S., "Sistem Pendeteksi Wajah Manusia pada Citra Digital" , Tesis Program Studi Ilmu Komputer Jurusan MIPA, Universitas Gadjah Mada, Yogyakarta, 2004.
[11] Ho. W. H and Watters. P. A," Identifying dan Blocking Pornographic Content" International Conference on Data Engineering (ICDE '05). 2005.
[12] Wang. Y, Wang.W, and Gao. W, "Research on the Discrimination of Pornographic dan Bikini Images" Seventh IEEE International Symposium on Multimedia (ISM'05), 2005.
[13] Still, J. D., Dohse, T., and Dohse K. C. "Touch table augmented with skin detection". Poster presented at the Emerging Technologies Conference, Ames, IA. April, 2007.
[14] Hu. W, Wu. O, Chen. Z, Fu. Z, and Maybank. S, "Recognition of Pornographic Web Pages by Classifying Texts dan Images" IEEE transactions on pattern analysis dan machine intelligence, vol. 29, no. 6, June, 2007.
[15] Agbinya. J. I, Lok. B, Wong. Y. S and Da Silva. S, "Automatic Online Porn Detection dan Tracking" Faculty of Engineering, University of Technology, Sydney, 1 Broadway, Sydney, 2007.
[16] Dwiyana, "Deteksi Kulit sebagai Penyaring Konten Gambar di Internet", Skripsi Jurusan Ilmu Komputer Universitas Pendidikan Indonesia, 2009.
[17] Andoko, " Perancangan program simulasi deteksi wajah dengan Support vector Machines – Viola Jones", Teknik Informatika – Matematika, Universitas Bina Nusantara, Jakarta, 2010.
[18] A Arihutomo, M., "Rancang Bangun Sistem Penjejakan Objek Menggunakan Metode Viola-Jones untuk Apiliasi Eyebot", Proyek Ahir Jurusan Telekomunikasi PENS-ITS, Surabaya, 2010.
[19] Pusat Bahasa Departemen Pendidikan Nasional, "Kamus besar bahasa Indonesia", Jakarta, 2008

DESIGN OF GEOGRAPHIC INFORMATION SYSTEM FOR TRACKING AND ROUTING USING DIJKSTRA ALGORITHM FOR PUBLIC TRANSPORTATION

Muh. Aristo Indrajaya
Institute of Technology Sepuluh Nopember
Surabaya, Indonesia
aristocool@yahoo.com

Achmad Affandi
Institute of Technology Sepuluh Nopember
Surabaya, Indonesia
affandi@ee.its.ac.id

Istas Pratomo
Institute of Technology Sepuluh Nopember
Surabaya, Indonesia
istaspra@ee.its.ac.id

Abstract— **The ability to perform vehicle tracking is very useful in daily life - today, such as security on personal vehicles, public transportation systems, fleet management and other mass transit. In this study, we designed an application of Geographic Information Systems (GIS) that will be applied to public transport services. This system provides real-time position tracking of each vehicle (taxi) and capable of providing a taxi with the best category for passengers using Dijkstra's algorithm. This system can be helpful, especially for passengers who are often too long waiting for a taxi that had been booked and also helps the driver to save fuel consumption because the taxi drivers do not have to drive across town to get the passengers and are just waiting for confirmation sent by this system.**

Keywords—Dijkstra, GPS, GIS, Tracking, Routing.

I. INTRODUCTION

Global growth in the number of vehicles is expected to increase along with economic growth and the number of middle class society is increasing, such as in China and India. Although the growth in the number of vehicles in addition to the positive impact that the increasing number of middle and upper class residents, but the development of a tracking system (tracking) of a vehicle which is also a very important part in a transport system is still lacking. The use of tracking systems on the mode of transport will be very useful for a variety of aspects including safety and economy in private vehicles, mass transport systems, commercial vehicle, and so forth.

On public transport services, especially taxis, often encountered a problem where the passengers have to wait very long to get a taxi that had been booked through the service provider. This generally occurs at rush hour where traffic jams often occur so taxis were booked sometimes be stuck in traffic so that the lower the level of service a taxi operator. Another problem that often occurs in the driver taxi in which a taxi driver had to drive around far enough to get the passengers, causing increased fuel costs.

The main objective of our research is to build a system capable of providing the service automatically and instantly to the passenger taxi. By using this system the position and velocity of each taxi will be monitored through the application of GIS (Geographic Information System) web-based. To be able to serve a taxi booking automatically, then the system is implemented Dijkstra's algorithm that serves to find a taxi that is most suitable for passengers based on the parameters within the prospective passengers of the taxi and the traffic levels nearby occurs so that passengers will get a taxi that had been

ordered in the not so long. Another benefit to be gained is a taxi driver does not have to drive around to different places to get the passengers because the system will immediately send location information so that passengers actually increase fuel efficiency and improve services for passengers.

II. STATE OF THE ART

A. Automatic Vehicle Location (AVL)

Automatic vehicle location system is a computer-based vehicle tracking vehicles [6]. The current position of each vehicle will be monitored and will be forwarded to the control center.
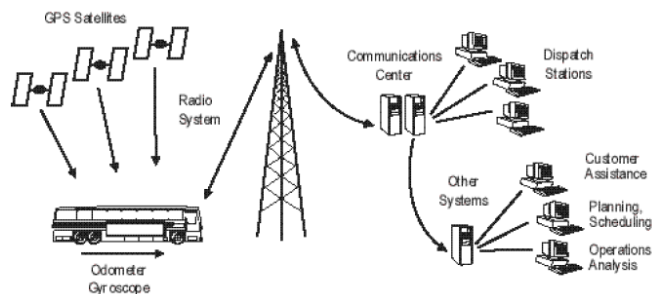

Fig 1. Working principle AVL.

Generally, the vehicle position information will be stored on the vehicle for which can last for several seconds. Position information can be forwarded to the control center in the form of raw data or after processing by the device on the vehicle before it is transmitted.

Agent or transportation company has implemented AVL systems to help them in many ways. By implementing this system, the many benefits that can be taken as from the operational side, the system will help meet the schedule accuracy, improve the efficiency of the services, facilities integrated system and reduce the number of supervisors (supervisors) in the field. The benefits that can be taken in terms of communication and security is a radio system that has replaced the old, reducing voice communication via mobile data terminals and improve response time to incidents and emergencies.

B. Global Positioning System

GPS is a system that serves to determine the location on the earth's surface with the aid of alignment by satellites [10]. GPS uses satellite data to calculate the accuracy of the position of

the earth. All GPS works the same way but they look very different and have different software. Very significant differences between the various GPS receivers is the number of satellites that can simultaneously communicate with the receiver. Most described the 12-channel receiver, which means the device is able to communicate with 12 satellites. GPS older models only able 8 or 5 channels, but with the latest models of receivers capable of communicating with 14-20 satellites.

Number, position and signal strength of satellites allows the GPS to calculate the error rate. This error rate can be a good guide to know how accurate the readings done by GPS and an error rate that can be tolerated from a GPS device is under 10 m (ideally below 5 m).

GPS data recording is generally the same in all units. GPS receivers automatically record the data into its memory based on time elapsed or the distance of the movement that occurs. It is generally termed as trackpoints. GPS receivers can often be used as a complete navigation tool, not only offers driving directions and the location in detail but also offers a navigation tool that can help users when it will move from one place to another. Most receivers have been equipped with digital compass. Digital compass work based on data from satellites and this is not a compass made of magnet and will only work when the user starts to move.

C. Geographic Information System

Geographic information systems (GIS) originally evolved from two independent disciplines, namely: digital mapping and database. The development of digital cartography as a result of growing world of design, especially CAD (Computer Aided Design) since the 1960s. Similarly, the development of the use of data base management systems, especially database or Database Management Systems (DBMS) that enables the integration of spatial data and non-spatial contribute to accelerate the development of GIS. In a further development of GIS involves various disciplines such as remote sensing, photogrammetry and surveying.
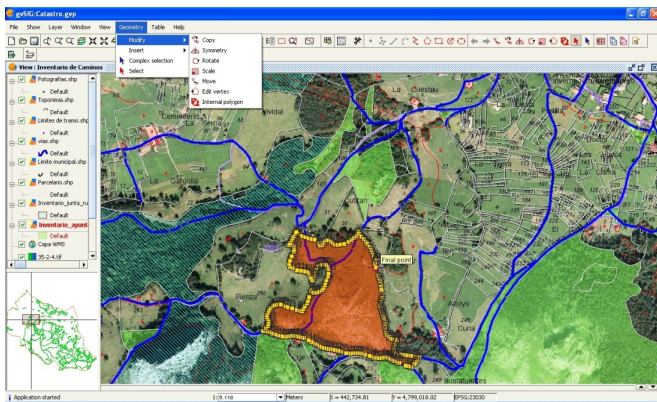

Fig 2. Example of GIS.

Today the use of GIS has been highly integrated with daily life. Geospatial technologies that work behind the scenes has helped either directly or indirectly projects and government programs. The map feature is currently available in almost every information system. Ranging from information services

(service) to address the search needs, something very difficult thing happened in the era of the 1980s in Indonesia.

D. Dijkstra Algorithm

Dijkstra's algorithm invented by Edsger Dijkstra in 1959, is a graph search algorithm that solves the shortest path problem that originates from one node to a graph with node weights can not be negative [7]. The analysis was performed by examining the node with the smallest weight and put it into the set of solutions to the initial search origin node requires knowledge of all the paths and weight, so it is necessary exchange of information with all the vertices. Dijkstra algorithm has a simple nature and plates (straightforward), according to the working principle greedy. Constituent elements of the greedy algorithm is:

1. The set of candidates, C

   This set contains elements that have a chance to form a solution. On the issue of the shortest path in the graph, this candidate set is the set of vertices in the graph.

2. The set of solutions, S

   This set contains the solution of the problems were resolved and the elements consist of elements in the set of candidates but not all of them, or in other words, the solution set is upabagian from the set of candidates.

3. The selection function

   The selection function is a function that will elect any candidate which allows to produce the optimum solution for every step.

4. The feasibility function

   The feasibility function will check whether a candidate has been elected violate the constraint or not. If a candidate violates the constraint then the candidate will not be incorporated into the solution set.

5. The objective function

   The objective function will maximize or minimize the value of the solution. The goal is to choose one course the best solution from each member of the set of solutions.

Figure 3.10. below is an example of an undirected graph consisting of 5 dots and 7 pieces of track connecting between two points. Djikstra algorithm is used to find the shortest distance from a point to another point on the undirected graph.
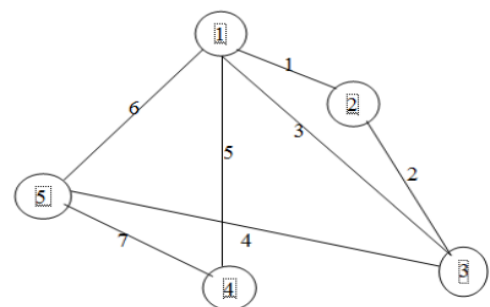

Fig 3. The example of undirectional graph

Based on the example of undirected graph above specified search starting point is the point 1 with the goal of 4 points and will look for the shortest distance that can be taken from point 1 to get to the point 4. The following is an explanation table graph using the Dijkstra's algorithm:

Path	Initial Path					Point	I(i,j)				
	1	2	3	4	5						
	0	0	0	0	0		1	2	3	4	5
1	1	0	0	0	0	1	∞	∞	∞	∞	∞
1-2	1	1	0	0	0	2	1	∞	∞	∞	∞
2-3	0	1	1	0	0	3	3	2	∞	∞	∞
3-5	0	0	1	0	1	4	5	∞	∞	∞	7
5-4	0	0	0	1	1	5	6	∞	4	∞	∞

TABLE I. Explanation of the graph using Dijsktra algorithm.

Completion Dijkstra path algorithm point 1 to point 4 has been completed as described above and the table according to the calculation graph search algorithm dijkstra appropriate procedural steps. In the first line of all successor in the set of 0 means to give value to a point source route to be used for all routes and ketidakterbatasaan another point, stating the fact that it is not known any trajectory.

For further because of point 1 as the source track then it is definitely elected. So it turned into a status set 0. 1. Point 1 will be check points directly neighboring ie points 2, 3, 4 and 5. From there dijkstra will choose who has the lowest weighting towards the next point. Elected point 2 with a weight of 1, sets the status of 0 is changed to 1 and so on. Then search the shortest distance of the above, obtained shortest path based search dijkstra from point 1 to 4 is via direct point 1 point 4 with the weight trajectory 5.

III. SYSTEM DESIGN

The system to be built consists of the android smartphone-based GPS receivers that are placed on each vehicle called on-board unit (OBU) and a server unit that serve receive position information from each GPS receiver and display it through a web-based service. The system works by monitoring in real time of the position of the vehicle and the level of traffic density.
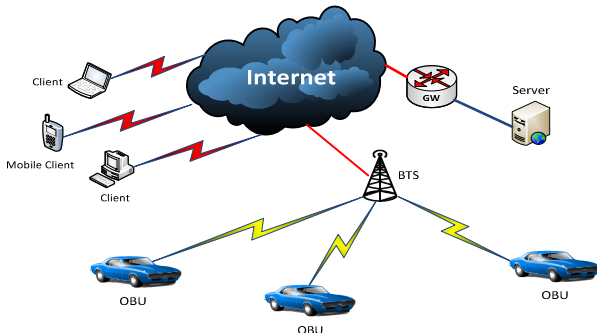

Fig 4. The design of system architecture

GPS receivers used in this system is a smartphone with Android operating system. Data from GPS feature on a smartphone will be sent to the server, using the application B'trace. Besides being able to track the position of a smartphone, this application will send the data of latitude and longitude in real time to a server. Data transmitted by the GPS receiver will be stored in the database of the server used. When passengers access the application pages, the system will show the position of each taxi is available on a web page based on latitude and longitude of the data collected from around the GPS receiver of each taxi.
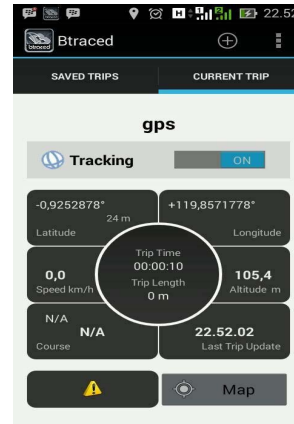

Fig 5. The tracking application

To be able to find the vehicle that best suits the passengers, then the system will use dijkstra's algorithm. Dijkstra's algorithm to be used in this system using the position of the vehicle as well as the density of traffic on urban streets as the parameters to be taken into account to find the most appropriate vehicle for passengers. If the taxi with best categories have been found, then the system will automatically send information about the position of passengers to taxi drivers through a service-based push e-mail.

IV. DISSCUSION AND CONCLUSION

The data will be sent to the server is the data that has been processed first by the GPS receiver before being sent to the server via communication celular services (GSM). Transmitted data is the data latitude and longitude to be used by the server to map the position of each taxi on a google map based map application. Latitude and longitude data that has been sent by the GPS receiver and stored into a database which will be processed by the server to determine the position of the nearest taxi with passengers.

This system will be tested in urban areas within the period that adjusted to the level of traffic density occurs. This system will be tested in two conditions. First in the event of high traffic density is at 07:00 AM - 03:00 PM. Second, when the current traffic conditions back smoothly ie at 05:00 PM - 09:00 PM. In this test, the designed system will be compared with the existing system services to know the service improvement that occurs based on the waiting time of each passenger on a taxi that has been booked.
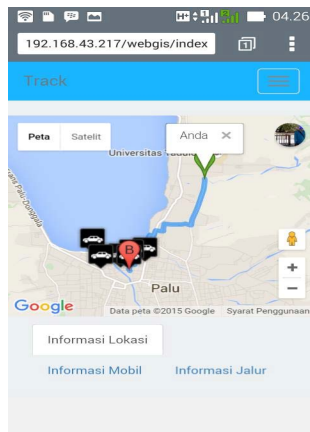
Fig 6. Application user interface

Dijkstra's algorithm is applied to the system will be able to solve the problem of finding the best with the taxi to the criteria based on the parameters of the taxi with the shortest distance to the passenger and traffic levels that occur in an area. These applications provide benefits not only to passengers where passengers are not too long waiting for a taxi he had a message but also provide benefits for taxi drivers where the close proximity of the passengers will save time and fuel consumption.

REFERENCES

[1] Aloquili O., Elbanna A., Al-Azizi, A. (2009), "Automatic Vehicle Location Tracking System Based on GIS Environment", *The Institution of Engineering and Technology*, Vol. 3, No. 4, pp. 255-263.

[2] Cho H.J., & Cho M., (2013), "Effective Position Tracking Using B-Spline Surface Equation Based on Wireless Sensor Networks and Passive UHF-RFID", *IEEE Transactions on Instrumentation and Measurement*, Vol. 62, No. 9.

[3] Dat H. P., Drieberg M., Cuong C.N. (2013), "Development of Vehicle Tracking System using GPS and GSM Modem". *IEEE Conference on Open Systems*, Sarawak.

[4] Davis S. (2007), "GIS for Web Developers", The Pragmatic Programmers.

[5] Jerath K., & Brennan, N. (2012), "GPS Free Train-Based Vehicle Tracking on Road Networks", *American Control Confrence*, Faimont Queen Elizabeth, Montreal.

[6] Johnson M.C., & Thomas, L.E. (2000), "Automatic Vehicle Location Successful Transit Aplications", U.S. Department of Transportations, Washington, DC.

[7] Joyner D., Nguyen, V.H., Cohen, N. (2011), "Algorithmic Graph Theory".

[8] Lammle T., (2007), "Cisco Certified Network Associate Study Guide", Wiley Publishing, Inc., Indianapolis.

[9] Lee S., Tewolde G., Kwon J., (2014), "Design and Implementation of Vehicle Tracking System Using GPS/GSM/GPRS Technology and Smartphone Application", *IEEE World Forum on Internet of Things*.

[10] McWilliam N. (2005), "GIS, GPS and Remote Sensing", The Expedition Advisory Centre Royal Geographical Society 1 Kensington Gore, London.

[11] Odom W., (2007), "CCENT/CCNA ICND1 Official Exam Certification Guide", Cisco Press, Indianapolis.

[12] Sathiamoorthy M. (2009), "On GPS Tracking of Mobile Devices", *International Conference on Networking and Services*".

[13] Yi Z., Ding W., Yanfei Y. (2009), "On Dynamic Scheduling of Vehicles Based on GPS / GIS / RFID", *Department of Computer Science & Technology*, Harbin.

[14] Yuan Gannan, Zhang Zhi and Guan Shang Wei. (2008), "Research and Design of GIS in Vehicle Monitoring System", *Harbin Engineering University*, Harbin.

Application and Data Level Interoperability on Virtual Machine in Cloud Computing Environment

Soffa Zahara
Faculty of Electrical Engineering
Institut Teknologi Sepuluh Nopember
Surabaya, Indonesia
soffa.zahara@gmail.com

Istas Pratomo
Faculty of Electrical Engineering
Institut Teknologi Sepuluh Nopember
Surabaya, Indonesia
istaspra@ee.its.ac.id

Djoko Suprajitno Rahardjo
Faculty of Electrical Engineering
Institut Teknologi Sepuluh Nopember
Surabaya, Indonesia
djokosr@ee.its.ac.id

Abstract—**The rapid development of internet nowadays impact on increasing many applications that utilizing cloud computing technology for the sake of organization. Increasing requirements in applications caused by inevitable business process growth in organization enabling a tendency to switch from old cloud provider to more reliable one. However, in practice, application functionality failures often occur in case of migrating process to new cloud system due to several circumstances e.g. vendor lock-in problem. This paper introduces a new method for system migration testing between two cloud providers. The goal is to determine the interoperability level of application and data in virtual machine within hypervisor system that moves from one cloud provider to another cloud provider. The contribution of this paper is to provide a reference test method for measuring the interoperability between the two cloud systems were migrated.**

Keywords—interoperability; virtual machine; cloud migration

I. INTRODUCTION

The rapid development of internet technology today impact on many organizations that began to shift from using physical infrastructure to cloud computing services to support the business process needs. The emergence of several cloud computing service providers that offer a range of benefits are taking part in the increasing usage of cloud computing technology, especially in the industrial field.

Increasing business processes and operational needs also better additional features offered by other cloud providers such as cheaper price, more reliable system, higher system performance, more secure system and other benefits make organization has tendency to move their service or can be called a migration from one cloud provider to another.

Yashpalsinh and Kirit [9] specified three type services of cloud computing i.e. IaaS (Infrastructure as a Service), SaaS (Software as a Service), and PaaS (Platform as a service). In the term of IaaS environment, the tiniest component that can be moved to another environment is virtual machine [1]. In virtual machine migration process there is a step called virtual machine image conversion that makes the image can be used in other system. However, the success of the virtual machine conversion process from one system to another does not guarantee the success of the migration process. Parameters such as network configuration, CPU, memory, security,

application and original data structure may have changed in the migration process. In migrating system process from one cloud provider to other cloud provider in which there are some applications in previous cloud that have been running, needs a testing method to measure the level of interoperability between two cloud systems, so that all components in the previous system such as operating system, security system, application and the data stored, can be run appropriately with its functionality in the new system.

TIOSA [1] is a virtual machine interoperability testing method based on Open Data Center Alliance (ODCA). The drawbacks of TIOSA's method is only test the functionality of the operating system and hypervisor also have not tested on a specific level of functionality such application and data on the new system, so TIOSA does not suit the evaluation of interoperability in actual system, especially in the industrial field.

The purpose of this study is to introduce a new method that test interoperability at the level of application and data running on virtual machine system, between two different cloud providers. In this study will also be conducted simulation interoperability testing using the method proposed. The benefits of this research is to give a reference about interoperability testing method between cloud systems that more specific to the application and data, so it can be implemented in the field of industry according to business process.

II. INTEROPERABILITY AND CLOUD COMPUTING TEORY

Internet has become a thing that cannot be separated from all aspects of human life. Utilization of various Internet technologies e.g. [7] that used Internet approach as new marketing strategy mix for business development with E-business, also [8] that designed Home Health Internet of Things as a novel health monitoring for the elderly people that stay at home due to several circumstances.

The latest trend in the field of information technology is cloud computing that migrates physical computing resource e.g. server and data storage to huge data centers [9] through internet.

There are several characteristics of cloud computing [9] such us data, applications or other services that provided by cloud computing can be accessed easily by using internet with a simple browser also high level IT abilities are not required in case of implementation or maintenance. Due to the term of high availability, multiple sites usage can ensure the reliability and scalability of cloud computing service. The other characteristics are easier maintenance because the application does not need to be installed on each user's computer and the payment is based on the facilities were used, also the system performance can be monitored easily. The last but not least is security. In cloud computing environment, security can be either equal with traditional system or better.
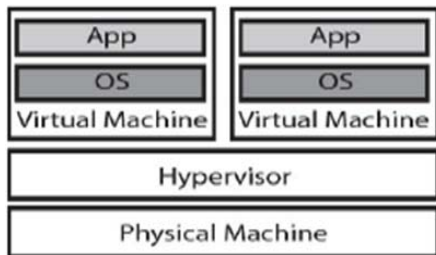
Fig. 1. Virtualization Principle[4]

Virtualization technology is the main key that enabling the emergence of cloud computing paradigm. Fig. 1 illustrates several virtual machines can be run simultaneously on one physical machine. Virtual machine migration is one of the virtualization capabilities allowing system to be transferred transparently from one physical host to another without losing system features [4]. In general, migration processes were done by moving or transfer the application along with the entire virtual machine system including CPU, memory, disk from the source system to the destination system.

Since virtual machine migration utilized for managing applications also its resources in the data center and cloud virtualized systems, it also enables system environment to relocate dynamically to other systems in a faster execution and more reliable way [2].

DMTF defines three types of virtual machine migration operation [2]. First, level 1 migration. Virtual machine system that will migrate must be ensured in the same product or architecture along with the destination system because this type of migration only runs on a particular virtualization product. The cycle is 'suspend' state in source system followed by 'reboot' state in the destination system. Live migration mechanism is possible to run on level 1.

Second, level 2 migration that support different hypervisors migration. The cycle is 'shut-down' state in source system followed by 'reboot' state in the target system.

The most flexible level for the virtual machine migration is level 3 that can be run on multiple families of virtual hardware but this type of migration still impossible due to several reasons.

Interoperability becomes one of critical factors. Cloud interoperability makes easily m*ig*ration and integration

process of applications and data between cloud service providers[5]. There are several attributes of interoperability between systems classified by LISI (Levels of Information System Interoperability) [5] :

1) Procedure

Several standard such us application development regulation, product development guidance, hardware and software standards could impact the interoperability level.

2) Applications

The critical aspect for application attribute is how well application running on different systems and platforms in accordance with its functionality.

3) Infrastructure

Infrastructure attribute shows the level of connectivity between systems and applications as well as how systems interact with other applications.

4) Data

This attribute means ability and flexibility of data format that run across systems environment became the main concern of interoperability.

TIOSA (Virtual Machine Interoperability Testing at an OS and Application Level) [1] is a method to measure system interoperability between two different hypervisors. TIOSA method using greybox-based testing method focusing on applications and operating systems verification. TIOSA testing method [1] included:

1) Structured and Repeated Process Models

a) Interoperability Check

Determine the possibility of migration between two hypervisors by collecting metadata required for the migration process.

b) Virtual Machine copy process of two hypervisor in a private cloud

This process ensures the virtual machine converted successfully and can be run on hypervisor target in accordance. The results of all tests that have been carried out is still within the limits of tolerable state
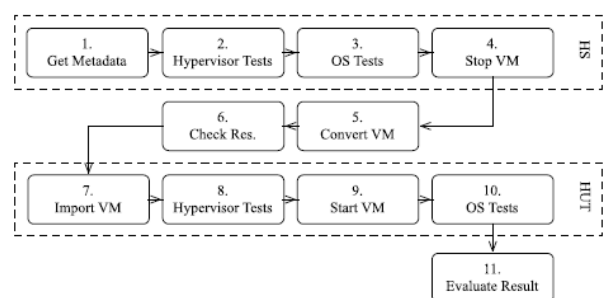

Fig. 2. TIOSA Method[1]

2) Test result measurement

The test results are grouped in several categories:

a) SUCCESS

Success status can be given if after migration process there is no changes in the term of several hypervisors and operating system parameters in target systems. All of the hypervisors, virtual machines, and operating systems run perfectly in new systems.

b) WARNING

The condition if after migration process there is a change but not too intrusive compared with the main functionality.

c) FAILURE

There are significant changes and not appropriate with the functionality of the system prior to the migration process.

3) Metrics comparative evaluation

There is a comparative evaluation metrics to determine indicators of the overall results of testing.

Implementation of TIOSA testing method uses combination of several cloud infrastructure products for virtualization e.g. VMWare, Citrix Xen, KVM and Microsoft Hyper-V. The total combined migration is 12 combinations for each operating system. The operating systems used in the implementation are CentOS 6.2, Ubuntu 12.0.4, and Microsoft Windows 2008 R2 64-bit. Figure 3 depicts the final result of the migration process with 36 combinations.
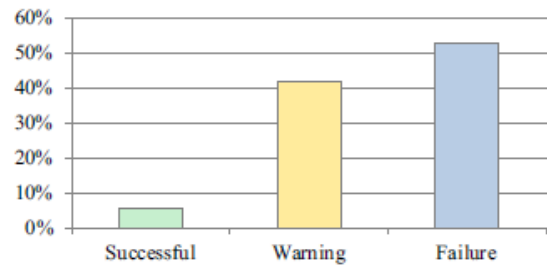

Fig. 3.   Final Result of TIOSA Testing

The drawbacks of TIOSA testing method are only testing interoperability at the level of the hypervisor and operating system, and have not been tested at the level of certain applications and data running on the system, so that TIOSA method cannot be implemented optimally for interoperability testing on the system that are in the industry.

III.   PROPOSED METHOD

The method proposed in this paper is the further development method of TIOSA that will add additional stages on the process of virtual machine migration in the cloud system. Application and data testing in both system also migration impact evaluation stage are being added in proposed method indicated by the numbers 2, 12, and 13.

Figure 4 depicts the proposed new interoperability method testing of virtual machine migration.
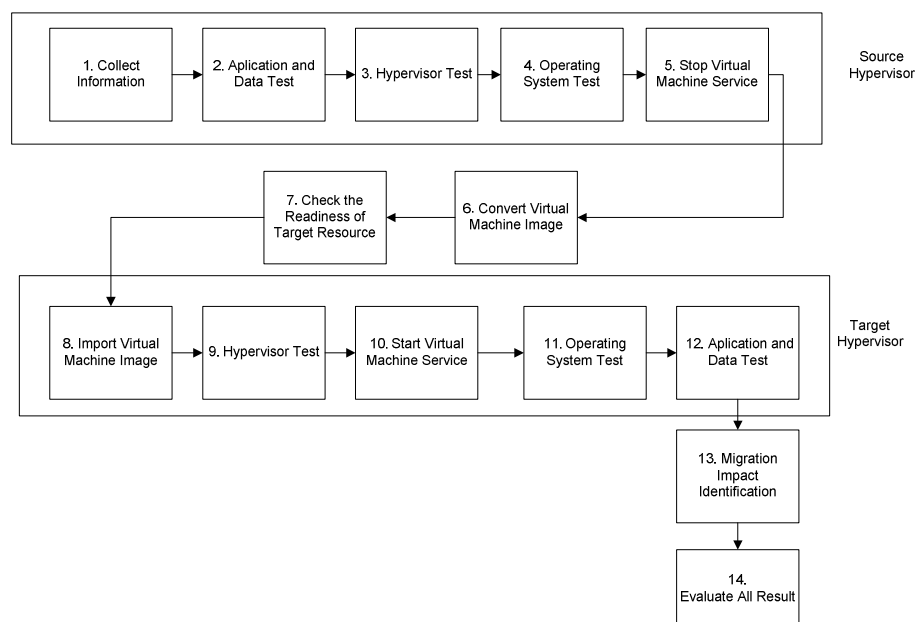

Fig. 4.   Proposed New Method

The process of collecting information relating to the possibility of migration between the hypervisor source and target such as the availability of virtual machine conversion application that supports the two systems to migrate and conversion application checking process that will be used whether support OVS (Open Virtualization Format) or not will become the early stage.

After collecting information between two hypervisors, the next stage is testing the application functionality and data consistency in accordance with the business processes running in the system. Hypervisor parameter test e.g. network management and storage in source hypervisor will be the next stage. Operating system test will perform by testing several attributes like the version of the kernel, network connectivity, user management as well as other parameters including other information resources.

Once all the above stages done, virtual machine service will be stopped and start to converting image using tool that available depend on hypervisor product used. Citrix Xen tool converter is one of the tools provided by Citrix that aims to convert the image in case of migration. Checking resource stage aims is to ensure readiness in the target hypervisor environment to start migration process. Virtual machine image import process can be done in an automated way using tools that are connected to the network between two hypervisor or by manually copying the image directly to target hypervisor. Hypervisor test followed by operating system test will performed after the convert process done. The last stage in target hypervisor is application functionality and data consistency test.

Migration impact identification process will measure several parameters in case of decreasing or increasing system performance after migration process. Final evaluation will be done by measuring and determining the test scores results of all the test data that have been obtained. Furthermore, the entire test results will be classified according to the level of interoperobility level.
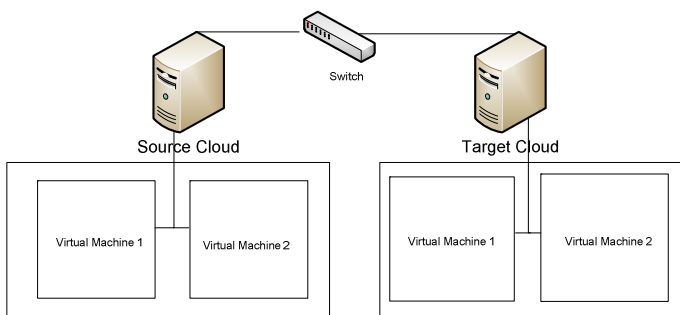

Fig. 5. Proposed Testing Environment

Figure 5 depicts the testing system design of the proposed method. Source cloud and target cloud environment are simulated using separate physical server that connected to network by switch.

Hypervisor in each cloud environment manages two virtual machines that contain operating systems, applications, and databases. In the migration process virtual machine image from source cloud will be converted using appropriate convert tool depend on their hypervisor type. The images will be transferred to target cloud through local network.

IV. DISCUSSION AND CONCLUSION

Based on the studies that have been done, there are several comparisons between TIOSA and the proposed method specified on the Table 1.

TABLE I.   COMPARISON OF TIOSA METHOD AND PROPOSED METHOD

No	TIOSA Method	Proposed Method
1	Does not tested at the level of application functionality	Will test at the level of application functionality
2	Does not tested at the level of data consistency in database	Will test at the level of data consistency in database
3	Does not be able to identify the impact of the migration process on the system	Will able to identify the impact of the migration process on the system
4	Does not approach the interoperability of migration system in the industry	Approach the interoperability of migration system in the industry

Data collection process will be conducted based on several test set for each testing components i.e. hypervisor test set, operating system test set, application functionality set test, data consistency test set also performance impact test set. Those tests are performed repeatedly before and after migration process to obtain data accuracy. Overall result will be achieved by classifying all of aforementioned test above to determine the level of interoperability.

In this paper we proposed further development method for interoperability testing between the two systems that migrate on different hypervisors. The method we propose has some benefits from the TIOSA's method because it test at the level of functional applications and data consistency that running on the system. Moreover, the proposed method can identify the performance impact caused by the migration process. This method can be used by organizations that want to test the interoperability between cloud systems in their system.

REFERENCES

[1] L. Alexander, K.Gregory, M. Michael, S. Ryan, R. Jannis, C. Enrique, and V P. Gopan , "TIOSA: Testing VM Interoperability at an OS and Application Level," *IEEE International Conference on Cloud Engineering.,* pp. 245-252, December 2014.

[2] Open Data Center Alliance(ODCA), "Implementing the Open Data Center Alliance Virtual Machine Interoperability Usage Model". Available : http://www.opendatacenteralliance.org

[3] Lewis, Grace A, "Role of Standards in Cloud-Computing Interoperability," *IEEE 46th Hawaii International Conference on System Sciences.,* pp. 1652-1661, January 2013.

[4] S. Anja, and D. Waltenegus "Does Live Migration of Virtual Machines cost Energy?"*, 2013 IEEE 27th International Conference on Advanced Information Networking and Applications,* pp. 514-521, March 2013.

[5] D. Scoot, B. Albert, B.M. James, and S. Man-Talk "Cloud to Cloud Interoperability,".*2011 6th International Conference on System of Systems Engineering,* pp. 258-263, June 2011

[6] vSphere 5 Documentation Center, "Introduction to VMware vSphere Virtual Machines,". Available : https://www. pubs.vmware.co

[7] D. Jovevski, Tijan. E, and P. Karanikić, "Internet Marketing Strategies and ICT as a common ground for business development," *MIPRO, 2010 Proceedings of the 33rd International Convention,* pp. 1120-1125, May 2010.

[8] P.P.Ray, "Home Health Hub Internet of Things (H3IoT): An architectural framework for monitoring health of elderly people," *2014 International Conference on Science Engineering and Management Research (ICSEMR),* pp. 1-3, November 2014.

[9] J.Yashpalsinh, and M. Kirit, "Cloud Computing - Concepts, Architecture and Challenges," *2012 International Conference on Computing, Electronics and Electrical Technologies [ICCEET],* pp. 877-880, March 2012.

Effect of Electromagnetic Radiation on Rice Plant Growth in Microgravity Environment

Arda Surya Editya
Institute of Technology Sepuluh Nopember
Surabaya, Indonesia
ardasurya@gmail.com

Istas Pratomo
Institute of Technology Sepuluh Nopember
Surabaya, Indonesia
istaspra@ee.its.ac.id

Gatot Kusrahardjo
Institute of Technology Sepuluh Nopember
Surabaya, Indonesia
gatot-kus@ee.its.ac.id

Abstract— **The existance of wireless technology indirectly take huge positive and negative effect on all organism on this earth especially plant. On previous research held by Racuciu, Lftode, and Miclauss said there is an effect on corn plant growth which treated by electromagnetic waves in 1 GHz frequency. The objective of this research is to prove the effect of electromagnetic waves on the plant in microgravity environment. In this research, 2.4 GHz electromagnetic waves were used and the testing environment will be used clinostat. The result on this research proved that there is an effect between electromagnetic waves 2.4 GHz on plant especially rice plant in microgravity environment. The main effect that we discovered is faster growth than normal condition.**

Keywords—Electromagnetic, Microgravity, Plant.

I. INTRODUCTION

Earth is the place all of creature and organism live within e.g. human, animal and plant. Plant is one type of living creature that has many benefits for humankind. Indonesia is one of the agricultural countries where most of the plant population due to tropical climate and soil texture that encourages farming predominately. Furthermore, Indonesian staple food is rice that derived from rice plant (*Oryza Sativa*).

Nowadays, a lot of researchs have been done to develop superior rice seedlings aiming to produce more rice in order to meet the food demand of Indonesian people, as we know rice fields getting smaller due to a lot of building and housing, especially in urban areas. Along with the development of information technology, many new technologies that facilitate human life, one of them is the wireless communication technology. With this technology allows humans to communicate remotely by using electromagnetic waves as a medium. The increasingly widespread use of this technology in everyday life, the impact on the number of BTS (Base Terminal Station). Of course as more BTS established, it will bring a great impact to the living beings who live around the Tower. During these studies that examine the effect of radiation of electromagnetic waves only focuses on a man, so the researchers rarely examined the impact of electromagnetic radiation for animals and plants.

Outer space environment where humans rarely to think about the impact of the space environment on the lives of living beings. This is due to the difficulty to build the same conditions as in space. At this time, we can build a condition where the condition is nearly resembling the conditions in outer space with a tool called clinostat. According Fathona et al. [4] reported that Clinostat built with the intention of creating a zero-gravity environment. From the facts presented above, researchers interested to research that aims to find the relationship between the development of the rice plants for space environment and radiation of electromagnetic waves.

II. STATE OF THE ART

Research on the effects of electromagnetic waves on plant growth had previously been done by Racuciu, Lftode and Miclaus [1] with the electromagnetic wave frequency of 1 GHz on corn and produce data as well as the period of exposure to a different microwave can affect seed germination and plant development started with the process mobile, such as mitosis. Study the effects of microwave exposure is important because they are worried about the effects that occur not only on the human body or a different animal, but also in plant organisms. As a result of this experimental study, we can say that the lower thermal oven 1 GHz microwave exposure is capable of initiating mutagenic effects and inhibition of cell proliferation and differentiation in seeds exposed. This indicates that there is an influence of electromagnetic waves on the growth and development of plants, further on previous research conducted by Igor Petrov Yu, Tatyana V. Moisseva and Elvira V. Morozova about [5] the effect of microwaves on plant wave results showed that there was accelerated growth of the seeds to plant without changing the cell structure of the plant. From both research before we can know that there is the influence of electromagnetic waves on the crop but research to investigate more about the influence of electromagnetic waves on this plant. On this paper researchers try to apply electromagnetic waves effects to plants in microgravity environment / space environment.

A. Clinostat

As quoted in the book made by the United Nations Programme on Space Applications Clinostat can be defined [2] assorted clinostats been developed, differing in the number of axes of rotation and operation mode with respect to the speed and direction of Clinostat form there is a form of two-dimensional (2-D), or an axis, Clinostat has a single rotational axis, which runs perpendicular to the direction rotation. of gravity vector. A Clinostat three-dimensional (3-D) has two axes of rotation, which is perpendicular to one another. Clinostat this type runs at a constant speed and in a constant direction, specifically called Clinostat 3-D. However, if the two-axis rotating at different speeds and in different directions. The present study concentrates on the comparison between different devices in order to determine the condition of the simulation is right for the object being treated. Clinostat can be equipped with the capacity for microscopy, online measurement of kinetic or chemical fixation samples during rotation. A rotation on Clinostat often called "clinorotation". Further [2] Clinostat movement analysis based on classical mechanics of the rotation and non-inertial frame. Rotation of

Clinostat generate fictitious force because there is a framework that is rotated coordinate system and the coordinates of the stationary frame. Both frameworks Clinostat rotated at a rate equal to the angle of the rotary axis, which is depicted as a dotted line as shown in Figure 1.
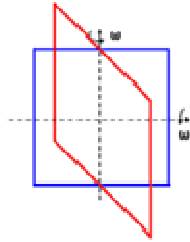

Figure 1. Clinostat Design

Figure above can describe with this equation:

$$F' = F - F_{Cent} - F_{Cor} - F''$$ (1)

With F is the force relative to the frame of reference that is stationary, F 'style relative to the reference frame rotating which is two order clinostat, Fcent a centrifugal force, F 'style which is caused by changes in rotational speed against time and Fcor is the Coriolis force generated when particle moving in a framework that is playing. Decrease Equation (1) is analogous to the two coordinate frame where XYZ is a framework that is silent and X'Y'Z 'framework that is playing is shown in Figure 2. The zero point of the second frame these coordinates coincide. Suppose framework X'Y'Z 'moves with a constant angular velocity ω, and we place a particle at the point P and the vector A.
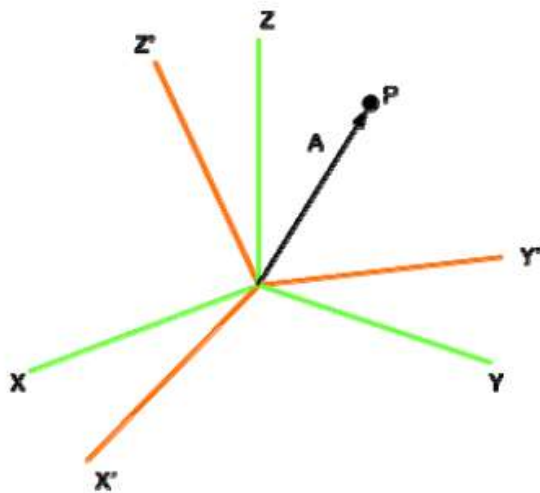
Figure 2. The intersection of the lines of force

By applying some conditions on Clinostat then some fictitious force would disappear or zero so that the fictitious force which is still in force is centrifugal force. Fcor koriolis style will be zero because the particles do not move to the coordinate frame is rotated; F " style caused by changes in rotational speed will be zero because the coordinate frame rotating speed ω be

made permanent; and we assume no frictional force or the influence of external forces so that F is equal to zero. Thus the force experienced by the particles only fictitious centrifugal force which is directed away from the rotary axis radially with a large following.

$$F_{cent} = m\omega^2 r$$

where m is mass and r is the radius. Because the quantity of the desired radius and acceleration are known, then we can determine the angular velocity of the DC motor so that the sample is placed on Clinostat will accelerate considerably smaller than the acceleration of gravity. DC motor speed is set by applying a PWM method, namely the setting powering the motor by regulating the time the motor off and on, or so-called duty cycle settings D.

$$D = \frac{T_{on}}{T_{on} + T_{off}} 100\%$$

Ton is the time motto tons and Toff is the time the motor off. This setting performed by the microcontroller by providing digital state 0 and 1 on the DC motor during a certain period in accordance with the calculation of the duty cycle D in Equation (3). Thereby forming microgravity environment.

B. Rice Plant (Oriza Sativa)

The rice plant is a plant that is used as a staple food, especially for the people of Indonesia. Even plants in nearly all parts of Indonesia are rice paddy which illustrates that the importance of this for the people of Indonesia.

Today many breeding of rice so that rice varieties more and more stuff. In general, the rice began to grow around 5-6 months. [4] The growth of the rice plant is divided into three phases: (1) vegetative (early growth until the formation will panicles / primordia); (2) reproductive (primordia until flowering); and (3) maturation (flowering to mature grain).

Figure 3. Phase Growth Rice Plant

C. Gravity Effect on Plant

The effect of gravity was very influential on plant growth as quoted in the book made by the United Nations Programme on Space Application argued that Gravity-dependent growth is based on a highly complicated stimulus-response chain. The physical signal of gravity has to be transformed into a biochemical signal, which leads to a physiological response. Gravity is a force that acts on mass. A mass has to be transported in the gravitational field in order to create

sufficient energy for the activation of a biological sensor. In order to transfer this signal at the level of a single cell, a mass which is denser than the surrounding medium must exist. This heavier mass sediment under the influence of gravity, thereby activating gravity specific receptors. Candidates for sedimenting mass are either intracellular statoliths or the entire cell mass (protoplast).9 The process that perceives gravity is called graviperception. Figure I shows a typical gravitropic response of a plant.
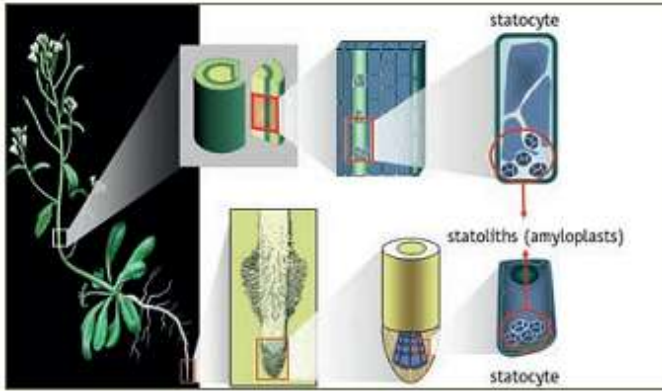
Figure 4. Growth of root plants with gravity vector

Furthermore, in United Nations Programme on Space Application also argued gravity is the stimulus that uses plants to grow roots toward the vector of gravity (below), retaining the plants in the ground, and to sprout in the opposite direction of the gravity vector (above), out of the land toward the sun. To understand the "up" and "down" is required for the survival of plants on earth.

It is also very necessary for all life on earth because photosynthesis necessary for the production of food and oxygen.

III. SYSTEM DESIGN

In the process of designing this experiment we will use three research objects and 2.4 GHz frequency electromagnetic waves to prove that there are significant electromagnetic wave frequency of 2.4 GHz on the growth of plants in the environment microgravity. The third subject may explain below:

1. Subject A = Rice plants are treated with electromagnetic waves and also microgravity environment.

Figure 5. Subject A

2. Subject B = Rice who just put in the microgravity environment.

Figure 6. Subject B

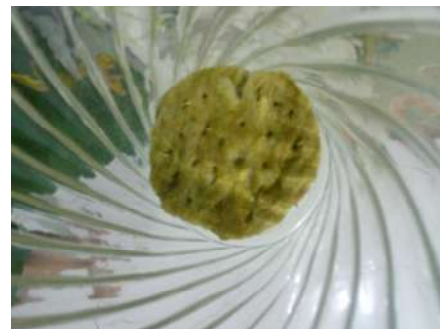3. Subject C = Rice grown without the use of electromagnetic radiation and microgravity environment.

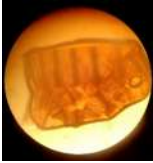Figure 7. Subject C

IV. RESULT

Based by research above we have result in subject A growth of Rice plant is faster than subject B and subject C because as past research who did by Racuciu, Lftode and Miclaus that use 1 GHz electromagnetic waves used on corn plant it can make corn plant growth faster and result of subject A is related with past result research. In microgravity electromagnetic wave have a role to make plant growth faster in microgravity.

In Subject B that provide by microgravity environment growth of rice plant is more slow than subject B because microgravity take effect on rice plant.

In subject C the rice plant planted in normal condition and the growth of rice plant is growth normally.

Of the three subjects are studied, it can be obtained as follows:

Subjek A	Subjek B	Subjek C
1. Growth Faster.	1. Growth more slow than normal.	1. Growth normal.

2. Growth with Kemotropism (root move to the nutrition way)	2. Growth with Kemotropism (root move to the nutrition way)	2. Growth with Geotropism (root move because gravity)
3. Result of root cell Figure 8. Root Cell Cell structure different with normal condition.	3. Result of root cell Figure 9. Root Cell Cell Structure more smaller than normal condition.	3. Result of root cell Figure 10. Root Cell Cell Structure normal.

V. CONCLUSION

Based on research that have been done, we encountered problem that this research has not been able to present more profound data because the limited facilities used during the study. In addition, the research data is still limited to rice plant. In general, the possibility of the result will be able to be applied to all plant because on previous research that performed by Racuciu, Lftode and Miclaus present the same data, but the research conducted by Racuciu, Lftode and Miclaus using normal environment. Different of past study with the present study we use a microgravity environment. With this research we add new knowledge about research in microgravity environment, because of that we can conclude :

1. With the 2.4 GHz frequency electromagnetic radiation can accelerate the growth of this is due to electromagnetic wave radiation heats the plant cells so that photosynthesis can be optimized.
2. With the 2.4 GHz frequency electromagnetic radiation can help plants to live in an environment microgravity (space) so as to allow for the existence of extraterrestrial life.

VI. FUTURE WORK

In future work research hope other work can prove if electromagnetic with different frequencies 1 GHz or 2,4 GHZ wil take same effect with past research. Also researcher hope research with space environment ore much that can be new knowledge about space environment and make a calculation to possible live in space.

REFERENCES

[1] R. Mihaela, l. Cora and M. Simona, "1GHz Low-thermal Microwaves Effect on Miotic Division of Vegetal Tissues," International Conference and Exposition on Electrical and Power Engineering (EPE 2014), October 2014.

[2] Fathona LW, Surrachman A, dkk, "Clinostat Tiga Dimensi sebagai Simulator Microgravity untuk Berbagai Eksperimen Tanpa Bobot," ITB Journal ISSN : 2085-2517, February 2011.

[3] H. L. Krauss, C. W. Bostian, and F. H. Raab, Teacher's Guide to Plant Experiments in Microgravity, New York: United Nations, 2013.

[4] Makarim Karim dan Suhartatik E.. Morfologi dan Fisiologi Tanaman Padi. November, 2009.

[5] Petrov Igor Yu, Moiseeva Tatyana V. and Morozova Elvira V., "A Possibility of Correction of Vital Proccess in Plant Cell With Microwave Radiation", International Conference and Exposition on Electrical and Power Engineering.August,1991

A Conceptual Framework of Engaged Digital Workplace Diffusion

Sarifah Putri Raflesia, Dinda Lestarini, Kridanto Surendro
School of Electrical Engineering and Informatics
Bandung Institute of Technology
syarifahpr@gmail.com, dinda.lestarini@gmail.com, surendro@gmail.com

Abstract---**Digital workplace creates challenges to improve the way people do their business. By using it, organization is able to collect, process, and provide data faster, share knowledge, enforce their employee to communicate and collaborate with any devices. Digital workplace can be enabled by implementing many recent technologies such as big data, cloud computing, search-based application, and internet connection. But in this paper, we argue that technology is not enough to help organization to do its business and reach its goal. According to these argument, we propose the conceptual framework of digital workplace diffusion. This conceptual framework integrates diffusion theory, user's engagement, and controls. Controls are contained IT governance, risk manangement, compliance. We believe that user engagement and control are one of keys for successful digital workplace diffusion. User engagement measurement is able to show the degree of employees' understanding and acceptance to the digital workplace. Meanwhile control is used to help organization in managing, monitoring, ensuring digital workplace is aligned to the requirements and regulations.**

Keywords--- digital workplace; digital workplace diffusion; user engagement;technologies.

I. INTRODUCTION

In information age, technology changes rapidly. New technologies can change the way people work and it becomes new challenge to begin improvement.The digital workplace is meant to be a virtual equivalent to the physical workplace[1] where employees can work anywhere by using any devices, share knowlege, and browse data faster. This idea is based on the used of several recent trends, Bring Your Own Devices (BYOD), Internet of Things (IoT), people-centric work methods, and analytics [2] which help employees to collaborate, do tasks, and activities effectively.

In this paper, we propose a conceptual framework to digital workplace diffusion. Beside adding the technologies and diffusion theory which can help organization to implement digital workplace, we propose user engagement-centric and controls in order to succeed well transformation. Employees must understand and accept digital workplace to bring a succesful digital workplace diffusion.

According to previous research, there is a positive correlation between full user involvement and participation with system success [3]. It becomes the reason for us to consider the focus on user engagement, we believe that the more users engage, the more chance for digital workplace diffusion to be success.

II. LITERATURE REVIEW

In this section, we will describe and discuss about related theories towards digital workplace diffusion.

A. Digital workplace

Digital workplace is a coordination between technology, process and people [1]. Digital workplace enables employees to work effectively from anywhere, at any time, on any device, and it provides an internet-like participative mode and user experience no matter where their location [4].

Digital workplace creates employees' ability to do their job by collaborating, communicating and connnecting with others [5]. To achieve this goal, we need technologies as support. Digital workplace is focused on developing an application for mobile environment. The integration of four technologies; mobile, big data, cloud computing, and search-based application enable us to achieve the desirable feature of digital workplace [6].

B. Diffusion

Technological diffusion is a multi-stage process comprised of adoption. It uses and widespread in corporation or society [7]. Roger describes diffusion as the process by which an innovation is communicated through certain channel over time among the members of a social system. There are four elements of diffusion. Those are (1) innovation, (2) communication, (3) time, and (4) social system.

Innovation is defined as an idea, practice, or object that is perceived as new by an individual or other unit of adoption [8]. Innovation is about figuring out how to add value for an organization. Innovation is the act with idea and succesfully bringing them to life to solve problem and create ooportunities [9].

In order to introduce the innovation, we need communication channels. It defines as which media to

transfer the messages from one individual to another in social system[8].

The third element of diffusion is time. We can find time dimension of diffusion in the innovation-decision process. The innovation-decision process is essentially an information-seeking and information-processing activity in which the individual is motivated to reduce uncertainty about the advantages and the disadvantages of the innovation. Fig.1 shows five stages of innovation decision process[8].

The last element of diffusion is social system which defines as environment where the diffusion occurs. The members or units of a social system maybe individuals, informal groups, organizations, and/or subsystems. Diffusion is a kind of social change because the decision to adopt or reject an innovation will lead to changes in structure and function of social system[8].
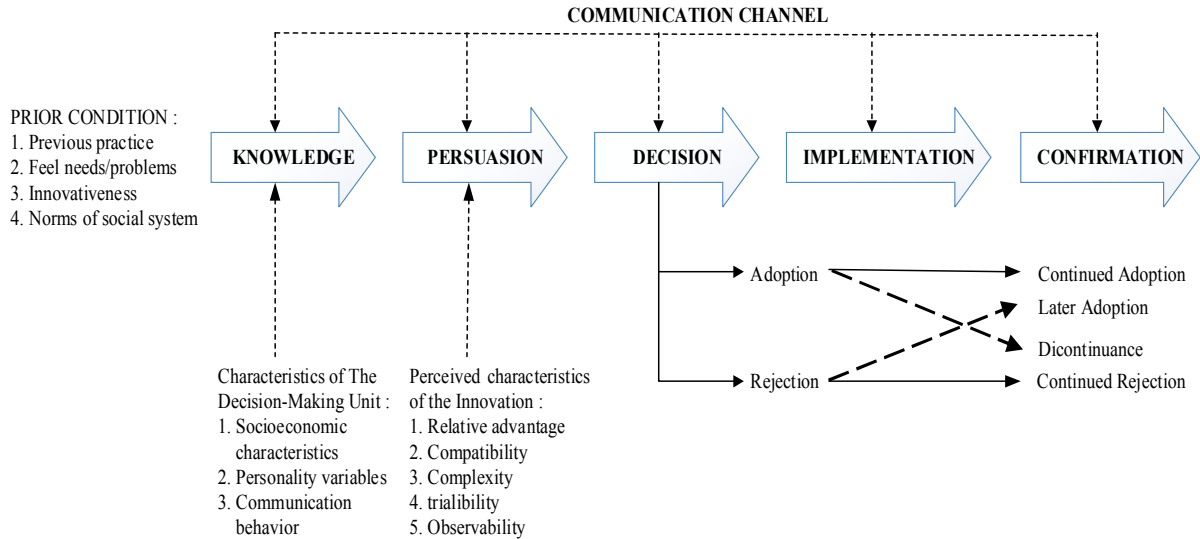
Fig. Innovation Decision Process [8]

C. User engagement

In order to engaged digital workplace, we need to ensure that users are involved and participated. These are compressed as user engagement. User engagement is defined as the quality of the user experience that emphasises the positive aspects of the interaction. It is not just about usability but it also contains how users invest time, attention, and emotion when they are connected to the system [10]. It matters because it is related to the confirmation of adoption status. When a user is engaged, it means they will more understand about what they should do and they will admit the value of whole system and there will be a chance to the innovation to be well adopted. User engagement has become an issue in the implementation of IT. It is a cognitive aspect which represents of positive emotion like enjoy and willingness [11]. It will suddenly cause the internal satisfaction. According to previous research, user engagement has 6 attributes, focused attention, aesthetic, novelty, perceived usability, endurability, felt involvement [12]. Table 1 shows the list of engagement attribute and description. This attributes will be used to measure user engagement of digital workplace.

TABLE I. DESCRIPTION OF USER ENGAGEMENT ATTRIBUTES

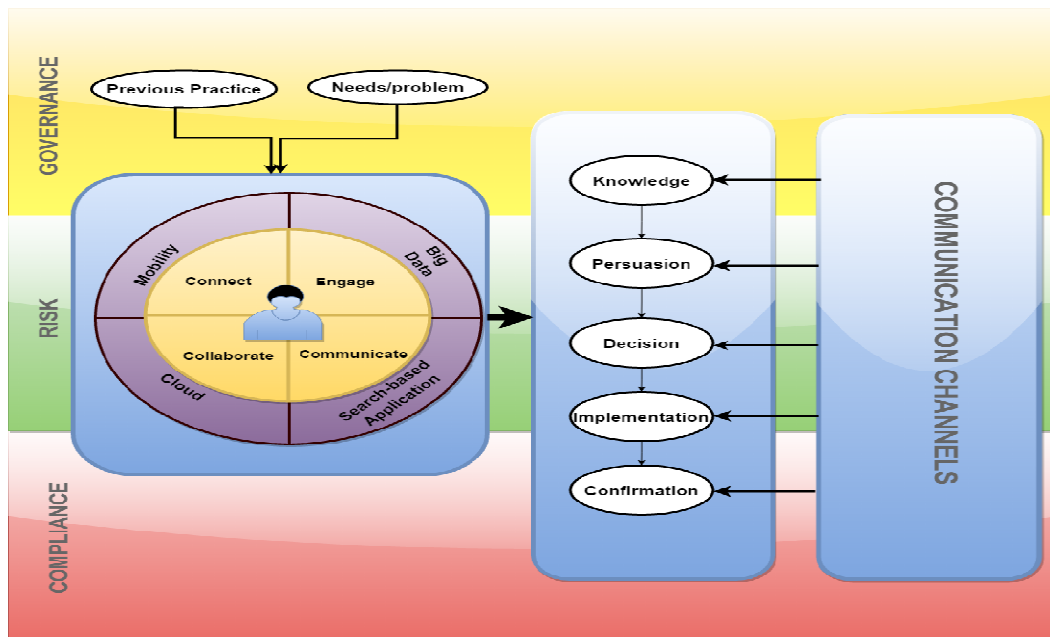| Attributes	Description
Focused attention	The state of total absorption in situation, and full attention [13]
Aesthetics	Aesthetic is defined as the feeling of beauty when a user interact to the system[14].
Novelty	The feeling of surprise and excitement when interacting to interface [12]
Perceived usability	It is defined as the perception when system is not beautiful means the system is not usable. [15]
Endurability	This attribute is defined as the state when the system is worth to try again in the future [16]
Felt involvement	The feeling of self relevance which affects attention [17]

Fig.2. Conceptual framework of Digital Workplace Diffusion

I. DESIGN OF CONCEPTUAL FRAMEWORK FOR DIGITAL WORKPLACE DIFFUSION

In this part, we will introduce the conceptual framework for digital workplace diffusion. As we can see fig.2, this model contains integration between diffusion theory, digital workplace concept, and user engagement. This two concepts lie on control which responsible to manage risks, compliance, run good IT governance along digital workplace diffusion.

A. Initial Stage

Before we decide to use the innovation, we have to identify where we are now. This activity enable us to define current status, future target, and how digital workplace helps organization to reach its goal. The common reasons of digital workplace diffusion are awareness and organization needs. It is an awareness if organization becomes more active in improving and monitoring the IT trends. In this state, organization is more open to digital workplace because it has advanced understanding to the advantage of implementing digital workplace.

Organization needs are caused by dissatisfaction to current practice. In this state, organization would examine a new technology to fulfill its needs. Digital workplace diffusion enables the organization to improve the used of technology from a previous state to desired state. It involves new technologies and employees's habits which are enable the core competencies of digital workplace.

B. Digital Workplace Technology

Nowadays, many new technologies emerged to support business. Those technologies, such as cloud computing, big data, mobile, and search-based application, create opportunity for organization to create a digital workplace. Along with those technology, we also need to consider business goal and capability of organization in order to build a digital workplace that can be accepted by employees and give a poitive impact for organization.

Digital workplace is focused on developing application in mobile environment. Cloud computing enables people to access data or applicationby using any devices which is already used by employee, such as PC, tablet or smart phone. It also enables people to connect and work together no matter where they are.

Organization also needs many data to support its business. These data comes from many different source and in different format. Big data helps employee to collect, process and visualize data faster. Given the amount of data involved, we need to develop search-based application in order to help employee access those data faster.Integration of those technologies will make a big improvement to organization's performance.

C. Innovation Decision Process

In this part, we will discuss about innovation decision process. It contains knowledge, persuasion, decision, implementation and confirmation. In every activity, there will be communication channel to facilitate us to introduce and give understanding about the digital workplace to employees as adopters.

1. Knowledge

In this stage, we will introduce the idea of digital workplace to the decision making unit. The decision making unit is represented as IT manager or IT supervisor. This

stage is an important state because it determines how the process will be proceeded and it mattes because if decision making unit is failed to recieve the basic understanding about benefits and business impact of digital workplace, they will reject to use it. According to this issue, we have to focus on how we present the idea. Moreover we have to take concern at socioeconomics, personality variables, and communication behavior in order to identify the type of adopter. It matters to help us in choosing suitable communication channels.

Socioeconomics is about how to identify education level, income, and occupation. Moreover, personality variables is used to find personality type. At this activity we can use five factor model (FFM). FFM is widely known as psychology model to identify human personality. This model contains openness to experience, conscientiousness, extraversion, agreeableness, neuroticism.

After we identify employees' personality type, we can continue to check on communication behavior. It contains three characteristics; communication quality, the extent of information sharing between employees, and participation in planning and goal settings [18]. After we analyze three characteristics of decision making unit, we can find the type of digital workplace adopter.

According to the type of adopters, we may choose communication channels to present the digital workplace. Earlier adopter will more interest in cosmpolite mass media channel. Meanwhile, later adopter will more interest in cosmopolite interpersonal channel.

2. Persuasion

Persuasion stage aims to form the attitude of decision making units toward digital workplace. After they gain some understanding about digital workplace through knowledge stage, they will more involve with the idea of digital workplace. They will find more information about digital workplace. Table 2 shows the characteristics of digital workplace which have to be covered. Finding the characteristics of digital workplace as innovation is important to decrease the degree of uncertainty for individual. In this stage, we can use interpersonal channel to communicate with decision making unit.

TABLE 2. CHARACTERISTICS OF DIGITAL WORKPLACE

Characteritics	Description
Relative Advantage	How digital workplace increasing user engagement and job satisfaction which can lead to productivity and profit organization
Compatibility	Digital workplace meets orgaization needs and must be compatible with existing value and system
Complexity	Digital workplace must be easy to be understood and used. Additionally, along the implementation and use, there will be many changes which come from business and technical, so digital workplace must be easy to customizable
Trialability	At the persuasion stage, the idea of digital workplace seems to be uncertain, to minimize the risk which will lead to rejection, we must add prototype. By using prototype, we can present and demonstrate digital workplace. Moreover, we must enable the users to try or even use it to prove the list of advantages.
Observability	As we discuss at trialability section, we enable the organization to try the prototype and understand the mechanism. It will ensure that organization are able to check on what digital workplace can do for the organization.

3. Decision

Organization will decide to adopt or reject the implementation of digital workplace for their organization at decision stage. In this stage, we will use interpersonal communication channel.If the organization decides to adopt, we may prepare the requirements to implement the suggested innovation. In contrary, the rejection can be a passive and active rejection. Passive rejection is the state when organization refuses to adopt innovation at the first presentation of innovation. Meanwhile the active rejection is defined as the state when the organization considers to adopt the innovation but at the end organization decides to not implementing the innovation [8].

4. Implementation

When organization decides to adopt digital workplace, the next step is to implement it in organization. The organization and developer must discuss IT infrastructure, configuration, standard operations, and set up a support system to ensure the digital workplace runs properly.We also need to communicate the changes which is caused by implementation of digital workplace to all employees. In this stage, we can combined interpersonal and mass media communication channel.

5. Confirmation

After implementing digital workplace in organization, we have to review and monitor the impact of digital workplace implementation. It will ensure that organization make a right decision. Organization can reverse the decision, if they find the implementation of digital orkplace has failed to boost the disired performance.

In this stage, we also proposeuser engagement measurement. Implementation of IT, including digital workplace needs full participation of employees as users. We propose the use of user engagement measurement which is formulated by Heather O'Brien. Using this measurement, we will measure every atributes of user engagement.

D. Control

This part descibes about control as the element to help organization in managing, controlling, and ensuring the digital workplace diffusion is aligned to the internal and external standard. Internal standard can be organizational standards policies and procedures, while external standard can be a government's regulation.

1. IT Governance

We need IT governance along the implementation of digital workplace as an innovation. IT governance helps organization to ensure the use of IT is effective, efficient, and meet its goals. IT governance enables organization to fix organization's culture issue along with digital workplace as IT product implementation, and measure IT and business performance. Digital workplace as IT product requires an enterprise-wide focus, by implementing digital workplace organization must have solution for issues which are related to business and strategic. There are many frameworks which are related to IT governance, such as COBIT, ITIL, etc. Every organization is unique, so we can discuss with the board about what kind of IT Governance that might be suitable.

2. Risk Management

Every project has risk and if it is being left uncertainty and ignored, it will become seeds of failures for organization. Digital workplace diffusion is big project with high level of cost, risk management must be run to help organization in identifying, monitoring, prioritizing, minimizing risk, formulating guide, strategy, and policy, and more important is providing solution of risks using technology, human and organization resources. There are many framework for IT risk management, such as Cobit, Coso's Enterprise Risk Management (ERM), Risk Management Framework (RMF), etc.

3. Compliance

The implementation and operation of digital workplace must comply to organization policy and regulation in which it is implemented. When we decided to use digital workplace, we must define all the relevant rules and regulations, such as privacy law, Data Protection Act (DPA) etc. Thereafter, those rules and regulations along with organization policy will serve as guideliness for developer to develop the digital workplace. In operation of digital workplace, we also need to monitor employee's compliance to organization policy and regulation to avoid misuse of digital workplace.

IV. CONCLUSION

In this proposal, diffusion theory is suggested as an approach in introducing and implementing digital workplace. We also propose the use of user engagement-centric and control. User engagement-centric helps organization to measure the degree of user involvement and acceptance to digital workplace. Meanwhile, control which contains IT governance, risk management, and compliance

help organization to align digital workplace and its business, evaluate, and monitor the activities in digital workplace. Futher research of this proposal is validation of the model and the impact of digital workplace to organization culture.

REFERENCES

[1]   N.Dotson, Building a Better Digital Workplace., San Fransisco, CA, CMSWire.

[2]   D.Lavenda, "What Gartner Wants You to Know About the New Digital Workplace." Internet : http://www.cmswire.com/social-business/what-gartner-wants-you-to-know-about-the-new-digital-workplace/, May 28, 2015 [Sep. 5, 2015].

[3]   M.I.Hwang and R.G.Thorn, "The effect of user engagement on system success: a meta-analytical integration of research findings." *Information and Management Journal*, vol.35, pp.229-336, Apr.1999.

[4]   J. Mcconnell, "Digital Workplace - Trends and Transformation," Washington D.C, 2013.

[5]   F. Herrera et al, "The digital workplace: Think, share, do,"Deloitte, Canada, 2011.

[6]   M.White."Digital workplaces: Vision and Reality".*Business Information Review,*vol.29, 205-214, Des.2012

[7]   M.S. Elliott and K.L. Kraemer. Computerization Movements and Technology Diffusion: From Mainframes to Ubiquitous Computing. New Jersey : American ociety for Information Science and Technology. 2008.

[8]   E.M.Rogers. *Diffusion of Innovations*. New York: Free Press, 2003.

[9]   R.B. Tucker. Innovation is Everybody's Business: How to Make Yourself Indispensable in Today's Hypercompetitive World.Hoboken, NJ : John Wiley & Sons, 2011, pp.12-13.

[10]   J.Lehmann, M.Lalmas, E. Yom-Tov, G.Dupret,"Model of User Engagement,"in *UMAP'12 Proceedings of the 20th international conference on User Modeling, Adaptation, and Personalization*,Montreal, CA, 2012, pp.164-175.

[11]   B.Laurel,*Computer as Theater*. Boston, MA : Addison-Wesley Longman, 1993.

[12]   H.L.O'Brien and E.G.Toms,"The Development and Evaluation of a Survey to Measure User Engagement," *Journal of the American Society for Information Science and Technology*, vol.61, pp. 50-69, Jan 2010.

[13]   M.Jennings, "Theory and models for creating engaging and immersive e- commerce websites,"in *SIGCPR '00 Proceedings of the 2000 ACM SIGCPR conference on Computer Personnel Research*, New York, USA, 2000, pp. 77-85.

[14]   R.Hunicke, M. LeBlanc, R.Zubek, "MDA: A Formal Approach to Game Design and Game Research," in *Proceedings of the 2004 AAAI Workshop on Challenges in Game Artificial Intelligence*, San Jose, USA, 2004.

[15]   O.Eliav and T. Sharon, "Usability in Israel,"in *Global Usability*,I.Douglas and L.Zhengjie, Eds.London : Springer, 2011, pp.169-194.

[16]   Y.Hung, W.Li, Y.S Goh,"Integration of Characteristics of Culture into Product Design: A Perspective from Symbolic Interactions,"in*Cross-Cultural Design, Methods, Practice, and Case Studies*,vol. 8023.P.L.P.Rau, Ed. Berlin:Springer,2013, pp.208-217.

[17]   R.L.Celsi and J.C.Olson."The Role of Involvement in Attention and Comprehension Processes."*Journal of Consumer Research*, vol.15, pp.210-224, Sep.1988.

[18]   J. J.Mohr and R.E.Spekman, "Characteristics of Partnership Success : Partnership Attributes, Communication Behavior, and Conflict

Resolution Techniques." *Strategic Management Journal,*
vol.15,pp.135-152, Feb.1994.

A Conceptual Framework for Implementing Gamified-Service to Improve User Engagement by Using ITIL

Sarifah Putri Raflesia
School of Electrical Engineering and Informatics
Bandung Institute of Technology
Bandung, Indonesia
Syarifahpr@gmail.com

Kridanto Surendro
School of Electrical Engineering and Informatics
Bandung Institute of Technology
Bandung, Indonesia
Surendro@gmail.com

Abstract--- Gamified- Service is defined as a service support which used ITIL and gamification model to boost the motivation of service support employees. Along the implementation of service support, organizations find the challenge which is related to human resource who deliver the service. Pressure at workplace and personal issues become trigger to decrease their productivity. According to this fact, standard service support is not enough. We need persuasive approach to guarantee that employees are totally engaged. In other side, to ensure that good service support is implemented, we need best practices of IT Service Management, it is Information Technology Infrastructure Library (ITIL). This research is focused on creating a framework to build, implement, and maintain good service support with full engaged employee.

Keyword---gamification;ITIL;service support;user engagement

I. INTRODUCTION

Most of organizations in this era implement information technology (IT) to help their activities run more effective and efficient. But, there are always unexpected incidents and problems during the use of IT. Those unexpected situation can slow the activities down, so that there will be delay time which will cause disappointment of end users as stakeholder. It is why we need service support to fix the IT incident and problem.

The implementation of service support needs best practice that is able to ensure standard service support is well designed. In this research, we use Information Technology Library (ITIL). But, we think that best practice is not enough because it just handles the mechanism of how to deliver good service support, it can not handle the employees of service support's motivation. Moreover, it can not ensure the engagement between employees and the system they use. Base on this finding, we need other persuasive approach.

Gamification model is the use of game design in non-game context[1]. This model is used as persuasive approach to motivate users of system in order to reach the system owner's goal. By using gamification, we can increase productivity of service support employees.

Naturally, human like challenges, games appeal to the players because there are challenges and uncertainties. Scientists who research about human's brain around the world agree that challenge – achievement - reward loop promotes production of dophamine. It can create satisfaction and reinforce desire to play [2].

This research focuses on the integration of ITIL and gamification model. The representation of the integration is a conceptual framework to build, implement, and monitor gamified- service. We believe that full engagement of employees will increase the productivity.

II. LITERATURE REVIEW

A. ITIL

ITIL is document that presents best practices to manage the implementation of IT service. ITIL explains the detail of management and IT operations such as incident management, problem management, change management, configuration management, and availability management. The latest version of ITIL is ITIL 3.0 which has been published in 2007 by Office of Government (OGC). It contains 5 phases of service lifecycle.

- Service Strategy
- Service Design
- Service Transition
- Service Operation;
- Continual Service Improvement

B. Service Support

The service support first presents in previous version of ITIL, version 2.0. It covers main cores of ITIL processes which are responsible to support the IT services. In the latest ITIL, it will be represent as service operation. Service support covers the concepts below :

- Service desk
  To run ITIL processes, we need a function. Service desk is a function to provide communication between users and IT employees. The roles and responsibilities of service desk are senior service desk manager, service desk manager, service desk supervisor, and service desk analyst [3].

Service desk primary tasks are providing solution of IT infrastructure incident, request, problem,etc. Moreover, service desk is a single and first line which communicate with users in order to provide information about status of incident, request, problem, etc, and give guidance and solution to users.

- Incident management
Process defines as set of structured activities and tasks that produce a specific goal [4]. ITIL processes have been specified. Such as incident management, it has been specialized to manage incident. Incident Management is often the first process when introducing the ITIL framework to a Service Desk, and offers the most immediate and highly cost reduction and quality gains [5].

- Problem management
This process contains activities to diagnose the root cause of incident. It also responsible to maintain problem information and resolution. So that organization is able to minimize incident.

- Configuration management
Process configuration management is a system that integrate all tools and provides critical data on improvement opportunities [6]. It eliminates a lot of manual works and produce better stability, predictability, and maintainability.

- Change management
Process change management is defined as set activities to ensure the standard procedure are used to control changes.

- Release management
The release management contains planning, designing, building, configuration, and testing hardware and software releases to create a set of release components.

C. Gamification

Many organizations have implemented gamification model in order to motivate their employees while doing their tasks. Last four years, gamification has been discussed. Many applications have been using gamification, such as Nike+ Running, GoJek, and Foursquare. Gamification helps the organization to gain costumer 's satisfaction. It is not about a user interface design, but it is about how to reach the goal with fun way. Gamification enables win – win solution between organization and employees [7]. Organization can reach their goal, and employees are able to get the internal satisfaction, like full engaged system, reward, and reputation.

Based on research, job satisfaction, high loyalty, and productivity of employees are stimulated by good internal service and organization policy [8]. It means issues which are related to employees satisfaction is critical in helping organizations reach their goals and business such as satisfying their costumers.

D. User Engagement Measurement

User engagement is defined as the quality of the user experience that emphasises the positive aspects of the interaction. It is not just about usability but it also contains how users invest time, attention, and emotion when they are connected to the system [9].

According to the previous research, user engagement attributes are focused attention, aesthetic, novelty, percieved usability, endurability, felt involvement[10]. By using user engagement scale (UES), we can get the score of each attributes. While, the accumulation of every score is the degree of user engagement. But, it is also available for us to present the result as the score of each attributes in order to simply identify which attribute is being a focus to evaluation.

E. Service Life Cycle Development

In Application Management Document which is one of ITIL product shows SDLC as an approach to manage service application[11]. The steps of SDLC are :

- Feasibility study
In this first step, we will do a set of practices to ensure that service is feasible to be implemented.

- Analysis
Implementation of service support needs the analysis about what is the current and desired state of selected process or function, and how do we reach the desired state. Moreover, we have to do some research and observe about stakeholder's needs and system requirements.

- Design
After we gather the stakeholder's needs and system requirements, we will create desired process business scheme. In this step, it is possible for us to build prototype in order to give better understanding to stakeholders about the system which will be deployed.

- Testing
The prototype or design that have been created in previous step will be tested. In this step, we will ensure that design is well designed and meet the stakeholder's needs and system requirements.

- Implementation
In this step , the design which has been created will be transformed to application. After the application is coded, we need to test and if the application has been agreed by stakeholder, we will set up the infrastructures to support the application.

- Evaluate
After the application has been set up, we need to evaluate the system periodically in order to find bugs and errors.

- Maintenance
When the bugs and errors have been listed, we need to fix the system. In this step, we must ensure that system run properly. Moreover, along the maintenance, we have opportunities to gather information and monitor the system in order to find a challenge for improvement.

III. FRAMEWORK DESIGN

A. Gamification Framework Design

From literature study [12] [13], we design gamification framework that will be used to develope game mechanincs on service system. Figure 1 shows the presentation of model.

functional and non-functional tests. Additionally, this step will engage the end users to try the system.

- Monitor
  In this step, we need to ensure that gamification elements and mechanics work properly and meet the agreements.

B. Proposed Conceptual Framework for Building Gamified-Service

The conceptual framework gamified- service is deal with two framework which have been explained and created at previous section. Fig 2. We can see the combination of SDLC and gamification model design

Fig. 1. Gamification framework design

The steps of gamification framework are :

- Initialization
  In this step, we need to know which part of process that must be gamified. Moreover, we need to identify who will join the project and form teams.
- Analysis
  After we identify what process that will be improved or built, we need more detail and deeper analysis about current state of process and what is the desired state, after that we need to identify who are the users of system. Identifying users is needed because we need to choose game elements. Moreover, in this steps we have to discover what kind of technology that will be used.
- Design
  In the analysis step, we have identified who are the users. In this design step we will design game element that will be used. Such as designing badges, virtual contents, etc.
- Colaborate
  After the elements are ready, we will integrate the element to the system and create game mechanics. Game mechanics is about how a game operate, what are applied rules, and how the players interact to the game[14]. In gamified- service perspective, this component defines tasks and actions that user can do to system.
- Testing
  In this step, we will test the the design or prototype. We will present the design and let the system owner to fully check the correctness.
- Implementation
  If the design is accepted and the tests are success. We will continue to implementation step. In this step, the full gamification model will be deployed. After the deployment, the second tests will be held. It includes
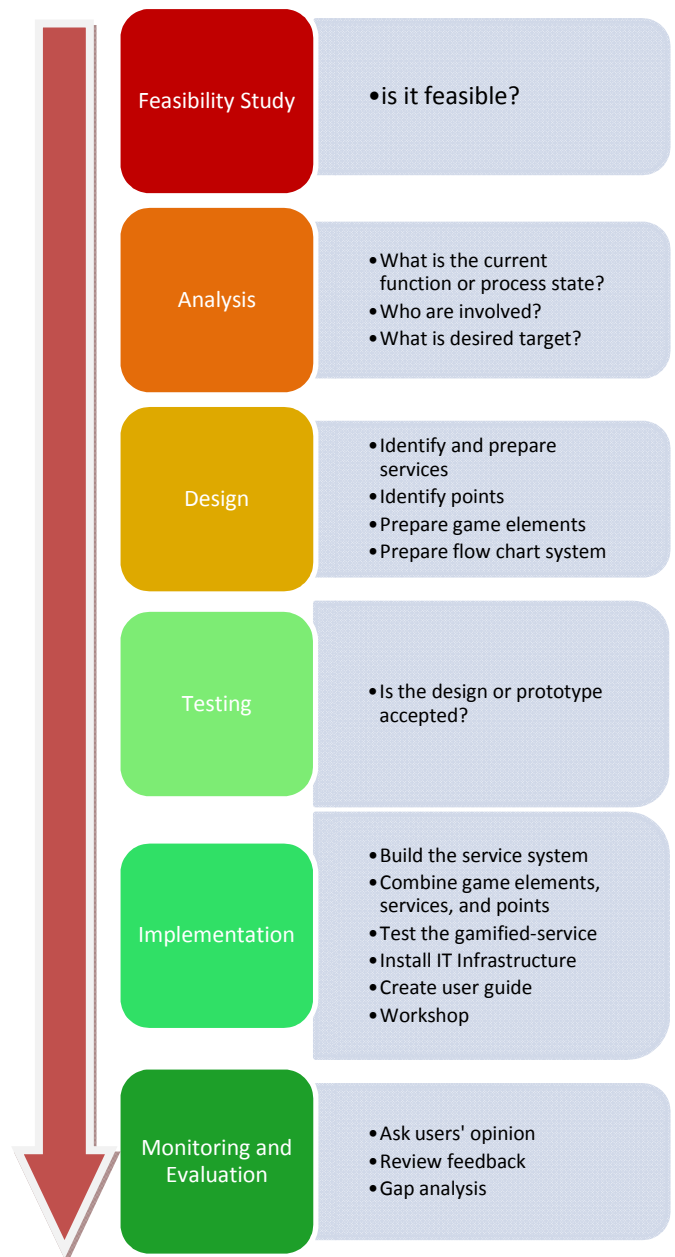
Fig. 2. Conceptual framework for Implementing Gamified-Service

The steps of conceptual framework for gamified-service are:

- Feasibility Study
  This step deals with the study to identify feasibility status of implementation gamified service. We need to identify the benefits of implementing gamified-service.
- Analysis
  If we find that gamified- service is feasible to be implemented. We can continue to analysis step. This step is focused on what is the current state of process or function that will be integrated with gamification model. We need to identify indicators in Table 1to simply assess current state of service support[15] :

TABLE 1 BASIC EVALUATION INDICATORS FOR
SERVICE SUPPORT

Indicators	Explanation
Response time	Response user's calls as soon as possible
Call rate	Rate of request for help (RFH) that comes from service desk
Records of request call	Numbers of the events and insidents recorded by service desk
Rate of complains	Assessing the service desk whether handling incident
Accuracy of incident classification	Assessing the service desk whether handling accidents by the defined categories
Growth rate of desk insident	The rate that incidents could not be processed
Rate of incident handling	Remote processing rate when service desk recieves the RFH
First call completion rate	Connected rate when user first calls

Moreover, we have to identify who are the users and then we identify user engagements, motivation, opinions and stakeholder's needs which are related to their view about the system. After gathering the stakeholder's needs and user's opinions, we need to identify their desired target.

- Design
  In this step, we prepare service and gamification contents. We also need to design rules for every actions. Below are activities of design:
  - Identify and prepare service
    This part deals with identification service features which are based on ITIL concept
  - Identify Points
    In this activity, points are identified. Points are used to get contents and stimulate elements

  - Prepare game elements
    After identify the service and points we will prepare what are game elements that will be integrated to the service system.
  - Create flow chart system
    After preparing all requirements, we need to create a process business of gamified- service. If needed, we can create prototype to deliver the design and gamified- service mechanism to system owner.
- Testing
  The design has been created and we can continue to the testing step. In this step, we need to present our design to system owner to ensure the design meets their requirements.
- Implementation
  The design that has been created and accepted will be transformed to service application. In this step, we will also do activities below :
  - Combine game elements, service, and points
    In this activity, every elements which has been choosen will be combined with rules.
  - Testing gamified- services
    In this activity, we have to complete functional test, non-functional test, user acceptance test (UAT). The goal of functional test is ensuring the gamified- service runs properly without errors. Based on ITIL, we may use diagnostic hooks which provide informations to fix errors. While, non-functional testing is more advance. It will test the degree of security, performance, usability, etc. When functional and non-functional test are done, we may engage the users to run UAT. This final test will direct to approval or rejection.
  - Set up IT infrastructure
    To run gamified- service we need other support technologies such as hardware and network. In this activity, we will engage IT Technical Expert.
  - Create user guide
    User guide is needed to provide guidance to users. It helps users to understand and operate the gamified-service.
  - Giving workshop and training
    This activity is important because it is the best way to help user to operate and understand system.
- Monitor and Evaluate
  We need to monitor system activity to ensure that system run properly. The other activities that we should do in this step are :
  - Asking user's opinion
    In order to gather information about user engagement, we need to interview system users. Their opinions are needed to identify what should be fixed and improved.
  - Review feedback
    After gather the information from users, we can set up solution to fix or improve the system.

- Gap analysis

First, we need to review the degree of user engagement. We can use user engagement measurement to ensure that we reach one of gamified-service goals. In order to assess the quality of service support, we can do assessment based on table 1. In the analysis step, we have the information about the state before the implementation. To ensure that we meet the goals, we can compare the state before and after implementation.

IV CONCLUSION

Service support employees must be fully engaged to the system because they responsible to communicate with users in order to help users fix incidents, problem, etc. If they can not engaged to the system, then it will cause slow response to the request, event-handling, incident, etc. Engagement deals with employees' motivation, involvement, and participation. So, we propose conceptual framework which integrate ITIL and gamification model. By using gamification in service support, the engagement will be increased and may return benefits to organization such as internal satisfaction, costumer trust, etc. This framework can be used to do some future research in gamified- service, like implementing mobile gamified-service or gamification system for costumers.

REFERENCES

[1] S.Deterding, D. Dixon, R. Khaled, L. Nacke, "From Game Design Elements to Gamefulness: Defining "Gamification" ," , 2011.

[2] G. Zichermann and C. Cunningham, *Gamification by design: implementing game mechanics in web and mobile apps*. Sebastopol, Calif.: O'Reilly Media, 2011.

[3] D. Knapp, *A guide to service desk concepts*, 3rd ed. Boston, MA: Course Technology, Cengage Learning, 2010.

[4] T. H. Davenport, *Process innovation: reengineering work through information technology*. Boston, Mass.: Harvard Business School Press, 1993.

[5] Q. Wang, J. Song, L. Liu, X. Luo, and E. Xinhua, "Building IT-based incident management platform," *5th International Conference on Pervasive Computing and Applications*, 2010.

[6] J. Bon, *Foundations of IT service management based on ITIL*, 2nd ed. Holland: Van Haren Publishing, 2005.

[7] A.Narayanan, *Gamification for Employee Engagement*, UK : Impackt Publishing, 2014.

[8] J.K.Heskett, J.O.Jones, et.al., *Putting the Service-Profit Chain to Work*, USA :Harvard Business Review, 1994.

[9] J.Lehmann, M.Lalmas, E. Yom-Tov, G.Dupret,"Model of User Engagement," in *UMAP'12 Proceedings of the 20th international conference on User Modeling, Adaptation, and Personalization*, Montreal, CA, 2012, pp.164-175.

[10] H.L.O'Brien and E.G.Toms,"The Development and Evaluation of a Survey to Measure User Engagement," *Journal of the American Society for Information Science and Technology*, vol.61, pp. 50-69, Jan 2010.

[11] Office of Government Commerce OGC, Application Management, UK : The Stationary, 2002.

[12] [12] P.Herzigg, M.Ameling, et.al. " *Gamification in Education and Business*. Springer International Publishing, 2015.

[13] S. Harris and K. O'Gorman, *Mastering Gamification : Customer Engagement in 30 days : the Revolutionary way to Attract Customers, Keep Them Coming Back for More, and take Your Business to the Next Level*, UK : Impackt Publishing, 2014.

[14] A.Ernest and A.Rollings, *Fundamentals of Game* Design, USA : Prentice Hall,2006..

[15] Z. Yao and X. Wang, "An ITIL based ITSM practice: A case study of steel manufacturing enterprise," *2010 7th International Conference on Service Systems and Service Management*, 2010.

The Implementation of Communication System Based on FPGA

Lv Hong
Anhui Jianzhu University
He Fei,China
yanjiusheng176@163.com

Hua Zhi-Xiang
Anhui Jianzhu University
He Fei,China
huaxzyl@163.com

Pan Fei
Anhui Jianzhu University
He Fei,China
1065517780@qq.com

Li Xiao-Xuan
Anhui Jianzhu University
He Fei,China
1577631944@qq.com

Yu Yong-Lin
Anhui Jianzhu University
He Fei,China
405041850@qq.com

Tao Xin-Wen
Anhui Jianzhu University
He Fei,China
847563982@qq.com

Abstract—At present , CDMA is used mainly for civilian mobile communications technology. But most of CDMA communication devices are designed by using special CDMA communications chips; FPGA (Field-Programmable Gate Array) is not used in CDMA system. The proposed new method of this paper is that a CDMA system can be designed by using VHDL in the Quartus II based on FPGA. The m-sequence for direct spread spectrum and Walsh-Coded Modulation has been adopted in this system.

Keywords—FPGA, CDMA, Communication, VHDL, Spread Spectrum

I. INTRODUCTION

FPGA is a further development based on PAL, GAL, CPLD and some other programmable devices. It is developed as a semi-custom circuit in the field of ASIC (Application Specific Integrated Circuit). FPGA can solve the lack of custom circuits and overcome the disadvantages of limited number of programmable gate. Moreover, VHDL is able to be a standardized hardware description language and it is widely used .The certainty is that it has many advantages that are not available in other hardware description languages. To sum up, the VHDL language has the following main advantages: (1) Powerful functions and diverse design approaches. (2) It has excellent hardware description abilities and transplant abilities. (3)Design description does not depend on devices. (4) The programs are easy to share and reuse.

A. CDMA technology

On the basis of spread spectrum communication technology (a branch of digital technology), a new sophisticated wireless communications technology had developed, namely, CDMA technology had occurred. The basic principles of CDMA technology are spread spectrum technology. Spread Spectrum Communication, a hybrid of spread spectrum technology and communication technology, is one of various communication methods. The data signal has a certain bandwidth by modulation, to expand the bandwidth of the data signal with a high-speed pseudo-random code, and then the signal is sent after multicarrier modulation. Receivers use the same pseudo-random code to deal with the signal so as to get the original narrow-band signal.

B. The principle of CDMA communication

The Shannon theory is:

$$C=W\log_2(1+S/N) \tag{1}$$

Where, C is Channel capacity(bit/s ） ;W is Signal bandwidth (Hz); S/N is Signal-noise ratio.

The channel capacity is proportional to the signal bandwidth according to equation (1). When the channel capacity is a fixed value, the bandwidth W is wide enough to obtain high quality of transmission in the case of a smaller S/N. So the original signal can transform into a random signal like white noise by using the pseudo-random spreading code. We spread the bandwidth of digital date information using high-speed spreading code，the design of CDMA system is based on this theory.

II. SYSTEM STRUCTURE

In this system, the address code adopts a fourth order Walsh code to modulate information. When t=0, each bits of the Walsh code is 1, and each bits is 0 if the Walsh code XOR with 1111.From this, we can know orthogonal sequence codes with different length can be mixed according to certain rules. Besides, m sequence is used for spreading code. In a cycle, m sequence only has a sharp auto-correlation peak so that its orthogonality is very good.

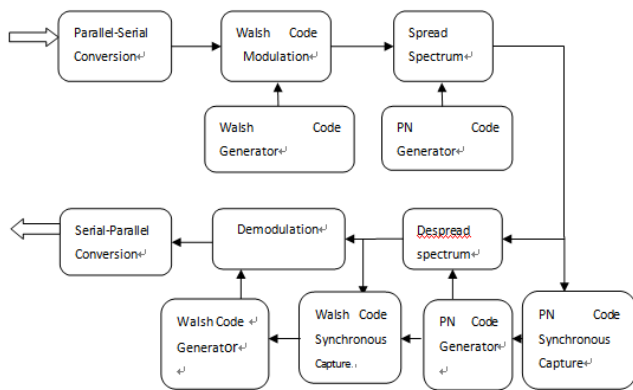The construct of proposed CDMA system is shown in Fig. 1.

Fig. 1 The construct of CDMA system

The CDMA system is divided into ten modules, respectively Parallel-Serial Conversion, Serial-Parallel Conversion, Walsh Code Modulation, Walsh Code Generator, Spread Spectrum, PN Code Generator, Despread Spectrum, PN Code Synchronous, Demodulation and Walsh Code Synchronous. But in practical projects, it needs another three modules, namely, Information Input, Information Output and Frequency Division. The thirteen modules are described in the following.

(1)Information Input Module：Enter the information into the chip of FPGA for later processing. In this system, 8 bit-input keys signal and a send key signal were entered into the chip and the module could recognize the information.

(2)Parallel-Serial Conversion Module: In this module, 8 bits parallel data from the output of information input module transform into serial data one by one. It adds 0 as a start bit in the beginning of data during conversion and adds 1 as a stop bit at the end of data. Moreover, parity bit is added to penultimate bit. So the output of a data block has 11 bits.

(3)Walsh Code Generator Module: The module generates 4 bits Walsh Code cyclically.

(4)Walsh Code Modulation Module: The serial data from the output of Parallel-Serial Conversion Module NXOR with Walsh code, thus modulating the serial information.

(5)PN Code Generator Module: The output code is generated by 6 series carry flip-flops; the structure is shown in Fig. 2. From checking table we can see the feedback coefficient of m sequence Generator is 103. So the corresponding characteristic equation is $f(x) = x6+x+1$, and there is feedback lines in first level and sixth level. The sixth order m sequence Generator could generate 63 states.The sequence is PN(t)=111111010101100110111011010010011100010111100101000110000100000.
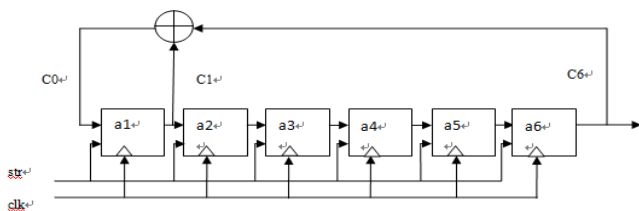
Fig. 2 Sixth Order m Sequence Generator

If all of bits from the original sequence of register are 0, the bits of output sequence are also 0. Then m sequence generator will enter a deadlock state.

In order to output PN code correctly, the state has to make at least one 1 in original registers.

(6)Spread Spectrum Module: Each signal output from the modulation Module XOR with PN sequence, and then sends the result.

(7)Frequency Division Module: The clock is divided to a desired frequency so that we could get many clocks which enable other modules operate normally.

(8)Despread Spectrum Module: Using the same PN sequence to XOR with the received signal data, so we can remove spreading code before data recovery. This is the first step to restore data.

(9)PN Code Synchronous Module: Owing to inconsistent PN code at the receiving end, the system cannot be restored modulated data directly. The function of this module is synchronous adjustment of PN code to makes the despread spectrum module working properly. The process diagram is shown in Fig. 3.
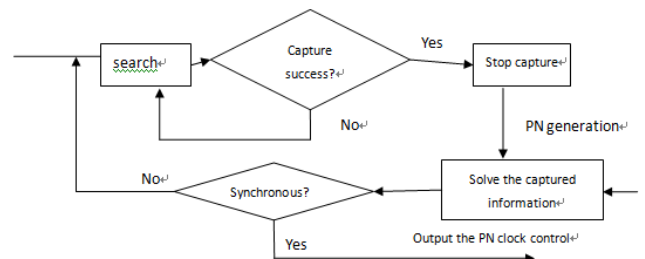
Fig. 3 The process of PN Code Synchronous

(10)Walsh Code Synchronous Module: The function is synchronous adjustment of Walsh code. The procedure is shown in Fig. 4.
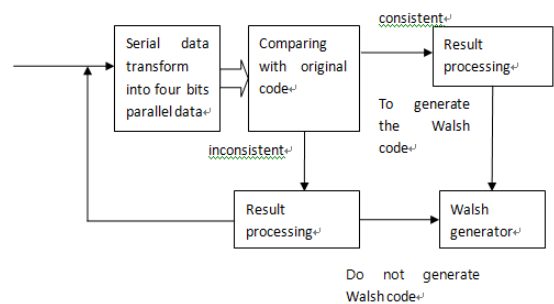

Fig. 4 The procedure of Walsh Code Synchronous

(11)Demodulation Module: The received signal XNOR with Walsh Code in this module.

(12)Serial-Parallel Conversion Module: Turning the output information into parallel data, and checking the Parity bit to determine if it is right.

(13)Information Output Module: Send the data from Serial-Parallel Conversion Module to the external 4 bits digital tubes.

III. Experimental Results

Information Input Module：This module consists of 5 mini modules, there are data_key、juhe、qian_c、querenyans and queren, as shown in Fig. 5. The functions of the data_key are change output state of register when pressed the key and restoring when falling edge of the sending signal key_fa comes (The original output is 1,and the output changes into 0 when pressed the key). The juhe module output the 8 bits parallel data. In qian_c module, the data 00000000 is outputted in parallel before the power is ready to be energized and pressed the first sending key. And sending the data from juhe immediately while press the first key. The querenyans module sending the eleventh bit of each data and output a rising edge after sent the eleventh bit when pressed sending key. Besides, the queren module sends the 8 bits data to the follow module when querenyans module output the rising edge.
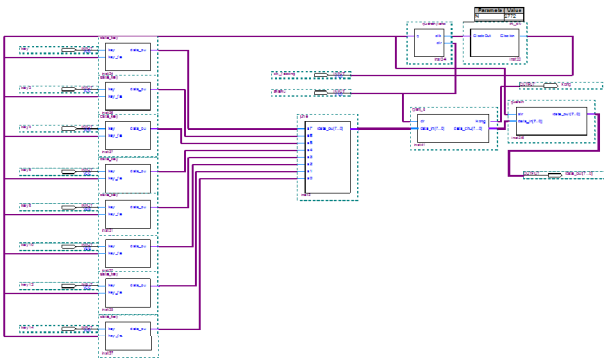
Fig. 5 Input Module

The simulation waveform is shown in Fig. 6.
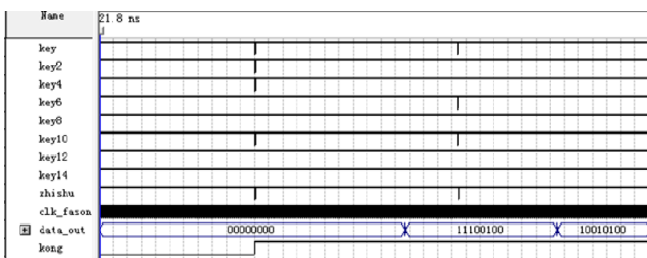
Fig. 6 The simulation waveform of system input

Parallel-Serial Conversion Module: The module structure is relatively simple. 8 bits parallel data transform into serial data and it adds start bit 0、ending bit 1 and parity bit among the data. Component instantiation figure is shown in the following illustration.

Fig. 7 Parallel-Serial Conversion Module

The simulation waveform is shown in Fig. 8.
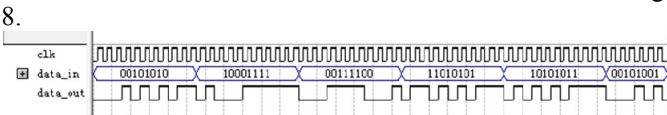
Fig. 8 The simulation waveform of Parallel-Serial Conversion

Walsh Code Generator Module: As shown in Fig. 9.
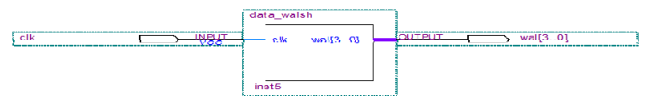
Fig. 9 Walsh Code Generator Module

The simulation waveform is shown in Fig. 10.
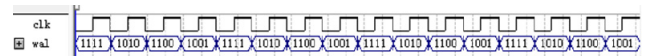
Fig. 10 The simulation waveform of Walsh Code Generator

Walsh Code Modulation Module: The modulation module consist of 3 mini modules, there are tiaozhi、walsh_bing and xiaomoci, as shown in Fig. 11. The data from Parallel-Serial Conversion XNOR with Walsh code in tiaozhi module. The function of walsh_bing is turning the 4 bits parallel data into serial data after modulation. Furthermore, the xiaomoci is to remove burrs among data.
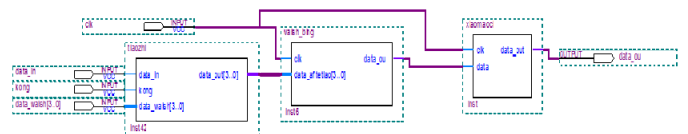

Fig. 11 Walsh Code Modulation Module
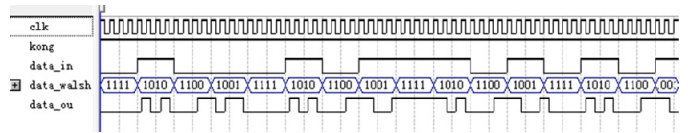
The simulation waveform is shown in Fig. 12.

Fig. 12 The simulation waveform of Walsh Code Modulation

PN Code Generator Module: This module includes PN_zhi mini module and frequent mini module. The PN_zhi initializes PN Code Generator Module and the frequent generates PN code. The structure is shown in Fig. 13.
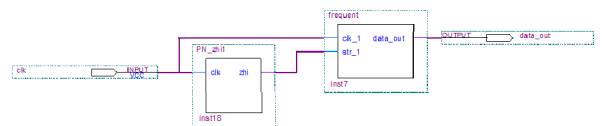

Fig. 13 PN Code Generator

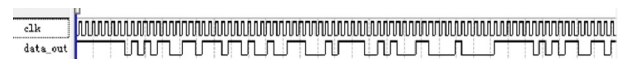The simulation waveform is shown in Fig. 14.

Fig. 14 The simulation waveform of PN Code Generator

Spreading and dispreading System: PN Code Synchronous Module module can be divided into two mini module, they are PN_tb and xinxuan. Spreading module 、 despreading module and PN Code Synchronous Module constitute a Spreading and Despreading System, as shown in Fig. 15.
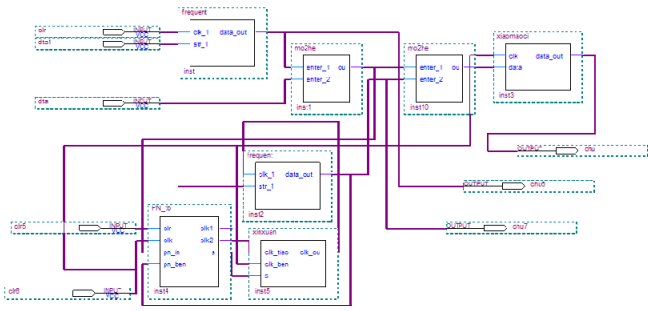
Fig. 15 Spreading and Despreading System

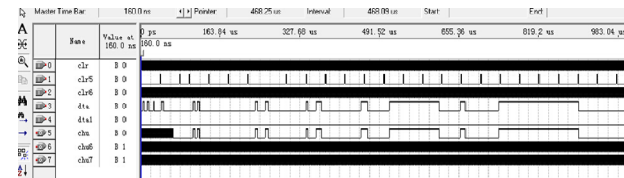The simulation waveform is shown in Fig. 16.

Fig. 16 The simulation waveform of Spreading and Despreading System

Demodulation Module: The output signal from spreading module XNOR with Walsh code and this module consists of three mini modules, they are walsh_tb 、 panbie and jietiao. The function of walsh_tb is turning the 4 bits serial data into parallel data. It makes a comparison between the output data from walsh_tb and original value of Walsh code generator in the panbie module. The jietiao module is to restore the output data from Parallel-Serial Conversion Module.

Modulation and Demodulation System: PN Code Generator 、 modulation and demodulation constitute a Modulation and Demodulation System, as shown in Fig. 17.
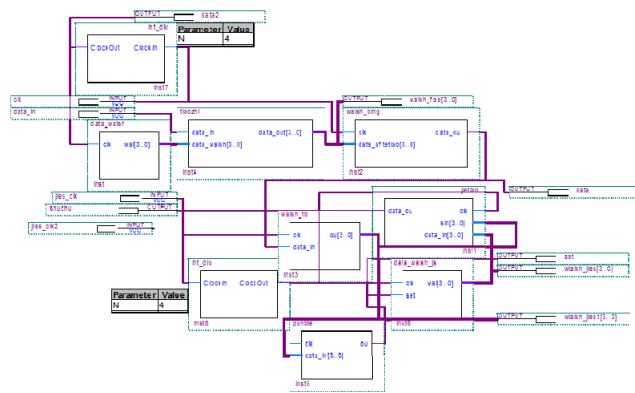

Fig. 17 Modulation and Demodulation System

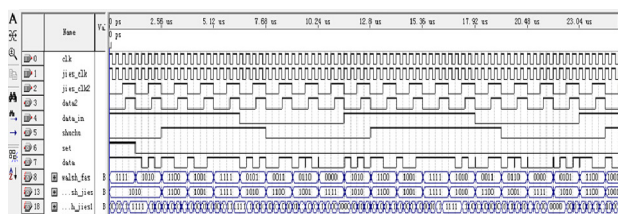The simulation waveform is shown in Fig. 18.

Fig. 18 The simulation waveform of Modulation and Demodulation System

IV. CONCLUSION

According to the requirements of the design task, we have learned the basic principles of CDMA system and knew lots of correlation technique of FPGA. We apply the theoretical knowledge of the direct sequence spread spectrum system and skill of EDA tools to practical chip development. Implement a CDMA direct sequence spread spectrum system on EP2C5T144 in the Quaetus Ⅱ 11.0 from Altera Corporation, and simulate the main module. It turns out that the design of this system meets the requirement of main function.

REFERENCES

[1] Guo Lili, Li Beiming, and Dou Zheng. FPGA design of spread-spectrum communication system. National Defense Industry Press (2013)

[2] Pan Song. Practical courses in EDA Technology. Science Press (2002)

[3] Wang Yuyin. Digital Electronic Technique. Higher Education Press(2012)

[4] Wan Long. EDA technology and application. Tsinghua University Press (2011)

[5] Huang Xiaojuan, and Wang Fuming. An FPGA-based design of CDMA digital baseband system [J]. Electronic Test (2011)

[6] Lu Kunsheng, and Xia Yinqiao. CDMA Mobile Communication Experiment. Tsinghua University Press (2012)

[7] Li Xiaomei. The design and implement of DS communication system based on FPGA [D]. Dalian University of Technology (2009)

[8] Hu Zaizhou. A carrier synchronization design and hardware design of wireless CDMA communication system. University of Electronic Science and Technology (2009)

[9] Luo Xi. Research and digital implementation on modulation and demodulation technology in CDMA system [D]. University of Electronic Science and Technology (2008)

[10] Tang Jianqiang, Xia Yong, and Xia Ming. A implementation of CDMA digital cordless PABX system using FPGA devices. Communication Technologies and development (1997)

[11] K Takeuchi, T Tanaka, T Kawabata.Performance Improvement of Iterative Multiuser Detection for Large Sparsely-Spread CDMA Systems by Spatial Coupling[J].IEEE Transactions On Information Theory.2015(No.4).1768-1794.

[12] Li, G.-D.;Meng, W.-X.;Chen, H.-H..I/Q Column-Wise Complementary Codes for Interference-Resistant CDMA Communication Systems[J].Systems Journal, IEEE.2015(No.1).4-12.

[13] Liu, Z.;Guan, Y.L.;Chen, H.-H..Fractional-Delay-Resilient Receiver Design for Interference-Free MC-CDMA Communications Based on Complete Complementary Codes[J].IEEE Transactions on Wireless Communications.2014(No.3).1226-1236.

[14] M. D. Kokate,T. R. Sontakke ,C. R. Bagul.Performance of RAKE-LMMSE Receivers in Wide-band Communication Systems[J].Wireless Personal Communications.2014(No.3).317-324

[15] G. Suchitra ,M. L. Valarmathi .BER Performance of Walsh‑Hadamard Like Kronecker Product Codes in a DS-CDMA and Cognitive Underlay System[J].Wireless Personal Communications.2013(No.3).2023-2043.

[16] Thomas Enkoskya, ;Branden Stoneb, , .A sequence defined by M - sequences[J].Discrete Mathematics.2014(Vol.333).35-38.

[17] Marcelo A.C. Fernandes;Dalton S. Arantes.Spatial and temporal adaptive receiver for DS-CDMA systems[J].AEU - International Journal of Electronics and Communications.2014(No.3).216-226.

Telemetry, Tracking and Command Subsystem for LibyaSat-1

Faisel EM M Tubbal[1,2], Akram Alkaseh[1,], and Asem Elarabi[1,3]

[1]Technological Projects Department, the Libyan Center for Remote Sensing and Space Science, Tripoli, Libya
[2]University of Wollongong, Australia
[3]Kyoto University, Japan
Femt848@uowmail.edu.au,   elkaseh1972@gmail.com,   asemelarabi@sk.kuee.kyoto-u.ac.jp

Abstract— **In this paper we present the design and the analysis of Telemetry, Tracking and Command Subsystem (TT&CS) for Libyan imaging mini-satellite (LibyaSat-1). This subsystem is the brain and the operating system of any satellite or spacecraft as it performs three important functions; tracking mini-satellite position, monitoring mini-satellite health and status and processing received and transmitted data. Moreover, the uplink and downlink budgets for s-band and x-band antennas are presented. We also designed s-band C-shaped patch antenna for command receiver (2.039 GHz). Electromagnetic simulation was performed to this antenna High Frequency Structure Simulator (HFSS). Our results show that the s-band C-shaped patch antenna achieves high gain of 6.45 dB and wide bandwidth; i.e., 1500 MHz. The achieved simulated return loss is -19.6 dB at a resonant frequency of 2.039 GHz.**

Keywords—mini-satellite; TT&C; transponder; telemetry

I. INTRODUCTION

Polar orbiting mini-satellites have a wet mass ranging from 100 to 500 kg and are sun-synchronous. They operate at Low Earth Orbit (LEO) at altitudes of 700 to 1000 km [1]. Compared to conventional, medium and mini sized satellites, as set out in Table I, they have lower mass, cost less, and consume less power. Mini-satellites are used for (i) remote-sensing; e.g., land imaging and weather forecasting, (ii) scientific research; e.g., ocean color and communication experiments, or (iii) telecommunications; e.g., rescue in ocean and for general purpose [2].

An example of a mini-satellite is the SATEX I project [3]. It is a Mexican experimental mini-satellite used for electronic telecommunications research at universities and multi-institutional environment. Another example is the SPOT satellites; i.e., SPOT 1, SPOT 2, SPOT 3, SPOT 4, and SPOT 5. They are French mini-satellites and their primary mission is obtaining earth's imagery for land-use, agriculture, forestry, geology, cartography, regional planning, and water resources. For example, SPOT 5 is a sun-synchronous imaginary mini-satellite that orbits at altitude 832 km. This satellite provides high resolution images for Libyan Centre for Remote Sensing and Space Science (LCRSSS) as part of commercial operations between France and Libya. Fig. 1 shows an image of Tripoli international airport in the capital of Libya with a resolution of 2.5 m. This image was captured by SPOT 5 in 2012 and it has been processed at LCRSSS.

TABLE I.   COMPARISON BETWEEN SATELLITES

Types	Mass (kg)	Cost (US $)	Power Consumption
Conventional	>1000	0.1-2 B	~ 1000 W
Medium	500-1000	50-100 M	~ 800 W
Mini	100-500	10-50 M	53.2W
Micro	10-100	2-10 M	35 W

Fig. 1.   An image of Tripoli international airport

Libyan national agency for scientific research is planning to have its own remote sensing satellite [4]. Therefore, Libyan Satellite project (LibyaSat-1) is planning to develop a mini--satellite program to meet the requirements of LCRSSS. The main aim of this project is to be the first earth observation mini-satellite to serve the needs of Libya and African countries, in the fields of natural resources management and agriculture. Moreover, the main mission of the LibyaSat-1 under the remote sensing program is to monitor terrestrial, marine environment, desertification and resources throughout Libyan landscape and its surrounding waters and possibly over other regions of the world for international cooperation. It is also recognized as an opportunity to validate new technologies in telecommunications, space science and allows achieving skilled human resources for all mini-satellite subsystems.

A critical subsystem of mini-satellite that provides a communication link with the ground stations is Telemetry, Tracking and Command (TTC) Subsystem. It also allows gathering and sending information to help in determining the satellite's orbit and to download images from payloads to control center [5]. An example of a ground station in Libya is Murezeq ground station which receives images and information from SPOT 5; see Fig. 2. In this paper, we focus on the design and requirements of telemetry, tracking and command subsystem for LibyaSat-1. We will present and discuss all

key requirements for T&C subsystem and image date downlink. These requirements include T&CS architecture, X-band subsystem architecture conceptual design, hardware components, operation requirements, components requirements and link analysis. We also present s-band patch antennas design for up and downlink communications. The LibyaSat-1 characteristics shown in Table II are considered when designing T&CS requirements.
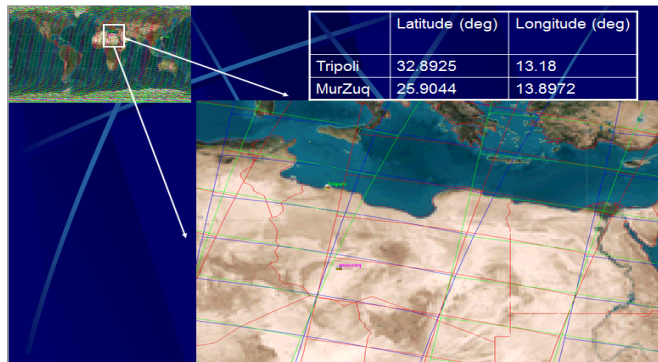

Fig. 2. The geographical locations of Tripoli and Murezeq

II. TELEMETRY, TRACKING AND COMMAND SUBSYSTEM

The aim of this project is to design, construct, implement and test of a RF subsystem to be used on a digital communication link at 2.039 GHz (s-band uplink) and 2.215 GHz (S-band, downlink), for the LibyaSat-1 mini-satellite. The system consists of transmitters, receivers, transponders and antennas. We present and analyse the link budget and the T&C architecture. Hardwar components with their characteristics and performance are also presented. LibyaSat-1 characteristics shown in Table II are considered when designing T&CS requirements.

TABLE II. LIBYASAT-1 CHARACTERISTICS

Mission Orbit	775 km circular, sun synchronous orbit.
Satellite lift-off (Wet) weight	no more than 300 kg.
Mission life	5 years minimum.
Resource of power	solar sell and battery.
Launcher	Falcon 1e.
Data storage volume	no less than 80Gbits.
Satellite reliability	0.6 at the end of the 5-year mission
Swath:30km GSD : 2.5m (PAN) , 10m(MS).	Swath:30km GSD : 2.5m (PAN) , 10m(MS).
Satellite power	3% margin at the end of the 5-year mission.
Downlink rate (x-band	no more than 150 Mbps.
Downlink rate (s-band)	no more than 2.0 Mbps (State-of-Health and Scientific Data).
Attitude control	3-Axis Stabilization.

A. An Overview

TT&C subsystem receives commands from Command and Data Handling subsystem (CD&H) and provides health and status of the satellite to CD&H. It also performs antenna pointing and mission sequence operations for each stored software. All these operations are done through communications between the satellite and ground station using telemetry, command and tracking signals.

1) Telemetry.

As shown in Fig. 3 telemetry is a set of signals that have one-way direction from satellite to ground station. These signals are the taken

measurements on board the mini- satellite of the status of the spacecraft resources, health; i.e., temperatures, voltages, and currents. It also measures the attitude, scientific data, images, spacecraft orbit and timing data for ground navigation etc. Then all these measurements are sent to the control Centre through the ground station by RF system.

2) Command

A set of one-way signals that are sent from ground station to the mini- satellite in space. This links is used either for controlling the payload or for sending commands to control the satellite and its attitude at the critical phase. When the solar cells is deployed, commends are then sent to turn on equipment that was off during launching phase; i.e., records and payloads. After the deployment of the solar cells, the mini- satellite should operate automatically and less command will be sent.

3) Tracking

For tracking the satellite to accurately locate its orbit, the same link is used to receive different measurements. These measurements include the time taken by RF signals for trip; i.e., station – satellite – station, frequency shift because of the satellite velocity, and the antenna orientation with respect to azimuth and elevation. By using all the aforementioned measurements, the accurate location of the satellite can be determined.
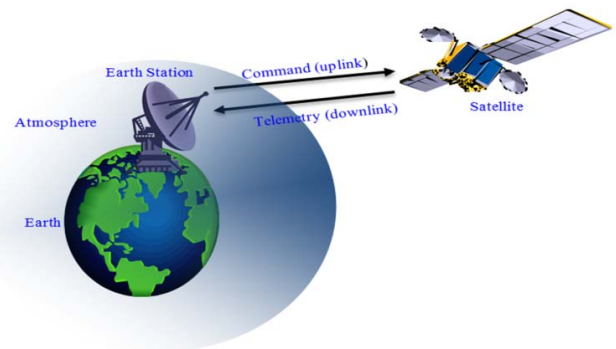

Fig. 3. Communication links between satellite and ground station

B. TT&C Architecture

As shown in Fig. 4, S-band TT&C subsystem consists of two TT&C s-band antennas, RF Distribution Unit (RFDU) and two transponders. Each transponder has a receiver, transmitter and duplexer. These two transponders are used to backup each other and to provide RF channels for mini- satellite tracking, telemetry, ranging and command. The duplexer at each transponder is used to switch between receiver and transmitter.
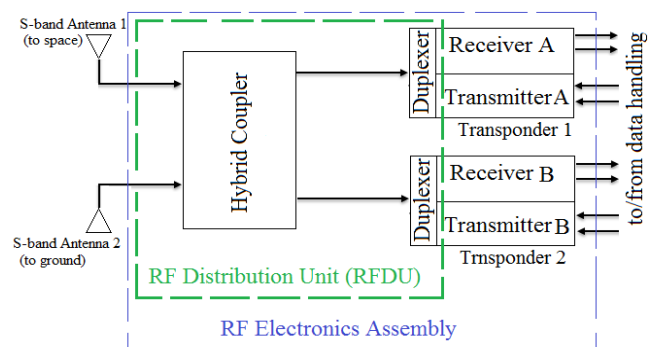

Fig. 4. Mini- satellite TT&C subsystem block diagram

1) Transponder

Two transponders in TT&C subsystem are used to backup each other and to provide RF channels for mini- satellite tracking, telemetry, ranging and command. This redundancy ensures that the TT&C subsystem has reliability should one of transponders fail. In addition, the duplexer at each transponder is used to switch between receiver and transmitter. The requirements and parameters of TT&C transponder (s-band command receiver and s-band telemetry transmitter) of the LibyaSat-1 are shown in Table III. The command receiving sensitivity is −110dBm, noise figure is less than 6 dB and the output power of the s-band telemetry transmitter is about 5 W. Transponders are connected to both antennas via hybrid coupler which distributes signals in both directions; see Fig.4. The polarization of these antennas should be Circular Polarization (CP). This is important as it achieves the best signal strength and mitigates multipath fading.

TABLE III.   PARAMETERS OF S-BAND COMMAND RECEIVER AND TELEMETRY TRANSMITTER FOR LIBYASAT-1

S-band Command Receiver	
Frequency	2.039 GHz
Sensitivity threshold for <10-6 bit error rate	-110 dBm
Receiver noise figure, maximum over temperature	< 6 dB
Signal modulation	BPSK +PM
Data Rate	32 kbps
S-band Telemetry Transmitter	
Frequency	2.215 GHz
Output power	5 W
Transmitter error vector magnitude	<10 %
Signal modulation	BPSK
Maximum transmit data rate	2Mbps

2) S-band antennas

As mentioned earlier, s-band command receiver and telemetry transmitter antennas should have resonant frequencies of 2.039 and 2.215 GHz respectively. To this end, we have designed s-band C-shaped patch antenna using the High Frequency Structure Simulator (HFSS) [6-8]. This antenna for s-band command receiver and operates at resonant frequency of 2.039 and meet all aforementioned requirements. For telemetry transmitter, we will purchase s-band antenna that provides the specifications mentioned in Table III above.

a) 2.039 GHz C-shaped patch antenna

Fig. 5 shows the 3D model of s-band C-shaped antenna for command receiver. The dimensions of the upper and lower patches are 69.2×24.4 and 46.8×7.3 mm^2 respectively. Three shorting pins are connected at the edges of the upper patch and are located between upper patch and 122×122 mm^2 ground plane. Their main purpose is to achieve a wide impedance bandwidth at small antenna size.
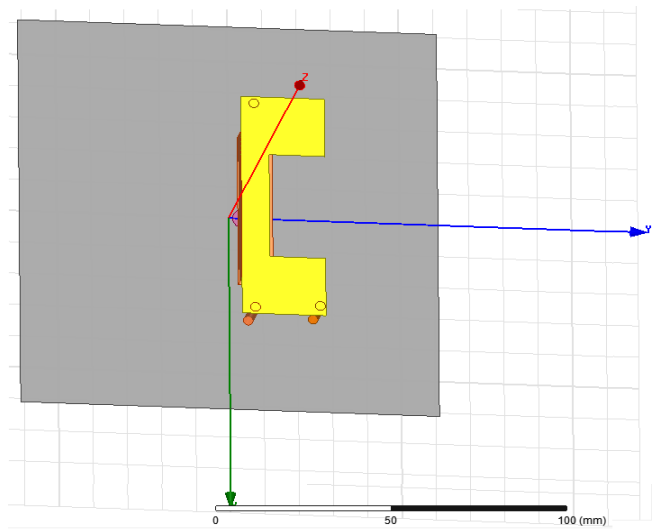

Fig. 5.   Geometry of 2.039 GHz C-shped patch antenna

Fig. 6 presents the 3D gains of the s-band C-shaped patch antenna at 2.039 GHz. We see that the antenna has a high gain of 6.4 dB and a uniform radiation pattern. Fig. 7 shows the return losses over varying frequencies for s-band C-shaped antenna. The antenna has a wide -10 dB bandwidth; i.e., 1500 MHz (1.8-3.3 GHz). The return loss at resonant frequency of 2.039 GHz is about -19.6 dB.
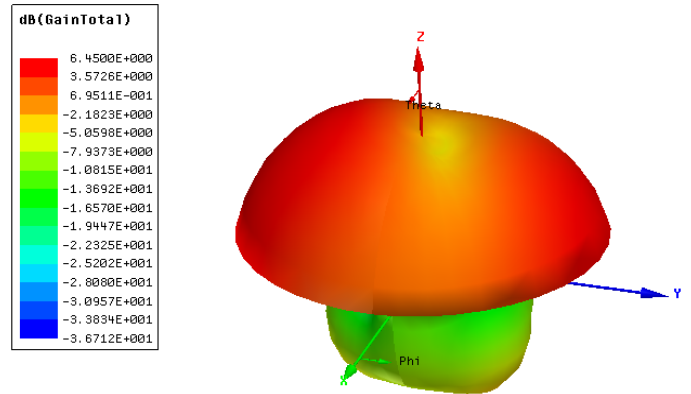

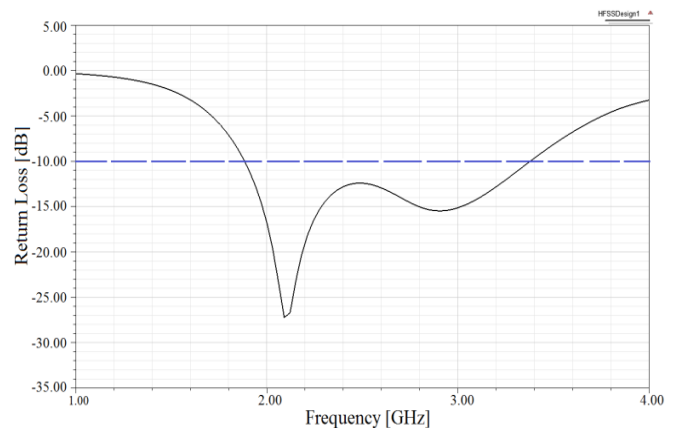Fig. 6.   3D gain of C-shaped patch antenna at 2.039 GHz

Fig. 7.   Simulated return losses (S$_{11}$) of C-shaped patch antenna

3) Passive components

Passive components that are used in TT&C subsystems are filters, hybrids, diplexers, and transmission lines. A band pass filter with 2.215 GHz center frequency and bandwidth of 50 MHz is used for a telemetry transmitter. The same band pass filter is used by the command receiver but at center frequency of 2.039 GHz. The coupler or divider provides a frequency range that covers 2.039 and 2.215 GHz at coupling rate of 3dB and a maximum insertion loss of 0.4. Another passive component is diplexer which has a maximum insertion loss of 0.5, minimum isolation of 30 dB and frequency range covers 2.039 and 2.215 GHz. Moreover, low loss cables and waveguides are used as transmission lines.

III. IMAGE DATA DOWNLINK

We now study the key requirements of image data downlink for LibyaSat-1. These requirements include real time transmission, store and dump transmission, the center frequency of x-band transmission, data rate, and type of coding scheme. Fig. 8 shows the architecture design of x-band subsystem for LibyaSat-1 including the x-band antenna and its pointing mechanism. Moreover, the downlink budget of x-band subsystem is presented in Table VI.
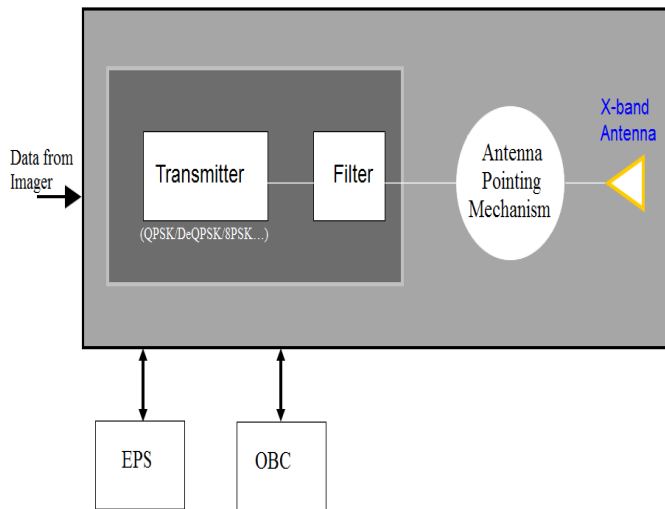

Fig. 8. X-band subsystem architecture

A. Real Time Transmission

The x-band communication link shall be with at least 6 dB link margin in clear sky with a cross-track viewing angle < ±30 degrees toward the ground station. Moreover, the ground station elevation angle should be >20 degrees and passes where maximum elevation angle of ≥30 degrees.

B. Store and Dump Transmission

The store-and-dump transmission capability shall be provided to process the data that is not dumped in real-time downlink.

C. Resonant Frequency of X-band Antenna

The centre frequency of the x-band transmission antenna shall be 8.150 GHz with a minimum gain of 10 dB. The bandwidth of this antenna must be about 150 MHz and should provide right hand circular polarization (RHCP). Next we provide more details about this antenna.

D. Data Rate and Coding Scheme

The data rate shall be 150 Mbps for the operation in QPSK/DeQPSK/8PSK/ mode. The proposed coding scheme is Reed-Solomon (255,223) that implemented in the imager.

IV. MUREZEQ GROUND STATION

This ground station is a multi-mission ground station which was installed by LCRSSS in 2007. The main aim of this station is to send commands to satellites in space and receive images back from these remote sensing satellites; i.e., SPOT 5 and ENVISAT. It uses 5.4 m x-band sub-system dish antenna a diameter of 5.4 m; see Fig. 9. It features an innovative Cassegrain feed and sub-reflector design which leads to high gain, low noise and high antenna efficiency. It feeds with LNA, mono-pulse tracking, and equipment to receive remote sensing data, including a GPS location and timing system. The characteristics of this x-band antenna are set out in Table IV.

Murezeg ground station has five sub-systems as following:

➢ Antenna sub-system: dish, feed and LNA, pedestal X\Y, control unit, wind gauge, and GPS antenna.

➢ RF sub-system: fixed frequency conversion from X-band to S-band, RF splitters, and programmable frequency conversion from S-band to FI 720MHz.

➢ Base band sub-system: demodulation, auto-tracking, time reference, test and measure equipment.

➢ Supervision sub-system: monitor and control of all equipment, management of tracking sequences, and interface with orbital data source.

➢ Infrastructure sub-system: radome, temperature and humidity control equipment, and UPS.

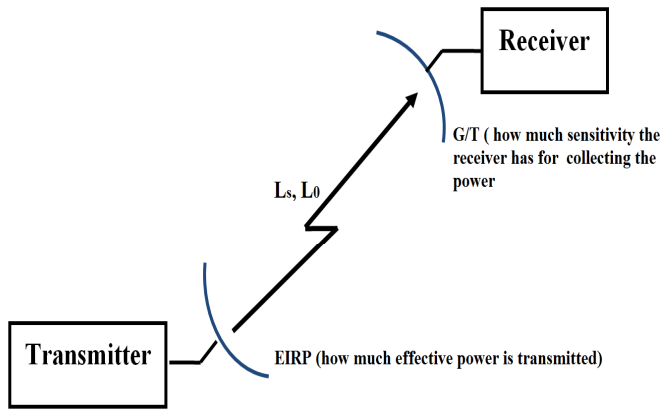Fig. 9. X-band dish antenna at Murezeq station

All the functions of Murezeq ground station are performed by the RF sub-system, baseband sub-system, and supervision sub-system. It is main objective is to receive data directly from French satellites; i.e., SPOT 5, 6 and 7, at frequency of 8.15 GHz with the occupied bandwidth of ≤ 250 MHz, the bit data rate of 310 Mbps (Reed Solomon coding included), the EIRP of 26 dBW, a minimum flux density of -123 dB/m^2, and the modulation used is D-QPSK. Nevertheless, it has the ability to receive from other satellites such as Envisat ASAR, GPS, and Vsat. Moreover, the system can automatically track the satellites, acquire, demodulate and archive the telemetry from remote sensing satellites.

TABLE IV.   CHARACTERISTICS OF X-BAND DISH ANTENNA

Parameter	Specification
Diameter of dish	5.4 m
Frequency	8000 – 8500 MHz
LNA gain	≥ 40 dB
Polarization	R/L HCS selectable
G/T at 5^0 elevation	30.5 dB/K
Side lobes	< 14 dB

A. *Link Budget Analysis*

We now provide a link analysis for x-band downlink and s-band up and downlinks. As mentioned above, the C-shaped patch antenna is proposed to be used for s-band uplink for command receiver. Currently the LCRSSS is using a parabolic antenna for uplink communication with SPOT 5 as command transmitter. This antenna operates at a resonant frequency of 2.039 GHz and provides high directivity. Moreover, it has a diameter of 2.4 m and an aperture efficiency of 0.65%. Although the designed C-shaped patch antenna provides a gain of 6.45 dBi, we have used a gain of 5 dB in the link budget calculation as a worst case scenario. The link budgets for s-band up and down links and x-band image downlink are presented in Table V and VI. Fig. 10 shows the key parameters of the link analysis. These parameters are calculated using the equations in [9] as following,

Fig. 10. Key parameters of a link analysis

$$G_t = 10 \times \log(e_A \left(\pi D / \lambda\right)^2) = 32.3 \; dBi.$$

With a maximum transmitted power of 100W and feeder loss of 1dB, the EIRP is:

$$EIRP = G_t + P_T - L_{co} = 32.3 + 10 \times \log(100) - 1 = 51.3 \; dBW.$$

At satellite altitude of 775 km and elevation angel of 10°, the slant range is equal to:

$$= \sqrt{r^2 - (R_e \cos \emptyset)^2} - R_e \sin \emptyset = 2315 \; km$$

The power flux density radiated from the ground station to the satellite can be calculated as following:

$$\beta = \frac{P_t G_t}{4\pi d^2} = EIRP - 10 \times \log(4\pi d^2) = 51.3 - 138.$$
$$= -86.98 \; dBW/m^2$$

The uplink space loss is equal to:

$$L_s = \left(\frac{c}{4\pi df}\right)^2 = 147.55 - 20\log(d) - 20\log(f) = -165.93 dB$$

The received power at the satellite:

$$P_r = EIRP + G_r + L_a + L_s = 51.3 + 5 - 11.5 - 165.93 = -121.13 dBW$$

The system noise temperature (T_s) of the satellite communication link is the sum of the antenna noise (290K), line loss noise (35K) and receiver noise (289K).

The noise power at the receiver can be calculated to be:

$$N_o = kT_s = -228.6 + 27.9 = -200.7 \; dB/Hz$$

The carrier to noise density ratio is equal to:

$$\frac{C}{N_o} = -121.13 + 200.7 = 79.57 \; dB - Hz$$

The receiver figure of merit (G/T)= 5-27.88 = -22.88 dB/K.

At uplink data rate of R=32 kbps, the ratio of received energy per bit (Eb) to noise density (No) is equal to:

$$\frac{E_b}{N_o} = P_r + 228.6 - 10\log(T_s) - 10\log(R) = 34.52 \; dB.$$

Modulation and coding techniques are very important for link budget calculation, satellite system with BPSK/PM technique and bit error rates (BER) of <10[-6], the required Eb/N[0] can reach to 15.8 dB.

TABLE V.   S-BAND UP AND DOWNLINK BUDGETS

Feature	Uplink	Downlink
Frequency	2.039 GHz	2.215 GHz
Satellite Altitude	775 km	775 km
Elevation Angel (deg)	10^0	10^0
Transmitter Power(Pt)	20 dBW	7 dBW
Ground Sation Antenna Gain (Gt)	32.3 dB	6.4 dB
EIRP Power	51.3 dBW	13.4 dBW
Space Loss	-165.93 dB	-166.63 dB
Atmospheric Losses	-0.5 dB	-0.5 dB
Rain Loss	-0.5 dB	-0.5 dB
Polarization Loss	-0.3 dB	-0.3 dB
Pointing Loss	-0.2 dB	-0.2 dB
On-Board Losses	-10 dB	-4.5 dB
System Noise Temperature(Ts)	27.9 dB/k	24.6 dB/k
Satellite Antenna Gain	5 dB	5 dB
Figure of Merit (G/T)	-22.88 dB/k	-18.2 dB/k
Bite rates	32 Kbps	2000 Kbps
C/No Received	79.57 dB-Hz	77.07 dB-Hz
Eb /No Received	34.52 dB	14 dB

Bit Error Rate (BER)	10^{-5}	10^{-5}
Required Eb /No	11.8 dB	9.6 dB
Implementation Loss	-2.5 dB	-1 dB
Margin	20.72 dB	3.4 dB

TABLE VI.   X-BAND DOWNLINK BUDGET

Link Parameters	Data
Frequency	8.1 GHz
Elevation Angle	20^0
Satellite Altitude	775 – 800 km
Satellite slant range	1723 km
Bit rate	150 MHz
Transmitter power	6 W
Transmitter imperfection losses	-2.5 dB
Transmitter feed losses	-0.5 dB
Antenna gain	15 dBi
EIRP	19.7 dBW
Propagation loss	-175.4 dB
Atmospheric losses	-1.5 dB
Rain losses	-0.5 dB
Polarization losses	-0.2 dB
Pointing losses	-0.3 dB
G/T ground station	32 dB/k
Eb/N0 received	20.7 dB
GS implementation losses	-2.0 dB
Eb/N0 achieved	18.7 dB
Eb/N0 required	6.5 dB
TM margin	12.23 dB

V. CONCLUSION

We have presented a conceptual design of telemetry, tracking and command subsystem for LibyaSat-1. The most important characteristics of TT&C subsystem were presented in this paper, explaining the uplink and downlink budgets. We also presented the design of s-band C-shaped patch antenna for command receiver. Simulation results show that the C-shaped patch antenna has a return loss that is well below -10 dB at the operational frequency of 2.039 GHz, and achieves an impedance bandwidth of 1500 MHz. The achieved simulated 3D gain is 6.4 dB at 2.039 GHz. We have obtained a margin > 3 dB, which means the calculation of link budget is good and within the range. In addition, the calculated and estimated values for budget links are acceptable and within the range for a real current model satellite.

REFERENCES

[1] C. Underwood, V. Lappas, A. D. S. Curiel, M. Unwin, A. Baker, and M. Sweeting, "Science Mission Scenarios Using "PALMSAT" Pico-Satellite Technology," presented at the 18th Annual AIAA/USU Conference on Small Satellites, Logan, Utah, 2004.

[2] F. EM. M. Tubbal, R. Raad, and K-W. Chin, "A Survey and Study on the Suitability of Planar Antennas for Pico Satellite Communications " unpublished.

[3] E. Pacheco, J. L. Medina, R. Conte, and J. Mendieta, "Telemetry and command subsystem for a Mexican experimental microsatellite," IEEE Conference on Aerospace Big Sky, MT, United State pp. 3/1159-3/1165 vol.3, 2001.

[4] A. Elarabi, A. Elkaseh, A. Abughufa, S. Ben Rabha, A. Turkman, and M. Alayeb, "Libyan CubeSat for monitoring desertification and deforestation," 5th Nano-Satellite Symposium University of Tokyo, Japan, pp. 1-4, November. 2013.

[5] D. Cinarelli and P. Tortora, "TT&C system for the ALMASat-EO microsatellite platform," IEEE First AESS European Conference on Satellite Telecommunications (ESTEL) Rome, Italy, pp. 1-6, October 2012.

[6] High Frequency Structure Simulator (HFSS) [online] available: http://www.ansys.com/.

[7] F. EM. Tubbal, R. Raad, K-W. Chin, and B. Butter, "S-band Shorted Patch Antenna for Inter Pico Satellite Communications," IEEE 8th International Conference on Telecommunication System, Services and Application, Bali, Indonesia, pp. 1-4, October, 2014.

[8] F. EM. Tubbal, R. Raad, K-W. Chin, and B. Butters, "S-band Planar Antennas for a CubeSat," International Journal on Electrical Engineering and Informatics, vol. 7, December 2015.

[9] W. J. Larson and J. R. Wertz, Space Mission Analysis and Design: Microcosm Press, California, USA 1999.

Performance Analysis of 10-Gigabit-capable Passive Optical Network (XGPON) with Splitting Ratio of 1:64

Nana Rachmana Syambas, Rahadian Farizi
Telecommunication Research Group, School of Electrical and Informatics Engineering, ITB
Jl. Ganesha No.10 Bandung 40132 Indonesia
Email : nana@stei.itb.ac.id

Abstract—**In this paper explains about performance analysis of 10-Gigabit-capable Passive Optical Network (XGPON) with splitting ratio 1:64. The software tool called Optisystem is used to simulate the network topology. The transmitter uses a laser components with NRZ modulation scheme and the transmitter power is adjusted to maximum power according to the ITU-T standards. The transmission channel, used a fiber optic cable Single Mode Fiber (SMF) G.652C with a length of 20 km, as maximum length of XGPON technology, and the cable attenuation of 0.47 dB/km for wavelengths 1270 nm. The result concluded that based on link budget, rise time and BER analysis, the performance of XGPON technology with 1:64 splitting ratio is suitable to be implemented for provide broadband services.**

Keywords—**Optical Network**, **GPON, XGPON**

I. INTRODUCTION

Needs of broadband servises is emerging in the near future. The broadband servises and co-existence with existing technologies are the general requirements from network operations to direct PON evolution. Operators worldwide are seeking to increase revenue by developing bandwidth-consuming services. New business models, an exemplified service is HDTV, which requires about 20 Mbit/s per channel such as broadcast TV and radio, video on demand, home online game, interactive E-learning, remote medical services and next-generation 3D TV will dramatically increase bandwidth demand. PON technology development was so diverse, among others is XGPON which has bite rate up to 10 Gbps.

A passive optical network is a network that uses point-to-multipoint fiber to the end-points in which unpowered optical splitters are used to enable a single optical fiber to serve multiple end-points. A XGPON consists of an optical line terminal (OLT) at the originating service provider, transmission channel which consist of optical cable and splitter, and a number of optical network units (ONUs), near end users.

In downstream scheme, XGPON uses data rate 10 Gbps and wavelengths 1575-1580 nm. In upstream scheme, uses data rate 2.5 Gbps and wavelength 1260-1280 nm, comply to ITU-T 987 standard.

Maximum distance of the optical cable between OLT and ONU on the XGPON architecture is 20 km with splitting ratio until 1:256. This ratio is bigger than the GPON architecture that has maximum splitting ratio is 1:32. General block diagram of XGPON topology using 1:64 splitter shown on figure 1. Downstream bite rate is 10 Gbps and upstream bite rate is 1,25 Gbps, according to ITU-T standard.
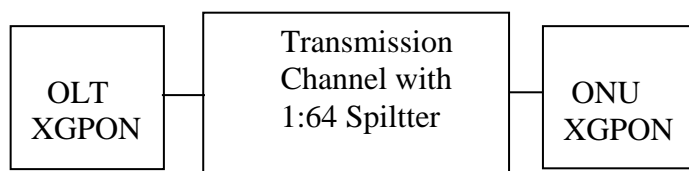

Figure 1. General block diagram of XGPON

A. Optical Line Terminal (OLT)

OLT consist of transmitters and optical amplifiers devices. The transmitter using a DFB laser with power 12.5 dBm. Modulator is Mach-Zender modulator with NRZ coding and extinction ratio is 25 dB. The circuit of OLT devices can be seen as in figure 2. The Optical amplifier is 20 dB and the upstream receiver device has -29.5 dBm sensitivity comply to the standard ITU-T. The receiver device uses a PIN photodetector and a low pass filter with 1270 nm cut-off frequency. Detail diagram of OLT XGPON can be described as on figure 2.

Optical Line Terminal (OLT)

Figure 2. XGPON Transmitter

B. Transmission Channel

XGPON transmission channel uses the standard ITU-T G.652C fiber optic cable. The worst cable attenuation according to the ITU-T G.652C standard is 0.47 dB/km at 1260 nm wavelength and the maximum length of the cable is 20 km. The splitter 1:64 places on the remote node as shown on figure 3.
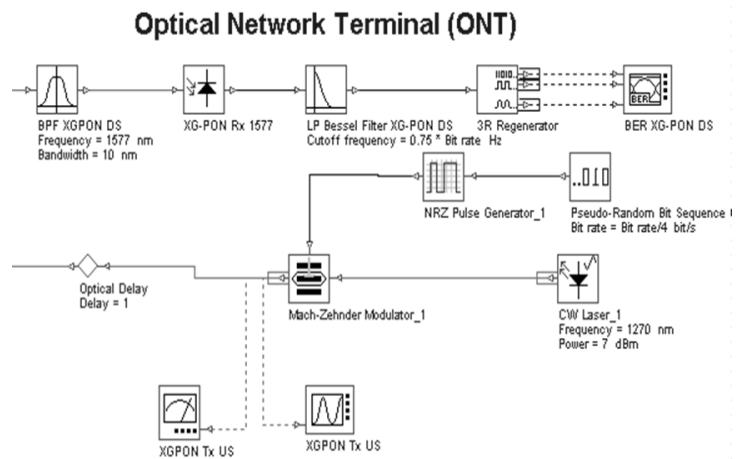
Passive Splitters

Figure 3. XGPON transmission channel

C. Optical Network Unit (ONU)

Optical network unit consist of downstream and upstream receiver devices. The downstream receiver uses photodetector PIN and low pass filter, which has a sensitivity of -21.5 dBm and *low pass filter* with 1577 nm cut-off frequency, according to the standard ITU-T. The upstream transmitter using a DFB laser with 1270 nm wavelength has power is 7 dBm. Modulator is Mach-Zender modulator with NRZ coding and extinction ratio is 25 dB. The signal is also amplified by the optical amplifier with gains of 20 dB. Configuring the XGPON ONU can be seen in figure 4.
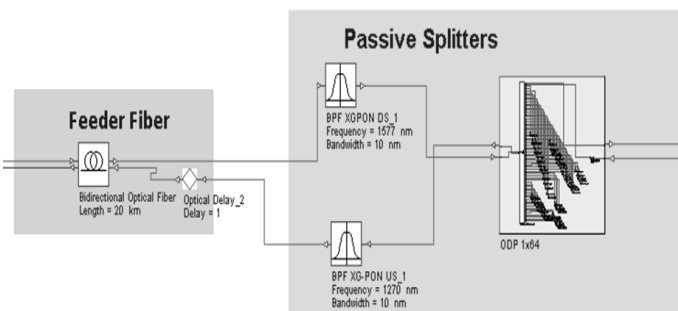
Optical Network Terminal (ONT)

Figure 4. XGPON Optical Network Unit

II. PERFORMANCE ANALYSIS

The analysis was performed by calculating the link budget and rise-time budget of the end – to-end system to see whether these parameters meet the requirements of the basic quality of the network connection. Link budget calculation determines the suitability of the power to the receiver sensitivity, and rise time budget tests the feasibility of the signal shape and dispersion effect. The design is simulated with software Optisystem to test its feasibility. The parameters tested in the simulation is the power received in each component, the ratio of the signal shape in

the receiver and the sender, BER and eye diagram form each receiver.

A.Link Budget

The result of measurement indicates that on the downstream side, the average power at the transmitter is 9.35 dBm, and the power at the receiver is -15.7 dBm. The power on the receiver side is greater than the sensitivity of the receiver (-21,5 dBm). It has 6 dB difference that more than 5 dB minimal margin. Based on this fact that received signal is upper the sensitivity threshold, performance of downstream network is declared visible.
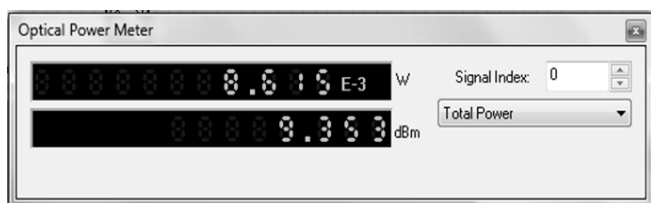
Figure 5. the downstream transmitter power
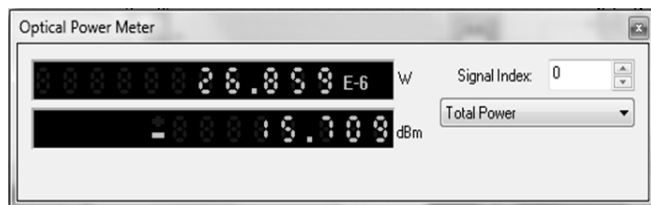
Figure 6. the downstream receiver power

On the upstream side, the link budget analysis is done by observing the power at the transmitter at ONU and the receiver at OLT. The observed power can be seen in figure 7 and figure 8.
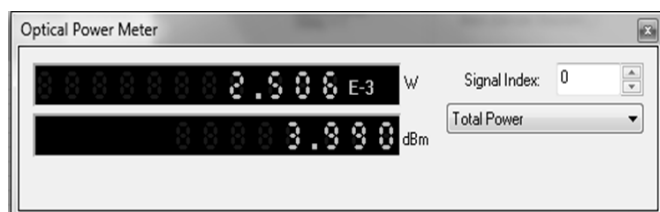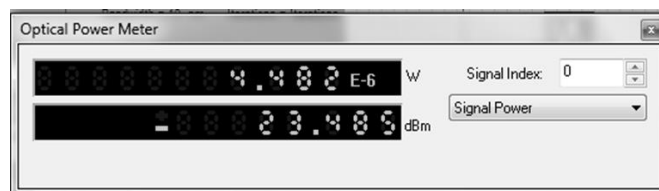

Figure 7. the upstream transmitter power

Figure 8. the upstream receiver power

The measurement result on the upstream side that the transmitter power is 3.99 dBm and the receiver power is -23.4 dBm. The power at the receiver is greater than the sensitivity of the receiver (-29.5 dBm), it has 6 dB difference that more than 5 dB minimal margin. Based on this fact that received signal is upper the sensitivity threshold, performance of upstream network is declared visible .

Both the downstream and the upstream connections are feasible due to the receiver signal detected on the upper threshold of receiver sensitivity.

B. Rise-time Budget

Rise-time budget analysis is done by observing the signal shape of a transmitter and receiver. Rise-time budget is said to be viable if the rise-time changes do not exceed 70% of the original time. Rise-time values can be observed from the time it takes to rise from 10 to 90% of the maximum value. Connection is feasible if the rise-time value change does not exceed 70% of the signal period. In the XGPON connection, use a bit rate of 10 Gbps, the signal bit period is calculated:

$$T_b = \frac{1}{10 \times 10^9} = 0{,}1 \, ns$$

So the rise-time change the maximum allowed is 70% Tb, which is 0.7x0.1= 0.07 ns.
Observations form of signals on the downstream side can be seen in figure 9 and figure 10, while on the upstream side can be seen in figure 11 and figure 12.
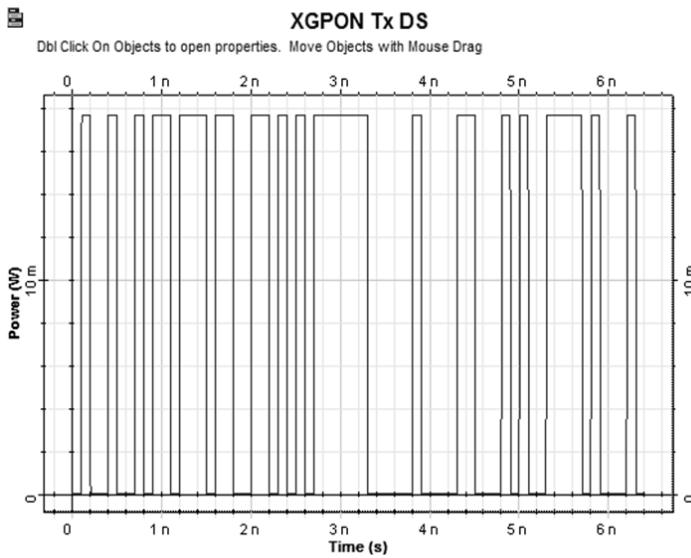
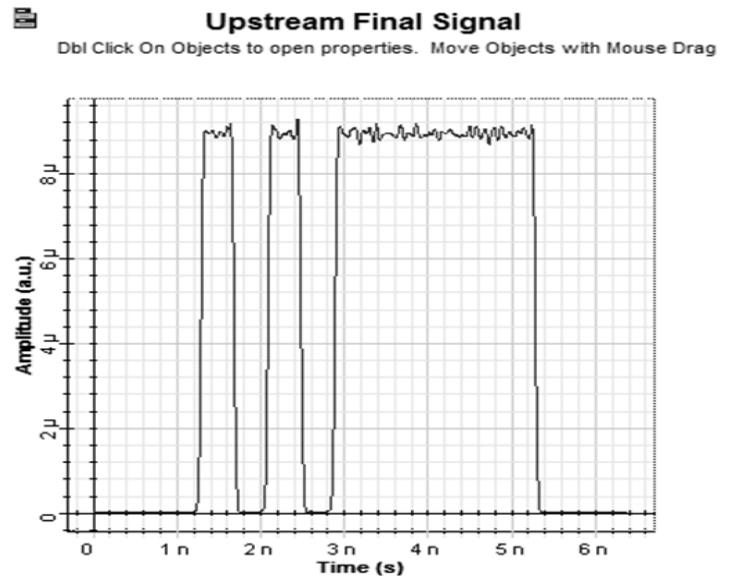Figure 9. The downstream transmitter signal
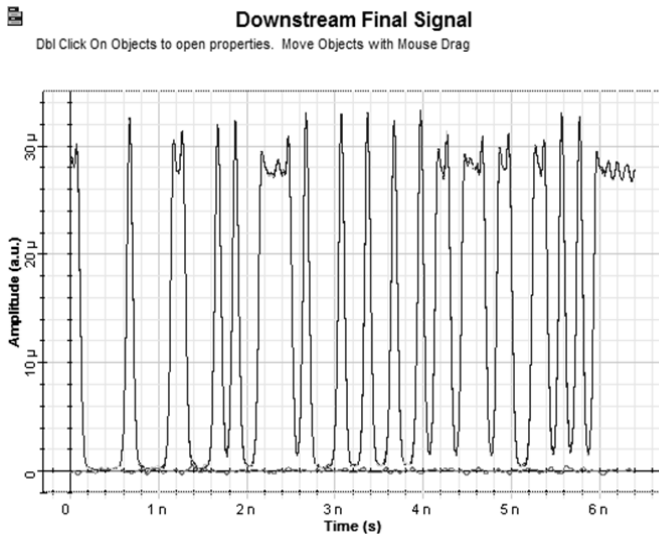

Figure 10. The downstream receiver signal

Figure 11. The upstream transmitter signal
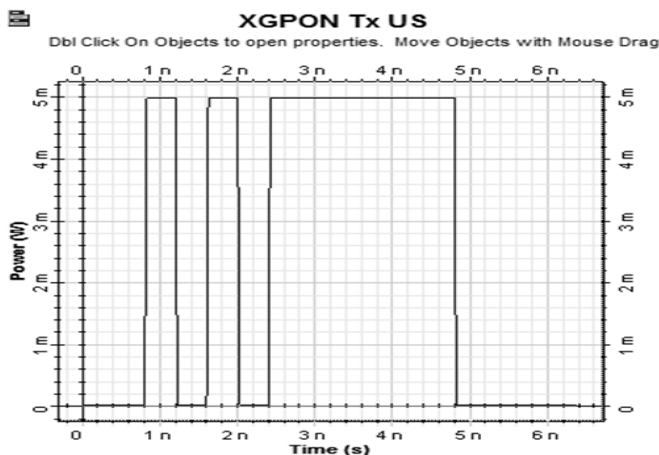

Figure 12. The upstream receiver signal

In the downstream, the value of the observed rise time on the transmitter is 4.69 x 10^{-3} ns, while the receiving side observed rise time is 5.96 x 10^{-2} ns. Both numbers are smaller than the permitted rise time, therefore, in the downstream connection, the XGPON declared eligible.

In the upstream, the value of the observed rise time on the transmitter is 1.4 x 10^{-2} ns, while the receiving side, observed rise time is 5.31 x 10^{-2} ns. That way, in the upstream connection, the XGPON is said to be feasible.

C. BER Analysis

The BER Analyzer generates the eye diagram on the output downstream and the output upstream. By analysed the eye diagram, the distorsion, the jitter and the BER can be determined. Figure 13 and figure 14 shown the output of BER analyzer.

Eye diagram as the output BER Analyzer shows is very clear both for downstream and upstream, that means the communication performance of the XGPON is very good.

Interm of distorsion and jitter, the output eye diagram of the signal in downstream side is better than the upstream side. However, these distortion and jitter look are still very small so that

communication can be declared eligible for XGPON configuration.

Figure 13. Eye diagram of output downstream

Figure 14. Eye diagram of output upstream

III. CONCLUSION

The design of optical communication systems by using XGPON technology with splitting ratio of 1:64 is suggested to be implemented due to good performance. The simulation results showed that the link budget analysis indicates that the received power at downstream and upstream receivers are -15.7 dBm -23.4 dBm respectively. Both numbers are greater than the sensitivity of the receiver components. Rise-time analysis and BER also showed signs of having very small distorsion and easy to read the output eye diagram.

REFERENCES

[1] S.B. Weinstein *et al.*, *The Comsoc Guide to Passive Optical Networks*. NJ: John Wiley & Sons Inc., 2012.
[2] *Gigabit-capable Passive Optical Networks (GPON): Physical Media Dependent (PMD) layer specification,* ITU-T G.984.2, 2003.
[3] *10Gb/s Ethernet PassiveOptical Network*, IEEE 802.3av, 2009.
[4] F. J. Effenberger, "The XG-PON System: Cost Effective 10 Gb/s Access", *J. Lightw. Technol.*, vol. 29, no. 4, pp. 403-409, Feb. 2011.
[5] *10-Gigabit-capable Passive Optical Networks (XG-PON): Physical Media Dependent (PMD) Layer Spesification,* ITU-T G.987.2, 2010.
[6] J. Li dan G. Shen, *Cost Minimization Planning for Passive Optical Networks*, 2008.
[7] S. Jain *et al.*, "World's First XG-PON Field Trial," *J. Lightw. Technol.,* vol. 29, no.4, pp. 524-528, Feb. 2011.
[8] B. Zhu *et al.*, *Coexistence of 10G-PON and GPON Reach Extension to 50-km with Entirely Passive Fiber Plant*, Amerika Serikat: Optical Society of America, 2011.
[9] Y. Lee *et al*., "Fast Management of ONUs Based on Broadcast Control Channel for a 10 Gigabit-Capable Passive Optical Network (XG-PON) System," *J. Commun. And Networks*, vol. 15, no. 5, pp. 538-542, Oktober 2013.
[10] J. Kim *et al*., "Design and Performance Analysis of Passively Extended XG-PON with CWDM Upstream," *J. Lightw. Technol*., vol. 30, no. 11, pp. 1677-1684, Juni 2012.
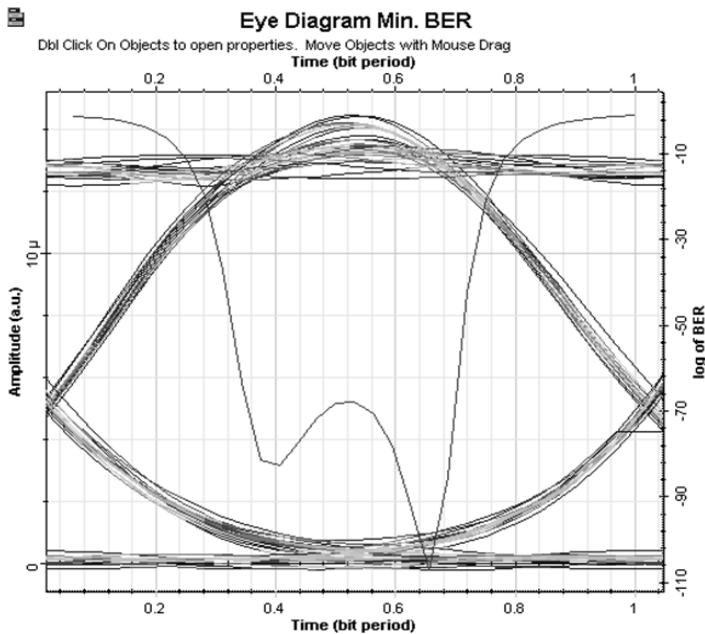
Link Failure Analysis in SDN Datacenter Using RipL-POX Controller

Iffah Kholidatun Nisrina, Andre Aginsa, Elsa Vinietta, and Nana Rachmana Syambas

School of Electrical Engineering and Informatics

Institut Teknologi Bandung

iffahnisrina@gmail.com, andreaginsa@gmail.com, elsa.vinietta@gmail.com, nana@stei.itb.ac.id

Abstract— **In a SDN-based data center network, the controller used greatly affects the behavior of the network. In this paper, the observation is conducted to describe the effect of various link failure scenarios to data center network performance using the Ripl-POX controller. Results shown in this paper can be used as a consideration for both controller selection or building for managing the data center and switch replacement method selection.**

This paper shows the effect of one to three switches that is turned down simultaneously on overall bandwidth. The simulation is done on 4k-fat tree data center network on mininet environment with RipL-POX as controller.

Keywords—data center, fat tree, Mininet, RipL-POX

I. INTRODUCTION

The data center is a facility used to store data. The data that we get in the cloud are physically located in the datacenter. Companies and other Internet network users also put its data in the datacenter because of its large capacity and high level of its security. Besides, datacenter must also be lit and can be accessed at any time.

The total number of network-connected devices is increasing significantly and also the Cloud Computing model make the world of enterprise has the option to store big data in the cloud, which creates more of data to store and process. So it is necessary upgrade our network to deal with this issue.

SDN is one trend that is popular and discussed to be implemented on existing networks, especially in the datacenter. SDN is a new approach to networking in which network control is decoupled from the data forwarding function and is directly programmable. The result is an extremely dynamic, manageable, cost-effective, and adaptable architecture that gives administrators unprecedented programmability, automation, and control [1].

But in the real world we often find switches that have been unsuitable and should be replaced or performed updating the firmware on the switch. To do this we must turn off the switch you want to change. At a datacenter availability and reliability is very important to be maintained so as to shut down the switch, we must do the planning right. To carry out this plan we need to calculate the effect of each switch to the datacenter performance.

II. RELATED WORK

There are some research in SDN controller. The simulation in Mininet of SDN network using POX controller has been performed in [2]. The result of the research is the simulation of SDN network, contain one switch, one controller, and 3 hosts. Communication and bandwidth performance between nodes of the network is analyzed using ping and iperf command. [2] have stated that it is possible to design the SDN network using POX controller. Another work using POX Controller has been proposed in [3] about shortest path routing and [4] about limitation of POX controller.

In [5], simulation using Floodlight controller has been done. The scenario of the simulation is when the controller fails, there are algorithm for fault recovery. Fault recovery algorithm was simulated in Mininet using Floodlight controller. The result is performance analysis of that algorithm, latency and throughput. [6] is another work related to Floodlight controller.

Another research about simulation SDN in Mininet is [7] that used NOX controller. [7] proposed the system to reduce switch and controller in OpenFlow network. The network that need to be reduced is data center network. The simulation was performed using two datacenter network traffic, tree and fat-tree topology. In both cases, switch reduction was performed successfully. Research about NOX controller is also performed in [8] and [9].

Comparison of performance between two controller has been performed in [10]. The processing time is analyzed using Opendaylight and Ryu controller. Scenario of simulation took in two topologies, fat tree and internet topology zoo. Throughput was also one of analysis parameter, but there was no difference in throughput compared to number of host and type of topology. Other works about Ryu controller performance has been done in [11] and [12] and another work about Opendaylight controller has been performed in [13].

[14] propose the algorithm for load balanced multipath in fat tree data center network. The implementation of the algorithm was simulated using Mininet with another controller. Beacon controller was used to take performance data. Throughput and delay was analyzed to measure the performance. The result of the research is the proposed algorithm is better than legacy multipath load balanced algorithm.

The same with [2], this paper is the future work that will perform the simulation of more complex network performance and use different controller. The use of specific controller is proposed, the same with [2]-[14]. Analyzing fat tree topology in data center is also proposed in this paper. But another work will be done, this paper propose to analyze the impact of link failure to network performance.

III. SIMULATION METHODS

In the present paper we will analyze the effect switches that are shuted down to the overall bandwidth of the system. It would be very useful if we want to replace the switch in a datacenter. Of course, if we want to do the replacement or renewal of the switch, the switch must be turned off and this will greatly affect the existing traffic. When simulate switch off, we will shut down the entire link that is connected to the switch so that no incoming or outgoing packet switch.

Data center network used in this paper is fat tree topology. Fat tree topology is one of data center topology that provide the efficient communication between the host. The advantages of fat tree topology is the capability of multipath routing. The topology that is used is 4-pod fat tree topology (Figure 1). The hierarchical layer of the network include core switch, aggregation switch, edge switch, and host. Simulation of link failure will be performed in core and aggregation switch.
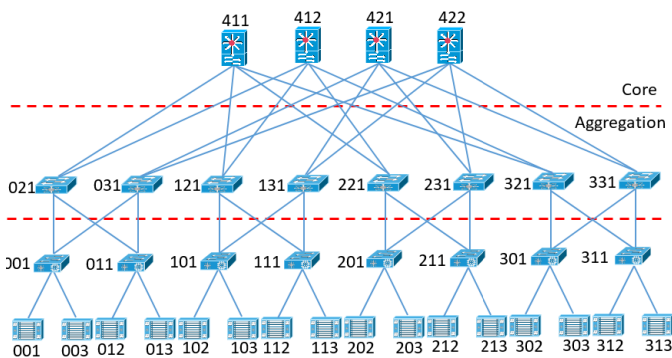

Figure 1 Data Center Network

The most important thing in simulating SDN network is the controller. There are several controller that can be simulated in Mininet. OpenFlow Controller is used to manage the entire data center network. RipL-POX (Ripcord-Lite for POX) is one of OpenFlow controller that can perform multipath routing in the topology. We use RipL-POX controller [15] to simulate this fat tree topology. The Ripl-POX controller is set with mode reactive and random routing. Other tools beside Mininet and RipL-POX that is used is Wireshark. Wireshark will be used to capture the packet flow of the network.

Simulation will be performed in each scenario and the performance will be measured. There are two types of performance, measuring input output packet in some time and measuring bandwidth in all the link. While measuring input output packet, the scenario is simulated and use Wireshark to capture the input and output packet within a time, but the test is not performed in all the link, only some link that represent the link failure. In this test, we can compare the performance of each link when the links fail. The second measurement is measuring bandwidth in all the link. The purpose of this test is to compare the bandwidth between two host when the link failure and when the all the link is up. So, we can calculate the performance reduction and analyze the effect of link failure with bandwidth between two host.

A. Measuring Bandwidth

We will simulate the measurement bandwidth when there is a down switch and see the impact to the total bandwidth. When there are one or more switches turned off, it would reduce the value of bandwidth variously. At this time our research will turn off one and up to three switches at once with different combinations. The combination includes:

- 1 Aggregation Switch (Switch 021) down
- 2 Aggregation Switch (Switch 021 & 121) down
- 3 Aggregation Switch (Switch 021, 121, & 221) down
- 1 Core Switch (Switch 411) down
- 1 Core Switch and 1 Aggregation Switch (Switch 021 & 411) down
- 2 Core Switch (Switch 411 & 412) down

As we have mentioned before, when we turn off a switch, there will be no packet to the switch or derived from the switch, in other words all links connected to the switch is off. In this simulation we will turn off the link between the switches. Suppose for the first case one Aggregation switch (example switch 021) is turned off, then the realization of the simulation are link 021-001 turned off, link 021-021 turned off, link 021-411 turned off, and link 021-412 turned off.

B. Measuring I/O packet

To measure overall data center network performance in each scenario, bandwidth test on every host pair has been done. In mininet, iperf test is used to obtain the value.

In the simulation, we also concerned about the performance fluctuation over a period of time in a specific node or host pair. Another mininet command, ping flood (ping -f) is used on host pairs to generate traffic, and I/O graph feature included in Wireshark is used to obtain the aggregation of input and output bandwidth over a period of time.

IV. SIMULATION RESULT AND ANALYSIS

The result of the simulation is divided into two parts, measuring bandwidth and measuring I/O packet.

A. Number of turned off switches vs. performance

The value of bandwidth that we get on each scenario will be compared with the entire bandwidth when all switch turns on, so it will give us the percentage of bandwidth performance as shown in Table 1.

Table 1 Bandwidth Result

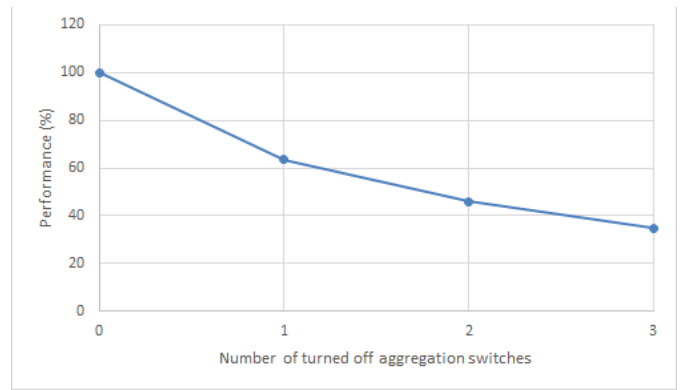| Scenario	Performance
1 Aggregation Down	63.60 %
2 Aggregation Down	45.94 %
3 Aggregation Down	34.80 %
1 Core Down	57.80 %
1 Core and 1 Aggregation Down	55.77 %
2 Core Down	42.80 %

Figure 2 Number of turned off aggregation switches vs. Performance
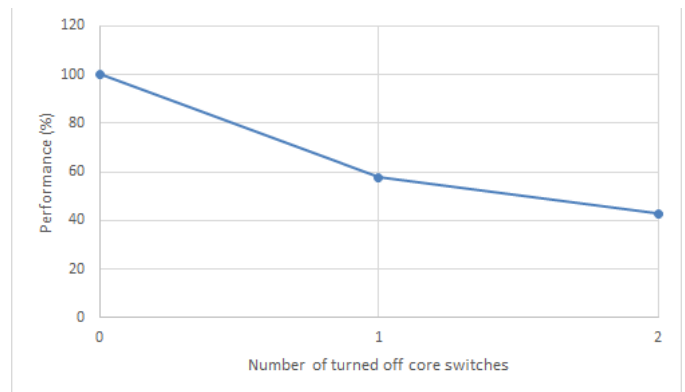

Figure 3 Number of turned off core switches vs. Performance
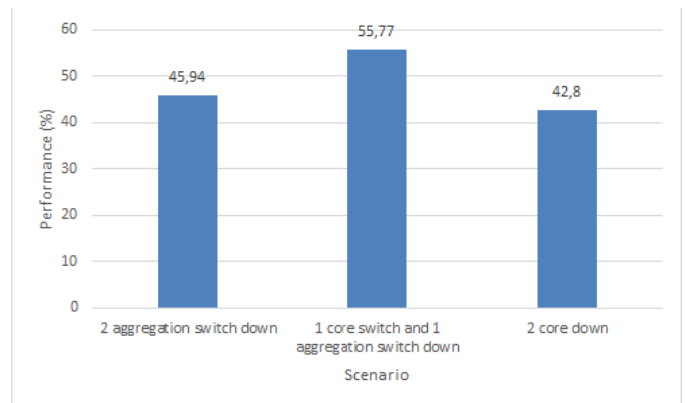

Figure 4 Performance of 2 turned off switches with different scenario

We can see that core switches will give more influence for the decrease in bandwidth compared to aggregation switches. And the more we turn off the switches, the performance of the bandwidth will decrease more. The comparison of the number of turned off switches with performance can be seen in Figure 2, 3, and 4. It is because

aggregation switch connect closer to the host so the connection possibility between two host will reduce. The more aggregation switch turned off, the connection possibility reduce more. So it affect the connection bandwidth in the entire network. The same with turned off core switch. The more core switch is turned off, the bandwidth also decrease.

B. *Position of turned off switch to respective host vs. performance*

- 1 Aggregation switch down

The simulation is performed in 3 test, ping flood host in the same pod (Figure 5), different pod (Figure 6), and other pod (Figure 7).
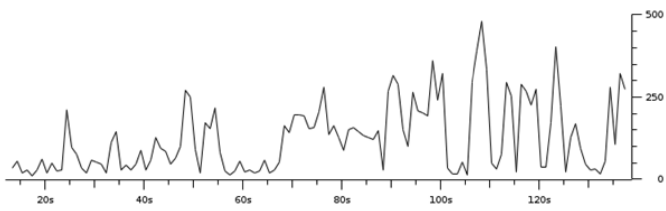

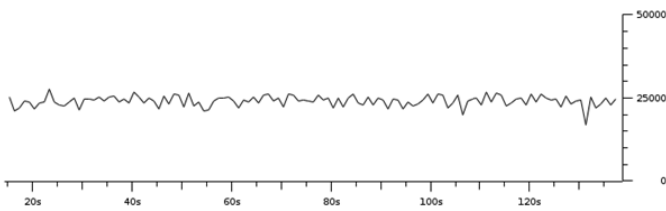Figure 5 I/O Packet Same Pod

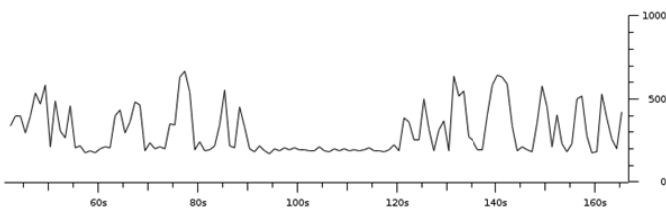Figure 6 I/O Packet Different Pod

Figure 7 I/O Packet Other Pod

- 2 Aggregation switch down

The results of the simulation are the I/O packet when ping flood between 2 host.
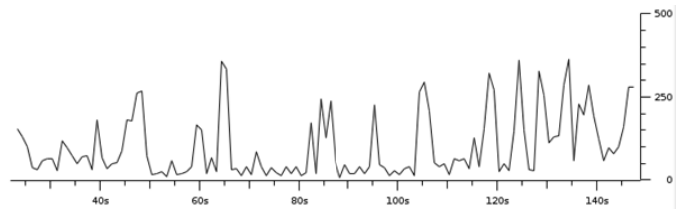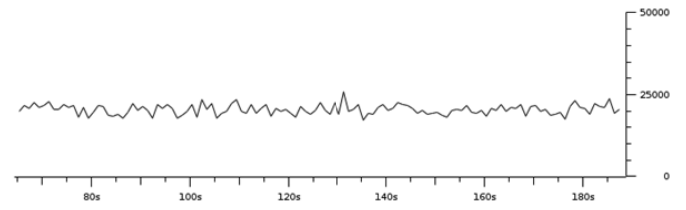

Figure 8 I/O Packet Same Pod
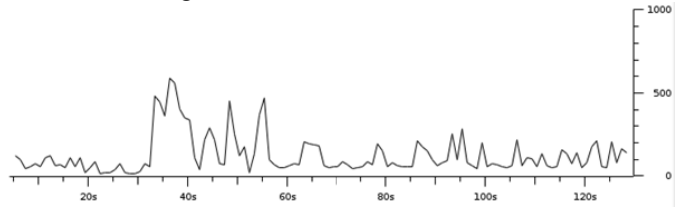

Figure 9 I/O Packet Different Pod

Figure 10 I/O Packet Other Pod

- 3 Aggregation switch down

Figure 11, 12, and 13 below are the results of the simulation when 3 aggregation switches down.
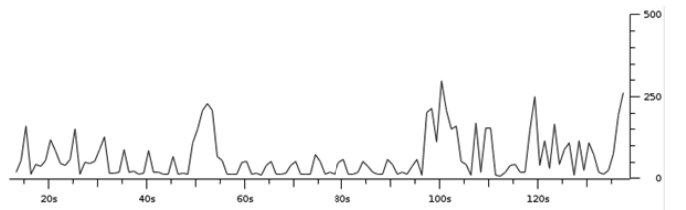

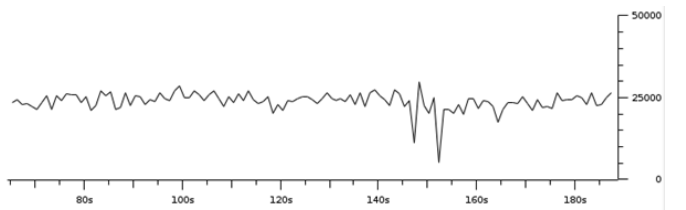Figure 11 I/O Packet Same Pod

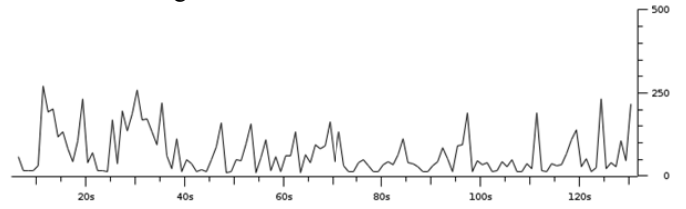Figure 12 I/O Packet Different Pod

Figure 13 I/O Packet Other Pod

- 1 Core Switch down

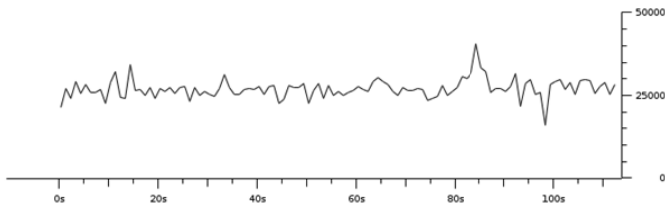   Figure 14 and 15 are the simulation result of one core switch down.
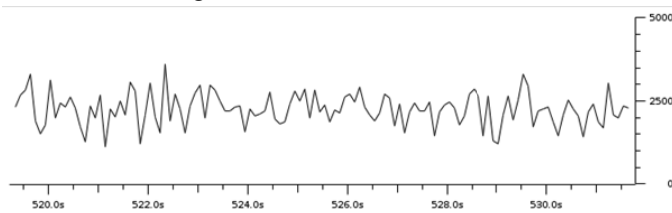

Figure 14 I/O Packet Same Pod

Figure 15 I/O Packet Different Pod

- 1 Core and 1 Aggregation switch down

    Figure 16, 17, and 18 are the result of one core switch and one aggregation switch down.
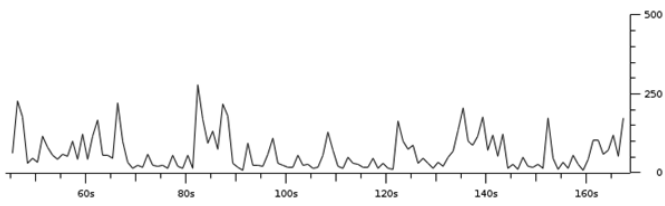

Figure 16 I/O Packet Same Pod
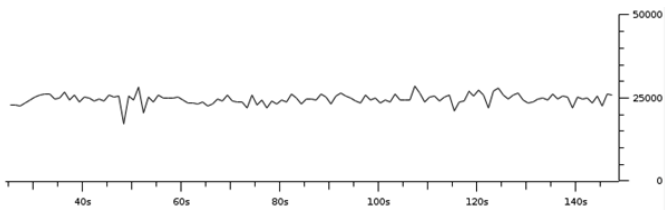
Figure 17 I/O Packet Different Pod
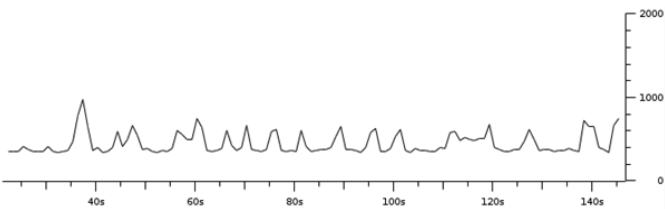
Figure 18 I/O Packet Other Pod

- 2 Core switch down

    Figure 19 and 20 are the simulation result of two core switches down.
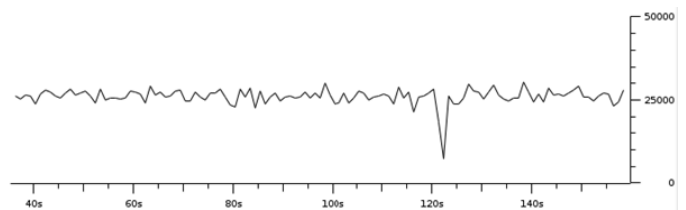
Figure 19 I/O Packet Same Pod
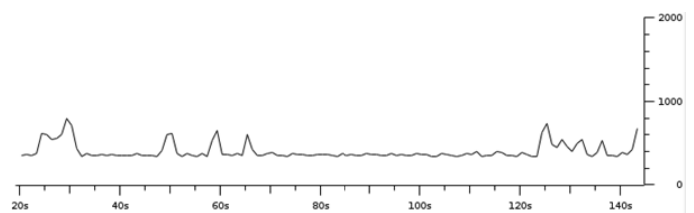
Figure 20 I/O Packet Different Pod

The simulation results above stated time in second (X axis) and the number of packets per kilo byte (Y axis). Wireshark capture the packet flow in the destination host. The number of delivered packet is affected by turned off switch. The amount of sent packet will reach the value of about 25 MByte when most of the package is delivered in the destination host. However, if the connection has the possibility to pass the turned off switch, there will be a decrease in the number of packets sent. The reduction varies depending on the connection that is built between the core and/or aggregation switches. The closer the host to the turned off switches, the greater number of packet that is not sent at the destination host. If the core switch is off, then the number of packet that is delivered will be decreased evenly across the network. The number of packets transmitted can only reach 2.5 MByte only. Failure that happens in aggregation switches aggravate packet delivery performance. Significant loss in performance does not occur in the entire networks but only the connection that close with the aggregation switches. The number of packets received is only about 250 KByte. But in other parts of the network that are not affected by the turned off aggregation switches, transmitted packet will still maintain about 25 MByte.

V. CONCLUSION

Experiments have been done in 4k data center network with the RipL-POX controller. It can be concluded that the failure on the core switch causes a greater loss to the data center network performance compared to the failure on the aggregation switch with the remaining performance value of 57.8% and 63.6%, respectively.

The more switch is turned off, the more bandwidth loss is caused in the data center. Performance of one turned off aggregation switch is 63,6%, two turned off aggregation switches is 45,94%, and three turned off aggregation switch is 34,8%. Performance of one turned off core switch is 57,8% and two turned off core switches is 42,8%. Combination of turned off aggregation and core switches, only reach 55,77% of the maximum performance. The results presented in this paper can be used not only as a consideration to determine the replacement method selection of the network elements to minimize traffic loss but also as a consideration for other researchers to develop more advanced controller that provide better fault tolerant for fat tree topology that supports multipath routing in data center.

REFERENCES

[1] "SDN Migration Consideration and Use Cases," https://www.opennetworking.org/images/stories/downloads/sdn-resources/solution-briefs/sb-sdn-migration-use-cases.pdf. 2014. Open Networking Foundation.

[2] L. R. Prete, C. M. Schweitzer, A. A. Shinoda, and R. L. S. Oliveira. "Simulation in an SDN Network Scenario Using the POX Controller," IEEE Colombian Conference Communications and Computing (COLCOM), 2014.

[3] R. Jmal and L. C. Fourati. "Implementing Shortest Path Routing Mechanism Using OpenFLow POX Controller," International Symposium on Networks, Computer and Communications, 2014.

[4] F. Keti and S. Askar. "Emulation of Software Defined Networks Using Mininet in Different Simulation Environment," 6th International Conference on Intelligent Systems, Modelling and Simulation (ISMS), 2015.

[5] D. Li, L. Ruan, L. Xiao, M. Zhu. "High availability for Non-stop network controller," IEEE 15th International Symposium World of Wireless, Mobile, and Multimedia Networks (WoWMoM), 2014.

[6] M. Afaq, S. U. Rehman, and S. W. Cheol. "Visualization of Elephant Flows and QoS Provisioning in SDN-Based Networks," 17th Asia-Pasific Network Operations and Management Symposium (APNOMS), 2015.

[7] M. Koerner and O. Kao. "Multiple Service Load-Balancing with OpenFlow," 13th International Conference on HIgh Performance Switching and Routing (HPSR), 2012.

[8] A. Xie, X. Wang, W. Wang, and S. Lu. "Designing a Disaster-resilient Network with Software Defined Networking," 22nd International Symposium of Quality of Service (IWQoS), 2014.

[9] A. S. Iyer, V. Mann, and N. R. Samineni. "SwitchReduce: Reducing Switch State and Controller Involvement in Openflow Network," IFIP Networking Conference, 2013.

[10] C. Metter, S. Gebert, S. Lange, T. Zinner, P. Tran-Gia, and M. Jarschel. "Investigating the Impact of Network Topology on the Processing Times of SDN Controllers," IFIP/IEEE International Symposium Intregated Network Management (IM), 2015.

[11] F. Lopez-Rodriguez and D. R. Campelo. "A Robust SDN Network Architecture for Service Providers," IEEE Global Communications Conference (GLOBECOM), 2014.

[12] S. Liao, X. Hong, C. Wu, B. Wang, and M. Jiang. "Prototype for Customized Multicast Services in Software Defined Networks," 22nd International Conference on Software, Telecommunications and Computer Networks (SoftCOM), 2014.

[13] Z. K. Khattak, M. Awais, and A. Iqbal. "Performance Evaluation of OpenDaylight SDN Controller," 20th IEEE International Conference on Parallel and Distributed Systems (ICPADS), 2014.

[14] E. Jo, D. Pan, J. Liu, and L. Butler. "A Simulation and Emulation Study of SDN-Based Multipath Routing for Fat-Tree Data Center Network," Winter Simulation Conference (WCS), 2014.

[15] Ripcord-Lite for POX: A simple network controller for OpenFlow-based data centers. https://github.com/brandonheller/riplpox

The Simulation of SDN Network Using POX Controller: Case in Politeknik Caltex Riau

Suci Ramadona[1], Beni Ari Hidayatulloh[2], Dwina Fitriyandini Siswanto[3],Nana Syambas[4]
School of Electrical & Informatics Engineering
Institut Teknologi Bandung
Jl. Ganesha 10 Bandung, Indonesia
suci.ramadona@gmail.com[1], beni.ari@s.itb.ac.id[2], dwina.fitri@students.itb.ac.id[3], nana@stei.itb.ac.id[4]

Abstract— **The growing internet network has led to the more complex design, management, and operational. The situation is getting harder because there are various protocol and hardware used in the networks. In order to overcome an easier network management and to obtain a better scalability, Software Defined Network (SDN) is used. SDN gives solution by applying an centralized network technology and separating the control plane and the data plane. The communication between the planes are controlled using the OpenFlow Protocol. This research using the POX Controller which is integrated with Mininet to do the simulation of SDN network in Politeknik Caltex Riau. In this SDN network two components, hub and switch, are compared.**

Keywords—network management, Sofyware Defined Network, Centralized Network, Control Plane, Data Plane, OpenFlowm, POX Controller, Mininet.

I. INTRODUCTION

The internet service and technology have grown with various complexity, design, management and operational that cause various skill level emerge as well. A problem arise when there are various and different hardware and protocols in a network. In recent years, Software Defined Network (SDN) has been applied by several big companies to produce and utilize their own hardware for the sake of the ease of management and development of their network. SDN has new design, architecture and technology compare to the traditional conventional network. SDN network is considered as one of the main proposal for the viability of the internet in the future[1]. The concept of SDN technology is separating the control plane and the data plane in order to give the optimization solutions in management and scalability[2][3]. Many advanced development of SDN has been emerged nowadays [4]-[8].

The requirements of a secure, robust, and resilient SDN controller has been identified and the state-of-the-art open-source SDN controllers also have been analyzed with respect to the security of their design[9]. This contribution highlights the gap between the potential security solutions for SDN controllers and the actual security level of current controller designs[9]. Two issues about the performance of SDN, which are: a) the impact of SDN on raw performance (in terms of throughput and latency) under various workloads, and b) whether there is an inherent performance

penalty for a complex, more functional, SDN infrastructure have been analyzed[10]. The results indicate that SDN does have a performance penalty, however, it is not necessarily related to the complexity level of the underlying SDN infrastructure[10].The OpenFlow protocol, which allows the creation of applications for Software Defined Networks, has been a new standard to make a network programmable based on the protocol specification[1]. To do the network programming, an interface is needed. That interface is known as API (Application Programming Interface). API follows the OpenFlow open standard based on its version. .POX Controller is one of the SDN controller which support the OpenFlow version 1.0 only. This is one of the first controller which developed to support SDN network.

This research will use POX Controller which is integrated with Mininet to do the simulation of the SDN network in Politeknik Caltex Riau as the test case. This research is important since the existing network of Politeknik Caltex Riau is still conventional network system. In order to migrate the conventional network to SDN, a simulation should be conducted first to asses the feasibility of applying SDN to the Politeknik Caltex Riau network.

The organization of this paper is constructed as follows: Related works are shown in Section II. The Software Defined Networking simulation system is presented in Section III. Section IV discuss about the scenario of SDN simulation. Section V presents the simulation while the results and discussion is presented in Section VI. Section VII will conclude this paper.

II. SOFTWARE DEFINED NETWORK SIMULATION SYSTEM

A. Software Defined Network

In traditional network devices, the decision making occur in its own interior, or the packet routing network is defined by algorithms previously calculated generally closed, with difficult or impossible modification, once implemented on network equipment makes its own decisions to send the packet [1]. While in the SDN, slightly different approach is implemented. Table 1 shows the comparison between conventional network and SDN.

**Table 1.** Comparison Between SDN and Conventional Networking [3]

	SDN	Conventional
Features	decoupled data and control plane, and programmability	a new protocol per problem, complex network control
Configuration	automated configuration with centralized validation	error prone manual configuration
Performance	dynamic global control with cross layer information	limited information, and relatively static configuration
Innovation	easy software implementation for new ideas, sufficient test environment with isolation, and quick deployment using software upgrade	difficult hardware implementation for new ideas, limited testing environment, long standardization process

Figure 1 shows the SDN reference model. The control layer bridges the application layer and the infrastructure layer, via its two interfaces. For downward interacting with the infrastructure layer (i.e., the south-bound interface), it specifies functions for controllers to access functions provided by switching devices. The functions may include reporting network status and importing packet forwarding rules. For upward interacting with the application layer (i.e., the north-bound interface), it provides service access points in various forms, for example, an Application Programming Interface (API). SDN applications can access network status information reported from switching devices through this API, make system tuning decisions based on this information, and carry out these decisions by setting packet forwarding rules to switching devices using this API [3].

The application layer contains SDN applications designed to fulfill user requirements. Through the programmable platform provided by the control layer, SDN applications are able to access and control switching devices at the infrastructure layer. Example of SDN applications could include dynamic access control, seamless mobility and migration, server load balancing, and network virtualization OpenFlow Protocol [3].

B. OpenFlow Controller

OpenFlow was proposed by Stanford University, its initial goal is to meet demand validation of new proposed architecture and network protocols on commercial equipment. Thus, it is possible to implement a technology able to promote innovation in the network core, through the execution of test networks in parallel with production networks. The OpenFlow proposal promotes the creation of SDN, using common elements of network such as switches, routers, access points or even personal computers [1].
OpenFlow is a SDN protocol that allows a network administrator to control the route of the data packets in a switch. In the conventional network, the non-openflow network, each switch only forwards the data packets based on Network Layer work standards.It communicates with switch over a secure channel. It defines message format and
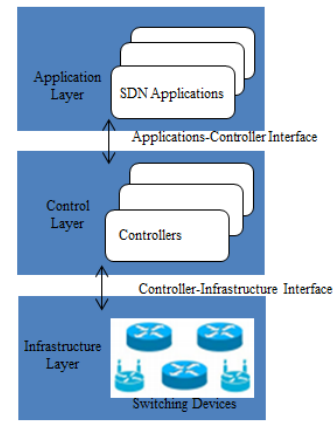
Fig. 1. SDN Reference Model: a three-layer model, ranging from an infrastructure layer to a control layer to an application layer, in a bottom-up mannerArchitechture [3]

purpose of control channel is update flow table. The logic is executed at controller.

OpenFlow describes two different management approaches to populate flow tables: proactive and reactive. Reactive mode is applied when incoming packets do not match any flow entry. Packets are sent to the controller, which installs rules back into the switch. Alternatively, the controller may install proactively flow entries into the switch according to user policies, before packets arrive. Reactive approach is a more powerful model because the controller can implement some kind of logic that cannot be represented into flow tables. In contrast, proactive mode yields to better performance because it avoids the extra latency on the first packet of the flow. In practice, applications may implement a combination of both, where some traffic is handled proactively and some is handled reactively. This hybrid mode would provide zero-latency forwarding for particular flows while still preserve fine-grained traffic control for the rest of the traffic.

Flow-based forwarding through OpenFlow consolidates functionalities of layer-specific hardware into a single device, which essentially involve packet forwarding based on a general definition of flow [5].

C. POX Controller

The main component of a Software Defined Networks is the SDN controller, called a network operating system. The controller is what defines the nature of the SDN paradigm. It is the responsible component for concentrating communication with all programmable elements of the network, providing a unified view of the network. Currently there are several SDN controllers. To develop applications, the programming language in which the controller was developed is essential, as well as its architecture and complexity [1].

POX Controller is one of the SDN controller which support the OpenFlow version 1.0 only. This is one of the first controller which developed to support SDN network.
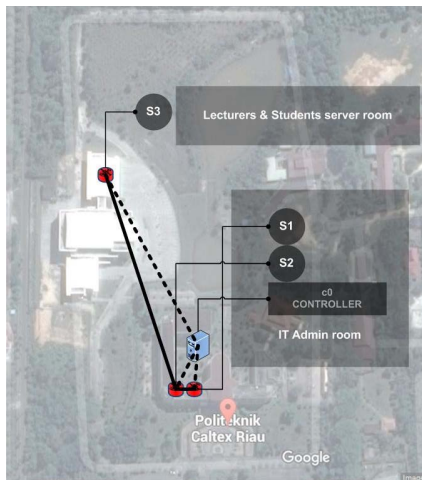
Fig. 2. Software Defined Network (SDN) using POX Controller Topology at Politeknik Caltex Riau
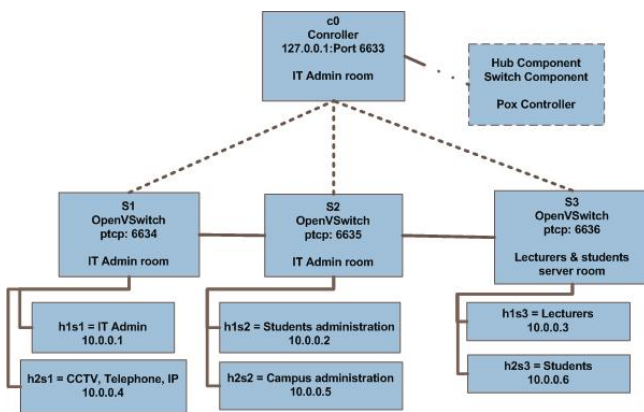

Fig. 3. Simulation Scenario

D. Mininet [1]

SDN architecture multiple components are required in its infrastructure. Initially we need a controller machine running a network operating system, for example NOX or POX. Subsequently, forwarders elements are necessary that have separated control plan with some programming interface, in this case the OpenFlow.

Furthermore, it is still required an entire physical infrastructure that links these forwarders elements and controller over a secure channel for the creation of a Software Defined Networks.

But not always a researcher has an infrastructure to conduct their experiments, since it has a high cost. To deal with this problem you can use a specific simulator. The Mininet is a tool to simulate the Software Defined Networks that allows quick prototyping of a large virtual infrastructure network with the use of only one computer. It enables you to create virtual prototypes of scalable networks based on software such as OpenFlow, using primitive Virtualization Operating System. With these primitives, it allows you to create, interact and customize prototypes for Software Defined Networks in a very quick way.

It is possible to perform with the Mininet debugging tests and problem solving, which can be benefited from having a complete trial network on a laptop or PC. It provides, intuitively, tools for developing learning networks in the area. Its interface enables the use in research and in classes fo the practical use of techniques and networking solutions.

III. SIMULATION SCENARIO

The simulation scenario consists of a three OpenFlow switches with linear topology (S1, S2, S3) connected to six hosts (h1s1, h1s2, h1s3, h2s1, h2s2, h2s3) and to a controller POX. This controller has two created components called Hub and Switch. Figure 3 shows the implementation of this scenario in the PCR buildings, S1 and S2 are located in the IT Admin room while S3 is located in the lectures & students room. Figure 4 shows this simulation scenario where host h1s1, h2s1 are connected to the switch s1 and have a role as IT admin server and cctv, telephone and IP server respectively. Host h1s2 and h2s2 are connected to the switch s2 and have a role as students administration and campus administration respectively. Host h1s3 and h2s3 are connected to the switch s3 and have a role as lectures server and students server respectively.

IV. SIMULATION

After the topology has been created, the virtual network SDN is ready and the POX will be able to remotely connect to it on a host machine or in the own VM Mininet Virtual Machine. Mininet implementation of the simulation scenario is shown in Table 2.

The version, specification, feature, state and table entries of the ovs switch can be found by using the command ovs-vsctl and ovs-ofctl show <switch> in the ssh terminal when the topology have been formed. The ovs-vsctl program configures ovs-vswitch by providing a high-level interface to its configuration database. ovs-vsctl connects to an ovsdb-server process that maintains an Open vSwitch configuration database. Using this connection, it queries and possibly applies changes to the database, depending on the supplied commands. Then, if it applied any changes, by default it waits until ovs-vswitchd has finished reconfiguring itself before it exits. The ovs-ofctl program is a command line tool for monitoring and administering OpenFlow switches. It can also show the current state of an OpenFlow switch, including features, configuration, and table entries. It should work with any OpenFlow switch, not just Open vSwitch. Table 3 shows the specification of one of the ovs switch, s2.

A. Hub Components

A component that acts as a hub, which is replicating the received and sent packets to all its output ports is also prepared. This hub component will be used in the scenario as shown in Fig 3. It is interesting to note how it is structured as a component in POX and how it works with the OpenFlow packages and messages. Table 4 shows the Mininet implementation of hub in POX controller.

B. Switch Components

This component has a switch action as self-study part that learns the path as the packets arrive at the switch. In other words, it is a simple switch that learns the ways of their hosts. The interesting part of this component is to see how this one works with messages `ofp_flow_mod` that installs entries in the flow table of an OpenFlow switch. This kind of behavior makes the switch run the packages commutation much faster than the previous component. Table 5 shows the Mininet implementation of switch in POX controller.

V. RESULTS AND DISCUSSION

After running the Hub component (Table 4) or Switch component (Table 5), the network then monitored by the POX controller. Analyzing network behavior with some commands in the CLI of Mininet while run the wireshark, the following results are obtained.

A. Ping

It was found that using the two components designed to the controller POX, successful pings are obtained. Ping is a utility that uses ICMP protocol to test the connectivity between the devices. Its operation consists of sending packets to the destination equipment and in the "listening" of the responses. Table 6 shows the ping results from Mininet.

B. RTT and Delay

Then the comparison of Round Trip Time (RTT) between using the hub component and a switch component in POX controller are shown. Round-trip time (RTT) also called round-trip delay, is the time required for a signal pulse or packet to travel from a specific source to a specific destination and back again. In this context, the source is the computer initiating the signal and the destination is a remote computer or system that receives the signal and retransmits it. Figure 6 shows the RTT between the hub and switch in POX controller.

Delay is the amount of time needed to do transmission from the source to the destination. Delay can be calculated using formula as follows,

$$Delay\ (s) = \frac{Average\ Round\ Trip\ Time\ (RTT)}{2}$$

The successfully captured hub average RTT is 0.031743129 seconds therefore,

$$Hub\ Delay\ (s) = \frac{0,031743129}{2} = 0.015871565\ s$$

The successfully captured switch average RTT is 0,094515557 seconds therefore,

$$Switch\ Delay\ (s) = \frac{0,094515557}{2} = 0,047257778\ s$$

C. Bandwidth

The bandwidth is also analyzed. Table 7 shows the comparison of the obtained bandwiths between two components of POX controller. In the tests between hosts, the bandwidth was greater in the execution using switch

Table 2. Simulation scenario impementation in Mininet

```
mininet@mininet-vm:~$ sudo mn –topo linear,3,2
-mac –switch ovsk –controller
=remote
*** Creating network
*** Adding controller
*** Adding hosts:
h1s1 h1s2 h1s3 h2s1 h2s2 h2s3
*** Adding switches
s1 s2 s3
*** Adding links
(h1s1, s1) (h1s2, s2) (h1s3, s3) (h2s1, s1)
(h2s2, s2) (h2s3, s3) (s2, s1) (s3, s2)
*** Configuring hosts
h1s1 h1s2 h1s3 h2s1 h2s2 h2s3
*** Starting controller
c0
*** Starting 3 switches
s1 s2 s3
*** Starting CLI:
```

Table 3. the specification of one of the ovs switch, s2

```
mininet@mininet-vm:~$ sudo ovs-ofctl show s2
OFPT_FEATURES_REPLY (xid=0x2) :
dpid:0000000000000002
N_tables :254, n_buffers:256
Capabilities: FLOW_STATS TABLE_STATS PORT_STATS
QUEUE_STATS ARP_MATCH_IP
Actions: OUTPUT SET_VLAB_VID SET_VLAN_PCP
STRIP_VLAN SET_DL_SRC SET_DL_DST SET_NW_SRC
SET_NW_DST SET_NW_TOS SET_TP_SCR SET_TP_DST
ENQUEUE
1 (s2-eth1): addr:0a:6b:3c:f7:5f:e1
     config:   0
     state :   0
     current : 10GB_FD COPPER
     speed : 10000 Mbps now, 0 Mbps max
2 (s2-eth2): addr:f6:53:e2:b6:aa:30
     config :  0
     state :   0
     current : 10GB-FD COPPER
     speed: 10000 Mbps now, 0 Mbps max
3 (s2-eth3) : addr:42:e1:c1:91:ac:be
     config :  0
     state :   0
     current : 10GB-FD COPPER
     speed : 10000 Mbps now, 0 Mbps max
4 (s2-eth4) : addr:02:0e:0f:36:ba:5c
     config :  0
     state :   0
     current : 10GB-FD COPPER
     speed : 10000 Mbps now, 0 Mbps max
LOCAL (s2) : addr:de:9e:a6:57:02:48
```

Table 4. Mininet implementation of Hub component in POX controller

```
mininet@mininet-vm:~$ cd pox
mininet@mininet-vm: ~/pox$ sudo su
root@mininet-vm:/home/mininet/pox# ./pox.py
log.level –DEBUG misc.of_tutorial
POX 0.2.0 (carp) / copyright 2011-2013 James
McCauley, et al.
DEBUG:core:POX 0.2.0 (carp) going up...
DEBUG:core:Running on Cpython (2.7.6/Mar 22
2014 22:59:38)
DEBUG:core:Platform is Linux-3.13.0-24-generic-
i686-with-Ubuntu-14.04-trusty
INFO:core:POX 0.2.0 (carp) is up.
DEBUG:openflow.of_01:Listening on 0.0.0.0:6633
```

component, since this component has an action of self-learning analyzing the way as the packets arrive at the switch using entries in the flow table, and when the next packets arrive, it already knows the path which provides the increasing of the bandwidth between the hosts, without need to always flood the network with packets to discover its destiny.

D. Throughput

Now the comparison of throughput between hub and switches component is considered. Throughput refers to how much data can be transferred from one nodes to another in a given amount of time. The following formula is the formula used to calculate the percentage of throughput,

$$\% \ throughput = \frac{successfully \ transferred \ data}{total \ data} \ x \ 100\%$$

For the hub, by using Wireshark capturing, the total data is 950478 Bytes where the successfully transferred data is 856428 Bytes. Therefore the percentage of hub throughput is calculated as follows,

$$\% \ throughput = \frac{856428 \ \text{Byte}s}{950478 \ \text{Bytes}} x \ 100\% = 90,10\%$$

For the switch, by using Wireshark capturing, the total data is 2926670 Bytes where the successfully transferred data is 2694410 Bytes. Therefore the percentage of switch throughput is calculated as follows,

$$\% \ throughput = \frac{2694410 \ \text{Bytes}}{2926670 \ \text{Bytes}} x \ 100\% = 92,06\%$$

The calculation above shows that, although the hub has slightly smaller value than the switch, both hub and switch has a good value of throughput percentage, which is above 90%. Figure 7 and 8 show the Bits/Tics and throughput performance of POX controller, respectively.

E. Mean Data Rate

Mean data rate shows the value of the average speed of the data transmission. Average throughput value is calculated at the beginning to build a data connection until data is received successfully. Mean Data Rate can be calculated by using the formula as follows[11],

$$Mean \ Data \ Rate \left[\frac{kbit}{s}\right] = $$
$$\frac{user \ data \ transferred \ [kbit]}{tdata \ transfer \ complete - tdata \ transfer \ start}$$

For the Hub, by using Wireshark capturing, user data transferred is obtained 856428 Bytes and the time between the first and the last packet is obtained 29,255 seconds therefore,

$$Hub \ Mean \ Data \ Rate = \frac{856428 \ Bytes}{29,255 \ sec} = \ 29,27458554 \ KBps$$

Table 5. Mininet implementation of Switch component in POX controller

```
mininet@mininet-vm:~$ cd pox
mininet@mininet-vm: ~/pox$ sudo su
root@mininet-vm:/home/mininet/pox# ./pox.py
log.level –DEBUG misc.switchrun
POX 0.2.0 (carp) / copyright 2011-2013 James
McCauley, et al.
DEBUG:core:POX 0.2.0 (carp) going up...
DEBUG:core:Running on Cpython (2.7.6/Mar 22 2014
22:59:38)
DEBUG:core:Platform is Linux-3.13.0-24-generic-
i686-with-Ubuntu-14.04-trusty
INFO:core:POX 0.2.0 (carp) is up.
DEBUG:openflow.of_01:Listening on 0.0.0.0:6633
```

Table 6. Mininet ping results (a) Hub (b) Switch

(a)
```
mininet> pingall
*** Ping: testing ping reachability
h1s1 -> h1s2 h1s3 h2s1 h2s2 h2s3
h1s2 -> h1s1 h1s3 h2s1 h2s2 h2s3
h1s3 -> h1s1 h1s2 h2s1 h2s2 h2s3
h2s1 -> h1s1 h1s2 h1s3 h2s2 h2s3
h2s2 -> h1s1 h1s2 h1s3 h2s1 h2s3
h2s3 -> h1s1 h1s2 h1s3 h2s1 h2s2
*** Results: 0% dropped (30/30 received)
```

(b)
```
mininet> pingall
*** Ping: testing ping reachability
h1s1 -> h1s2 h1s3 h2s1 h2s2 h2s3
h1s2 -> h1s1 h1s3 h2s1 h2s2 h2s3
h1s3 -> h1s1 h1s2 h2s1 h2s2 h2s3
h2s1 -> h1s1 h1s2 h1s3 h2s2 h2s3
h2s2 -> h1s1 h1s2 h1s3 h2s1 h2s3
h2s3 -> h1s1 h1s2 h1s3 h2s1 h2s2
*** Results: 0% dropped (30/30 received)
```

Table 7. Mininet bandwidth results (a) Hub (b) Switch

(a)
```
*** Iperf: testing TCP bandwidth between h1s1
and h2s3
***    Results:    ['4.28    Mbits/sec',    '4.48
Mbits/sec']
```

(b)
```
*** Iperf: testing TCP bandwidth between h1s1
and h2s3
***    Results:    ['1.76    Gbits/sec',    '1.76
Gbits/sec']
```

For the Switch, by using wireshark capturing, user data transferred is obtained 2694410 Bytes and the time between the first and the last packet is obtained 63,402 seconds therefore,

$$Switch \ Mean \ Data \ Rate = \frac{2694410 \ Bytes}{63,402 \ sec} = 42,49723983 \ KBps$$

VI. CONCLUSIONS

In this paper, simulation of SDN network using POX controller for case Politeknik Caltex Riau has been presented. The topology of the SDN network for Politeknik Caltex Riau is designed and then the simulation is done using mininet. In this SDN network two components, hub and switch, are compared. The RTT, delay, bandwidth, throughput and mean data rate of the two components are compared. From the simulation, we obtained that the
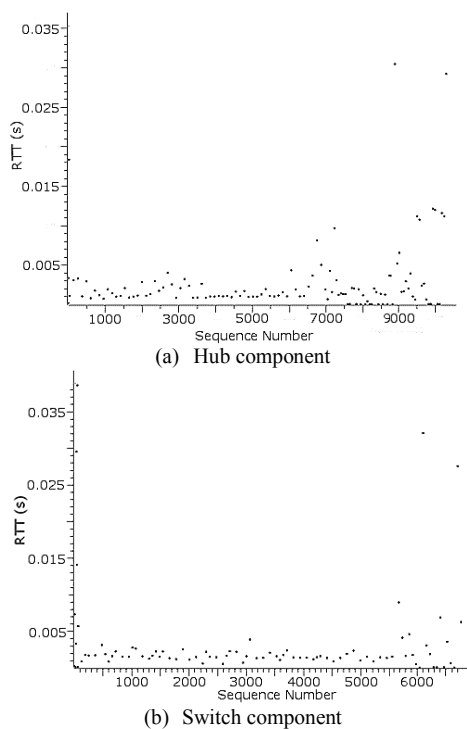
(a) Hub component

(b) Switch component

Fig. 6. Round Trip Time of POX controller

(a) Hub

(b) Switch

Fig. 7. Bits/Tick of POX controller

(a) Hub

(b) Switch

Fig. 8. Throughput of POX controller

average RTT and the delay of hub have smaller value than the switch. The bandwidth of the switch is greater than the bandwidth of the hub. Both hub and switch has a good value of throughput percentage, which is above 90%, although the hub has slightly smaller value than the switch. Last, the mean data rate of the hub is smaller than the mean data rate of the switch.

REFERENCES

[1] Rodrigues Prete, L.; Schweitzer,C.M.; Shinoda A.A.; Santos de Oliveira, R.L, "Simulation in an SDN network scenario using the POX controller", IEEE Columbian Conference Communication and Computing (COLCOM), 2014.

[2] Wenfeng Xiam Yonggang Wen. Senior Member, IEEE, Chuan Heng Foh, Senior Member, IEEE, Dusit Niyanto, Member, IEEE, and Haiyong Xie, Member, IEEE, " A Survey on Software-Defined Networking", IEEE Communication Surveys & Tutorial, VOL. 17, NO.1, First Quarter 2015.

[3] Nakayama, H.; Mori,T.; Ueno,S.; Watanabe,Y.; Hayasi, T., " An Implementation Model and Solutions for Stepwise Introduction of SDN", 16th Asia-Pacific Network Operations and Management Symposium (APNOMS), 2014.

[4] Marcel Caria, Admela Jukan, and Marco Hoffmann, " A Performance Study of Network Migration to SDN-enabled Traffic Engineering",Globecom 2013- Communication QoS, Reliability and Modeling Symposium, 2013.

[5] Izquierdo-Zaragoza, J,-L,; Fernandez-gambin, A,; Pedreno-Manresa,J.-J,; Pavon-Marino,P, "Leveraging Net2Plan planning tool for network orchestration in OpenDaylight", International Conference on Smart Communications in Network Technologies (saCoNet), 2014.

[6] Yao-Yu Yangm Chao-Tung Yang, Shuo-Tsung Chen, Wi-Hsun Chenng, and Fuu-Cheng Jiang, " Implementation of Network Traffic Monitor System with SDN", IEEE 39th Annual International Computersm Software & Applications Conference, 2015.

[7] Tamal das, Marcel Caria, and Admela Jukan, Marco Hoffmann, " Insights on SDN Migration Tracetory", IEEE ICC 2015- Netxt generation Networking Symposium, 2015.

[8] Heleno Isolani, P, "Interactive Monitoring, Visualization, and Configuration of OpenFlow-based SDN", IEEE International Symposium on Integrated Network Management, 2015.

[9] Scott-Hayward, S, "Design and Deployment of Secure, Robust, and Resilient SDN Controllers", IEEE Conference on Network Softwarization, 2015

[10] Gelberger, A et al., "Performance Analysis of Software-Defined Networking (SDN)", IEEE 21st International Symposium on Modeling, Analysis & Simulation of Computer and Telecommunication Systems, 2013.

[11] S. Haryadi, *Telecommunication Service and Experience Quality*, Bandung: Lantip Safari Media, 2013.

Effect of Material Thickness on Resonance Characteristics of Anisotropic Artificial Circular Dielectric Resonator

Hepi Ludiyati[1,2], Andriyan Bayu Suksmono[1], Achmad Munir[1]
[1]Radio Telecommunication and Microwave Laboratory
School of Electrical Engineering and Informatics, Institut Teknologi Bandung
[2]Department of Electrical, Politeknik Negeri Bandung
Bandung, Indonesia
hepi_ludiyati@yahoo.com, suksmono@stei.itb.ac.id, munir@ieee.org

Abstract—In the case of the artificial circular dielectric resonator which is encapsulated in a circular waveguide, the resonance characteristic is determined not only by a resonator thickness but also by a novel anisotropic permittivity value and a radius of a circular waveguide. In this paper, the relationship of its parameters is calculated and analyzed. The calculation is done by using the mathematical formulation which is derived from Maxwell's equations with proper boundary condition. The research is focused on the influence of the resonator thickness to the TM resonance characteristics of artificial circular dielectric resonator. The results show, the ability of novel anisotropic in ρ direction increase due to a radius of a circular waveguide enhancement for TM_{01} wave mode, whilst, the ability increase due to a radius of a circular waveguide reduction for TM_{11} wave mode. A novel permittivity in ρ direction is effective reduce the resonant frequencies for thin resonator thickness.

Keywords—anisotropic permittivity; artificial dielectric material; artificial circular dielectric resonator; Transverse Magnetic; resonance characteristic

I. INTRODUCTION

Artificial dielectric materials are proposed by the researches to answer the telecommunication equipment needs notably the microwave equipment at this time. Numerous unique properties from the material such as a dielectric material with a permittivity less than unity [1], a dielectric material with a refractive index less than unity [2], and a dielectric material with a huge permittivity [3] are studied and implemented in several microwave devices. Mostly, the dielectric materials are proposed to miniaturize the size of microwave devices, thus more easy to be connected to the integrated networks.

In 2003, the artificial dielectric material with anisotropic permittivity was proposed [4]-[8]. The proposed material had a relative permittivity tensor which a relative permittivity was a function of direction in a rectangular coordinate system. Some prototypes of the proposed material were implemented in the bandpass microwave filters. The proposed material was not only successfully in lowering the resonance frequencies of

the devices, but also rejecting unwanted wave modes in the microwave filters.

In [4], anisotropic permittivity of artificial dielectric material was introduced by a relative permittivity in x, y, and z direction. The ability of the anisotropic permittivity had been investigated when the material was applied as a microwave resonator. In [4], the characteristic resonance in TE resonance modes were studied when the resonator was encapsulated in a rectangular waveguide. One of the scientific contribution of this research was a mathematical formulation for analyzed the mutual coupling between the microwave resonators. As a future work of the research, in this paper, another unique anisotropic permittivity of the artificial dielectric material is introduced. Different from [4]-[8], a proposed anisotropic permittivity has different values in a cylindrical coordinate system. Henceforth, this material is called as the artificial circular dielectric material.

The study of the artificial circular dielectric material is begun in 2012 [9]. The paper has been published with the focus on a capability artificial circular dielectric resonator to select the resonant mode which is required. Some property of a natural dielectric material has been modified artificially to obtain a unique characteristic of the resonator. Some prototype of the resonator is proposed too which the prototype is etched above of a natural dielectric material as metal strips with some gaps. The investigation result shows that the resonator configuration consists of 1 strip with 4 gaps and of 2 strips with 4 gaps in different gap position has the lowest resonant frequency of $TE_{01\delta}$ wave mode.

The study of artificial circular dielectric material is continued in [10]. In [10] a mathematical formulation of artificial circular dielectric resonator which is encapsulated with a d thickness in a circular waveguide is reported. It formulation is derived from Maxwell's equations in Transverse Electric (TE) wave modes. The paper consist of a derivation of the scalar Helmholtzt equation and its solution for TE resonance wave mode, the electric field and magnetic field equations inside the resonator, an impedance wave of resonator and propagation constants in outside and inside of

resonator. In [10], the resonance characteristics of three successive TE resonance modes are explored, and the results shows that the relative permittivity in radial direction is more influence in lowering the resonance frequencies of the resonator.

The extension of [10] is proposed in [11] with the focuses on a mathematical formulation for Transverse Magnetic (TM) resonance mode of artificial circular dielectric resonator. A potentially of every novel anisotropic permittivity in lowering the resonance frequencies of the resonator are analysis. In the results, we found that the good impact is shown by a novel permittivity in z in which it is capable to reduces resonant frequencies of the conventional resonator with a natural dielectric material up to 65.22% for TM_{01} resonance mode. The results are a beneficial for resonance mode selection when the proposed resonator is implemented in a microwave device.

The resonator thickness as an essential parameter on the resonance characteristic of artificial circular dielectric resonator is not yet explored more in a previous paper. In this research, the influence of the parameter in two successive TM wave modes are investigated. The investigations are based on a mathematical formulation which is derived from Maxwell's equations in curl forms. By defining a proper boundary condition for a circular waveguide with radius of a, an equation which relate a resonator thickness of d, a resonance frequency and novel anisotropic value is determined and calculated. The resonance frequency for some values of a resonator thickness (d) is calculated by the equation and analyzed, specific only for a novel anisotropic permittivity in a radial direction. The whole of the process will be presented in the following section.

II. Breaf Overview of Anisotropic Permittivity in Artificial Circular Dielectric Material

As we know, the electromagnetic materials such as conductor, dielectric and magnetic are commonly used in several microwave devices. Every material has different characteristics and gives different utility or functionality. For instance, a dielectric material will polarize if it's fed by the external electric field source. In this case, the electrons in a dielectric will move in a bounded region, but in other hand this characteristic cause a dielectric material is able to store the electric energy. One of utilization of a dielectric material is hold the electrons between two conductors in order to avoid a direct contact or a short circuited.

In a natural dielectric material, the characteristics of the material are given by a relative permittivity value. The permittivity is isotropic and commonly is less than 10 [13]. Different from a natural dielectric material, the artificial circular dielectric material is introduced by anisotropic permittivity . In this case, a value of relative permittivity is a function of a direction in a cylindrical coordinate system. The anisotropic permittivity of artificial circular dielectric material is written in a matrix form as

$$[\varepsilon] = \varepsilon_0 \begin{bmatrix} \varepsilon_\rho & 0 & 0 \\ 0 & \varepsilon_\phi & 0 \\ 0 & 0 & \varepsilon_z \end{bmatrix} \qquad (1)$$

In a vector form or a tensor, (1) become

$$[\varepsilon] = \varepsilon_0 \varepsilon_\rho \vec{a}_\rho + \varepsilon_0 \varepsilon_\phi \vec{a}_\phi + \varepsilon_0 \varepsilon_z \vec{a}_z \qquad (2)$$

where :

ε_0 = a permittivity in free space

ε_ρ = a relative permittivity in ρ direction

ε_ϕ = a relative permittivity in ϕ direction

ε_z = a relative permittivity in z direction

In this research, the permeability of the proposed material is equal to a permeability of free space ($\mu = \mu_0$).

As a consequence, the Maxwell's equations for the proposed material are given by

$$\nabla \times \vec{E} = -j\omega\mu_0\vec{H} \qquad (3)$$

$$\nabla \times \vec{H} = j\omega[\varepsilon]\vec{E} \qquad (4)$$

Equation (2) and (3) are applicable for a sinusoidal source with the equation is given by

$$\vec{E}(z,t) = E_0 e^{j(\omega t - \beta z)}\vec{a}_\rho \qquad (5)$$

The source is assumed as an electric field polarizes in ρ direction and propagates in z direction. Figure 1 is a cylindrical coordinate system to guide our understanding of anisotropic permittivity properties. There are three unity vectors, i.e. $\vec{a}_\rho, \vec{a}_\phi$, and $\vec{a}_z$ as a unity vector in a radial direction, a unity vector in a ϕ direction, and a unity vector in a z direction, respectively.
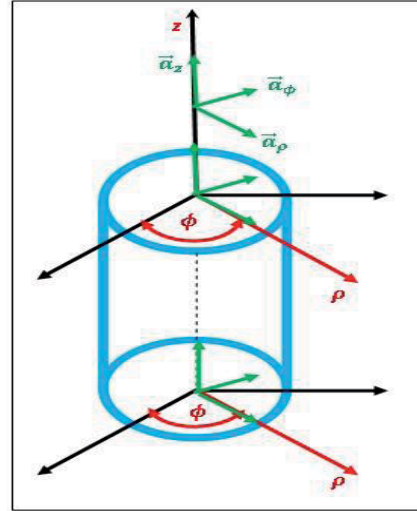
Fig. 1. A cylindrical coordinate system with three unity vectors.

By applying the operation of a curl equation in a cylindrical coordinate system to (2) and (3), the following equations will be obtained

$$\left[\frac{1}{\rho}\frac{\partial E_z}{\partial \phi} - \frac{\partial E_\phi}{\partial z}\right]\vec{a}_\rho + \left[\frac{\partial E_\rho}{\partial z} - -\frac{\partial E_z}{\partial \rho}\right]\vec{a}_\phi + \left[\frac{1}{\rho}\frac{\partial}{\partial \rho}(\rho E_\phi) - \frac{1}{\rho}\frac{\partial E_\rho}{\partial \phi}\right]\vec{a}_z = -j\omega\mu_0(H_\rho\vec{a}_\rho + H_\phi\vec{a}_\phi + H_z\vec{a}_z) \qquad (6)$$

and

$$\left[\frac{1}{\rho}\frac{\partial H_z}{\partial \phi} - \frac{\partial H_\phi}{\partial z}\right]\vec{a}_\rho + \left[\frac{\partial H_\rho}{\partial z} - \frac{\partial H_z}{\partial \rho}\right]\vec{a}_\phi + \left[\frac{1}{\rho}\frac{\partial}{\partial \rho}(\rho H_\phi) - \frac{1}{\rho}\frac{\partial H_\rho}{\partial \phi}\right]\vec{a}_z = \left(\varepsilon_\rho E_\rho \vec{a}_\rho + \varepsilon_\phi E_\phi \vec{a}_\phi + \varepsilon_z E_z \vec{a}_z\right) \tag{7}$$

From (6) and (7), the differential equations for the artificial circular dielectric will be described and the equations will be simplified to determine further characteristics of the artificial dielectric resonator in a TM resonance mode.

III. THE RESONANCE CHARACTERISTIC OF ARTIFICIAL CIRCULAR DIELECTRIC IN TM RESONANCE MODES

For the electromagnetic wave propagates in a z direction, Transverse Magnetic (TM) modes are indicated by the component of a magnetic field in z direction is zero $\left(\vec{H}_z\right)$. The artificial circular dielctric material is placed encapsulating in a circular waveguide as shown in Fig. 2. Hence, from (6) and (7) which is set $\vec{H}_z = 0$ and by applying some mathematical manipulations will be obtained the scalar Helmholtz equation for artifcial circular dielectric resonator. The equation is written as

$$\frac{1}{\rho}\frac{\partial}{\partial \rho}\left(\rho\frac{\partial E_z}{\partial \rho}\right) + \frac{1}{\rho^2}\left(\frac{k_\rho \sqrt{\varepsilon_\phi}}{k_\phi \sqrt{\varepsilon_\rho}}\right)^2 \frac{\partial^2 E_z}{\partial \phi^2} = -k_\rho^2 \frac{\varepsilon_z}{\varepsilon_\rho} E_z \tag{8}$$

In the artificial circular dielectric resonator, we define two the wave numbers that are $k_\rho^2 = \omega^2 \mu_0 \varepsilon_0 \varepsilon_\rho - \beta^2$ and $k_\phi^2 = \omega^2 \mu_0 \varepsilon_0 \varepsilon_\phi - \beta^2$. For a conventional dielectric resonator, the wave number has only one, i.e. $k^2 = \omega^2 \mu_0 \varepsilon_0 \varepsilon_r - \beta^2$, which ε_r is a relative permittivity of a natural dielectric material.
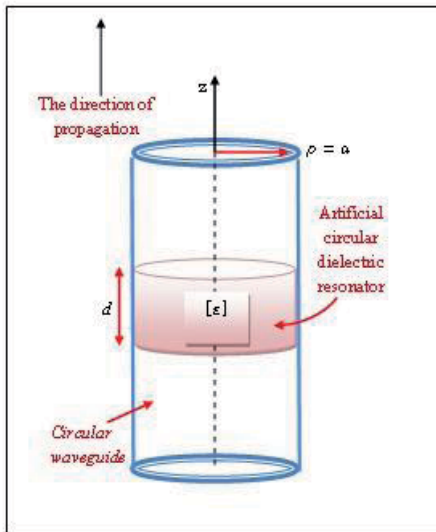

Fig. 2. Artificial circular dielectric resonator with the thickness of d is encapsulated in a circular waveguide with the radius $\rho = a$

There are several steps to determine the related equation between a resonator thickness (d), resonance frequency, and permittivity $\left(\varepsilon_\rho, \varepsilon_\phi, \varepsilon_z\right)$, i.e.

- Determine a solution for the scalar Helmholtz equation in (8) by using the separation of variable method in a cylindrical coordinate system. In this step, E_z in (8) can be written as a function of ρ and ϕ.

$$E_z = R(\rho)\Phi(\phi) \tag{9}$$

From the first step, by applying some mathematical manipulation, the following equations are obtained

$$R = C_1 J_n\left(k_\rho \frac{\sqrt{\varepsilon_z}}{\sqrt{\varepsilon_\rho}}\rho\right) + C_2 N_n\left(k_\rho \frac{\sqrt{\varepsilon_z}}{\sqrt{\varepsilon_\rho}}\rho\right) \tag{10}$$

where C_1 and C_2 are constants, and J_n and N_n are Bessel and Neumann functions, respectively, and

$$\Phi = A_1 \cos\left(\frac{k_\phi \sqrt{\varepsilon_\rho}}{k_\rho \sqrt{\varepsilon_\phi}}n\phi\right) + A_2 \sin\left(\frac{k_\phi \sqrt{\varepsilon_\rho}}{k_\rho \sqrt{\varepsilon_\phi}}n\phi\right) \tag{11}$$

where A_1 and A_2 are constants, whilst $\cos\left(\frac{k_\phi \sqrt{\varepsilon_\rho}}{k_\rho \sqrt{\varepsilon_\phi}}n\phi\right)$

and $\sin\left(\frac{k_\phi \sqrt{\varepsilon_\rho}}{k_\rho \sqrt{\varepsilon_\phi}}n\phi\right)$ are the standing waves which are defined for Bessel functions in $\rho < a$ and Neumann functions in $\rho > a$, respectively. By substituting (10) and (11) to (9) and its solution is taken only in a sinusoidal function for simplification, the solution of (9) in a time domain is written as

$$E_z(z,t) = E_{0z} J_n\left(k_\rho \frac{\sqrt{\varepsilon_z}}{\sqrt{\varepsilon_\rho}}\rho\right)\cos\left(\frac{k_\phi \sqrt{\varepsilon_\rho}}{k_\rho \sqrt{\varepsilon_\phi}}n\phi\right)e^{j(\omega t - \beta z)} \tag{12}$$

- Next, determine the wave impedance of the artificial circular dielectric resonator and thus it will be used for determine the wave impedance in outer and inner the resonator. The purpose is to determine the mathematical formulation to correlate three parameters which will be used to analyze the influence of the resonator thickness on the resonance characteristics of the artificial circular dielectric resonator. The similar step in [5] that is a short-open termination of the resonator by a flat conductor is used to determine the solution. All of the steps yield the following equations, i.e.

$$\frac{\beta}{\varepsilon_\phi}tan\left(\beta\frac{d}{2} - \frac{s\pi}{2}\right) = \alpha \tag{13}$$

$$\beta = \sqrt{\left(\frac{\omega}{c}\sqrt{\varepsilon_\rho}\right)^2 - \left(\frac{X_{np}}{a}\frac{\sqrt{\varepsilon_\rho}}{\sqrt{\varepsilon_z}}\right)^2} \tag{14}$$

and

$$\alpha = \sqrt{\left(\frac{X_{np}}{a}\right)^2 - \left(\frac{\omega}{c}\right)^2} \tag{15}$$

where β is the phase constant, in the artificial circular dielectric, it depends on novel anisotropic permittivity values and a root of the Bessel function, X_{np}. For two successive TM$_{np}$ modes, its values are 2.405, and 3.832. In a conventional dielectric resonator case, (13),(14) and (15) become

$$\frac{\beta}{\varepsilon_r}tan\left(\beta\frac{d}{2} - \frac{s\pi}{2}\right) = \alpha \tag{16}$$

where α obtained from (15) and β is obtained by

using the formula :

$$\beta = \sqrt{\left(\frac{\omega}{c}\sqrt{\varepsilon_r}\right)^2 - \left(\frac{X_{np}}{a}\right)^2} \quad (17)$$

The resonance frequency, f_r can be set by using $\omega = 2\pi f_r$. Equations (12), (13), and (14) will be calculate to investigate the influence of a resonator thickness   to resonance characteristics on TM resonance modes in next section.

IV. CALCULATION, RESULTS, AND ANALYSIS

In order to investigate the influence of a resonator thickness on the resonance characteristic of artificial circular dielectric resonator, a radius of a circular waveguide is set in three values, i.e. 10 mm, 15 mm, and 20 mm. The calculation of a resonance frequency is done when artificial circular dielectric resonator has a novel permittivity in ρ direction $\left(\varepsilon_\rho\right)$, which in every calculation, ε_ρ is set 15 while $\varepsilon_\phi = \varepsilon_z = 5$.

Fig. 3. Resonant frequency as a function of resonator thickness of TM_{01} for three values of a circular waveguide radius *10mm, 15mm,* and *20 mm*
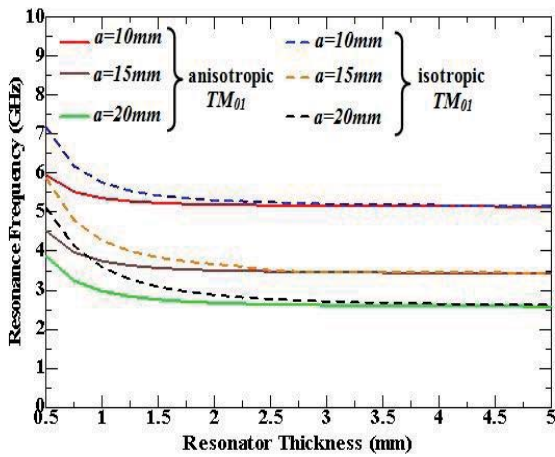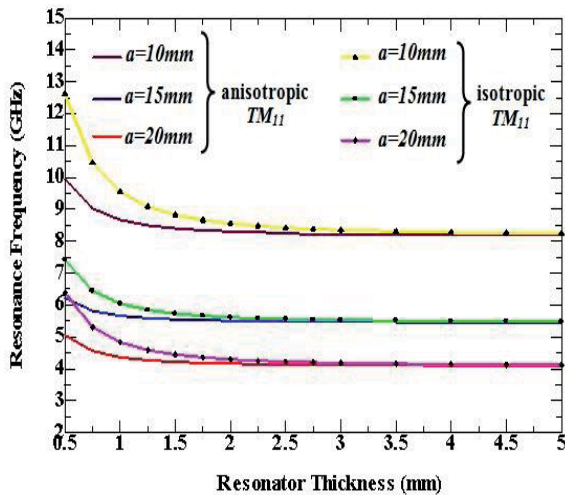

Fig. 4. Resonant frequency as a function of resonator thickness of TM_{11} for three values of a circular waveguide radius *10mm, 15mm,* and *20 mm*

The resonator thickness d is set from 0.5 mm to 5 mm for two successive TM wave modes, i.e TM_{01} and TM_{11}. In this mode, the cut off frequency of a hollow circular waveguide itself is 11.483 GHz, and 18.296 GHz for a radius, a = 10mm, 7.655 GHz, and 12.198 GHz for a radius, a = 15mm, and 5.742 GHz, and 9.148 GHz for a radius, a = 20mm , respectively. The calculation results are compared to a conventional resonator one which uses a natural dielectric material.

The results of resonant frequency as a function of resonator thickness d for TM_{01} wave mode and TM_{11} wave mode are plotted in Figures 3, and 4. From the results, it can be seen that when the anisotropic permittivity in ρ direction (ε_ρ) is higher than ε_ϕ and ε_z, the resonant frequencies of artificial circular dielectric resonator are lower than the resonant frequencies of a conventional dielectric resonator. For TM_{01} wave mode, the ability of novel anisotropic in ρ direction is increase due to a radius of a circular waveguide enhancement, whilst for TM_{11} wave mode, the ability of novel anisotropic in ρ direction is increase due to a radius of a circular waveguide reduction.   A novel anisotropic permittivity in ρ direction is effective reduce the resonant frequencies for the thickness of resonator is less than 0.15 times of the radius of a circular waveguide for TM_{01} and TM_{11}, and the lowering of resonant frequencies in both of TM wave modes are effective for the thin resonator thickness.

V. CONCLUSION

This paper investigates the influence of a resonator thickness on the resonance characteristic of artificial circular dielectric resonator with novel anisotropic permittivity in ρ direction. We derived the formulation to calculate the resonant frequencies of two first TM wave modes, i.e TM_{01} and TM_{11} when the artificial circular dielectric resonator is encapsulated in a circular waveguide. From the results, we conclude that on TM_{01} wave mode, the ablity of novel anisotropic in ρ direction is increase due to a radius of a circular waveguide enhancement, whilst on TM_{11} wave mode, the ablity is increase due to a radius of a circular waveguide reduction. A relative permittivity in ρ direction is effective reduce the resonant frequencies for the thickness of resonator is thin.

REFERENCES

[1] K. C. Gupta, "Narrow-beam antennas using an artificial dielectric medium with permittivity less than unity," *Electronic Letters 14th,* Vol. 7, No. 1, pp. 16-18, Dec. 1970.

[2] J. Brown, "Artificial dielectric having refractive indeks less than unity," *Institution Monograph 15th*, pp. 51-62, May. 1953.

[3] I. Awai, H. Kubo, T. Irobe, D. Wakamiya, A. Sanada, "An artificial dielectric material of a huge permittivity with novel anisotropy and its application to a microwave BPF," *IEEE MTT-S Digest,* Philadelphia, USA, Vol. 1, pp. 301-304, 2003.

[4] H. Kubo, I. Awai, T. Iribe, A. Sanada, A. Munir, "Artificial dielectric composed of metal strips and calculation method of the permittivity and permeability," *IEEJ Trans. FM.*, vol. 123, no. 3, pp. 265-272, Mar.

2003. (*in Japanese)*

[5] I. Awai, H. Kubo, T. Iribe and A. Sanada, "Dielectric resonator based on artificial dielectrics and its application to a microwave BPF," in *32ndEuropean Microwave Conference Proc.,* Milan, Italy, pp. 1045-1048, Sept. 2002.

[6] I. Awai, A. Munir, N. Hamanaga and A. Sanada, "Artificial dielectric rectangular resonator with great anisotropic permittivity and its waveguide application," *in 2003 Asia-Pacipic Microwave Conference Proc.,* Seoul, Korea, pp. 1752-1755, Nov. 2003.

[7] I. Awai, A. Munir, H. Kubo and A. Sanada, "A TE$_{108}$-mode waveguide filter made of artificial dielectric resonators," in *5th Asia-Pacipic Engineering Research Forum on Microwaves and Electromagnetics Theory Proc.,* Fukuoka, Japan, pp. 145-151, Jul. 2004.

[8] A. Munir, N. Hamanaga, A. Sanada, H. Kubo and I. Awai, "Improvement of spurious property of waveguide bandpass filter based on artificial dielectrics, " *in 34th European Microwave Conference Proc.,*

[9] R.H Basuki, H. Ludiyati, A. Munir, "Artificial circular dielectric resonator with resonant mode selectability," *7th International Conference on Telecommunication Systems, Services, and Applications (TSSA),* 2012.

Amsterdam, Netherlands, pp. 1005-1007, Oct. 2004.

[10] H. Ludiyati, A. Bayu Suksmono, and A. Munir, "Basic theory of artificial circular resonator encapsulated in a circular waveguide and its theoretical analysis," *Proceeding of 3rd International Conference and Instrumentation, Communication, Information Technology and Biomedical Engineering (ICICI-BME)*, pp. 392-395, Bandung, Indonesia, Nov. 2013.

[11] H. Ludiyati, A. Bayu Suksmono, and A. Munir "TM wave mode analysis of circular dielectric resonator with anisotropic permittivity,*"* PIERS *Proceeding,* Guangzhou, China, pp. 230-233, August 25-28, 2014.

Simulation of Network Migration to Software-Defined Network
Case Study : ITB Ganesha Campus

Mukti Rahim[1], Muhammad Rizky Hikmatullah[2], GedeArna Jude Saskara[3], Nana Rachmana S[4]
School of Electrical Engineering and Informatics
InstitutTeknologi Bandung, Jl. Ganesha 10 Bandung 40132, Indonesia
[1]Email: mukti_r@yahoo.com, [2]Email: muhammad.rizky3012@gmail.com,
[3]Email: jude_saskara@yahoo.com, [4]Email: nana@stei.itb.ac.id

Abstract— Internet networking's growing lead to complexity in the design, management, and operations. Software Defined Network (SDN) is the answer to all the challenges of the complexity of today's networks. By conducting the separation between the control plane and the data plane, SDN administrator facilitate the network in the process of optimization, perform network management and has better scalability in its provisioning. This is the basis for this paper to be able to implement it at ITB network that still use the conventional network. Implementation of network migration is tailored to the specifications of the network needs at ITB.

Keywords— SDN, Network, ITB, control, data

I. INTRODUCTION

The development of technology is currently very rapid, particularly in the field of network technology development. With all the challenges in terms of network complexity that exists today, Software Defined Network (SDN) be a reliable solution for future network developments. With the method of separation of control plane and data plane, process optimization and network management can be done easily, and can improve better scalability.

In Bandung Institute of Technology conventional network is still used, using 3 servers at the center of a grid placed in different buildings and are connected to each other. These conditions allow the various problems making network management and data migration if there is damage to one of the servers. Moreover, with the development of the user at ITB every year, this network will also provide new problems in terms of development and scalability.

By using the SDN network, is expected to address the various problems that will occur at the ITB campus network. Moreover, with the centralized controller, network management will be easy to do without having to perform the configuration on each server because the server will follow the rule that has been in the settings on the controller. The network planning process using Net2Plan applications in building design that will be designed and implemented. And simulated using POX controller in Mininet.

II. BACKGROUND

A. Software Defined Network

Software Defined Networking (SDN) is a new concept in design, architecture and management of computer networking. SDN is the basic concept of separation (decouple) between the network control plane to the forwarding plane to facilitate the optimization of the data, perform management to scalability. This system is necessary because in the world of networking is actually no use of a balance between control plane to the forwarding plane.

Control plane and data plane have different functions within the application. For example in the application of network switches in the figure II.1, forwarding plane more unused resource compared to the control plane. Another example is a firewall where the control plane is more dominant than the forwarding plane of unused resources. Departing from here then SDN into solutions that can offset the use of both control plane and data plane.
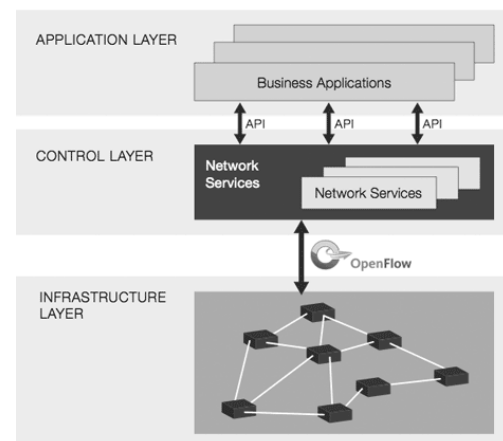

Fig. 1. SDN Architecture

SDN based network has several differences become advantages over conventional network that can be seen in terms of features, network configuration and performance. The differences include features, configuration, performance and even in innovations. In SDN, we can decoupled data and control plane so we can configure automatically with

centralized validation. For more innovations, we can make easy software implementation for new ideas, sufficient test environment with isolation, and quick deployment using software upgrade. While in conventional networking we are difficult to implement for new ideas, limited testing environment, and long standardization process because it's have limited information and relatively static configuration. And also conventional networking still use manual configuration that can be error when we configure it.

B. Net2Plan[2]

Net2Plan is a free and open-source Java tool devoted to the planning, optimization and evaluation of communication networks [7]. It was originally thought as a tool to assist the teaching of communication networks planning courses. Eventually, it has converted into a powerful network planning tool for the academia and industry [7], together with a growing repository of network planning resources.

Net2Plan is built on top of an abstract network representation, so-called network plan, based on seven abstract components: nodes, links, routes, traffic demands, protection segments, shared-risk groups and network layers. The network representation is technology-agnostic, thus Net2Plan can be adapted for planning networks in any technology. Technology- specific information can be introduced in the network representation via user-defined attributes attached to any of the abstract components mentioned above.

Current version of Net2Plan (0.2.3, March 2014, available for download in [3]) provides six different tools: offline network design, traffic matrix design, three post-analysis simulator (network resilience, connection-admission control, and time-varying traffic), and a reporting tool. For this work, we focus on the offline network design tool.

This tool is targeted to evaluate the network designs generated by built-in or user-defined offline network design algorithms, deciding on aspects such as the network topology, the traffic routing, link capacities, protection routes and so on. If needed, those algorithms based on constrained optimization formulations (i.e. ILPs) can be fast-prototyped using the open- source Java Optimization Modeler library (JOM), to interface from Java to a number of external solvers such as GPLK, CPLEX or IPOPT.

The word "offline" means that all the variables in the network design are supposed to be known deterministic values. For instance, in our study, this could be a snapshot of the network (topology and end-to-end average traffic), although in reality network conditions fluctuate along time.

The workspace of the window is divided into three areas: input data, execution and reporting (right area), plot area (top-left area), and warning area (bottom-left area). In Net2Plan, network designs can be completed incrementally, modifying the current network design, that the user can inspect visually in the "Network Topology" panel, and the "Edit network plan" tab. When the offline design tool starts, the current network design is empty. Then, the user can modify it (i) using manual editions in the "Network Topology" panel or the "Edit network

plan" tab, (ii) loading existing designs and/or traffics demands, (iii) applying offline design algorithms (that take the current network design, and return a modified design that becomes the current design).

C. Mininet

Mininet is an emulator, where mininet capable of running as host devices, switches, routers, and links interconnecting media in a linux kernel. Mininet using the basic concept of virtualization to create a single system looks to be like a complete system, running in the kernel, system, and the same user code. Mininet behave not just as a real machine; but can also perform remote ssh and run the program (any program that has been installed on the Linux operating system). A program created to send packets through the ethernet interface, to be able to provide a connection speed and delay parameters. Packet will be processed through an interface such as switches, routers, or other intermediary device.

III. DESIGN IMPLEMENTATION

When designing a network, especially network on a widespread scale necessary supporting data to help provide more in depth information both about the condition of the current network, or the estimated time at which a network that we create can be used in a considerable period of time. Data such as traffic internet network is still functioning on the network, then the number of users that exist today are very helpful to perform calculations in the planning of the network to be built in the future.

A. Network Plan
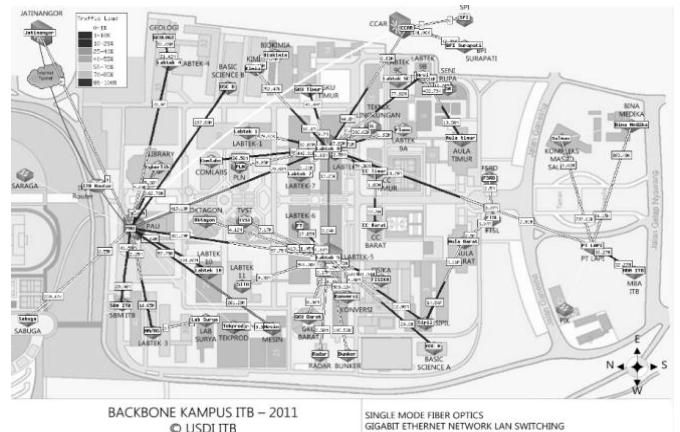
Fig. 2. Existing Network of ITB

Figure 2 describe existing network of ITB. It seemed that the network is still use the conventional concept where there are three central servers that are connected each other but working separately with each device holds full control over their function and performance.

B. Traffic Data

Data traffic is used and referenced in this journal is the traffic on the internet core network ITB namely PAU Building, Labtek VIII and V Building Labtek Ganesha ITB.

Data traffic is taken is the use of inbound and outbound traffic from August to October 2015.

TABLE I. TRAFFIC BETWEEN PAU AND LABTEK 8

PAU/Labtek 8	Inbound (Mbps)	Outbound (Mbps)
August	25.78	105.15
September	75.11	165.27
October	57.95	177.29

TABLE II. TRAFFIC BETWEEN PAU AND LABTEK 5

PAU/Labtek 5	Inbound (Mbps)	Outbound (Mbps)
August	39.59	70.59
September	43.33	101.19
October	35.19	99.77

TABLE III. TRAFFIC BETWEEN LABTEK 5 AND LABTEK 8

Labtek 5/Labtek 8	Inbound (Mbps)	Outbound (Mbps)
August	17.39	1.53
September	11.07	1.16
October	7.58	1.25

Based on the data traffic over, the data are then processed using net2plan application to get the design we want to build. After receiving all the data that we need such as metric topology, metric of capacity and traffic, followed by simulating network with mininet.

IV. SIMULATION

A. Net2Plan

Net2Plan used to determine future network needs. By entering some input into Net2plan, we obtained images SDN network topology. Design of network topology obtained can be seen in the following picture.
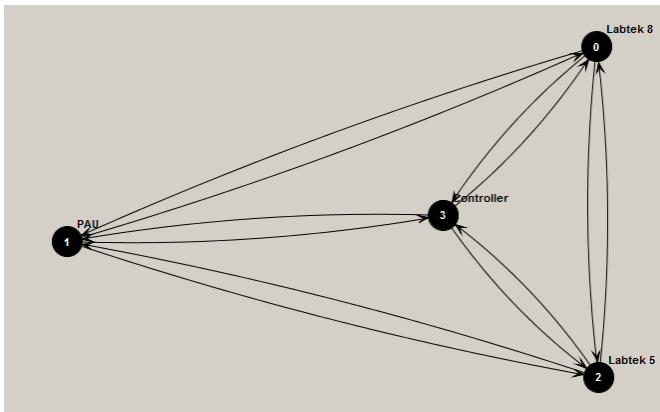

Fig. 3. Network Topology Based SDN

Judging from figure 3, there are two links mounted between the corresponding link. This illustrates that these links act as each inbound and outbound traffic in a node.

B. Mininet

The first step to doing this is to run performance calculations to simulate appropriate putty net2plan topology. Which in net2plan uses 1 controller and 3 OpenFlow switches.

For the simulation of each switch is connected to the PC or commonly known as the host. Syntax as follows :

"sudo mn - - topo linear, 3 - -switch ovsk - -controller remote".

Which in switch_ctrl.py program are as follows python script :

```
def _handle_idealpairswitch_packetin (event):
 packet = event.parsed

 # Learn the source and fill up routing table
 table[(event.connection,packet.src)]= event.port
 dst_port=table.get((event.connection,packet.dst))

 if dst_port is None:
   send_packet(event, of.OFPP_ALL)
   log.debug("Broadcasting %s.%i -> %s.%i" %
     (packet.src, event.ofp.in_port, packet.dst, of.OFPP_ALL))
 else:
   msg = of.ofp_flow_mod()
   msg.idle_timeout = 10
   msg.hard_timeout = 30
   msg.match.dl_dst = packet.src
   msg.match.dl_src = packet.dst
   msg.actions.append(of.ofp_action_output(port = event.port))
   event.connection.send(msg)
   msg = of.ofp_flow_mod()
   msg.idle_timeout = 10
   msg.hard_timeout = 30
   msg.match.dl_src = packet.src
   msg.match.dl_dst = packet.dst
   msg.actions.append(of.ofp_action_output(port = dst_port))
   event.connection.send(msg) log.debug("Installing %s.%i -> %s.%i
AND %s.%i -> %s.%i" %
     (packet.dst,dst_port,packet.src,event.ofp.in_port,
     packet.src,event.ofp.in_port,packet.dst,dst_port))
```

V. ANALYSIS

A. Net2Plan Analysis

And with traffic as described in the previous chapter. With the Shortest Path algorithm CFA Fixed Utilization in net2plan obtained the following result :

- Metric Topology

TABLE IV. METRIC TOPOLOGY

Metric	Value
Number of nodes ($|N|$)	4
Number of unidirectional links ($|E|$)	12
Average node degree	3
Average link distance (km)	0.500
Network diameter (hops)	1
Network diameter (km)	0.500
Average shortest path distance (hops)	1.000
Average shortest path distance (km)	0.500
Connected topology?	Yes
Bidirectional topology (links)?	Yes

Bidirectional topology (links & capacities)?	No
Simple topology?	Yes

- Capacity Metric

TABLE V. CAPACITY METRIC

Metric	Value
Maximum capacity installed in a link (Erlangs, Mbps)	295.48 (295475.34)
Minimum capacity installed in a link (Erlangs, Mbps)	2.09 (2087.04)
Average capacity installed in a link (Erlangs, Mbps)	105.29 (105284.69)
Total capacity installed in a link (Erlangs, Mbps)	1263.42 (1263416.27)
Capacity module size (Erlangs, Mbps)	0.001 (1.00)

- Traffic Metric

TABLE VI. TRAFFIC METRIC

Metric	Value
Total offered traffic (Erlangs, Mbps)	758.05 (758049.76)
Total carried traffic (Erlangs, Mbps)	758.05 (758049.76)
Average offered traffic per demand (Erlangs, Mbps)	63.17 (63170.81)
Average carried traffic per demand (Erlangs, Mbps)	63.17 (63170.81)
Blocked traffic (%)	0.000
Avg. number of hops	1.000

From the results of network design using Net2plan application traffic design results in traffic that can be carried (Carried traffic) the traffic offered (offered traffic) is the same because it does not happen blocking or restriction of traffic which blocked traffic on the design results 0%.

B. Performance Analysis Using Mininet

To analyze the performance of the SDN that we have built, we use wireshark application to determine the flow of traffic on the topology simulation on campus ITB SDN. Our network performance measurement is the network delay and throughput. After running wireshark capture pinging from h1 to h2 (Host 1 to Host 2) for 10 minutes 25 seconds. From the results of capture will get a summary as follows :

```
PING 10.0.0.2 (10.0.0.2) 56(84) bytes of data.
64 bytes from 10.0.0.2: icmp_seq=1 ttl=64 time=2005 ms
64 bytes from 10.0.0.2: icmp_seq=2 ttl=64 time=996 ms
64 bytes from 10.0.0.2: icmp_seq=3 ttl=64 time=0.053 ms
64 bytes from 10.0.0.2: icmp_seq=4 ttl=64 time=0.089 ms
64 bytes from 10.0.0.2: icmp_seq=5 ttl=64 time=0.083 ms
64 bytes from 10.0.0.2: icmp_seq=6 ttl=64 time=0.109 ms
64 bytes from 10.0.0.2: icmp_seq=7 ttl=64 time=0.096 ms
64 bytes from 10.0.0.2: icmp_seq=8 ttl=64 time=0.067 ms
64 bytes from 10.0.0.2: icmp_seq=9 ttl=64 time=0.093 ms
64 bytes from 10.0.0.2: icmp_seq=10 ttl=64 time=0.046 ms
```

From wireshark obtained data as follows :

TABLE VII. SUMMARY WIRESHARK

Traffic	Capture
Packets	1240
Between first and last packet	625.98 sec
Avg. Packets/sec	1.981
Avg. Packet size	95.92 bytes
Bytes	118944
Avg. bytes/sec	190.01
Avg. MBit/sec	0.002

The average round trip time of the ping is 5.2 ms which the first and second ping requires a long time due to be forwarded to the controller.
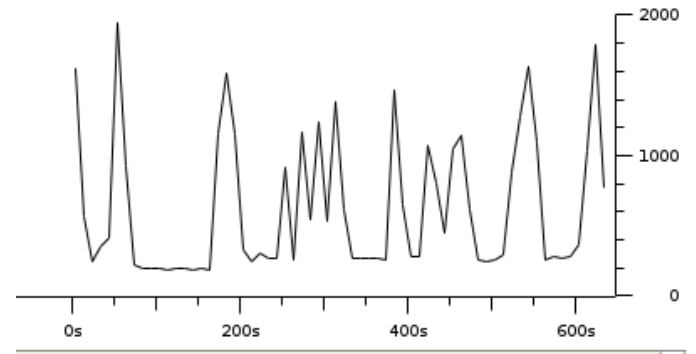

Fig. 4. Traffic Graph at Controller

At figure 4. showing the flow of network traffic that occurs on the controller which can be taken from the graph analysis that any particular interval of OpenFlow switch forwarding the data to the controller and check the appropriate rules on flow table that is programmed into the controller.
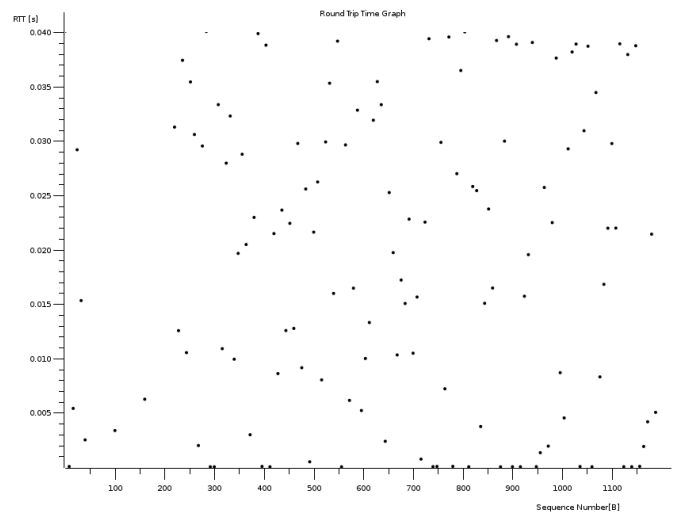

Fig. 5. Round Trip Time at Controller

Figure 5 is round trip time graph on loop back controller which, on the Y-axis is Round Trip Time (RTT) and the X

axis is sequence number. From the graph, it can be analyzed the delivered time for each packets are very fast with maximum RTT is 0.04 second.
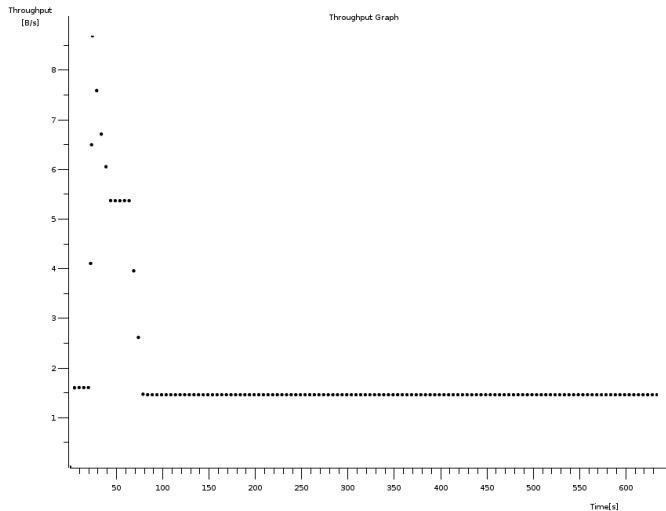

Fig. 6. Throughput at Controller

Figure 6 show the output results of throughput on wireshark which is on the X axis is the packet transmission time and the Y axis is the amount of throughput out in units of bits per second (bps). From the graph, we can see in the first 100 seconds when packet is delivered, there is increased throughput due to the exchange of information between the switch and the controller for the process of identifying and matching each packets sent by the rules that exist in the flow table on the controller. Once the package is sent according to the existing rules on the flow table controller, then the packets can be forwarded to the destination. And if the packets is not in accordance with the existing rules, then the packet will be dropped.

From the data Table VII. obtained delay from switch:

$$delay = \frac{Average\ RTT}{2} = \frac{5.207}{2} = 2.6\ \text{ms}$$

It also obtained throughput from switch values as follows :

$$Troughput = \frac{The\ amount\ of\ data\ sent}{time\ data\ delivery}$$
$$= \frac{118944\ byte\ x\ 8}{625.979\ sec} = 1520,1\ \text{bit/second}$$

VI. CONCLUSION

In this paper, we have presented design migration network to SDN and simulation of SDN performance. The simulation using Mininet. As a result from the simulation by using a network design Net2Plan, blocking traffic obtained at 0% which explains that the network is designed to be able to serve the needs of the service including at the time of use at peak hours. The simulation results obtained using mininet 2.6 ms delay and throughput 1520 bps.

REFERENCES

[1] Ediansyah, Pories, " Desain dan Implementasi Testbed OpenFlow ITB", Thesis Megister, 2013

[2] Jose Luiz Izquiarado, "Leveraging Net2Plan planning tool for networkorchestration in OpenDaylight", 978-14479-5196 3 14/ $31-00/ 2015.

[3] Net2Plan – The open-source network planner [Online]. Available: http://www.net2plan.com/ [Last accessed: April 2014]

[4] Marcel Caria," A performance Study of Networks Migration to SDN enabled Traffice Engineering, Globecom Communication QoS,Reliability and Modelling Symposium, 2013.

[5] Open Network Foundation, "Migration Tool and Metrics",Migration Working Group, ONF-TR 507.

[6] Open Network Foundation, "SDN Security Consideration in the Data Centre", ONF Solution Brief, October 2013.

[7] P. Pavon-Marino and J.L. Izquierdo-Zaragoza, "Net2Plan: An open-source network planning tool for bridging the gap between academia and industry," *IEEE Network*, in press.

[8] Rohit Mehra, "Is Your Enterprise Campus Network Ready for SDN? ",IDC #248956, June 2014.

[9] WenfengXiamYonggang Wen. Senior Member, IEEE, ChuanHengFoh, Senior Member, IEEE, DusitNiyanto, Member, IEEE, and HaiyongXie, Member, IEEE, " A Survey on Software-Defined Networking", IEEE Communication Surveys & Tutorial, VOL. 17, NO.1, First Quarter 2015

Network Migration to SDN
Using Pareto Optimal Resilience Controller (POCO):
Case Study in the UPI Network

[1)]Arif Indra Irawan, [2)]Maya Rahayu, [3)]Fidyatun Nisa, [4)]Nana Rachmana Syambas

School of Electrical&InformaticsEngineering
Institute Technology Bandung
Bandung, Indonesia
arif.indra.irawan@gmail.com, mayaaarahayu@yahoo.com, fidyatunnisa@gmail.com nana@stei.itb.ac.id

Abstract— **Campus is one of the environment that needs a good network connectivity because it has a lot of user and require a rapid information exchange on a large scale. To equal the increasing number for those necessaries, the network becomes more complex and complicated, so it is difficult to manage the complex network. SDN is presented to facilitate the process of network control by separating control plane and data plane to optimize the performance of a network. In this paper, we will discuss about the migration of campus network (study case UPI) to SDN network. The main focus of this paper is about best controller placement by using POCO Algorithm that have MATLAB framework. We use node to controller maximum latency and controller imbalance parameter as consideration to find best controller placement.**

Keywords—SDN, University Network, POCO, Pareto Optimal Resilience, Network Migration

I. INTRODUCTION

Campus is the environment that needs network connectivity with a good performance. It is because a lot of users in campus area need a rapid information exchange on a large scale to support education process at that campus. In fact, many campuses in Indonesia still have inadequate network performance that may obstruct the education process at those campuses. The problems of campus network are throughput problem, latency, the lack of network capacity, the difficulty of managing network on a large campus, etc. Various studies have been done to fix any problems on campus network, such as in paper [1] that discuss about planning system and analysis for distribution network to the university in China. Then, Hasson, Shawkat, et al [2] do research to increase the information sharing on Iraqi Universities network with e-government architecture using data warehouse technique.

Many solutions to optimize the network to serve the users. In addition, the large capacity and data transfer rate in a network become primary demand for users to use the network technology. One of the technologies is SDN. SDN is a new network paradigm that separate the control and forwarding plane, so SDN is expected to fix the network problems that increasingly complex. Various studies have been done to

optimize the network by using SDN, such as Hub Yunnan, et al [3] who optimize the reliability of the network using SDN, Armenia, et al [4] who make analysis about scalability of MAN network with hybrid traffic, and Affirm Salami, et al [5] who explain about SDN network optimization with a focus of controller placement problem.

In this paper, we will overcome the problem at one of campuses in Indonesia with a network migration planning from the existing network to SDN network. The main focus of this paper is about controller placement by using POCO algorithm. Pareto-Optimal Resilient Controller Placement (POCO) is a toolset on MATLAB to determine the controller placement based on network resilient and latency parameter [6]. This paper use UPI campus network.

II. EXISTING NETWORK OF UPI

A. Problems of UPI Network

UPI (Universitas Pendidikan Indonesia) is a campus located in West Java, which has a central campus in Bandung, and secondary campuses in many areas such as Tasikmalaya, Cibiru, Sumedang, Purwakarta, etc. ICT development at UPI began in 1990, and began the internal ICT management by Dir. TIK UPI in 2001. The recently of internal ICT development and the increasing of UPI users (students, lecturers, and employees) pop up the various network problems at UPI, such as [7] :

- Not yet available the mechanism for Quality of Service
- Not yet available the internal service level guarantee
- Not yet available the ticketing system for complaints
- Not yet available the procedure of installation-maintenance-repair-supporting device redundancies
- Not yet available the early warning system on the network disturbance
- The number of human resource available to manage the network is smaller than the covarage of network that need to serve
- Network capacity is always smaller than necessaries

- Utilization of ICT infrastructure is not optimal as its availability
- Become more complex-expensive–difficult to control
- The human resource is left by technology

B. Existing Network Topology of UPI

Based on the direct observation of Dir. TIK UPI, we acquired of the existing network topology as follows:
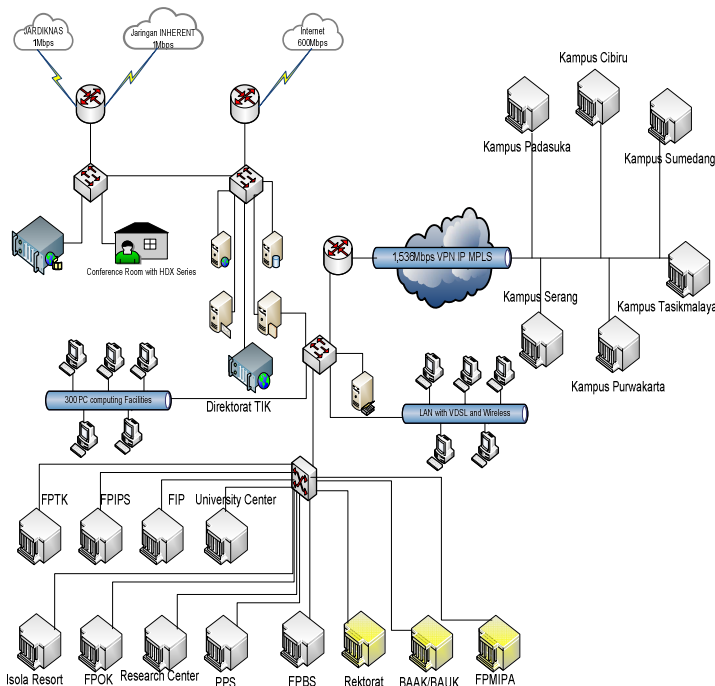

Fig. 1.   Network Topology of UPI [7]

Overall, UPI network consists of Core Layer, Distribution Layer, and Access Layer. Core layer in UPI is in Dir. TIK which has 600 Mbps bandwidth capacity providing by PT. Telkom and using two manageable Switches. Distribution layer include every faculties, units, and agency in UPI which is connected with Dir. TIK using fiber optic. Secondary UPI campuses in several areas are connected to Dir. TIK with VPN IP MPLS technology. Access layer in UPI provide access for fixed user and mobile user. Connection for fixed user use UTP cable which has 100 Mbps capacity, and for mobile user use Access Point (AP) which has 54 Mbps bandwidth capacity for each AP.

C. Data User of UPI Network

Here is the data user of UPI network at each Institutions/Unit/Faculty in 2015 depends on UPI Annual Report in 2014 [8] which used as the input for the node weight in POCO:

Table 1.   The number of user data UPI

No	Faculty/ Unit/ Institution	Number of user			Total
		Student	Lecturer	Employee	
1	FIP	3719	199	37	3955
2	FPIPS	3821	125	23	3969
3	FPBS	3221	213	28	3462
4	FPMIPA	3080	207	40	3327
5	FPTK	3131	167	39	3337
6	FPOK	2357	81	22	2460
7	SPS	3876		24	3900
8	University Center	-	-	±69	±69
9	Research Center	-	-	28	28
10	Rector Office	-	-	±24	±24
11	BAAK/BAUK	-	-	126	126
12	K. Cibiru	1146	37	25	1208
13	K. Sumedang	1006	25	14	1045
14	K.Purwakarta	807	28	12	847
15	K. Tasikmalaya	977	27	10	1014
16	K. Serang	983	26	8	1017
17	K. Padasuka	2357	81	22	±2460
18	Dir. TIK	-	-	53	53
19	ISOLA Resort	-	-	±100	±100
Total					±32401

III. POCO ALGORITHM

The *POCO* is a toolset that available in *MATLAB*. It is used to compute resilient Pareto-based optimal controller placement. It can used to find the best solution of all controller placements [6]. The best solutions according to the particular requirements can be selected from the possible placements. Usually, *POCO* gives no recommendation for a particular placement, but gives the set of Pareto-optimal placements. It enables the networks operators to choose which one is appropriate for their best need of placement. In particular, they also can choose how many controller failures should be covered by a resilient placement.

A. Program Structure

The *POCO*'s program structure contains functions as shown in Figure 1. The functions and scripts can be classified into four group such as : input, config, calculation, and output.

B. Graphical User Interface

POCO provides a Graphical User Interface (GUI) to make easily control, evaluate and illustrate its results.

C. POCO Capabilities

As an algorithm to fix controller placement and resilience problem, POCO has this following capabilities :
- Evaluation : *POCO* demonstrate the different evaluation methods about placement of a variable

number of controller for failure free scenario, controller outages, and node outages.

- Visualization : *POCO* shows the difference resilience issues. Several important placements can be selected quickly.
- Analysis : *POCO* can be used to analyze the difference placement options and to find the most adequate controller placement for any particular requirements
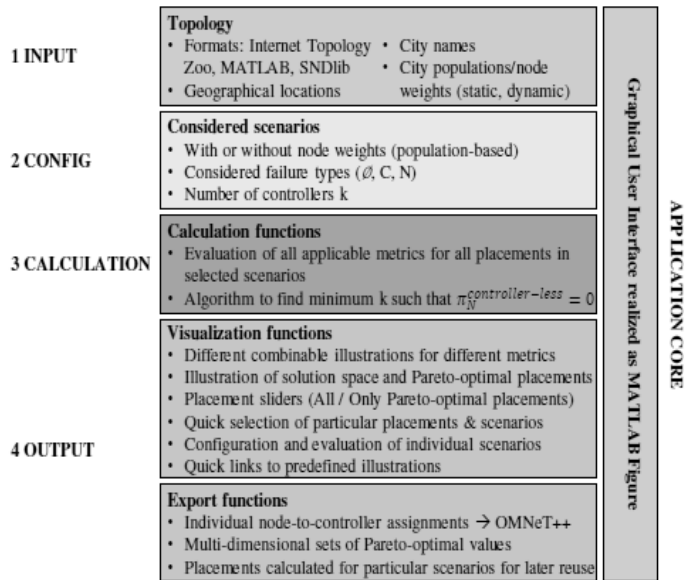

Fig. 2. Program Structure of POCO [6]

IV. RESEARCH SCHEME

A. Problem Formulation

From the various problems on UPI network, we focus to overcome for several problems as follows :

- Not available the mechanism of Quality of Service
- Not available the internal service level guarantee
- Become more complex –expensive – difficult to control

To overcome the problems above, based on paper by David Hock, et all [9], some of primary keys will be discussed in this paper are :

- Node to controller latency
- Controller Imbalance

B. Research Stage

Based on literature study from white paper NEC [10], these following are some steps for planning or designing NetworkVirtualization (NV) and SDN:

- Define NV and SDN

- Identify the primary opportunities for implementing NV and SDN
- Identify the key metrics
- Define the scope of possible solutions
- Evaluate NV and/or SDN solutions
- Test and certify solutions
- Integrate with the existing environment
- Educate the organization
- Evaluate professional services
- Eliminate organizational resistance
- Perform a POC
- Obtain management Buy-In

From the results of literature study above, we make the planning stage of research in this paper as follows:
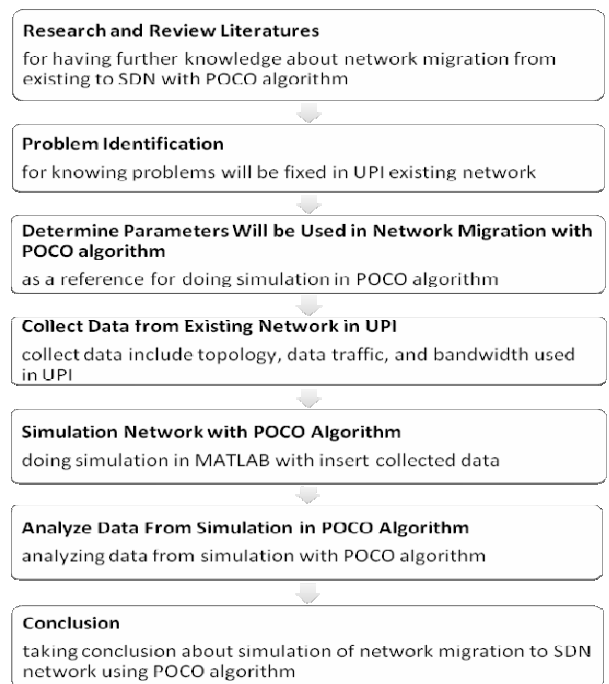

Fig. 3. Research Stage

V. DESIGN AND SIMULATION

For its network, UPI chooses star topology. This following is UPI topology which is being input to be simulated with POCO:
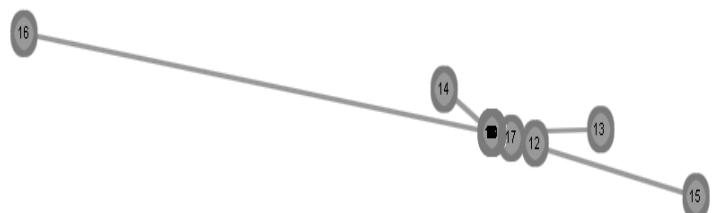

Fig. 4. Network Topology of UPI

According to the network problems which is mentioned above, it appears that the network infrastructure utility of UPI is not optimal. In some cases, the lack of electricity causes the device outage, as happened in FPBS FPOK and FPTK. We use 3 controllers for network SDN to anticipate the outage due to failure of the power source.

By using POCO, we try to find the best controller placement with k=3 as the number of controller we used. The result is in figure 6:
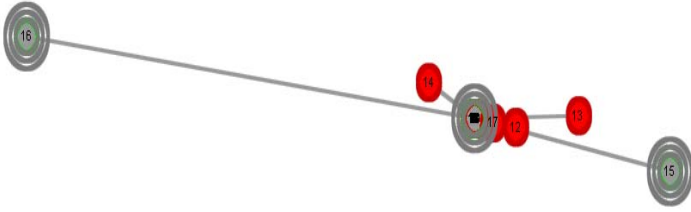

Fig. 5.   Node Heat Map of UPI Star Topology

Based on figure 5 that show controller-less nodes heat map, we can see that the red color indicates nodes in that topology has very bad latency and bad controller imbalance. For further information, the graph in figure 6 shows us tradeoff between maximum node to controller latency and controller imbalance in failure free case. And this is the graph result of that topology:
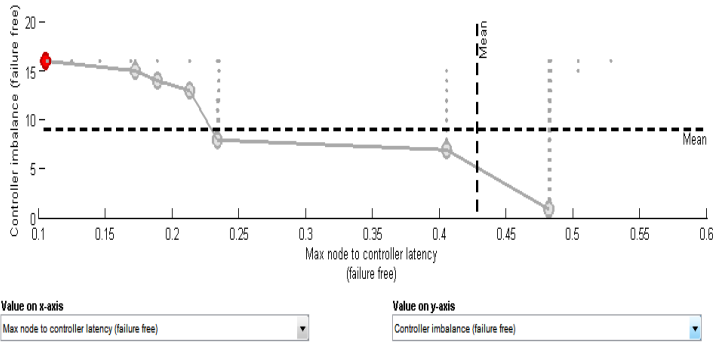

Fig. 6.   Trade Off Between Max Latency and Controller Imbalance in UPI Star Topology

Value in maximum node to controller latency (x axis) is based on percentage of diameter, $\pi_{\emptyset}^{\text{max latency}}$. Values in controller imbalance parameter (y axis) show the difference between maximum numbers of node that controller handle and minimum number of node that other controller handle, $\pi_{\emptyset}^{\text{imabalance}}$. The calculation for that value shown in this formulation below [11]:

$$\pi^{\text{max latency}}(\mathcal{P}) = \max_{(v \in \mathcal{V})} \min_{(p \in \mathcal{P})} d_{v,p} \quad (1)$$

$$\pi_{\emptyset}^{\text{imbalance}}(\mathcal{P}) = \max_{(p \in \mathcal{P})} n_p^{\emptyset} - \min_{(p \in \mathcal{P})} n_p^{\emptyset} \quad (2)$$

That graph show if that topology has very bad latency moreover in best placement controller depending on controller imbalance parameter.

Therefore, we created new topology to decrease max latency in UPI network in star topology. We made UPI half mesh topology based on UPI mesh topology. First, we choose failure free case with number of controller k=3, and concern in node to controller latency and controller imbalance parameter to find best controller placement. Although the infrastructure utility in UPI network is not optimal, the case outage device is rarely happened. So, we use failure free case to find best controller placement. This is the result of best placement from UPI mesh topology:
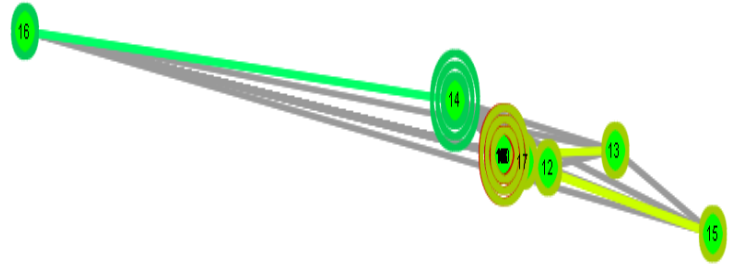

Fig. 7.   Best Controller Placement based on UPI Mesh Topology
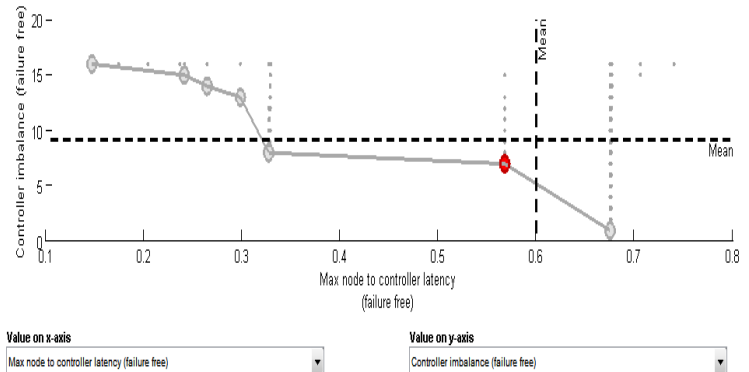
This is graph from that topology:

Fig. 8.   Graph from UPI Mesh Topology

In this trade off graph between maximum latency and controller imbalance, we choose the red node which near with mean value of maximum node to controller latency and controller imbalance parameter, so we can get best controller placement depending of both parameter. The result from that trade off, we found that the best controller placement is in node 1 (FIP Faculty), 5 (FPTK Faculty), and 14 (Purwakarta Secondary Campus).

For link efficiency purpose, we delete some edge which connected two nodes and both of those nodes not directly connected with the controller. After that, we get UPI half mesh topology which has good node to controller latency and good in controller imbalance parameter but has efficient edge number. Here it is UPI half mesh topology in figure 9 and UPI central campus topology in figure 10.
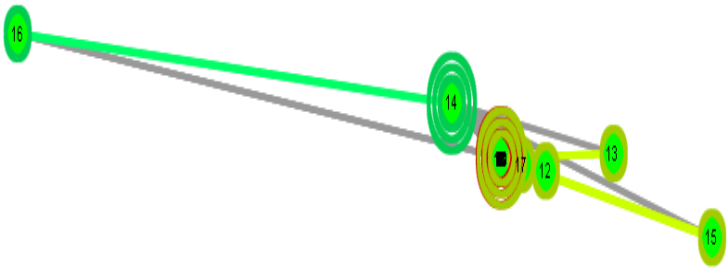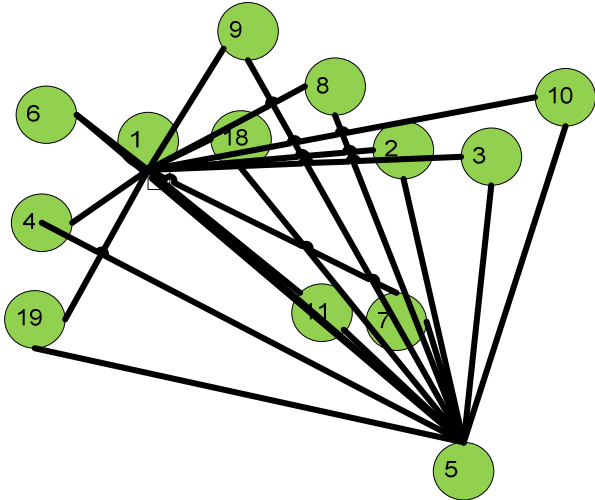
Fig. 9.   UPI Half Mesh Topology

Fig. 10. UPI Central Campus Topology

Figure 9 and 10 show that UPI half mesh topology has better result in latency and controller imbalance parameter indicated than UPI star topology but has more link efficiency than UPI mesh topology.

VI. ANALYSIS

By using POCO, we simulate some scenarios. The first scenario is free failure and the second is outage scenario.

1. Free failure scenario

Figure 11 shows us the graph of UPI half mesh topology based on node to controller and controller imbalance parameter. The circles are connected to each other as shown in the graph below shows the pareto optimal between the controller imbalance and node to controller latency. The more balanced the controller will increase the node to the controller latency. Placement controller design that we recommend is 1,5,14. From the graph, the placement controller will generate the balance of trade off between imbalance and node to controller latency. The value imbalance controller on the placement of the controller we recommend is 7, which means a big difference in the number of nodes is handled by the controller most and least at 7 nodes. The maximum latency nodes to controller have a value of 57 percent of the diameter UPI half mesh topology.
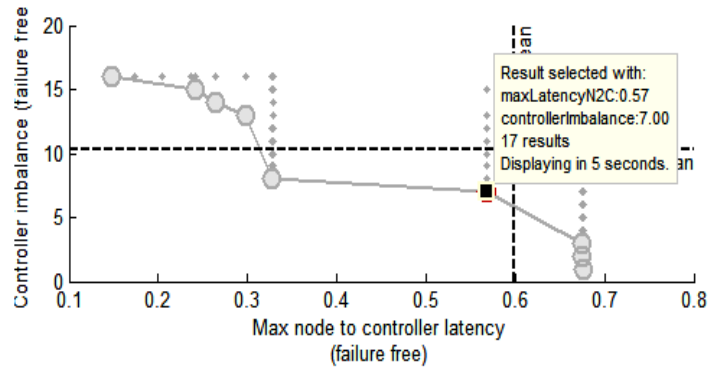

Fig. 11.   Trade Off Between Max Latency and Controller
Imbalance in UPI Half Mesh Topology

2. Outage scenario
   a. Up to k-1 controller failure case

Figure 12 show us, graph from half mesh topology based on max node to controller latency (up to k -1 controller failure) and max node to controller latency (failure case). The graph tell us, tradeoff between max latency node to controller latency (up to k-1 controller failure) and max node to controller (free failure case) still in the pareto optimal. The maximum latency node to controller (up to k-1 controller failure) is 66 percent of the diameter of UPI half mesh topology and maximum latency node to controller (free failure) is 59 percent of the diameter UPI half mesh topology. Figure 13, show us controller imbalance in the network SDN symbol on controller number 14 stated the controller imbalance have low value and the symbol is not obvious imbalance controller owned by controller number 1 or controller number 5.
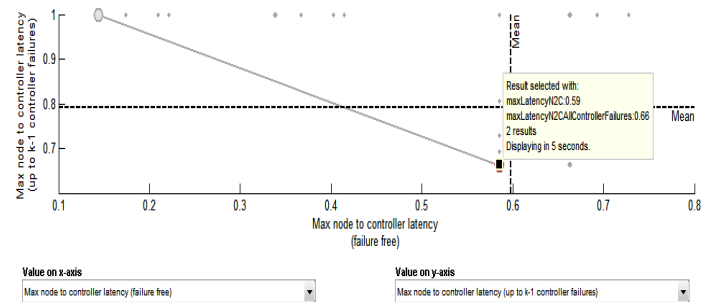

Fig. 12.   Trade Off Between Max to Node Controller Latency
0.66(up to k-1 controller failure) and Max to Node Controller in
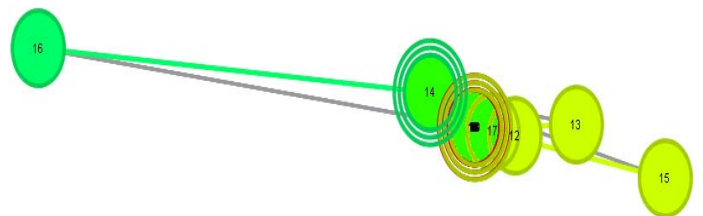UPI Half Mesh Topology

Fig. 13.   Controller imbalance up to k-1 controller failure

Figure 14 show us graph from UPI half mesh topology based on controller imbalance (up to k-1) and max to node controller (free failure case). The graph shows us the placement controller still in the pareto optimal. The value controller imbalance (up to k-1) is 15 and the maximum node to controller latency is 59 percent of the diameter UPI half mesh topology.
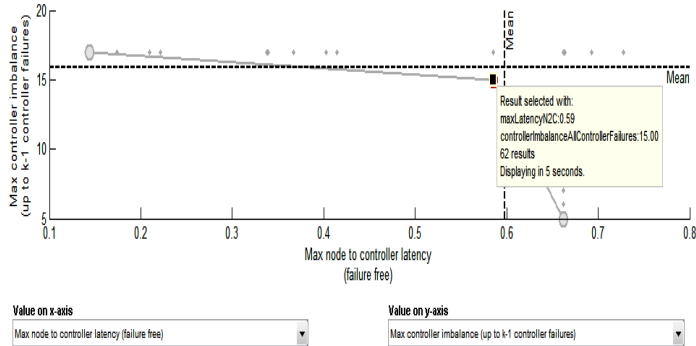

Fig. 14. Trade Off Between Max Controller Imbalance (up to k-1) controller failure and Max to Node Controller in UPI Half Mesh Topology

b. Up to 2 node failure
Figure 15 show us tradeoff controller less node up to two node failure and max node to controller latency. The controller less node up to node failure is zero and the nodes to controller have a value of 59 percent of the diameter UPI half mesh topology. The result show us, the placement controller not in pareto maximal if up to two node failure but all the remaining node is still connected to controller.
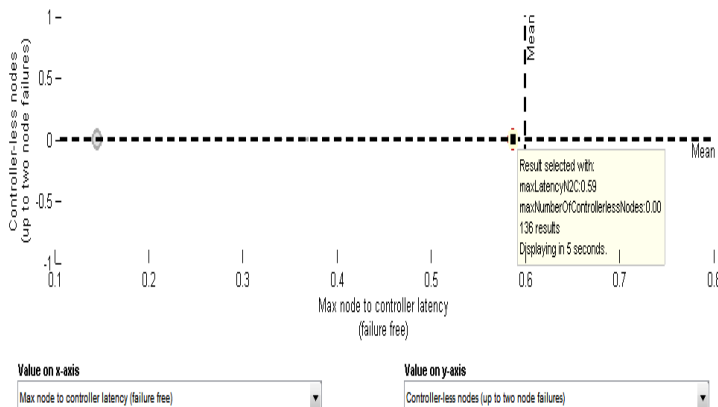

Fig. 15. Trade Off Between Max to Node Controller Latency (up to k-1 controller failure) and Max to Node Controller in UPI Half Mesh Topology

VII. CONCLUSION

Depend on our simulation with Pareto-Optimal Resilience Controller (POCO), we choose three best placement controller based on maximum node to controller latency and controller imbalance in UPI. We recommended to build half mesh topology because there is bad maximum node to controller latency in existing UPI network (star topology). The result form our simulation in POCO in free failure case, show maximum node to controller latency decrease to 57 percent of the diameter UPI half mesh topology. The value imbalance controller on the placement of the controller is 7.

In controller failure up to k-1 case, the result node to controller latency and controller imbalance still in pareto optimal. In up two node failure case, the controller less node up to node failure is zero and the node to controller have a value of 59 percent of the diameter UPI half mesh topology. From that result, POCO show us that best placement controller is in node 1 which represent Fakultas Ilmu Pendidikan (FIP) location, node 5 which represent Fakultas Pendidikan Teknologi Kejuruan (FPTK) location, and UPI Purwakarta secondary campus.

References

[1] Wei Tao, Su Jian, Liu Jun, Cui Yanyan, "Research and Development and Application of Distribution-Network Planning Calculation & Analysis System", Power System Technology (POWERCON), 2014 International Conference.

[2] Mohamed M.A, "E-Government Architecture Uses Data Warehouse Techniques to Increase Information Sharing in Iraqi Universities", E-Learning, E-Management and E-Services (IS3e), 2012 IEEE Symposium.

[3] Hu Yannan, Gong Xianyang, "On Reliability Optimized Controller Placement for SDN", Communications, China (Volume 11, Issue: 2), 2014.

[4] Rameina Veislari, Carla Raffaeli, "Scalability Analysis of SDN Controlled Optical Ring MAN with Hybrid Traffic", Communications (ICC), 2014 IEEE International Conference, Sydney, NSW, 2014.

[5] Afrim Sallahi, Marc St-Hilaire, "Optimal Model for the Controller Placement Problem in Software Defined Networks", Communications Letters, IEEE (Volume:19 , Issue: 1), 2015.

[6] David Hock, Steffen Gebert, Matthias Hartmann, Thomas Zinner, Phuoc Tran-Gia, "POCO-Framework for Pareto-Optimal Resilient Controller Placement in SDN-based Core Networks", Network Operations and Management Symposium (NOMS), 2014 IEEE.

[7] Munir, Holin Sulitstyo, Asep Wahyudin, Dedi Rohendi. (2010). Gerbang Teknologi Infrormasi dan Komunikasi. Bandung: UPI PRESS.

[8] Laporan Tahunan Universitas Pendidikan Indonesia Tahun 2014. Bandung, 2015.

[9] David Hock, Matthias Hartmann, Steffen Gebert, Thomas Zinner, Phuoc Tran-Gia, "POCO-PLC: Enabling Dynamic Pareto-Optimal Resilient Controller Placement in SDN Networks", Computer Communications Workshops (INFOCOM WKSHPS), 2014 IEEE Conference.

[10] Ashton, Metzler, & Associates. How to Plan for Network Virtualization and SDN. NEC : Loverage Technology & Talent for Success.

[11] David Hock, Matthias Hartmann, Steffen Gebert, Michael Jarchel, Thomas Zinner, Phuoc Tran-Gia, "Pareto-Optimal Resilient Controller Placement in SDN-based Core Networks", Proceedings of the 2013 25th International Teletraffic Congress (ITC), 2013.

FMCW-based SAR Transmitter for Remote Sensing Application and Its Characterization

Edwar and Achmad Munir

Radio Telecommunication and Microwave Laboratory
School of Electrical Engineering and Informatics, Institut Teknologi Bandung
Bandung, Indonesia
munir@ieee.org

Abstract—Remote sensing based on radar technology has been gaining popularity in last decade. The flexibility to be operated in both day and night is the main benefit of this remote sensing technology. Active remote sensing using synthetic aperture radar (SAR) is the one of technique to do the observation, and an aircraft is one of platform that has been used to be installed by the radar device. The development of FMCW-based SAR transmitter for Unmanned Aerial Vehicle (UAV) is the interest point focused in this paper. An UAV is a small aircraft that is operated remotely. The choice of components for SAR transmitter is considered to be as compact as possible so it could be installed in a UAV. The components such as chirp generator, Voltage Controlled Oscillator (VCO), mixer, combiner/splitter, and RF power amplifier have been selected with performance, size, and power consumption consideration. Each component has been characterized and then integrated each other as a system in 3 layers of 100mm x 100mm board.

Keywords—SAR; UAV; remote sensing; FMCW; transmitter front-ends

I. INTRODUCTION

Remote sensing is a science and art of obtaining information about an object, area, or phenomenon through the analysis of data acquired by a device that is not in contact with the object, area, or phenomenon under investigation [1]. The information of the target can be acquired by capture their electromagnetic wave emission and reflection. From the properties of the target's electromagnetic wave, like their wavelength, magnitude, and polarization, we could recognize the real physical characteristic of the target. Remote sensing is mostly use for earth observation purposes which the system does monitoring the environmental and climate phenomenon.

In remote sensing field, there are two techniques that are usually used to obtain information from the target; the first is passive remote sensing technique and the second is active remote sensing technique. In the passive technique, the device does not need to transmit the electromagnetic waves to detect the targets. They only use a receiver antenna to do the detection because the targets naturally emit the electromagnetic waves which bring the information of the targets property. The example application is the radiometry [2]. While the active technique need to transmit and receive the electromagnetic waves in their detection process. Their applications are like ocean and forest observation [2]-[3]. This paper focus is the design and measurement of the active remote sensing device using radar concept.

The using of radar for remote sensing purposes is not a new invention in remote sensing field. Radar is known as a part of a war device at first. But since the battle era was ended, the radar application started to be developed towards the wider purposes. In their development, radar devices have been working in various platforms, such as ground-based radar and airborne radar. Recently, radar also has been installed in an UAV (Unmanned Aerial Vehicle) [4]. For UAV radar, there are restrictions in developing the devices due to limitation of the vehicle physical size and their ability to lift the payload.

Meanwhile, radar application is often identified as a high power application because they consume so much power especially to generate the radar pulse. Generally, overall radar system is consists of signal generator, transmitter, duplexer, receiver, and controller [5]. This research focus is the radar transmitter, the part where the generated radar pulses will be carried to radio frequency, must be consists of high powered devices. In this research, the focus is directed to design the small radar transmitter system which also have small power consumption rate relatively for SAR application.

In this paper, the research idea and progress will be explained into four chapters, where the chapter 1 will explain about the background and the idea of this research, while the chapter 2 will explain about related theories to this research. Next in chapter 3, the implementation and measurement results will be presented, and the last, chapter 4, will conclude the entire this research activity.

II. OVERVIEW OF SAR AND UAV

A. Synthetic Aperture Radar

Radar is a way to detect the object by using electromagnetic signal in radio frequency range. It works by transmitting the electromagnetic signal and process the received signal which is reflected back to the radar receiver from the target. From that reflection signal we can extract any information about the target's characteristics.

Synthetic Aperture Radar (SAR) is a technique to get the better mapping resolution using radar device. The idea of this technique is to synthesize the real size of the antenna aperture by using the movement from small aperture antenna which the synthetic aperture technique will generate similar result with the real one. The SAR payload is mostly use in air-borne and space-borne radar system. Fig. 1 below describe how the airborne SAR works
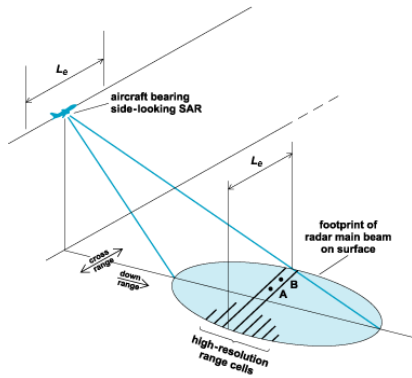
Fig. 1.   How synthetic aperture radar works [6]

Basically, from its configuration, radar is classified into 2 types, mono-static and bi-static radar, as shown in Fig. 2. This classification depends on the use of the transmitter and receiver antenna. If the radar uses same antenna for transmitting and receiving the signal, it means the radar using the mono-static configuration. However, if the transmitter antenna and receiver antenna are used separately to each other, then the radar is working in bi-static configuration.
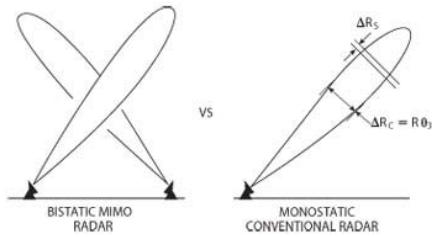

Fig. 2.   Bistatic vs monostatic radar [7]

In this paper, the radar waveform that is used is FMCW waveform. It means the transmitter will continuously emit the electromagnetic signal as long as the detection processes are running. So, to receive the reflected signal from the target, the radar uses another identical antenna with the transmitter ones. It is natural that every FMCW-radar has bi-static configuration. CW radar is the basic of FMCW radar where the block system is supposed to be illustrated in Fig. 3 [8]
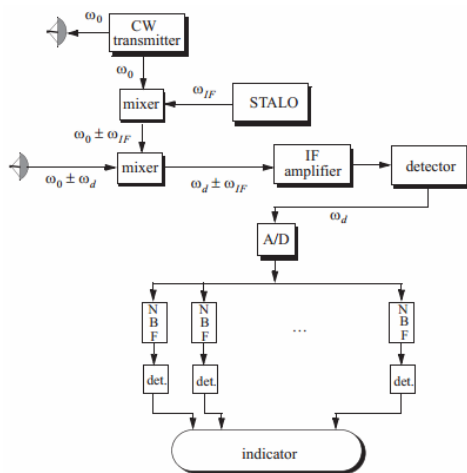

Fig. 3.   CW radar block system

Generally in radar transmitter system, there are few parts, like oscillator, mixer, and amplifier. In this research, those parts have been arranged into this transmitter block system in Fig. 4. An oscillator is a device who yields oscillation frequency. This oscillation frequency is usually used as carrier frequency in telecommunication system. This carrier signal which carries information signal, which in radar system is the chirp signal. While a mixer is a component in telecommunication device which join the information signal and the carrier signal. Further, an amplifier is used to increase the magnitude of the signal. The purpose of this amplifying process is to yield stronger signal which could be transmitted in far distance.
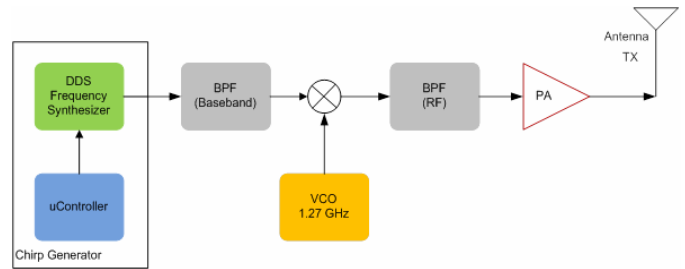
Fig. 4.   SAR Transmitter Block System

The digital chirp generator is used in this research. This is the result from previous research which DDS IC AD9850 is used to generate the FMCW signal. The DDS IC has been controlled by a single microcontroller.

B. *Unmanned Aerial Vehicle*

An UAV is an aircraft which has no man who drives in it. They are also known as drone. This aircraft is controlled remotely. UAV has many purposes, from military purposes (as spy aircraft) until for research and environment monitoring. The appearance of UAV can be seen in Fig. 5.

Fig. 5.   Unmanned aerial vehicle (UAV)

The use of UAV could save the cost if we want to do monitoring using airborne platform.

III.   CHARACTERIZATION AND DISCUSSION

A. *FMCW-based SAR Transmitter*

General design of FMCW radar has been described by Fig. 2. In this part, the FMCW-based SAR transmitter and its characterization will be explained. The diagram block of FMCW-based SAR transmitter is illustrated in Fig. 6.

Fig. 6. Block diagram of FMCW-based SAR transmitter

The FMCW waveform is generated by using digital technique. For the implementation, the system uses DDS (Direct Digital Synthesizer) IC, AD9850. The AD9850 has been chosen because its flexibility if user wants to change the produced frequency. To create the complex waveform, which consists of in-phase and quadrature waveform, the number AD9850 used is two, where the one to another has 90° degree phase difference.
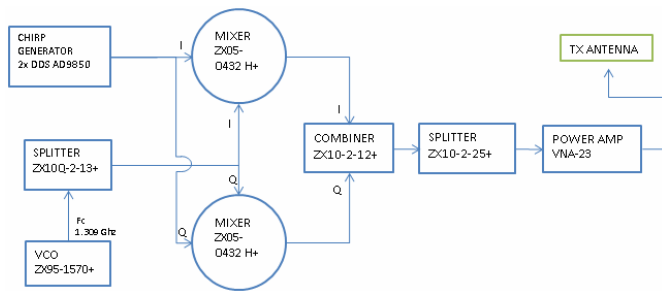
B. VCO Characterization

VCO (Voltage Control Oscillator) is used to generate the operation frequency in this FMCW radar. As determined as radar specification in Table 1, the VCO in this FMCW radar system will generate the carrier frequency of 1.27 GHz. The ZX95-1570+ from Minicircuit has been chosen as VCO in this research. Fig. 7 shows the appearance of the module.

Fig. 7. ZX95-1570+, VCO from Minicircuit [9]

The VCO module can be controlled from 1250 MHz to 1570 MHz. This module has 5V supply voltage. The characterization process of this module is shown in Fig. 8
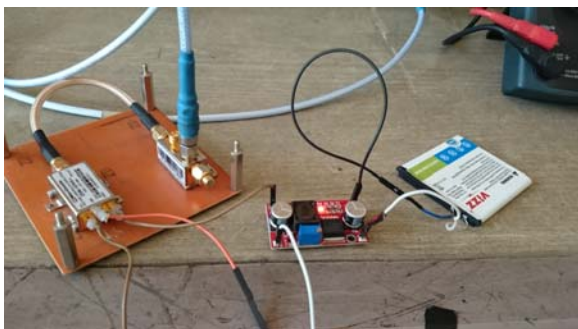
Fig. 8. Measurement process of ZX95-1570+

At Fig. 9, to control the output VCO output frequency, a DC-DC Step Up was used in the practice. The step-up module contains IC LM2577 which its power is supplied by using a single Li-Ion battery. The step-up output voltage has been set to around 6.37V to yield the wanted frequency value.
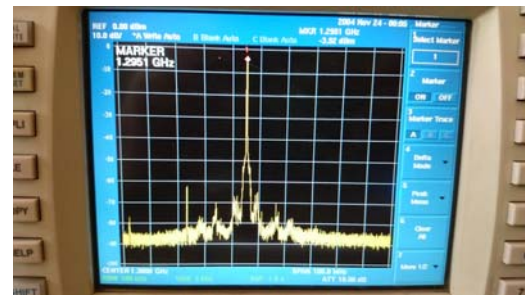
Fig. 9. Characterization result of ZX95-1570+

C. 2-Way 90° Splitter Characterization

The 90° difference splitter is needed to split the produced frequency from VCO into in-phase and quadrature modes, which will be mixed with DDS output signals. The splitter used is ZX10Q-2-13+ from Minicircuit as shown in Fig. 10.

Fig. 10. ZX10Q-2-13 2-way splitter [10]

This splitter module has been tested and measured. The characterization results are shown in Figs. 12 and 13 for port 1 and port 2, respectively.
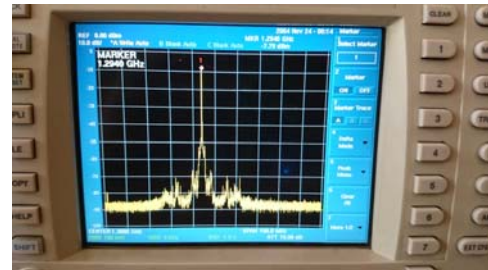
Fig. 11. Output of port 1
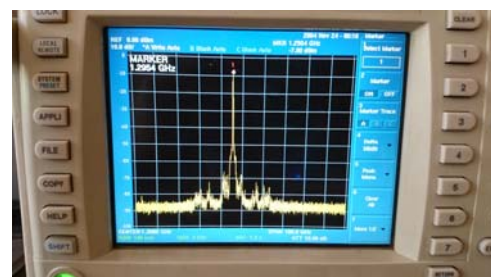
Fig. 12. Output of port 2

From the characterization results, there are a frequency discrepancy between port 1 and port 2, where it should not be different between each other. The port 1's output showed frequency of 1.240GHz, meanwhile port 2's output showed frequency of 1.254GHz. There is about 14MHz difference between these both ports.

D. Mixer Characterization

The Mixers are used to mix the both outputs from DDS IC and VCO. The ZX05-U432H+ from Minicircuit is chosen as mixer device in this system. The picture of mixer module is shown in Fig. 13.

Fig. 13. Mixer ZX05-U432H+ [11]

The mixer module has been tested for its performance. The inputs are from DDS IC and VCO. However, in measurement process, input from DDS IC has been changed into output from spectrum analyzer. The characterization results of mixer module are shown in Figs. 14 and 15 for In-phase and Quadrature, respectively.

Fig. 14. Output of In-phase mixer

Fig. 15. Output of Quadrature mixer

E. RF Power Amplifier Characterization

It is common if a radar signal need to be amplified. The main purpose of amplification process is to increase the range of detection. The RF power amplifier module used is VNA-23 as shown in Fig. 16. This module could amplify the signal up to 18 dB. The characterization result of RF power amplifier is shown in Fig. 17.
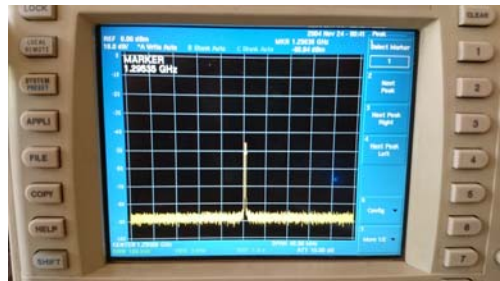

Fig. 16. An RF power amplifier VNA-23 [12]
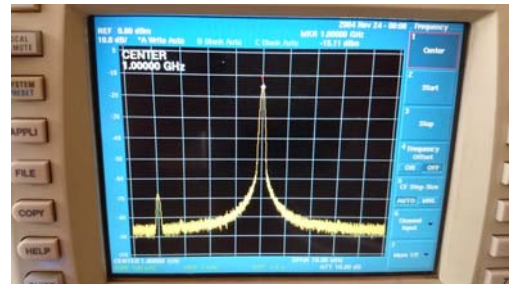
Fig. 17. VNA-23 RF power amplifier characterization at frequency of 1GHz

IV. CONCLUSION

The development of FMCW-based SAR transmitter has been demonstrated and characterized experimentally. The components of SAR transmitter such as VCO, mixer, combiner/splitter, and RF power amplifier, has been selected with less cost and relatively small in size. However, there was unwanted result at the 90° splitter output in which there is different result between their both output ports. Meanwhile the amplifier has gain value about 17dB. This value is enough to do monitoring using radar device which installed in an UAV.

REFERENCES

[1] M. Skolnik, *Radar Handbook*,3rd ed. McGrawHill, 2008.

[2] J. T. S. Sumantyo, "Development of circularly polarized synthetic aperture radar (cp-sar) onboard small satellite", PIERS Proceedings, Marrakesh, MOROCCO, March 20-23, 2011

[3] Kramer Herbert J.,Observation of The Earth and Its Environtment – Survey of Missions and Sensors, 4th Edition, Springer-Verlag, 2002

[4] Y. Yilong and S. Xuezheng, "The Synthetic Aperture Radar Transmitter Used In An Unmanned Vehicle", 3rd International Asia-Pacific Synthetic Aperture Radar (APSAR), 2011

[5] N. Yoshiaki, N. Hideo, O. Makoto, H. Mizutamari, N. Katsuhiko, and T. Kaoru, "Japanese Earth Resources Satellite-1 Synthetic Aperture Radar", Proceedings of IEEE, Vol. 79, No. 6, 1991

[6] http://www.geos.ed.ac.uk/homes/s0094539/CE757765FG0010.gif, accessed by October 2015

[7] http://www.microwavejournal.com/ext/resources/images/Figures/2013/1 M27/1M27F5x350.jpg, accessed by October 2015

[8] B. R. Mahafza, *Radar Systems Analysis and Design Using MATLAB*, 3rd ed., CRC Press, 2012

[9] ZX95-1570+ Datasheet

[10] ZX10Q-2-13 Datasheet

[11] ZX05-U432H+ Datasheet

[12] VNA-23 Datasheet

[13] Bowick Chris, RF Circuit Design, Newness, 1982

Implementation of Load Balancing and Automatic Failover for Application Internet Banking

Raka Yusuf
Computer Science Faculty
Mercubuana University
Indonesia
raka@mercubuana.ac.id

Abstract— **Nowadays application needs to always on and never get downtime. If your application has downtime, you will lose your business. Load balancing and automatic failover become the way that Bank XYZ choose to support their new application, Internet Banking. In the implementation they use the technology from F5 with their product BIG-IP LTM and BIG-IP GTM. Internet Banking in Bank XYZ can perform well and never get down time anymore because they have failover and balancing method for the traffic. After the implementation, Bank XYZ get 30% of improvement in page loading performance. They will get more if they can use more features from the device.**

Keywords—Load balancing; Automatic Failover; F5; Internet Banking

I. INTRODUCTION

Business development leads business application. When a company grows up, it must be ready to develop more in its application. The development is not only to adjust the application according to the business needs but also to make a reliable level of application availability. The availability become the most important things when your company already has a great business. The application needs to be ready all the time. There is no excuse for down time. Fulfillment is aimed at the high-availability network infrastructure and application systems. In addition, it is necessary also the redundancy of network devices and servers used, so that if something happens then the business does not stop because there is no back up. To maximize this, the devices used must have feature load sharing and automatic failover. Load sharing is used to help divide the existing traffic of applications on devices that are used so that the device is not burdened with the amount of traffic. While automatic failover is used when one server fails, it can automatically move to the next device without disrupting the activity of the applications used so as not to disrupt business.

Bank XYZ want to implement their new application named internet banking which is the new generation from the old one. They want to make the business grows up with this application. To fulfill their goals, they want to implement a device that have load sharing and automatic failover feature.

The process for making the infrastructure that can be work as above is starts with an assessment of the overall existing network devices to obtain preliminary data on the conditions that exist today. It will be the basis for laying and also the addition of devices that will support the desired goal.

The team observe the location found that in fact it has been using the technology that already had load sharing features in it. But its use is not maximized because the device is only one. In making load sharing, there are must be minimal two devices because they need to share the traffic. They will switch in taking the process of incoming traffic. There is not failover mechanism also because the devices is only one so if it is failed, the system will failed and the business will stop.

In addition, the team also found that the needs of the case study site in performing failover not only for their primary application is Internet banking but for other applications which can support the passage of the internet banking application.

II. THE THEORY

A. Load Balancing

Load balancing is an even division of processing work between two or more computers and/or CPUs, network links, storage devices or other devices, ultimately delivering faster service with higher efficiency. Load balancing is accomplished through software, hardware or both, and it often uses multiple servers that appear to be a single computer system (also known as computer clustering). Management of heavy Web traffic relies on load balancing, which is accomplished either by assigning each request from one or more websites to a separate server, or by balancing work between two servers with a third server, which is often programmed with varied scheduling algorithms to determine each server's work. Load balancing is usually combined with failover (the ability to switch to a backup server in case of failure) and/or data backup services.

System designers may want some servers or systems to share more of the workload than others. This is known as asymmetric loading. Large telecommunications companies and others with extensive internal or external networks may

use more sophisticated load balancing to shift network communications between paths and avoid network congestion. Results include improved network reliability and/or the avoidance of costly external network transit. [1]

B. Automatic Failover

Automatic failover is a resource that allows a system administrator to automatically switch data handling to a standby system in the event of system compromise. Here, automatic describes the failover process. By definition, most failover processes are programmed to operate automatically. Automatic failover is a best practice for systems that experience damage or lose vital connectivity during various scenarios, such as storms and natural disasters. Organizations may use automatic failover systems to protect against data loss in such situations, which are often referred to as disaster recovery plans or emergency planning. An automatic failover system allows for immediate off-site handling of database and server setups, ensuring seamless operations if an original system site is under attack by a storm or other disaster. [2]

C. Round Robin Algorithm

As name implies, it is simplest load balancing algorithm uses the time slicing mechanism. It works in the round trip where a time is divided into slices and is allotted to each node. Each node has to wait for their turn to perform their task. This algorithm has less complexity as compared to the other two algorithms. Open source simulation software knows as cloud analyst uses this algorithm as default algorithm in the simulation. This algorithm has less complexity as compared to the other two algorithms. This algorithm simply assigns the jobs in round robin fashion without considering the load on different machines. Though the algorithm is very simple, there is an additional load on the scheduler to decide the size of time slice and it has longer average waiting time, higher context switches higher turnaround time and low throughput. [3]

III. OVERVIEW OF PRODUCT AND SOLUTION

A load balancer is a device that acts as a reverse proxy and distributes network or application traffic across a number of servers. Load balancers are used to increase capacity (concurrent users) and reliability of applications. They improve the overall performance of applications by decreasing the burden on servers associated with managing and maintaining application and network sessions, as well as by performing application-specific tasks.

Load balancers are generally grouped into two categories: Layer 4 and Layer 7. Layer 4 load balancers act upon data found in network and transport layer protocols (IP, TCP, FTP, UDP). Layer 7 load balancers distribute requests based upon data found in application layer protocols such as HTTP.

Requests are received by both types of load balancers and they are distributed to a particular server based on a configured algorithm. Some industry standard algorithms are:
• Round robin
• Weighted round robin
• Least connections
• Least response time

Layer 7 load balancers can further distribute requests based on application specific data such as HTTP headers, cookies, or data within the application message itself, such as the value of a specific parameter.

Load balancers ensure reliability and availability by monitoring the "health" of applications and only sending requests to servers and applications that can respond in a timely manner. [4]

High availability refers to the ability of a BIG-IP® system to process network traffic successfully. The specific meaning of high availability differs depending on whether you have a single BIG-IP device or a redundant system configuration:
• Single device

When you are running the BIG-IP system as a single device (as opposed to a unit of a redundant system), high availability refers to core services being up and running on that device, and VLANs being able to send and receive traffic. For information on configuring a single device for high availability, see Configuring fail-safe. The remainder of this chapter is not applicable to systems configured as single devices.
• Redundant system configuration

When you are running the BIG-IP system as a unit of a redundant system configuration, high availability refers to core system services being up and running on one of the two BIG-IP systems in the configuration. High availability also refers to a connection being available between the BIG-IP system and a pool of routers, and VLANs on the system being able to send and receive traffic. For information on configuring a redundant system for high availability, see the remainder of this chapter.

A redundant system is a type of BIG-IP® system configuration that allows traffic processing to continue in the event that a BIG-IP system becomes unavailable. A BIG-IP redundant system consists of two identically-configured BIG-IP units. When an event occurs that prevents one of the BIG-IP units from processing network traffic, the peer unit in the redundant system immediately begins processing that traffic, and users experience no interruption in service. [5]

A. Infrastructure Design

Implementation is done by using the BIG-IP Local Traffic Manager. The device BIG-IP Local Traffic Manager is a network device that serves to organize and manage data traffic either towards or coming out of multiple device servers or networks. The device server or network can be a web server, cache servers, routers, firewalls and proxy servers. With the F5 LTM is the integrated application system is expected to be more reliable, higher value of high availability and reduce server load and bandwidth.

The main feature that will be implemented is Analytics (also called Application Visibility and Reporting). Analytics (also called Application Visibility and Reporting) is a module on BIG-IP ® system that you can use to analyze the performance of web applications. AVR provides detailed metrics such as transactions per second, client server and latency, response time and throughput, as well as sessions. You can view metrics for applications, virtual servers, pool,

URLs, and additional detailed statistics on traffic of applications running through the BIG-IP system.

Transaction Counter to the response code, user agent, HTTP methods, and IP address provide statistical analysis of traffic going through the system. With these AVR we can capture traffic for inspection and have the feature to send alerts so we can troubleshoot more easily.

Moreover, it will also feature implemented Global Traffic Manager (GTM). Global Traffic Manager (GTM) This increases the performance and availability of applications by directing the user to the data center nearest or best-performing data center. Using the high-performance features of DNS, BIG-IP GTM has a high level scalability and can secure DNS infrastructure from DDoS attacks, and provide real-time complete DNSSEC solution. GTM can be configured as a full-proxy and DNS server.
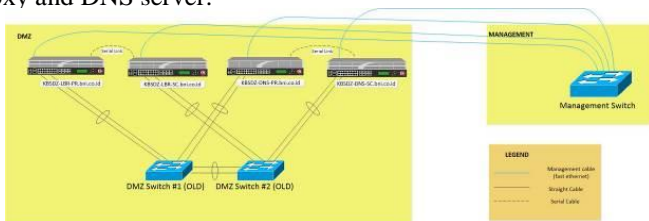

Figure 1. Infrastructure Design

Each server F5 BIG-IP LTM has an Ethernet connection to each switch DMZ as much as 2 pieces. The connections are made so that the total bandwidth Ether Channel obtained becomes large. Vlan in the DMZ switch that is configured VLAN tag (4, 101, 105, 109, and 140) were allocated to VLAN server. Additionally, both servers F5 BIG-IP LTM is configured active-standby so that if one of the servers F5 BIG-IP LTM impaired then the user can still access the virtual servers provided by F5 BIG-IP LTM is. As for F5 BIG-IP GTM is configured active-active, either the existing resource record in the Zone List, and PTR which is in Zone List, all will sync.

IV. THE CONFIGURATION

The basic configuration includes the hostname, Domain Name, Management IP Address and mask, Self IP Address VLAN External, Self IP Address VLAN Internal, Self IP Address VLAN new_ibank (application internet banking), Self IP Address VLAN synchronization, Self IP Address VLAN Management, DNS Servers, NTP Servers, Authentication Server.

A. Parameter Configuration Server for Load Balancing in F5 LTM

Parameter Configuration Server for Load Balancing in F5 LTM Virtual Server Host Name is the Pool Name, Host Port and Protocol, Load Balancing Pool and listening ports, and Load Balancing Method used is round robin.

B. High Availability Configuration in F5 LTM

Configuration is done by making access to the system menu and then to high availability by using an administrator account on both devices F5 LTM. Then from the menu, choose the vlan synchronization administrator that was created earlier. Configuration synchronization between the two devices F5 is done manually through the menu Device Management and then select the option to synchronize with a device that has been defined previously.
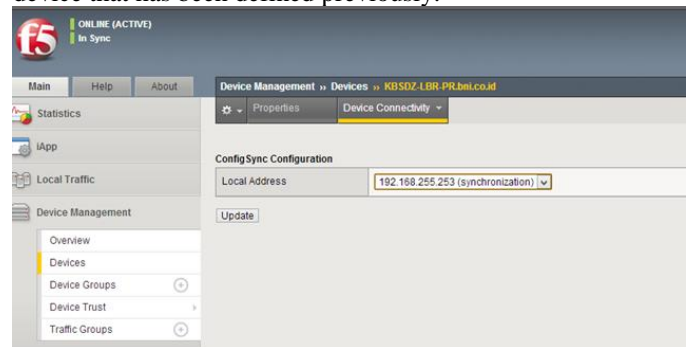
Figure 2. High Availability Configuration Part 1
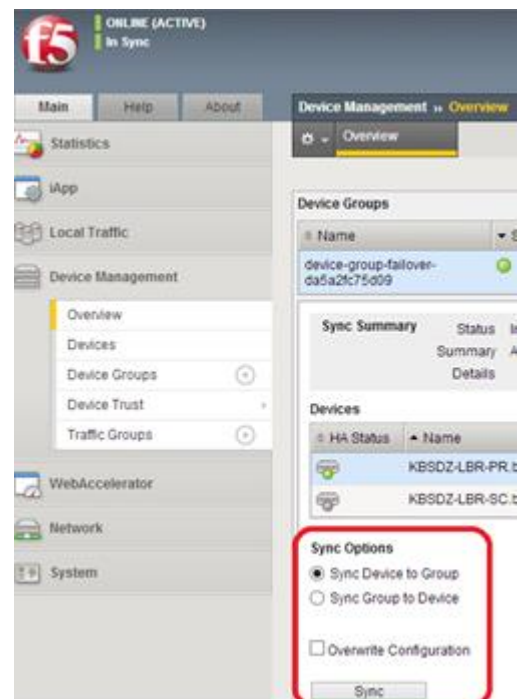
Figure 3. High Availability Configuration Part 2

C. Parameter Configuration Server in F5 GTM

Parameter configuration for F5 GTM are Host name, domain name, Management IP Address and mask, Self IP Address VLAN Listeners, NTP Servers, and Authentication Server. F5 BIG IP GTM used to have one piece of interface used to provide a link connection to the DMZ Switch DC BNI, also one piece interface for management needs to Switch Management DC BNI.

D. Active-Active Configuration in F5 GTM

In performing state active-active configuration for the two devices GTM F5, then the administrator needs access to the Certificate. After that put configuration as in Figure 4 for SSH.

Figure 4. Command Configuration through SSH

V. RESULT AND RECOMMENDATION

Result of the implementation is great because Bank XYZ can launch the new application, intenet banking well and it is already publish and being used by all of the customers. The response is faster than before and already has redudancy for the device.

System menu and Device Certificates. Next on the Secondary GTM do Renew Certificate via the menu System and Device

Figure 6 Traffic Flow

In Figure 6, we can see that the two web servers are being load balanced by BIG-IP LTM. Application and DB servers are clustered themselves and transaction between weband APP/DB servers are processed through switch (Bypassed F5).

It is also improves the performance of the access of the web application from the application. In F5 we called it web accelerator.

Figure 7. Capture before implementation

Figure 8 Capture after implementation

The test environment gets about 30% of improvement for page load performance. Contents analysis most of contents of web servers is java and CSS.. The features recommended to enhance more user experience are enable CSS Reordering, enable JavaScript Reordering, enable CSS Inlining, enable JAvaScript Inlining, and optimize image. And also implement more feature from F5 through the device.

References

[1]   https://www.techopedia.com/definition/4197/load-balancing

[2] https://www.techopedia.com/definition/27075/automatic-failover

[3] Ajit, M. M., & Vidya, M. G. (2013). VM Level Load Balancing in
     Cloud Environment. IEEE.

[4] https://f5.com/glossary/load-balancer

On Relay Selection in Cooperative Communications

Ferzia Firdousi

Department of Electrical Engineering
EME, National University of Sciences and Technology
Rawalpindi, Pakistan
ferziafirdousi@ceme.edu.pk

Abstract- **Cooperative relaying, or forwarding data on behalf of another node, saves energy. It is mostly used when the direct data transmission fails. It can form a perfect ad-hoc distributed network. Using a reservation based MAC protocol like TDMA delivers the system from control frames like RTS and CTS. Albeit being underrated, use of TDMA can result in energy conservation. Consequently we propose protocol formulating a cooperative relay using TDMA. Keeping in mind the need of modern wireless technology, the protocol will also be decentralized. Thus the paper presents a system which is autonomous and energy efficient; the nodes which decide to relay failed transmissions, do so on their own and not as a mandatory feat unlike previous cooperative systems. It also uses relays non-redundantly. The results achieved are compared to IrcMAC and C-TDMA and prove that a decentralized network though is difficult to design, can conserve energy more efficiently. Moreover, an improved SNR and throughput have been observed, with a moderate data rate of 5.5Mbps.**

Keywords-autonomous, cooperative, TDMA, relayTable, energy efficiency

I. INTRODUCTION

A large coverage area accommodates more users. Many of those users are placed far away from each other; so much so that they are not able to hear each other. In such a case, cooperative relaying can be used for forwarding the data packets between such users with the help of other nodes. These are called relay nodes. This forms the basis of ad-hoc networks as well.

It has been observed that there are generally three types of cooperative communications; cooperative diversity, cooperative MIMO and cooperative relaying. Cooperative diversity and MIMO increase the diversity gain because they forward data irrespective of the need for it or not. Contrastingly, cooperative relaying forwards data only in case of failure of data transmission via direct

link; thus diversity gain remains one [1], energy is conserved [2], and relay nodes are used efficiently. In most cases it is more beneficial than the other two methods.

Khalid et al [3] propose a cooperative relaying, IrcMAC, in which the source decides upon optimal relay for cooperation based on coherence time of the paths; whichever paths, direct or indirect, has less coherence time is chosen for cooperation. This protocol incurs a lot of overhead, and increases delay. The time taken to get the response from all the relays is large; an entire transmission path has to be decided before transmission can actually take place.

In [4], authors observe that two signals should be send to the destination. For this purpose a direct signal and an indirect signal are forwarded. The indirect signal is chosen by a bargaining game between source and all the relay nodes. Whichever relay node wins the game is used for forwarding data via a second (indirect) path. Thus destination receives two signals which are combined later. This forms an unwanted redundancy and results in energy wastage. On top, the delay encountered in choosing an optimal relay is also quite large.

In [5] the use of C-TDMA is suggested. For data transmission failure, all the other remaining nodes of the network relay the same data packet in their own time slots. Having received several data packets, destination can combine the signals via maximal ratio combining (MRC). This protocol makes efficient use of TDMA. Since all the other nodes relay data unnecessarily, this protocol fails to advocate efficient energy conservation. Even with the diversity gain being equal to the number of nodes, there is a lot of redundancy.

More often than not, it is assumed that the potential relay nodes are situated in between the

source and a destination and are always willing to cooperate. Most literature found in this regard patently assumes the same, which is an unfitting supposition to make. Protocol described in [6] denies this fact by claiming that only one parameter cannot determine the optimal relay for any given transmission. Further proving this point, the paper has used distance, SNR, and throughput to determine the optimal relay in cooperative system.

The main ideas extracted from the reviews include:

- Mostly relays are used redundantly.
- Using more than one relays increases overhead energy wastage considerably [7].
- Contention-based MAC uses up a lot of energy [8] as compared to reservation-based MAC.
- Relays, by design, do not lie between the source and destination.
- An autonomous system is needed to fully utilize properties of the distributed network [9].

Thus the idea developed and proved in this paper with the help of simulations in Matlab is that a potential relay is the one which is in hearing distance from both source and destination. This makes it self-reliant when relaying a packet. In simple words, only those nodes which lie between the source and destination and are able to receive data from both are good enough to forward a packet to the destination. This concept is very essential in a distributed and decentralized system and is explained in detail later.

In a decentralized system, no nodes are controlled by any other nodes like in other centralized and distributed systems [10]. They don't usually communicate with each other except for broadcast of data packets for transmission. Therefore no nodes have any idea whether other nodes are capable of relaying or not. Although, this provides a perfect ground for a decentralized system, this is also very difficult to design a cooperative system in it. Furthermore, BER, SNR and throughput are used for justification of a potential relay node. The protocol is called decentralized TDMA, and is compared to IrcMAC and C-TDMA.

The rest of the paper is laid out as follows: system preliminaries are described in the section II, followed by a description of the proposed protocol in section III, section IV describes the simulation and analysis and conclusion is presented in section V.

II. SYSTEM PRELIMINARIES

A. Hello packets:

In order to confirm whether a node is within hearing distance of other nodes (source and/or destination), it needs to have received a data packet from that node beforehand. This criterion is fulfilled by HELLO packets. These are regularly sent out by each node to discover other and vice versa [11]. They are transmitted at the data rate of 5.5Mbps which is standard data rate for our protocol. This offers a transmission range of approximately 50m. Therefore any nodes lying in this range of a certain node will receive its HELLO packet and update their relayTables.

This is necessary for later autonomously deciding whether a node is a potential relay or not. At the failure of a signal transmission, every node which previously received HELLO packets from both the source and the destination, considers itself to be a potential relay. Thus autonomy is maintained and delay is reduced.

B. RelayTable:

Each node maintains a comprehensive table, denoted as the *relayTable*. The purpose for creating it is to keep a record of data/hello packets received from other nodes. The columns in this table are shown in Table 1 where the first column is a list of all the nodes surrounding the concerned node. The second and third column defines the distance, as calculated by RSSI (explained in later sections) for these nodes. The fourth column represents the time slot assigned.

Table 1: relayTable stored by each node

Address of nodes	Distance from nodes	RSSI received from nodes	Time slot occupied by the source nodes

III. PROPOSED PROTOCOL

Channel slots are allocated to nodes with the help of the TDMA protocol. Fig. 1 shows flow of the proposed protocol. Channel allocation is followed by hello packet transmission which helps in updation of relayTables before data is transmitted. Once the data transmission starts, each node keeps hearing to see if they can receive the data that is broadcasted. After successful data transmission, ACK is send back to the source node from the destination node. Nodes which hear the data transmission also keep a tab of the ACK broadcast.
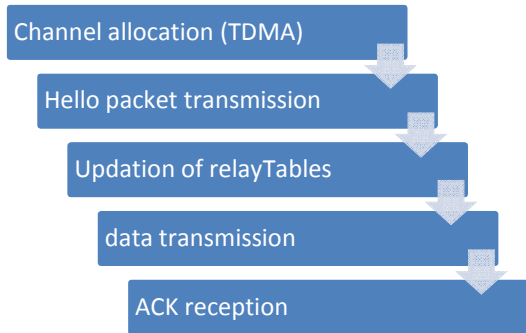
Figure 1: Proposed Protocol

Figure 2: Protocol to be followed in case of data transmission failure

In case of failure in data delivery between two nodes during transmission, i.e. no reception of ACK, cooperative relaying is used as is described by the Fig. 2. A potential relay needs to be found, but since the system is self-reliant, this task has to be done by the all the nodes themselves.

In order to understand which nodes are potential relays, it is necessary to understand the placement of nodes in a network. A node gathers information about the placement of the source and destination acquired through HELLO packets. As shown in Fig. 3, the third node has information regarding source node alone acquired by reception of a HELLO packet from source alone. Conventionally, in case of data packet failure, it should wait for an ACK from destination. But since it never received a HELLO packet from destination, so even in case of no ACK reception, it will not consider itself a potential relay and discard the data packet.

As a result of the previous argument, one might think that a node placed somewhere in the middle of source and destination may be good enough for relay transmission. Fig. 4 proves this wrong by showing that a node placed somewhere in the middle of source and destination, still may not be a potential relay if it is out of the listening range of source and destination i.e. if it is still does not receive a HELLO packet.

In conclusion, as shown in Fig. 5, only a node placed between source and destination and which is in listening distance to either of them, will receive a HELLO packet from both. This way it can consider itself to be a potential relay node when cooperative transmission is needed. It can also safely be conceived that such a node will autonomously relay failed data to the desired destination in case of transmission failure because it will hear a data transmission but no ACK reception. Thus an autonomous and decentralized system is made. Relaying from a node takes place during the time slot allocated to it.
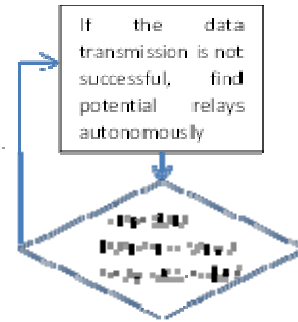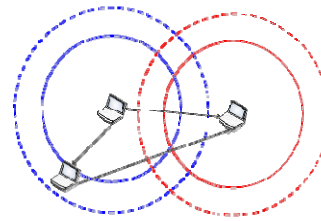

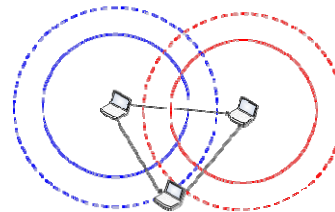Figure 3: Scenario 1: Relay node is placed to the left of source node

Figure 4: Scenario 2: Relay node is placed between source and destination but cannot receive HELLO packets from either one
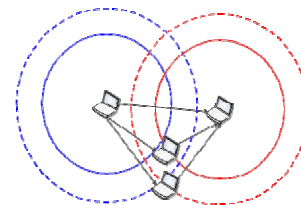

Figure 5: Scenario 3: Relay node is placed between source and destination, and receives a HELLO packet from both

IV. SIMULATION AND ANALYSIS

In this section, we develop analytical models for IrcMAC, C-TDMA and our decentralized MAC protocol in terms of network throughput, SNR and delay. For simulation purposes an area of 100m x 100m is selected and 16 nodes are randomly placed in it as illustrated by Fig. 6. The input data used for the calculation of SNR, BER and throughput is summarized in Table 2.
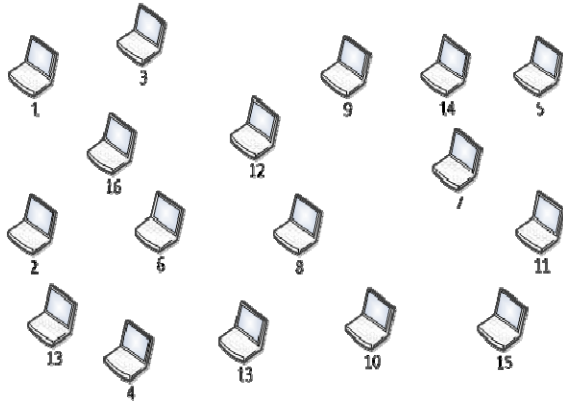
Figure 6: A network layout showing nodes placed randomly

In order to derive the throughput of decentralized TDMA, we have considered only 16 nodes with a channel divided into 16 time slots. for all the 16 nodes, a signal is forwarded and BER, SNR and throughput are calculated. With n as path loss exponent, R as the transmission rate, N_o as noise power spectral density, d as the distance, P_t as the transmitted power, P_r representing the received power and A as the constant of proportionality, SNR is calculated by (2) and maximum throughput is given by (3).

$$SNR = \frac{AP_t}{N_o R d^n} \qquad (2)$$

$$Throughput_{max} = R * \log_2(1 + \frac{P_r}{N_o R}) \qquad (3)$$

Table 2. Summary of input data values

Transmitted Power	22mW
Data rate	5.5Mbps
Spectral Noise density	$1x10^{-9}$

Fig. 7 compares saturation throughput as a function of source to destination distance. For distances of less than 50 m, the source-destination overlapping area is large and hence encompasses larger number of potential relay nodes for transmission.
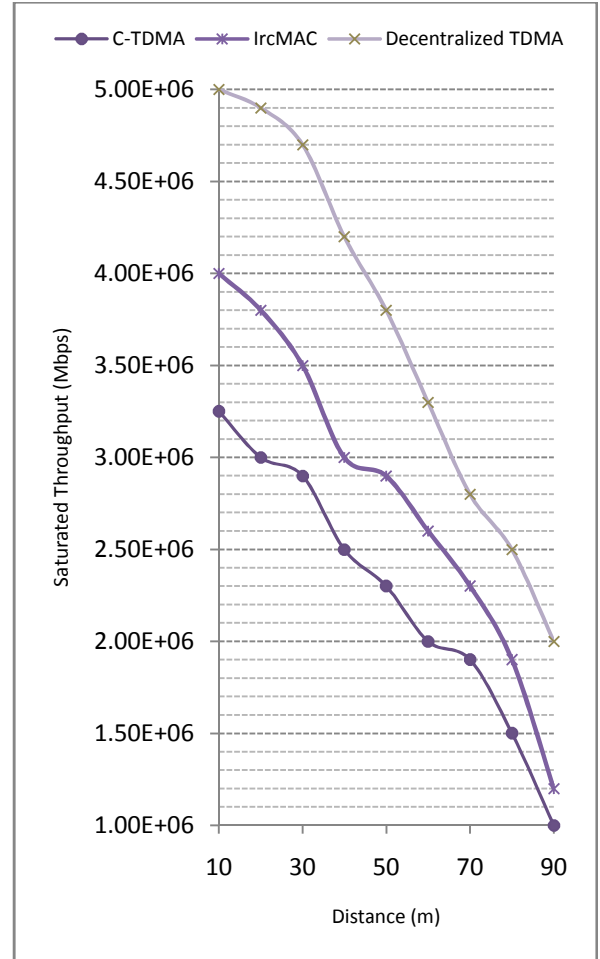

Figure 7: Saturated Throughput versus Distance

In case of data failure for one node, C-TDMA waits for an entire channel frame to forward that data packet from all of the remaining nodes (relays) and as a result throughput decreases because not all of the nodes will be able to relay effectively. It becomes easier for IrcMAC because it already has information about direct and indirect paths, and knows which relay node to use. But as the distance between source and destination increases, even relay nodes become difficult to use and overall throughput for IrcMAC starts to fall. Decentralized TDMA yields an excellent throughput since it not controlled by source. Relaying is only used when needed i.e. when transmission via direct link fails. The overall throughput of decentralized TDMA stays high. And the nodes which relay the data are autonomous.

BER is shown as a function of distance in Fig 8. Overall BER is lesser for decentralized TDMA. Although IrcMAC uses only a direct or indirect link for transmission, but for an indirect path chosen for distances above 50m, the coherence time is still large

enough to incur a large BER. C-TDMA yields the worst result since it keeps relaying data, irrespective of the fact whether any of relayed packets are helping in decreasing the BER or not.
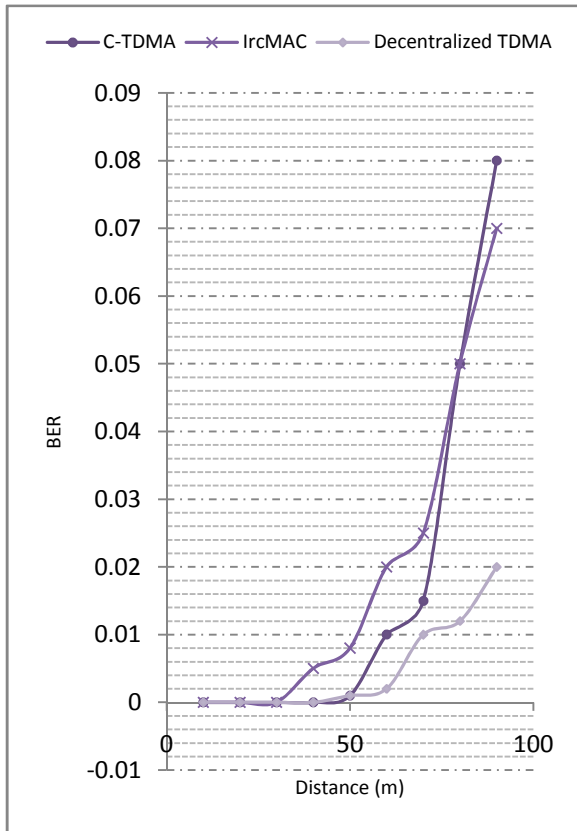

Figure 8: BER versus Distance

Fig. 9 shows the delay as a function of distance. Undoubtedly, the delay encountered in decentralized TDMA is the least. IrcMAC and C-TDMA yield a large delay because in C-TDMA, when relaying data packets and entire channel frame duration is used and IrcMAC waits for a transmission path to be decided upon and setup at the start of transmission which puts delay at the very beginning of the transmission.

Overall, the protocol devised in this paper not only acts autonomously, it also does not have to wait for a command from source node; all nodes have equal power and freedom to relay or not to relay. This way the delay decreases. Throughput increases because the relayed signal travels only through a better indirect path than the one used before. No RTS/CTS are used which means energy is highly conserved and SNR is also improved for the new path chosen.
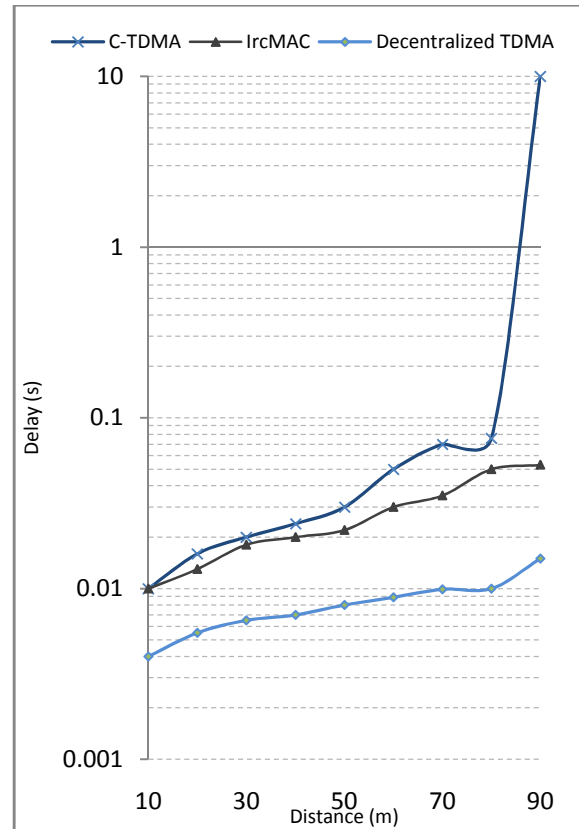

Figure 9: Delay versus Distance

V. CONCLUSION

The paper concentrates on making a cooperative relaying protocol to suit the decentralized and distributed nature of today's modern wireless system. TDMA is used since it suits the network's cooperative need to conserve energy. The protocol specifically focuses on the fact that to make a decentralized network it was necessary to limit the placement of nodes so only that each node that fulfills the criteria of being a potential relay is consequently considered a one. The technique also fulfills the need for a system's robustness because no nodes, potential or not, has any way of informing the other nodes about this.

The results obtained prove that the throughput of the nodes which were potential relays were close to the data rate requirements. Moreover, implementation of the protocol allows a network to be formed where two nodes which were communicating did not need to be within each other's hearing range. Hence a large coverage area is also formed without using more power and energy than before. The results also help in situating TDMA as yet another strong suitor for a cooperative MAC protocol.

REFERENCES

[1] Helmut Adam, Wilfried Elmenreich, Christian Bettstetter, Sidi Mohammed Senouci, "CoRe-MAC: A MAC-Protocol for CooperativeRelaying in Wireless Networks", Global Telecommunications Conference, 2009. GLOBECOM 2009. IEEE, Nov. 30 2009-Dec. 4 2009, Page(s) 1 - 6

[2] Giuseppe Anastasi, Marco Conti, Mario Di Francesco, Andrea Passarella, "Energy Conservation in Wireless Sensor Networks: a Survey", Ad Hoc Networks, volume 7, May 2009, Pages 537–568, doi:10.1016/j.adhoc.2008.06.003

[3] Murad Khalid, Yufeng Wang, Ismail Butun, Hyung-jin Kim, In-ho Ra and Ravi Sankar, "Coherence time-based cooperative MAC protocol for wireless ad hoc networks", EURASIP Journal on Wireless Communications and Networking 2011, 2011:3

[4] Beibei Wang, Zhu Han, K.J. Ray Liu, "Distributed Relay Selection and Power Control or Multiuser Cooperative Communication Networks Using Stackelberg Game", IEEE TRANSACTIONS ON MOBILE COMPUTING, VOL. 8, NO. 7, JULY 2009

[5] Zhuo Yang, Yu-Dong Yao, Xiaochen Li, Di Zheng, "A TDMA-Based MAC Protocol with Cooperative Diversity", IEEE COMMUNICATIONS LETTERS, VOL. 14, NO. 6, JUNE 2010

[6] Md. Rasel Rana, Md. Faruque Hossain, Md. Kamrul Hasan, Md. Uzzal Hossain, Md. Obaidur Rahman, "Distance-Aware Reliable Relay Selection Provisioning in Wireless Cooperative MAC Protocol", Strategic Technology (IFOST), 2014 9th International Forum on, 21-23 Oct. 2014, Page(s): 156 - 160

[7] Virag Shah, Neelesh B. Mehta, Raymond Yim, "The Relay Selection and Transmission Trade-off in Cooperative Communication Systems", Wireless Communications, IEEE Transactions on , June 2010, (Volume:9), Page(s):2505 – 2515

[8] Wei Ye, John Heidemann, Deborah Estrin, "An Energy-Efficient MAC Protocol for Wireless Sensor Networks", I NFOCOM 2002. Twenty-First Annual Joint Conferences of the IEEE Computer and Communications Societies. Proceedings. IEEE , 2002, Page(s): 1567 - 1576 vol.3

[9] Damien Magoni, Jean Jacques Pansiot, "Analysis of the Autonomous System Network Topology", ACM SIGCOMM Computer Communication Review (Impact Factor: 1.12). 07/2001; 31(3):26-37. DOI: 10.1145/505659.505663

[10] Chisa Takano, Masaki Aida, "Stability and Adaptability of Autonomous Decentralized Flow Control in High-Speed Networks", IEICE Transactions Communications, Volume E86-B, No. 10, October 2003, Pages: 2882-2890

[11] Beakcheol Jang, Jun Bum Lim, Mihail L. Sichitiu, "An asynchronous scheduled MAC protocol for wireless sensor networks", Mobile Ad Hoc and Sensor Systems, 2008. MASS 2008. 5th IEEE International Conference on, Date of Conference: Sept. 29 2008-Oct. 2 2008, Page(s): 434 – 441

Design of Microstrip Antenna based on Different Material Properties

Anis Nabihah Ibrahim[1], Rozlan Alias[1,2,a]

[1] *Faculty of Electric and Electronic Engineering, Universiti Tun Hussein Onn Malaysia, 86400 Batu Pahat, Johor, Malaysia*

[a]*rozlan@uthm.edu.my*

Keyword: Microstrip, substrate,

Abstract. This paper describes different substrate used in design the microstrip antenna which will be operating in WLAN. Two type of substrate investigate in this paper which is FR4 and Roger4350. The frequency chosen for the microstrip antenna is 2.4GHz and it has been chosen from IEEE 802.11 which is for the Wireless Fidelity (WiFi) network.

Introduction

An antenna can be defined as a transducer that can transmit or receive electromagnetic waves. Antennas also can be viewed as deviced that convert between circuit power and radiated power carried in a electromagnetic wave. Antenna are usually reciprocal device, as they have the same radiation characteristics for receiving transmiting [1].

Microstrip patch antenna in recent years emerged a lot in different field of communication such as mobile communication, satellites, wireless local area networks etc. Many techniques have been implemented by researchers like cutting slots, different patchs shapes and notch are used [2].

Previous researches have shown that microstrip patch antennas have number of advantage such as low profile, easy to fabricate and comformability to mounting hosts also size, return loss reaction and bandwidth enhancement and impedance matching are major design consideration for applications of microstrip antennas. Microstrip antenna consists of very small conducting patch which is built on a ground plane separated by dielectric substrate. The patch is generally made of conducting material like copper that can be any possible shape [3].

In this paper, the aim is to investigated the comparison between microstrip feeding technique for two different substrate using specific frequency 2.4GHz has been designed and simulated using CST software and using experiment method to compare performance of each substrate.

Antenna Configuration and Design

This antenna allows the operation of the Wireless Local Area Network (WLAN) at the frequency of 2.4GHz. The typical shapes of the patch antenna are circular, ellipse [4],[5] and rectangular [6],[7]. This project will design the rectangular shape of the microstrip antenna with the microstrip feed line. This antenna prototype has a simple structure feed by 50Ω microstrip line. Figure 1 show the dimension the purpose antenna used for simulated and experiment study. The substrates for the design is FR4 and Roger4350 which has dielectric constant of 4.4, 3.66 and height of substrate (h) is 1.6mm and 1.525mm. The dimension of propose antenna demonstrate in figure 1. CST 14.5 package is used to obtain return loss, impedance, and radiation pattern. Table 1 illustrate detail dimension for both substrate.
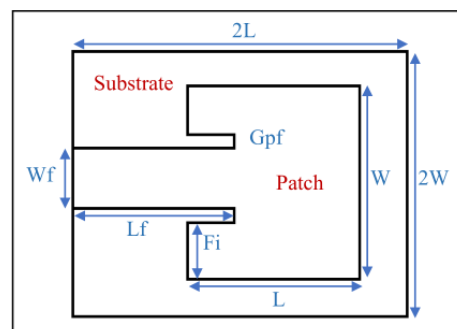

Figure 1: Microstrip antenna design

Where
W   = Width of patch.
L   = Length of patch.
Wf   = Width of feed.
Lf   = Length of feed.
Gpf   = Gap between patch and feed.
Mt   = Thickness of the copper layer on dielectric substrate
Fi   = Inset-fed length.

Table 1: Dimension of Substrate

Type of Substrate	Length (mm)	Width (mm)
FR4	29.44	38.04
Roger 4350	33.05	41.75

Result and Discussion

Discussion is focused on exploring the antenna performance by different material properties of substrate. A comparative analysis is presented by using both the physically existing and the theoretical substrates. In the upcoming sections, detailed insights on both geometric and materialistic effects on antenna performance are discussed.

Return Loss. The proposed antenna is simulated and measure using different substrate namely, FR4 and Roger4350. Figure 2 show the return loss for FR4 using simulation and measurement method.

Based on Figure 2, the return loss for Flame Retardant 4 (FR4) substrate is about -27dB while the return loss for Roger4350 is about -37dB. Based on the simulation result in Figure 2, it shows that the Roger4350 substrate have a better performance in return loss because the value is more that -10dB. Besides that, the operating frequency is 2.4GHz for both of the substrates. Figure 4.28 shows the comparison between the measurement result of return loss for Flame Retardant 4 (FR4) substrate and Roger4350 substrate.
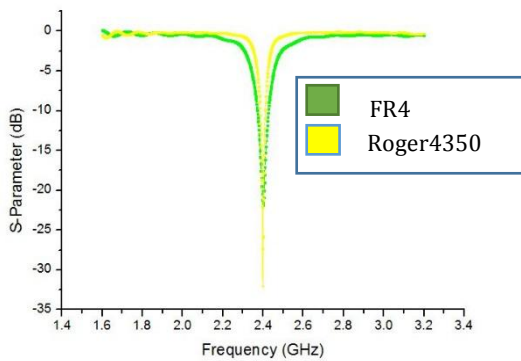

Figure 2: Return Loss Comparison for different substrate using simulation

Figure 3 show the comparison of return loss of the purposed antenna for Roger4350 using simulation and measurement method. Based on 3, it shows that the result for Flame Retardant 4 (FR4) have a good performance in return loss value which is about -37.32dB while for the Roger4350 is -16.34dB. The resonance frequency for simulation result for both materials is 2.4GHz while the measurement result for Flame Retardant 4 (FR4) substrate is 2.46GHz and the measurement result for Roger4350 substrate is 2.418GHz. The value of return loss shows the big differences where the value for Flame Retardant 4 (FR4) substrate was

increase from -23dB to -37.32dB while for the Roger4350 substrate was decrease from -33dB to -16.34dB. This problem might be caused during the fabrication process. When soldering the feeder, there is too much solder and the extra solder act as a radiation element.
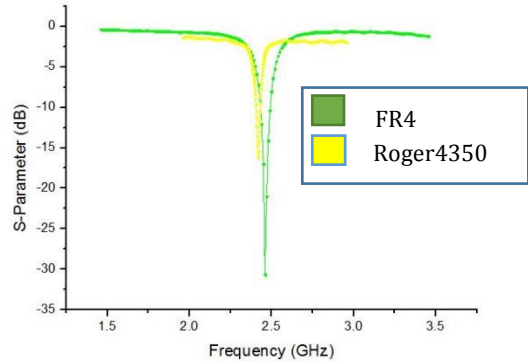

Figure 3: Return Loss comparison for different substrate using mesurement method.

Radiation Pattern.

The proposed prototype has been designed to provide uniform radiation patterns on the broadside of the radiating surface. Figures 4 and 5 show the 2D plots of the radiation pattern using simulation and measurement for different substrate. Figure 6 shows the comparison of the measurement result for the radiation pattern between FR4 and Roger4350.
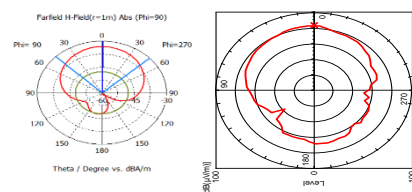

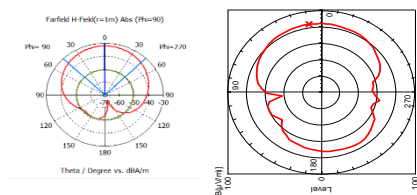Figure 4: Radiation pattern for FR4 using simulating and measurement

Figure 5: Radiation pattern for Roger4350 using simulating and measurement
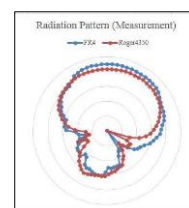

Figure 6 : Comparison of measurement result for radiation pattern between FR4 and Roger4350

Input Impedance. The measured input impedance of fabricated antenna for Flame Retardant 4 (FR4) substrate and Roger 4350 substrate was shown in Figure 7 and 8 below. From the observation, the measured input impedance for Flame Retardant 4 (FR4) substrate is $0.072-j5.1692\Omega$ while for Roger4350 substrate is $62.456-j11.656\Omega$. The value for Roger4350 impedance does not matching with 50Ω and the value is slightly different with the simulation result.
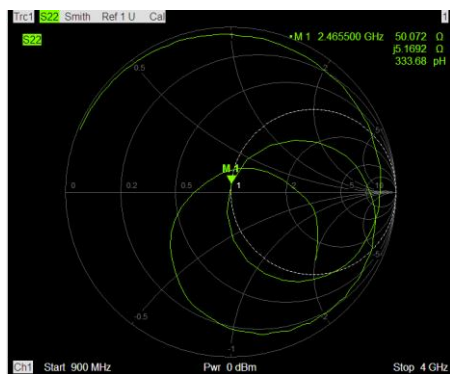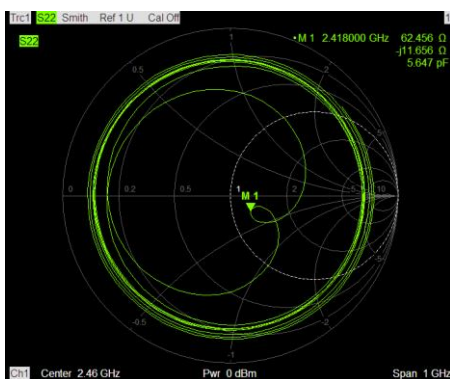

Figure 6: Input Impedance for FR4 substrate

Figure 7: Input Impedance for Roger 4350

Voltage Standing Wave Ratio (VSWR).
The measurement result of Voltage Standing Wave Ratio (VSWR) for Flame Retardant (FR4) substrate was shown in Figure 9 below. The measurement result for Flame Retardant 4 (FR4) is 1.0350 and Voltage Standing Wave Ratio (VSWR) for Roger4350 substrate was shown in Figure 10 below. The measurement result for Roger4350 is 1.3697. From the result, the value for measurement result was higher than simulation result. The variation is for the Flame Retardant 4 (FR4) substrate is 0.14 while the variation for the Roger4350 substrate is 0.27. This different value might cause by the present of the reflected power in the fabricated antenna.

The reflected power increases the magnitude reflection coefficient and caused increment in the value of VSWR since the VSWR is proportional to the magnitude coefficient. However, the antenna is in good performance as the value of VSWR is less than 2.
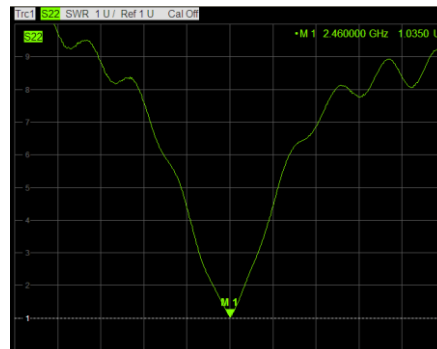
Figure 9: VSWR for FR4
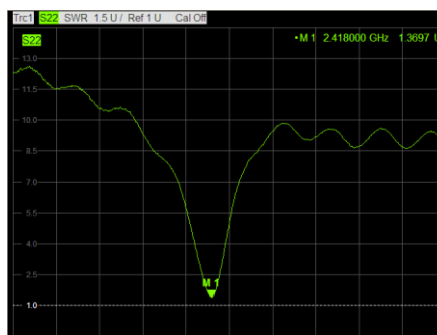
Figure 10: VSWR for Roger 4350

Conclusion
Microstrip patch antenna was chosen because of the advantages compared to conventional antennas. Conventional antennas are large and not suitable for mobile communications. There are several advantages of the microstrip patch antenna such as good in radiation pattern and have a compact shape. Besides that, the microstrip patch antenna have a low-profile design, light, and easy to fabricate. In this project, a microstrip patch antenna for Wireless Local Area Network (WLAN) application was presented. The main objective of this project is to design a microstrip patch antenna which will be operating at 2.4GHz have been achieved. From the result of simulation and measurement of the fabricated antenna design, the microstrip patch antenna provides good result compared to the conventional antenna. The results of return loss, input impedance and also Voltage Standing Wave Ratio (VSWR), shows the agreement between the measurement of the fabricated antenna and the simulation of the antenna design. There are slight differences between the simulation and the measurement results.

Soldering process of the SMA Connector and the microstrip feed line of the antenna design might effects the measurement readings. Besides that, cable loss during the measurement process also contributes to this factor.

References

[1]   Ibrahim Turki Nasar, Small Design for 2.4GHz Application, University of South Florida, 2010.

[2]   Kiram Jaim, Keshav Gupta, Different Substraye use in Microstrip Patch Antenna-A Survey, School of Computing Science and Engineering (2012) 2319-7064.

[3]   Harish Langgar, Bharti Gupta, Comparative study of Microstrip Patch Antenna for Microstrip Feed Line and Different Substrate, International Journal of Engineering Trends and Technology(IJETT), Volume 7 2014.

[4]   N. P. Agra wall, G. Kumar, and K. P. Ray, "Wide-band planar monopole antennas," IEEE Trans. Antennas Propag., vol. 46, no.2, pp. 294–295, Feb. 1998.

[5]   L. Jianxin, C. C. Chiau, X. Chen, and C. G. Parini, "Study of a printed circular disc monopole antenna for UWB systems," IEEE Trans. Antennas Propag., vol. 53, no. 11, pp. 3500–3504, Nov. 2005.

[6]   M. J. Ammann and Z.-N. Chen, "Wideband monopole antennas for multi-band wireless systems," IEEE Antennas Propag. Mag., vol. 45, no. 2, pp. 146–150, Apr. 2003.

[7]   M. J. Ammann and Z. N. Chen, "A wide-band shorted planar monopole with bevel," IEEE Trans . Antennas Propag., vol. 51, no. 4, pp. 901–903, Apr. 2003.

Web Design Education Based on Gamification

Yoppy Sazaki, MT
Faculty of Computer Science
Sriwijaya University
Palembang, Indonesia
yoppysazaki@gmail.com

Arief Rahmansyah
Faculty of Computer Science
Sriwijaya University
Palembang, Indonesia
ariefrahmansyah@hotmail.com

Muhammad Syahroyni
Faculty of Computer Science
Sriwijaya University
Palembang, Indonesia
msyahroyni@hotmail.com

Abstract— **Implementation of gamification is very broad, all sectors of life can implement the concept of gamification, including the education sector. Jagoanilmu.com use based gamification design criteria, certificate, leaderboard, quiz, badge and free course. Web design based gamification to make understand the lessons better, and reduce stress players.**

Keywords— *gamification, Jagoanilmu.com, Web design.*

I. INTRODUCTION

Playing games make people happy and addicted to keep playing it. In contrast with other activity such as sports, study or work. Although some people may enjoy their activity than playing games. However, many people got stressed while studying or working than playing games. The difference between playing games and other activities lies in the pleasure of people (users) find on the games, as a game designed to please players.

The concept of gamification is which the elements and game design was applied to activities other than playing games. The purpose is to make activity that does not include in games becomes fun and interesting. The term of gamification was introduced by Nick Pelling on 2002 (http://zefcan.com/2013). The gamification's concept was popular on 2010, but the concept of gamification has been used before the term itself was introduced. The concept of gamification will be applied become an alternative learning application in media learn to deliver learning materials to people who expected to be useful for improving the quality of education so that add a sense of self confidence.

Gamification implementation is very wide, all sectors of life can implement the concept of gamification, including the educational sector [2]. The concept of gamification is very interesting to examine, one of which is to improve the quality of learning in education.

II. RESEARCH METHODOLOGY

The gamification is applied in educational system to observe the behavior students. How the students get the lessons, how far they get in touch to the system, and how much they are get attracted to the system.

The purpose of this research are:

1. Implement the application based on gamification to improve the learning quality thereby increase people's understanding of the knowledge.

2. Make the knowledge easier to learn and to understand by students.

The benefit of this research are:

1. Improve the student's self confidence in learning though it is difficult and need hard work.

2. Make students more understand about the learning materials.

Observation Method

In this method, will be study about how the system works and observe the design of gamifications that already exist.

The Design of Gamification

The design of gamification that meets criteria is as follows [1]:

1. Fun: Gamification which focused on education or learning materials needs deliver the learning values using feast method to make students feel enjoyed.

2. Loyalty: Gamification gives rewards to the players or students if only the players or students reach certain points.

3. Status: Status shows everything what has been achieved by players or students. There are 2 kind of status, they are badges and leaderboard.

   a. Badges: Symbol which indicates that the player or student has a certain ability and recognized to other players or students.

   b. Leaderboard: Score board which shows points of each players or students, the purpose is to motivate the players or students to be highest scorer.

4. Administrator: In every games, no matter what player thinks, the administrator will always be the winner of the games. If the game is well-designed and the illusion of winning is vital to motivating players or students. In other words, the development and the design of gamification must be suitable to what players or students need, as a fun game, interesting, creative and has educational values to improve knowledge of players or students.

The concept of gamification by following five-steps process [3]:
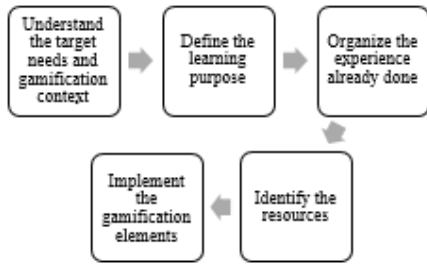
III. RESULT AND ANALYSIS

The website which based on gamification created namely jagoan ilmu, the address is http://www.jagoanilmu.com. Jagoan ilmu's features are:

1. Free course: There are 3 courses, they are data communication, computer network, and computer network security. The materials of each course such as power point presentation, animations or videos.

2. Leaderboard: Each players or students will be get some points and compete each other to be highest scorer.

3. Quiz: Each players or students must be following the quiz in certain modules of each course. The purpose of the quiz is to observe how far the player's or student's understanding to the learning materials.

4. Badge: Each players or students will get certain badge as fit as their progress.

5. Certificate: Each players or students will get the certificate if completed each course.

Fig. 1. Coming Soon Jagoan Ilmu's Interface

Fig. 2. Jagoan Ilmu's Features

A. Courses

The jagoan ilmu's courses are based on bachelor degree. The learning materials are such as power points, animations and videos.

B. Jagoan Ilmu's Scheme
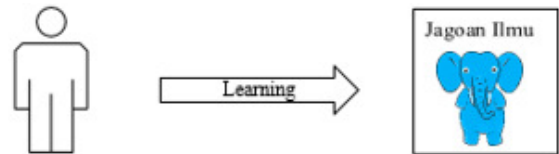
Learning:
1. Each module has main materials
2. Some modules have additional materials in attachment that can be downloaded
3. Some modules have quiz to test player's or student's understanding
4. Each module has different points depend on module's difficulty

Read Materials:
1. Each player or student who read materials will be get some points
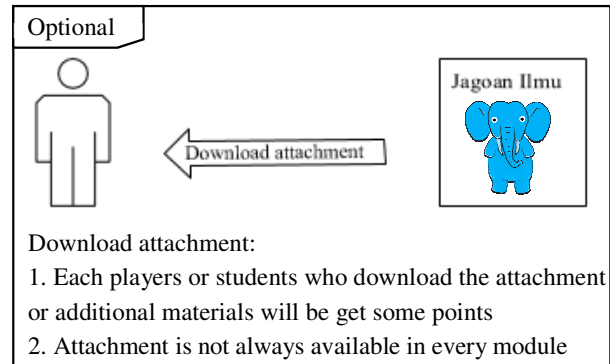
Download attachment:
1. Each players or students who download the attachment or additional materials will be get some points
2. Attachment is not always available in every module
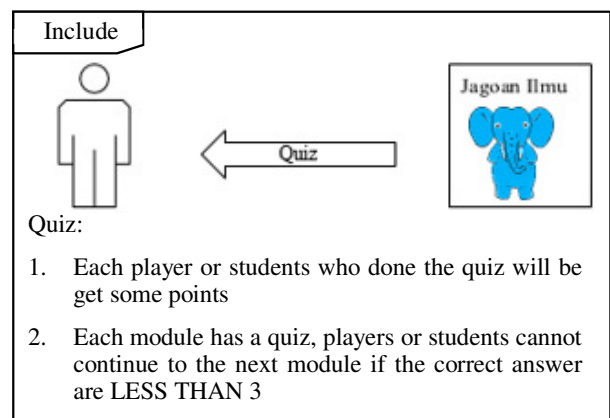
Quiz:

1. Each player or students who done the quiz will be get some points

2. Each module has a quiz, players or students cannot continue to the next module if the correct answer are LESS THAN 3

Achievement 1:

1. Players or students will be get achievement 1 "Welcome" after completing user profile biodata

Achievement 2:

1. Players or students will be get achievement 2 "First Step" after completing the module 0. Module 0 is the first module in the system, it contains the tutorial video about the gamification

Achievement 3:

1. Players or students will be get achievement 3 "The Challenger" after completing first module in any course

Achievement 4:

1. Players or students will be get achievement 4 "Bronze Medal" after completing 2 modules with perfect points

Achievement 5:

1. Players or students will be get achievement 4 "Silver Medal" after completing 3 modules with perfect points

Achievement 6:

1. Players or students will be get achievement 6 "Gold Medal" after completing 4 modules with perfect points

Achievement 7:

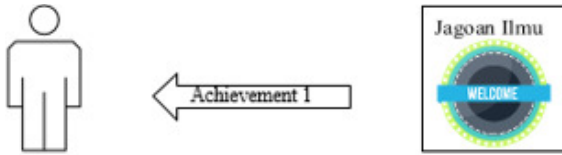1. Players or students will be get achievement 7 "Platinum Medal" after completing 5 modules with perfect points

Achievement 7:

1. Players or students will be get certificate for every course completion

IV. CONCLUSION

The conclusion of this research are as follows:

1. Help players or students to mastering the lessons packaged in the game form.
2. Reduce the stress level of players or students in learning materials.
3. The existence of gamification learning make players or students feel better than conventional learning.
4. Encourage players or students to socialize each other to share the achievements and also compete each other through leaderboard points.

REFERENCES

[1] Zichermann, Gabe and Cunningham, Christopher, *Gamification by Design*, O'Reilly Media. Canada, First Edition, ISBN. 978-1-449-39767-8, August 2011. (*references*)

[2] Miller, Craig. (2013). *The Gamification of Education*. Development in Business Simulation and Experiential Learning.

[3] Huang, Wendy Hsin-Yuan and Soman, Dilip, *A Practitioner's Guide to Gamification of Education*, Rotman School of Management. Toronto, 10 December 2013.

[4] Swacha, Jakub and Baszuro, Pawel. (2013). *Gamification-Based E-Learning Platform for Computer Programming Education.* X World Conference on Computers in Education.

[5] Harsono, Ma'ruf, *Pengaruh Bermain Game Terhadap Perkembangan Remaja*, Surya University. Serpong, Maret 2014.

[6] Stott, Andrew and Neustaedter, Carman. (2015). *Analysis of Gamification in Education*. School of Interactive Arts and Technology, Simon Fraser University.

[7] Gonigal, Jane Mc, *Reality is Broken: Why Game Make Us Better and How They Can Change The World*, The Penguin Press. New York, ISBN. 978-1-59420-285-8, 2011.

[8] Whyte, Moira. (2013). *Gamification in Higher Education*. MA Games Design.

[9] Gee, James Paul, *What Video Games Have to Teach Us About Learning and Literacy*, Palgrave Macmillan. New York, First Edition, ISBN-13. 978-1-4039-8453-1. ISBN-10: 1-4039-8453-0. December 2007.

[10] Enders, Brenda and Kapp, Karl. (2013). *Gamification, Games and Learning: What Managers and Practitioners Need to Know*. The eLearning Guild.

[11] Glover, Ian. (2013). *Play As You Learn: Gamification as a Technique For Motivating Learners*. Proceedings of World Conference on Educational Multimedia.

[12] Beier, Lars. (2014). *Evaluating The Use of Gamification in Higher Education to Improve Students Engagement*. Technische Universtat Dresden.

[13] Gonzalez, Carina and Area, Manuel. (2013). *Breaking The Rules: Gamification of Learning and Educational Materials*. Proceedings of the 2nd International Workshop on Interaction Design in Educational Environments.

[14] Schell, Jesse, *The Art of Game Design*, Elesevier Inc. United States of America, ISBN. 978-0-12-369496-6. 2008.

[15] Hamari, Juho and Koivisto, Jonna. (2015). *Why Do People Use Gamification Services?*. International Journal of Information Management.

[16] Cechanowicz, Jared. Gutwin, Carl. Brownell, Briana and Goodfellow, Larry. (2013). *Effects of Gamification on Participation and Data Quality in a Real-World Market Research Domain*. University of Saskatchewan.

[17] Caponetto, Ilaria, Earp, Jeffrey and Ott, Michela. (2014). *Gamification and Education: A Literature Review*. ITD-CNR

Implementation of Parallel Duplicate Address Detection (PDAD) Mechanism for Macro Handover on HMIPv6

Hamzah U. Mustakim
School of Informatics and Electrical Engineering
Bandung Institute of Technology
Bandung, Indonesia
arekpanjen@gmail.com

TutunJuhana
School of Informatics and Electrical Engineering
Bandung Institute of Technology
Bandung, Indonesia
tutun.j@gmail.com

Abstract— **The ever growing number of mobile devices for internet communication has led to developing Mobile IPv6 (MIPv6) and all of its extentions such as Hierarchical Mobile IPv6 (HMIPv6) that has been introduced for reducing latency and data loss in micro or local handover with employs Mobilty Anchor Point (MAP). But, the problems still occur for macro handover or inter-MAP handover.In this paper we purpose to implement Parallel Duplicate Address Detection (PDAD) on HMIPv6 to reduce latency within macro handover process.**

Key words: HMIPv6, macro handover, PDAD.

I. INTRODUCTION

Mobile IPv6 is an enhancement to IP network which allows devices to roam freely on the Internet while still maintaining the same IP address [1]. The Mobile-IP architecture defines various entities that called the Home Agent (HA), Foreign Agent (FA), Correspondent Nodes (CN), Mobile Node (MN), AccessRouter (AR). Each Mobile Host is associated with a home network as indicated by its permanent IP address. When the mobile node is in its home network, it is counted as a normal host when receiving and sending packets and communicates via standard IP routing mechanisms. If the mobile node moves and changes location to a new network, it will have a new IP address besides its original IP address. The major advantages of MIPv6 is the MN can moves to the other networks without changing the IP address, the mobile nodes change their point-of-attachment to the Internet and allows mobile devices to move from one network to another by maintaining existing connections [2].

Although MIPv6successfuly delivers data from CN to the MN either at the Home Network (HN) or at the Foreign Networks (FN), MIPv6still suffers fromhandover latency problems [3]. The handover latency happens because three major causes, they are Movement detection delay time, Address configuration time and Duplicate Address Detection (DAD) delay time, and Binding Update (BU), in which DAD occupies most of the delay that is recorded as 1000ms approximately and affects the handover efficiency badly. Therefore, lots of studies have been proposed to reduce the handover latency, such as Fast handovers for Mobile IPv6 [4].

In order to reduce handover latecy and signaling delay some researchers have been developedaextention of MIPv6 that called HMIPv6. This extention using new entity called MAP that work as a HA. If a MN moves off the HN to a FN, the MN generates two temporary addresses, Local CoA (LCoA) and a Regional CoA (RCoA). The MN registers newly generated RCoA and LCoA with the HA and the MAP. Then, the MAP intercepts the packets destined to the RCoA and tunnels them to the LCoA. If the MN moves inside the domain of a MAP, the MN has to register an LCoA only with the MAP [5]. Then the MN continues to communicate without registration with the HA and the CN. Moreover, signaling latency is reduced rather than MIPv6 which the MN registers with the HA because the MN is closer to the MAP than the HA. HMIPv6 performs efficiently in micro mobility when the MN moves access routers into a MAP domain. HMIPv6 leads to longer handover latency with more packet loss than MIPv6 when macro-handover occurs because the MN has to register two CoAs [6].

II.RELATED WORK

HMIPv6 is developed to support MIPv6 for global mobility management with employs MAP that reduce latency for local or micro handover effectively. But the ploblems are occur when the MN make a macro mobility or inter-MAP handover such as DAD latency withing new MAP. In the following, we will discuss the existing technique to reducing latency in inter-MAP handover and to improve DAD.

2.1 Fast inter-MAP Handover

In 2009 Zheng Wang et al proposed a scheme with recognizing MN's movement to a new MAP while still staying in the current MAP, the MN can prepare for the handover in advance. As for HMIPv6, another reason for long inter-MAP handover delay is that local movement is not "localized". That is inter-MAP movement is actually incurred by inter-AR movement just as the local movement within the same MAP. So to inform the AR of the movement is the only requirement for early time of the inter-MAP handover.
Considering the pre-handover mechanism, the other procedure of handover can be carried out simultaneously while performing the inter-AR handover [7].

2.2 Fast Macro-Handover Scheme (FMHS)

Sung-Hyun Nam et al proposed a scheme that reduce bindingupdate cost, in which a MN sends binding update (BU) messageincluding the newly obtained RCoA to the previous MAPinstead of its own HA where several MAPs existin the administration domain [6].

2.3 Optimistic DAD

In Optimistic DAD process, the MN can use the nCoA before DAD, but if the DAD result finds that this address is already in use, the address will not be available to the MN and to the user immediately. The advantage of Optimistic DAD is that it can interoperate with standard DAD without adding new devices [8].

2.4 Advance DAD

Advance DAD keeps a list of duplicate-free IPv6 addresses at an AR pool. Each AR generates an address randomly and performs DAD. After checking the uniqueness of the address, the AR stores the address in Passive Proxy Cache and the AR acts as the address of the passive proxy cache. If the AR monitors that another node performs DAD on the same address in its pool, the AR removes that address in its cache, generates a new address, and performs

DAD to keep the list of unique addresses constant [8].

2.5 Parallel DAD

In 2011, M. H. Masud et al proposed Parallel DAD. When MN moves to another network, it will requests parallel for several CoA to its neighboring network as in figure 1. If the MN moves within the time period, it will configure the cached CoA without delay. In this way PDAD takes time only for initial transition and do not need any time for subsequent transition and address configuration. PDAD mechanism reduces the configuration time of MIPv6. After the time expired the routers will refresh their cache [9][10][2].
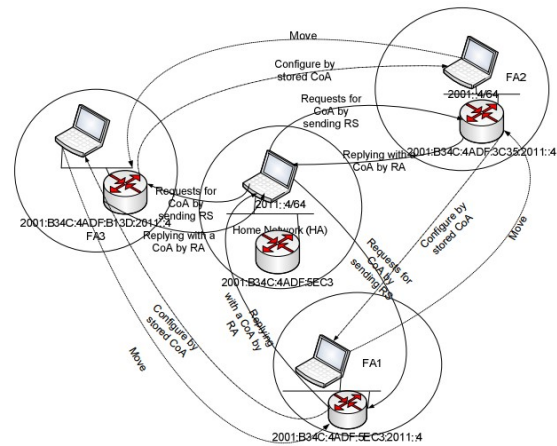
Figure 1. PDAD Mechanism [10]

III. PROPOSED SCHEME

In this section, we will describe our scheme to implement PDAD for macro mobility in inter-MAP handover. This scheme is similar to PDAD mechanism in MIPv6, if a MN moves within a MAP to another network with different MAP then MN will ask RCoA from foreign networks MAP by requesting router solicitation (RS) simultaneously. By request from MN, each MAP in foreign network will generate a unique RCoA to MN and store it to their ache for several times. After MN moves and arrived to new network, MN will use the RCoA from its network MAP. So, with this sceme MN does not need to request RCoA again.Its will reduce signaling time and DAD process time. After completing this process, the MN will receives unique LCoA from MAP as normal procedure in HMIPv6.

IV. FUTURE WORK

In our future work, we will perform simulative evaluation of inter-MAP handover in HMIPv6 using OMNeT++.

V. CONCLUTION

We have proposed a scheme to reduce latency for macro mobility in HMIPv6 using PDAD mechanism for inter-MAP handover. This scheme eliminatesRCoA requesting process and DAD time when MN in the new network.

REFERENCES

[1] Zhijun Yang; Min Zhang; YinghuaCai, "A New Mobile IP Architecture and Routing Mechanism," in *Wireless Communications, Networking and Mobile Computing, 2008. WiCOM '08. 4th International Conference on* , vol., no., pp.1-4, 12-14 Oct. 2008.

[2] Barbudhe, A.K.; Barbudhe, V.K.; Dhawale, C., "Comparison of Mechanisms for Reducing Handover Latency and Packet Loss Problems of Route Optimization in MIPv6," in *Computational Intelligence & Communication Technology (CICT), 2015 IEEE International Conference on* , vol., no., pp.323-329, 13-14 Feb. 2015.

[3] Al-Farabi, K.M.; Kabir, M.H., "Reducing packet loss in Mobile IPv6," in *Computer and Information Technology (ICCIT), 2011 14th International Conference on* , vol., no., pp.38-43, 22-24 Dec. 2011.

[4] Yu-Hsuang Chen; Tin-Yu Wu; Wei-Tsong Lee, "A Novel Mechanism to Improve Handover Efficiency Considering the Duplicate Address Occurs in HMIPv6," in *Advanced Information Networking and Applications (WAINA), 2011 IEEE Workshops of International Conference on* , vol., no., pp.658-663, 22-25 March 2011

[5] H. Soliman, et al., "Hierarchical Mobile IPv6 mobility management," RFC4140, August, 2005.

[6] Sung-Hyun Nam; Hyunwoo Hwang; Ju-Hyun Kim; Kyung-Geun Lee, "Fast Macro Handover in Hierarchical Mobile IPv6," in *Network Computing and Applications, 2009. NCA 2009. Eighth IEEE International Symposium on* , vol., no., pp.323-326, 9-11 July 2009.

[7] Zheng Wang; Xiaodong Li; Baoping Yan, "Fast Inter-MAP Handover in HMIPv6," in *Education Technology and Computer Science, 2009. ETCS '09. First International Workshop on* , vol.3, no., pp.918-922, 7-8 March 2009.

[8] Yu-Hsuang Chen; Tin-Yu Wu; Wei-Tsong Lee, "A Novel Mechanism to Improve Handover Efficiency Considering the Duplicate Address Occurs in HMIPv6," in *Advanced Information Networking and Applications (WAINA), 2011 IEEE Workshops of International Conference on* , vol., no., pp.658-663, 22-25 March 2011.

[9] Masud, M.H.; Anwar, F.; Mohamed, O.M.; Bari, S.M.S.; Salami, A.F., "A Parallel Duplicate Address Detection (PDAD) mechanism to reduce handoff latency of Mobile Internet Protocol version 6 (MIPv6)," in *Mechatronics (ICOM), 2011 4th International Conference On* , vol., no., pp.1-6, 17-19 May 2011.

[10] Masud, M.H.; Anwar, F.; Bari, S.M.S.; Mohamed, O.M., "Enhancement of handoff latency reduction mechanism of mobile internet protocol version 6 (MIPv6)," in *Computer and Communication Engineering (ICCCE), 2012 International Conference on* , vol., no., pp.700-705, 3-5 July 2012.

A High Availability (HA) MariaDB Galera Cluster Across Data Center with Optimized WRR Scheduling Algorithmof LVS - TUN

Bagus Aditya, Tutun Juhana

School of Electrical Engineering and Informatics
Institute of Technology Bandung
Jl. Ganesa No. 10 Bandung, IndonesiaPhone: +62-22-2502260 Fax: +62-22-2534222
E-mail: bagus.aditya.it@gmail.com, tutun@stei.itb.ac.id

Abstract—**Data availability and reliability is very important along with the growth of information and communication technology services today. Needs of the powerful and affordable database system infrastructure to be the most considered thing by the application service provider. This paper presents the powerful and scalable database open source solution infrastructure which can be distributed across the data center in the world to provide any application or content services. Database infrastructure in this paper using MariaDB Galera Cluster which geographically distributed across data center and Linux Virtual Server (LVS)- Tunnel with optimized weighted round robin algorithm as the load balancer. Optimization in this weighted round robin algorithm are focused on assignment value of weight, based on the condition of database server status. The condition include total active thread (active connected client) and Query per Second Average.**

Keywords—**MariaDB Galera Cluster, LVS-TUN, Geo Load Balancing**

I.INTRODUCTION

[13]High availability is essential for any organizations interested in protecting their business against the risk of a system outage, loss of transactional data, incomplete data, or message processing errors. Servers don't run forever. Hardware components can fail. Software can crash. Systems are shutdown for upgrades and maintenance. Whatever the reason, when a server goes down, the applications and the business processes that depend on those applications stop. For a business interested in being available at all times, HA clustering is a practical solution. High availability clusters allow the application and business process to resume operations quickly despite the failure of a server and ensure business is not interrupted. High availability clusters are simple in principle. Two or more servers are joined or clustered together to back each other up. If the primary server goes down, the clustering system restarts the application on one of the other servers in the cluster, allowing the business to continue operating normally. The servers are connected using a network or serial interface so they can communicate with each other. With this kind of clustering there is no need to modify the application.

The principal of this High availability solution inspired us to design the powerful and scalabe Database system as a core of the business. The clustered database server distributed across data center in some country. This method is to reduce the risk in a data center (i.e. bomb,fire, power outage, netowork maintenance,etc.) , so there will no failure response at the system or application because of down database server.

In this paper we used MariaDB as database server. [1]MariaDB is based on the open source MySQL code. It is a branch, or fork, of the source code. Then to clustering the database server we used Galera Cluster. [9]Galera from Codership is a multi master cluster implementation for MySQL and MariaDB.

[16]Load balancer for clustered database server distributed across data center, we used Linux Virtual Server is a software tool that directs network connections to multiple servers that share their workload, which can be used to build highly scalable and highly available services. Prototypes of Linux Virtual Server have already been used to build many sites of heavy load on the Internet, such as Linux portal www.linux.com, sourceforge.net and UK National JANET Web Cache Services.

II. RELATED WORK

1. MariaDB Galera Cluster

[9]Galera from Codership is a multi master cluster implementation for MySQL and MariaDB.Multi master clustering is a type of clustering that allow writes to any server in the cluster, but avoids the complexities of distributed locking, shared disk systems and substitutes these with a more advanced replication system.Galera use the InnoDB Storage Engine of the database server and a

compact library is used to communicate between the involved database servers.

[9]To run Galera, no additional services than the Galera enabled database servers themselves are needed. In a Galera Cluster, all servers are active and database requests can be addressed to anyone of them. This means that the system is always on. As all servers are active, no recovery is needed when an application switch from using one server to the other. From an availability point of view, this is a great benefit. As there is no shared resources and as all the servers are equal, the issues with a single point of failure is removed.

[9]In terms of scalability, this also has tremendous benefits, as the writes may be scaled beyond a single server. Due to Galera using Optimistic locking, scalability can be retained even for writes, despite the fact that all servers hold the same data. In a Cloud environment, elasticity is key. The ability to add, and remove, servers as they are needed. The ability to replace a server with a different one, while still keeping the service running is necessary in a cloud. Also, the ability to optimize the size of each server in a cloud to create the most cost effective setup is another key. Galera allows all this, servers can be added and remove from an existing cluster while the system is fully online .

2. Linux Virtual Server (LVS)

Linux Virtual Server (LVS) is an open source project which developed by Wensong Zhang. Linux Virtual Server has ability to load balance the workload of the multiple server which running Linux kernel based operating system. [13]Load balancing is a computer networking method for distributing workloads across multiple computing resources, such as computers, a computer cluster, network links, central processing units or disk drives. Load balancing aims to optimize resource use, maximize throughput, minimize response time, and avoid overload of any one of the resources.

[16]Linux Virtual Server directs network connections to the different servers according to scheduling algorithms and makes parallel services of the cluster to appear as a virtual service on a single IP address. Client applications interact with the cluster as if it were a single server. The clients are not affected by interaction with the cluster and do not need modification. Scalability is achieved by transparently adding or removing a node in the cluster. High availability is provided by detecting node or daemon failures and reconfiguring the system appropriately.

In this paper we used IPVS is a software which developed by LVS project that implement advanced IP load balancing software inside the linux kernel. [16]IPVS implements transport-layer load balancing, usually called Layer 4 LAN switching, as part of the Linux kernel. IPVS runs on a host and acts as a load balancer in front of a cluster of servers.

There are 3 IP load balancing techniques developed by LVS. There are LVS/NAT, LVS/TUN and LVS/DR. Each techniques has different purposes and implementation technique [16]. LVS/NAT usually used whenLBserver receive request from client at internet/intranet (via Virtual IP (VIP)) then rewrite the request to Real server which connected at private network then real server sending reply back via Lbserver to be forwarded to client. This technique has good security because of the network of real server separated from client because Lbserver acts as gateway. LVS/TUN usually used when LBserver receive request from client at internet (via Virtual IP (VIP)) then forward the request to Real server which connected in any network (WAN/LAN) via tunneling IP then real server sending reply directly to client.[16]The real servers can have any real IP address in any network, and they can be geographically distributed, but they must support IP tunneling protocol and they all have one of their tunnel devices configured with VIP.

LVS/DR has setup and testing is the same as LVS-Tun except that all machines within the LVS-DR (ie the director and realservers) must be on the same segment (be able to arp each other). [16]The load balancer and the real servers must have one of their interfaces physically linked by an uninterrupted segment of LAN such as a HUB/Switch. The virtual IP address is shared by real servers and the load balancer. All real servers have their loopback alias interface configured with the virtual IP address, and the load balancer has an interface configured with the virtual IP address to accept incoming packets.

In this paper we used LVS/TUN to load balance the workload of MariaDB Galera Cluster which distributed across data center which located in separate geography. This method was used because of high availability reason. When real server distributed across data center which located in separated country, it can reduce the possibility risk of natural disaster or political issue which can affect the condition of data center. In the other research, load balancer actually can be distributed also in separated data center as failover server using heartbeat, but in this paper we only focused in the real server which distributed accross data center.

III. IMPLEMENTATION

The infrastructure of mariaDB galera cluster across the data center with LVS/TUN as load balancer is shown below.
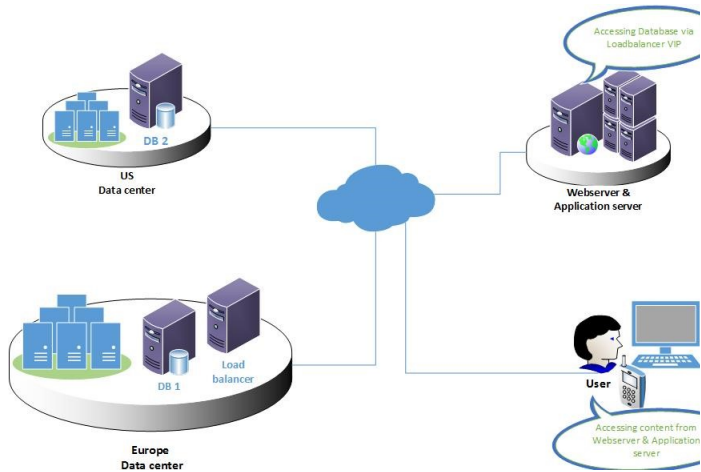
Fig. 3.1 Network Infrastructure

In the above figure shown that DB1 and DB2 located at different data center. In the implementation we used dedicated server hosting at Europe and US which act as Loadbalancer (LVS) and Real Server (DB) with this following detail of server specification :
CPU: AMD Athlon™ X2
(Dual-Core, 2x 1.8 GHz)
Main Memory : 4 GB DDR2
Hard Disks : 2x 320 GB SATA
Link : 100 Mbit/s
Bandwidth guaranteed :100 Mbit/s
External Connections:550 Gbit/s
Operating System CentOS 6

Below is the detail of network Interfaces :

Load Balancer (Location at Europe)
eth0   : 62.75.222.15
eth0:1 : 62.75.223.25

Real Database Server 1 (DB1)(Location at Europe)
eth0   : 62.75.202.135
tunl0 : 62.75.223.25

Real Database Server 2 (DB2)(Location at US)
eth0   : 69.64.38.77
tunl0 : 62.75.223.25

On above details, shown IP address 62.75.223.25 as Virtual IP which shared by load balancer to real database server. This VIP is accessed by application server to access the database server.

Flow Request at Network Diagram

At network diagram above is shown that when user requesting content at application server, the application server sending query to load balancer to selected real database server. [16]The load balancer encapsulates the packet within an IP datagram and forwards it to a dynamically selected real database server. When the real database server receives the encapsulated packet, it decapsulates the packet and finds the inside packet is destined for VIP that is on its tunnel device, so it processes the request, and returns the result to the application server directly. Then, application server replying content to the user.

This implementation usually has an issue at forwarding request to selected real server. This because there are some of ISPs at data center doesn't support IP tunneling protocol. They block spoofing IP activity because of security reason.

IV. PROPOSED ALGORITHM OF HIGH AVAILABILITY MARIADB GALERA CLUSTER WITH OPTIMIZED WRR SCHEDULING ALGORITHM OF LVS-TUN

LVS has some scheduling algorithms to distribute the workload to the real server. There are static and dynamic scheduling algorithms. Round robin (rr) and weighted round robin (wrr) algorithm are included in static algorithms. Then, another dynamic algoritms are least connection (lc), weighted least connection (wlc), etc. The algorithms has strengthness and weakness depends on the infrastructure and the service/application which running in the real server. In this case, we made optimization at weighted round robin (wrr) algorithm at LVS to share the workload of MariaDB Galera Cluster distributed across data center in separated country.

[16]The weighted round-robin scheduling is designed to better handle servers with different processing capacities. Each server can be assigned a weight, an integer value that indicates the processing capacity. Servers with higher weights receive new connections first than those with less weights, and servers with higher weights get more connections than those with less weights and servers with equal weights get equal connections.In the implementation of the weighted round-robin scheduling, a scheduling sequence will be generated according to the server weights after the rules of Virtual Server are modified. The network connections are directed to the different real servers based on the scheduling sequence in a round-robin manner.

We use wrr algorithm because in the implementation, this algorithm is commonly used and more stable than another dynamic algorithms. Additionally we can easily customized the weight of real server destination depends on the MariaDB status and condition.Actually, LVS has dynamic algorithms to check status and condition of the real server. But, the algorithm is running for common server or application infrastructure. In this paper, firstly we check the real status of MariaDB server. Then after
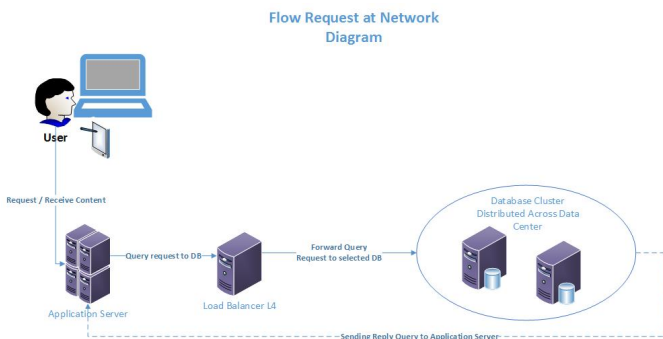
knowing the variable status that indicates the best performance of server, we sort the server based on those value of performance variable status.After all, run the algorithm script in every 3 seconds to update the status of the real server. This explanation can be shown in the following flow chart.
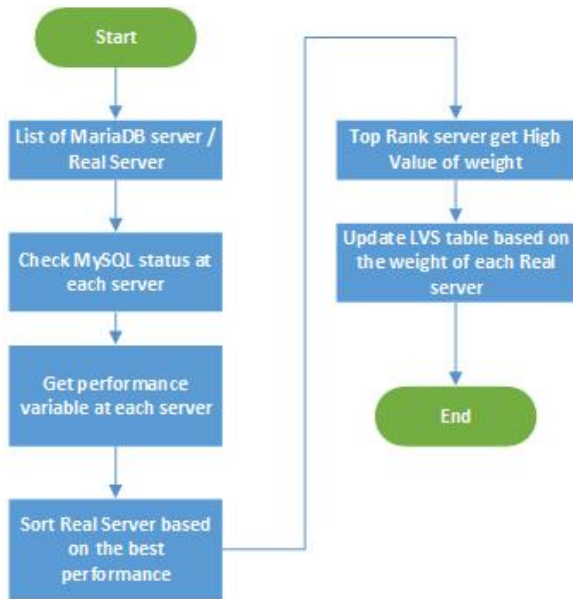

Fig. 3.1 Flow Chart Optimizing wrr in LVS table

This algorithm script is running in the crontab of load balancer server to automatically update the LVS table.This crontab of this script is executed in every 3 seconds. The details of algorithm script to optimize the LVS table is shown below.
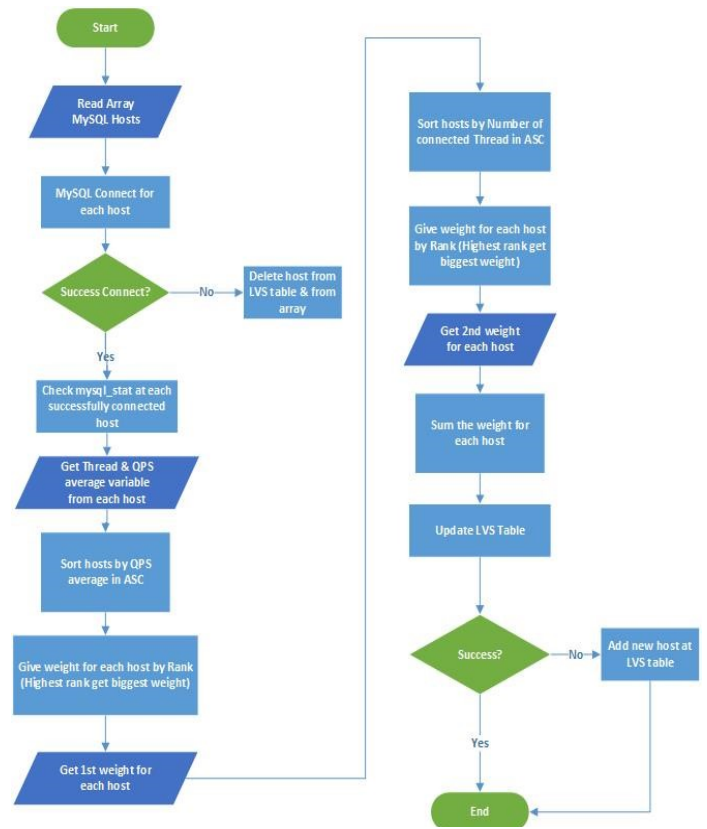
Fig. 3.2 Flow Chart Detail of optimizing wrr in LVS table

At those algorithm we used connected thread and query per seconds average as variable of MariaDB server performance. Connected thread variable indicates the total client that actively connected to MySQL server's thread. So, in this case we can know server capacity's status. If the server has free capacity we can use it as priority server. Then, query per second average indicates that the server load status. If this value has high value, this means the server is busy. Then if server is busy it will execute query longer. So, we can conclude that if the value of average query per second of the server is low we can use it as priority server.

Then as the principal of weighted round robin scheduling algorithm, the top priority server will be assigned to higher weight. After all server has been assigned the weight then it will update the LVS table, so the load balancer can decide then forward the query request to selected priority server.

V. SIMULATION

Infrastructure implementation and simulation of High Availability MariaDB Galera Cluster with optimized wrr algorithm was tested in the real hosted dedicated server in some data centers as described at point III. At simulation test, we were using 2 servers as client which located at the different data center which running sysbench to generate OLTP (online transactions processing) benchmark test to the database server.

The first server generate OLTP transactions through load balancer with various threads, then the second server generate OLTP transactions directly with constant thread to the priority database server based on the weight that has been assigned before depend on the server condition. We're using the second server to simulate when the priority database serveris busy, can it handle the newtransaction which coming from load balancer? Then, how is the performance (throughput/response)?

OLTP benchmark that has been generated from the first server was using various threads starting from 8 until 512 threadswith 10000 maximum requests to 2 million rows of sample data in the database server. The result of benchmarks is shown in the following graph.
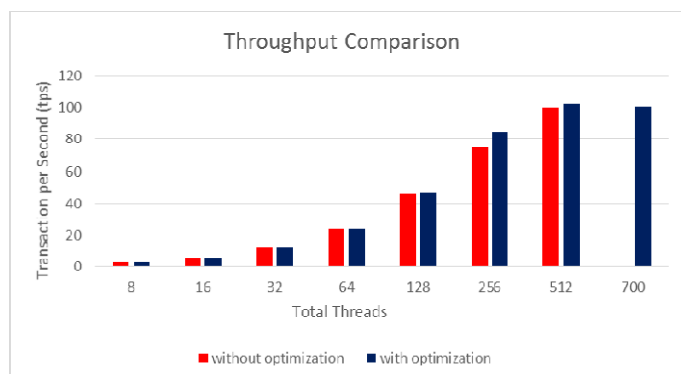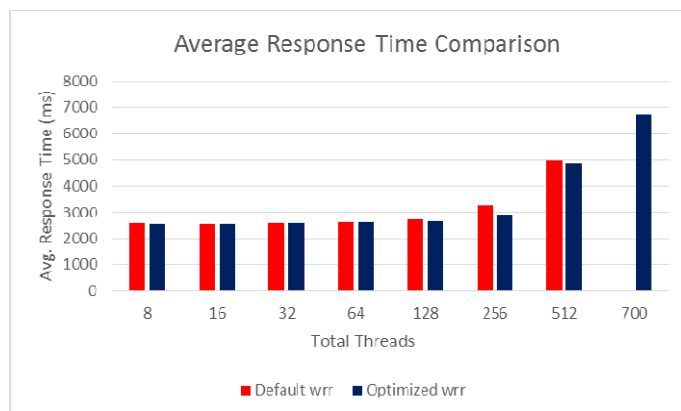

Fig. 5.1 Transaction per Second graph

Fig. 5.2 Avg. Response Time Graph

The result of benchmark simulation, shows that the optimized wrr algorithm can handle more threads and the response time is faster than the default wrr algorithm. At the default wrr simulation, when the load balancer receives more than 512 thread, the connection to MySQL server was lost. It means that the default wrr algorithm can not handle the transaction because the priority server is very busy. After we use optimization in the wrr algorithm, when the clustered database server has different load capacity, it can normalize and balancing the load at the each server so the transaction can be handled.

VI. CONCLUSION

The proposed optimization wrr algorithm at LVS/TUN infrastructure of high availability MariaDB Galera Cluster can be work effectively in the dynamic environment (i.e internet). Because when every server connected to the cloud environment, especially in this case of paper we use clustered database server across data center, the load capacity and the condition of server can be dynamically changed. There are many conditions that make priority server busy and not available anymore to handle the new transaction request, i.e. system security attack, data center trouble (i.e fire, power outage, network maintenance), etc. The automated changes at wrr algorithm is very helpful to adapt the condition of dynamic environment (i.e internet) at the clustered database server which distributed across data center in the different geographical location.

VII. REFERENCE

[1] Bartholomew,Daniel."MariaDB vs.MySQL" in MariaDB whitepaper. September. 2012
[2] Chaurasiya,Vijay, Dhyani,Prabhash,Munot,Siddharth."Linux Highly Available (HA) Fault-Tolerant Servers" in 10th International Conference on Information. DOI Technology.10.1109/ICIT.2007.58
[3] Daryapurkar,Akshay , Mrs. Deshmukh,V.M. "Efficient Load Balancing Algorithm in Cloud Environment" in International Journal Of Computer Science And Applications Vol. 6, No.2, Apr 2013
[4] Dua,Ruchika, Bhandari,Saurabh. "Recovery in Mobile Database System". University of Missouri Kansas City.2006
[5] FromDual."High-availability with Galera Cluster for MySQL".www.fromdual.com
[6] Ingo,Henrik. "How to evaluate which MySQL High Availability solution best suits you" in Percona Live MySQL Conference and Expo.2013
[7] TungYang,Chao, TzuWang,Ko, Li,KuanChing , and Lee,Liang-Teh. "Applying Linux High-Availability and Load Balancing Servers forVideo-on-Demand (VOD) Systems". Tatung University. K.Aizawa,Y. Nakamura, and S. Satoh (Eds.): PCM 2004, LNCS 3332, pp. 455–462, 2004
[8] MarkLogic. High Availability & Disaster Recovery. MarkLogic Data sheet
[9] MariaDB. "MariaDB and MySQL Clustering with Galera" in MariaDB whitepaper
[10] MAZILU,Marius Cristian."Database Replication" in Database Systems Journal vol. I, no. 2/2010
[11] Mohy,Ahmed , Makarem,Mohamed Abul."A Robust and Automated Methodology for LVS Quality Assurance".Egypt.2009
[12] Moniruzzaman,A. B. M. , Hossain,Syed Akther. "A Low Cost Two-Tier Architecture Model for High Availability Clusters Application Load Balancing" in International Journal of Grid and Distributed Computing Vol.7, No.1 (2014), pp.89-98

[13] Moniruzzaman,A. B. M. , Md.Waliullah , Rahman, Md.Sadekur ."A High Availability Clusters Model Combined with Load Balancing and Shared Storage Technologies for Web Servers" in International Journal of Grid Distribution Computing Vol.8, No.1 (2015), pp.109-120

[14] Ni,James.   "System   High   Availability Architecture".Conning Technology.2008

[15] Oracle."MySQL: A Guide to High Availability".A MySQL Strategy Whitepaper.2015

[16] Zhang,Wensong ."Linux Virtual Server for Scalable Network Services". National Laboratory for Parallel & Distributed Processing Changsha, Hunan 410073, China

Non-Intrusive Load Monitoring Using Bluetooth Low Energy

[1)]Arif Indra Irawan, [2)]Tutun Juhana
School of Electrical&InformaticsEngineering
Institut Teknologi Bandung
Bandung, Indonesia
arif.indra.irawan@gmail.com, tutun@stei.ac.id

Abstract—**The energy consumption in residential has been increasing over the past years. Many researches about energy saving which uses information and communication technology have been presented to conserve electrical consumption. Providing residents with information on their energy consumption has become a feasible option to promote energy saving in residential sector. In this paper, a home energy monitoring system using Bluetooth Low Energy (BLE) and sensor non-invasive, is described. The authors designed a system based on BLE and non-invasive sensor so monitoring process of electrical parameter such as voltage RMS, current RMS, real power, apparent power and power factor is realized.**

Keywords— **Smart homes; Energy measurement;** *Bluetooth Low Energy; Nonintrusive appliance load monitoring (NIALM)*

I. INTRODUCTION

Nowadays, the level of energy consumption in the residential has increased excessively. One of the most influential factors on electrical energy consumption comes from inefficient use of electrical appliances such as air conditioner, electric lights, and other home appliances. Technology which can improve electrical energy efficiency is required to overcome energy growth due to the increasing number of population.

One of technology which increase efficiency energy in residential is smart sensors. smart sensor can detect people in the room. If there is people in the room, electrical appliances can automatically turn-on but when no one in the room electrical appliance will be turn-off. Another example is electrical monitoring energy. Information of their electrical consumption can make user change their electrical consumption habit. As the result, user can reduce their consumption rater while operator can avoid overload [1]. Non-Intrusive Load Monitoring (NILM) algorithm aims to separate the aggregated energy consumption signal from each appliance. That algorithm can measured electrical parameter in centralized point using a simple hardware but smart software [2]. NILM become more powerful than the other technology such as smart socket because have lower implementation cost than smart other technology.

In 2010, Bluetooth Special Interest Group (SIG) published their core specification 4.0 including Bluetooth Low Energy (BLE) technology or commonly known as Bluetooth Smart. This low-range radio communications have technical specification that make BLE can run for years only with batteries supply. This makes BLE becomes the leader to Internet of Things [3]. Qualcomm Inc., one of the leading electronics companies in the world, has completed acquisition of the two companies Bluetooth (Stonestreet One LLC. and CSR plc) also indicated that the BLE will be widely applied to various kinds of electronic devices even in smart home area.

The rest of this paper is organized as follows. Section 2 outlines of the related issues. In Section 3, we describe the requirements and features of our proposed energy monitoring system in detail. Section 4 discusses the implementation of research and describe muwhat we have done, and section 5 concludes the paper and mentions our future work.

II. RELATED WORK

Research on the application of BLE has been applied in several fields. In the biomedical field Bin Yu *et al* are applying technology BLE on electrocardiogram monitoring system [4], Bin Yu *et al* use BLE to transmit ECG signal data from sensor node to a smartphone. Furthermore, Zhe-Min Lin *et al* apply the BLE on blood pressure monitoring system is the same as the proposed system of Bin Yu, BLE is used to transmit blood pressure measurement data to a smartphone [5]. Whereas in the farming field, Rajagopal G *et al* propose BLE technology in smart farming, BLE is used to transmit data to the microcontroller; cloud performs real-time intelligence operation and transmits control commands to the microcontroller [6]. While Raphael Frank *et al* proposes BLE on VANET applications, smartphone which is equipped by a BLE radio is used to transmit information between vehicles [7]. In home automation system field, Shiu Kumar *et al* present a low-cost Smart Living System, which uses Android based user interface for control of home appliances. Devices such as light, temperature sensors, gas sensors, motion detection sensors and alarms are well integrated using Siren, nRF24l01+radio module. User can access the system by using Bluetooth connection or the Internet connection, with additional features such as user authentication and voice

activation makes system more secure [8].

In the area energy management system, based on the transmission medium to the main control, there are kind two approaches the first one is wired network such as Power Line Carrier (PLC) and the other is wireless network such as Radio Frequency (RF). In the wired network, transmission cables are used to transmit signals from the main control to the household appliances have a high level of complexity of the installation that causes the wireless technology becomes more widely used due to the installation process easier and more flexible than the wired network. Dhiren Tejani *et al* measure the energy conservation across 4 homes using a Z-Wave home automation system, wireless technology that makes regular household products, like lights, door lock and thermostats "talk" each other, and show an 18,70% decrease in energy consumption when the home automation system acts to manage the power consumption of the devices in the home [9]. Aoi Hashizume *et al* introduce Home Energy Management System (HEMS), an energy monitoring system using sensor network in residential homes. The system is consist of the smart power strip node, sink node, gateway, DB server, and Web server. The smart power strip nodes measure the energy consumptions for the connected home appliance. Sink node aggregates the energy consumption data from smart power strip nodes. Gateway receives data from sink node and writes data to the DB. When web server is accessed, trend charts visualization is obtained data from DB server [10]. Seek Young Cho et al designing intelligent LED lighting system with a smartphone that has the BLE feature, the user can perform monitoring and/or controlling LED lighting system manually from a smartphone. Smart LED lighting system consists of five function blocks including microcontroller, wireless communication interface (used BLE), LED driver, LED light source and power supply. In order to monitor the environmental information, a multi-sensor module consisting of an ambient light sensor, temperature sensor and a motion sensor are combined into microcontroller that enables LED lighting system can be controlled automatically so as to make the LED lighting systems are becoming more intelligent, energy efficient and convenient lighting system [11].

III. SYSTEM ARCHITECTURE

A. System requirements

Our system performs the aggregate of the energy consumption in residential homes, using NILM to separate the energy consumption of each home appliance and visualizes it into a comprehensible form. Fine data visualization is realized to allow residents to understand the details of their energy consumption so they can pay attention about their daily energy usage. To achieve the goal which is described above, some requirement will be discussed below:

1) Sensor nodes are used to monitor energy consumption is non-invasive so deployment of the systems become easier which is not disrupting existing energy power system.
2) Sensor nodes also require a low power wireless communication technology to reduce maintenance costs.
3) For make user easier to know about their power consumption, it requires a sensor node which can process data in a real time.
4) To reduce errors within the process of monitoring the electrical appliance, it required a good NILM algorithm.
5) To meet the demand for visualization of their electric energy consumption habits, it requires a good user interface and data base for storing measurement data.

B. System architecture

We focus on the development of effective, simple to use, and affordable electrical monitoring energy which integrates the Bluetooth Low Energy technology. The structure of the whole system of BLE Non-Intrusive Load Monitoring is shown in Fig.1
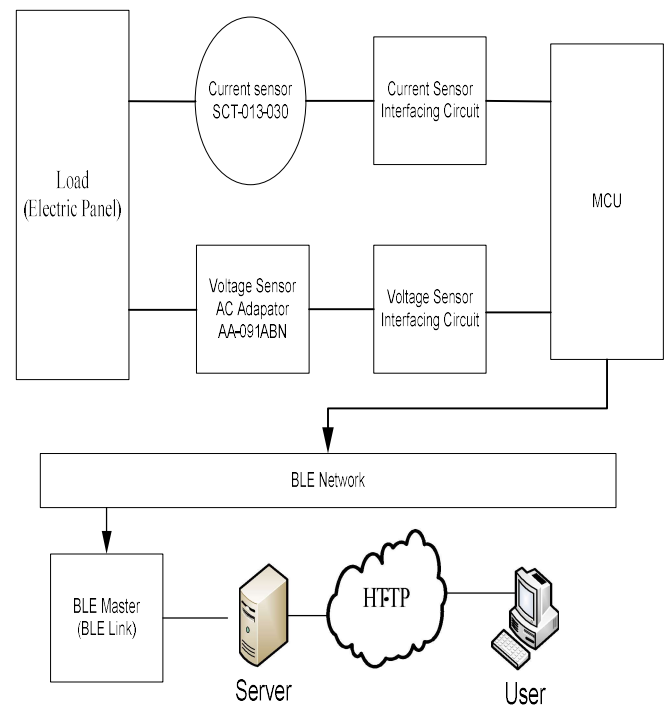
Fig 1. System Block Diagram

The electrical energy monitoring process begins with taking electrical current and voltage analog data from the load.. Then, data will be transmitted to signal conditioning circuit that acts as a signal conditioner. The signal conditioning circuit consists of two parts which is the current interfacing circuit and voltage interfacing circuit.

The Micro Control Unit (MCU) will convert analog signal from interfacing circuit to digital signals, processing electrical variables (such as voltage, current, power factor, real power and apparent power) and transmit data to the server through the network BLE

Server will store data from the MCU, processing NILM algorithm that is used to separate the electrical quantities of each appliance and develop web pages that will be rendered by user.

IV. PRELIMINARY RESULTS

In this section, we will describe what we have done in our ongoing research both in terms of hardware and software.

A. Hardware Development

The hardware device used in this paper was inspired by the open-source hardware that can be accessed [12] with some changes to accommodate requirement of this paper. Fig. 1 shows that there are 5 main building hardware: sensor module, signal conditioning circuit, Micro Control Unit, BLE network and server.

1) Sensor Module

To get the energy consumption of all household appliances, we need information about elctrical current and voltage, for electrical current measurement is used non-invasive current sensor SCT-013-030 while AC adapter AA-091ABN is used to obtain voltage information. Current sensor will convert AC electric current of 0-30 A to 0-5VAC and voltage sensor will convert 220VAC to 9VAC. Both the sensor output will be fed to the signal conditioning circuit

2) Signal Conditioning Circuit

MCU can not directly process the output of the sensor module. Therefore, it requires a signal conditioning circuit. There are two sets of signal conditioning which is signal conditioning circuit voltage and current signal conditioning circuit. The main function of signal conditioning circuit is to scale down signal voltage and adds offset voltage.

a. Current interfacing circuit

Current interface circuit consists of 3 resistors and 1 capacitor, as shown in Fig. 2. Resistors R2 and R3 form a voltage divider circuit which divide 5V supply voltage to 2.5 V. It is used to add offset voltage for current sensor output. Capacitor is used to reduce the voltage ripple. Resistor R4 and the burden resistor of the current sensor form a voltage divider circuit to the sensor output.
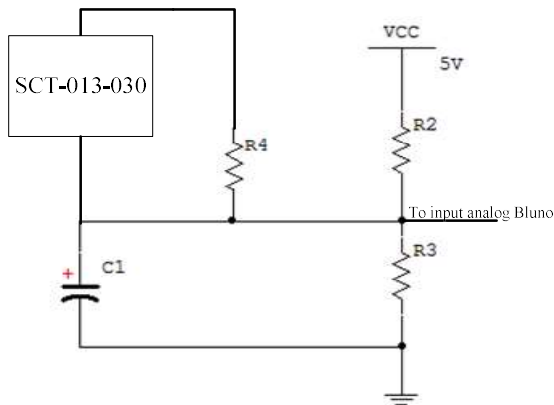

Fig 2. Current Interfacing Circuit

b. Voltage interfacing circuit

Voltage signal conditioning circuit as in Figure 3 consists of 4 resistors and 1 capacitor. R1 and R2 serve as a voltage divider output AC adapter, while R3 and R4 will add offset voltage for AC adapter output. capacitor serves to reduce the voltage ripple.
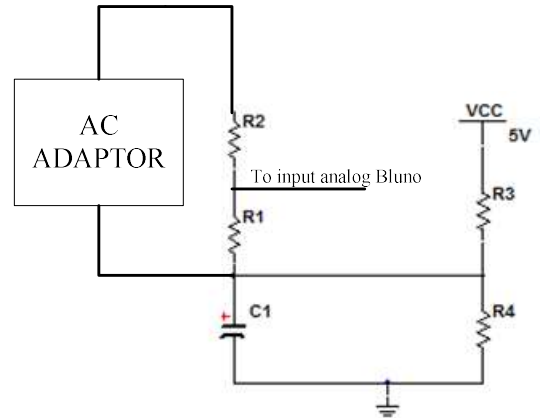

Fig 3. Voltage Interfacing Circuit

3) Micro Control Unit

Micro Control Unit (MCU) module that we use is Bluno which is a combination between Arduino Uno and Bluetooth 4.0/BLE chip (TI CC2540). Bluno will process ADC, calculating electrical power and transmits signals to the server via the BLE.

4) BLE Network

BLE network consists of Bluno and BLE link. Bluno acts as slave Bluetooth while BLE Link as master Bluetooth. Data received by the BLE link will be transmitted to the server via the USB micro cable using serial communication protocol.

5) Server

Server consists of web server that develop web pages and database server that stores data regularly from sensor module. Server will connect to Wi-Fi network which is allows user to monitor their electrical energy consumption from internet.

B. Software Development

There are two parts software block building that proposed by this paper, software block building on MCU side and software building on server side. MCU software block building is used to read data from the signal conditioning circuit then calculates voltage RMS, current RMS, real power and apparent power. To calculate voltage RMS and current RMS, we use equation (1), using equation (2) for real power measurement, using equation (3) for apparent power and using equation (4) for power factor measurement. u(n) is sampled instance of u(t), i(n) is sampled instance of i(t) and N is number of samples [13].

$$U\,rms = \sqrt{\frac{\sum_{n=0}^{N-1} u^2\ (n)}{N}} \qquad (1)$$

$$P \equiv \frac{1}{N} \sum_{n=0}^{N-1} u(n) \times i(n) \qquad (2)$$

$$Apperent\ Power = RMS\ Voltage\ \times RMS\ current \quad (3)$$

$$Power\ Factor = \frac{Real\ Power}{Apparent\ Power} \qquad (4)$$

After MCU obtain data such as voltage RMS, current RMS, apparent power and power factor. That data will be sent to the BLE chip (TI CC22540) in Bluno using serial communication. BLE chip and BLE link forms BLE network, BLE chip acts as slave and BLE link acts as master. Micro USB cable is used to transmit data from BLE link to server. Figure 4 shows voltage RMS, current RMS, apparent power and power factor from MCU software block building..
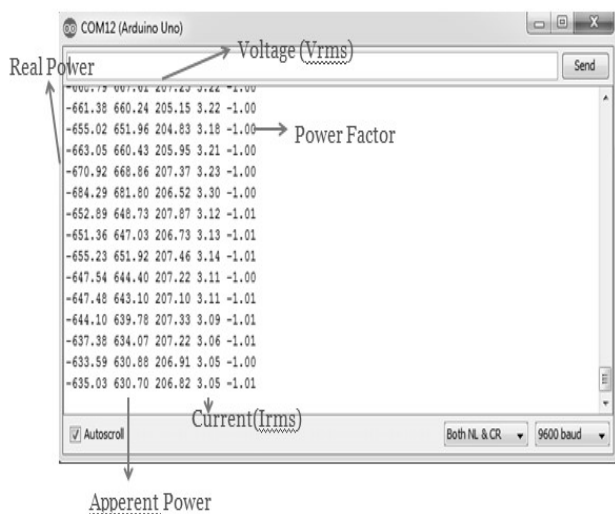

Fig 4. Data from the processing of the MCU through Arduino IDe

V. CONSLUSION AND FUTURE WORK

Energy monitoring system using the network BLE has been implemented at a cost of about 90USD, and uses open hardware design. The system uses a non-invasive sensor which is the installation process will be easier than we use of invasive sensors. The system has been able to measure current RMS, voltage RMS, real power and apparent power and transmit that data to the server.

In the next paper will be embedded algorithms NILM so system can distinguish power consumption of each appliance household . Furthermore, will be developed interactive web pages so users can aware about their consumption of electrical energy and increase the conservation of electrical energy

REFERENCES

[1] H.K. Alfares, M.Nazeruddin, "Electric load forecasting: literature survey and classification methods," *International Journal of Systems Science,* vol. 33, no.1, pp. 23-34, 2002.
[2] Hart. G. W., "Nonintrusive Appliance Load Monitoring," *Proceeding of the IEEE*, vol.80, no.12. Dec 1992.
[3] Decuir, J. "Introducing Blueooth Smart: Part 1: A look at both classic and new technologies", *Consumer Electronics Magazine, IEEE*, Vol:3 no1, pp. 12-18, Jan 2014.
[4] Bin Yu, Xu Lisheng, Yongxu Li. "Bluetooth Low Energy (BLE) Based Mobile Electrodiagram Monitoring," *2012 International Conference on Information and Automation*, ICIA, pp. 763-767, June 2012.
[5] Zhe-Min Lin, Cheng-Hung Chang, Nai-Kuan Chou, Yuan-Hsiang Lin, "Bluetooth Low Energy (BLE) based blood pressure monitoring system," *2014 International Conference on Intelligent Green Builidng and Smart Grid (IGBSG)*, IGBSG, pp.1-4, April 2014.
[6] Rajagopal, *et al*, "Low Cost Cloud Based Intelligent Farm Automation System Using Bluetooth Low Energy," *Humanitarian Technology Conference (R10-HTC),* pp. 127-132, Aug 2014.
[7] Frank. R., Bronzi. W., Castagnani. G., Engel. T., "Bluetooth Low Energy: An alternative technology for VANET applications," *Wireless On-demand Network Systems and Services,* WONS, pp.104-107, April 2014.
[8] Kumar. S., Seong Ro Lee., "Android based smart home system with control via Bluetooth and internet connectivity," *The 18th IEEE International Symposium on Consumer Electronics (ICSE 2014)*, pp. 1-2, June 2014.
[9] Tejani. D., A.M.A.H. H., Al-Kuwari, Potdar. V., "Energy Conservation in Smart Home," *IEEE International Conference on Digital Ecosystems and Technologies (IEEE DEST 2011)*, pp.241-256, June 2011.
[10] Hashizume. A., Mizuno. T., Mineno. H., "Energy Monitoring System using Sensor Network in Residential House," *2012 26th International Conference on Advanced Information Networking and Applications Workshops*, pp. 595-600, 2012.
[11] Cho.Y. S, Kwon. J., Choi. S., Park. D., "Development of smart LED lighting system using multi-sensor module and bluetooth low energy Technology", *Sensing, Communication, and Networking (SECON),* SECON, pp.192-193, June 30- July 3 2014.
[12] How to build an arduino energy monitor-measuring mains voltage and current [Online]. Available: http://www.openenergymonitor.org
[13] AC Power Theory-Advanced math [Online]. Available: http://www.openenergymonitor.org

Migration Strategies of Terrestrial Digital TV Broadcasting in Indonesia

Case Study West Java Area

Hadi Putra Masrul
School of Electrical Engineering & Informatics
Bandung Institut of Technology
Bandung, Indonesia
hadi.masrul@gmail.com

Hendrawan
School of Electrical Engineering & Informatics
Bandung Institut of Technology
Bandung, Indonesia
hend@stei.itb.ac.id

Abstract— The Indonesian government has determined DVB-T as a standard for free to air terrestrial digital TV in Indonesia. Migration to digital technology is done to get a better broadcasting quality and increase the efficiency of spectrum use. This paper describes the strategy of allocating frequency channels to digital broadcast TV taking into account the sustainability of the existing analogue TV services by considering the effect of interference arising from the displacement of frequency channels for area of West Java.

Keywords—DVB-T; Digital; Television, Migration; Strategy; Planning

I. Introduction

TV broadcasting history in Indonesia began when TVRI (state TV broadcaster) launched as the first broadcasting station in 1962. As time goes by, broadcasting TV in Indonesia began to flourish with the emergence of several private TV station, which operates both nationally and locally. However, analog TV technology that is still used today in the world of TV broadcasting in Indonesia can no longer accommodate the growing number of TV stations and higher broadcast-quality requirements. This is due to limited available frequency spectrum, where one frequency channel can only be allocated to one analog service only. Granting broadcasting licenses with limited frequency spectrum available will only cause a decrease in the quality of the broadcast due to interference. Therefore, the use of technology in the world of digital TV broadcasting Indonesia urgently needed.

Based on digital broadcasting technology roadmap designed by the Ministry of Communications and Information Technology, the migration of broadcasting digital technology is planned to be realized in 2018 nationally [1]. The migration process requires the design of the distribution of the allocation of frequency channels for the needs of digital TV broadcasting. Allocating channel for digital TV transmitters need to pay attention to the sustainability of the existing analogue TV services, the effect of interference caused

This study will examine aspects of the interference caused by the allocation of digital channels for existing analog TV stations to areas of western Java. The results of this study can be used as a reccomendation for the Ministry of Communication and Information of Indonesia in the implementation of digital TV services in Indonesia.

II. Reasearch Design

This research will discuss the strategy for the preparation of digital TV broadcasting migration in West Java, covering aspects of the potential of interference due to digital channel assignment to existing analog TV stations.

A. Interference Observation

Research observes interference between analog broadcasting system using PAL-G standard against DVB-T digital broadcasting system. Possible interference between two broadcasting systems. The possibility of interference between the two systems were observed in UHF band IV (channels 28-37) and UHF band V (Channel 38-45) which has been allocated to digital broadcasting [2]. The influence of interference observed was Co-Channel Interference (CCI) and Adjacent Channel Interference (ACI) in the adjacent areas.

Two conditions of possible interference is observed, ie interference to broadcast analog signals PAL-G by the DVB-T transmitters and interference to digital TV broadcasting DVB-T by PAL-G transmitters in West Java area.

Analog transmitters whixh are considered can be seen in the following table:

Table I observed analog transmitter

No	Stasiun Pemancar	Kanal
Bandung, Cimahi, Padalarang, Cianjur		
1	LPP (TVRI)	40
2	Trans TV	42
3	Trans 7	44
4	Global TV	46
Garut, Tasikmalaya		
1	TPI	28
2	SCTV	30
3	RCTI	34
Cirebon, Indramayu		
1	SCTV	36
2	RCTI	38
3	ANTV	42
4	TPI	44
5	Indosiar	46
Sumedang		
1	TPI	31
2	RCTI	33

Meanwhile, DVB-T transmitters which are considered in this study is in accordance with the allocation scenario which has been set by the Ministry of Communications and Information Technology for West Java area as shown in Table II.

Table II. Digital TV frequency allocation in West Java

No	Wilayah Layanan	Kanal Frekuensi
1	Bandung, Cimahi, Padalarang, Cianjur	29, 32, 35, 38, 41, 44
2	Purwakarta	28, 31, 34, 37, 40, 43
3	Sukabumi	28, 31, 34, 37, 40, 43
4	Pelabuhan Ratu	29, 32, 35, 38, 41, 44
5	Cianjur Selatan	30, 33, 36, 39, 42, 45
6	Cirebon, Indramayu	29, 32, 35, 38, 41, 44
7	Garut. Tasikmalaya	28, 31, 34, 37, 40, 43
8	Sumedang	30, 33, 36, 39, 42, 45
9	Majalengka	SFN dengan wilayah layanan Cirebon
10	Kuningan	SFN dengan wilayah layanan Cirebon
11	Ciamis	SFN dengan wilayah layanan Garut, Tasikmalaya

III. ANALYSIS

A. Channel interference of analog broadcasting by digital broadcasting channels

From observations it appears that a number of the same frequency channel used by the existing analog TV transmitters are used also for broadcasting digital TV on adjacent territory, causing the potential for co-channel interference.

Contour calculation shows that the limit values of the Protection Ratio parameter can not be met so that the interfering-signal interfere with the reception of the desired signal in the service area of the analog TV stations. Possible co-chennael interference in the west java area can be shown in the table below:

Table III. Potential for co-channel interference in the service zone of West Java

No	Titik Pengamatan	Kanal UHF
1	[Bandung/Sukabumi]	[40/40]
2	[Bandung/Purwakarta]	[40/40]
3	[Bandung/Garut]	[40/40]
4	[Bandung/Sumedang]	[42/42]
5	[Bandung/Jakarta]	[42/42]
6	[Bandung/CianjurSel]	[42/42]
7	[Cirebon/Sumedang]	[36/36]
8	[Cirebon/Sumedang]	[42/42]
9	[Garut/Sumedang]	[30/30]
10	[Sumedang/Garut]	[31/31]
11	[Sumedang/Purwakarta]	[31/31]

Observation of interference include adjacent channels located above (N + 1) and under (N-1) between the two adjacent areas. The results show that there are seven possible potential adjacent-channel interference. Contour calculation shows that the protection ratio value can not be met so that the interfering-signal interfere with the reception of the desired signal in the service area of the analog TV stations.

Worst interference occurs at frequency channel of analog TV stations in the service area of Cirebon caused by DVB-T transmitters in the service area of Sumedang. Potential adjacent-channel interference that occurs can be seen from the following table:

Table IV. Potential of adjacent-channel interference in the service zone of West Java

No	Titik Pengamatan	Kanal UHF
1	[Garut/Bandung]	[28/29]
2	[Garut/Bandung]	[30/29]
3	[Garut/Bandung]	[34/35]
4	[Sumedang/Cirebon]	[33/32]
5	[Cirebon/Sumedang]	[38/39]
6	[Cirebon/Sumedang]	[44/45]
7	[Cirebon/Sumedang]	[46/45]

Frequency channel migration process from analogue TV station experiencing interference should be a priority to be

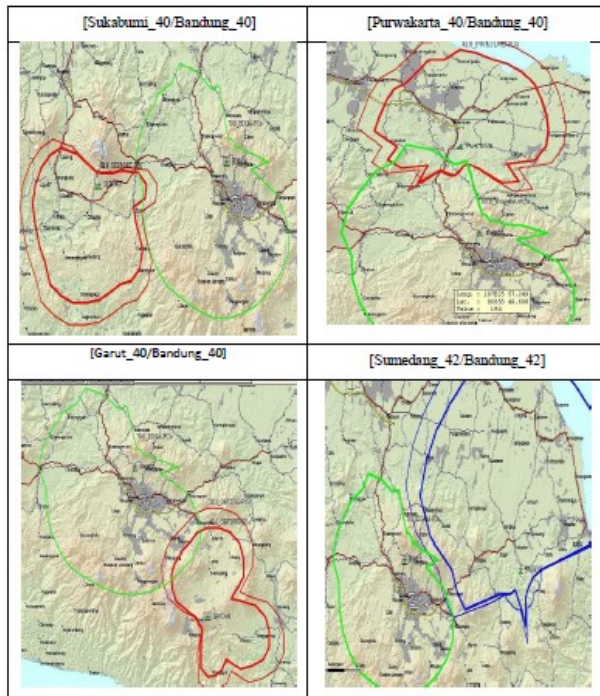transferred to the allocation of frequencies for digital broadcasting.

Fig. 1. Potential Interference Simulation Results [DVB-T/PAL-G]

B. Interference on digital broadcasting channel by analog channel

From the observation, it appears that there are 3 frequency channels allocated for digital broadcasting in the region of Sumedang potentially interferenced by analog broadcasting from Cirebon region. This is because the protection ratio value can not be met so that the interfering-signal interfere with the reception of the desired signal in the Sumedang services. Criteria potential for co-channel interference (CCI) occurs in channels 36 and 42 in which the coverage area of the interfering-signal from analog transmitters in the service area of Cirebon enters the coverage area of minimum field strength of DVB-T transmitters in the service area of Sumedang. Meanwhile, potential criteria for adjacent-channel interference (ACI) occur in channel 45 for the allocation of the digital broadcasting in the region of Sumedang. Interfering-signal from analog transmitters in the service area of Cirebon enters the coverage area of maximum interference field strength of digital broadcast signals in the area of Sumedang significantly. Channel of digital broadcasting frequencies potentially interferenced by existing analog broadcasting frequency channel, used after the existing analog broadcast frequency

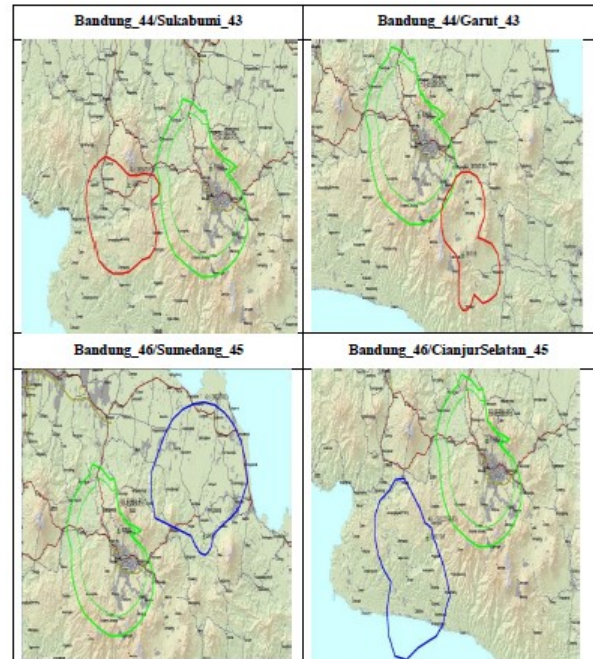channel is migrated to the determined digital channel allocation.

Fig. 2. Potential Interference Simulation Results [PAL-G/DVB-T]

C. Planning of the distribution of frequency channels of analog TV stations to the digital frequency channels

Ministry of Communications and Information has established planning for frequency allocation of digital TV and mapping group of frequencies for each service area. West Java consists of 11 service areas with 3 groups of frequencies used.

Based on the conditions and digital frequency allocation in the service zone of West Java, it is recommended that grouping of TV stations to digital TV services is as follows:

Table V Classification of existing national TV stations to digital broadcasting

Grup	Stasiun TV
Grup 1	LPP : TVRI
Grup 2	MNC GROUP (LPS: RCTI, MNC TV, Global TV)
Grup 3	Trans Corp (LPS: Trans TV, Trans 7)
Grup 4	VIVA Media Group (LPS: ANTV, TV One)
Grup 5	LPS: SCTV, Indosiar, Metro TV
Grup 6	LP Komunitas

IV. Conclusions

1. The potential for the greatest interference occurs on co-channel analog TV transmitters with DVB-T transmitters in West Java.

2. TV stations which are within the criteria of co-channel and adjacent channel interfering are prioritized to be migrated to digital channels. While digital frequency channel potentially inteferenced by existing analog frequencies should be used after the existing analogue frequency channels have moved to the allocated digital frequency

References

[1] [1] "__", White Paper: Migration Broadcasting System Analog to Digital Broadcasting Systems, Directorate General of Post and Telecommunications, pp 2-3, 13-16, 26-28, 34-36, 43-45

[2] [2] "__", "Regulation of the Minister of Communication and Information of the Republic of Indonesia number 39 of 2009", the Ministry of Communications and Information Technology, Jakarta 2009

[3] [3] "__", Final Report: Expert Consulting Services for Implementation of the Advanced Program TV & Radio Broadcasting Digital nationally. Ensemble Indonesia. 2010

Video Processing for Traffic Monitoring Application Using Optical Flow Technique

Bagas Abisena Swastanto[1], Hendrawan[2],
School of Electrical Engineering & Informatics
Bandung Institut of Technology
Bandung, Indonesia
[1]bagasabisena@gmail.com
[2]hend@stei.itb.ac.id

Abstract— **Traffic jam has been a problem in big cities in Indonesia. The placement of monitoring cameras in the street has become one of the solutions to deal with the congestion problem. This study proposes a computer vision system that is capable of extracting important data from the camera. The important data is the average speed of vehicles and the classification of road density in an interval of time. The system is designed to use motion tracking techniques with optical flow to estimate the speed of the vehicle. Optical flow is able to calculate displacement and velocity of the vehicle that occurred between frames. The speed is then used as the basis for the classification of road density at the time. The accuracy of calculation of the velocity was 78.96% in the morning and 41.91% at night. The system manages to calculate the average speed and classification of traffic density on the road. Results calculation and classification of the traffic state of the roads can be properly displayed on the mobile browser Android-based smartphone.**

Keywords— *optical flow, Lucas-Kanade, calculation of vehicle speed, traffic information, traffic monitoring.*

I. INTRODUCTION

Traffic jam and congestion in major cities in Indonesia has been a problem that almost faced every day. Addition of travel time to reach a destination due to congestion resulting in losses in terms of time and fuel. This time loss if converted into economic losses estimated at 5.8 trillion in Indonesian currency per year [1].

Highway authority has sought many ways to cope with the congestion problem. Solutions based on the implementation and installation of CCTV has been attempted. However CCTV can only provide visual information only. The system monitors the state of existing roads is currently only displays the image or the video stream from the CCTV installed on the highway. Therefore, arise an idea to add the functionality of existing CCTV cameras with the software. The system proposed in this study has the ability not only to display video and images, but also be able to "think". The system is able to calculate the velocity of the vehicle captured by the camera and then classify state of the road based on the density of the traffic on the road derived from some calculation.

Visual information coupled with two additional information (speed and road density) into a traffic information is very useful for many people. In order to provide benefits to road users, this information should be easily accessible by the users. Because mobile devices have become common owned by many people, access via mobile web will be very interesting.

This research describes the extraction of traffic information by the software based on computer vision techniques of optical flow. Optical flow detects the movement of vehicles on the road by comparing two frames of the video, then the distance traveled by the vehicle is determined and finally the average speed of the vehicles is derived using method which will explained in the next section. This information will then be used as the basis for classification of the traffic state which is stored and can be accessed through mobile devices.

II. BASIC THEORI

Motion or movement is directly related to the change in position relative to the spatial elements or the movement captured by the camera. The technique of identifying the object to be observed on the video stream is called motion tracking. Motion is detected using features which can be easily extraced from each frame. Edge is a good feature to be used in detecting motion from the frame of the video. Edge is identified by detecting discontinuities in brightness of pixels in a digital image. When an edge is seen from two different directions perpendicular to each other then this point is called the corner and is a unique feature, which can be used as a feature in motion tracking.

There are several algorithms to detect corners one of which is a Harris detection algorithm and then refined as Shi-Tomasi detection algorithm [2].

Optical flow is a technique in performing motion tracking. Optical flow represents image changes that occurred during the movement in the time interval dt and optical flow field is a field that represents the speed of movement of the three-dimensional image of an object in two dimensions [3]. Optical flow computation based on the following assumptions:

 a. Brightness value of the object to be constant over time.

 b. Points around the object move in the same behavior

Every movement produces displacement and velocity, and any speed is adjusted on each pixel in the frame. Displacement means how distance traveled pixels in the current frame relative to the previous frame. When all the pixels in a frame associated with the speed of the optical

flow is categorized as dense optical flow. Conversely, sparse optical flow method requires that only specific points that will be assosiated with a speed so that only those points that will be traced.

Lucas-Kanade algorithm is an algorithm that implements sparse optical flow technique and is based on three assumptions:

    a. *Brightness constancy.* such as optical flow assumption in general, the value of the brightness of the object to be constant over time

    b. *Temporal persistence.* The movement should be fast enough in a very short time.

    c. *Spatial coherence.* The dots around the object must be in one surface, and one same movement [4].

III. SYSTEM DESIGN

This section describes the design stage which has the objective to provide additional traffic information from CCTV already on the road. This system is designed with the following features:

1. Calculate the velocity of the vehicle.
2. Classify the traffic density based on average speed.
3. Store the information into a server which can be accessed through mobile.

Features (1) and (2) is realized with computer vision software. While the feature (3) is realized with a web server that is specially formatted to be displayed on mobile web browser client. Figure 1 shows the overall system design.
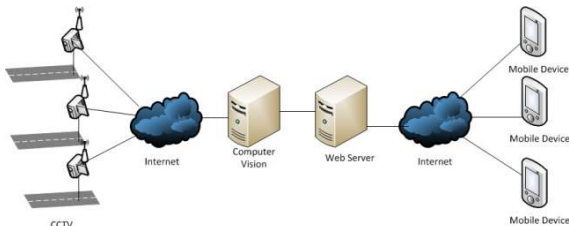

Fid. 1. System Diagram.

IV. SYSTEM IMPLEMENTATION

A. Computer Vision Module

1) Acquisition Frame

Optical flow will process two corresponding frames, therefore it will acquire two sequenced framea (frame i and frame i+1) from the camera video stream as shown in Figure 2. Optical flow can only process the frame with one color channel, therefore 3 color channel (R, G, B) on the frame acquired from the camera video stream is converted into one color channel (greyscale). The next is to determine the region of interest (ROI) of the second frame. ROI serves to limit the area in the frame to be processed in the optical flow.

Fig. 1. Two Adjacent Frame (a) Frame i (b) Frame i+1

2) Motion Speed Estimation

The calculation of the velocity used in this research is a sparse optical flow method of Lucas-Kanade. Sparse optical flow is chosen instead of dense optical flow techniques because the former gives computation time faster than the latter one. Corner detection algorithm that is used in this research is the Shi-Tomasi algorithm. Table 1 summaries the algorithm to calculate the velocity.

Table 1. The velocity calculation algorithm

Acquisition frames i and i+1 from the stream.
Detect corners with Shi-Tomasi algorithm
Apply sparse optical flow in the frame i and i+1 with the Lucas-Kanade algorithm to capture the movement of the vehicle.
Calculate the magnitude of the velocity vector as a result of sparse optical flow processing.
Averaged magnitude of the velocity vector to generate global speed of movement between the frame i and frame i+1.

Figure 3 is the result of a process of optical flow on the two frames that have been acquired in the image of x and y.

Fig. 2. Results of Optical Process Flow

The lines in the figure is a representation of the vector displacement in units of pixels. The magnitude of the displacement vector is calculated based on the euclidean distance as in equation 1.

$$d(x,y) = \sqrt{(x_2 - x_1)^2 + (y_2 - y_1)^2} \qquad (1)$$

Table 2 and 3 shows the magnitude of the displacement vector as a result of calculation using optical flow method on the two frames in Figure 2 (a) and Figure 2 (b).

Table 2. Magnitude Vector 1-20

Vector	Magnitude (pixels)	Vector	Magnitude (pixels)
1	3,04138	11	5,5227
2	5,02495	12	5,5
3	5	13	5,5227

4	4,527695	14	5,5227
5	4,60977	15	5,5227
6	2,061555	16	5
7	3,04138	17	5,5
8	5,5227	18	5,5227
9	4,03113	19	5,5
10	5,5227	20	5

Table 3. Magnitude Vector 21-37

Vector	Magnitude (pixels)	Vector	Magnitude (pixels)
21	6	31	5,5227
22	5,099	32	5,5227
23	5,5227	33	5,02495
24	5,5227	34	5,5
25	4,527695	35	5,5227
26	5,5227	36	6,0208
27	4,5	37	4,527695
28	4,03113		
29	5,02495		
30	6,0208		

Then each of the vectors are averaged to obtain the average global displacement. The term global used because the displacement measured is the transfer of the entire pixel from frame i to frame i+1, instead of the transfer of a moving object. In other words, if there are three objects moving at the time, the displacement represents a moving average of the three objects. Using data form Table 2 and 3, the average displacement is obtained:.

$$\Delta d = 5,024594$$

Because the movement of the object occurs in a very narrow time interval, the velocity of the vehicle is expressed in the instantaneous speed. The travel time is 33 ms or 0,033 s because the video frame rate is 30 frames / sec

$$V = \frac{\Delta d}{\Delta t}$$

$$= \frac{5,024594}{0,033}$$

$$= 153,3604 \text{ pixel/sec}$$

The last step needed is to change the speed unit in metric units. Displacement conversion from pixels to meters or kilometers is needed. Scale conversion is obtained by comparing the length of the road captured by the camera in pixels with a path length in metric.

$$1 \; piksel = {}^{1}\!/_{12} \; meter$$

Then speed can be obtained:

$$v = 12,42076 \; m/s$$

Or in km / h :

$$v = 44,71476 \; km/jam$$

Value speed above will be used as the basis for determining the classification of the density of the highway.

3) Calculation of average Movement Speed

Average moving speed is obtained by calculating the mean of the row of instantaneous movement speed obtained during the time interval t. Implementation is done by looping functions of optical flow during the time interval t. The resulting instantaneous velocity at the end of the function of optical flow is stored into a cache and the function is performed repeatedly. Here's the workflow of the above process:
  a. Perform optical flow in the frame i and i+1
  b. Instantaneous speed calculated
  c. Instantaneous speed is stored in the cache
  d. Perform optical flow in the frame i+1 and i+2
  e. Instantaneous speed calculated
  f. Instantaneous speed is stored in the cache
  g. Etc.

By the time the program runs until the specified interval, a row of instantaneous velocity stored in the cache on average. The average yield was concluded as the average speed of vehicles on the interval 0 to t. Average results are rounded to the nearest integer. Of the value of the speed obtained after the classification of road density can be determined. Classification of congestion levels are selected based on average speed (vrata) and decision making is determined simply by conditional logic as follows:
  a. 0 km/h ≤ vrata < 10 km/jam → heavy traffic jam
  b. 10 km/h ≤ vrata < 20 km/jam → light heavy traffic jam
  c. 20 km/h ≤ vrata < 30 km/jam → busy traffic
  d. vrata ≥ 30 km/h → smooth traffic

4) Output and Traffic Data Delivery

At the end of each interval t, the result of the classification of the following road density with an average speed is stored in XML format. In addition to xml format, the system will also produce data in the form of a single frame image capture results at the end of the interval t and capture the video footage during the interval t-5 to t. The third data has a small footprint. Xml data takes up hard drive space for 1KB, the image of the video ~ 10kb and 300kb. The third data is transmitted to the web server to be delivered via the web.

B. Web Server

The function of this section is to display traffic information to the public via the web. The public can access the information by mobile browser on their smartphone device.
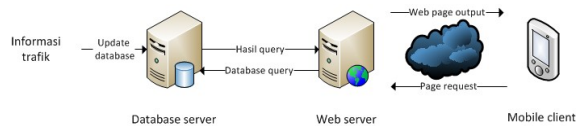

Fig. 3. Web Server Diagram.

Figure 4 shows how the scheme to deliver information over the web. The first database server will always do an update every latest traffic information. When people type in the url website traffic information, then their mobile browser will

send an HTTP request to the server. Web server performs a database query asking for the latest traffic information from the database server, and database server is a web server replying to a query with the latest information. Lastly web server providing HTTP response and the HTML body containing traffic information. HTML formatted in such a way to display small resolution mobile browser.

V. RESEARCH RESULTS

The system has good accuracy in the morning and afternoon, but bad at night. Accuracy is good enough here means the system is still able to classify the density of roads in the appropriate category despite the speed calculation results deviate from the true value. However, when viewed from the context of the system as a means of measuring the velocity of course, then the system is not accurate enough.

System can perform calculations in real time on the third scenario, but there is a delay of 11 ms for each calculation of optical flow in the fourth scenario. It can be concluded that the system is able to perform calculations in real time or with a small delay.

Table 4. Accuracy of System

Morning	Night
78,96%	41,91 %

Table 5. Processing Time

Test Scenario	Average Processing Time (milisekon)
Heavy Traffic	32,27
Light Traffic	44,14

Fig. 4. Web Appearance

VI. REFERENCES

[1] JICA and National Development Planning Agency (BAPPENAS), "The Study on Integrated Transportation Master Plan (SITRAMP) for the Jabodetabek Phase 2," Jakarta, Technical Report 2004.

[2] Jianbo Shi and Carlo Tomasi, "Good Features to Track," in *9th IEEE Conference on Computer Vision and Pattern Recognition*, June 1994.

[3] Milan Sonka, Vaclav Hlavac, and Roger Boyle, *Image Processing, Analysis, and Machine Vision*, 3rd ed. Toronto: Thomson, 2008.

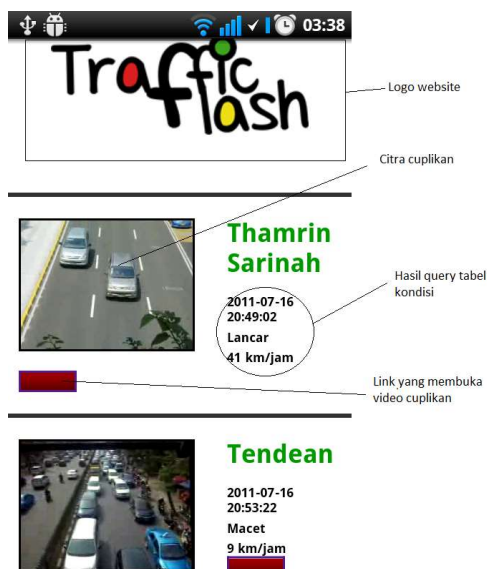[4] Gary Bradski and Adrian Kaehler, *Learning OpenCV*. Sebastopol: O'Reilly, 2008.